

# **UC Berkeley**

## **SEMM Reports Series**

### **Title**

Characterization and representation of pulse-like ground motions using cumulative pulse extraction via wavelet analysis

### **Permalink**

<https://escholarship.org/uc/item/2np8n4bs>

### **Authors**

Lu, Yuan  
Panagiotou, Marios

### **Publication Date**

2013-02-01

Report No.  
UCB/SEMM-2013/01

Structural Engineering  
Mechanics and Materials

---

---

Characterization and Representation of Pulse-like  
Ground Motions Using Cumulative Pulse Extraction  
via Wavelet Analysis

By

Yuan Lu and Marios Panagiotou

---

---

February 2013

Department of Civil and Environmental Engineering  
University of California, Berkeley

## Abstract

This paper presents an iterative method for extracting multiple strong pulses imbedded in historical pulse-like ground motion records. The method results in a representation of the pulse-like part of the ground motion record comprised of the sum of the extracted pulses. Each of the pulses is identified via wavelet analysis using the M&P wavelet based on the waveform developed by Mavroeidis and Papageorgiou (2003). The method is applied to the fault-normal horizontal component of 40 pulse-like ground motion records from 13 historical earthquakes, with magnitudes ranging from  $M_W6.3$  to  $M_W7.9$ , 36 of which were recorded at a distance less than 10 km from the fault rupture. The results of the study indicate that out of a total of 40 records, 34 have more than one predominant pulse. The representation of the ground motion records is evaluated by comparing the linear single-degree-of-freedom displacement spectra for periods ranging between 0.5 and 10 s. The effect of the following parameters of the pulse extraction method on the extracted pulses and resulting representation of the records are studied: (a) the number of extracted pulses (varying from one to three) used in the representation of the record; (b) the type of time-domain (velocity or acceleration time history of the motion) at which the analysis is conducted; and (c) the three weighting functions used in the wavelet analysis. Finally, suggestions are provided for choosing a combination of the above three parameters to achieve different level of representation of the records at different ranges of periods.

*Description of Appendices:* Appendix A1 includes the parameters of the three extracted pulses from each of the six CPE methods investigated; Appendix B1 to B6 include figure sets containing the plots of the time history as well as the SDOF linear spectral response for the extracted pulses and representation  $S_3(t)$  computed by each of the six methods (one figure set per method) studied for each of the 40 records.

## Table of Contents

Introduction.....	1
Motivation.....	3
Cumulative Pulse Extraction (CPE) Method .....	6
Pulse Identification Using Wavelet Analysis .....	8
M&P Wavelets.....	9
Literature Review of Wavelet Analysis Used for Pulse Identification.....	11
Description of the 40 Pulse-like Ground Motion Records Studied .....	12
Extracted Pulses and Results Using the CPE <sub>V-EN</sub> method .....	12
Evaluation of Pulse Representation by SDOF Response.....	19
Effect of Type of Time Domain and Weighting Function of Wavelet Analysis .....	21
Conclusions.....	27
Data and Resources.....	29
References.....	30
Appendix A1: Parameters of the three extracted pulses from each of the six CPE methods investigated .....	A1 - 1
Appendix B1: Time history and linear spectral response of three extracted pulses using the CPE <sub>V-AR</sub> method for 40 motions .....	B1 - 1
Appendix B2: Time history and linear spectral response of three extracted pulses using the CPE <sub>V-EN</sub> method for 40 motions .....	B2 - 1
Appendix B3: Time history and linear spectral response of three extracted pulses using the CPE <sub>V-AM</sub> method for 40 motions .....	B3 - 1
Appendix B4: Time history and linear spectral response of three extracted pulses using the CPE <sub>A-AR</sub> method for 40 motions .....	B4 - 1
Appendix B5: Time history and linear spectral response of three extracted pulses using the CPE <sub>A-EN</sub> method for 40 motions .....	B5 - 1
Appendix B6: Time history and linear spectral response of three extracted pulses using the CPE <sub>A-AM</sub> method for 40 motions .....	B6 - 1

## **Introduction**

The last five decades has seen much research conducted on the identification, characterization, and analysis of pulse-like ground motions. Compared to broadband motions, these motions contain distinct and strong acceleration, velocity, and displacement pulses, which result in large demands in the response of structures. The pulse-like characteristic of such motions is commonly found in many near-fault ground motions and is closely related to forward directivity effects [when the ground motion recording station is in the direction of the fault rupture (Housner and Trifunac 1967, Aki 1968, Somerville and Graves 1993)]. The first near-fault pulse-like ground motion record was obtained during the 1957 Port Hueneme, California, earthquake (Housner and Hudson 1958) approximately 8 km from the epicenter. Since then, many pulse-like near-fault ground motions have been recorded and studied. The dominant period, amplitude, and the shape of the pulses included in near-fault ground motions depend on earthquake source characteristics (i.e. earthquake magnitude and fault mechanism) and site effects (Somerville et al. 1997, Mavroeidis and Papageorgiou 2002, Bray and Rodriguez-Marek 2004, Rodriguez-Marek and Bray 2006).

The effect of pulse-like ground motions on structural response has been investigated in numerous studies, starting with Bertero et al. (1978). Such studies include the response of single-degree-of-freedom (SDOF) structures (Veletsos et al. 1965, Chopra and Chintanapakdee 2001, Makris and Black 2003, Mavroeidis et al. 2004), multi-degree-of-freedom (MDOF) structures (Anderson and Bertero 1987, Alavi and Krawinkler 2004), and long-period structures (first-mode period greater than 2 s) such as tall buildings (Hall et al. 1995, Krishnan et al. 2006, Olsen et al. 2008, Calugaru and Panagiotou 2012a), seismically base-isolated low- and high-rise structures (Makris 1997, Hall and Ryan 2000, Jangid and Kelly 2001, Komuro et al. 2005, Calugaru and Panagiotou 2012b), and structures with a predominant sliding or rocking mode of response (Newmark 1965, Makris and Zhang 2001, Gazetas et al. 2012). A common finding in these studies is that the response to pulse-like ground motions strongly depends on the relative characteristics of the structure (periods, yield strength, and type of nonlinear force-displacement relation) and of the pulses (dominant period, amplitude, and shape).

Several different methods have been developed to characterize and mathematically represent pulse-like ground motions. Common methods to determine the predominant pulse of historical pulse-like near-fault motions include visual inspection of the ground motion time

history, matching of a mathematical pulse representation and the recorded ground motion in the time domain, and matching of the linear SDOF spectral response of the pulse representation with that of the recorded ground motion. Krawinkler and Alavi (1998) used a combination of the aforementioned methods and matching of linear and nonlinear response of MDOF systems to determine the predominant pulse. Somerville (1998) and Bray and Rodriguez-Marek (2004) determined the predominant pulse period based on zero-crossing in the velocity time history. Menun and Fu (2002) used nonlinear regression to fit four types of pulses to the velocity time history of records. Mavroeidis and Papageorgiou (2003) developed a waveform and manually fitted this to the ground motions records by trial and error to optimize the agreement between the pulse representation and the record in terms of velocity and displacement time history as well as in terms of peak spectral velocity. More recent studies have used wavelet analysis, more specifically the continuous wavelet transform, either in the velocity or in the acceleration time domain to identify pulses included in pulse-like ground motions (Baker 2007, Yaghmaei-Sabegh 2010, Vassiliou and Makris 2011). A detailed overview of the variations of wavelet analysis methods used for pulse identification is presented in the section titled *Literature Review of Wavelet Analysis Used for Pulse Identification*.

Although most investigations have focused on identifying one pulse with an associated dominant period,  $T_P$ , in pulse-like ground motions, the existence and classification of multiple distinct pulses of significantly different  $T_P$  in historical records has also been investigated. Mavroeidis and Papageorgiou (2003) utilized a sum of two and three velocity pulses to create pulse representations for two records. Makris and Black (2003) identified, by visual inspection and fitting in the acceleration time history, two distinct pulses in each of two records they studied. Vassiliou and Makris (2011) showed that by using wavelet analysis in the acceleration time domain, the extracted pulse properties (i.e. dominant period, amplitude, and oscillatory character) depend on the type of wavelet and weighting functions used in the wavelet analysis. In comparison to the method proposed in this paper, neither the Makris and Black (2003) nor the Vassiliou and Makris (2011) studies used a combination of multiple pulses to represent ground motion records with more than one predominant pulse. Moustafa and Takewaki (2010) developed simple models for near-fault ground motions using an enveloped oscillatory time history with up to three dominant frequencies. However, their study did not identify the

predominant pulse periods in historical records and did not account for pulses that had little or no overlap in the time domain.

This paper presents a cumulative pulse extraction (CPE) method for extracting multiple pulses from a pulse-like ground motion time history whereby the sum of the extracted pulses forms a representation of the motion; here, wavelet analysis is used to identify pulses. The CPE method is applied to 40 historical pulse-like records, 36 of which recorded at less than 10 km from the fault rupture (near-fault). The level of representation of the 40 records is measured by the difference between the linear SDOF spectral response to the pulse representation and to the historical record, for periods ranging between 0.5 and 10 s. The effect of the following parameters on the properties of the extracted pulses and on the level of representation is studied: (i) the number of pulses, ranging between one and three, used in the pulse representation; (ii) pulse extraction in the velocity (V) or the acceleration (A) time history; and (iii) the weighting function [equal amplitude (AM), equal energy (EN), and equal area (AR)] used in the wavelet analysis. A total of six methods are studied in this paper:  $CPE_{V-AR}$ ,  $CPE_{V-EN}$ ,  $CPE_{V-AM}$ ,  $CPE_{A-AR}$ ,  $CPE_{A-EN}$ , and  $CPE_{A-AM}$ ; the first subscript (V or A) describes the time history in which the wavelet analysis is conducted and the second (AR, EN, and AM) refers to the weighting function used.

## Motivation

Figure 1 shows the acceleration and velocity time history, linear SDOF oscillator spectral acceleration ( $S_a$ ), and spectral displacement ( $S_d$ ) of three historical near-fault pulse-like records: (a) PRPC from the 2011, magnitude 6.3 ( $M_w$ 6.3), Christchurch, New Zealand, earthquake; (b) Parachute Test Site from the 1987,  $M_w$ 6.6, Superstition Hills, California earthquake; and (c) TCU52 from the 1999,  $M_w$ 7.6, Chi-Chi, Taiwan earthquake. Each of these three records is characterized by at least two distinct dominant pulse periods, which can be observed in the velocity time history and/or through local peaks in the spectral response.

For each of these three records, Figure 1 shows the time history and spectral response of two individual pulses – each of a single dominant period – as well as the sum (in the time domain) of the two extracted pulses. These pulses were extracted from the ground motion record using the  $CPE_{V-EN}$  method developed in this paper and are numbered according to the order of extraction. For the PRPC record, the two extracted pulses have a dominant period of  $T_{P,1} = 2.3$  s

and  $T_{P,2} = 4.6$  s, respectively. The peak spectral response of the two extracted pulses agrees well with the local peaks in the spectral response of the record; however, it is clear that neither of the two individual pulses can adequately represent the entire pulse-like part of the ground motion record or the spectral response of this record for the entire range of periods studied here. The composite pulse (shown in red) consisting of the sum of the two individual pulses results in good agreement with the velocity time histories as well as the  $Sa$  and  $Sd$  spectra (for  $T$  larger than 1.5 s) of the record. This is similarly observed in the Parachute Test Site and TCU052 records, where the two extracted pulses have dominant periods  $T_{P,1} = 2.2$  and  $T_{P,2} = 5.0$  s and  $T_{P,1} = 7.4$  s and  $T_{P,2} = 2.2$  s, respectively. Compared to the PRPC record, where the overlap of the two pulses is almost perfect (0.1 s difference in mid-time for the two pulses), the Parachute Test Site and TCU052 records have significantly smaller overlap in the pulses (4.4 s and 4.2 s difference in mid-time, respectively). It is readily understood that the presence of two pulses of significantly different dominant period as well as the type of overlap of these pulses is an important characteristic of a pulse-like ground motion that can significantly affect the response of a structure. Note also that for all three records, the pulse representation consisting of the sum of the two extracted pulses resulted in a poor agreement with that of the records in terms of spectral response for periods smaller than 1.5 to 2 s. The section titled *Effect of Type of Time Domain and Weighting Function of Wavelet Analysis* presents appropriate CPE methods that better extract pulses of shorter dominant period.

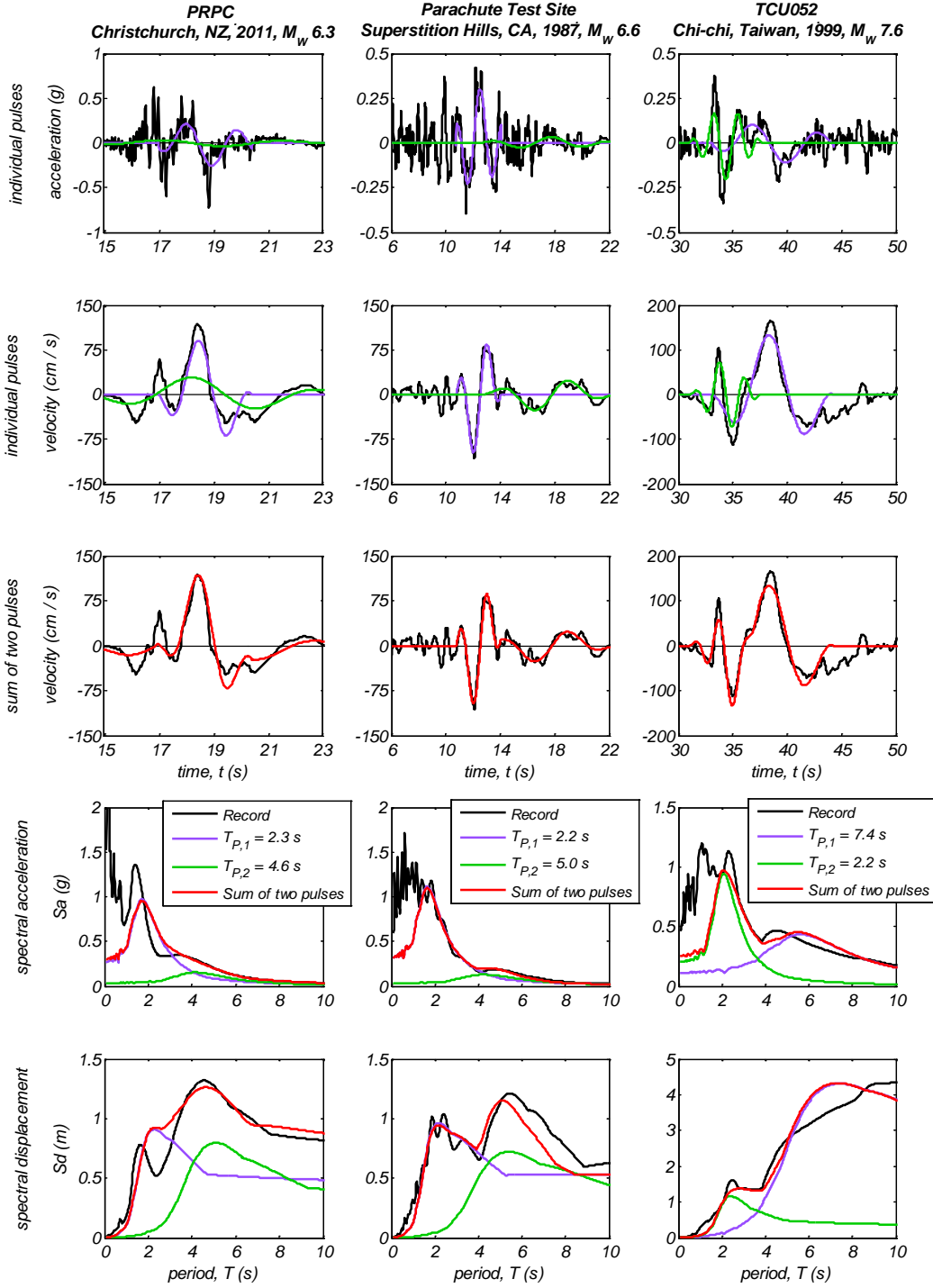


Figure 1. Acceleration and velocity time history, linear SDOF oscillator acceleration and displacement spectra (2% damping) of three historical pulse-like ground motions, as well as their representation using individual pulses and the sum (in the time domain) of two pulses.

## Cumulative Pulse Extraction (CPE) Method

The CPE method extracts multiple pulses from a ground motion record and represents the ground motion as the sum of the extracted pulses: one pulse is extracted in each iteration of the CPE. For a pulse-like ground motion time history  $S(t)$ , the CPE results in the following representation:

$$S(t) \approx S_N(t) = \sum_{i=1}^N P_i(t) \quad (\text{Eq. 1})$$

where  $S_N(t)$  is the pulse representation of  $S(t)$  using a sum of  $N$  pulses  $P_i(t)$  for  $i$  between 1 and  $N$ . Each pulse can be identified using a pulse identification method (e.g., visual pulse fitting, wavelet analysis) chosen by the user. The specific pulse identification method used in this paper is wavelet analysis as defined in the section titled *Pulse Identification Using Wavelet Analysis*. Next, the CPE<sub>V-EN</sub> method is applied to the Pacoima Dam (PCD) ground motion record from the 1971, M<sub>w</sub>6.6, San Fernando earthquake [shown in Figure 2] as an example of the CPE method. A description of the iteration steps of the CPE method follows.

**1<sup>st</sup> iteration:** To identify the first pulse,  $P_1(t)$ , the pulse identification method (wavelet analysis here) is applied to the PCD record.  $P_1(t)$  [shown in Figure 2 (a)] has dominant period  $T_{P,1} = 1.4$  s. After subtracting pulse  $P_1(t)$  from the PCD record, the residual motion is calculated as  $R_1(t) = S(t) - P_1(t)$  and is shown in Figure 2 (b).

**2<sup>nd</sup> iteration:** The second pulse  $P_2(t)$  is identified from the residual motion  $R_1(t)$  using the chosen pulse identification method. For the PCD record,  $P_2(t)$  is shown in Figure 2 (b) and has a dominant period  $T_{P,2} = 5.4$  s. At the end of this iteration, the residual motion  $R_2(t)$  is computed as  $R_2(t) = R_1(t) - P_2(t) = S(t) - [P_1(t) + P_2(t)]$ , which is shown in Figure 2 (c).

**$N^{\text{th}}$  iteration:** The  $N^{\text{th}}$  pulse  $P_N(t)$  is identified from the residual time history  $R_{N-1}(t) = R_{N-2}(t) - P_{N-1}(t) = S(t) - [P_1(t) + \dots + P_{N-1}(t)]$ . For the PCD record, Figure 2 (c) shows the third pulse  $P_3(t)$  which is identified from the residual  $R_2(t)$ .

Figure 2 (d) shows the pulse representation formed by the sum of the first two pulses,  $S_2(t)$ , and first three pulses,  $S_3(t)$ , compared to the original velocity time history,  $S(t)$ , of the PCD record. Figure 2 (e) and (f) show the  $S_a$  and  $S_d$  spectra for the original motion  $S(t)$ , three pulses  $P_1(t)$ ,  $P_2(t)$ , and  $P_3(t)$ , and pulse representations  $S_2(t)$ , and  $S_3(t)$ . As expected, the spectral

response of each individual extracted pulse has a global peak around the dominant period of the pulse [peak  $S_a$  at  $T = 1.1, 4.8$ , and  $0.45$  s and peak  $S_d$  at  $T = 1.4, 5.7$ , and  $0.6$  s for  $P_1(t)$ ,  $P_2(t)$ , and  $P_3(t)$ , respectively]. While the sum of two pulses,  $S_2(t)$ , approximates well the spectral response to the PCD record for  $T > 1$  s, the addition of the third pulse to form  $S_3(t)$  improves the approximation for  $T$  between  $0.5$  and  $1$  s.

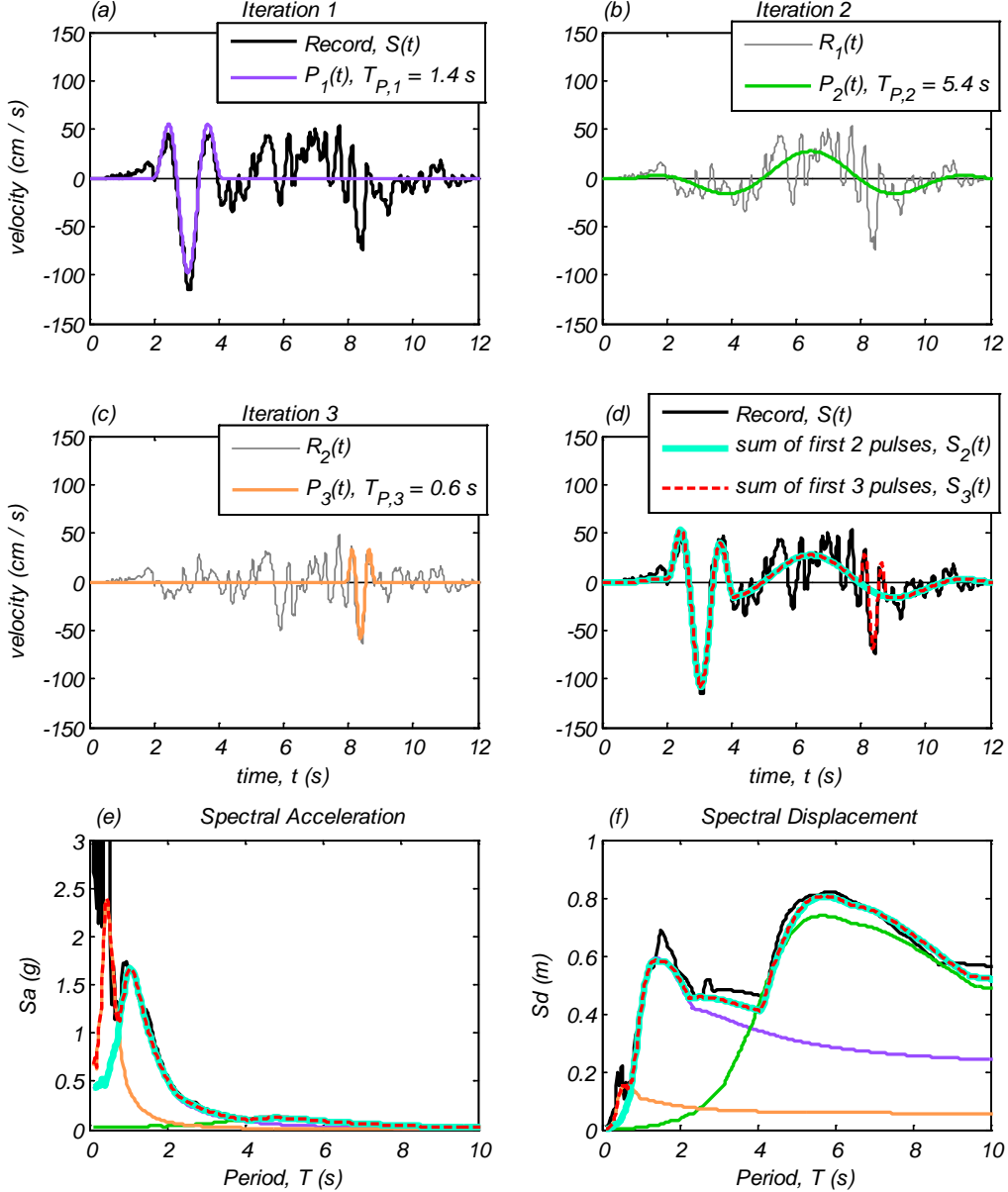


Figure 2. Extraction of three pulses from the PCD record using the CPEV-EN method; linear SDOF acceleration and displacement spectra of the record, each extracted pulse, and the pulse representations  $S_2(t)$  and  $S_3(t)$ .

## Pulse Identification Using Wavelet Analysis

Wavelet analysis is a tool for time and frequency decomposition of a signal (e.g. ground motion time history) using finite length signals, called wavelets, which have a narrow range of periods. Here, the dominant period of the wavelet is defined to be the period corresponding to the peak magnitude of the Fourier transform of the wavelet. For the purposes of pulse identification, the continuous wavelet transform is used to compute the relative degree of match between selected wavelets and the given ground motion time history,  $S(t)$ . The wavelet with the best match is the identified pulse. For all wavelets used in the analysis, a prototype wavelet, called the mother wavelet,  $\Phi(t)$ , is selected; the mother wavelet must satisfy the mathematical requirements of finite energy and zero mean (Mallat 2009). The wavelets  $\varphi_{s,l}(t)$ , are constructed by simultaneous scaling of the amplitude and the period of the mother wavelet, as well as by translating it in the time domain as follows:

$$\varphi_{s,l}(t) = w(s) \Phi\left(\frac{t-l}{s}\right) \quad (\text{Eq. 2})$$

where  $w(s)$  is the amplitude scale factor, called the weighting function,  $s$  is the period scale factor, and  $l$  is the magnitude of translation in time.  $w(s)$  can be selected to achieve a specific relation between the mother ( $\Phi$ ) and the child ( $\varphi_{s,l}$ ) wavelet. The three weighting functions studied here are: (a)  $w(s) = 1/s$ , called equal area (AR); (b)  $w(s) = 1/\sqrt{s}$ , called equal energy (EN); and (c)  $w(s) = 1$ , called equal amplitude (AM). As the names indicate, these weighting functions result in the following relationship between mother and child wavelet: (a)  $\int_{-\infty}^{\infty} |\Phi(t)| dt = \int_{-\infty}^{\infty} |\varphi_{s,l}(t)| dt$  for AR; (b)  $\int_{-\infty}^{\infty} \Phi^2(t) dt = \int_{-\infty}^{\infty} \varphi_{s,l}^2(t) dt$  for EN; and (c)  $\max(|\Phi(t)|) = \max(|\varphi_{s,l}(t)|)$  for AM. For a particular  $s$  and  $l$ , the relative match between the wavelet  $\varphi_{s,l}(t)$  and the signal  $G(t)$  [either the ground motion record  $S(t)$  or residual ground motion  $R_i(t)$  for the CPE method described above] is determined by the continuous wavelet transform as:

$$a_{s,l} = \frac{1}{\int_{-\infty}^{\infty} \varphi_{s,l}^2(t) dt} \int_{-\infty}^{\infty} G(t) \varphi_{s,l}(t) dt \quad (\text{Eq. 3})$$

In the case of discretized data such as ground motion records, the integral shown in Eq. (3) is computed numerically for all the pairs  $(s, l)$  of interest. Independent of the weighting function used, the identified pulse  $P(t)$  is chosen to be the wavelet with the coefficient  $a_{s,l}$  of peak magnitude, with the following expression for the pulse  $P(t)$ :

$$P(t) = a_{s,l} \varphi_{s,l}(t) = a_{s,l} w(s) \Phi\left(\frac{t-l}{s}\right) \quad (\text{Eq. 4})$$

Note that the term  $\int_{-\infty}^{\infty} \varphi_{s,l}^2(t) dt$  appearing in Eq. (3) normalizes the numerator, resulting in a dimensionless coefficient  $a_{s,l}$  that scales the child wavelet  $\varphi_{s,l}(t)$  to the identified pulse  $P(t)$ . This normalization allows the identified pulse to be that with the (a) largest area for AR; (b) largest energy for EN; and (c) largest amplitude for AM. In this study, the values of  $l$  for a ground motion  $G(t)$  range between the start time and end time of the ground motion, with a step equal to the time step of the ground motion.

## M&P Wavelets

The mother wavelets used in this study have the following expression:

$$\Phi(t, \gamma, \theta) = C_{\gamma\theta} \left[ \sin\left(\frac{2\pi}{\gamma}t\right) \cos(2\pi t + \theta) + \gamma \sin(2\pi t + \theta) \right] \left[ 1 + \cos\left(\frac{2\pi}{\gamma}t\right) \right]$$

(Eq. 5)

$$\text{for } (-\frac{\gamma}{2}) \leq t \leq (\frac{\gamma}{2})$$

where  $\gamma$  is the oscillatory character parameter and  $\theta$  is the phase parameter. The variables  $\gamma$  and  $\theta$  provide flexibility for the wavelet to adjust to the pulse shape in the original ground motion. The mother wavelet  $\Phi(t, \gamma, \theta)$  with a specific value  $\gamma$  has a dominant period equal to  $T_{p,\Phi} = \gamma / (\gamma + 0.5)$ . These wavelets, called the M&P wavelets, are the derivative of the waveform derived in Mavroeidis and Papageorgiou (2003). The constant  $C_{\gamma\theta}$  depends on the weighting function and is

defined such that: (a)  $\int_{-\infty}^{\infty} |\Phi(t, \gamma, \theta)| dt = 1$  for the equal area (AR) weighting function; (b)

$\int_{-\infty}^{\infty} \Phi(t, \gamma, \theta)^2 dt = 1$  for the equal energy (EN) weighting function; and (c)  $\max(|\Phi(t, \gamma, \theta)|) = 1$  for the equal amplitude (AM) weighting function. Figure 3 shows the time history for mother M&P wavelets for selected values of  $\gamma$  and  $\theta$  and EN weighting function.

To implement the wavelet analysis with the M&P wavelet for discrete values of  $\gamma$  and  $\theta$ , a separate wavelet analysis was performed for each pair of  $\gamma$  and  $\theta$ . This study used 40 pairs for the wavelet analysis, with values  $\theta = \{0, \pi/8, \pi/4, 3\pi/8, \pi/2, 5\pi/8, 3\pi/4, 7\pi/8\}$  and  $\gamma = \{1.0, 1.5, 2.0, 2.5, 3.0\}$ . The resulting wavelet for any  $s, l, \gamma$ , and  $\theta$  is:

$$\varphi_{s,l,\gamma,\theta}(t) = w(s) \Phi\left[\frac{(t-l)}{s}, \gamma, \theta\right] \quad (\text{Eq. 6})$$

The dominant period of wavelet  $\varphi_{s,l,\gamma,\theta}(t)$  is  $T_p = s[\gamma/(\gamma+0.5)]$ . Here, for each mother wavelet with a specific value of  $\gamma$ , the values of  $s$  are selected such that  $T_p = \{0.3, 0.35, \dots, 0.55, 0.6, 0.7, \dots, 25.0\}$  seconds. Clearly, the number of mother wavelets used determines the required computational effort; however, the smaller the number of mother wavelets, the larger the restriction on the shape and amplitude of the pulse that can be extracted.

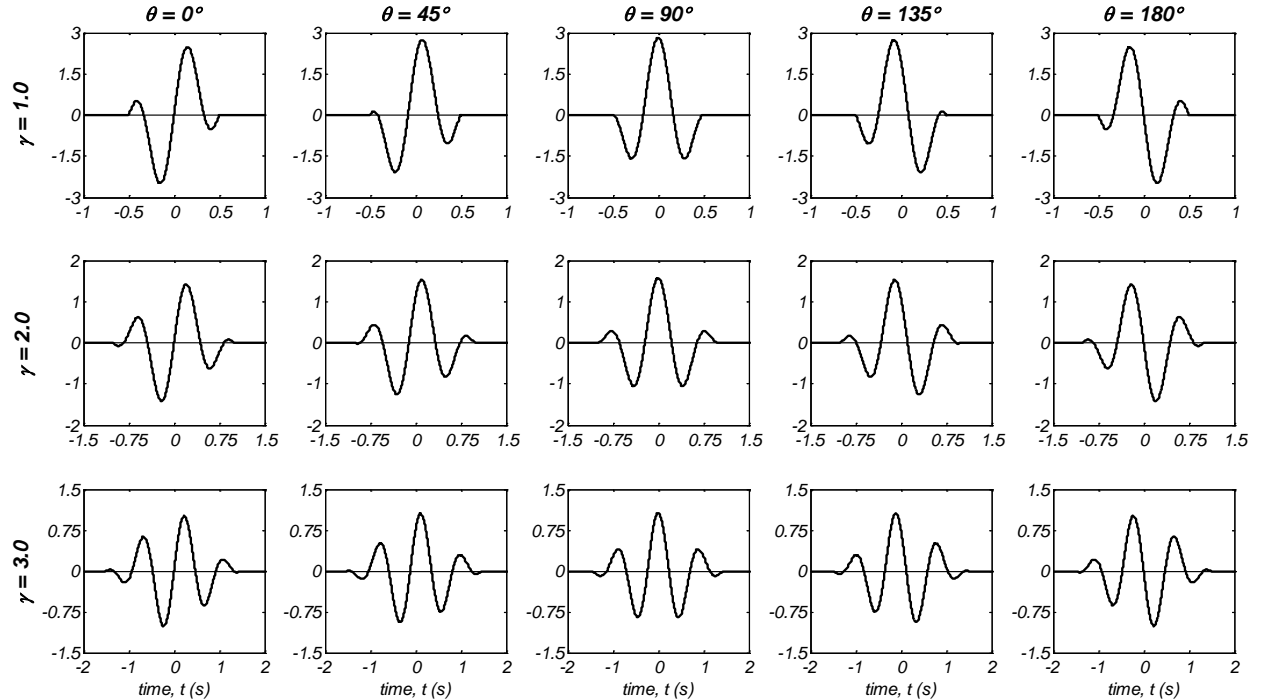


Figure 3. Selected M&P mother wavelets  $\Phi(t, \gamma, \theta)$  for the equal energy (EN) weighting function.

## Literature Review of Wavelet Analysis Used for Pulse Identification

Wavelet analysis using the continuous wavelet transform has been used for identification of pulses in ground motions by Baker (2007), Yaghmaei-Sabegh (2010), and Vassiliou and Makris (2011). Baker (2007) conducted wavelet analysis in the velocity time history to extract a single pulse for each motion, using the Daubechies wavelet order four as the mother wavelet and the equal energy weighting function. To attain flexibility in the extracted pulse shape, he used an iterative procedure: first, he determined the wavelet corresponding to the largest wavelet coefficient from the continuous wavelet transform. This wavelet was subtracted from the original ground motion to give the residual motion. For the subsequent iterations, the continuous wavelet transform was computed for the residual motion, restricted to the dominant period,  $T_P$ , of the first wavelet and temporal position within  $\pm T_P / 2$  of the first wavelet; the wavelet with the largest magnitude coefficient was chosen. The selected wavelet was subtracted from the current residual motion, and a new residual motion was computed for the next iteration. The final extracted pulse consisted of the sum of the 10 wavelets (all having the same dominant period  $T_P$ ), one from each of 10 iterations. Yaghmaei-Sabegh (2010) investigated other types of mother wavelets using the same method as Baker. In their work, Baker (2007) and Yaghmaei-Sabegh (2010) did not determine more than one pulse for a specific ground motion.

Vassiliou and Makris (2011) conducted the wavelet analysis in the acceleration time domain and investigated several mother wavelets, including the M&P wavelet used herein. In addition, they investigated the effect of the three weighting functions (studied here) on the identified pulses of a ground motion. This method was not iterative and, for each pair of type of mother wavelet and weighting function, an independent pulse was determined for each record. In contrast to the study presented here, they did not use a combination of multiple pulses to represent ground motion records.

## Description of the 40 Pulse-like Ground Motion Records Studied

Table 1 lists the 40 historical pulse-like ground motion records studied here, rotated to the fault normal (FN) direction. The specific earthquakes and their associated records are listed in ascending order of earthquake magnitude. The following parameters of the records are listed in Table 1: strike angle, distance from fault rupture ( $R_{rup}$ ), peak ground acceleration (PGA), peak ground velocity (PGV), peak ground displacement (PGD), and the shear wave velocity of the top 30 m of soil ( $V_{s30}$ ). These records were obtained from 13 different historical earthquake events with magnitudes varying from 6.3 to 7.9. All 40 ground motion records were recorded at a distance less than 25 km from the fault rupture,  $R_{rup}$ ; the  $R_{rup}$  is less than 10 km for 36 of those records. The PGV of the 40 records ranges between 44 and 185 cm / s with an average value of 97 cm / s.

## Extracted Pulses and Results Using the CPE<sub>V-EN</sub> method

This section presents the extracted pulses using the CPE method with wavelet analysis performed on the velocity time history using the equal energy weighting function [CPE<sub>V-EN</sub>] of the 40 records described above. For each record, a total of three pulses were extracted; the pulse period  $T_{P,i}$ , the pulse peak velocity  $v_{max,i}$ , and energy ratio  $E_{r,i}$  of these pulses are reported in Table 1; the M&P wavelet parameters ( $\gamma$ ,  $\theta$ , and  $l$ ) are reported in Appendix A1. The energy ratio  $E_{r,i}$  is defined as:

$$E_{r,i} = \frac{\int_{-\infty}^{\infty} P_i(t)^2 dt}{\int_{-\infty}^{\infty} S(t)^2 dt} \quad (\text{Eq. 7})$$

where the numerator and the denominator is the energy of the pulse  $P_i(t)$  and the original ground motion record,  $S(t)$ , respectively. Since the CPE<sub>V-EN</sub> extracts pulses in order of decreasing energy, the  $E_{r,i}$  is a metric of the importance of the pulse. A cut-off value of 7% for the energy ratio  $E_{r,i}$  was used to determine the pulses of significant energy, termed “predominant” pulses. These predominant pulses are shown as bold in Table 1. Although arbitrary, the 7% limit was chosen because it was found adequate to achieve a specific level of representation as discussed in the section titled *Evaluation of Pulse Representation by SDOF Response*.

Table 1. Parameters of 40 pulse-like ground motion records, fault-normal (FN) component, and three pulses extracted by the CPE<sub>V-EN</sub> method. The predominant pulses ( $E_{r,i} > 7\%$ ) are shown in bold.

EQ #	Earthquake Name	M <sub>w</sub>	Strike Angle (N°E)	Record #	Station name	$R_{rup}^{\dagger}$ (km)	$V_{s30}$ (m/s)	PGA (g)	PGV (cm/s)	PGD (m)	Three Extracted Pulses from CPE <sub>V-EN</sub> (Predominant pulses [ $E_r > 7\%$ ] are shown in bold)					
											$T_{P,I}$ (s) [ $E_{r,1} (\%)$ ]	$v_{max,I}$ (cm/s)	$T_{P,2}$ (s) [ $E_{r,2} (\%)$ ]	$v_{max,2}$ (cm/s)	$T_{P,3}$ (s) [ $E_{r,3} (\%)$ ]	$v_{max,3}$ (cm/s)
1	Christchurch, New Zealand 2011/02/22	6.3	57	1	PRPC	2.5	n/a	0.73	118	0.56	<b>2.3 [63]</b>	<b>90</b>	<b>4.6 [17]</b>	<b>29</b>	<b>1.6 [ 8]</b>	<b>32</b>
2	Imperial Valley 1979/10/15	6.5	143	2	EC County Center FF	7.3	192.1	0.18	54	0.38	<b>4.2 [68]</b>	<b>43</b>	<b>5.1 [14]</b>	<b>13</b>	1.5 [4.6]	14
				3	EC Meloland Overpass FF	0.1	186.2	0.38	115	0.40	<b>2.7 [82]</b>	<b>87</b>	<b>2.0 [ 8]</b>	<b>28</b>	0.8 [3.7]	28
				4	El Centro Array #4	7.0	208.9	0.36	78	0.59	<b>4.3 [86]</b>	<b>69</b>	1.3 [4.6]	25	3.5 [3.2]	14
				5	El Centro Array #5	4.0	205.6	0.38	91	0.62	<b>3.8 [82]</b>	<b>81</b>	2.9 [5.0]	21	1.0 [3.2]	24
				6	El Centro Array #6	1.4	203.2	0.44	112	0.67	<b>3.5 [91]</b>	<b>84</b>	7.7 [1.9]	7	1.0 [1.5]	19
				7	El Centro Array #7	0.6	210.5	0.46	109	0.46	<b>3.4 [81]</b>	<b>73</b>	0.7 [5.6]	33	1.4 [5.2]	23
				8	El Centro Array #8	3.9	206.1	0.47	49	0.37	<b>4.2 [72]</b>	<b>39</b>	2.6 [6.7]	13	4.8 [6.4]	9
				9	El Centro Differential Array	5.1	202.3	0.42	60	0.39	<b>3.8 [63]</b>	<b>43</b>	<b>5.4 [10]</b>	<b>16</b>	<b>4.4 [10]</b>	<b>12</b>
3	San Fernando 1971/02/09	6.6	105	10	Pacoima Dam	1.8	2016.1	1.43	116	0.31	<b>1.4 [51]</b>	<b>98</b>	<b>5.4 [18]</b>	<b>27</b>	<b>0.6 [ 8]</b>	<b>59</b>
4	Superstition Hills 1987/11/24	6.6	127	11	Parachute Test Site	1.0	348.7	0.42	107	0.51	<b>2.2 [69]</b>	<b>97</b>	<b>5.0 [13]</b>	<b>26</b>	0.8 [4.6]	33
5	Northridge 1994/01/17	6.7	122	12	Jensen Filter Plant	5.4	373.1	0.39	105	0.45	<b>2.7 [72]</b>	<b>74</b>	<b>1.1 [ 8]</b>	<b>43</b>	3.4 [5.8]	23
				13	Jensen Filter Plant Generator	5.4	525.8	0.52	67	0.43	<b>2.5 [75]</b>	<b>57</b>	<b>6.5 [ 8]</b>	<b>16</b>	0.7 [3.4]	24
				14	Newhall - Fire Sta.	5.9	269.1	0.72	121	0.35	<b>0.9 [35]</b>	<b>95</b>	<b>2.0 [23]</b>	<b>49</b>	<b>2.1 [19]</b>	<b>42</b>
				15	Newhall - W. Pico Canyon Rd.	5.5	285.9	0.43	88	0.55	<b>2.4 [77]</b>	<b>77</b>	1.0 [6.8]	30	2.0 [4.7]	24
				16	Northridge - 17645 Saticoy St	12.1	280.9	0.41	53	0.21	<b>1.8 [29]</b>	<b>47</b>	<b>1.5 [14]</b>	<b>26</b>	<b>1.5 [14]</b>	<b>26</b>
				17	Rinaldi Receiving Station	6.5	282.3	0.89	173	0.32	<b>1.2 [64]</b>	<b>129</b>	<b>1.8 [13]</b>	<b>48</b>	3.9 [6.4]	23
				18	Sylmar - Converter Station	5.3	251.2	0.59	130	0.53	<b>2.6 [46]</b>	<b>70</b>	<b>1.2 [15]</b>	<b>61</b>	<b>0.9 [12]</b>	<b>63</b>
				19	Sylmar - Converter Stat. East	5.2	370.5	0.84	117	0.39	<b>2.8 [57]</b>	<b>47</b>	<b>1.0 [11]</b>	<b>48</b>	<b>1.0 [ 8]</b>	<b>36</b>
				20	Sylmar - Olive View Med FF	5.3	440.5	0.73	123	0.33	<b>2.4 [66]</b>	<b>64</b>	<b>1.2 [16]</b>	<b>44</b>	1.6 [5.8]	23
				21	Tarzana, Cedar Hill	15.6	257.2	1.33	65	0.39	<b>5.8 [28]</b>	<b>27</b>	<b>1.6 [15]</b>	<b>42</b>	<b>1.9 [10]</b>	<b>23</b>

Table 1 cont.

EQ #	Earthquake Name	M <sub>w</sub>	Strike Angle (N°E)	Record #	Station name	R <sub>rup</sub> <sup>†</sup> (km)	V <sub>s30</sub> (m/s)	PGA (g)	PGV (cm/s)	PGD (m)	Three Extracted Pulses from CPE <sub>V-EN</sub> (Predominant pulses [E <sub>r</sub> > 7%] are shown in bold)					
											T <sub>P,1</sub> (s) [E <sub>r,1</sub> (%)]	v <sub>max,1</sub> (cm/s)	T <sub>P,2</sub> (s) [E <sub>r,2</sub> (%)]	v <sub>max,2</sub> (cm/s)	T <sub>P,3</sub> (s) [E <sub>r,3</sub> (%)]	v <sub>max,3</sub> (cm/s)
6	Loma Prieta 1989/10/18	6.9	128	22	LGPC	3.9	477.7	0.65	102	0.37	<b>2.9 [45]</b>	<b>53</b>	<b>1.2 [15]</b>	<b>65</b>	<b>0.9 [12]</b>	<b>57</b>
7	Kobe 1995/01/16	6.9	50	23	Takatori	1.5	256	0.68	169	0.45	<b>1.9 [50]</b>	<b>115</b>	<b>1.1 [16]</b>	<b>82</b>	<b>1.2 [13]</b>	<b>86</b>
8	Duzce, Turkey 1999/11/12	7.1	85	24	Duzce	6.6	276	0.35	61	0.45	<b>5.5 [60]</b>	<b>42</b>	<b>2.9 [12]</b>	<b>26</b>	<b>3.5 [9]</b>	<b>27</b>
9	Landers 1992/06/28	7.3	156	25	Lucerne	2.2	684.9	0.77	93	0.66	<b>4.8 [77]</b>	<b>76</b>	<b>10.5 [14]</b>	<b>19</b>	1.7 [3.2]	27
				26	Yermo Fire Station	23.6	353.6	0.24	56	0.48	<b>7.1 [68]</b>	<b>39</b>	<b>1.2 [11]</b>	<b>28</b>	2.8 [3.6]	10
10	Tabas, Iran 1978/09/16	7.4	40	27	Tabas	2.1	766.8	0.85	121	0.95	<b>4.7 [71]</b>	<b>101</b>	<b>3.8 [8]</b>	<b>31</b>	1.9 [3.2]	29
11	Kocaeli, Turkey 1999/08/17	7.5	92	28	Gebze	10.9	792	0.24	51	0.43	<b>5.4 [73]</b>	<b>41</b>	<b>8.5 [16]</b>	<b>12</b>	3.5 [4.4]	9
				29	Yarimca	4.8	297	0.27	49	0.44	<b>7.7 [39]</b>	<b>32</b>	<b>3.0 [20]</b>	<b>31</b>	<b>3.7 [9]</b>	<b>18</b>
12	Chi-Chi, Taiwan 1999/09/20	7.6	5	30	TCU052	0.7	579.1	0.38	165	2.04	<b>7.4 [70]</b>	<b>133</b>	<b>2.2 [11]</b>	<b>73</b>	<b>18.1 [8]</b>	<b>24</b>
				31	TCU054	5.3	460.7	0.16	60	0.61	<b>9.7 [61]</b>	<b>38</b>	<b>4.0 [11]</b>	<b>18</b>	10.6 [6.2]	10
				32	TCU065	0.6	305.9	0.83	129	0.94	<b>4.4 [51]</b>	<b>90</b>	<b>3.1 [8]</b>	<b>46</b>	12.7 [6.6]	24
				33	TCU067	0.6	433.6	0.52	84	0.96	<b>11.1 [40]</b>	<b>42</b>	<b>1.9 [17]</b>	<b>63</b>	1.8 [6.8]	32
				34	TCU068	0.3	487.3	0.56	185	3.50	<b>11.3 [78]</b>	<b>159</b>	<b>3.2 [10]</b>	<b>101</b>	22.0 [4.2]	23
				35	TCU075	0.9	573	0.33	89	0.87	<b>4.9 [65]</b>	<b>78</b>	<b>3.5 [8]</b>	<b>24</b>	<b>15.7 [7]</b>	<b>14</b>
				36	TCU087	7.0	473.9	0.13	44	0.65	<b>8.3 [74]</b>	<b>31</b>	<b>3.6 [7]</b>	<b>14</b>	4.5 [3.3]	8
				37	TCU101	2.1	272.6	0.21	68	0.73	<b>8.1 [69]</b>	<b>41</b>	<b>3.2 [10]</b>	<b>22</b>	5.3 [6.9]	13
				38	TCU102	1.5	714.3	0.30	109	0.88	<b>7.5 [54]</b>	<b>56</b>	<b>2.8 [18]</b>	<b>46</b>	1.5 [6.8]	48
				39	TCU103	6.1	494.1	0.13	62	0.86	<b>7.3 [70]</b>	<b>46</b>	<b>3.1 [10]</b>	<b>24</b>	<b>3.1 [7]</b>	<b>20</b>
13	Wenchuan, China 2008/05/12	7.9	43	40	Mianzuqingping	3.0	n/a	0.93	138	1.38	<b>7.7 [69]</b>	<b>79</b>	<b>2.5 [10]</b>	<b>40</b>	20.6 [5.7]	14

† Closest distance to fault rupture

Figure 4 (a) shows the periods of the extracted predominant pulses for each of the 40 records. Vertical dashed lines are used here to separate the records recorded in different earthquakes. Of the 40 records, 34 records have more than one predominant pulse; of these, 15 have a total of three predominant pulses. All records from earthquakes of  $M_W \geq 6.9$  include more than one predominant pulse. Figure 4 (b) shows the extracted predominant pulse periods plotted versus earthquake magnitude,  $M_W$ , along with the relationships between the two quantities from Mavroeidis and Papageorgiou (2003) and Baker (2007). The two curves fit decently to the period of the first extracted pulse from the 40 ground motion records. Better agreement was achieved using the relation developed in Mavroeidis and Papageorgiou (2003) for the  $M_W 7.6$  records (Chi-Chi, Taiwan earthquake), while both of these relations underestimated the extracted  $T_{P,I}$  for the  $M_W \leq 6.5$  records (Christchurch, New Zealand and Imperial Valley, California earthquakes) and overestimated it for the  $M_W 6.7$  Northridge, California, earthquake records. These relations do not

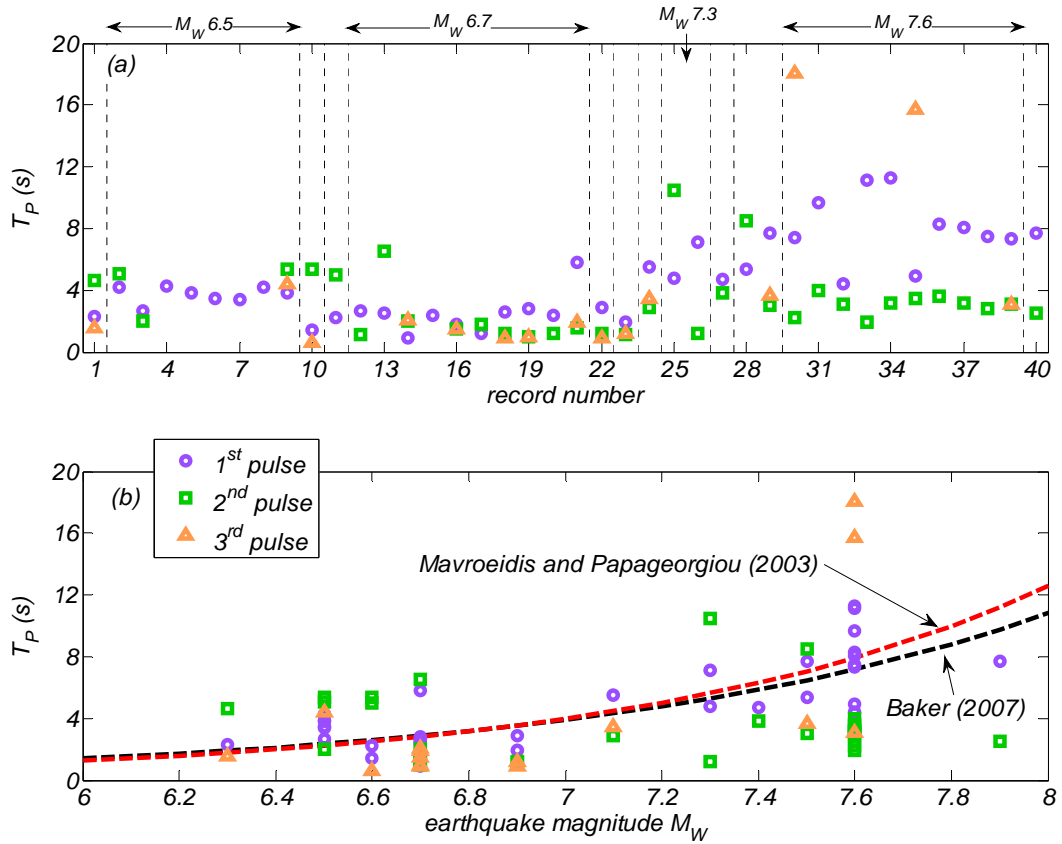


Figure 4. Periods  $T_P$  of predominant ( $E_{r,i} > 7\%$ ) pulses computed using CPEv-EN method: (a) for each record; and (b) versus earthquake magnitude  $M_W$ .

account for nonlinear site effects. The dominant periods of the first extracted pulse is, on average, 0.88 times that identified in both Mavroeidis and Papageorgiou (2003) and Baker (2007) for the motions that are considered both in their studies and herein. However, in most cases, the second and third predominant extracted pulses have dominant periods significantly different (either shorter or longer) than that of the first pulse and that predicted by the aforementioned relations. For the 40 records, the average  $T_{P,1} = 4.7$  s and average  $v_{max,1} = 70$  cm / s.

For the periods of the extracted predominant pulses, the ratio between the periods of pulse  $i$  and  $j$  is defined as  $r_{TP,ij} = \max(T_{P,i}, T_{P,j}) / \min(T_{P,i}, T_{P,j})$ . The ratios  $r_{TP,12}$ ,  $r_{TP,13}$ , and  $r_{TP,23}$  are shown in Figure 5. The average value of  $r_{TP,12}$  for the 34 records with more than one predominant pulse is 2.45, with the maximum and minimum value to be 5.9 (record #26 Yermo Fire Station) and 1.2 (record #16 17645 Saticoy St), respectively. For these 34 records, the average value of  $T_{P,2}$  was 3.3 s and that of  $v_{max,2} = 38$  cm / s (0.54 times  $v_{max,1}$ ).

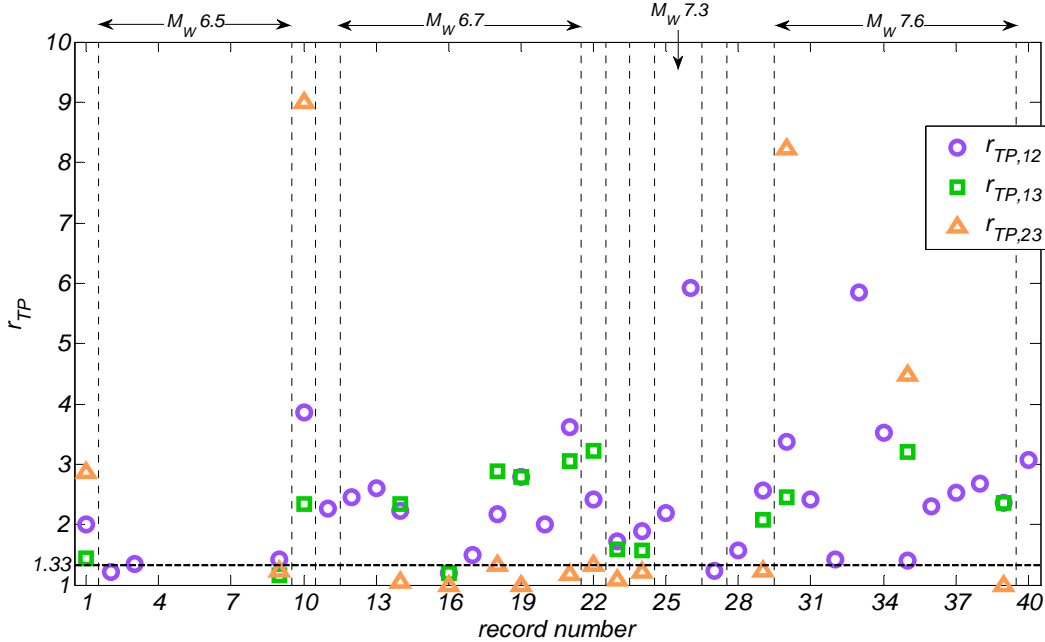


Figure 5. Ratio of largest to smallest periods between the first and second ( $r_{TP,12}$ ), first and third ( $r_{TP,13}$ ), and second and third ( $r_{TP,23}$ ) predominant pulses computed using CPEv-EN method.

Of the 15 records that have three predominant pulses, the period of the third predominant pulse was distinct (defined as either less than 0.75 or greater than 1.33 times that of the first and second predominant pulses) in only 4 records (#1 PRPC, #10 Pacoima Dam, #30 TCU052, and #35 TCU075).

For motions where the pulse-like part of the motion has a high oscillatory character, the third predominant pulse can be an extension of the previously extracted pulse; but due to the restrictions imposed by the pulse extraction method used – the shape of mother wavelet and the limited values of  $\gamma$  (oscillatory character parameter) of the mother wavelet – the pulse was extracted in multiple parts resulting in extracted pulses of similar dominant periods. The three extracted pulses for one of these records (record #14 Newhall Fire Station) is shown in Figure 6; the two pulses of similar period had little overlap and appear to be one pulse of a specific dominant period and larger number of cycles. For this motion,  $V_{s30}$  is 269.1 m / s; thus, nonlinear site effects are possibly a cause of the level of oscillatory character of this motion.

For the 40 records studied here, the average energy ratio of the first extracted pulse  $E_{r,1}$  was 64%, with a maximum of 91% (motion #6 El Centro Array #6) and a minimum of 28% (motion #21 Tarzana, Cedar Hill) [see Figure 7 (a) and Table 1]. For the 34 records that had more than one predominant pulse,  $E_{r,1}$  had an average value of 60% compared to an average value of 81% for the 6 records with only one predominant pulse. For these 34 records,  $E_{r,2} / E_{r,1}$  was on average 0.24, with a maximum of 0.66 for record #14 (Newhall Fire Station) and with a minimum of 0.10 for record #36 (TCU086) [see Figure 7 (b)]. For the 15 records that had 3 predominant pulses, the average  $E_{r,1}$  and  $E_{r,2}$  was 51% and 14%, respectively.

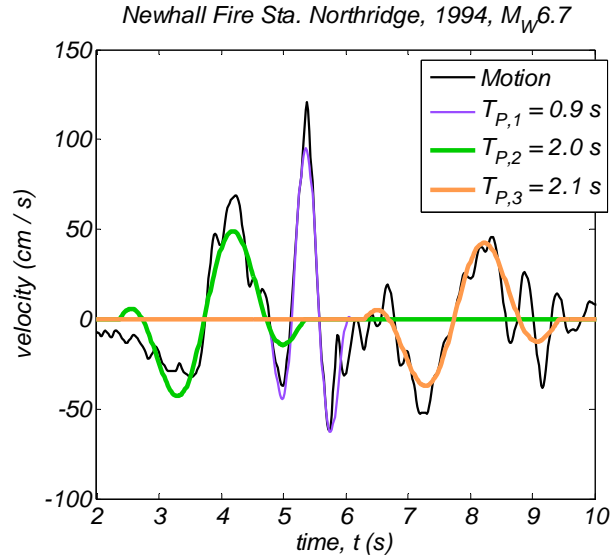


Figure 6. Three extracted pulses using the CPEv-EN method (two of which have similar periods) for Record #16 Newhall Fire Station from the  $M_w 6.7$  1994 Northridge, California earthquake.

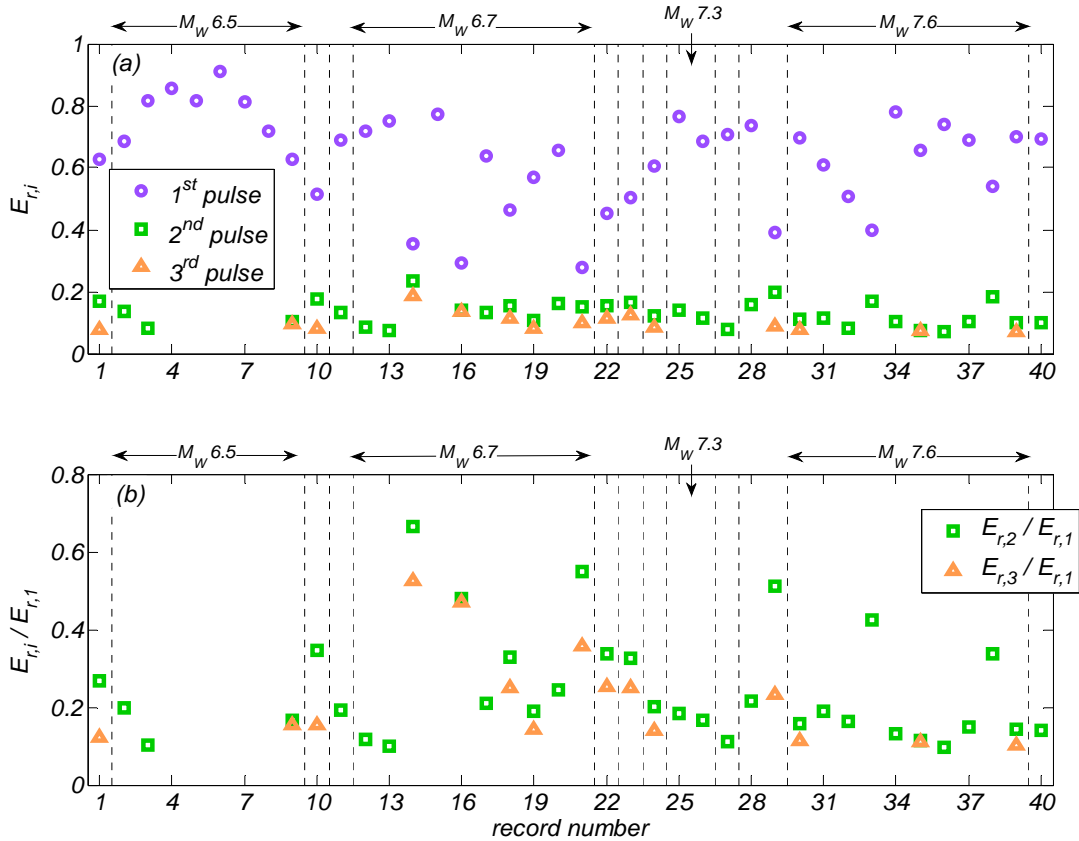


Figure 7. (a) Energy ratio  $E_{r,i}$ ; and (b) ratios  $E_{r,2}/E_{r,1}$  and  $E_{r,3}/E_{r,1}$  of predominant pulses computed using CPEv-EN method.

## Evaluation of Pulse Representation by SDOF Response

The metric used for the evaluation of the pulse representation  $S_N(t)$  of the ground motion record  $S(t)$  was the error in the linear spectral displacement of the SDOF oscillator subjected to  $S(t)$  and  $S_N(t)$  at 2% viscous damping ratio, defined as:

$$e_{Sd}(T) = \frac{|Sd[S(t), T] - Sd[S_N(t), T]|}{Sd[S(t), T]} \quad (\text{Eq. 8})$$

where  $Sd[S(t), T]$  and  $Sd[S_N(t), T]$  is the spectral displacement of the linear SDOF oscillator of period  $T$  subjected to  $S(t)$  and the corresponding  $S_N(t)$ , respectively.  $e_{Sd}^{\text{avg}}(T_1, T_2)$  is then defined as the average value of  $e_{Sd}(T)$  for  $T$  ranging from  $T_1$  to  $T_2$ .

Figure 8 shows the  $e_{Sd}^{\text{avg}}(1, 5)$  for  $S_1(t)$ ,  $S_2(t)$ ,  $S_3(t)$ , and  $S_P(t)$ , which are the pulse representations from the sum of one, two, three, and predominant ( $E_{r,i} > 7\%$ ) pulses, respectively, as extracted from each of the 40 ground motions records by the CPE<sub>V-EN</sub> method described in the previous section. The average value of  $e_{Sd}^{\text{avg}}(1, 5)$  for the 40 records was 0.41, 0.22, 0.17, and 0.20 for  $S_1(t)$ ,  $S_2(t)$ ,  $S_3(t)$ , and  $S_P(t)$ , respectively. For the pulse representation  $S_1(t)$ ,  $e_{Sd}^{\text{avg}}(1, 5)$  ranged between 0.13 (record #15 Newhall W Pico Canyon Rd) and 0.87 (record #33 TCU067). For  $S_2(t)$ ,  $e_{Sd}^{\text{avg}}(1, 5)$  ranged between 0.05 (record #12 Jensen Filter Plant) and 0.44 (record #31 TCU054), demonstrating the significant improvement in the level of representation achieved with  $S_2(t)$  compared to that with  $S_1(t)$ . The  $S_P(t)$  resulted in  $e_{Sd}^{\text{avg}}(1, 5)$  less than 0.44 for all motions. For the 11 records with  $M_W \geq 7.6$  (records #30 to 40 from Chi-Chi, Taiwan, and Wenchuan, China, earthquakes), the  $e_{Sd}^{\text{avg}}(1, 5)$  of  $S_1(t)$  and  $S_2(t)$  had an average value of 0.67 and 0.29, respectively, demonstrating the importance of considering the second extracted pulse for records from earthquake with large magnitudes. Other records where the second extracted pulse was very important were records #1, #14, #21, #24, and #29; record #1 was from the  $M_W = 6.3$  Christchurch, New Zealand, earthquake (the earthquake of smallest magnitude considered in this study).

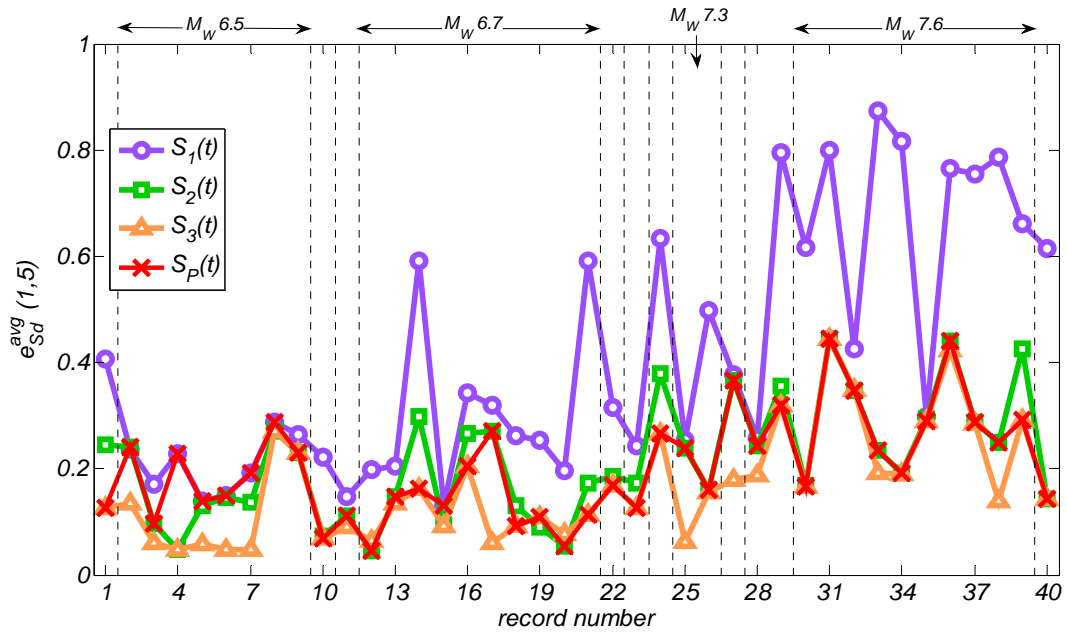


Figure 8. Average error in  $S_d$  for  $T = 1$  to  $5$  s,  $e_{Sd}^{\text{avg}}(1,5)$ , of four types of pulse representations from the CPE<sub>V-EN</sub> method.

## Effect of Type of Time Domain and Weighting Function of Wavelet Analysis

This section investigates the effect of two key parameters of the wavelet analysis used for pulse identification: (a) the type of time domain [acceleration (A) or velocity (V)] in which the wavelet analysis is conducted; and (b) the weighting function [equal amplitude (AM), equal energy (EN), and equal area (AR)] used. The CPE using wavelet analysis conducted with the six variations of the above parameters are termed  $CPE_{V-AR}$ ,  $CPE_{V-EN}$ ,  $CPE_{V-AM}$ ,  $CPE_{A-AR}$ ,  $CPE_{A-EN}$ , and  $CPE_{A-AM}$ . The first three extracted pulses and associated M&P wavelet parameters ( $\gamma$ ,  $\theta$ ,  $l$ ,  $a_{max}$ , and  $v_{max}$ ) for these six methods are listed in Appendix A1 to this paper. Also, the figures sets in Appendices B1 to B2 show the time history as well as the SDOF linear spectral response of the extracted pulses and  $S_3(t)$  for each of the 40 methods computed by each of the six methods.

Figure 9 shows the acceleration and velocity time histories of Record #34 TCU068 from the  $M_w 7.6$  Chi-Chi, Taiwan, earthquake and the corresponding three extracted pulses obtained by the four methods ( $CPE_{A-AM}$ ,  $CPE_{A-EN}$ ,  $CPE_{V-EN}$ , and  $CPE_{V-AR}$ ). The  $Sa$  and  $Sd$  of the record, individual pulses, and  $S_3(t)$  representation are also shown for each method. This figure illustrates the differences between the four methods in terms of extracted pulse period and level of agreement in spectral response. The  $CPE_{A-AM}$  method resulted in pulses periods ranging from 0.3 to 2.6 s. While the  $S_3(t)$  representation resulted in very good agreement with the record in terms of  $Sd$  for periods of  $T = 0.1$  to  $3.5$  [ $e_{Sd}^{avg}(0.1, 3.5) = 0.14$ ], the corresponding level of agreement for  $T \geq 3.5$  was very poor with  $e_{Sd}^{avg}(3.5, 10) = 0.67$ . The  $CPE_{A-EN}$  method extracted a strong 0.5 s acceleration pulse (second extracted pulse) and two other pulses of periods  $T_{P,1} = 2.9$  s and  $T_{P,3} = 9.0$  s; the  $e_{Sd}^{avg}(0.5, 10)$  for  $S_3(t)$  of this method was equal to 0.09.

The first and second pulses computed with  $CPE_{V-EN}$  method have similar (less than 25% difference) periods to the first and third pulses extracted with the  $CPE_{A-EN}$  method, but a third pulse of very long period  $T_{P,3} = 22.0$  s is additionally identified. While the  $CPE_{V-EN}$  method resulted in nearly excellent agreement of  $Sd$  with the record for  $T$  larger than 2 s [ $e_{Sd}^{avg}(2, 10) = 0.10$ ], the  $e_{Sd}^{avg}(0.5, 2) = 0.48$  with a maximum of 0.8 in that period range because no pulses of dominant period less than 3.2 s were extracted. Finally, the  $CPE_{V-AR}$  method extracted pulses with period larger than 7.5 s, resulting in the worst approximation of  $Sd$  for  $T < 7$  s.

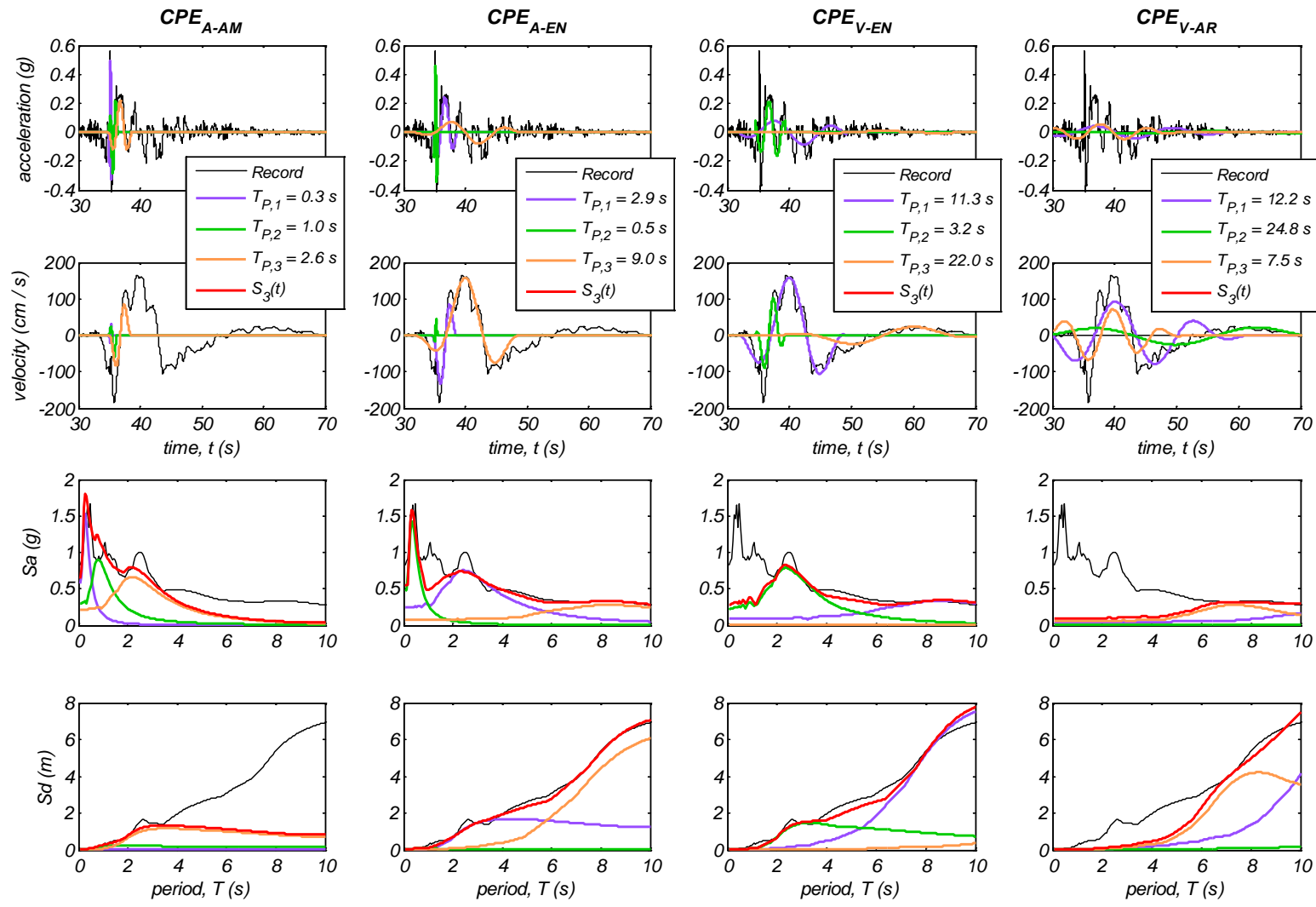


Figure 9. Pulses extracted using four CPE methods and their corresponding  $S_a$  and  $S_d$  (2% damping) for record #34 TCU068 from the Chi-Chi, Taiwan, 1999, M<sub>w</sub>7.6 earthquake.

Figure 10 shows the periods  $T_{P,max} = \max(T_{P,1}, T_{P,2}, T_{P,3})$  and  $T_{P,min} = \min(T_{P,1}, T_{P,2}, T_{P,3})$  of the three extracted pulses computed by each of the six methods for each of the 40 records. Table 2 lists the average  $T_{P,max}$  and  $T_{P,min}$  for all 40 records. Using the same weighting function, the methods operating in the velocity time domain (V) resulted in longer  $T_{P,max}$  and  $T_{P,min}$ , as expected. Independent of the time domain, the AM weighting function resulted in the smallest  $T_{P,max}$  and  $T_{P,min}$ , and the AR weighting function in the largest  $T_{P,max}$  and  $T_{P,min}$ .

Table 3 summarizes the average error metric  $e_{Sd}^{avg}(T_1, T_2)$  for the pulse representations  $S_1(t)$ ,  $S_2(t)$ , and  $S_3(t)$  of each of the six methods in the following five period windows  $(T_1, T_2) = 0.5 - 1$ ,  $1 - 2$ ,  $2 - 3$ ,  $3 - 5$ , and  $5 - 10$  seconds. Figure 11 presents the error  $e_{Sd}(T)$  averaged over all 40 motions versus SDOF oscillator period  $T$ . Table 3 and Figure 11 demonstrate that both parameters of wavelet analysis significantly affect the level of representation achieved, independent of the number of pulses used. For the  $0.5 - 1$  s and  $1 - 2$  s period ranges, the CPE<sub>A-EN</sub> resulted in the smallest  $e_{Sd}^{avg}$ , except for the case of  $S_3(t)$  in the  $1 - 2$  s period range where the  $e_{Sd}^{avg}$  was slightly smaller for CPE<sub>V-AM</sub>. The CPE<sub>A-AM</sub> method resulted in  $e_{Sd}(T)$  greater than 0.58 for  $T \geq 1.5$  s for the  $S_3(t)$ . This level of error reduces significantly for  $T = 0.1$  to  $0.5$  s, resulting in  $e_{Sd}^{avg}(0.1, 0.5) = 0.28$ , which is the smallest error in this period range among the six methods studied. For the period ranges  $2 - 3$  and  $3 - 5$  s, the CPE<sub>V-EN</sub> resulted in the smallest  $e_{Sd}^{avg}$ , except for the case of  $S_1(t)$  in the  $T = 2 - 3$  s period range where CPE<sub>V-AM</sub> resulted in slightly smaller error. For periods longer than 5 s, CPE<sub>V-EN</sub> also resulted in the smallest error for  $S_1(t)$  and  $S_2(t)$ ; the two smallest  $e_{Sd}^{avg}(5, 10)$  for  $S_3(t)$  are 0.10 and 0.11 from CPE<sub>V-EN</sub> and CPE<sub>V-AR</sub>, respectively.

Table 2.  $T_{P,max}$  and  $T_{P,min}$  averaged over the 40 records for each of the six CPE methods.

Pulse period (s)	Time domain	Weighting function		
		AR	EN	AM
$T_{P,max}$	Velocity (V)	10.3	6.9	4.2
	Acceleration (A)	4.5	2.7	0.9
$T_{P,min}$	Velocity (V)	3.1	1.9	1.1
	Acceleration (A)	1.1	0.6	0.4

The  $e_{Sd}^{\text{avg}}(T_1, T_2)$  for  $S_3(t)$  in any of the windows between  $T = 1$  and 5 s is less than 0.33 for methods CPE<sub>V-EN</sub>, CPE<sub>V-AM</sub>, CPE<sub>A-AR</sub>, and CPE<sub>A-EN</sub>. However, for records containing multiple strong short period ( $T_P < 1.0$  s) acceleration pulses (e.g., records #8, #19, #21, #24, #27, and #37), the CPE<sub>A-EN</sub> and CPE<sub>A-AR</sub> methods, and in some cases CPE<sub>V-AM</sub>, were unable to extract strong long period pulses ( $T_P > 5.8$  s) included in these records. [See the figure sets in Appendix B3, B4, and B5, respectively]. The CPE<sub>V-EN</sub> method results in the lowest  $e_{Sd}^{\text{avg}}(2,3)$  and  $e_{Sd}^{\text{avg}}(3,5)$ , with both values less than 0.2 for the  $S_2(t)$  representation (which is lower than the values for the  $S_3(t)$  representation of all other methods in these two period ranges). Since the CPE<sub>V-EN</sub> method results in the best approximation of  $Sd$  for  $T > 2$  s, a hybrid CPE method may be used to improve the  $S_3(t)$  representation in the 0.5 – 2 s period range: the first two iterations of the CPE method use the V-EN wavelet analysis, and the third iteration uses A-EN in order to capture important short-period acceleration pulses. However, investigation of such a method is outside the scope of this paper.

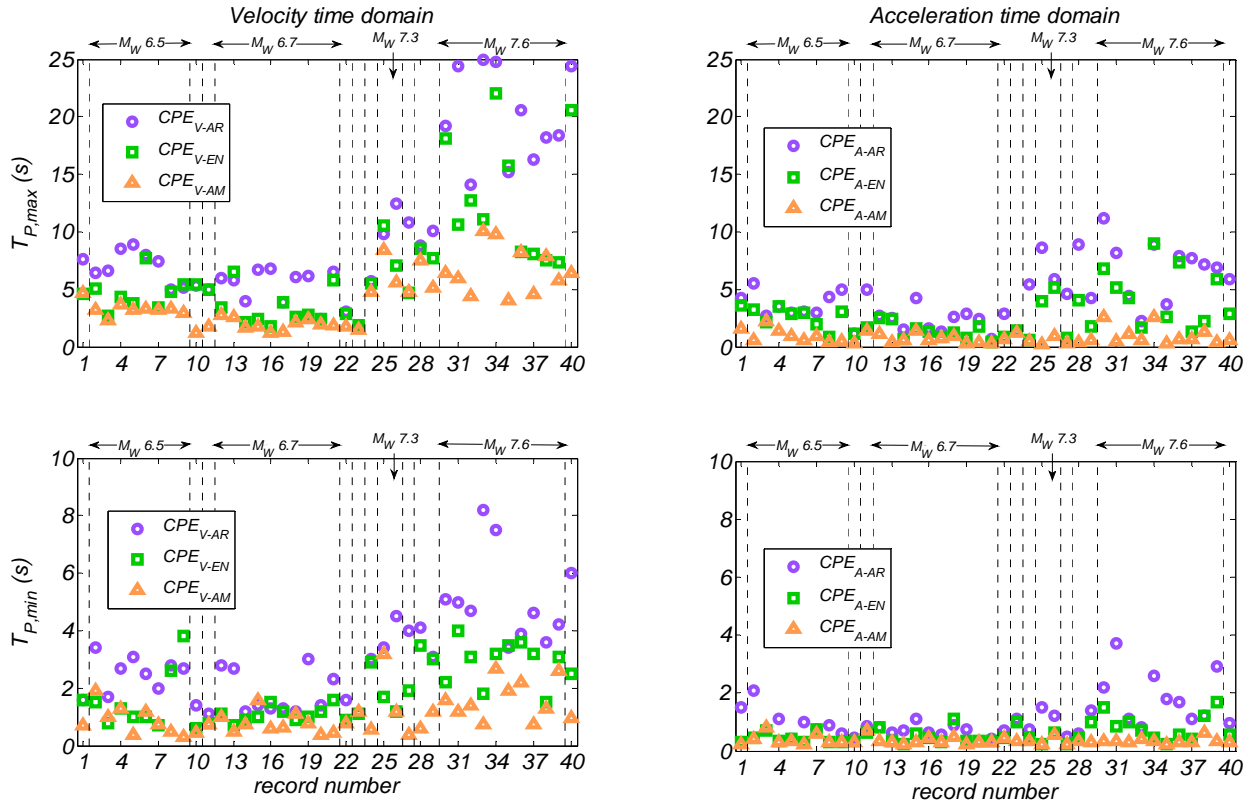


Figure 10. Maximum and minimum pulse period  $T_P$  among the first three pulses extracted using each of the 6 CPE methods.

Table 3.  $e_{Sd}^{\text{avg}}(T_1, T_2)$  for five different windows ( $T_1, T_2$ ) for the pulse representations of the 40 records computed using the six different methods.

Method for pulse extraction	Pulse representation	Average of $e_{Sd}^{\text{avg}}(T_1, T_2)$ over 40 motions for five windows ( $T_1, T_2$ ) of periods				
		0.5 – 1 s	1 – 2 s	2 – 3 s	3 – 5 s	5 – 10 s
CPE <sub>V-AR</sub>	$S_1(t)$	0.92	0.83	0.65	0.44	0.29
	$S_2(t)$	0.85	0.66	0.47	0.28	0.14
	$S_3(t)$	0.81	0.57	0.36	0.18	0.10
CPE <sub>V-EN</sub>	$S_1(t)$	0.80	0.63	0.42	0.29	0.20
	$S_2(t)$	0.64	0.42	0.19	0.13	0.12
	$S_3(t)$	0.53	0.33	0.15	0.10	0.11
CPE <sub>V-AM</sub>	$S_1(t)$	0.65	0.47	0.38	0.36	0.39
	$S_2(t)$	0.45	0.31	0.28	0.30	0.33
	$S_3(t)$	0.32	0.23	0.22	0.25	0.29
CPE <sub>A-AR</sub>	$S_1(t)$	0.80	0.68	0.50	0.38	0.33
	$S_2(t)$	0.53	0.40	0.31	0.25	0.27
	$S_3(t)$	0.40	0.26	0.20	0.21	0.24
CPE <sub>A-EN</sub>	$S_1(t)$	0.50	0.46	0.48	0.54	0.59
	$S_2(t)$	0.30	0.33	0.38	0.42	0.48
	$S_3(t)$	0.25	0.25	0.26	0.30	0.36
CPE <sub>A-AM</sub>	$S_1(t)$	0.51	0.74	0.85	0.88	0.87
	$S_2(t)$	0.38	0.60	0.74	0.81	0.81
	$S_3(t)$	0.35	0.57	0.71	0.79	0.80

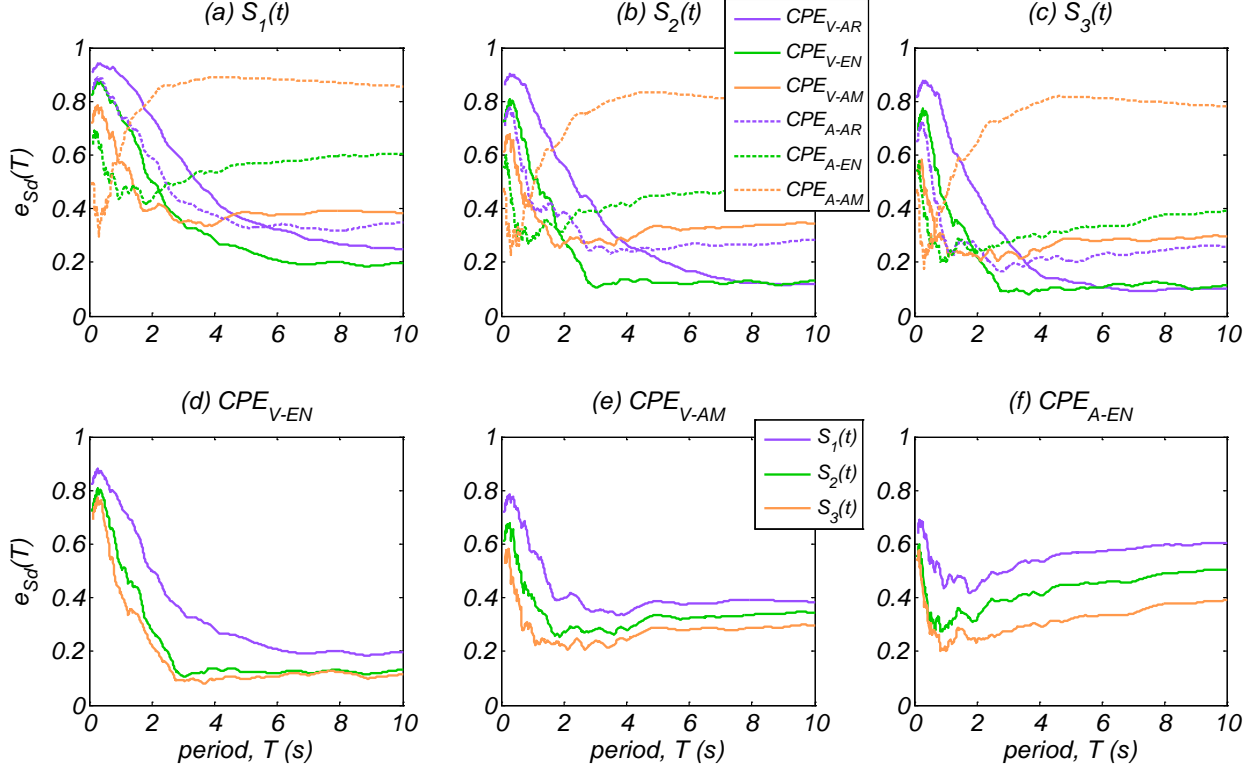


Figure 11. Errors in  $S_d$ ,  $e_{S_d}(T)$ , averaged over 40 records for the pulse representations: (a)  $S_1(T)$ , (b)  $S_2(T)$ , and (c)  $S_3(T)$  computed with each of the six considered CPE methods; and for the three pulse representations computed using the methods: (d)  $CPE_{V-EN}$ ; (e)  $CPE_{V-AM}$ ; and (f)  $CPE_{A-EN}$ .

## Conclusions

This paper presented an iterative method for extracting multiple pulses from a pulse-like ground motion in such a way that the sum of the extracted pulses composes a representation of the ground motion. Called the cumulative pulse extraction (CPE) method, this method was applied to 40 pulse-like ground motion records from 13 historical earthquakes of magnitudes ranging from 6.3 to 7.9, with distances from the fault rupture ranging between 0.1 km and 23.6 km (36 of which are within 10 km of the fault rupture). Wavelet analysis using continuous wavelet transform with the M&P wavelet was performed to extract one pulse per iteration of the CPE method; a total of three pulses were extracted for each ground motion record. The level of representation achieved for each of the 40 records was studied by comparing the linear SDOF spectral displacement response of the extracted pulse representation and that of the ground motion record for periods  $T$  ranging between 0.5 and 10 s. The paper also investigated the effect of the following parameters: (a) the number of pulses,  $N$ , used in the representation  $S_N(t)$  of the records; (b) the type of time-domain [velocity (V) or acceleration (A)] at which the wavelet analysis is conducted; and (c) the weighting function [equal area (AR), equal energy (EN), equal amplitude (AM)] used in the wavelet analysis. Six versions of the  $CPE_{d,w}$  method were studied; subscript  $d$  describes the time domain at which the wavelet analysis was conducted (V and A) and subscript  $w$  the weighting function used (AR, EN, and AM). Based on the results of the study the following conclusions are drawn:

1. The  $CPE_{V-EN}$  resulted in the determination of more than one predominant pulse (defined as pulses with energy more than 0.07 times that of the record) in 34 out of the 40 records, with three predominant pulses identified in 15 of those records. The first extracted pulse for the 40 motions had the following characteristics: dominant period  $T_{P,1}$  ranging from 0.9 to 11.3 s (with an average of 4.7 s), peak velocity ranging from 27 to 159 cm / s (with an average of 70 cm / s), and energy ranging from 28% to 91% that of the ground motion (average of 64%). These periods were on average of 0.88 times the pulse periods of the same motions identified in Mavroeidis and Papageorgiou (2003) and Baker (2007).

2. For the 34 records that had more than one predominant pulse based on  $CPE_{V-EN}$ , the energy of the first pulse was, on average, 0.60 times that of the ground motion, while the average value of the ratio of the dominant periods of the longer and the shorter among the first two extracted pulses was 2.45. For these motions the second extracted pulse had the following

characteristics (average values): dominant period of 3.3 s, peak velocity of 38 cm / s, and energy 0.13 times that of the ground motion.

3. For 11 out the 15 motions with three predominant pulses, the third pulse period  $T_{P,3}$  was 0.75 to 1.33 times that of the first or second pulse period. In many of these 11 motions, the third pulse was merely a continuation of the first or second extracted pulse and was extracted separately because of limits in the oscillatory character parameter,  $\gamma$ , used in the M&P wavelet. 8 out of these 11 motions were recorded at sites with  $V_{s30}$  less than 300 m / s; nonlinear site effects are assumed to have affected the high oscillatory character of these motions.

4. For the CPE<sub>V-EN</sub> method, increasing the number of pulses used from one [referred to as the  $S_1(t)$  representation] to two [ $S_2(t)$  representation] and to three [ $S_3(t)$  representation] improved the pulse representation of the records; the average error in spectral displacement response for SDOF oscillator periods between 1 and 5 s,  $e_{Sd}^{avg}(1,5)$ , was 0.41, 0.22, and 0.17, for  $S_1(t)$ ,  $S_2(t)$ , and  $S_3(t)$ , respectively. The level of reduction of  $e_{Sd}^{avg}(1,5)$  from  $S_1(t)$  to  $S_2(t)$  was even larger for records from the  $M_W$ 7.6 Chi-Chi, Taiwan, and the  $M_W$ 7.9 Wenchuan, China, earthquakes, which were the earthquakes of largest magnitude studied; the  $e_{Sd}^{avg}(1,5)$  for  $S_1$ ,  $S_2$ ,  $S_3$  for the  $M_W \geq 7.6$  records was 0.67, 0.29, and 0.26, respectively. For these records, the first extracted pulse period  $T_{P,1}$  ranged from 4.4 to 11.3 s (8.0 s on average), while  $T_{P,2}$  ranged from 1.9 to 4 s (3.0 s on average).

5. Both the time domain at which wavelet analysis is conducted and the weighting function used play an important role on the properties of the extracted pulses. For the same weighting function, wavelet analysis in the velocity time history identifies longer period pulses compared to wavelet analysis in the acceleration time history. For wavelet analysis performed in the same time domain, the weighting function AM results in the smallest period pulses and AR results in the largest period pulses.

6. The CPE<sub>A-EN</sub>, and CPE<sub>V-EN</sub> methods resulted in the best approximation of  $Sd$  for  $T = 0.5 - 2$  s [ $e_{Sd}^{avg}(0.5,2) = 0.25$  for  $S_3(t)$ ] and  $2 - 10$  s [ $e_{Sd}^{avg}(2,10) = 0.11$  for  $S_3(t)$ ], respectively. The methods CPE<sub>V-AM</sub>, CPE<sub>A-AR</sub>, and CPE<sub>A-EN</sub> result in a good approximation of  $Sd$  for  $T = 1$  to 5 s (on average less than 32% error); however, CPE<sub>A-EN</sub> and CPE<sub>A-AR</sub> (and to a lesser extent CPE<sub>V-AM</sub>) were not able to extract strong long-period (greater than 5.8 s) pulses in records that included many cycles of short period.

## Data and Resources

The 40 ground motion records listed in Table 1 were obtained from:

Record #1: <http://www.geonet.org.nz/> (last accessed September 2012)

Records #2-39: <http://peer.berkeley.edu/nga/> (last accessed January 2013)

Record #40: Provided by Dr. Y. Borzognia (March 2012)

The parameters ( $R_{rup}$ , strike angle etc.) for records #1 and #40 were obtained from:

1. Bradely, B. A. and Cubrinovsky, M. (2011). "Near-source strong ground motions observed in the 22 February 2011 Christchurch Earthquake." *Seismological Research Letters*, 82(6), 853-865.
2. Wen, Z., Xie, J., Gao, M., Hu, Y., and Chau, K. T. (2010). "Near-source strong ground motion characteristics of the 2008 Wenchuan Earthquake." *Bulletin of the Seismological Society of America*, 100(5B), 2425-2439.
3. Li, X., Zhou, Z., Yu, H., Wen, R., Lu, D., Huang, M., Zhou, Y., and Cu, J. (2008). "Strong motion observations and recordings from the great Wenchuan Earthquake." *Earthquake Engineering and Engineering Vibration*, 7(3), 235-246.

The cumulative pulse extraction method was implemented in MATLAB: MATLAB and Statistics Toolbox Release 2012b, The MathWorks, Inc., Natick, Massachusetts, United States.

All wavelet analysis was done with built-in `cwt()` function in the Wavelet Toolbox of MATLAB R2102b.

## References

1. Aki, K. (1968). "Seismic displacements near a fault." *Journal of Geophysical Research*, 73(16), 5359–5376.
2. Alavi, B. and Krawinkler, H. (2004). "Behavior of moment-resisting frame structures subjected to near-fault ground motions." *Earthquake Engineering & Structural Dynamics*, 33(6), 687–706.
3. Anderson, J. C. and Bertero, V. V. (1987). "Uncertainties in establishing design earthquakes." *Journal of Structural Engineering*, 113(8), 1709–1724.
4. Baker, J. W. (2007). "Quantitative classification of near-fault ground motions using wavelet analysis." *Bulletin of the Seismological Society of America*, 97(5), 1486–1501.
5. Bertero, V. V., Mahin, S. A., and Herrera, R. A. (1978). "Aseismic design implications of near-fault San Fernando earthquake records." *Earthquake Engineering and Structural Dynamics*, 6, 31–42.
6. Bray, J. D. and Rodriguez-Marek, A. (2004). "Characterization of forward-directivity ground motions in the near-fault region." *Soil Dynamics and Earthquake Engineering*, 24, 815–828.
7. Calugaru, V. and Panagiotou, M. (2012a). "Response of tall cantilever wall buildings to strong pulse type seismic excitation." *Earthquake Engineering & Structural Dynamics*, 41(9), 1301–1318.
8. Calugaru, V. and Panagiotou, M. (2012b). "Seismic responses of 20-story base-isolated and fixed-base RC structural wall buildings subjected to near-fault ground shaking." Report UCB/SEMM-2012/03, Earthquake Engineering Research Center, University of California, Berkeley.
9. Chopra, A. K. and Chintanapakdee, C. (2001). "Comparing response of SDOF systems to near-fault and far-fault earthquake motions in the context of spectral regions." *Earthquake Engineering & Structural Dynamics*, 30, 1769–1789.
10. Gazetas, G., Garini, E., Berrill, J. B., and Apostolou, M. (2012). "Sliding and overturning potential of Christchurch 2011 earthquake records." *Earthquake Engineering & Structural Dynamics*, 42(14), 1921–1944.
11. Hall, J. F., Heaton, T. H., Halling, M. W., and Wald, D. J. (1995). "Near-source ground motion and its effects on flexible buildings." *Earthquake Spectra*, 11, 569–606.

12. Hall, J. F. and Ryan, K. L. (2000). “Isolated buildings and the 1997 UBC near-source factors.” *Earthquake spectra*, 16(2), 393–411.
13. Housner, G. W. and Hudson, D. E. (1958). “The Port Hueneme Earthquake of March 18, 1957.” *Bulletin of the Seismological Society of America*, 48(2), 163–168.
14. Housner, G. W. and Trifunac, M. D. (1967). “Analysis of accelerograms – Parkfield earthquake.” *Bulletin of the Seismological Society of America*, 57(6), 1193–1220.
15. Jangid, R. S. and Kelly, J. M. (2001). “Base isolation for near-fault motions.” *Earthquake engineering & structural dynamics*, 30(5), 691–707.
16. Krawinkler, H. and Alavi, B. (1998). “Development of improved design procedures for near fault ground motions.” *SMIP98 Seminar Proceedings*, Oakland, CA.
17. Krishnan, S., Ji, C., Komatitsch, D., and Tromp, J. (2006). “Case studies of damage to tall steel moment-frame buildings in southern California during large San Andreas earthquakes.” *Bulletin of the Seismological Society of America*, 96(4A), 1523–1537.
18. Komuro, T., Nishikawa, Y., Kimura, Y., and Isshiki, Y. (2005). “Development and realization of base isolation system for high-rise buildings.” *Journal of Advanced Concrete Technology*, 3(2), 233–239.
19. Makris, N. (1997). “Rigidity-plasticity-viscosity: can electrorheological dampers protect base-isolated structures from new-source ground motions?” *Earthquake Engineering & Structural Dynamics*, 26(5), 571–591.
20. Makris, N. and Black, C. (2003). “Dimensional analysis of inelastic structures subjected to near fault ground motions.” Report EERC 2003-05, Earthquake Engineering Research Center, Berkeley, California, 96 pp.
21. Makris, N. and Zhang, J. (2001). “Rocking response of anchored blocks under pulse-type motions.” *Journal of engineering mechanics*, 127(5), 484–493.
22. Mallat, S. (2009). “A Wavelet Tour of Signal Processing: The Sparse Way.” Burlington, MA: Academic Press. 832 pp.
23. Mavroeidis, G. P., Dong, G., and Papageorgiou, A. S. (2004). “Near-fault ground motions, and the response of elastic and inelastic single degree-of-freedom (SDOF) systems.” *Earthquake Engineering & Structural Dynamics*, 33(9), 1023–1049.

24. Mavroelidis, G. P. and Papageorgiou, A. S. (2002). “Near-source strong ground motion: characteristics and design issues.” *Proc. of the Seventh U.S. National Conf. on Earthquake Engineering* (7NCEE), Boston, Massachusetts, 21–25 July 2002.
25. Mavroelidis, G. P. and Papageorgiou, A. S. (2003). “A mathematical representation of near-fault ground motions.” *Bulletin of the Seismological Society of America*, 93(3), 1099–1131.
26. Menun, C. and Fu, Q. (2002). “An analytical model for near-fault ground motions and the response of SDOF systems.” *Proc. of the 7th U.S. National Conf. on Earthquake Engineering*, Boston, MA.
27. Moustafa, A. and Takewaki, I. (2010). “Deterministic and probabilistic representation of near-field pulse-like ground motion.” *Soil Dynamics and Earthquake Engineering*, 30(5), 412–422.
28. Newmark, N. M. (1965). “Effects of earthquakes on dams and embankments.” *Geotechnique*, 15(2), 139–160.
29. Olsen, A., Aagaard, B., Heaton, T. (2008). “Long-period building response to earthquakes in the San Francisco Bay Area.” *Bulletin of the Seismological Society of America*, 98(2), 1047–1065.
30. Rodriguez-Marek, A. and Bray, J. D. (2006). “Site response for near-fault forward directivity ground motions.” *Journal of Geotechnical and Geoenvironmental Engineering*, 132(12), 1611–1620.
31. Somerville, P. and Graves, R. (1993). “Conditions that give rise to unusually large long period ground motions.” *The Structural Design of Tall Buildings*, 2(3), 211–232.
32. Somerville, P. G., Smith, N. F., Graves, R. W., and Abrahamson, N. A. (1997). “Modification of empirical strong ground motion attenuation relations to include the amplitude and duration effects of rupture directivity.” *Seismological Research Letters*, 68(1), 199–222.
33. Somerville, P. (1998). “Development of an improved representation of near-fault ground motions.” *SMIP98 Seminar Proceedings*, Oakland, CA.
34. Vassiliou, M. F. and Makris, N. (2011). “Estimating time scales and length scales in pulse-like earthquake acceleration records with wavelet analysis.” *Bulletin of the Seismological Society of America*, 101(2), 596–618.

35. Veletsos, A. S., Newmark, N. M., and Chelapati, C. V. (1965). "Deformation spectra for elastic and elastoplastic systems subjected to ground shock and earthquake motions." *Proceedings of Third World Conference on Earthquake Engineering, Wellington, New Zealand*, II, 663–682.
36. Yaghmaei-Sabegh, S. (2010). "Detection of pulse-like ground motions based on continues wavelet transform." *Journal of Seismology*, 14(4), 715–726.

**Appendix A1: Parameters of the three extracted pulses from each of the six CPE methods investigated**



Lu and Panagiotou -  
Appendix A1.xls

(Available electronically, or reproduced in segmented tables on the following pages)

\* Energy is defined as the integral of the velocity time history squared

\*\* Area is defined as the integral of the absolute value of the velocity time history

Record #	Ground Motion Record				Pulse #	CPE <sub>V-AR</sub>							
	$a_{max}$ (g)	$v_{max}$ (cm/s)	energy*	area**		$T_P$ (s)	$a_{max}$ (g)	$v_{max}$ (cm/s)	energy*	area**	$\gamma$	$\theta$ (°)	$l$ (s)
1	0.73	117.8	1.18	2.80	1	4.10	0.066	45.1	0.60	2.21	3.0	158	19.0
					2	1.60	0.228	62.5	0.44	1.17	3.0	45	18.2
					3	7.60	0.005	6.7	0.03	0.63	3.0	0	19.6
2	0.18	54.5	0.46	2.45	1	6.40	0.016	18.5	0.15	1.38	3.0	113	8.5
					2	3.40	0.049	29.1	0.20	1.16	3.0	113	7.6
					3	5.40	0.008	7.3	0.02	0.47	3.0	23	19.4
3	0.38	115.0	0.94	2.69	1	2.90	0.116	59.1	0.69	2.00	3.0	113	5.2
					2	1.70	0.114	33.5	0.13	0.67	3.0	45	4.7
					3	6.60	0.004	4.7	0.01	0.38	3.0	0	7.6
4	0.36	77.9	0.95	3.08	1	4.30	0.063	45.3	0.64	2.33	3.0	23	6.0
					2	8.50	0.006	8.4	0.04	0.86	3.0	158	9.2
					3	2.70	0.054	25.8	0.12	0.81	3.0	113	5.3
5	0.38	91.5	1.22	3.45	1	3.60	0.090	55.8	0.78	2.37	3.0	45	6.8
					2	8.90	0.006	9.3	0.06	1.02	3.0	0	10.8
					3	3.10	0.044	22.7	0.12	0.84	3.0	23	12.1
6	0.44	111.9	1.52	3.48	1	3.60	0.109	65.6	1.12	2.83	3.0	158	6.2
					2	8.00	0.009	12.5	0.09	1.16	3.0	113	9.2
					3	2.50	0.060	27.0	0.12	0.78	3.0	90	8.4
7	0.46	108.8	1.03	2.75	1	3.40	0.094	55.1	0.72	2.21	3.0	135	6.3
					2	7.40	0.008	10.4	0.05	0.90	3.0	90	9.3
					3	2.00	0.067	22.5	0.07	0.54	3.0	23	4.3
8	0.47	48.6	0.43	2.26	1	4.60	0.037	29.5	0.28	1.60	3.0	45	6.9
					2	2.80	0.033	16.1	0.05	0.53	3.0	68	5.4
					3	5.00	0.010	8.8	0.03	0.52	3.0	135	24.1
9	0.42	59.6	0.48	2.54	1	5.20	0.029	26.4	0.25	1.60	3.0	68	7.2
					2	2.70	0.049	23.0	0.10	0.73	3.0	135	5.7
					3	4.60	0.015	12.0	0.05	0.65	3.0	135	20.7
10	1.43	116.5	0.98	2.66	1	5.30	0.024	22.3	0.18	1.38	3.0	68	6.0
					2	1.40	0.264	63.6	0.40	1.05	3.0	135	3.2
					3	2.30	0.040	16.3	0.04	0.44	3.0	68	7.1
11	0.42	106.8	1.29	3.44	1	5.00	0.036	30.6	0.34	1.83	3.0	23	15.4
					2	1.90	0.219	67.8	0.67	1.58	3.0	0	12.5
					3	1.10	0.165	32.0	0.08	0.41	3.0	113	10.2
12	0.39	104.5	1.22	3.19	1	2.80	0.132	66.8	0.85	2.17	3.0	90	4.8
					2	6.00	0.010	10.1	0.04	0.72	3.0	158	7.1
					3	3.00	0.027	14.5	0.04	0.51	3.0	68	8.5
13	0.52	67.3	0.79	2.65	1	2.70	0.120	52.7	0.57	1.75	3.0	0	4.3
					2	5.80	0.011	11.0	0.05	0.74	3.0	68	4.1
					3	2.70	0.029	13.4	0.03	0.43	3.0	135	7.7
14	0.72	120.9	0.87	2.83	1	4.00	0.039	25.8	0.19	1.24	3.0	158	5.5
					2	1.20	0.261	55.0	0.25	0.77	3.0	68	4.7
					3	1.60	0.123	33.9	0.13	0.64	3.0	135	7.6

Appendix A1 – Parameters of the three extracted pulses from each of the six CPE methods

CPE<sub>V-AR</sub>

Record #	Ground Motion Record				Pulse #	CPE <sub>V-AR</sub>							
	$a_{max}$ (g)	$v_{max}$ (cm/s)	energy*	area**		$T_P$ (s)	$a_{max}$ (g)	$v_{max}$ (cm/s)	energy*	area**	$\gamma$	$\theta$ (°)	$l$ (s)
15	0.43	87.7	0.90	2.42	1	2.60	0.113	49.4	0.46	1.54	3.0	158	4.9
					2	6.70	0.011	13.5	0.08	1.05	3.0	68	6.6
					3	1.40	0.172	42.4	0.17	0.69	3.0	68	5.5
16	0.41	53.2	0.51	2.58	1	2.40	0.068	29.6	0.14	0.83	3.0	90	7.3
					2	6.80	0.006	6.2	0.02	0.52	3.0	0	11.2
					3	1.30	0.115	26.4	0.06	0.40	3.0	68	7.8
17	0.89	173.1	1.25	2.51	1	1.30	0.345	77.1	0.54	1.18	3.0	135	2.5
					2	3.90	0.030	20.8	0.12	0.95	3.0	113	2.8
					3	1.70	0.110	32.3	0.12	0.65	3.0	135	5.8
18	0.59	130.3	1.99	4.98	1	2.80	0.141	66.3	0.89	2.23	3.0	23	4.6
					2	6.10	0.013	13.9	0.08	0.99	3.0	68	4.3
					3	1.20	0.296	59.5	0.31	0.86	3.0	23	7.1
19	0.84	116.5	0.83	2.80	1	3.00	0.091	45.7	0.45	1.64	3.0	158	4.2
					2	6.20	0.008	9.0	0.03	0.65	3.0	113	4.9
					3	3.10	0.027	13.8	0.04	0.51	3.0	158	8.3
20	0.73	123.1	1.01	2.77	1	2.40	0.150	63.5	0.66	1.77	3.0	68	4.9
					2	1.40	0.163	40.0	0.15	0.65	3.0	68	4.4
					3	1.80	0.063	20.5	0.05	0.43	3.0	90	8.4
21	1.33	65.4	0.69	2.96	1	6.50	0.016	18.3	0.15	1.38	3.0	90	9.4
					2	2.30	0.061	24.6	0.09	0.66	3.0	113	7.5
					3	3.00	0.031	15.0	0.05	0.55	3.0	0	3.7
22	0.65	102.3	1.23	3.20	1	3.10	0.092	50.1	0.53	1.81	3.0	68	8.2
					2	1.60	0.131	37.8	0.16	0.70	3.0	90	8.9
					3	2.60	0.051	22.0	0.09	0.69	3.0	23	13.2
23	0.68	169.5	3.17	5.97	1	1.90	0.333	109.0	1.58	2.44	3.0	45	6.9
					2	1.10	0.444	82.0	0.54	1.08	3.0	158	6.2
					3	1.20	0.327	67.5	0.38	0.95	3.0	135	3.1
24	0.35	61.4	1.10	3.99	1	5.70	0.040	41.1	0.65	2.72	3.0	90	7.3
					2	3.70	0.038	23.7	0.15	1.05	3.0	158	13.4
					3	3.00	0.034	17.8	0.07	0.62	3.0	68	7.4
25	0.77	92.6	1.56	4.33	1	4.60	0.069	53.2	0.94	2.93	3.0	158	12.1
					2	9.80	0.012	20.1	0.27	2.30	3.0	68	18.0
					3	3.40	0.039	21.8	0.12	0.91	3.0	0	15.3
26	0.24	56.5	0.61	2.94	1	7.20	0.021	25.6	0.33	2.17	3.0	45	17.5
					2	4.50	0.022	17.0	0.09	0.90	3.0	135	21.5
					3	12.50	0.002	4.3	0.02	0.62	3.0	68	19.2
27	0.85	121.4	3.41	7.26	1	5.00	0.094	83.3	2.38	4.86	3.0	113	12.6
					2	4.00	0.041	28.6	0.22	1.33	3.0	113	24.1
					3	10.80	0.005	10.0	0.08	1.28	3.0	45	12.2
28	0.24	51.1	0.47	2.33	1	8.80	0.013	19.7	0.24	2.04	3.0	45	10.9
					2	4.10	0.036	25.2	0.18	1.22	3.0	45	7.1
					3	5.80	0.004	3.8	0.01	0.26	3.0	45	19.3

Record #	Ground Motion Record				Pulse #	CPE <sub>V-AR</sub>							
	$a_{max}$ (g)	$v_{max}$ (cm/s)	energy* (m <sup>2</sup> /s)	area** (m)		$T_P$ (s)	$a_{max}$ (g)	$v_{max}$ (cm/s)	energy* (m <sup>2</sup> /s)	area** (m)	$\gamma$	$\theta$ (°)	$l$ (s)
29	0.27	48.7	0.98	4.01	1	10.10	0.010	16.3	0.19	1.97	3.0	158	18.0
					2	5.50	0.026	24.3	0.23	1.58	3.0	135	18.1
					3	3.10	0.057	29.7	0.20	1.10	3.0	158	14.7
30	0.38	165.5	7.20	11.71	1	9.50	0.041	67.8	3.05	7.59	3.0	135	39.6
					2	19.20	0.006	20.9	0.61	4.81	3.0	158	49.0
					3	5.10	0.084	73.8	1.94	4.43	3.0	45	37.6
31	0.16	60.3	0.86	4.28	1	10.30	0.013	23.1	0.38	2.77	3.0	113	37.3
					2	24.40	0.001	4.6	0.04	1.35	3.0	23	44.2
					3	5.00	0.026	21.3	0.17	1.31	3.0	0	34.5
32	0.83	129.5	4.91	10.80	1	4.70	0.106	85.6	2.41	4.74	3.0	135	32.1
					2	14.10	0.006	14.1	0.20	2.38	3.0	158	35.5
					3	6.60	0.018	21.5	0.21	1.65	3.0	113	38.9
33	0.52	84.2	1.90	6.63	1	14.20	0.008	20.0	0.39	3.31	3.0	68	34.0
					2	8.20	0.017	24.4	0.34	2.36	3.0	135	35.0
					3	25.00	0.002	6.7	0.08	1.96	3.0	68	45.9
34	0.56	184.5	13.88	17.15	1	12.20	0.043	92.5	7.16	13.18	3.0	113	41.0
					2	24.80	0.006	25.7	1.12	7.44	3.0	113	51.6
					3	7.50	0.056	70.9	2.73	6.37	3.0	23	38.3
35	0.33	88.5	1.83	6.23	1	5.80	0.041	41.1	0.69	2.81	3.0	45	29.5
					2	15.20	0.005	13.0	0.19	2.37	3.0	158	34.1
					3	3.40	0.070	41.8	0.41	1.66	3.0	113	30.1
36	0.13	43.7	0.68	3.87	1	8.60	0.019	26.9	0.47	2.84	3.0	0	41.3
					2	20.60	0.001	3.8	0.02	0.96	3.0	0	44.1
					3	3.90	0.022	15.4	0.06	0.70	3.0	90	49.6
37	0.21	68.3	0.91	3.91	1	8.40	0.021	31.2	0.56	3.06	3.0	68	20.0
					2	4.60	0.025	20.3	0.13	1.09	3.0	68	16.6
					3	16.30	0.002	4.8	0.03	0.90	3.0	68	20.6
38	0.30	109.0	1.97	5.72	1	7.80	0.031	42.3	0.96	3.85	3.0	68	40.1
					2	3.60	0.059	35.4	0.33	1.53	3.0	23	36.1
					3	18.20	0.001	4.2	0.02	0.89	3.0	113	43.6
39	0.13	62.1	1.23	4.93	1	7.40	0.031	39.1	0.82	3.47	3.0	23	41.0
					2	18.40	0.002	5.2	0.04	1.14	3.0	135	40.9
					3	4.20	0.028	21.1	0.13	1.03	3.0	68	41.6
40	0.93	137.6	2.75	6.59	1	12.90	0.013	28.8	0.73	4.33	3.0	113	38.9
					2	6.00	0.053	53.4	1.24	3.84	3.0	158	39.7
					3	24.40	0.002	7.8	0.10	2.22	3.0	90	37.2

\* Energy is defined as the integral of the velocity time history squared

\*\* Area is defined as the integral of the absolute value of the velocity time history

Record #	Ground Motion Record				Pulse #	CPE <sub>V-EN</sub>							
	$a_{max}$ (g)	$v_{max}$ (cm/s)	energy*	area**		$T_p$ (s)	$a_{max}$ (g)	$v_{max}$ (cm/s)	energy*	area**	$\gamma$	$\theta$ (°)	$l$ (s)
1	0.73	117.8	1.18	2.80	1	2.30	0.256	90.4	0.74	1.29	1.0	135	18.7
					2	4.60	0.036	28.5	0.20	1.16	2.0	135	18.8
					3	1.60	0.122	32.0	0.09	0.47	2.0	23	16.7
2	0.18	54.5	0.46	2.45	1	4.20	0.066	43.2	0.31	1.14	1.0	45	7.0
					2	5.10	0.015	13.2	0.06	0.79	3.0	135	15.6
					3	1.50	0.055	13.9	0.02	0.25	3.0	23	9.5
3	0.38	115.0	0.94	2.69	1	2.70	0.189	87.4	0.77	1.46	1.0	90	5.0
					2	2.00	0.075	27.8	0.08	0.48	2.0	90	8.0
					3	0.80	0.210	27.6	0.03	0.20	2.0	23	5.2
4	0.36	77.9	0.95	3.08	1	4.30	0.104	69.0	0.82	1.86	1.0	45	6.2
					2	1.30	0.127	24.6	0.04	0.27	1.5	0	5.5
					3	3.50	0.028	14.1	0.03	0.32	1.0	158	14.3
5	0.38	91.5	1.22	3.45	1	3.80	0.138	81.0	0.99	1.93	1.0	45	6.8
					2	2.90	0.045	20.6	0.06	0.47	1.5	23	13.7
					3	1.00	0.133	24.1	0.04	0.28	3.0	90	8.0
6	0.44	111.9	1.52	3.48	1	3.50	0.161	84.3	1.38	2.45	1.5	0	6.4
					2	7.70	0.006	7.0	0.03	0.66	3.0	0	15.1
					3	1.00	0.123	19.3	0.02	0.18	2.0	0	5.9
7	0.46	108.8	1.03	2.75	1	3.40	0.128	73.4	0.84	1.87	1.5	135	6.3
					2	0.70	0.289	33.0	0.06	0.28	3.0	0	5.4
					3	1.40	0.098	22.9	0.05	0.38	3.0	23	6.1
8	0.47	48.6	0.43	2.26	1	4.20	0.058	38.6	0.31	1.27	1.5	23	6.6
					2	2.60	0.027	12.8	0.03	0.39	3.0	90	10.5
					3	4.80	0.011	9.0	0.03	0.51	3.0	135	24.1
9	0.42	59.6	0.48	2.54	1	3.80	0.077	42.6	0.30	1.04	1.0	158	5.9
					2	5.40	0.018	15.5	0.05	0.52	1.0	68	10.2
					3	4.40	0.016	12.2	0.05	0.63	3.0	135	20.7
10	1.43	116.5	0.98	2.66	1	1.40	0.412	98.2	0.50	0.85	1.0	90	3.1
					2	5.40	0.027	27.4	0.17	1.07	1.5	90	6.5
					3	0.60	0.584	59.3	0.08	0.22	1.0	90	8.4
11	0.42	106.8	1.29	3.44	1	2.20	0.301	96.7	0.89	1.37	1.0	158	12.4
					2	5.00	0.033	26.3	0.17	1.03	1.5	158	17.5
					3	0.80	0.256	32.8	0.06	0.29	2.5	0	9.9
12	0.39	104.5	1.22	3.19	1	2.70	0.150	74.1	0.88	2.02	2.5	90	4.8
					2	1.10	0.211	43.0	0.10	0.41	2.0	90	3.4
					3	3.40	0.042	23.3	0.07	0.49	1.0	68	8.7
13	0.52	67.3	0.79	2.65	1	2.50	0.136	57.1	0.59	1.71	3.0	23	4.5
					2	6.50	0.015	15.5	0.06	0.63	1.0	68	4.1
					3	0.70	0.191	23.5	0.03	0.19	3.0	68	6.9
14	0.72	120.9	0.87	2.83	1	0.90	0.651	95.2	0.31	0.53	1.0	113	5.4
					2	2.00	0.168	48.9	0.20	0.62	1.0	23	3.8
					3	2.10	0.138	42.4	0.16	0.57	1.0	23	7.9

Appendix A1 – Parameters of the three extracted pulses from each of the six CPE methods

CPE<sub>V-EN</sub>

Record #	Ground Motion Record				Pulse #	CPE <sub>V-EN</sub>							
	$a_{max}$ (g)	$v_{max}$ (cm/s)	energy*	area** (m)		$T_P$ (s)	$a_{max}$ (g)	$v_{max}$ (cm/s)	energy*	area** (m)	$\gamma$	$\theta$ (°)	$l$ (s)
15	0.43	87.7	0.90	2.42	1	2.40	0.235	77.4	0.69	1.26	1.0	0	5.1
					2	1.00	0.169	29.8	0.06	0.35	3.0	113	4.5
					3	2.00	0.072	23.6	0.04	0.29	1.0	113	10.4
16	0.41	53.2	0.51	2.58	1	1.80	0.159	46.6	0.15	0.52	1.0	68	7.2
					2	1.50	0.102	25.6	0.07	0.46	3.0	158	4.3
					3	1.50	0.098	26.1	0.07	0.46	3.0	68	9.7
17	0.89	173.1	1.25	2.51	1	1.20	0.697	129.2	0.80	0.97	1.0	135	2.5
					2	1.80	0.173	48.2	0.17	0.54	1.0	45	6.2
					3	3.90	0.036	23.2	0.08	0.56	1.0	68	2.5
18	0.59	130.3	1.99	4.98	1	2.60	0.161	70.0	0.92	2.18	3.0	23	4.6
					2	1.20	0.288	60.9	0.30	0.85	3.0	113	6.8
					3	0.90	0.421	63.2	0.23	0.60	2.5	158	3.7
19	0.84	116.5	0.83	2.80	1	2.80	0.103	47.2	0.47	1.62	3.0	0	4.4
					2	1.00	0.308	47.6	0.09	0.30	1.0	45	3.2
					3	1.00	0.207	35.6	0.07	0.31	2.0	135	6.3
20	0.73	123.1	1.01	2.77	1	2.40	0.150	63.5	0.66	1.77	3.0	68	4.9
					2	1.20	0.214	44.1	0.16	0.62	3.0	135	4.0
					3	1.60	0.083	22.8	0.06	0.43	3.0	45	8.2
21	1.33	65.4	0.69	2.96	1	5.80	0.027	27.4	0.19	1.16	1.5	68	9.1
					2	1.60	0.161	41.6	0.10	0.41	1.0	68	8.3
					3	1.90	0.069	22.9	0.07	0.51	3.0	113	4.2
22	0.65	102.3	1.23	3.20	1	2.90	0.102	53.2	0.56	1.79	3.0	90	8.4
					2	1.20	0.317	64.9	0.19	0.48	1.0	90	8.8
					3	0.90	0.464	57.2	0.14	0.35	1.0	0	10.2
23	0.68	169.5	3.17	5.97	1	1.90	0.361	114.5	1.60	2.29	2.5	23	6.8
					2	1.10	0.435	82.4	0.52	1.07	3.0	45	6.4
					3	1.20	0.426	85.8	0.40	0.77	1.5	135	3.1
24	0.35	61.4	1.10	3.99	1	5.50	0.043	42.0	0.66	2.70	3.0	113	7.7
					2	2.90	0.052	25.7	0.13	0.88	3.0	45	8.7
					3	3.50	0.047	26.6	0.09	0.58	1.0	113	14.8
25	0.77	92.6	1.56	4.33	1	4.80	0.108	75.9	1.19	2.34	1.0	158	12.0
					2	10.50	0.010	18.7	0.22	2.00	2.5	113	18.6
					3	1.70	0.103	27.1	0.05	0.29	1.0	45	10.7
26	0.24	56.5	0.61	2.94	1	7.10	0.034	39.4	0.42	1.73	1.0	68	18.0
					2	1.20	0.141	28.3	0.07	0.40	3.0	23	16.4
					3	2.80	0.022	10.5	0.02	0.35	3.0	23	26.6
27	0.85	121.4	3.41	7.26	1	4.70	0.115	100.6	2.41	4.10	2.0	90	12.3
					2	3.80	0.049	31.3	0.27	1.42	3.0	158	22.6
					3	1.90	0.087	29.2	0.11	0.64	3.0	68	13.4
28	0.24	51.1	0.47	2.33	1	5.40	0.046	40.9	0.34	1.37	1.0	113	8.0
					2	8.50	0.009	12.4	0.07	0.96	2.0	23	15.3
					3	3.50	0.016	9.2	0.02	0.35	2.5	0	11.4

Record #	Ground Motion Record				Pulse #	CPE <sub>V-EN</sub>							
	$a_{max}$ (g)	$v_{max}$ (cm/s)	energy* (m <sup>2</sup> /s)	area** (m)		$T_P$ (s)	$a_{max}$ (g)	$v_{max}$ (cm/s)	energy* (m <sup>2</sup> /s)	area** (m)	$\gamma$	$\theta$ (°)	$l$ (s)
29	0.27	48.7	0.98	4.01	1	7.70	0.030	32.0	0.38	1.67	1.0	0	18.7
					2	3.00	0.058	30.8	0.19	1.08	3.0	113	14.3
					3	3.70	0.029	18.2	0.09	0.81	3.0	23	24.1
30	0.38	165.5	7.20	11.71	1	7.40	0.111	133.4	5.01	6.12	1.0	113	38.8
					2	2.20	0.205	72.5	0.79	1.74	2.5	0	34.4
					3	18.10	0.009	23.8	0.57	3.58	1.5	0	49.4
31	0.16	60.3	0.86	4.28	1	9.70	0.023	37.9	0.52	2.28	1.0	90	36.5
					2	4.00	0.028	18.5	0.10	0.88	3.0	23	37.0
					3	10.60	0.007	10.2	0.05	0.73	1.0	0	56.0
32	0.83	129.5	4.91	10.80	1	4.40	0.119	90.0	2.50	4.67	3.0	135	32.1
					2	3.10	0.086	46.3	0.41	1.48	2.5	135	47.5
					3	12.70	0.013	24.3	0.32	1.98	1.0	158	35.2
33	0.52	84.2	1.90	6.63	1	11.10	0.023	42.4	0.76	2.92	1.0	68	33.5
					2	1.90	0.226	62.7	0.32	0.77	1.0	23	30.5
					3	1.80	0.112	32.4	0.13	0.64	2.5	0	33.8
34	0.56	184.5	13.88	17.15	1	11.30	0.086	158.8	10.84	11.13	1.0	113	40.6
					2	3.20	0.216	101.2	1.41	2.08	1.0	23	36.9
					3	22.00	0.008	23.4	0.58	3.49	1.0	0	55.3
35	0.33	88.5	1.83	6.23	1	4.90	0.103	78.3	1.20	2.40	1.0	45	29.5
					2	3.50	0.038	24.0	0.14	0.98	3.0	90	45.2
					3	15.70	0.006	14.0	0.13	1.42	1.0	23	35.6
36	0.13	43.7	0.68	3.87	1	8.30	0.024	31.4	0.51	2.48	2.0	0	41.4
					2	3.60	0.023	13.8	0.05	0.60	3.0	158	48.5
					3	4.50	0.011	8.4	0.02	0.45	3.0	158	36.7
37	0.21	68.3	0.91	3.91	1	8.10	0.030	41.0	0.63	2.50	1.5	45	19.4
					2	3.20	0.039	21.8	0.09	0.72	2.5	135	17.3
					3	5.30	0.014	12.8	0.06	0.82	3.0	158	29.9
38	0.30	109.0	1.97	5.72	1	7.50	0.044	55.7	1.07	3.13	1.5	45	39.5
					2	2.80	0.104	45.7	0.36	1.22	2.0	0	37.6
					3	1.50	0.205	47.5	0.13	0.45	1.0	135	47.5
39	0.13	62.1	1.23	4.93	1	7.30	0.042	46.0	0.86	2.79	1.5	0	40.6
					2	3.10	0.044	24.2	0.12	0.87	3.0	68	47.2
					3	3.10	0.037	20.4	0.09	0.74	3.0	113	38.1
40	0.93	137.6	2.75	6.59	1	7.70	0.066	78.8	1.91	3.80	1.0	135	39.4
					2	2.50	0.088	39.9	0.27	1.16	3.0	90	38.1
					3	20.60	0.004	14.2	0.16	1.82	1.0	90	38.7

\* Energy is defined as the integral of the velocity time history squared

\*\* Area is defined as the integral of the absolute value of the velocity time history

Record #	Ground Motion Record				Pulse #	CPE <sub>V-AM</sub>							
	$a_{max}$ (g)	$v_{max}$ (cm/s)	energy*	area**		$T_p$ (s)	$a_{max}$ (g)	$v_{max}$ (cm/s)	energy*	area**	$\gamma$	$\theta$ (°)	$l$ (s)
1	0.73	117.8	1.18	2.80	1	1.80	0.334	98.2	0.66	1.10	1.0	113	18.5
					2	4.70	0.056	42.7	0.32	1.24	1.0	113	18.4
					3	0.70	0.379	39.9	0.04	0.17	1.0	135	17.1
2	0.18	54.5	0.46	2.45	1	3.20	0.093	46.1	0.27	0.92	1.0	45	6.9
					2	1.90	0.071	21.9	0.03	0.26	1.0	68	9.5
					3	2.10	0.055	17.8	0.03	0.23	1.0	135	13.0
3	0.38	115.0	0.94	2.69	1	2.30	0.231	90.9	0.71	1.30	1.0	90	5.0
					2	1.00	0.202	32.8	0.04	0.20	1.0	113	5.9
					3	2.30	0.084	31.5	0.09	0.45	1.0	68	7.9
4	0.36	77.9	0.95	3.08	1	3.70	0.121	73.0	0.75	1.67	1.0	68	6.4
					2	1.30	0.151	31.9	0.05	0.26	1.0	68	5.7
					3	2.00	0.071	21.9	0.04	0.27	1.0	135	8.3
5	0.38	91.5	1.22	3.45	1	3.20	0.166	86.6	0.91	1.72	1.0	68	7.0
					2	1.30	0.159	31.9	0.05	0.26	1.0	135	8.7
					3	0.40	0.415	28.1	0.01	0.07	1.0	90	5.7
6	0.44	111.9	1.52	3.48	1	3.30	0.190	97.2	1.24	2.01	1.0	45	6.8
					2	1.20	0.168	32.9	0.05	0.24	1.0	68	6.1
					3	2.10	0.076	24.8	0.05	0.33	1.0	45	4.8
7	0.46	108.8	1.03	2.75	1	3.20	0.152	79.4	0.77	1.58	1.0	113	6.1
					2	0.75	0.340	41.6	0.05	0.19	1.0	68	5.1
					3	1.50	0.158	38.7	0.09	0.36	1.0	113	7.1
8	0.47	48.6	0.43	2.26	1	3.30	0.085	43.4	0.25	0.90	1.0	135	5.8
					2	1.10	0.155	27.7	0.03	0.19	1.0	113	8.1
					3	0.50	0.264	21.4	0.01	0.07	1.0	68	5.4
9	0.42	59.6	0.48	2.54	1	3.00	0.100	46.2	0.26	0.87	1.0	135	5.7
					2	0.70	0.237	25.6	0.02	0.11	1.0	45	6.9
					3	0.30	0.424	19.5	0.00	0.04	1.0	45	8.4
10	1.43	116.5	0.98	2.66	1	1.20	0.497	101.5	0.46	0.75	1.0	90	3.1
					2	0.55	0.702	61.7	0.08	0.21	1.0	68	8.3
					3	0.45	0.630	46.1	0.04	0.13	1.0	113	7.7
11	0.42	106.8	1.29	3.44	1	1.80	0.351	102.8	0.72	1.14	1.0	113	12.2
					2	0.90	0.339	47.2	0.08	0.27	1.0	135	13.5
					3	0.75	0.339	40.9	0.05	0.19	1.0	68	10.0
12	0.39	104.5	1.22	3.19	1	2.80	0.188	85.4	0.77	1.48	1.0	68	4.6
					2	1.00	0.310	53.0	0.11	0.33	1.0	90	6.6
					3	1.10	0.266	46.8	0.09	0.31	1.0	113	3.5
13	0.52	67.3	0.79	2.65	1	2.60	0.157	69.8	0.47	1.12	1.0	90	3.6
					2	2.30	0.115	43.2	0.16	0.62	1.0	113	6.5
					3	0.50	0.386	32.8	0.02	0.10	1.0	90	7.0
14	0.72	120.9	0.87	2.83	1	0.75	0.809	101.2	0.28	0.46	1.0	90	5.4
					2	1.40	0.250	57.0	0.17	0.50	1.0	68	4.1
					3	1.70	0.180	47.1	0.15	0.50	1.0	135	7.5

Record #	Ground Motion Record				Pulse #	CPE <sub>V-AM</sub>							
	$a_{max}$ (g)	$v_{max}$ (cm/s)	energy*	area**		$T_P$ (s)	$a_{max}$ (g)	$v_{max}$ (cm/s)	energy*	area**	$\gamma$	$\theta$ (°)	$l$ (s)
15	0.43	87.7	0.90	2.42	1	1.70	0.356	93.7	0.60	1.00	1.0	45	5.4
					2	1.80	0.114	35.0	0.08	0.39	1.0	90	4.2
					3	1.60	0.102	27.9	0.05	0.28	1.0	90	6.2
16	0.41	53.2	0.51	2.58	1	1.20	0.283	52.3	0.13	0.39	1.0	45	7.0
					2	0.85	0.319	41.8	0.06	0.22	1.0	45	3.7
					3	0.60	0.352	34.1	0.03	0.13	1.0	68	8.9
17	0.89	173.1	1.25	2.51	1	0.95	0.901	139.7	0.71	0.82	1.0	113	2.4
					2	1.30	0.263	52.9	0.14	0.43	1.0	45	6.2
					3	0.65	0.505	50.9	0.07	0.21	1.0	45	1.9
18	0.59	130.3	1.99	4.98	1	1.10	0.552	98.7	0.41	0.67	1.0	68	3.4
					2	1.30	0.442	93.5	0.43	0.75	1.0	113	6.8
					3	2.10	0.204	69.7	0.39	0.91	1.0	68	4.9
19	0.84	116.5	0.83	2.80	1	2.40	0.164	67.3	0.41	1.00	1.0	90	3.6
					2	0.80	0.361	49.2	0.07	0.24	1.0	90	3.7
					3	1.10	0.258	46.2	0.09	0.31	1.0	68	6.6
20	0.73	123.1	1.01	2.77	1	1.50	0.393	94.8	0.51	0.87	1.0	113	3.9
					2	2.00	0.163	52.9	0.21	0.65	1.0	68	7.4
					3	0.40	0.581	38.6	0.02	0.09	1.0	90	3.9
21	1.33	65.4	0.69	2.96	1	0.50	0.816	62.2	0.08	0.19	1.0	135	7.9
					2	0.45	0.743	50.7	0.05	0.14	1.0	135	4.7
					3	1.90	0.139	40.5	0.12	0.48	1.0	45	8.2
22	0.65	102.3	1.23	3.20	1	1.80	0.263	77.1	0.41	0.86	1.0	68	8.0
					2	0.80	0.464	63.3	0.12	0.31	1.0	90	10.4
					3	0.95	0.413	64.1	0.15	0.38	1.0	113	11.4
23	0.68	169.5	3.17	5.97	1	1.40	0.696	166.0	1.44	1.44	1.0	90	6.1
					2	1.50	0.417	101.9	0.59	0.95	1.0	68	8.1
					3	1.20	0.443	90.4	0.37	0.67	1.0	90	3.0
24	0.35	61.4	1.10	3.99	1	4.20	0.070	50.4	0.40	1.31	1.0	90	10.6
					2	4.80	0.057	44.4	0.36	1.32	1.0	113	4.6
					3	0.55	0.478	40.7	0.04	0.14	1.0	135	4.7
25	0.77	92.6	1.56	4.33	1	4.00	0.128	83.3	1.06	2.07	1.0	113	11.4
					2	3.20	0.060	31.3	0.12	0.62	1.0	113	14.1
					3	8.40	0.018	25.8	0.21	1.34	1.0	90	18.2
26	0.24	56.5	0.61	2.94	1	5.60	0.044	41.9	0.37	1.45	1.0	90	18.5
					2	1.20	0.189	38.4	0.07	0.28	1.0	90	16.6
					3	1.60	0.086	21.2	0.03	0.21	1.0	135	14.7
27	0.85	121.4	3.41	7.26	1	4.80	0.136	111.6	2.24	3.31	1.0	90	12.4
					2	0.40	0.818	52.0	0.04	0.13	1.0	68	10.5
					3	0.80	0.397	51.1	0.08	0.25	1.0	68	13.6
28	0.24	51.1	0.47	2.33	1	4.50	0.056	43.2	0.31	1.20	1.0	90	7.6
					2	7.50	0.013	17.1	0.08	0.80	1.0	90	12.2
					3	0.60	0.140	14.3	0.00	0.05	1.0	90	7.1

Record #	Ground Motion Record				Pulse #	CPE <sub>V-AM</sub>							
	$a_{max}$ (g)	$v_{max}$ (cm/s)	energy* (m <sup>2</sup> /s)	area** (m)		$T_P$ (s)	$a_{max}$ (g)	$v_{max}$ (cm/s)	energy* (m <sup>2</sup> /s)	area** (m)	$\gamma$	$\theta$ (°)	$l$ (s)
29	0.27	48.7	0.98	4.01	1	3.40	0.085	46.9	0.28	0.99	1.0	113	14.4
					2	5.20	0.043	38.2	0.28	1.23	1.0	90	20.6
					3	1.20	0.162	31.7	0.05	0.24	1.0	68	13.9
30	0.38	165.5	7.20	11.71	1	6.40	0.127	139.4	4.66	5.53	1.0	90	38.3
					2	1.60	0.348	95.2	0.54	0.94	1.0	90	33.7
					3	2.40	0.168	65.9	0.40	0.98	1.0	68	36.0
31	0.16	60.3	0.86	4.28	1	6.00	0.044	43.3	0.43	1.61	1.0	68	35.6
					2	5.40	0.028	23.7	0.12	0.80	1.0	45	40.6
					3	1.20	0.102	20.0	0.02	0.15	1.0	68	49.4
32	0.83	129.5	4.91	10.80	1	4.40	0.149	112.4	2.08	3.07	1.0	90	31.5
					2	2.40	0.189	77.5	0.54	1.15	1.0	90	36.1
					3	1.40	0.318	72.4	0.28	0.63	1.0	113	47.4
33	0.52	84.2	1.90	6.63	1	1.50	0.309	71.6	0.31	0.67	1.0	45	30.6
					2	0.75	0.376	46.0	0.06	0.21	1.0	113	28.2
					3	10.10	0.026	42.9	0.71	2.69	1.0	68	33.5
34	0.56	184.5	13.88	17.15	1	9.80	0.099	166.3	10.16	10.11	1.0	90	39.9
					2	2.90	0.242	114.4	1.44	2.06	1.0	68	37.2
					3	2.70	0.148	65.0	0.43	1.09	1.0	68	42.3
35	0.33	88.5	1.83	6.23	1	4.10	0.124	83.0	1.07	2.11	1.0	68	29.7
					2	1.90	0.116	36.0	0.09	0.42	1.0	113	30.2
					3	3.50	0.045	26.9	0.10	0.58	1.0	90	47.2
36	0.13	43.7	0.68	3.87	1	8.30	0.028	37.3	0.44	1.92	1.0	68	43.1
					2	2.20	0.055	19.9	0.03	0.27	1.0	113	44.4
					3	3.50	0.028	15.9	0.03	0.35	1.0	68	49.7
37	0.21	68.3	0.91	3.91	1	4.60	0.067	47.7	0.42	1.38	1.0	135	17.3
					2	4.20	0.040	28.5	0.13	0.74	1.0	90	20.7
					3	0.75	0.220	25.5	0.02	0.12	1.0	45	27.8
38	0.30	109.0	1.97	5.72	1	3.20	0.146	76.2	0.71	1.51	1.0	113	37.1
					2	1.30	0.233	49.3	0.12	0.40	1.0	113	47.5
					3	7.90	0.034	46.0	0.63	2.25	1.0	90	40.6
39	0.13	62.1	1.23	4.93	1	5.80	0.065	58.1	0.78	2.11	1.0	45	41.4
					2	3.80	0.046	26.9	0.11	0.64	1.0	135	47.7
					3	2.60	0.066	26.5	0.07	0.43	1.0	135	42.4
40	0.93	137.6	2.75	6.59	1	6.40	0.080	84.0	1.72	3.34	1.0	113	39.0
					2	2.60	0.106	44.8	0.20	0.72	1.0	68	39.2
					3	0.95	0.241	35.5	0.05	0.21	1.0	45	46.4

\* Energy is defined as the integral of the velocity time history squared

\*\* Area is defined as the integral of the absolute value of the velocity time history

Record #	Ground Motion Record				Pulse #	CPE <sub>A-AR</sub>							
	$a_{max}$ (g)	$v_{max}$ (cm/s)	energy*	area**		$T_p$ (s)	$a_{max}$ (g)	$v_{max}$ (cm/s)	energy*	area**	$\gamma$	$\theta$ (°)	$l$ (s)
1	0.73	117.8	1.18	2.80	1	1.50	0.262	68.8	0.50	1.19	3.0	113	36.5
					2	4.20	0.065	49.5	0.70	2.35	3.0	45	34.4
					3	2.70	0.040	18.5	0.07	0.59	3.0	90	34.3
2	0.18	54.5	0.46	2.45	1	3.40	0.054	34.2	0.26	1.30	3.0	158	23.6
					2	5.50	0.017	16.1	0.10	1.02	3.0	113	25.1
					3	2.10	0.035	12.4	0.02	0.31	3.0	90	24.4
3	0.38	115.0	0.94	2.69	1	2.70	0.135	66.0	0.80	2.02	3.0	45	23.3
					2	1.60	0.115	34.5	0.13	0.62	3.0	23	24.1
					3	0.75	0.183	25.7	0.03	0.22	3.0	158	25.0
4	0.36	77.9	0.95	3.08	1	3.50	0.086	54.4	0.70	2.16	3.0	135	22.5
					2	1.10	0.119	23.7	0.04	0.30	3.0	135	24.3
					3	2.30	0.033	14.0	0.03	0.36	3.0	135	22.9
5	0.38	91.5	1.22	3.45	1	3.00	0.117	65.6	0.85	2.20	3.0	158	23.5
					2	1.00	0.144	25.3	0.04	0.29	3.0	113	25.6
					3	0.40	0.282	21.6	0.01	0.10	3.0	0	25.1
6	0.44	111.9	1.52	3.48	1	3.10	0.139	73.3	1.25	2.70	3.0	90	22.9
					2	1.00	0.099	17.9	0.02	0.20	3.0	135	24.6
					3	2.70	0.033	16.5	0.05	0.50	3.0	23	25.6
7	0.46	108.8	1.03	2.75	1	3.00	0.113	61.7	0.77	2.10	3.0	45	21.7
					2	0.75	0.276	37.6	0.07	0.32	3.0	135	23.2
					3	1.40	0.120	30.6	0.09	0.48	3.0	45	22.8
8	0.47	48.6	0.43	2.26	1	4.30	0.042	33.2	0.32	1.61	3.0	135	21.2
					2	0.90	0.110	17.5	0.02	0.18	3.0	113	24.7
					3	2.70	0.034	17.2	0.05	0.52	3.0	158	21.9
9	0.42	59.6	0.48	2.54	1	5.00	0.032	29.6	0.29	1.66	3.0	158	21.6
					2	2.40	0.060	25.3	0.11	0.70	3.0	68	23.2
					3	0.60	0.189	19.3	0.02	0.14	3.0	90	25.5
10	1.43	116.5	0.98	2.66	1	1.10	0.374	74.7	0.42	0.93	3.0	45	24.6
					2	0.45	0.650	52.9	0.09	0.27	3.0	45	27.7
					3	0.45	0.383	29.3	0.03	0.16	3.0	90	26.6
11	0.42	106.8	1.29	3.44	1	1.70	0.259	75.2	0.72	1.52	3.0	90	17.6
					2	0.85	0.225	32.6	0.07	0.33	3.0	90	17.1
					3	5.00	0.036	32.8	0.36	1.86	3.0	135	16.4
12	0.39	104.5	1.22	3.19	1	2.70	0.153	72.7	1.01	2.26	3.0	68	14.4
					2	1.10	0.194	39.5	0.11	0.48	3.0	158	14.8
					3	0.80	0.211	29.5	0.05	0.27	3.0	113	16.6
13	0.52	67.3	0.79	2.65	1	2.50	0.136	61.9	0.65	1.75	3.0	135	16.6
					2	0.65	0.211	26.3	0.03	0.19	3.0	0	19.4
					3	1.00	0.112	19.6	0.03	0.23	3.0	68	17.1
14	0.72	120.9	0.87	2.83	1	0.70	0.532	70.6	0.23	0.55	3.0	0	25.1
					2	1.20	0.192	40.4	0.14	0.56	3.0	68	24.1
					3	1.50	0.130	33.2	0.12	0.59	3.0	90	25.6

Appendix A1 – Parameters of the three extracted pulses from each of the six CPE methods

CPE<sub>A-AR</sub>

Record #	Ground Motion Record				Pulse #	CPE <sub>A-AR</sub>							
	$a_{max}$ (g)	$v_{max}$ (cm/s)	energy*	area**		$T_P$ (s)	$a_{max}$ (g)	$v_{max}$ (cm/s)	energy*	area**	$\gamma$	$\theta$ (°)	$l$ (s)
15	0.43	87.7	0.90	2.42	1	2.00	0.170	59.8	0.50	1.38	3.0	113	15.3
					2	1.10	0.177	35.4	0.09	0.44	3.0	135	16.1
					3	4.20	0.029	21.0	0.14	1.05	3.0	90	13.3
16	0.41	53.2	0.51	2.58	1	1.30	0.139	34.7	0.10	0.50	3.0	0	19.7
					2	0.65	0.254	30.8	0.04	0.22	3.0	23	20.8
					3	1.60	0.099	28.8	0.09	0.52	3.0	135	20.6
17	0.89	173.1	1.25	2.51	1	0.95	0.571	95.6	0.61	1.05	3.0	68	9.1
					2	1.30	0.176	40.2	0.15	0.60	3.0	68	10.4
					3	0.55	0.331	35.0	0.04	0.21	3.0	0	9.3
18	0.59	130.3	1.99	4.98	1	2.60	0.162	74.0	1.01	2.22	3.0	113	23.0
					2	1.20	0.310	63.4	0.36	0.90	3.0	90	25.5
					3	0.90	0.400	61.3	0.25	0.66	3.0	90	24.1
19	0.84	116.5	0.83	2.80	1	2.90	0.102	50.5	0.55	1.74	3.0	90	22.7
					2	0.75	0.303	38.8	0.08	0.35	3.0	90	24.1
					3	0.85	0.194	31.8	0.06	0.30	3.0	0	25.3
20	0.73	123.1	1.01	2.77	1	2.40	0.158	68.6	0.76	1.86	3.0	45	23.6
					2	1.30	0.205	46.8	0.20	0.70	3.0	68	23.9
					3	0.35	0.475	30.6	0.02	0.12	3.0	23	24.7
21	1.33	65.4	0.69	2.96	1	0.70	0.315	39.5	0.07	0.31	3.0	45	24.6
					2	0.40	0.527	36.2	0.04	0.17	3.0	68	26.6
					3	0.65	0.263	28.9	0.04	0.22	3.0	90	25.6
22	0.65	102.3	1.23	3.20	1	2.90	0.107	56.4	0.63	1.85	3.0	45	16.2
					2	0.70	0.442	56.1	0.15	0.44	3.0	45	18.8
					3	1.30	0.200	48.6	0.20	0.71	3.0	158	17.6
23	0.68	169.5	3.17	5.97	1	1.30	0.531	121.5	1.36	1.83	3.0	68	25.2
					2	1.40	0.297	77.6	0.56	1.21	3.0	23	26.5
					3	1.10	0.338	69.6	0.35	0.86	3.0	23	24.1
24	0.35	61.4	1.10	3.99	1	5.40	0.046	44.9	0.74	2.75	3.0	45	14.2
					2	0.75	0.224	31.5	0.05	0.26	3.0	158	16.5
					3	2.90	0.051	27.0	0.14	0.89	3.0	135	16.7
25	0.77	92.6	1.56	4.33	1	3.70	0.093	64.4	1.02	2.67	3.0	23	30.2
					2	8.60	0.017	25.6	0.42	2.62	3.0	90	28.2
					3	1.50	0.082	22.3	0.05	0.38	3.0	135	31.7
26	0.24	56.5	0.61	2.94	1	5.90	0.029	32.2	0.40	2.12	3.0	158	29.1
					2	1.20	0.140	29.5	0.07	0.41	3.0	113	32.5
					3	3.10	0.021	12.4	0.03	0.43	3.0	158	30.9
27	0.85	121.4	3.41	7.26	1	4.60	0.109	93.4	2.65	4.80	3.0	23	21.2
					2	0.50	0.468	42.2	0.06	0.24	3.0	45	23.6
					3	0.75	0.292	38.4	0.08	0.33	3.0	68	24.7
28	0.24	51.1	0.47	2.33	1	3.90	0.040	29.4	0.22	1.28	3.0	158	16.4
					2	8.90	0.011	18.9	0.21	1.87	3.0	0	14.3
					3	0.60	0.096	11.0	0.00	0.07	3.0	0	19.1

Record #	Ground Motion Record				Pulse #	CPE <sub>A-AR</sub>							
	$a_{max}$ (g)	$v_{max}$ (cm/s)	energy* (m <sup>2</sup> /s)	area** (m)		$T_P$ (s)	$a_{max}$ (g)	$v_{max}$ (cm/s)	energy* (m <sup>2</sup> /s)	area** (m)	$\gamma$	$\theta$ (°)	$l$ (s)
29	0.27	48.7	0.98	4.01	1	3.20	0.060	35.8	0.27	1.28	3.0	158	24.3
					2	4.20	0.042	31.1	0.29	1.51	3.0	113	27.4
					3	1.40	0.107	28.0	0.07	0.44	3.0	23	24.9
30	0.38	165.5	7.20	11.71	1	5.30	0.095	94.0	3.10	5.57	3.0	158	66.1
					2	2.20	0.201	75.3	0.93	1.97	3.0	90	67.0
					3	11.20	0.023	46.4	1.63	5.88	3.0	45	61.7
31	0.16	60.3	0.86	4.28	1	8.20	0.019	28.9	0.45	2.65	3.0	158	62.6
					2	4.30	0.028	22.5	0.14	1.08	3.0	158	65.7
					3	3.70	0.022	15.1	0.06	0.62	3.0	23	73.4
32	0.83	129.5	4.91	10.80	1	4.40	0.119	97.9	2.79	4.82	3.0	23	63.8
					2	1.10	0.277	53.5	0.22	0.68	3.0	68	74.3
					3	1.90	0.153	49.5	0.35	1.12	3.0	90	67.9
33	0.52	84.2	1.90	6.63	1	2.20	0.116	49.2	0.35	1.21	3.0	0	65.3
					2	1.10	0.212	42.3	0.13	0.53	3.0	135	66.4
					3	0.80	0.237	32.2	0.06	0.31	3.0	90	65.2
34	0.56	184.5	13.88	17.15	1	8.90	0.072	120.3	8.52	11.98	3.0	158	63.7
					2	2.60	0.163	81.4	1.13	2.36	3.0	0	68.2
					3	5.00	0.052	46.8	0.74	2.65	3.0	135	65.0
35	0.33	88.5	1.83	6.23	1	3.70	0.086	59.3	0.86	2.45	3.0	158	63.4
					2	1.80	0.088	27.1	0.10	0.58	3.0	90	64.6
					3	3.60	0.039	26.4	0.17	1.06	3.0	158	71.1
36	0.13	43.7	0.68	3.87	1	7.90	0.022	30.7	0.52	2.80	3.0	113	65.8
					2	3.60	0.025	16.4	0.07	0.67	3.0	135	73.2
					3	1.70	0.035	10.7	0.01	0.21	3.0	135	72.3
37	0.21	68.3	0.91	3.91	1	7.70	0.024	35.0	0.63	3.02	3.0	23	31.9
					2	3.10	0.039	22.5	0.10	0.78	3.0	23	34.0
					3	1.10	0.080	15.5	0.02	0.20	3.0	68	41.0
38	0.30	109.0	1.97	5.72	1	7.20	0.036	47.0	1.08	3.83	3.0	135	65.3
					2	2.70	0.095	45.3	0.39	1.41	3.0	113	68.3
					3	1.20	0.167	38.6	0.12	0.51	3.0	0	74.4
39	0.13	62.1	1.23	4.93	1	6.90	0.036	43.2	0.91	3.44	3.0	113	66.2
					2	2.90	0.047	24.6	0.12	0.81	3.0	45	72.3
					3	3.10	0.041	21.7	0.11	0.80	3.0	90	68.4
40	0.93	137.6	2.75	6.59	1	5.90	0.058	60.7	1.54	4.14	3.0	68	106.7
					2	2.50	0.088	42.4	0.30	1.18	3.0	0	108.9
					3	0.95	0.142	23.7	0.04	0.26	3.0	68	114.0

\* Energy is defined as the integral of the velocity time history squared

\*\* Area is defined as the integral of the absolute value of the velocity time history

Record #	Ground Motion Record				Pulse #	CPE <sub>A-EN</sub>							
	$a_{max}$ (g)	$v_{max}$ (cm/s)	energy*	area**		$T_p$ (s)	$a_{max}$ (g)	$v_{max}$ (cm/s)	energy*	area**	$\gamma$	$\theta$ (°)	$l$ (s)
1	0.73	117.8	1.18	2.80	1	1.40	0.27	65.0	0.440	1.07	3.0	90	36.5
					2	0.30	0.40	24.2	0.006	0.04	1.0	135	36.9
					3	3.60	0.08	56.4	0.651	1.95	2.5	23	35.3
2	0.18	54.5	0.46	2.45	1	3.20	0.08	50.4	0.324	0.98	1.0	113	25.1
					2	0.45	0.12	9.9	0.003	0.05	3.0	135	27.0
					3	0.75	0.11	17.9	0.008	0.07	1.0	45	27.7
3	0.38	115.0	0.94	2.69	1	2.10	0.21	96.9	0.760	1.31	1.5	158	24.4
					2	0.70	0.20	24.3	0.031	0.20	3.0	90	25.0
					3	1.70	0.07	23.2	0.061	0.44	3.0	158	25.9
4	0.36	77.9	0.95	3.08	1	3.50	0.12	80.9	0.912	1.71	1.0	113	24.1
					2	1.10	0.12	24.1	0.042	0.30	3.0	23	24.4
					3	0.35	0.19	12.6	0.002	0.03	1.0	68	24.9
5	0.38	91.5	1.22	3.45	1	2.90	0.14	80.1	0.934	1.91	2.0	135	24.2
					2	0.40	0.38	30.8	0.016	0.08	1.5	45	25.3
					3	0.95	0.15	24.0	0.041	0.27	3.0	90	25.6
6	0.44	111.9	1.52	3.48	1	3.00	0.17	86.8	1.401	2.38	2.0	90	23.8
					2	0.60	0.24	26.8	0.017	0.10	1.0	68	25.2
					3	0.30	0.18	9.8	0.002	0.03	3.0	45	25.7
7	0.46	108.8	1.03	2.75	1	0.75	0.28	37.7	0.072	0.32	3.0	135	23.2
					2	2.00	0.19	83.5	0.482	0.88	1.0	135	23.2
					3	1.90	0.12	57.9	0.211	0.54	1.0	158	24.2
8	0.47	48.6	0.43	2.26	1	0.45	0.22	18.2	0.008	0.07	2.0	68	24.1
					2	0.85	0.13	18.5	0.020	0.16	2.5	90	24.9
					3	0.30	0.23	15.0	0.003	0.03	1.5	158	25.4
9	0.42	59.6	0.48	2.54	1	0.30	0.34	18.4	0.006	0.05	2.0	68	26.4
					2	0.55	0.20	19.9	0.015	0.12	3.0	135	25.5
					3	3.10	0.09	50.0	0.309	0.94	1.0	68	24.2
10	1.43	116.5	0.98	2.66	1	0.45	0.65	53.0	0.086	0.27	3.0	45	27.7
					2	1.10	0.43	97.7	0.501	0.86	2.0	23	24.8
					3	0.35	0.63	39.7	0.021	0.08	1.0	68	26.9
11	0.42	106.8	1.29	3.44	1	1.70	0.28	86.3	0.788	1.47	2.5	68	17.8
					2	0.75	0.32	39.1	0.068	0.23	1.5	90	17.4
					3	0.65	0.18	21.9	0.020	0.16	3.0	158	19.0
12	0.39	104.5	1.22	3.19	1	1.30	0.29	98.5	0.413	0.61	1.0	0	15.3
					2	2.50	0.12	55.9	0.516	1.56	3.0	158	14.9
					3	0.80	0.23	32.0	0.051	0.26	2.5	113	16.7
13	0.52	67.3	0.79	2.65	1	2.40	0.14	60.6	0.598	1.65	3.0	135	16.7
					2	0.50	0.34	41.4	0.028	0.10	1.0	23	19.8
					3	0.35	0.32	21.1	0.008	0.06	2.0	45	19.4
14	0.72	120.9	0.87	2.83	1	0.70	0.68	110.3	0.317	0.49	1.5	0	25.3
					2	0.45	0.41	32.3	0.031	0.16	3.0	45	27.1
					3	0.25	0.43	18.4	0.006	0.05	3.0	113	25.8

Record #	Ground Motion Record				Pulse #	CPE <sub>A-EN</sub>							
	$a_{max}$ (g)	$v_{max}$ (cm/s)	energy*	area**		$T_P$ (s)	$a_{max}$ (g)	$v_{max}$ (cm/s)	energy*	area**	(m)	$\gamma$	$\theta$ (°)
15	0.43	87.7	0.90	2.42	1	1.60	0.31	108.9	0.654	0.92	1.0	135	16.5
					2	0.60	0.11	12.1	0.006	0.08	3.0	0	16.5
					3	1.60	0.07	27.7	0.046	0.28	1.5	0	18.7
16	0.41	53.2	0.51	2.58	1	0.45	0.34	27.3	0.023	0.14	3.0	45	18.9
					2	0.65	0.26	28.9	0.041	0.22	3.0	90	20.9
					3	1.30	0.24	67.9	0.207	0.47	1.0	135	20.3
17	0.89	173.1	1.25	2.51	1	0.90	0.86	167.6	0.872	0.80	1.0	45	9.5
					2	0.30	0.48	26.7	0.014	0.09	3.0	158	10.4
					3	0.80	0.30	59.0	0.092	0.23	1.0	23	11.2
18	0.59	130.3	1.99	4.98	1	1.10	0.45	129.9	0.607	0.68	1.0	0	24.3
					2	1.20	0.38	82.9	0.451	0.85	2.0	68	25.7
					3	1.10	0.32	53.2	0.172	0.43	1.0	90	24.9
19	0.84	116.5	0.83	2.80	1	0.35	0.71	54.2	0.036	0.10	1.0	45	24.6
					2	0.40	0.48	35.8	0.020	0.09	1.0	68	26.3
					3	0.75	0.21	28.1	0.040	0.24	3.0	135	25.3
20	0.73	123.1	1.01	2.77	1	1.40	0.32	120.0	0.663	0.80	1.0	0	24.4
					2	0.35	0.53	33.2	0.022	0.12	2.5	45	24.7
					3	1.80	0.14	54.8	0.254	0.79	2.0	0	25.6
21	1.33	65.4	0.69	2.96	1	0.45	0.70	56.7	0.057	0.15	1.0	68	26.8
					2	0.40	0.59	59.8	0.046	0.11	1.0	0	25.2
					3	0.35	0.63	38.8	0.020	0.08	1.0	113	28.2
22	0.65	102.3	1.23	3.20	1	0.70	0.44	56.1	0.149	0.44	3.0	45	18.8
					2	0.45	0.51	42.7	0.054	0.22	3.0	23	20.2
					3	0.90	0.37	81.8	0.199	0.36	1.0	23	19.7
23	0.68	169.5	3.17	5.97	1	1.30	0.67	177.2	1.707	1.55	1.5	135	25.9
					2	1.00	0.42	73.6	0.382	0.85	3.0	113	24.4
					3	1.40	0.34	110.8	0.642	0.98	1.5	0	27.0
24	0.35	61.4	1.10	3.99	1	0.55	0.38	38.9	0.040	0.15	1.5	68	17.0
					2	0.50	0.30	28.8	0.021	0.12	2.0	45	16.5
					3	0.45	0.20	16.7	0.008	0.09	3.0	45	17.8
25	0.77	92.6	1.56	4.33	1	4.00	0.11	82.0	1.351	2.70	2.0	45	31.1
					2	0.30	0.28	20.2	0.004	0.03	1.0	158	32.6
					3	0.25	0.22	10.3	0.002	0.03	3.0	158	33.2
26	0.24	56.5	0.61	2.94	1	1.10	0.15	33.5	0.069	0.35	2.5	0	32.8
					2	0.65	0.15	19.8	0.009	0.07	1.0	45	34.3
					3	5.20	0.04	53.3	0.487	1.35	1.0	23	32.8
27	0.85	121.4	3.41	7.26	1	0.35	0.67	51.5	0.036	0.13	1.5	158	23.9
					2	0.25	0.61	27.3	0.012	0.08	3.0	23	24.2
					3	0.75	0.29	38.4	0.078	0.33	3.0	68	24.7
28	0.24	51.1	0.47	2.33	1	4.10	0.05	47.0	0.339	1.23	1.5	0	17.9
					2	0.55	0.15	15.8	0.005	0.05	1.0	113	19.4
					3	0.45	0.13	10.8	0.003	0.05	2.5	45	21.2

Record #	Ground Motion Record				Pulse #	CPE <sub>A-EN</sub>							
	$a_{max}$ (g)	$v_{max}$ (cm/s)	energy* (m <sup>2</sup> /s)	area** (m)		$T_P$ (s)	$a_{max}$ (g)	$v_{max}$ (cm/s)	energy* (m <sup>2</sup> /s)	area** (m)	$\gamma$	$\theta$ (°)	$l$ (s)
29	0.27	48.7	0.98	4.01	1	1.70	0.13	54.9	0.169	0.46	1.0	23	25.9
					2	1.80	0.13	51.2	0.163	0.49	1.0	45	26.8
					3	1.00	0.14	27.7	0.036	0.22	2.0	158	27.9
30	0.38	165.5	7.20	11.71	1	1.50	0.36	130.6	0.845	0.96	1.0	158	68.0
					2	6.80	0.11	189.8	8.102	6.32	1.0	158	68.1
					3	2.20	0.12	45.3	0.318	1.15	3.0	113	68.3
31	0.16	60.3	0.86	4.28	1	1.10	0.09	24.9	0.022	0.13	1.0	158	76.1
					2	0.85	0.08	12.5	0.009	0.12	3.0	113	69.1
					3	5.20	0.04	40.5	0.413	1.52	1.5	113	66.6
32	0.83	129.5	4.91	10.80	1	1.00	0.28	52.8	0.184	0.59	3.0	158	74.2
					2	4.20	0.12	95.9	2.554	4.50	3.0	23	64.0
					3	1.10	0.23	51.4	0.163	0.54	2.5	0	66.0
33	0.52	84.2	1.90	6.63	1	1.30	0.28	80.4	0.290	0.55	1.0	45	66.8
					2	0.70	0.37	47.4	0.062	0.20	1.0	68	65.6
					3	1.70	0.11	36.0	0.146	0.68	3.0	23	67.0
34	0.56	184.5	13.88	17.15	1	2.90	0.25	132.7	2.035	2.33	1.0	68	69.0
					2	0.45	0.46	44.7	0.031	0.11	1.0	135	69.2
					3	9.00	0.08	157.5	8.604	9.15	1.5	23	67.6
35	0.33	88.5	1.83	6.23	1	2.60	0.15	73.6	0.561	1.16	1.0	68	65.1
					2	0.35	0.22	13.3	0.005	0.05	3.0	90	68.7
					3	0.25	0.20	9.3	0.001	0.03	3.0	158	75.9
36	0.13	43.7	0.68	3.87	1	0.55	0.09	8.8	0.003	0.06	3.0	113	69.3
					2	7.30	0.03	38.7	0.522	2.27	2.0	158	68.7
					3	1.80	0.05	24.2	0.035	0.21	1.0	158	73.2
37	0.21	68.3	0.91	3.91	1	0.75	0.19	26.4	0.021	0.12	1.0	113	41.8
					2	1.30	0.10	35.8	0.054	0.22	1.0	0	36.2
					3	0.40	0.18	15.4	0.003	0.03	1.0	135	34.7
38	0.30	109.0	1.97	5.72	1	2.00	0.20	84.9	0.499	0.90	1.0	135	69.3
					2	1.20	0.18	42.9	0.124	0.49	2.5	0	74.5
					3	2.20	0.08	31.2	0.146	0.78	3.0	135	70.1
39	0.13	62.1	1.23	4.93	1	5.90	0.06	64.6	0.982	2.31	1.0	113	70.1
					2	1.70	0.07	30.6	0.053	0.25	1.0	158	75.5
					3	2.30	0.05	20.7	0.065	0.53	3.0	158	71.9
40	0.93	137.6	2.75	6.59	1	0.55	0.28	36.0	0.027	0.13	1.5	0	111.9
					2	2.90	0.14	96.7	0.897	1.37	1.0	158	109.9
					3	0.55	0.26	28.8	0.019	0.11	1.5	135	114.0

\* Energy is defined as the integral of the velocity time history squared

\*\* Area is defined as the integral of the absolute value of the velocity time history

Record #	Ground Motion Record				Pulse #	CPE <sub>A-AM</sub>							
	$a_{max}$ (g)	$v_{max}$ (cm/s)	energy*	area**		$T_p$ (s)	$a_{max}$ (g)	$v_{max}$ (cm/s)	energy*	area**	$\gamma$	$\theta$ (°)	$l$ (s)
1	0.73	117.8	1.18	2.80	1	0.25	0.40	16.3	0.002	0.023	1.0	113	37.0
					2	1.60	0.33	98.2	0.611	0.943	1.0	113	37.2
					3	0.30	0.29	15.0	0.003	0.025	1.0	113	38.0
2	0.18	54.5	0.46	2.45	1	0.40	0.13	7.9	0.001	0.023	1.0	90	27.1
					2	0.55	0.13	15.6	0.005	0.045	1.0	45	26.6
					3	0.40	0.12	9.1	0.001	0.022	1.0	113	27.3
3	0.38	115.0	0.94	2.69	1	0.80	0.32	55.2	0.084	0.233	1.0	45	25.2
					2	2.20	0.17	70.0	0.430	0.932	1.0	113	24.4
					3	0.85	0.14	25.7	0.019	0.116	1.0	45	25.8
4	0.36	77.9	0.95	3.08	1	0.30	0.23	15.0	0.002	0.024	1.0	45	24.9
					2	1.40	0.16	41.7	0.097	0.353	1.0	68	24.6
					3	0.40	0.14	8.6	0.002	0.025	1.0	90	25.8
5	0.38	91.5	1.22	3.45	1	0.40	0.40	24.2	0.013	0.071	1.0	90	25.3
					2	1.00	0.22	40.2	0.064	0.243	1.0	68	26.1
					3	0.35	0.16	10.5	0.002	0.022	1.0	113	25.2
6	0.44	111.9	1.52	3.48	1	0.55	0.27	32.4	0.020	0.094	1.0	45	25.2
					2	0.35	0.21	13.9	0.003	0.029	1.0	68	25.9
					3	0.25	0.21	8.0	0.001	0.015	1.0	90	25.0
7	0.46	108.8	1.03	2.75	1	0.60	0.37	33.9	0.038	0.149	1.0	90	23.4
					2	0.60	0.34	44.5	0.041	0.141	1.0	45	24.0
					3	1.00	0.15	27.3	0.030	0.165	1.0	68	24.8
8	0.47	48.6	0.43	2.26	1	0.30	0.25	11.3	0.002	0.025	1.0	90	25.4
					2	0.45	0.24	16.6	0.007	0.055	1.0	90	24.2
					3	0.30	0.20	8.9	0.001	0.019	1.0	90	25.1
9	0.42	59.6	0.48	2.54	1	0.30	0.37	16.9	0.005	0.037	1.0	90	26.4
					2	0.30	0.27	15.1	0.003	0.027	1.0	113	25.7
					3	0.50	0.24	18.5	0.009	0.068	1.0	90	26.0
10	1.43	116.5	0.98	2.66	1	0.30	0.75	48.6	0.025	0.077	1.0	45	27.9
					2	0.35	0.66	34.3	0.022	0.086	1.0	90	28.1
					3	0.30	0.63	29.0	0.014	0.064	1.0	90	27.0
11	0.42	106.8	1.29	3.44	1	0.70	0.34	36.3	0.051	0.187	1.0	90	17.5
					2	1.40	0.33	84.6	0.398	0.714	1.0	68	18.5
					3	0.80	0.28	33.5	0.049	0.195	1.0	90	19.3
12	0.39	104.5	1.22	3.19	1	1.10	0.32	75.4	0.213	0.432	1.0	45	15.4
					2	0.80	0.27	38.8	0.047	0.185	1.0	68	17.1
					3	0.35	0.26	13.2	0.003	0.033	1.0	90	16.9
13	0.52	67.3	0.79	2.65	1	0.40	0.37	27.7	0.012	0.066	1.0	68	19.9
					2	0.40	0.36	26.4	0.011	0.063	1.0	68	19.5
					3	0.30	0.28	15.4	0.003	0.028	1.0	113	20.7
14	0.72	120.9	0.87	2.83	1	0.60	0.83	88.5	0.179	0.308	1.0	68	25.5
					2	0.25	0.48	19.6	0.004	0.028	1.0	68	25.7
					3	0.50	0.44	40.6	0.033	0.122	1.0	113	27.3

Appendix A1 – Parameters of the three extracted pulses from each of the six CPE methods

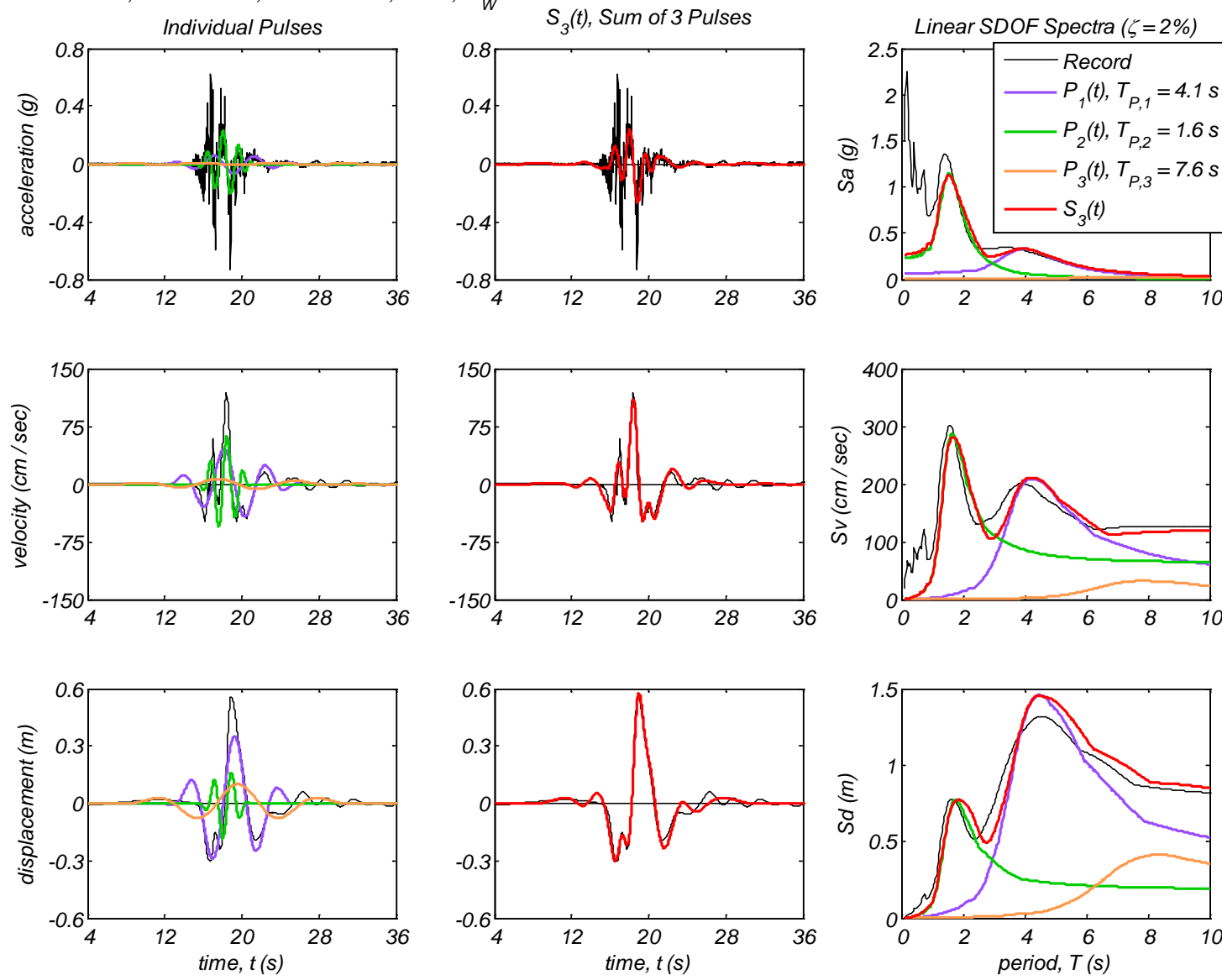
CPE<sub>A-AM</sub>

Record #	Ground Motion Record				Pulse #	CPE <sub>A-AM</sub>							
	$a_{max}$ (g)	$v_{max}$ (cm/s)	energy*	area**		$T_P$ (s)	$a_{max}$ (g)	$v_{max}$ (cm/s)	energy*	area**	$\gamma$	$\theta$ (°)	$l$ (s)
15	0.43	87.7	0.90	2.42	1	1.40	0.33	86.1	0.412	0.726	1.0	113	16.5
					2	0.30	0.13	6.0	0.001	0.013	1.0	90	16.6
					3	0.75	0.13	18.2	0.010	0.082	1.0	113	17.0
16	0.41	53.2	0.51	2.58	1	0.45	0.39	26.4	0.017	0.087	1.0	90	19.2
					2	0.45	0.37	30.9	0.017	0.084	1.0	68	20.9
					3	0.55	0.32	32.6	0.023	0.107	1.0	113	21.5
17	0.89	173.1	1.25	2.51	1	0.75	0.92	128.1	0.491	0.582	1.0	68	9.6
					2	0.30	0.56	25.5	0.011	0.056	1.0	90	10.6
					3	0.35	0.39	29.6	0.011	0.055	1.0	135	11.5
18	0.59	130.3	1.99	4.98	1	0.85	0.54	85.1	0.246	0.438	1.0	68	24.5
					2	1.00	0.44	82.1	0.268	0.495	1.0	113	25.9
					3	0.50	0.32	29.3	0.017	0.088	1.0	113	26.2
19	0.84	116.5	0.83	2.80	1	0.30	0.75	41.4	0.020	0.074	1.0	68	24.6
					2	0.35	0.51	33.0	0.015	0.070	1.0	68	26.3
					3	0.25	0.30	16.5	0.002	0.022	1.0	45	25.1
20	0.73	123.1	1.01	2.77	1	0.35	0.57	35.6	0.017	0.072	1.0	68	24.8
					2	0.40	0.44	26.0	0.015	0.075	1.0	90	25.0
					3	0.30	0.37	19.1	0.004	0.033	1.0	68	26.8
21	1.33	65.4	0.69	2.96	1	0.35	0.75	38.2	0.028	0.095	1.0	90	26.9
					2	0.30	0.68	40.8	0.016	0.061	1.0	135	25.2
					3	0.30	0.67	34.7	0.013	0.059	1.0	113	28.3
22	0.65	102.3	1.23	3.20	1	0.45	0.55	37.4	0.035	0.124	1.0	90	20.4
					2	0.65	0.49	59.8	0.093	0.235	1.0	68	19.4
					3	0.50	0.47	43.7	0.038	0.131	1.0	68	19.1
23	0.68	169.5	3.17	5.97	1	1.20	0.72	161.0	1.234	1.163	1.0	113	26.0
					2	1.00	0.49	74.2	0.304	0.542	1.0	90	24.8
					3	0.35	0.41	25.9	0.009	0.053	1.0	68	25.7
24	0.35	61.4	1.10	3.99	1	0.50	0.41	37.8	0.028	0.114	1.0	68	17.1
					2	0.40	0.36	21.7	0.010	0.063	1.0	90	16.6
					3	0.35	0.28	15.1	0.004	0.039	1.0	90	20.6
25	0.77	92.6	1.56	4.33	1	0.25	0.29	16.0	0.002	0.021	1.0	135	32.7
					2	0.25	0.28	12.8	0.002	0.019	1.0	68	33.0
					3	0.25	0.27	10.4	0.001	0.019	1.0	90	33.3
26	0.24	56.5	0.61	2.94	1	1.00	0.19	35.2	0.049	0.213	1.0	113	33.1
					2	0.55	0.15	15.5	0.005	0.051	1.0	68	34.3
					3	0.60	0.11	12.1	0.003	0.042	1.0	68	33.8
27	0.85	121.4	3.41	7.26	1	0.30	0.77	39.9	0.018	0.068	1.0	68	24.1
					2	0.25	0.71	28.9	0.008	0.041	1.0	68	24.3
					3	0.30	0.45	23.4	0.006	0.040	1.0	68	24.0
28	0.24	51.1	0.47	2.33	1	0.35	0.18	11.4	0.002	0.024	1.0	113	19.4
					2	0.45	0.14	9.7	0.002	0.032	1.0	90	21.3
					3	0.35	0.11	6.1	0.001	0.016	1.0	90	21.6

Record #	Ground Motion Record				Pulse #	CPE <sub>A-AM</sub>							
	$a_{max}$ (g)	$v_{max}$ (cm/s)	energy* (m <sup>2</sup> /s)	area** (m)		$T_P$ (s)	$a_{max}$ (g)	$v_{max}$ (cm/s)	energy* (m <sup>2</sup> /s)	area** (m)	$\gamma$	$\theta$ (°)	$l$ (s)
29	0.27	48.7	0.98	4.01	1	0.30	0.24	15.5	0.002	0.024	1.0	45	27.0
					2	0.60	0.21	23.5	0.013	0.085	1.0	113	25.7
					3	0.30	0.20	8.8	0.001	0.019	1.0	90	27.9
30	0.38	165.5	7.20	11.71	1	1.20	0.39	100.7	0.421	0.639	1.0	135	68.1
					2	2.60	0.17	81.0	0.680	1.274	1.0	113	68.0
					3	0.35	0.16	12.4	0.002	0.023	1.0	45	75.4
31	0.16	60.3	0.86	4.28	1	0.35	0.13	11.5	0.002	0.020	1.0	23	76.4
					2	0.45	0.13	8.8	0.002	0.029	1.0	90	69.4
					3	0.50	0.11	8.1	0.002	0.030	1.0	90	72.7
32	0.83	129.5	4.91	10.80	1	0.30	0.40	18.2	0.005	0.040	1.0	90	75.4
					2	0.75	0.33	38.0	0.060	0.210	1.0	90	65.0
					3	1.10	0.32	64.9	0.184	0.431	1.0	113	74.9
33	0.52	84.2	1.90	6.63	1	0.40	0.43	26.2	0.015	0.076	1.0	90	65.8
					2	0.45	0.36	39.8	0.024	0.088	1.0	158	67.0
					3	0.55	0.27	27.3	0.016	0.091	1.0	68	67.6
34	0.56	184.5	13.88	17.15	1	0.35	0.49	32.2	0.014	0.068	1.0	113	69.2
					2	1.00	0.29	62.5	0.135	0.330	1.0	135	69.2
					3	2.60	0.22	85.2	1.048	1.627	1.0	90	69.2
35	0.33	88.5	1.83	6.23	1	0.35	0.25	16.4	0.004	0.035	1.0	113	68.9
					2	0.25	0.24	9.0	0.001	0.017	1.0	90	76.0
					3	0.35	0.20	13.3	0.002	0.028	1.0	68	68.6
36	0.13	43.7	0.68	3.87	1	0.65	0.10	10.0	0.004	0.048	1.0	90	69.5
					2	0.30	0.10	5.6	0.000	0.010	1.0	68	68.9
					3	0.45	0.09	6.2	0.001	0.020	1.0	90	69.2
37	0.21	68.3	0.91	3.91	1	0.70	0.19	25.1	0.017	0.106	1.0	113	41.8
					2	0.35	0.19	12.3	0.002	0.026	1.0	113	34.7
					3	0.30	0.16	7.3	0.001	0.016	1.0	90	34.3
38	0.30	109.0	1.97	5.72	1	0.65	0.25	35.3	0.028	0.122	1.0	135	75.5
					2	1.30	0.22	43.3	0.135	0.413	1.0	90	69.4
					3	1.00	0.19	35.4	0.050	0.214	1.0	113	74.9
39	0.13	62.1	1.23	4.93	1	0.40	0.11	6.7	0.001	0.020	1.0	90	70.2
					2	0.40	0.11	9.4	0.001	0.020	1.0	135	70.5
					3	0.35	0.11	6.9	0.001	0.015	1.0	113	68.9
40	0.93	137.6	2.75	6.59	1	0.55	0.31	32.1	0.023	0.107	1.0	68	112.0
					2	0.30	0.30	16.3	0.003	0.029	1.0	68	116.0
					3	0.45	0.28	23.8	0.010	0.065	1.0	113	114.1

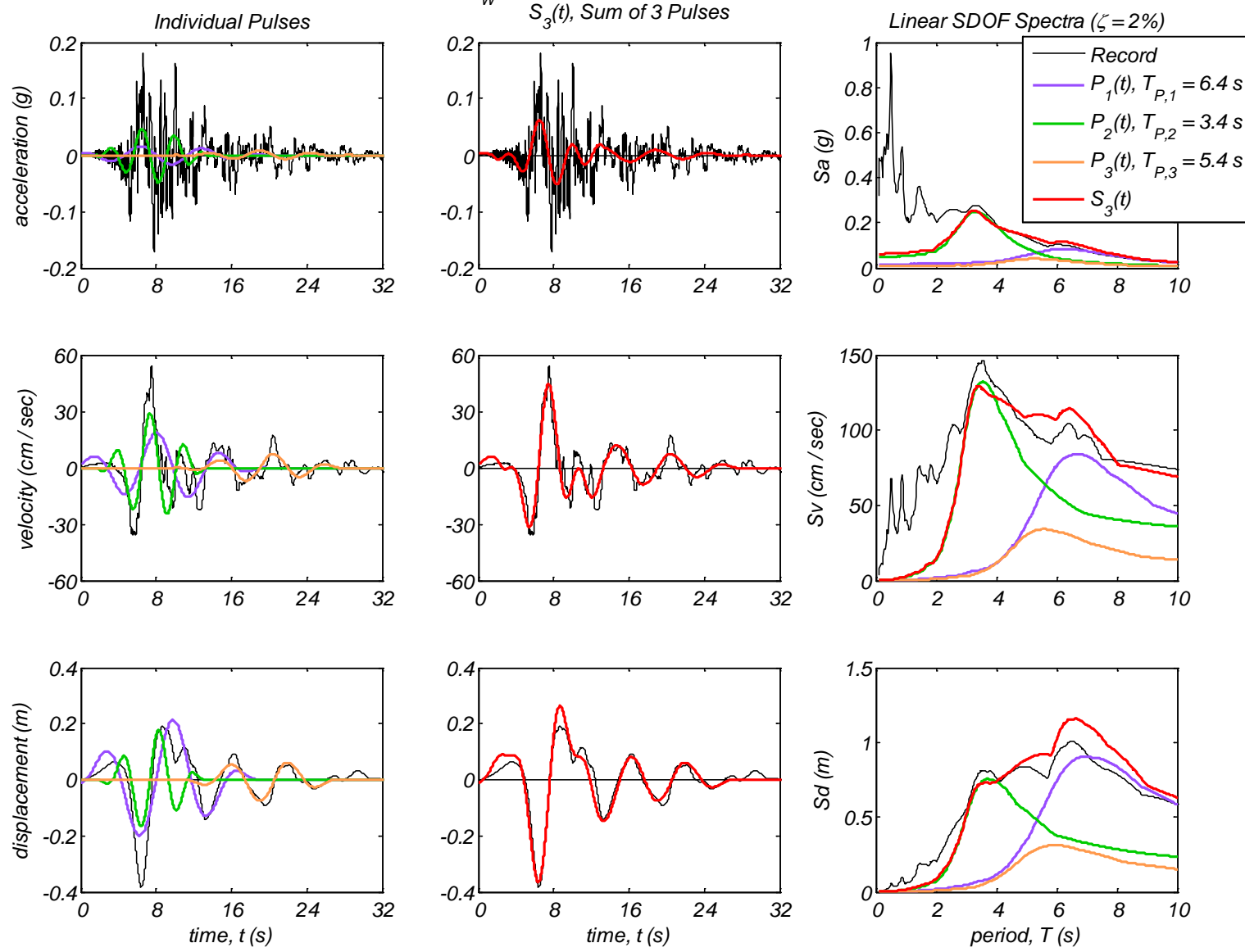
## Appendix B1: Time history and linear spectral response of three extracted pulses using the CPE<sub>V-AR</sub> method for 40 motions

Record #1: PRPC, Christchurch, New Zealand, 2011,  $M_W 6.3$

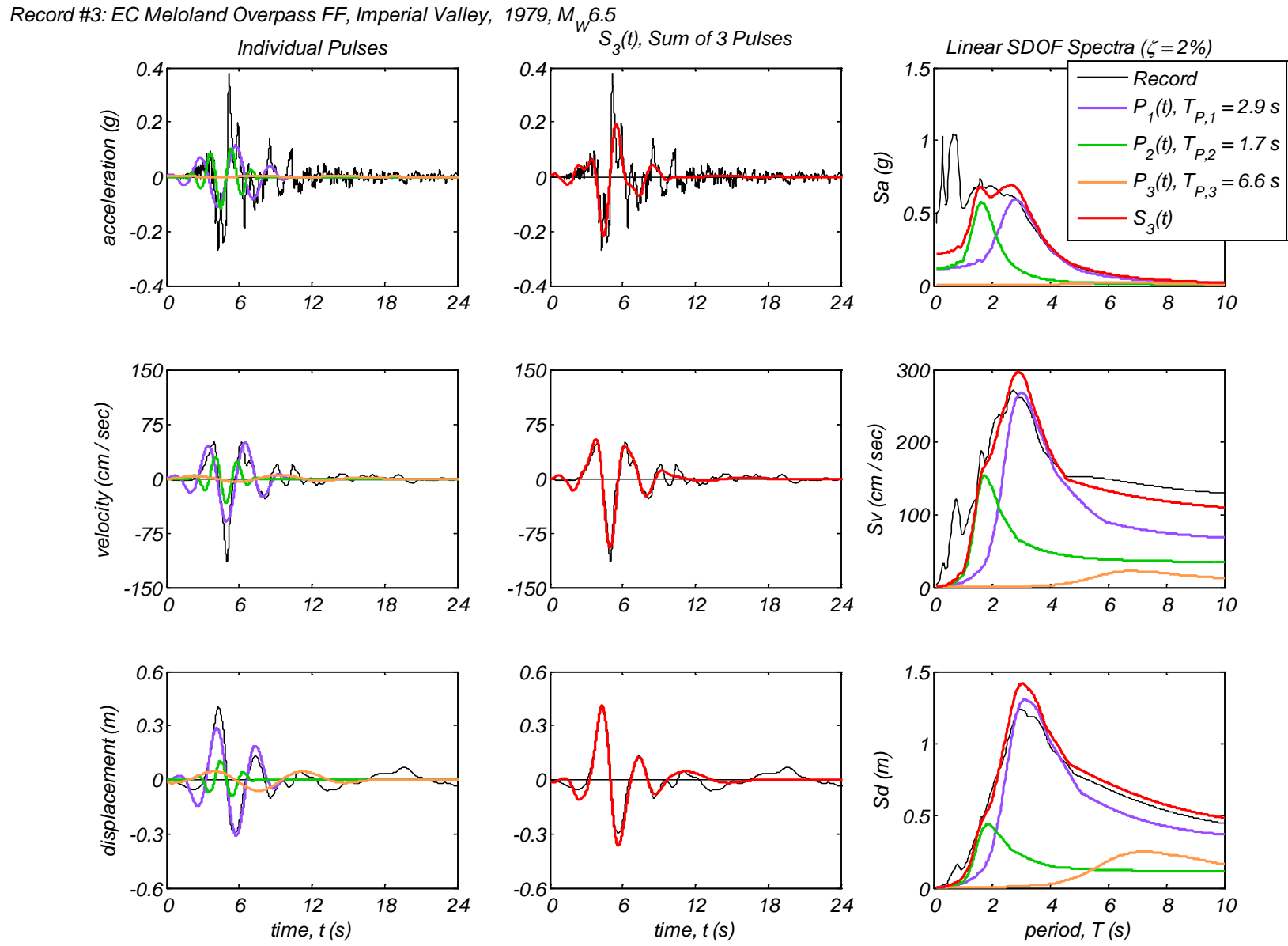


Appendix B1 – Time history and linear spectral response of three extracted pulses using the CPE<sub>V-AR</sub> method for 40 Motions

Record #2: EC County Center FF, Imperial Valley, 1979,  $M_W 6.5$



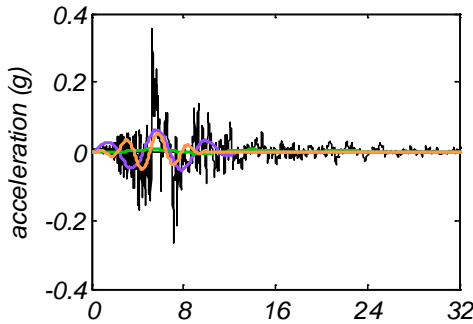
Appendix B1 – Time history and linear spectral response of three extracted pulses using the CPE<sub>V-AR</sub> method for 40 Motions



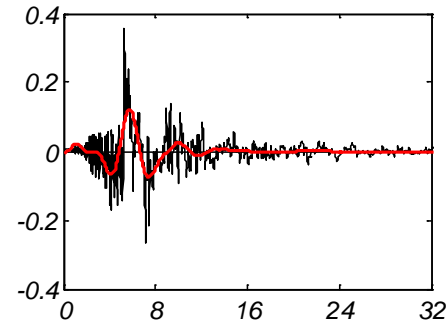
Appendix B1 – Time history and linear spectral response of three extracted pulses using the CPE<sub>V-AR</sub> method for 40 Motions

Record #4: El Centro Array #4, Imperial Valley, 1979,  $M_W 6.5$

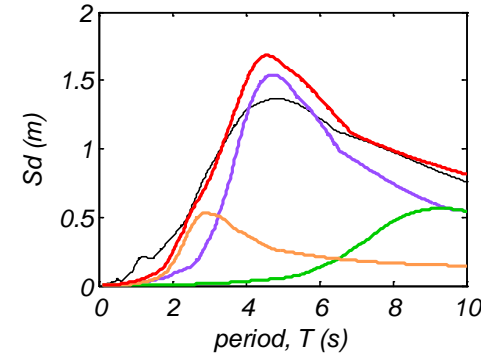
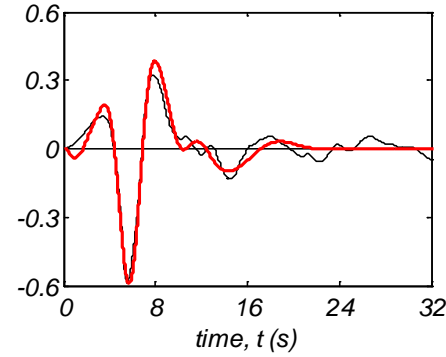
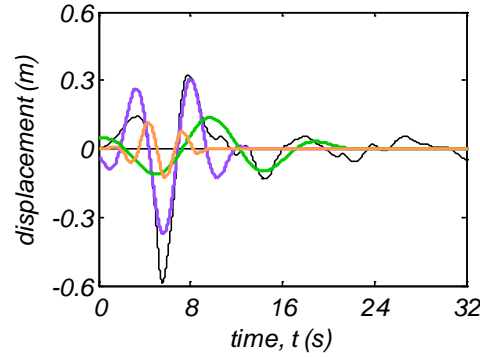
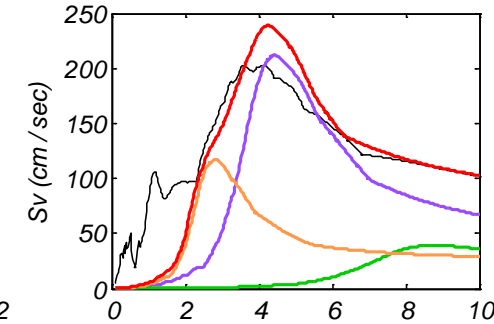
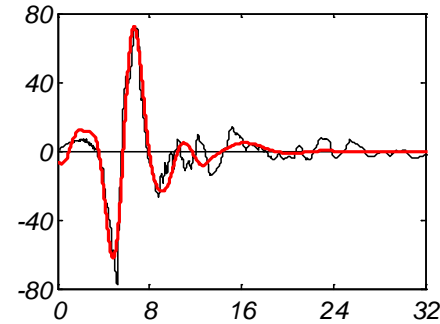
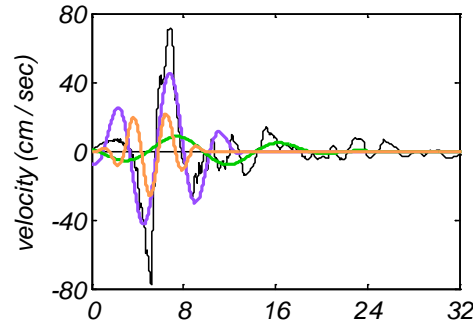
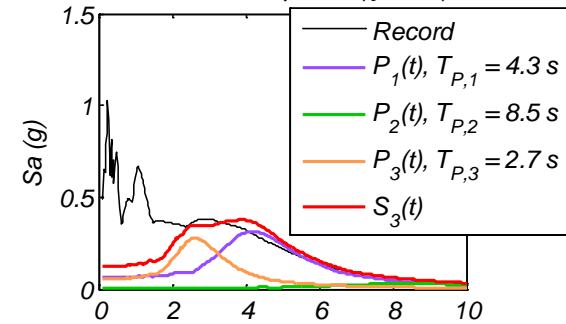
Individual Pulses



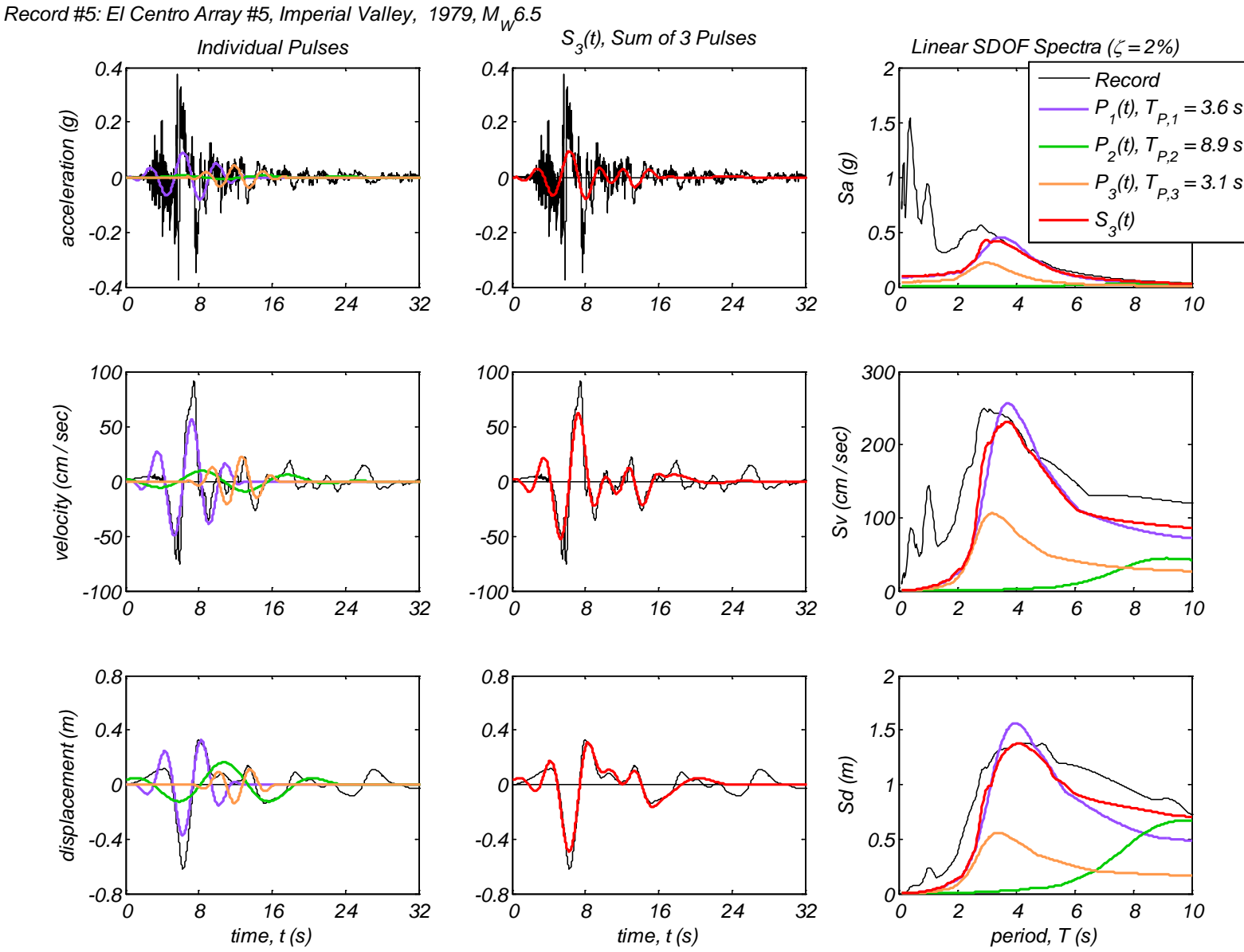
$S_3(t)$ , Sum of 3 Pulses



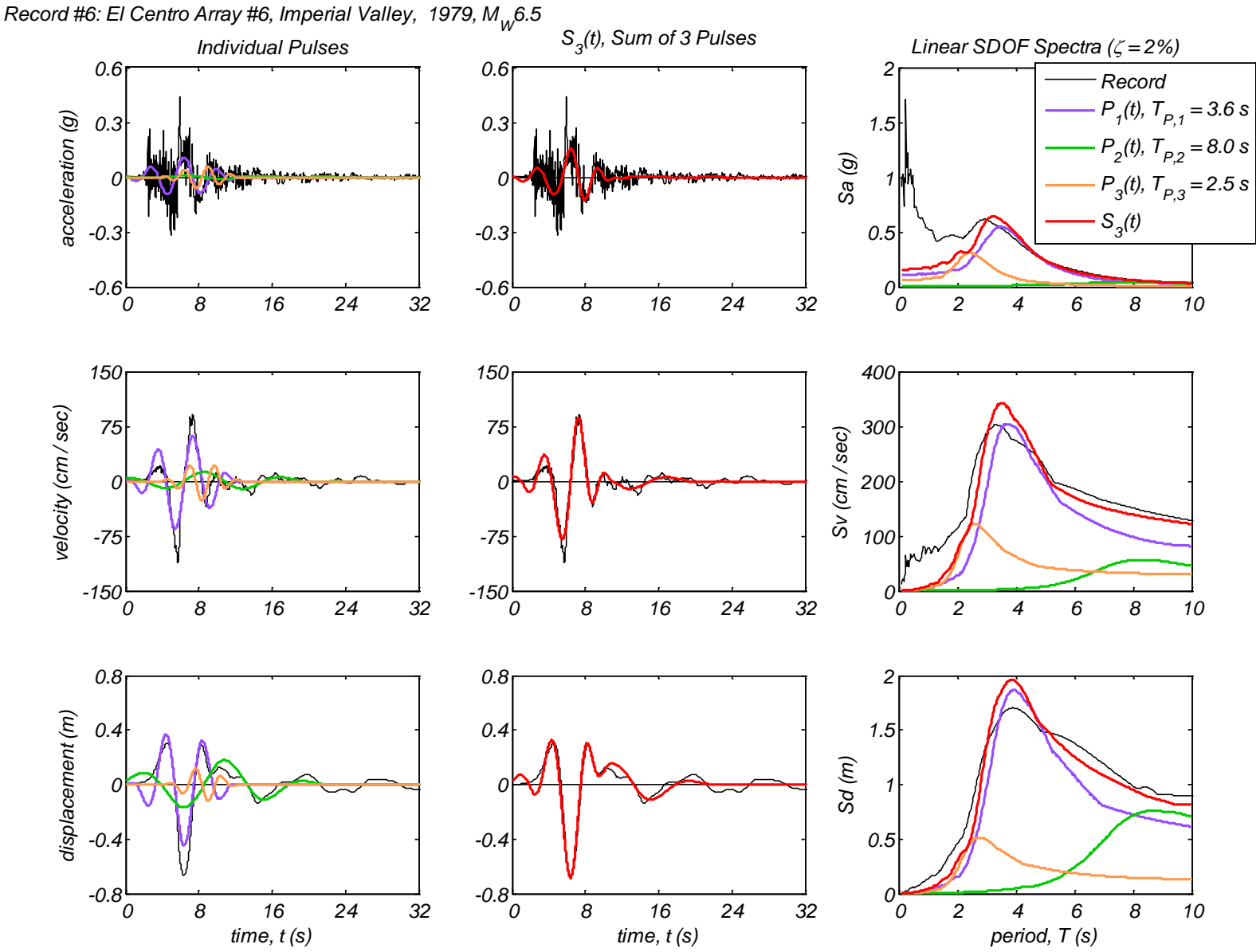
Linear SDOF Spectra ( $\zeta = 2\%$ )



Appendix B1 – Time history and linear spectral response of three extracted pulses using the CPE<sub>V-AR</sub> method for 40 Motions

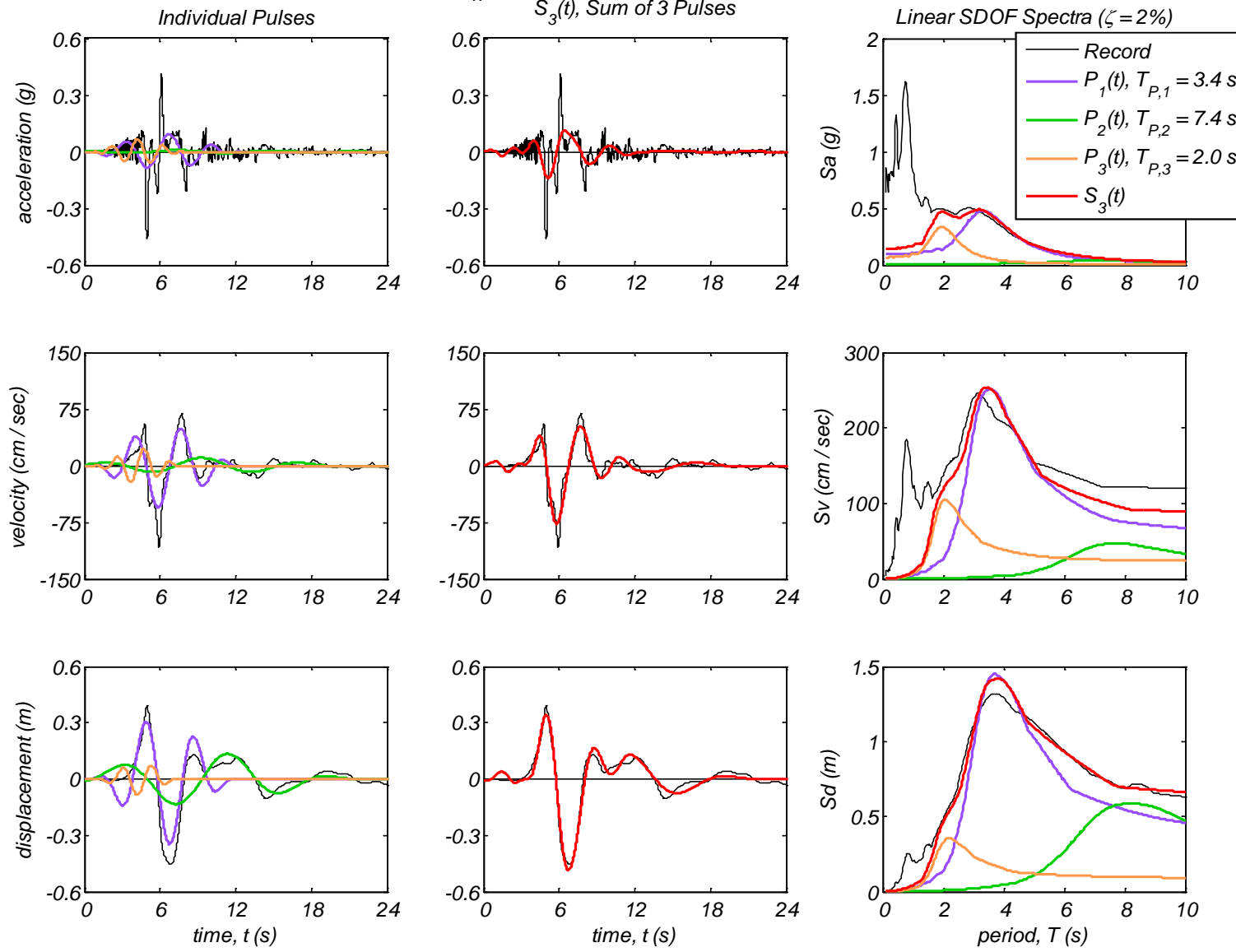


Appendix B1 – Time history and linear spectral response of three extracted pulses using the CPE<sub>V-AR</sub> method for 40 Motions

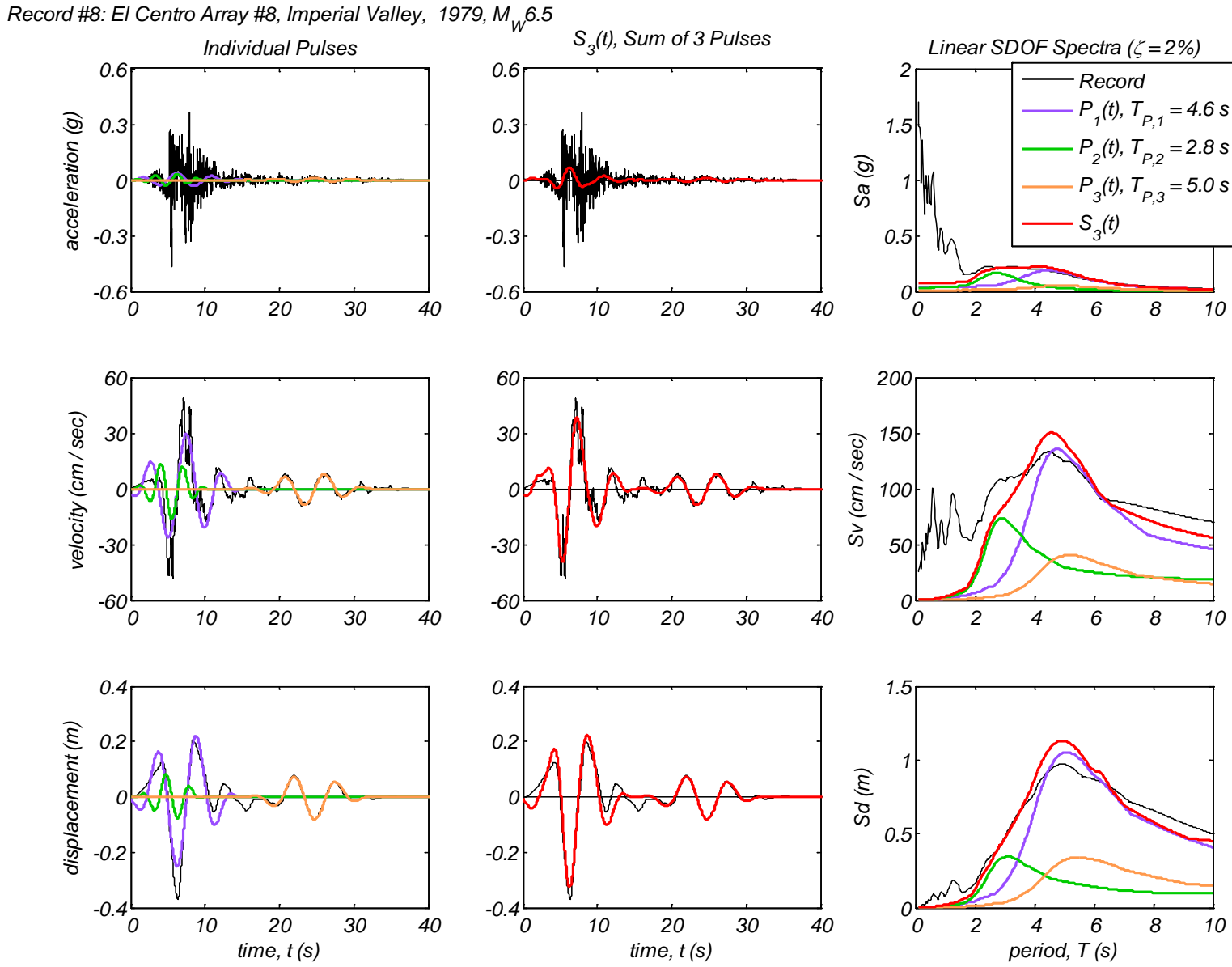


Appendix B1 – Time history and linear spectral response of three extracted pulses using the CPE<sub>V-AR</sub> method for 40 Motions

Record #7: El Centro Array #7, Imperial Valley, 1979,  $M_W 6.5$

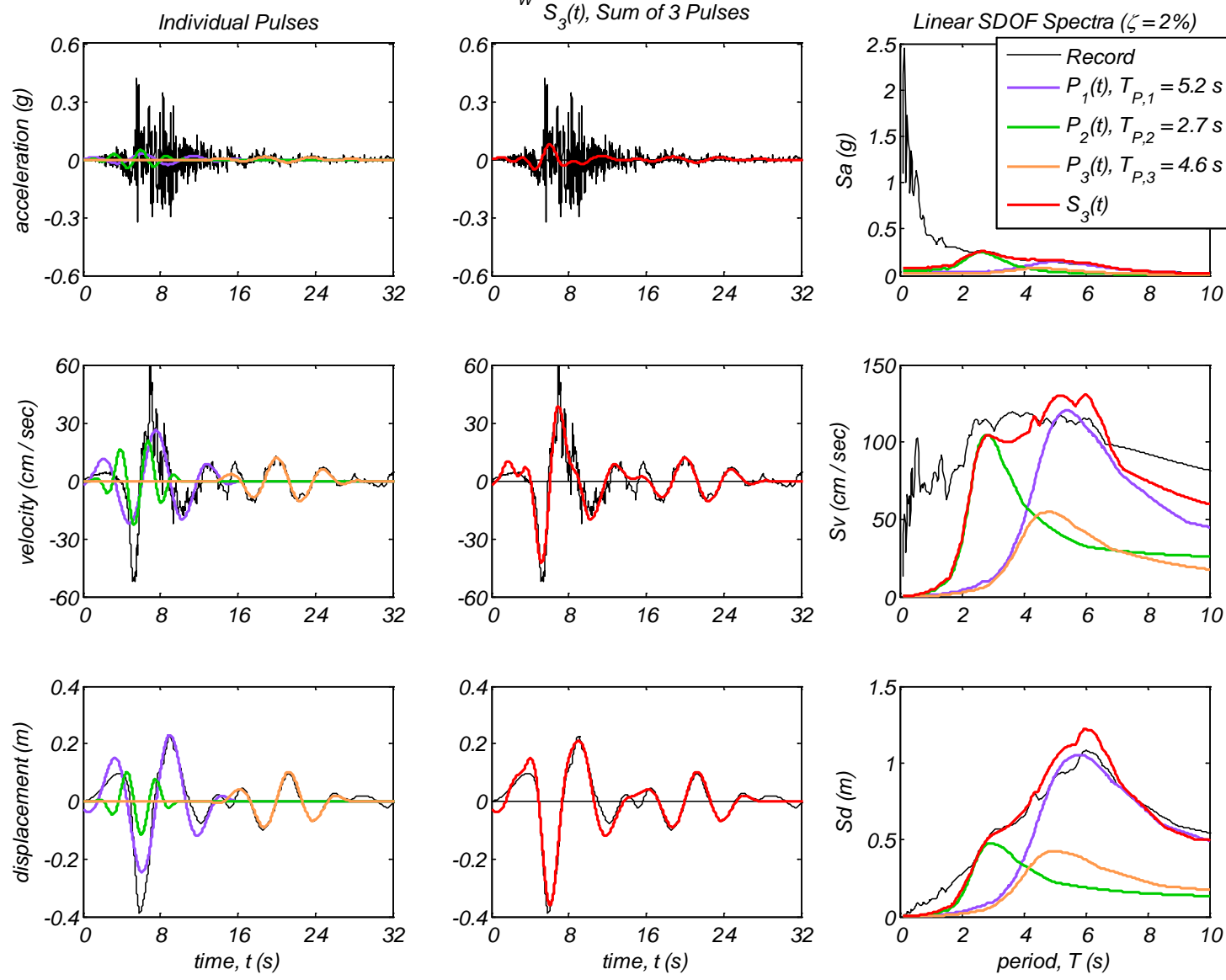


Appendix B1 – Time history and linear spectral response of three extracted pulses using the CPE<sub>V-AR</sub> method for 40 Motions

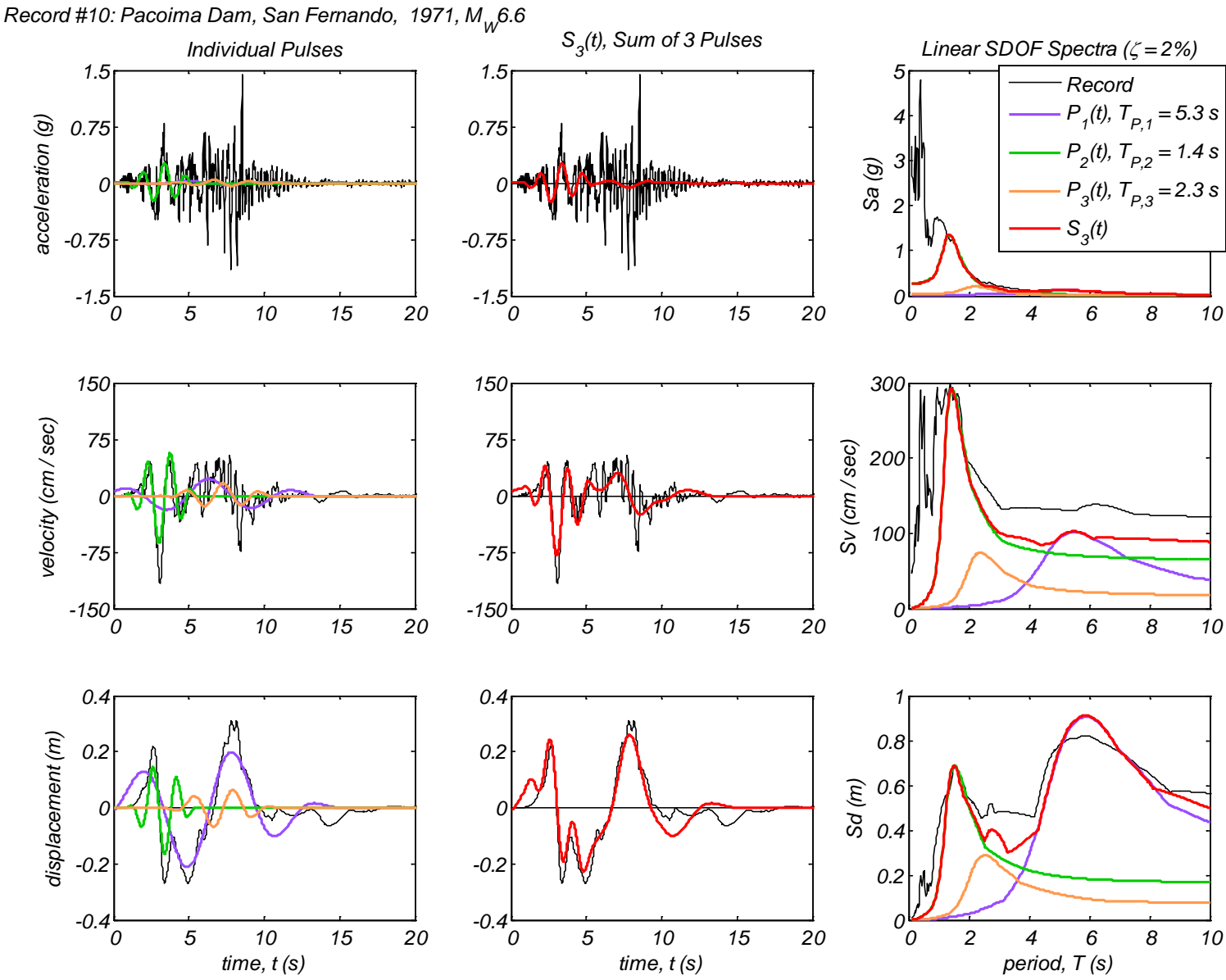


Appendix B1 – Time history and linear spectral response of three extracted pulses using the CPE<sub>V-AR</sub> method for 40 Motions

Record #9: El Centro Differential Array, Imperial Valley, 1979,  $M_W 6.5$

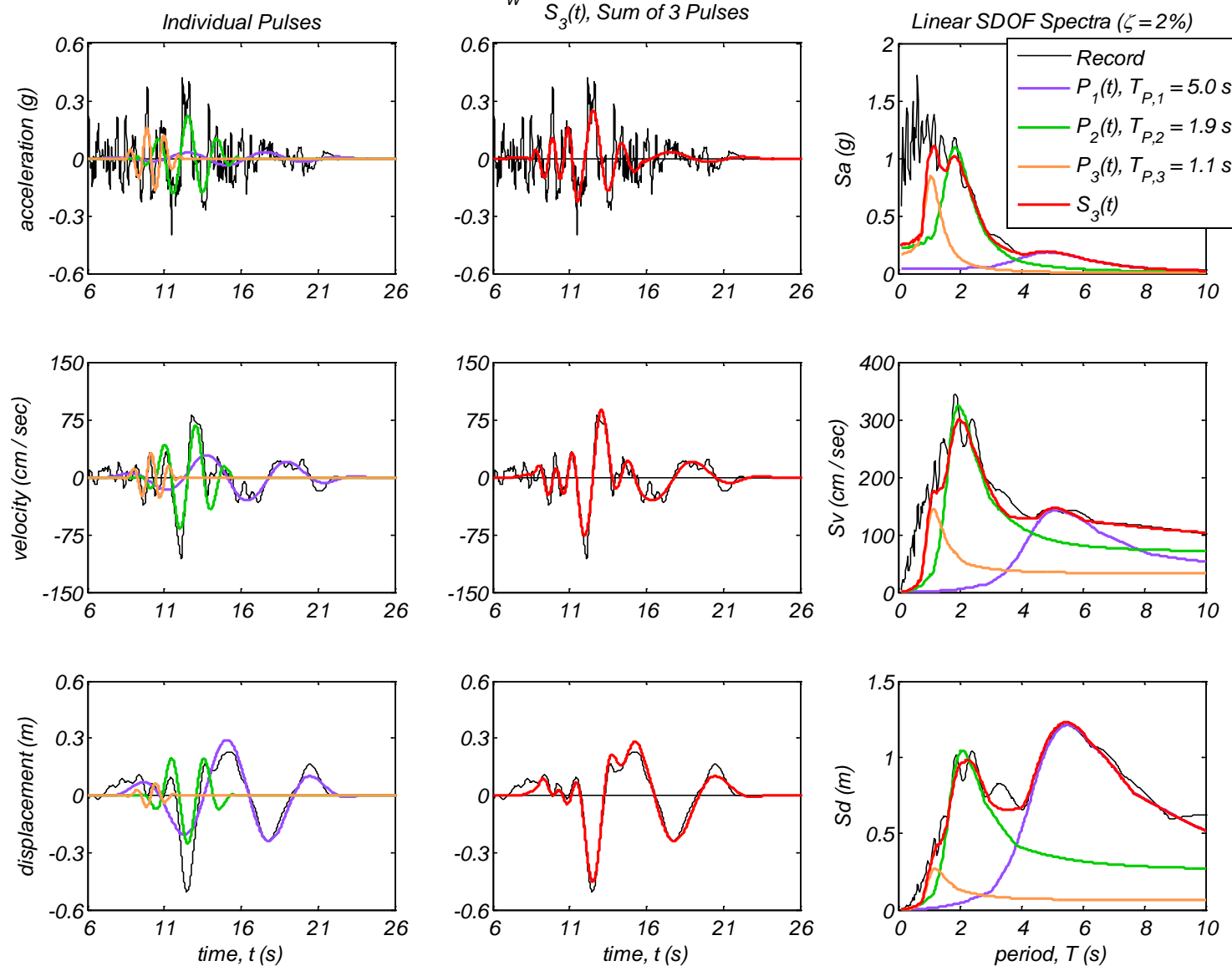


Appendix B1 – Time history and linear spectral response of three extracted pulses using the CPE<sub>V-AR</sub> method for 40 Motions

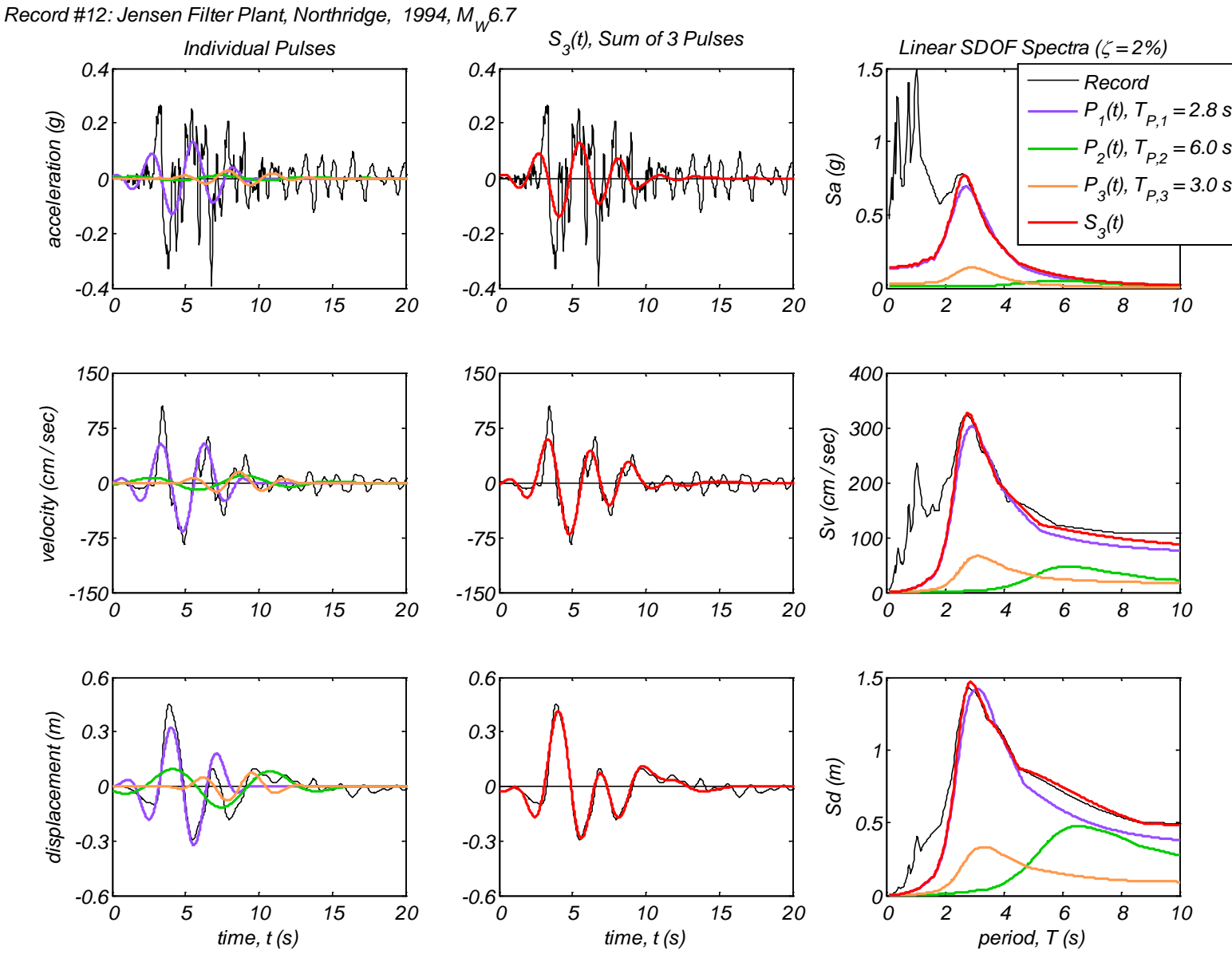


Appendix B1 – Time history and linear spectral response of three extracted pulses using the CPE<sub>V-AR</sub> method for 40 Motions

Record #11: Parachute Test Site, Superstition Hills(B), 1987,  $M_w 6.6$

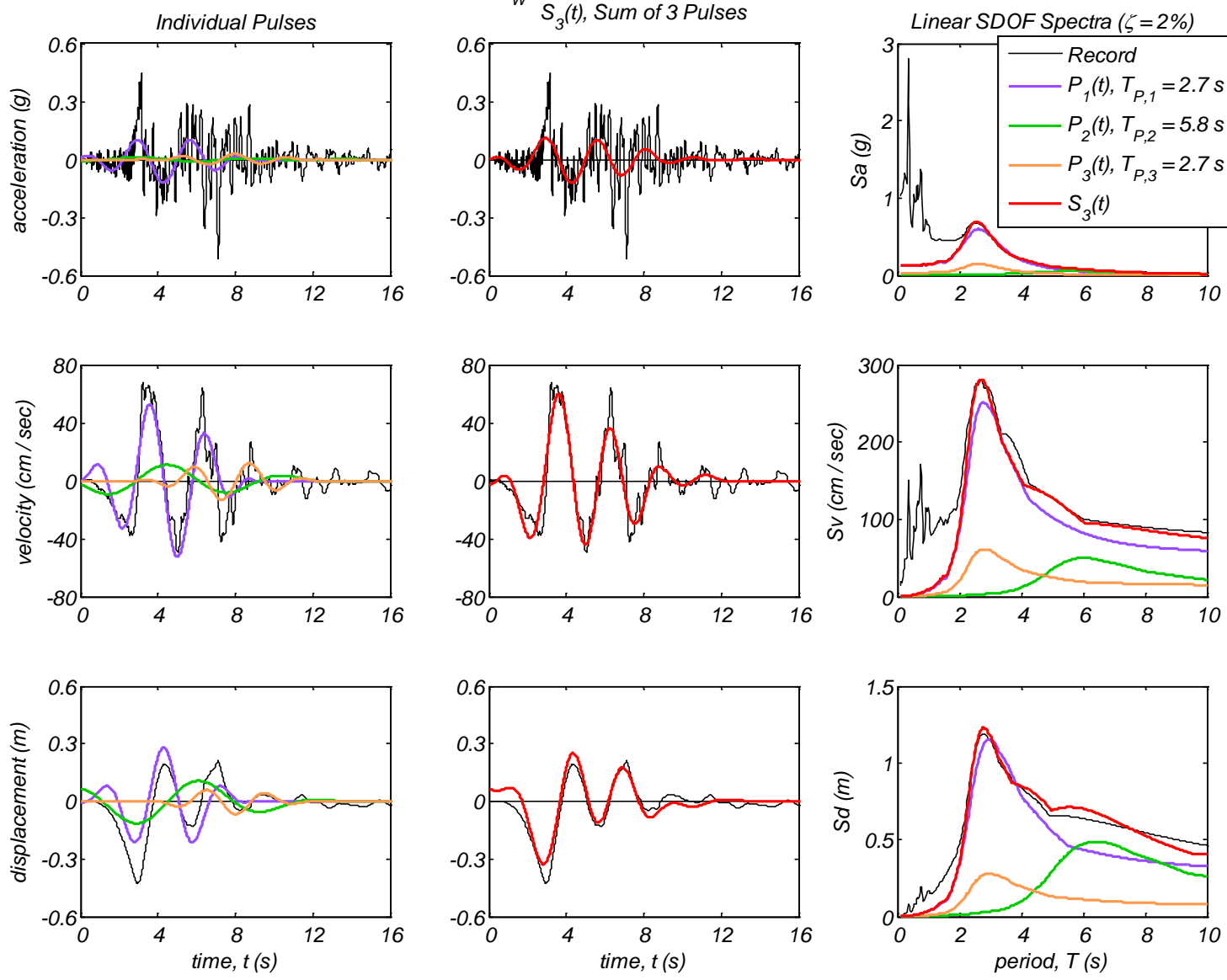


Appendix B1 – Time history and linear spectral response of three extracted pulses using the CPE<sub>V-AR</sub> method for 40 Motions

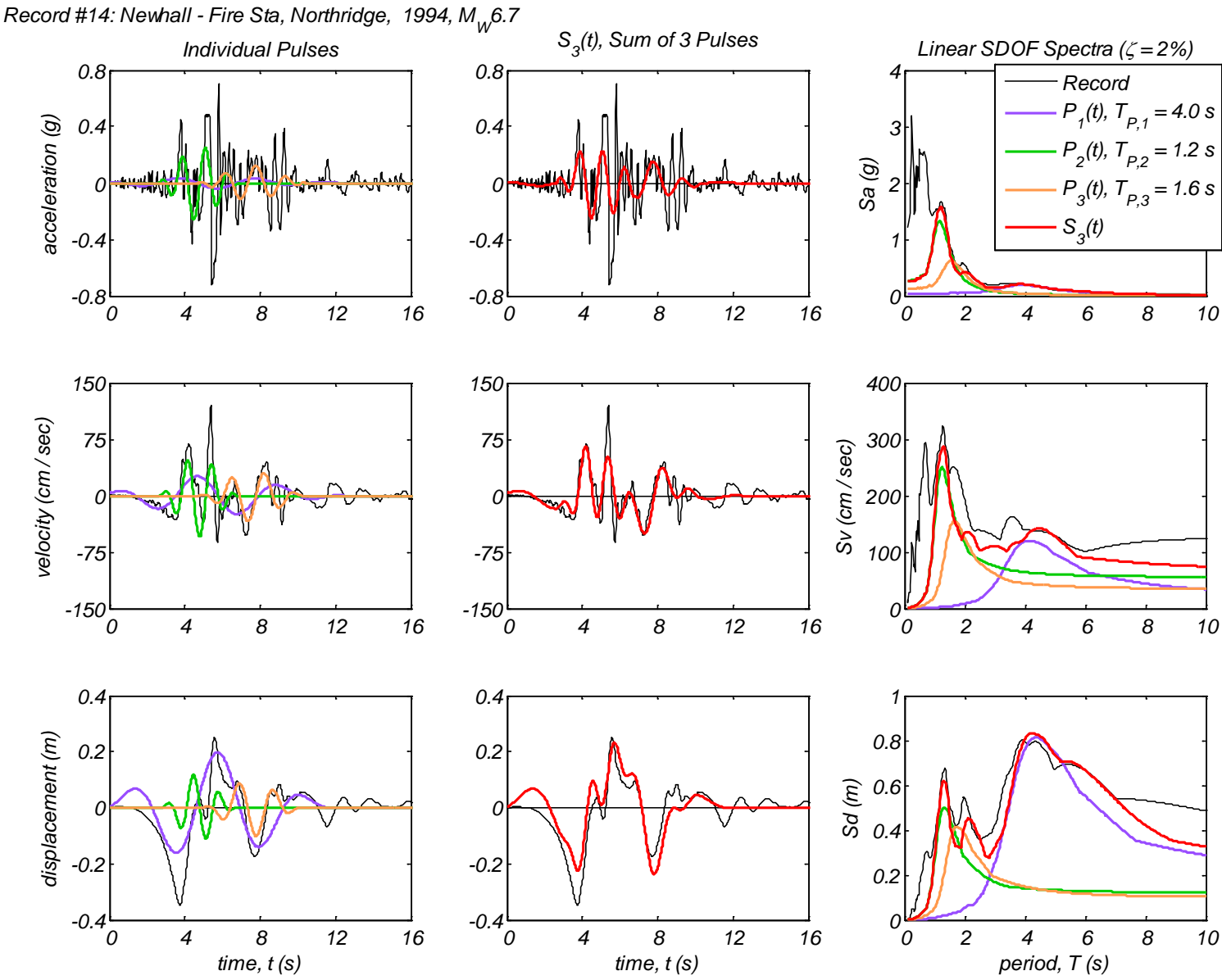


Appendix B1 – Time history and linear spectral response of three extracted pulses using the CPE<sub>V-AR</sub> method for 40 Motions

Record #13: Jensen Filter Plant Generator, Northridge, 1994,  $M_W 6.7$

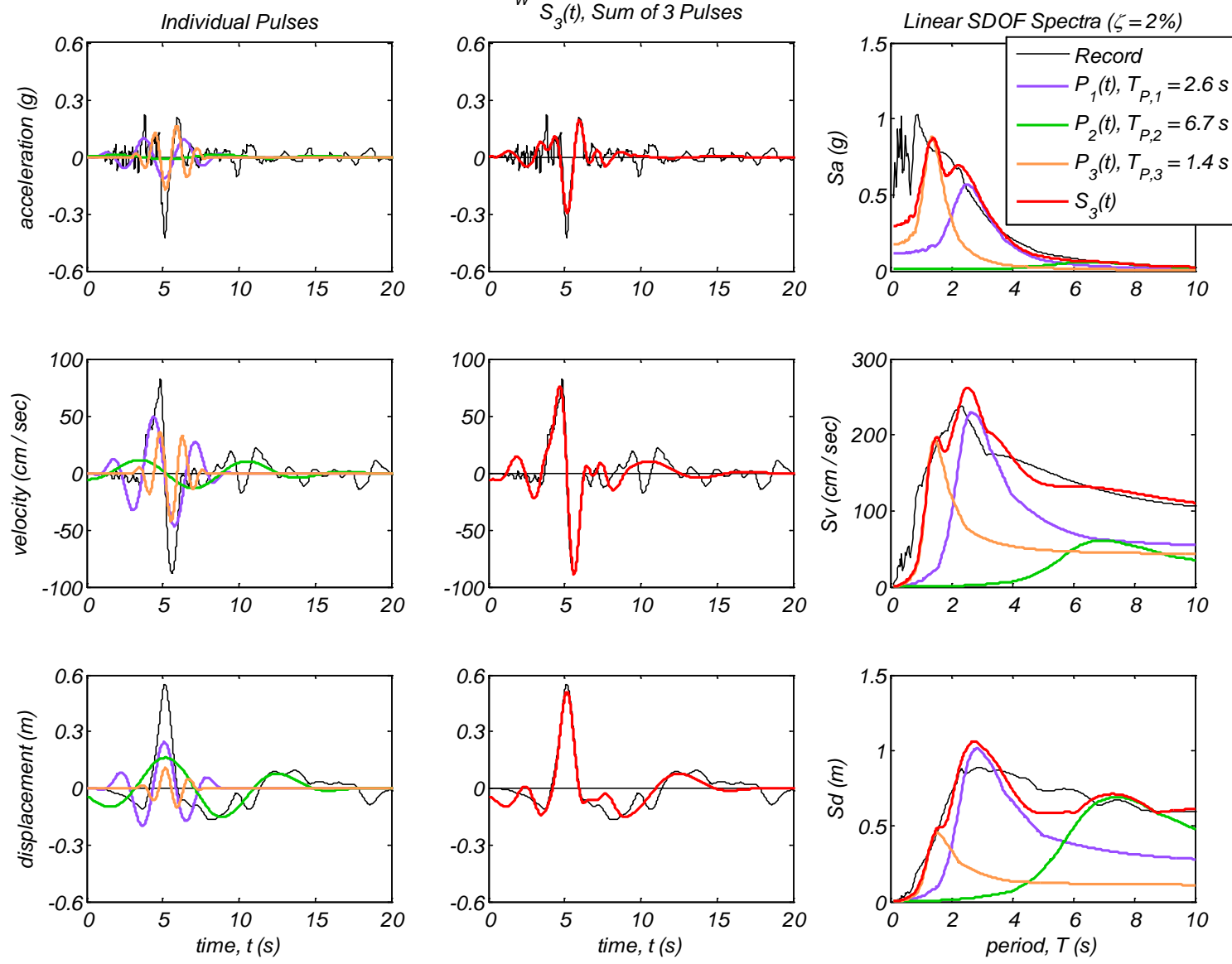


Appendix B1 – Time history and linear spectral response of three extracted pulses using the CPE<sub>V-AR</sub> method for 40 Motions

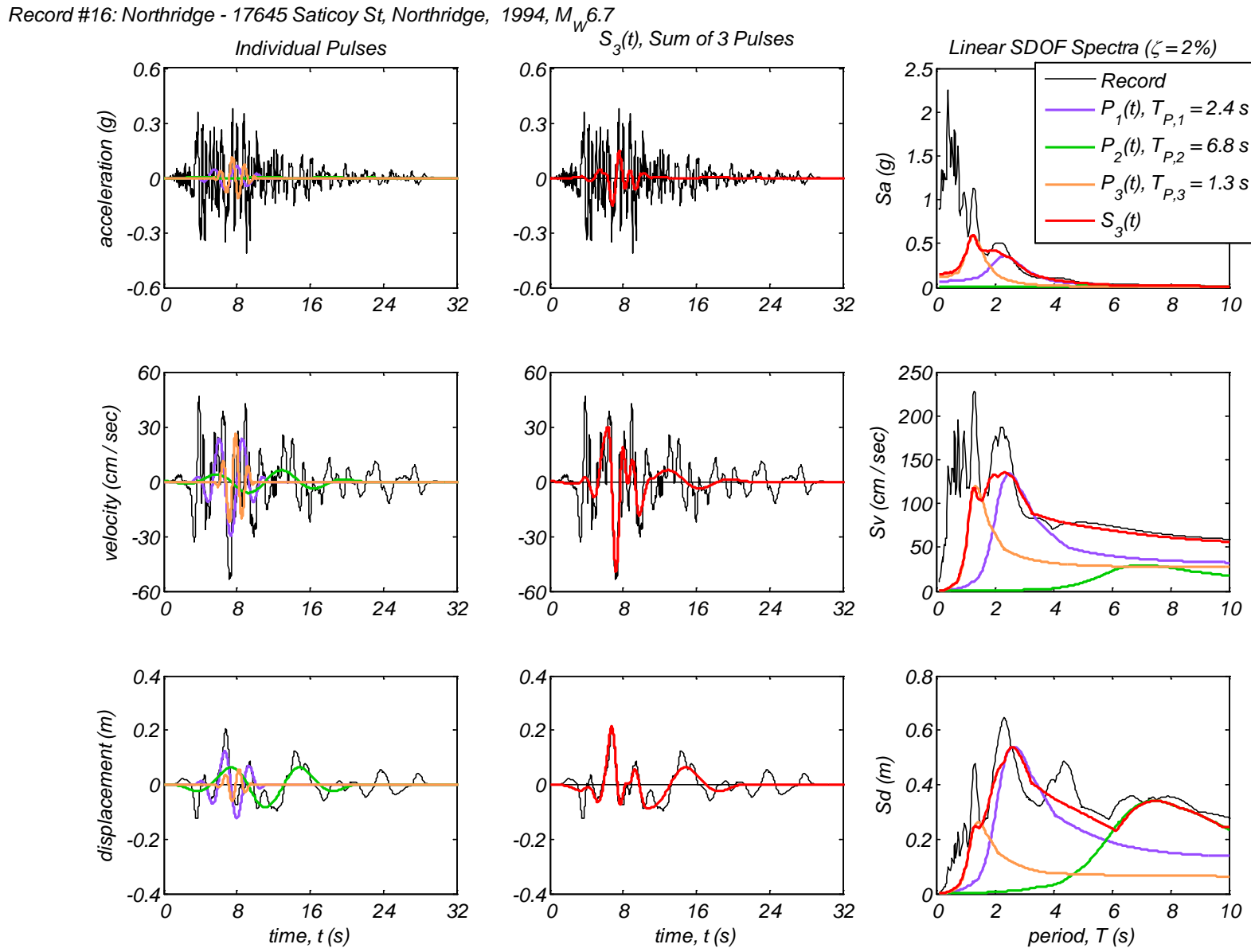


Appendix B1 – Time history and linear spectral response of three extracted pulses using the CPE<sub>V-AR</sub> method for 40 Motions

Record #15: Newhall - W. Pico Canyon Rd., Northridge, 1994,  $M_W$  6.7

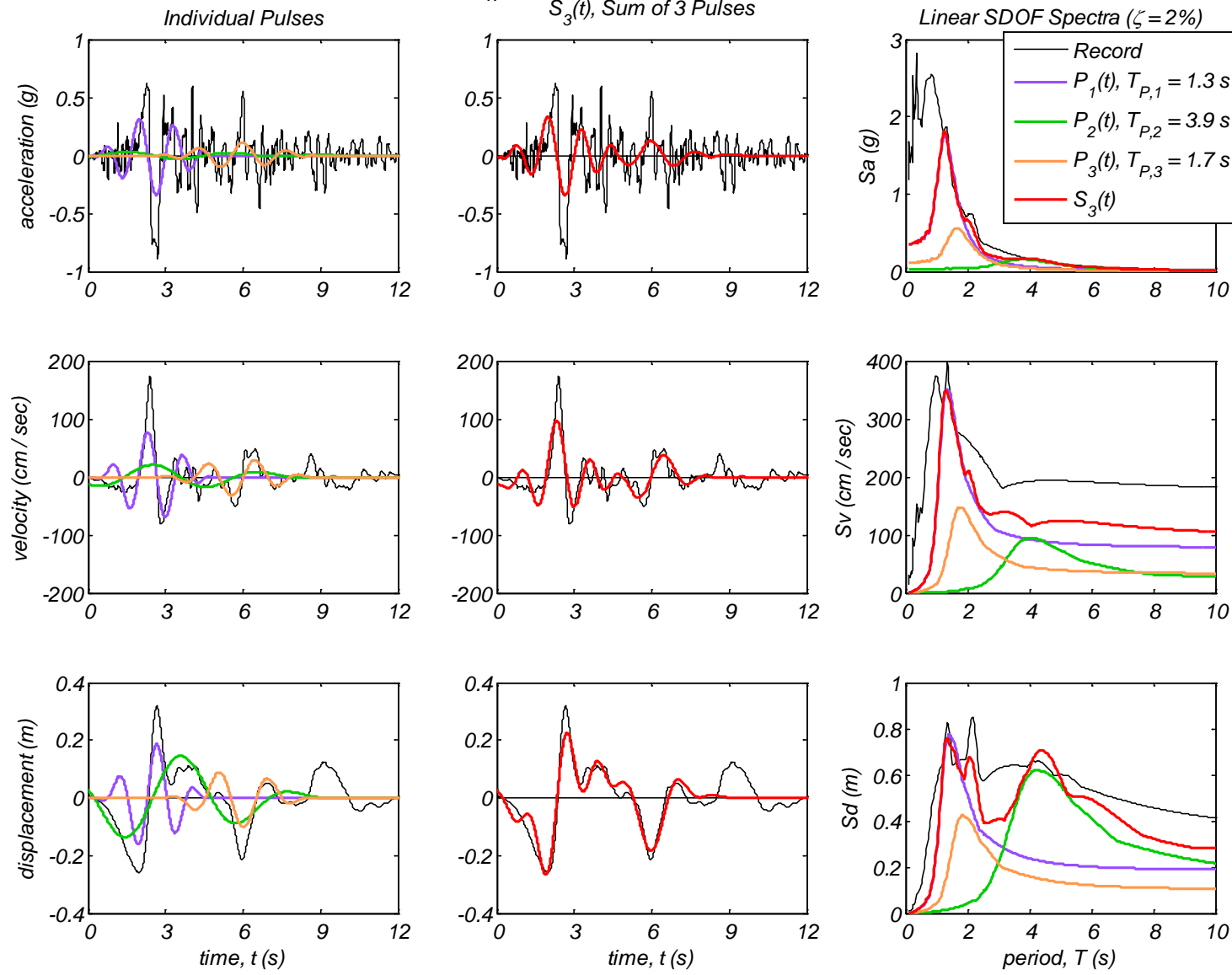


Appendix B1 – Time history and linear spectral response of three extracted pulses using the CPE<sub>V-AR</sub> method for 40 Motions

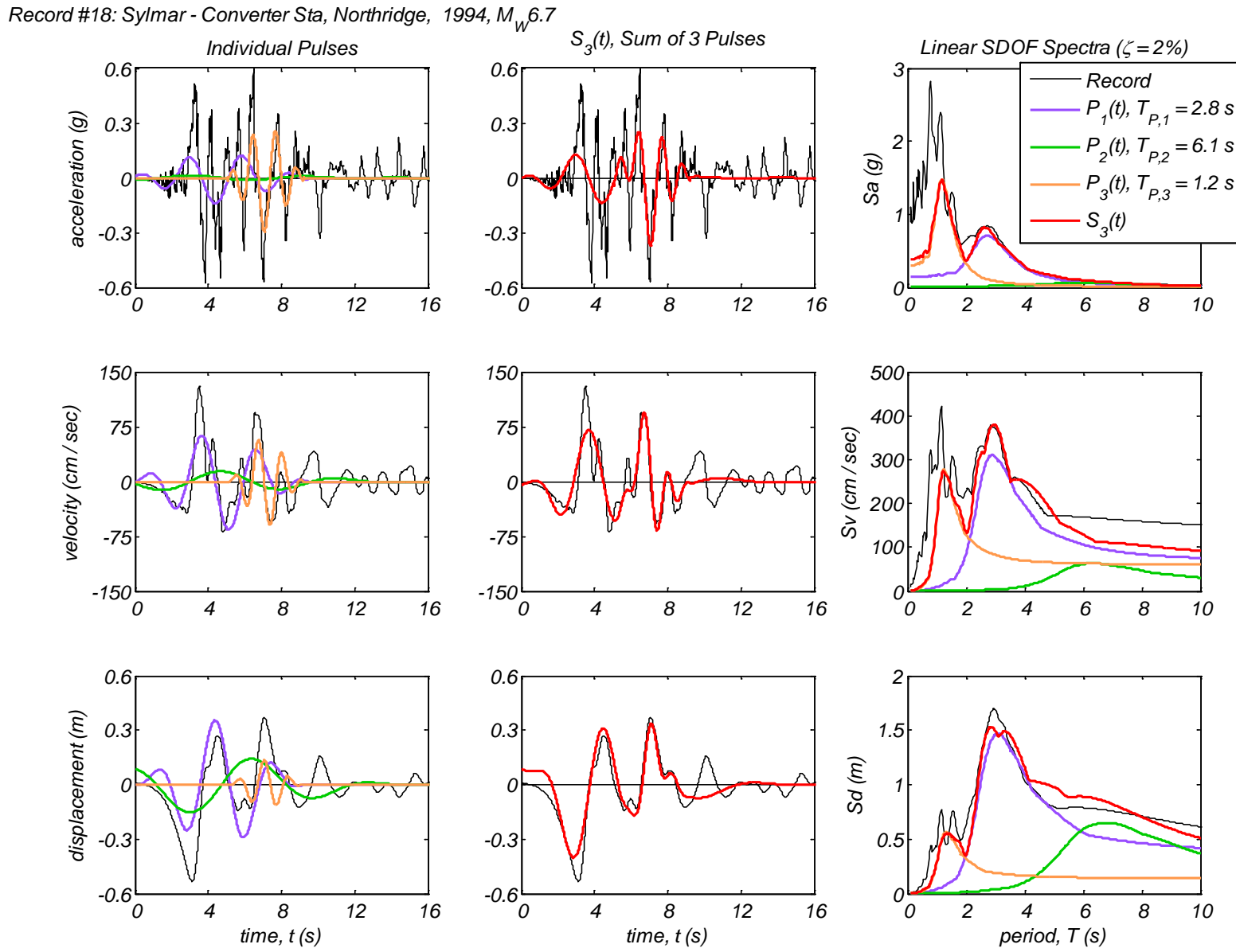


Appendix B1 – Time history and linear spectral response of three extracted pulses using the CPE<sub>V-AR</sub> method for 40 Motions

Record #17: Rinaldi Receiving Sta, Northridge, 1994,  $M_W 6.7$

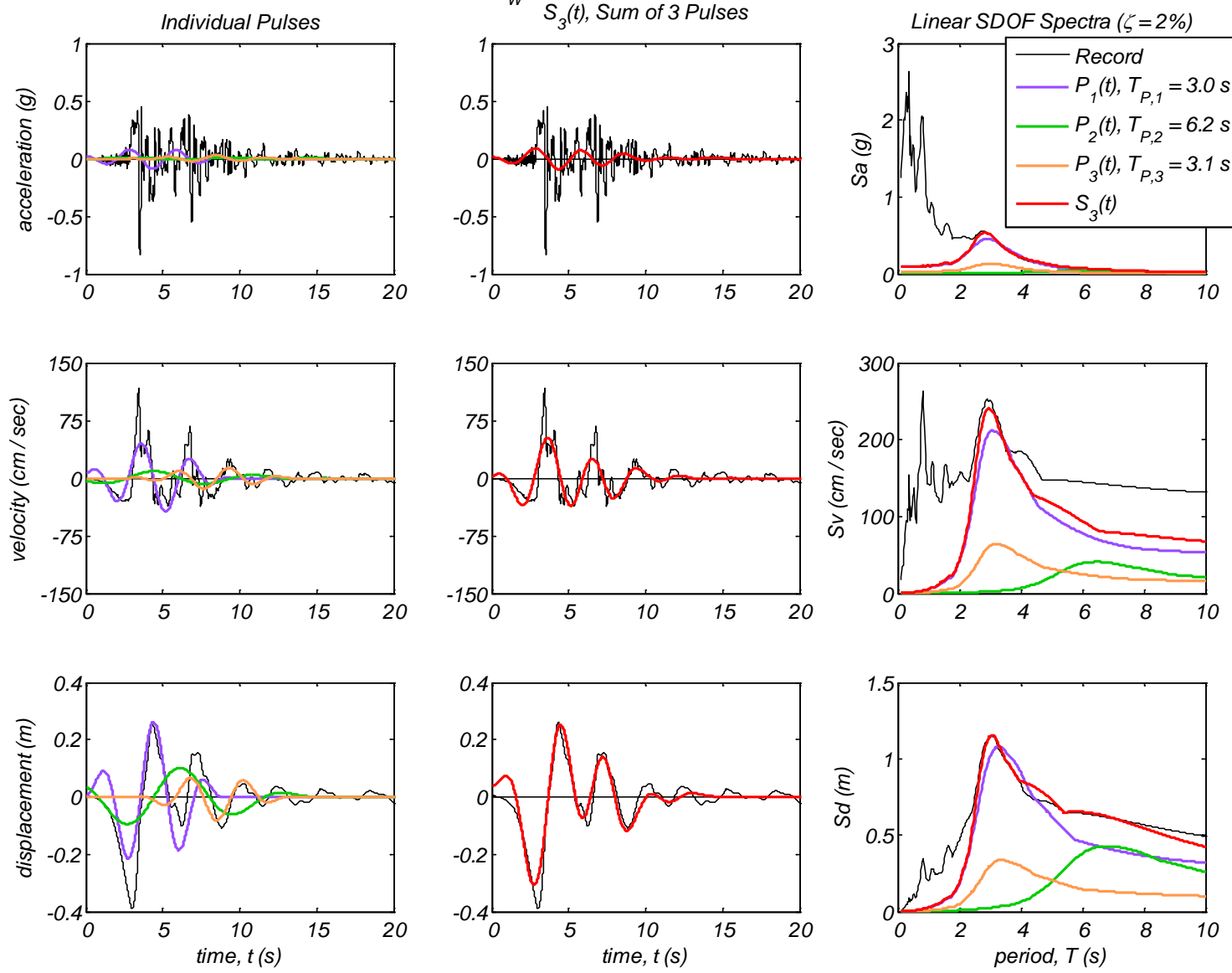


Appendix B1 – Time history and linear spectral response of three extracted pulses using the CPE<sub>V-AR</sub> method for 40 Motions



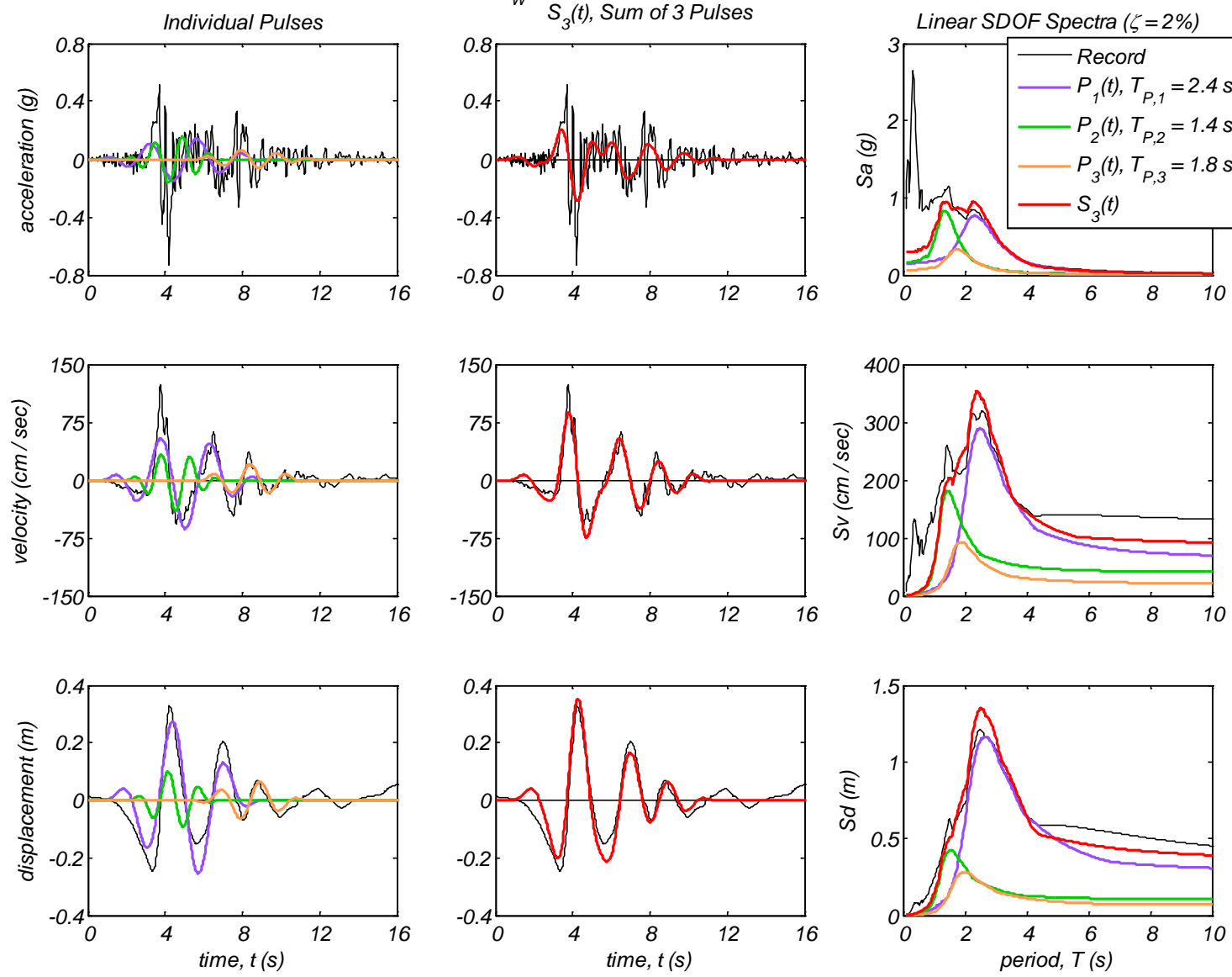
Appendix B1 – Time history and linear spectral response of three extracted pulses using the CPE<sub>V-AR</sub> method for 40 Motions

Record #19: Sylmar - Converter Sta East, Northridge, 1994,  $M_W 6.7$

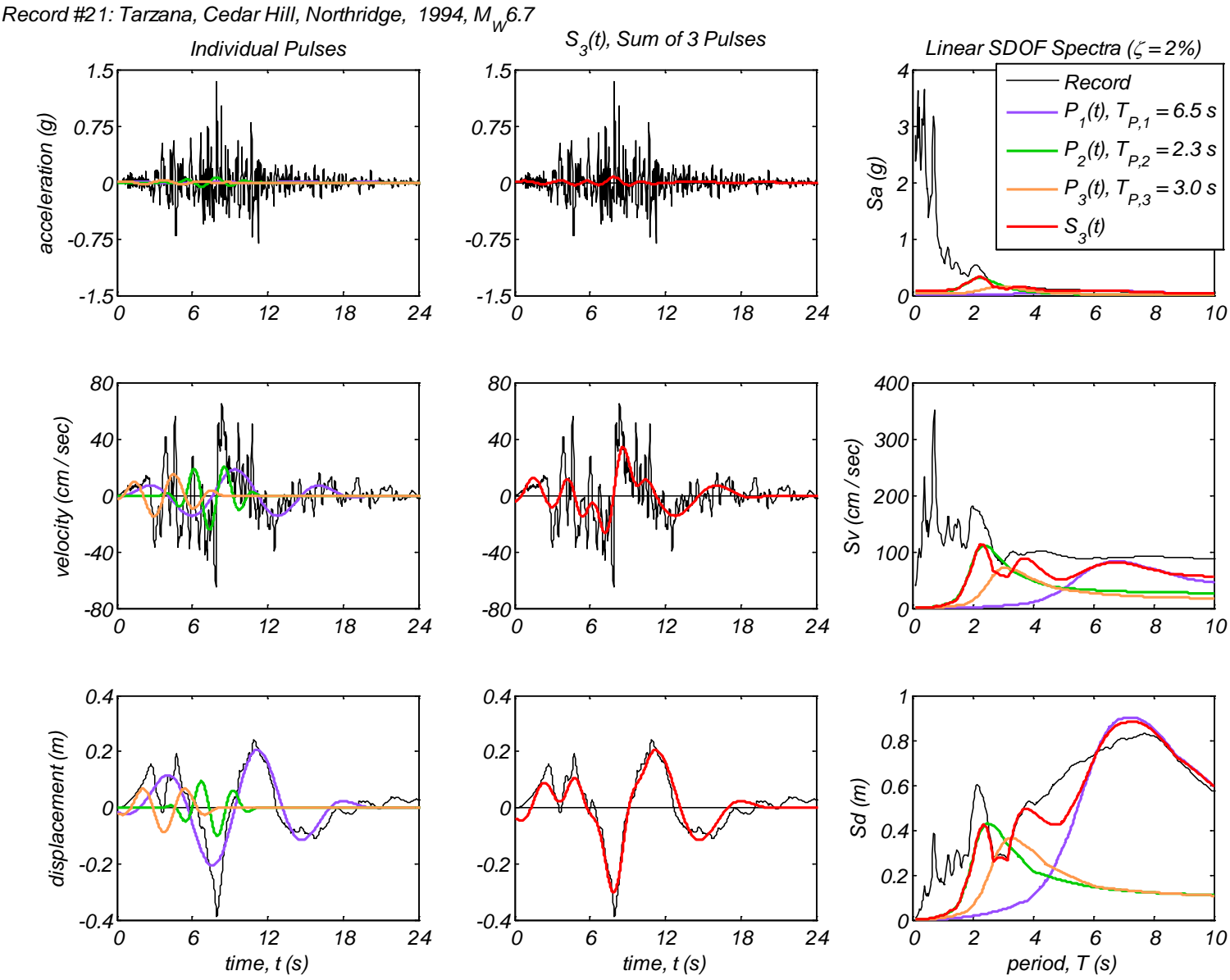


Appendix B1 – Time history and linear spectral response of three extracted pulses using the CPE<sub>V-AR</sub> method for 40 Motions

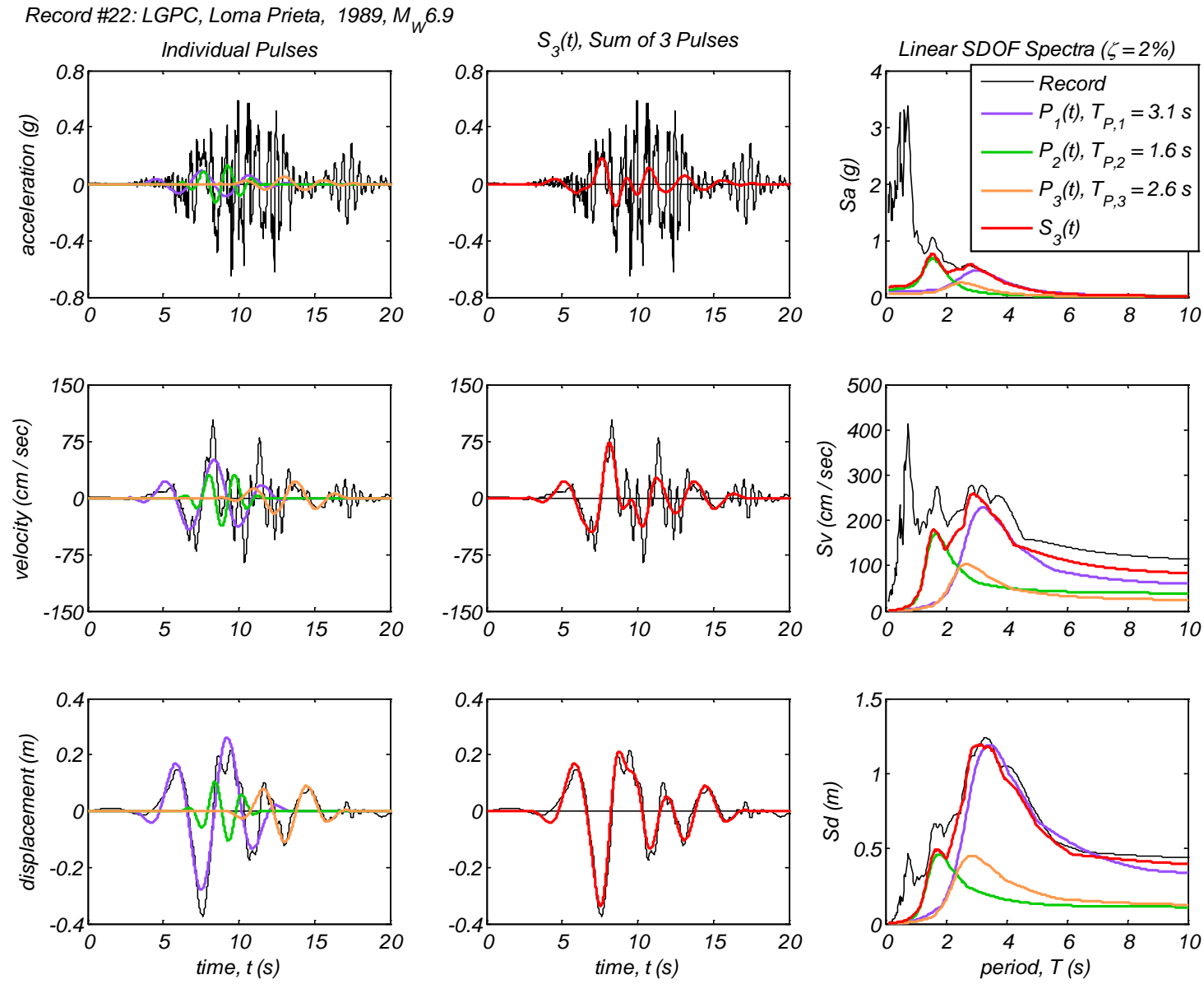
Record #20: Sylmar - Olive ViewMed FF, Northridge, 1994,  $M_W 6.7$



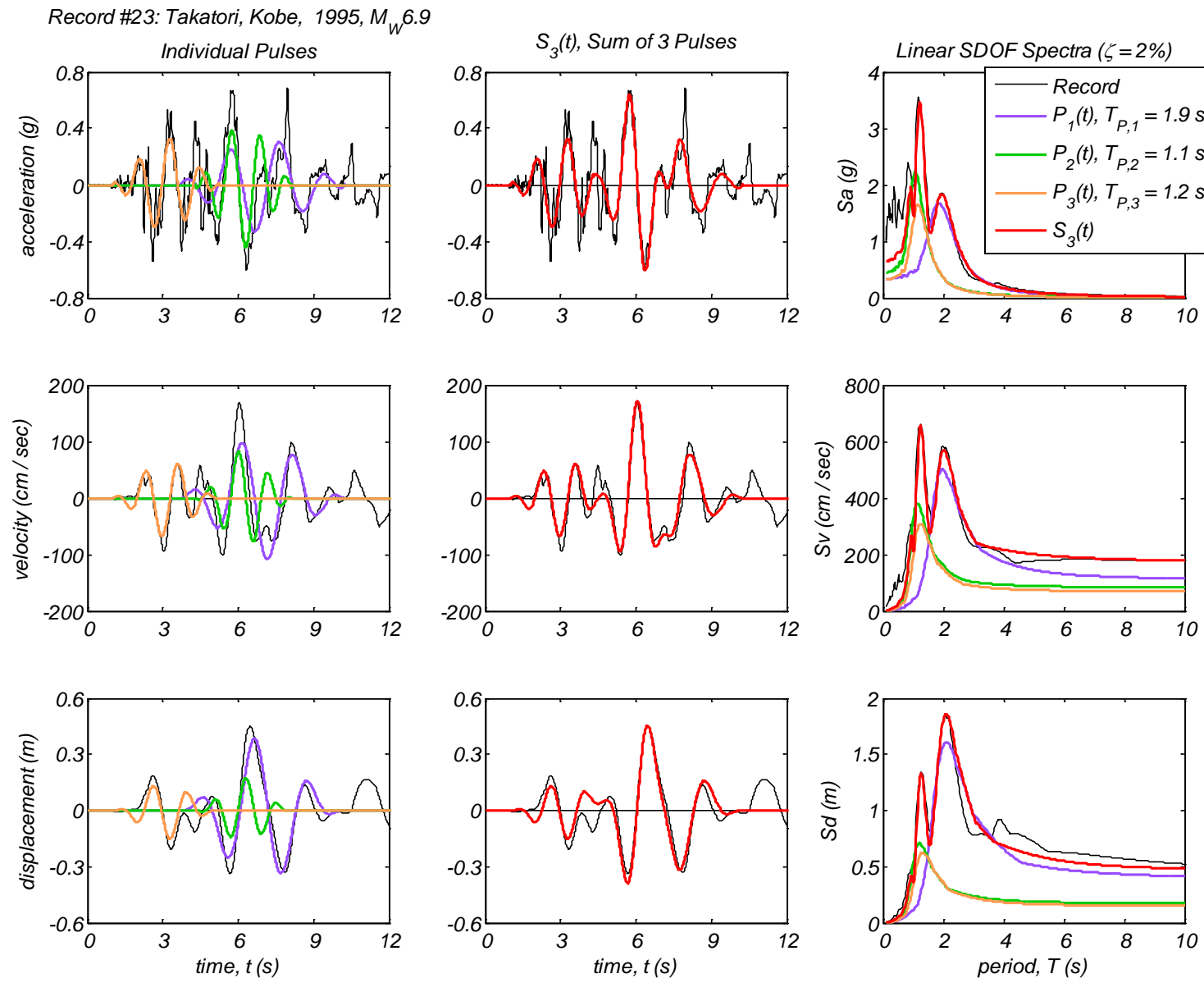
Appendix B1 – Time history and linear spectral response of three extracted pulses using the CPE<sub>V-AR</sub> method for 40 Motions



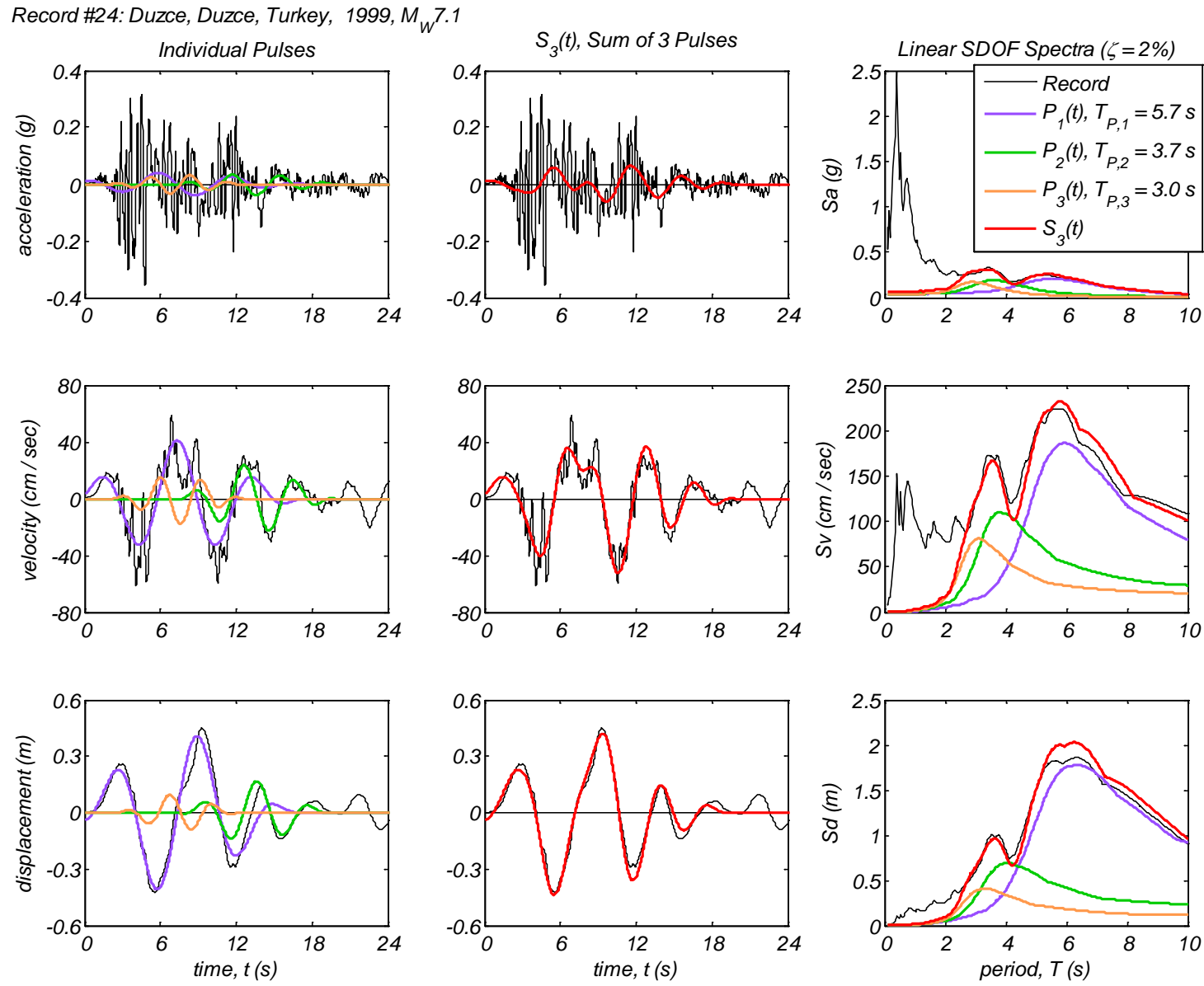
Appendix B1 – Time history and linear spectral response of three extracted pulses using the CPE<sub>V-AR</sub> method for 40 Motions



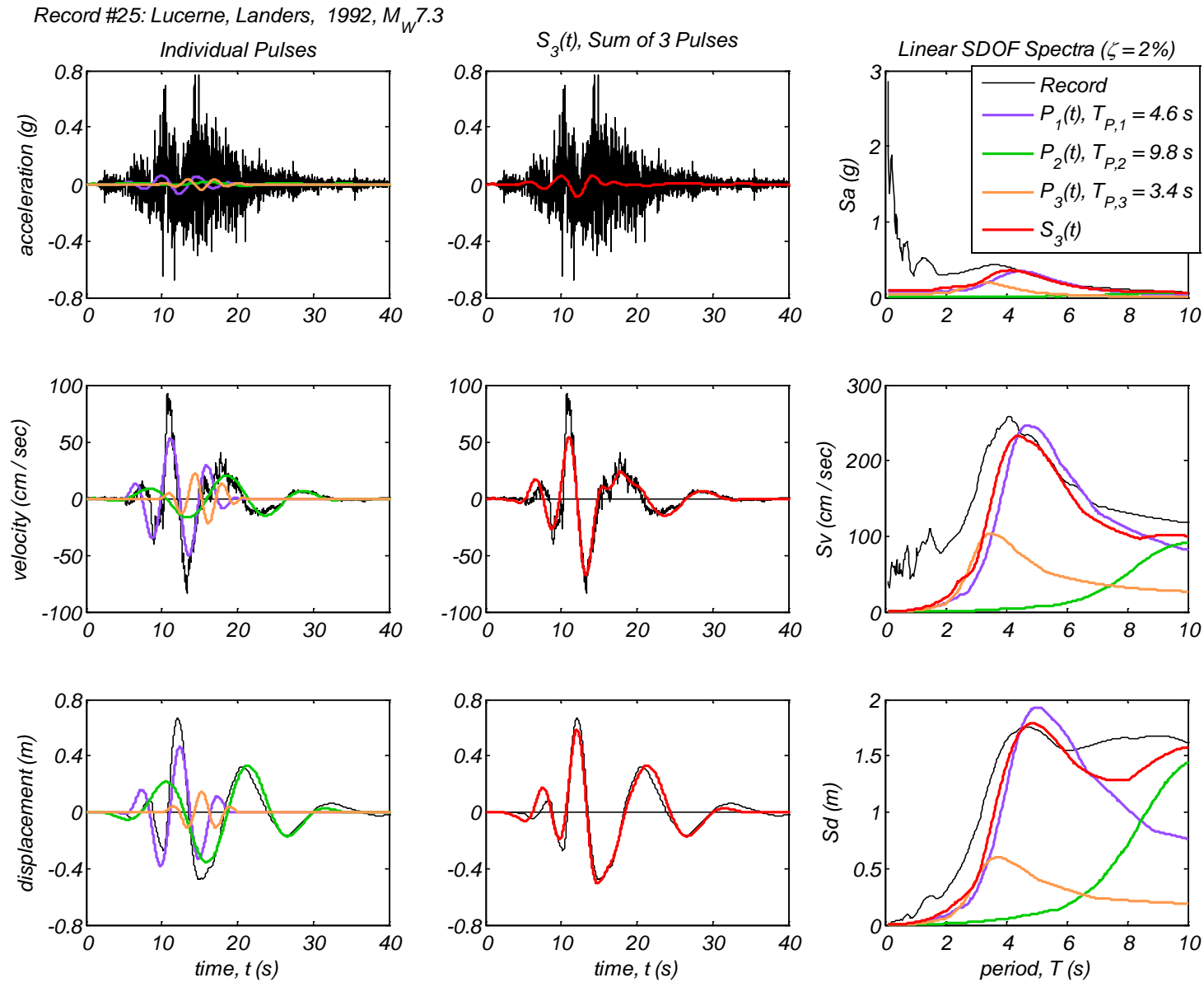
Appendix B1 – Time history and linear spectral response of three extracted pulses using the CPE<sub>V-AR</sub> method for 40 Motions



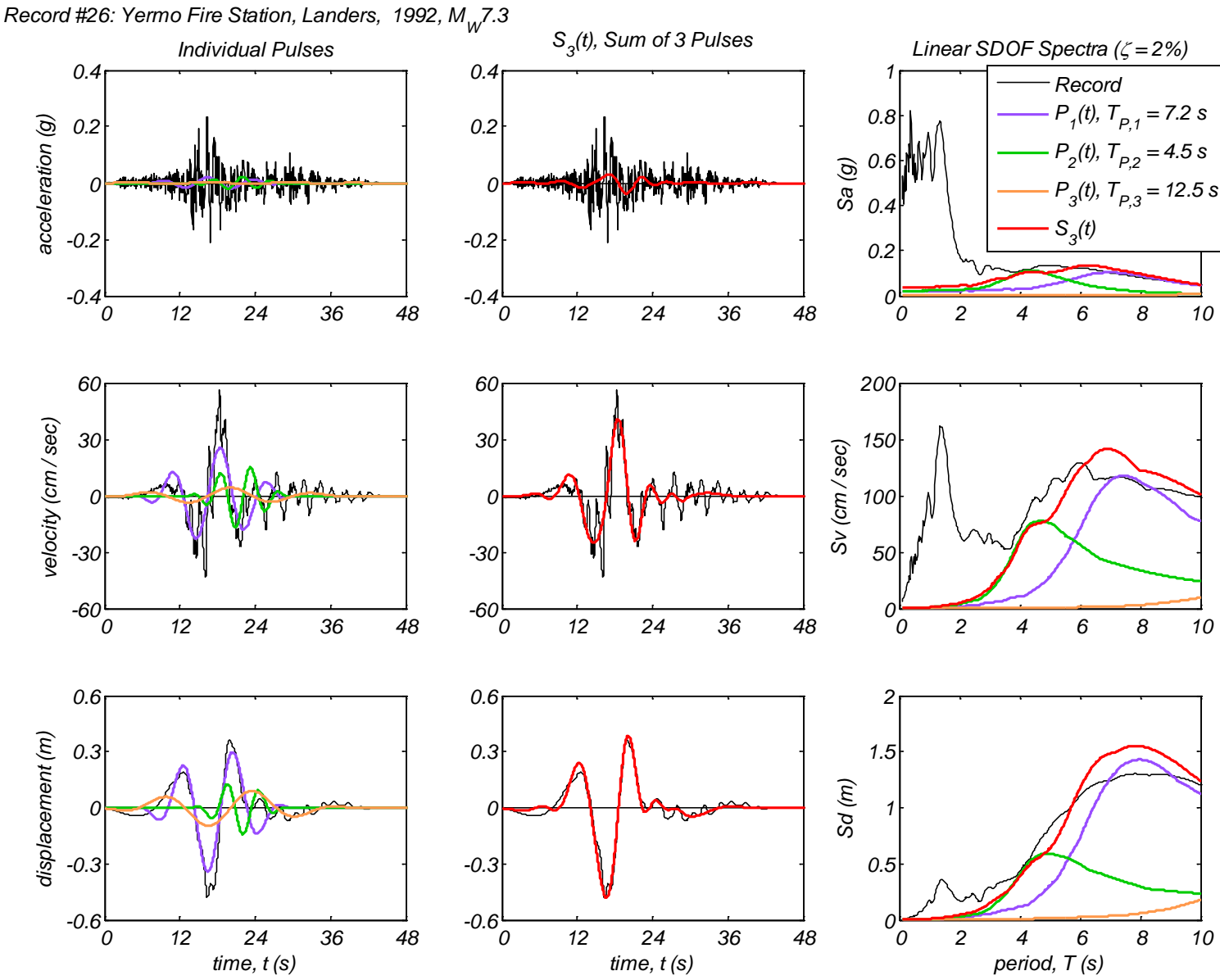
Appendix B1 – Time history and linear spectral response of three extracted pulses using the CPE<sub>V-AR</sub> method for 40 Motions



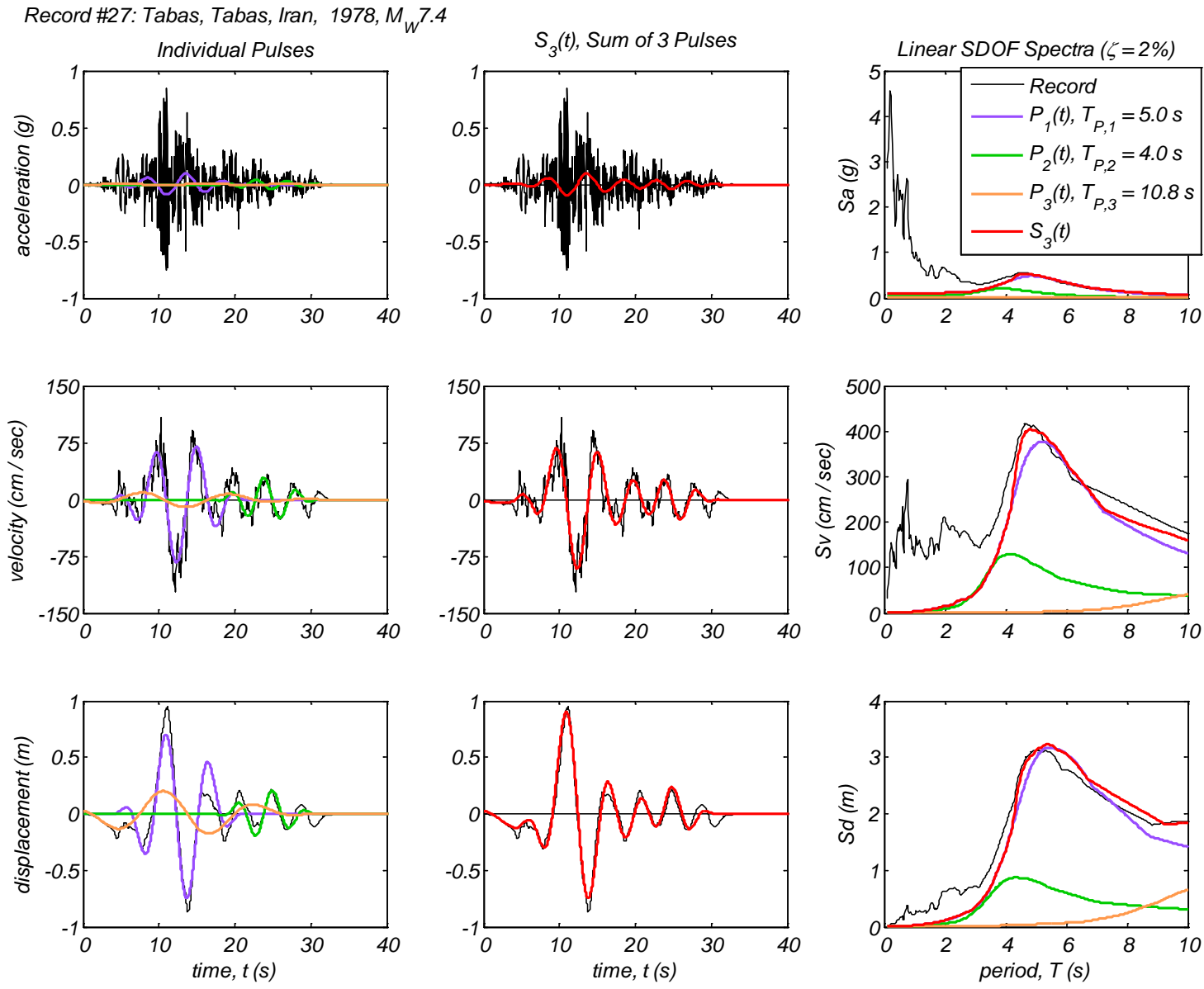
Appendix B1 – Time history and linear spectral response of three extracted pulses using the CPE<sub>V-AR</sub> method for 40 Motions



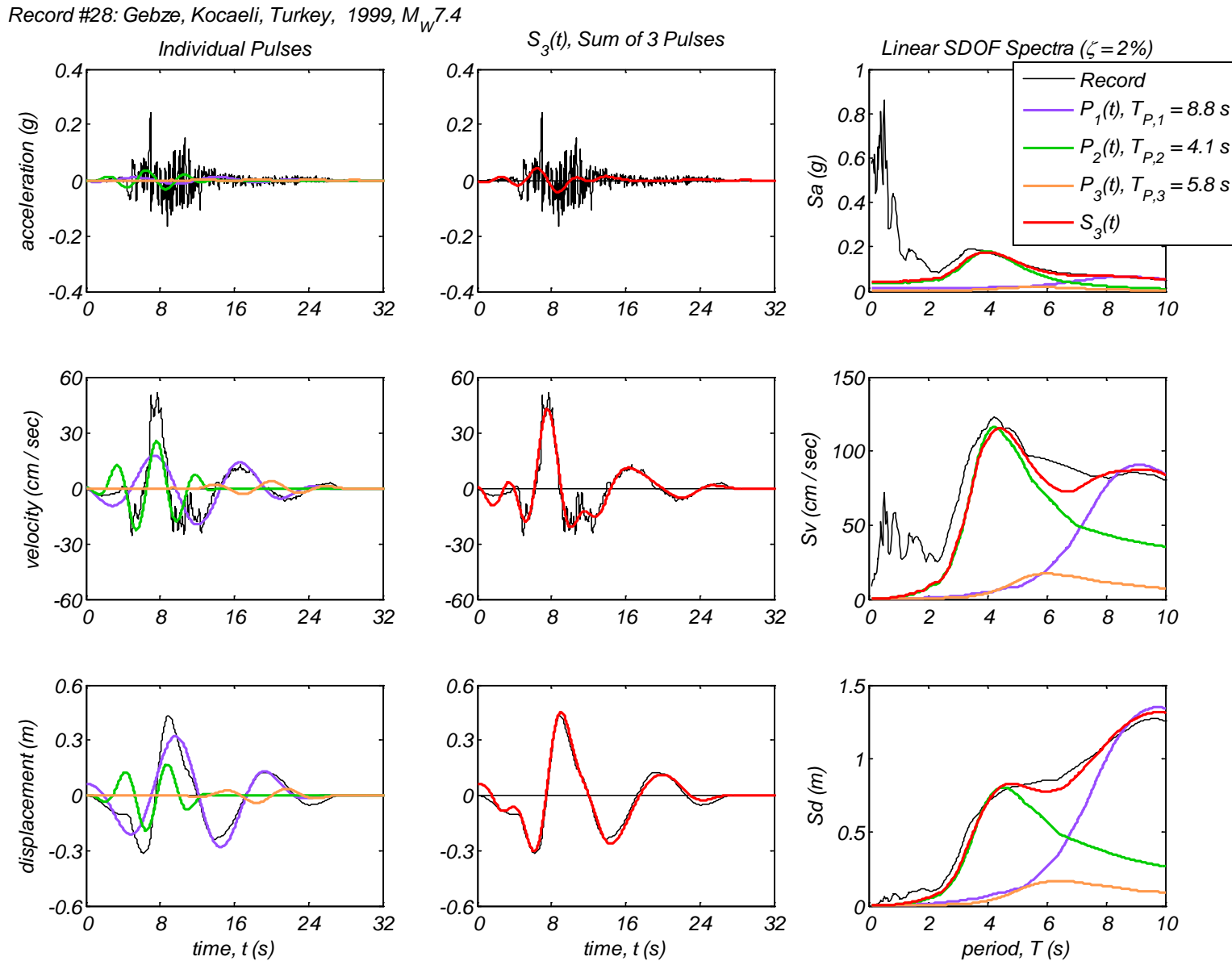
Appendix B1 – Time history and linear spectral response of three extracted pulses using the CPE<sub>V-AR</sub> method for 40 Motions



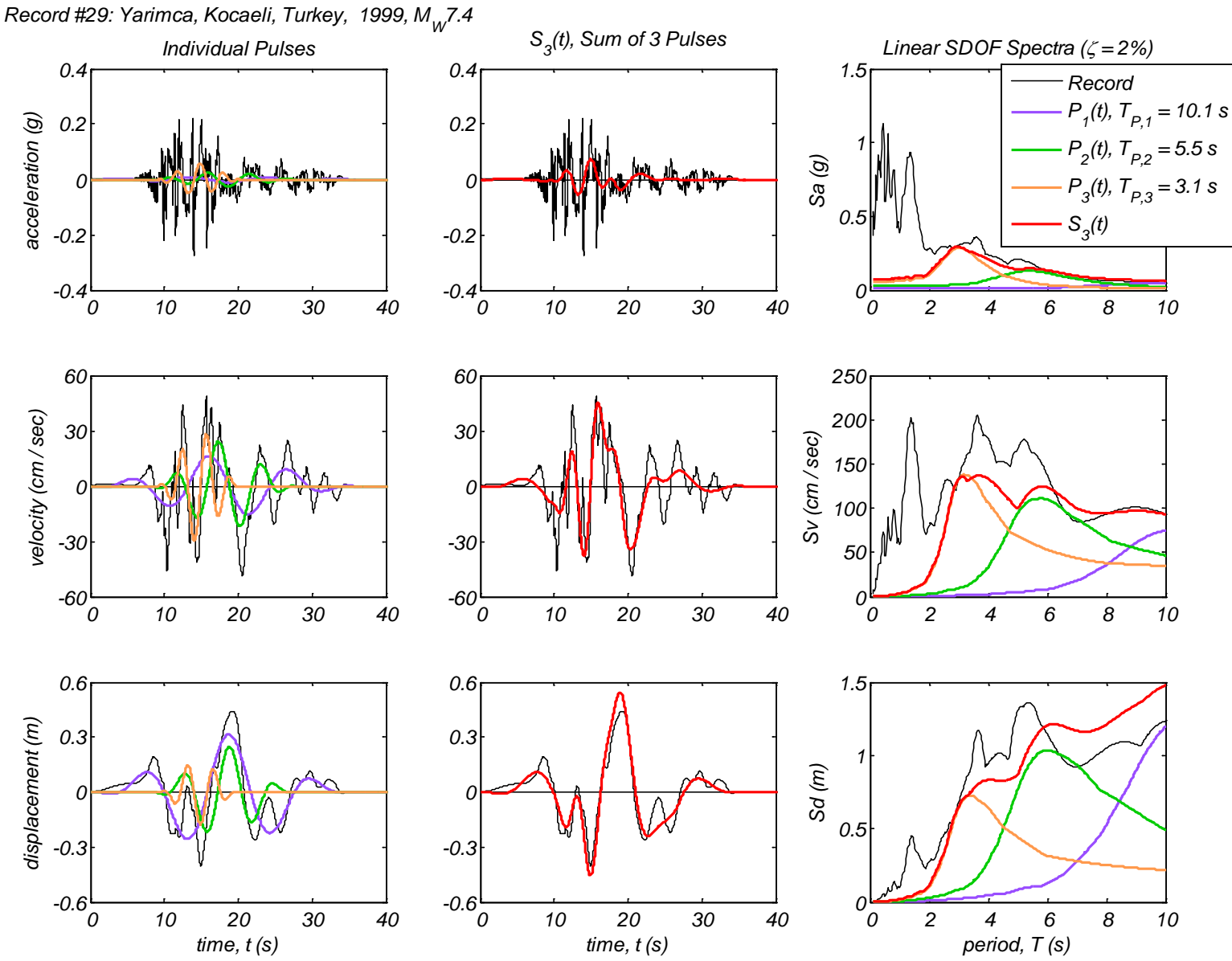
Appendix B1 – Time history and linear spectral response of three extracted pulses using the CPE<sub>V-AR</sub> method for 40 Motions



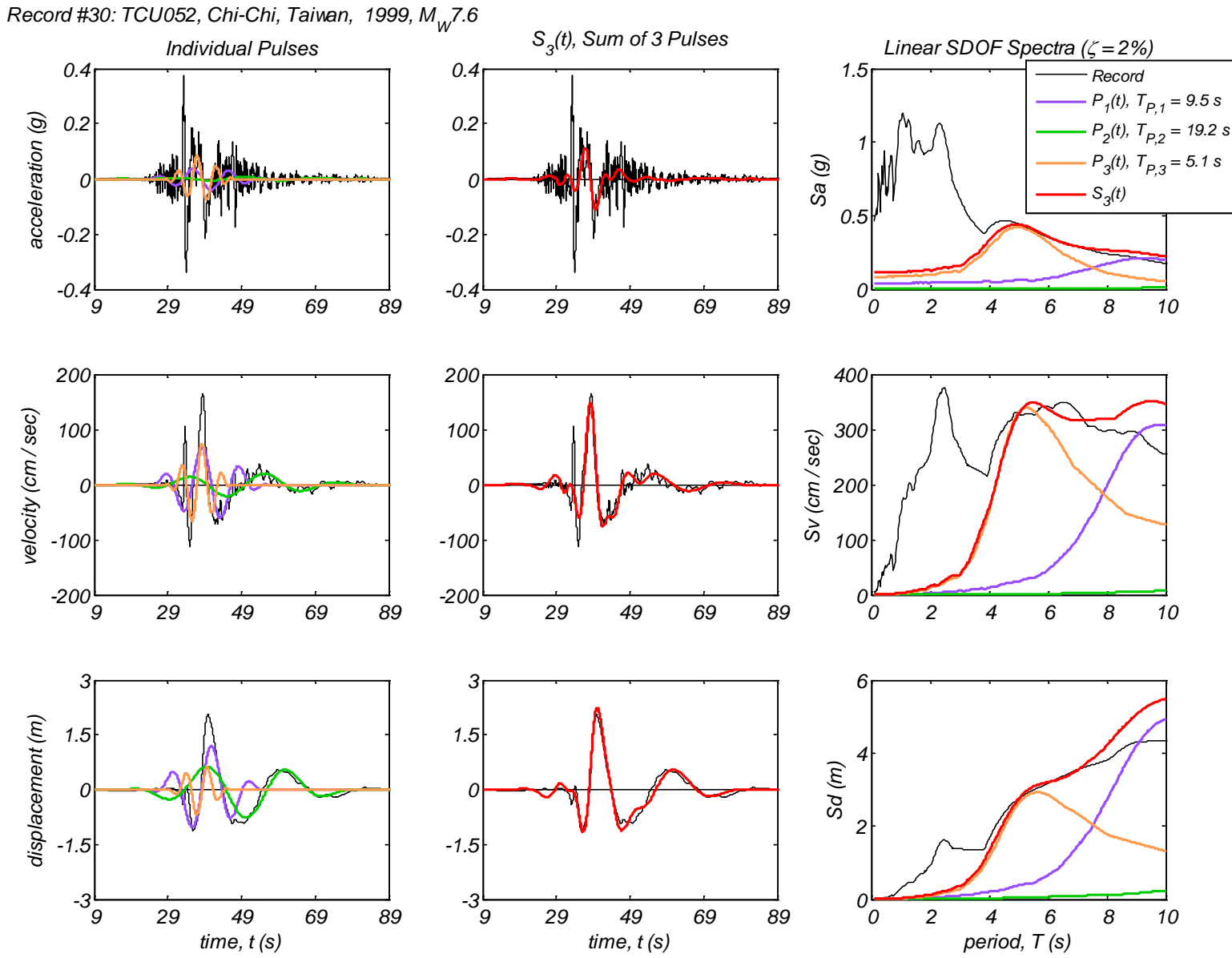
Appendix B1 – Time history and linear spectral response of three extracted pulses using the CPE<sub>V-AR</sub> method for 40 Motions



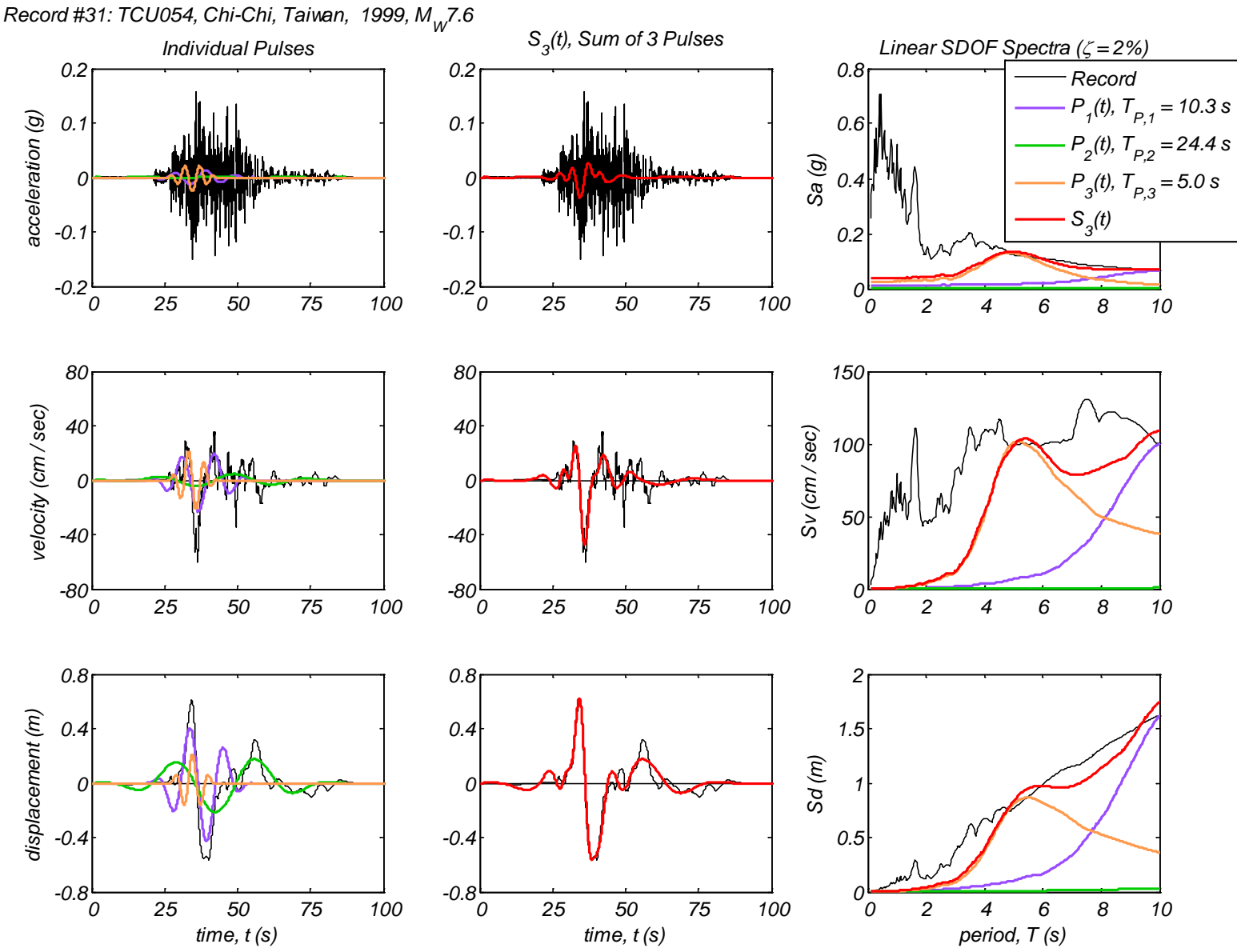
Appendix B1 – Time history and linear spectral response of three extracted pulses using the CPE<sub>V-AR</sub> method for 40 Motions



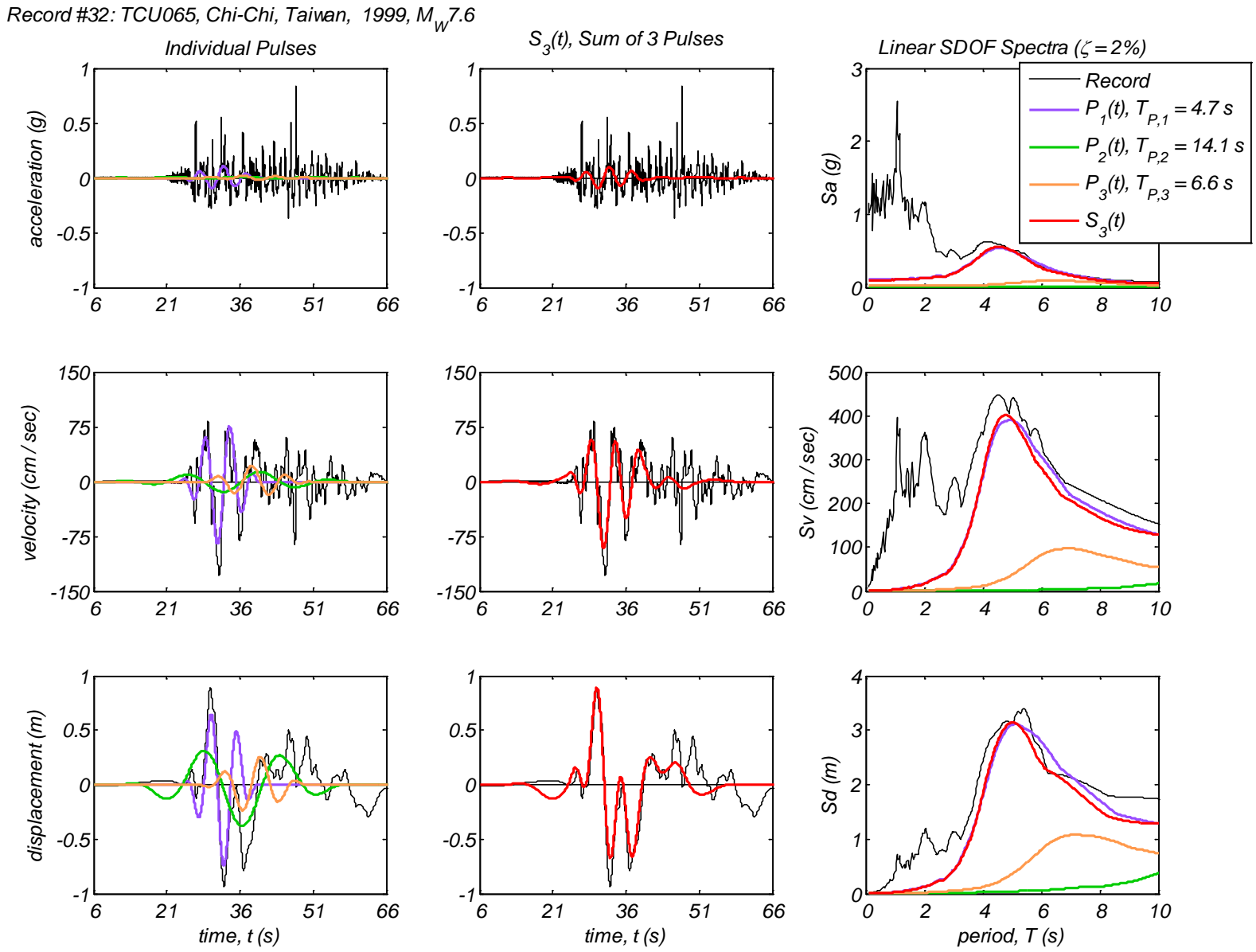
Appendix B1 – Time history and linear spectral response of three extracted pulses using the CPE<sub>V-AR</sub> method for 40 Motions



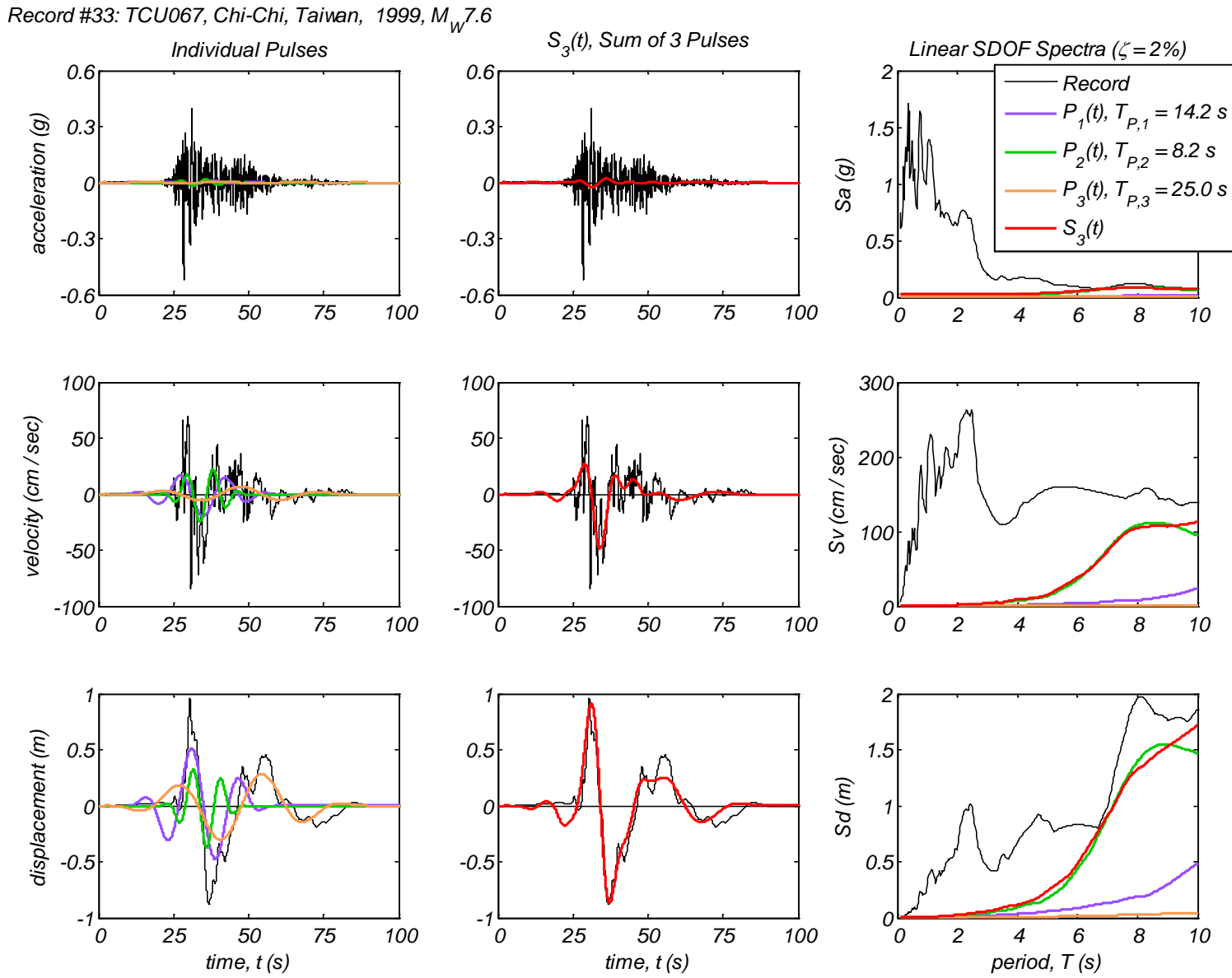
Appendix B1 – Time history and linear spectral response of three extracted pulses using the CPE<sub>V-AR</sub> method for 40 Motions



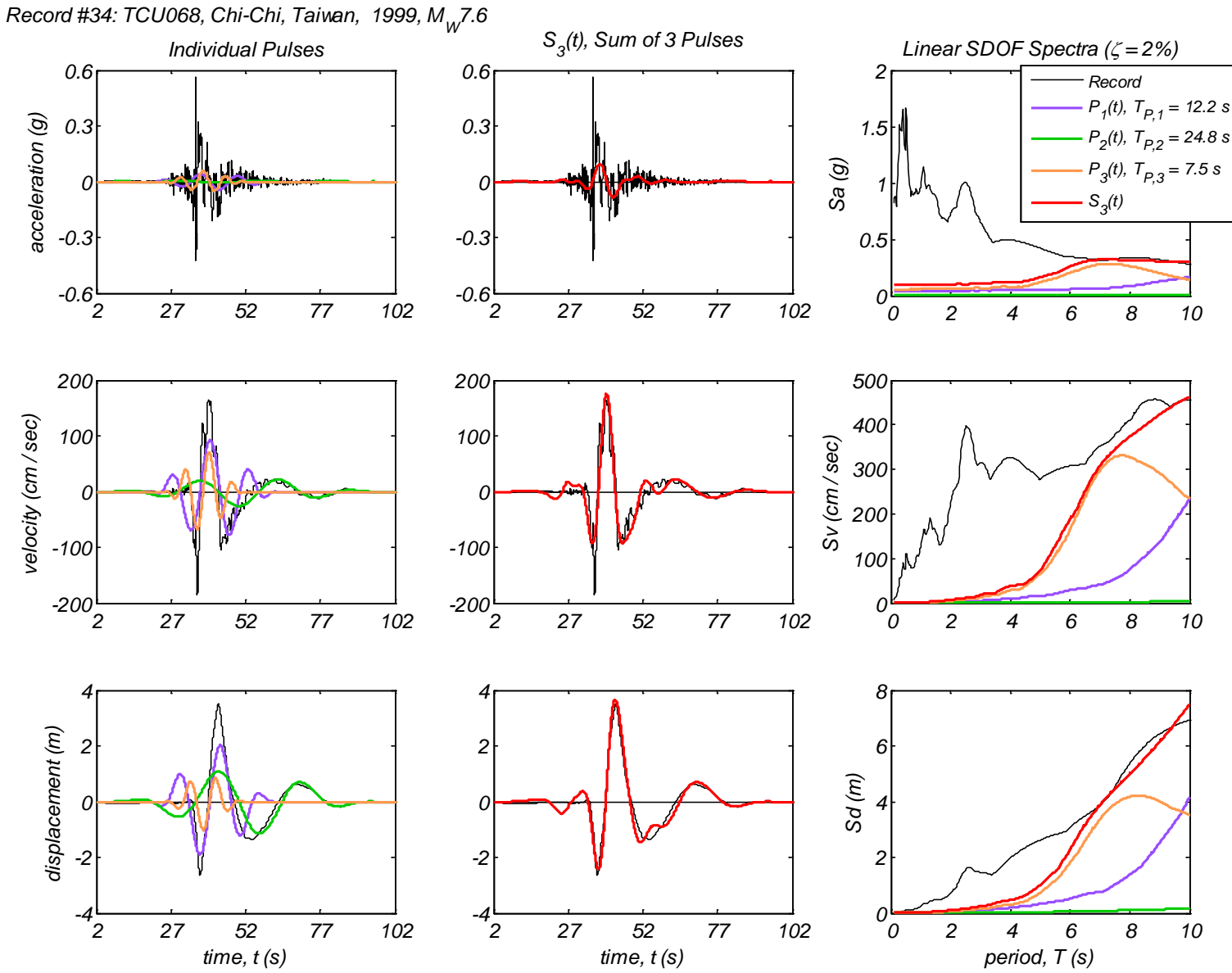
Appendix B1 – Time history and linear spectral response of three extracted pulses using the CPE<sub>V-AR</sub> method for 40 Motions



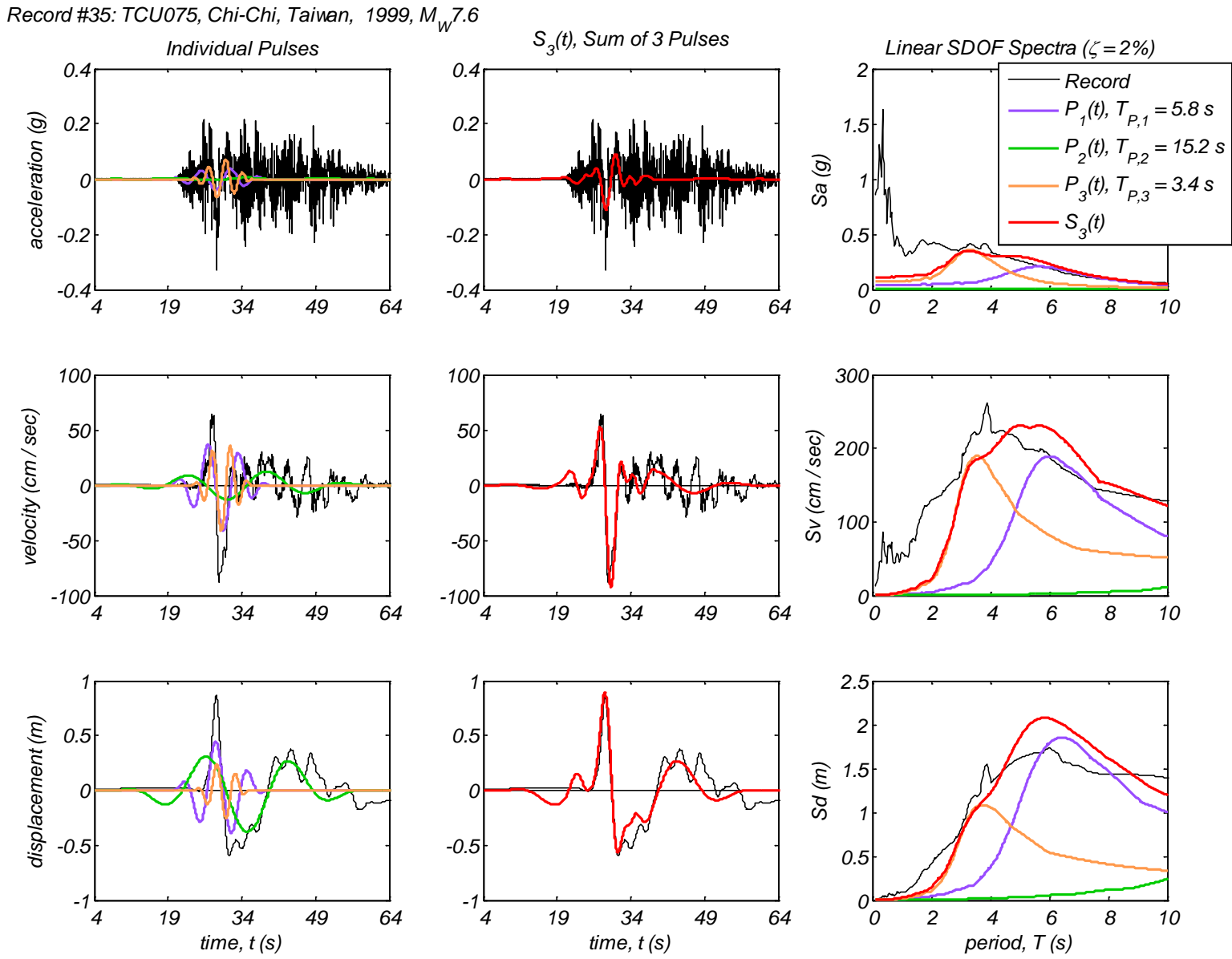
Appendix B1 – Time history and linear spectral response of three extracted pulses using the CPE<sub>V-AR</sub> method for 40 Motions



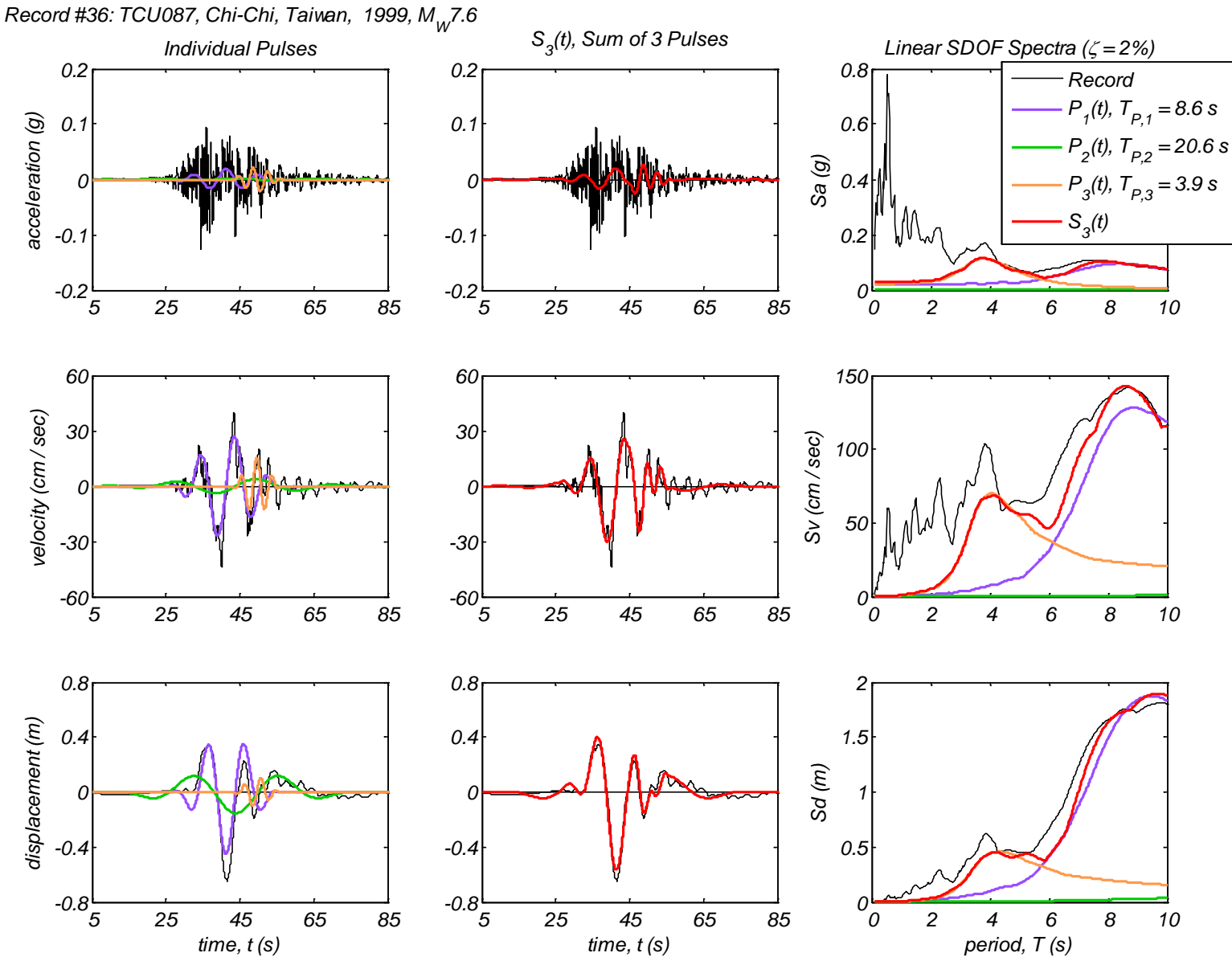
Appendix B1 – Time history and linear spectral response of three extracted pulses using the CPE<sub>V-AR</sub> method for 40 Motions



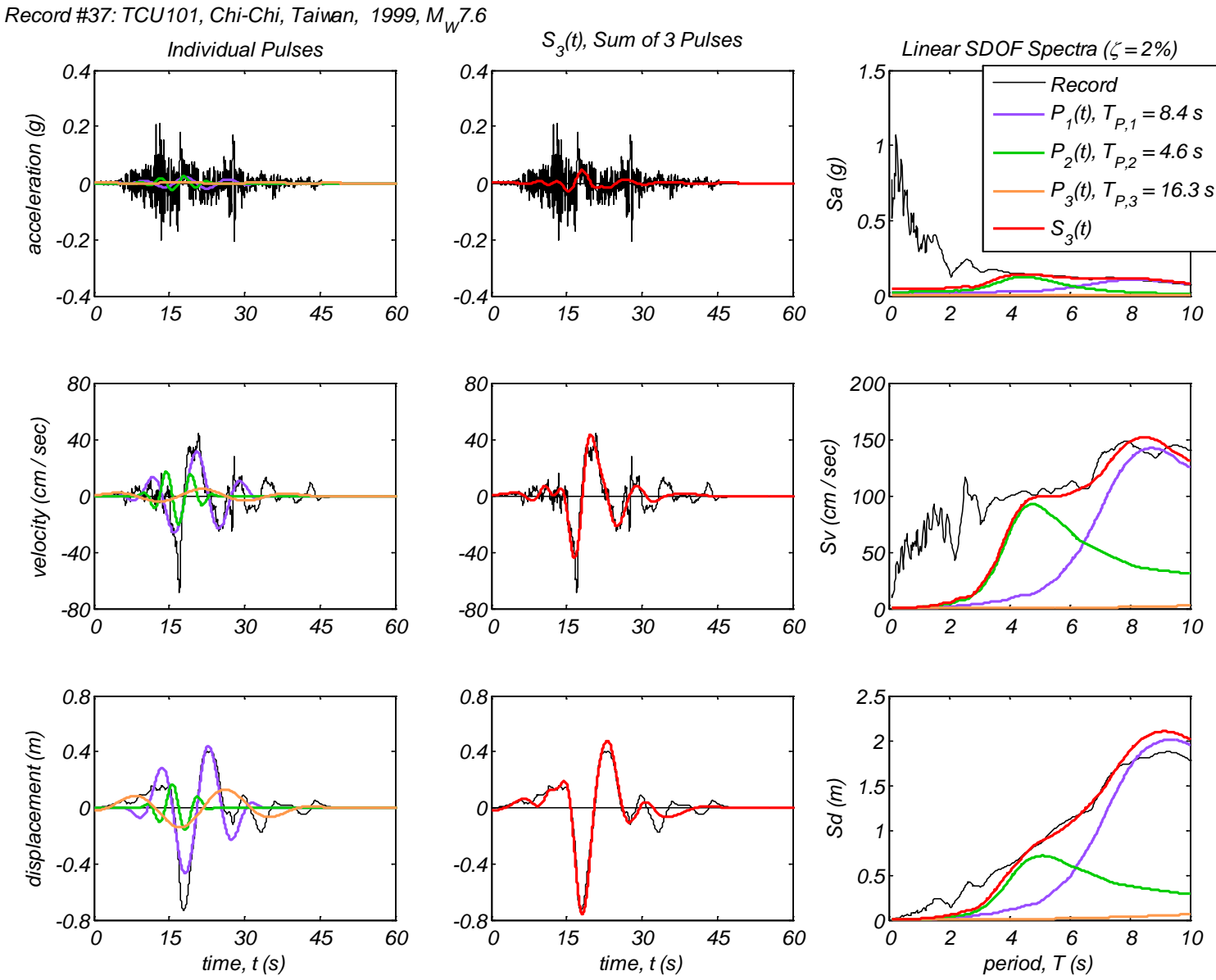
Appendix B1 – Time history and linear spectral response of three extracted pulses using the CPE<sub>V-AR</sub> method for 40 Motions



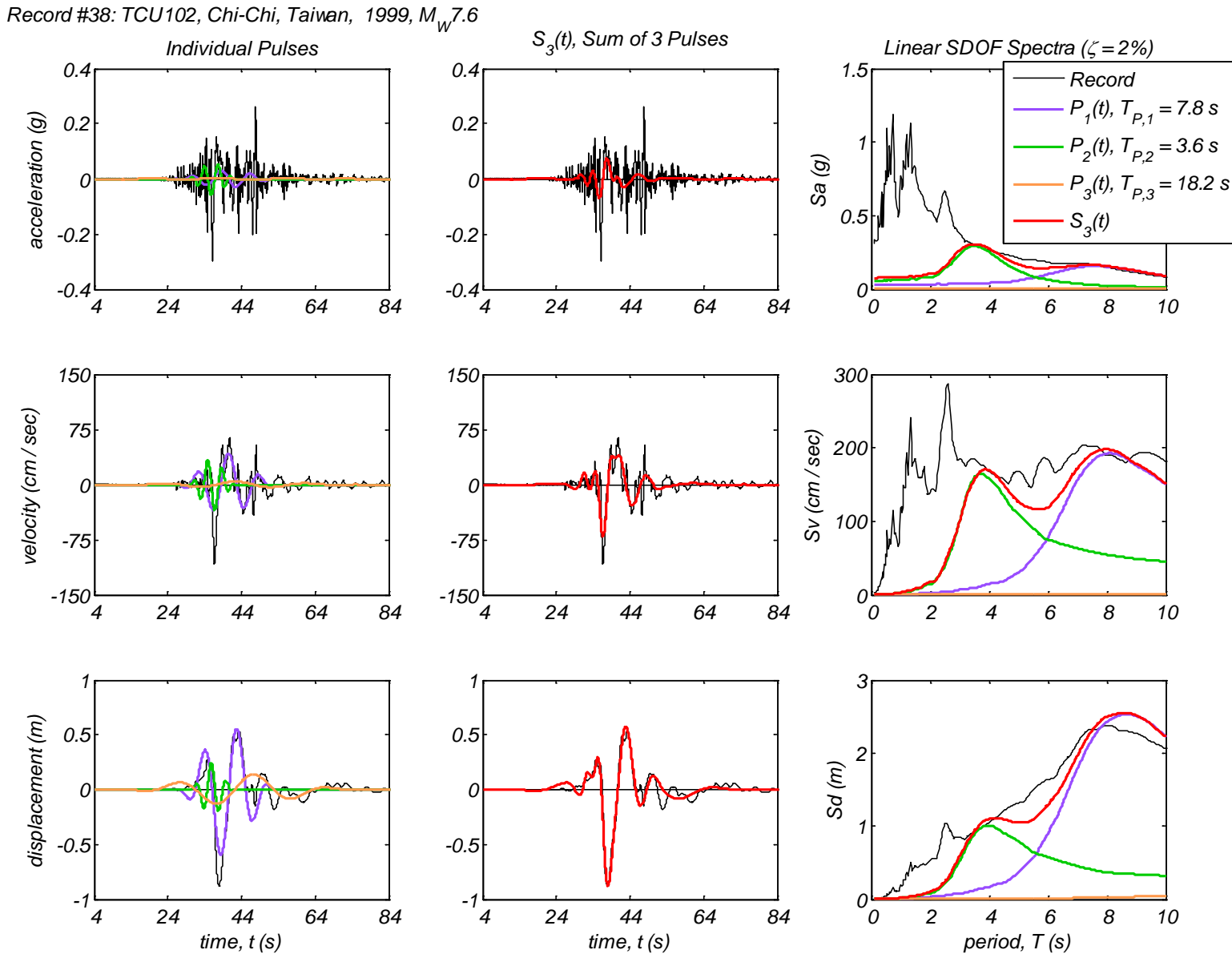
Appendix B1 – Time history and linear spectral response of three extracted pulses using the CPE<sub>V-AR</sub> method for 40 Motions



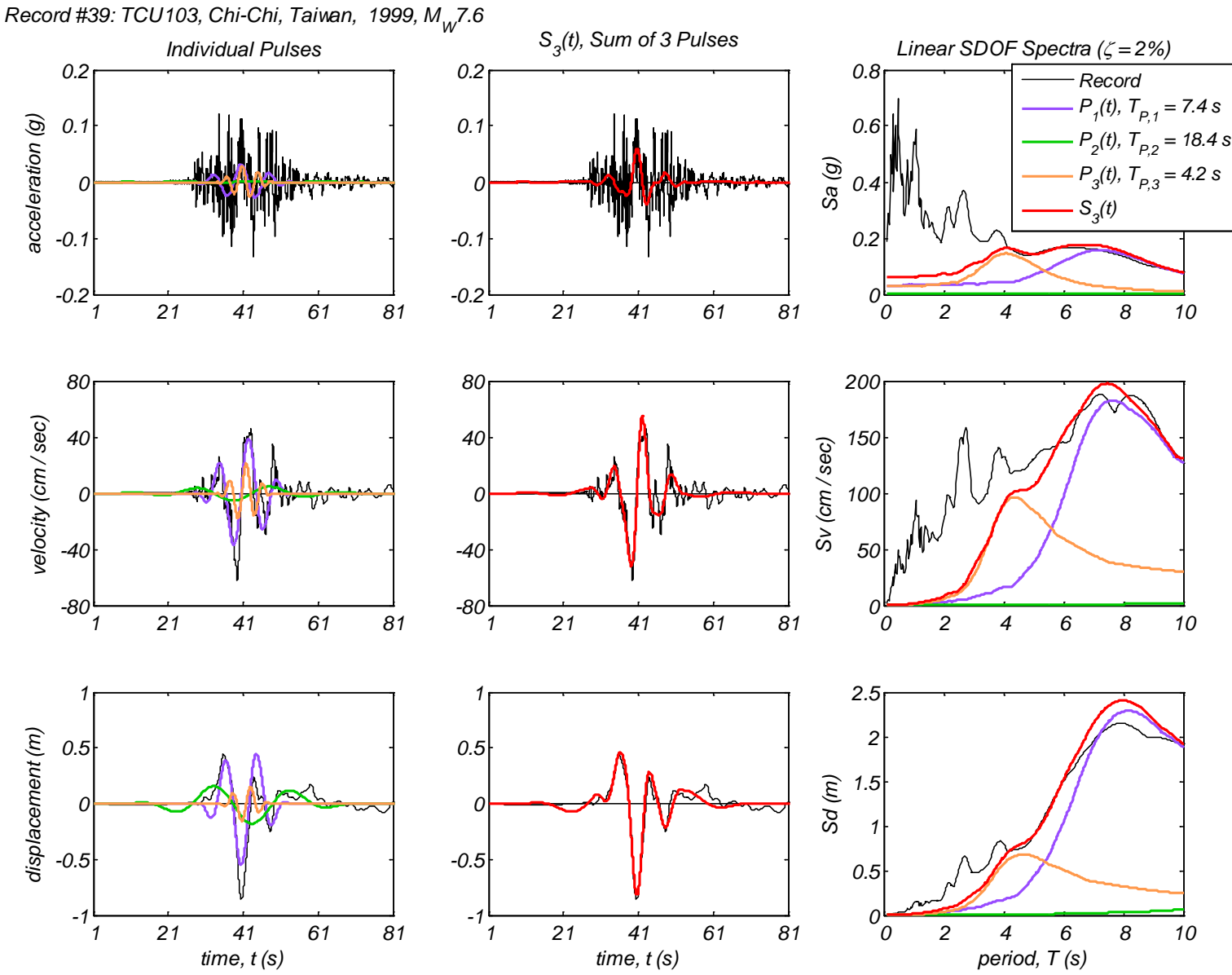
Appendix B1 – Time history and linear spectral response of three extracted pulses using the CPE<sub>V-AR</sub> method for 40 Motions



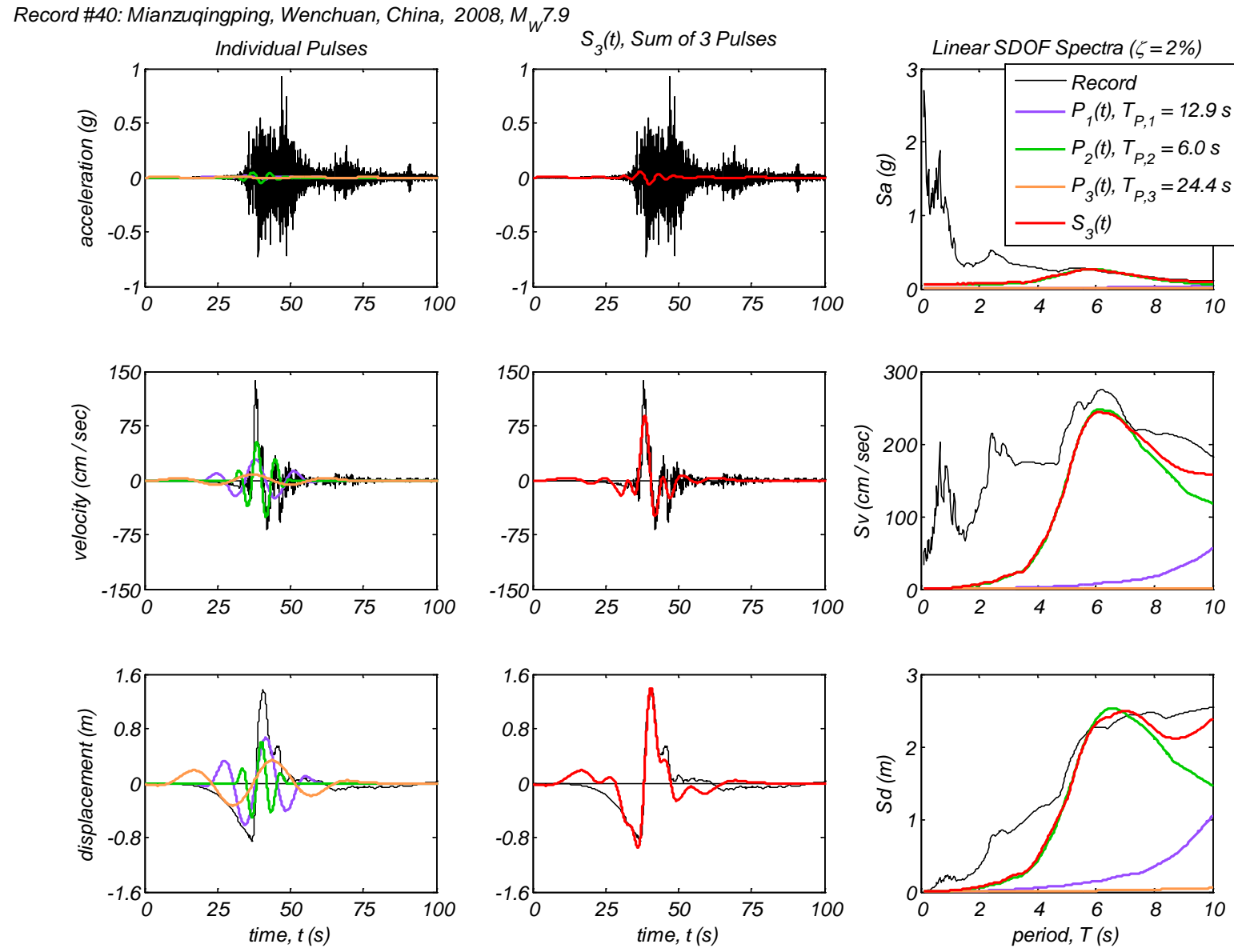
Appendix B1 – Time history and linear spectral response of three extracted pulses using the CPE<sub>V-AR</sub> method for 40 Motions



Appendix B1 – Time history and linear spectral response of three extracted pulses using the CPE<sub>V-AR</sub> method for 40 Motions

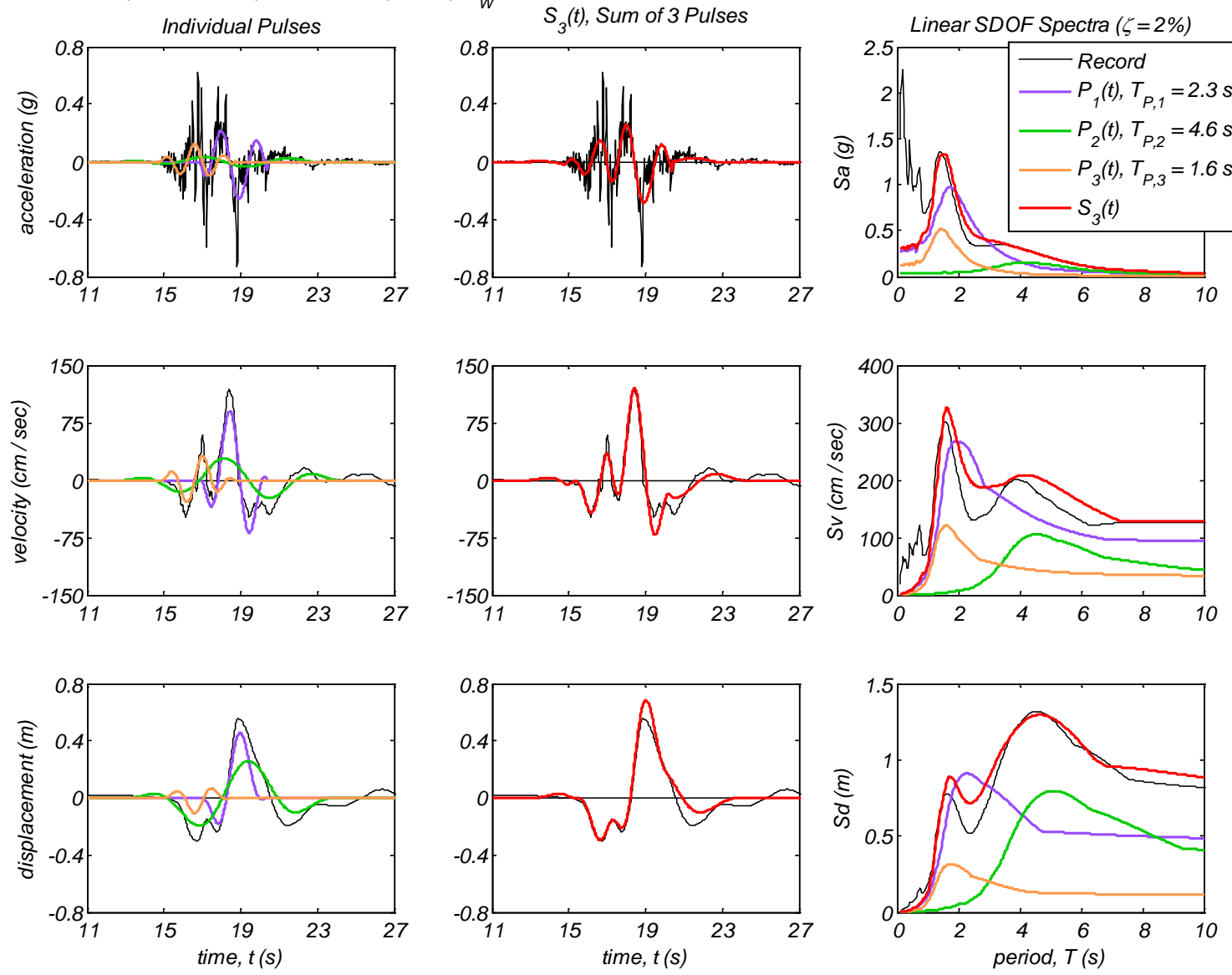


Appendix B1 – Time history and linear spectral response of three extracted pulses using the CPE<sub>V-AR</sub> method for 40 Motions



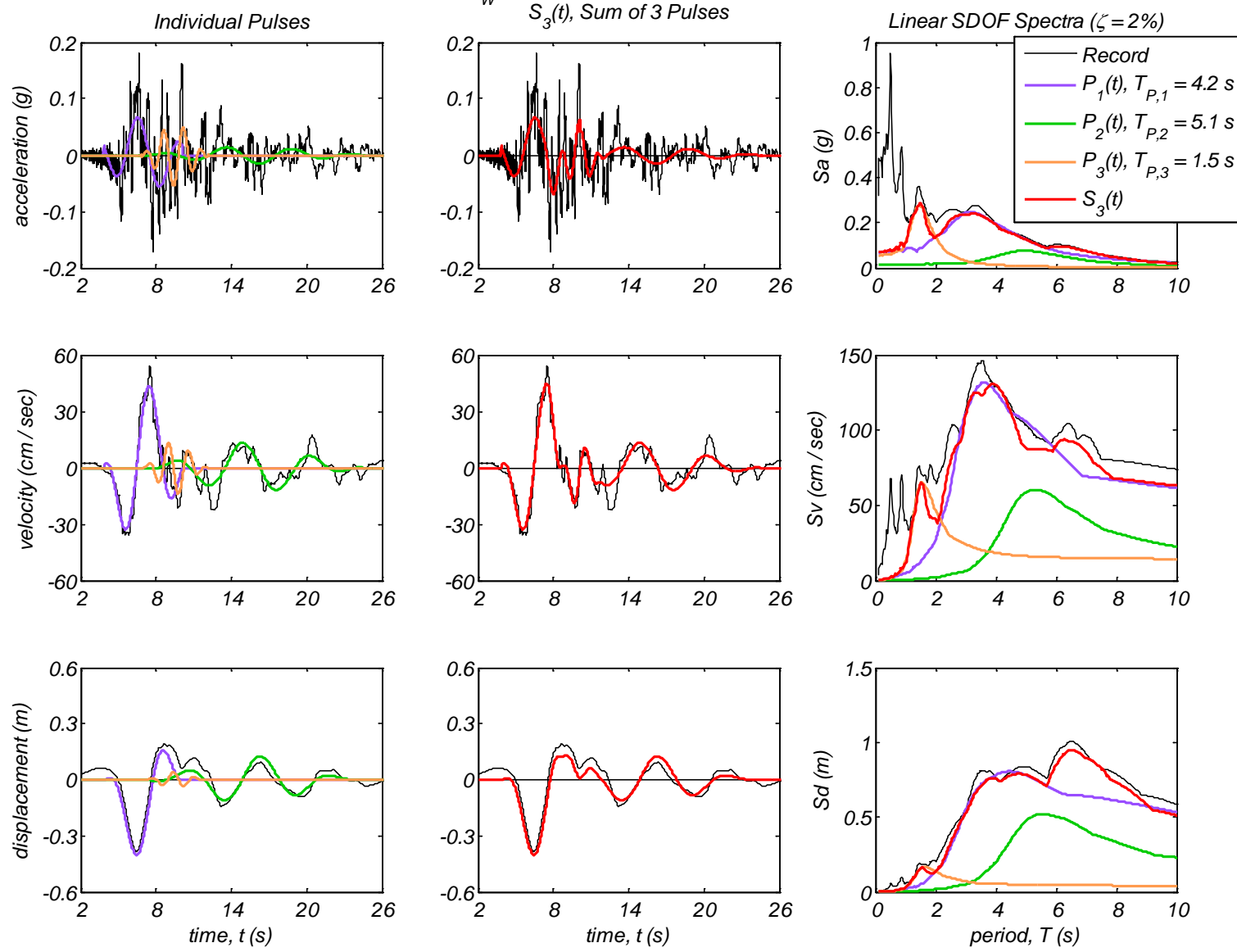
## Appendix B2: Time history and linear spectral response of three extracted pulses using the CPE<sub>V-EN</sub> method for 40 motions

Record #1: PRPC, Christchurch, New Zealand, 2011,  $M_W 6.3$

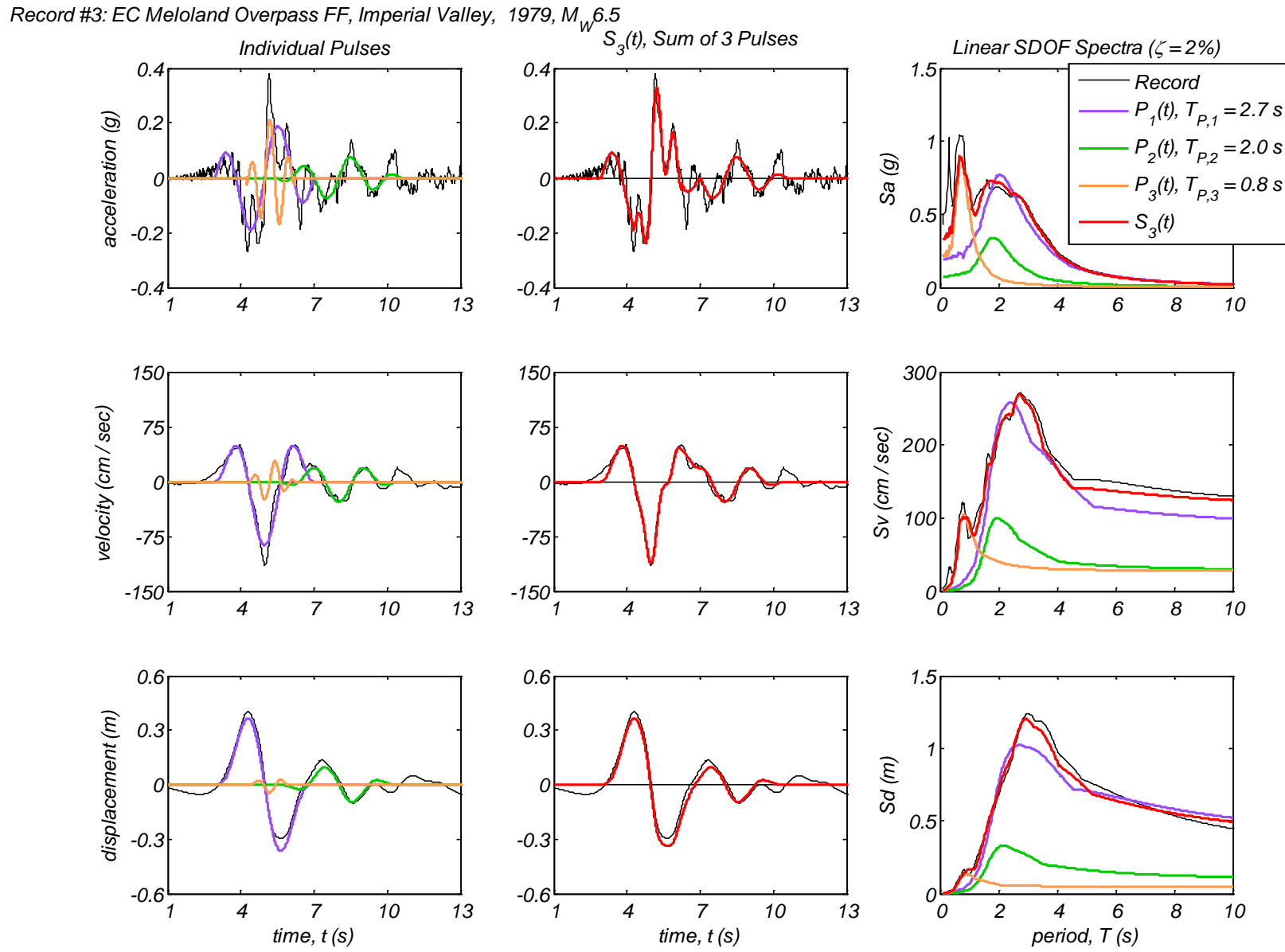


Appendix B2 – Time history and linear spectral response of three extracted pulses using the CPE<sub>V-EN</sub> method for 40 Motions

Record #2: EC County Center FF, Imperial Valley, 1979,  $M_W 6.5$

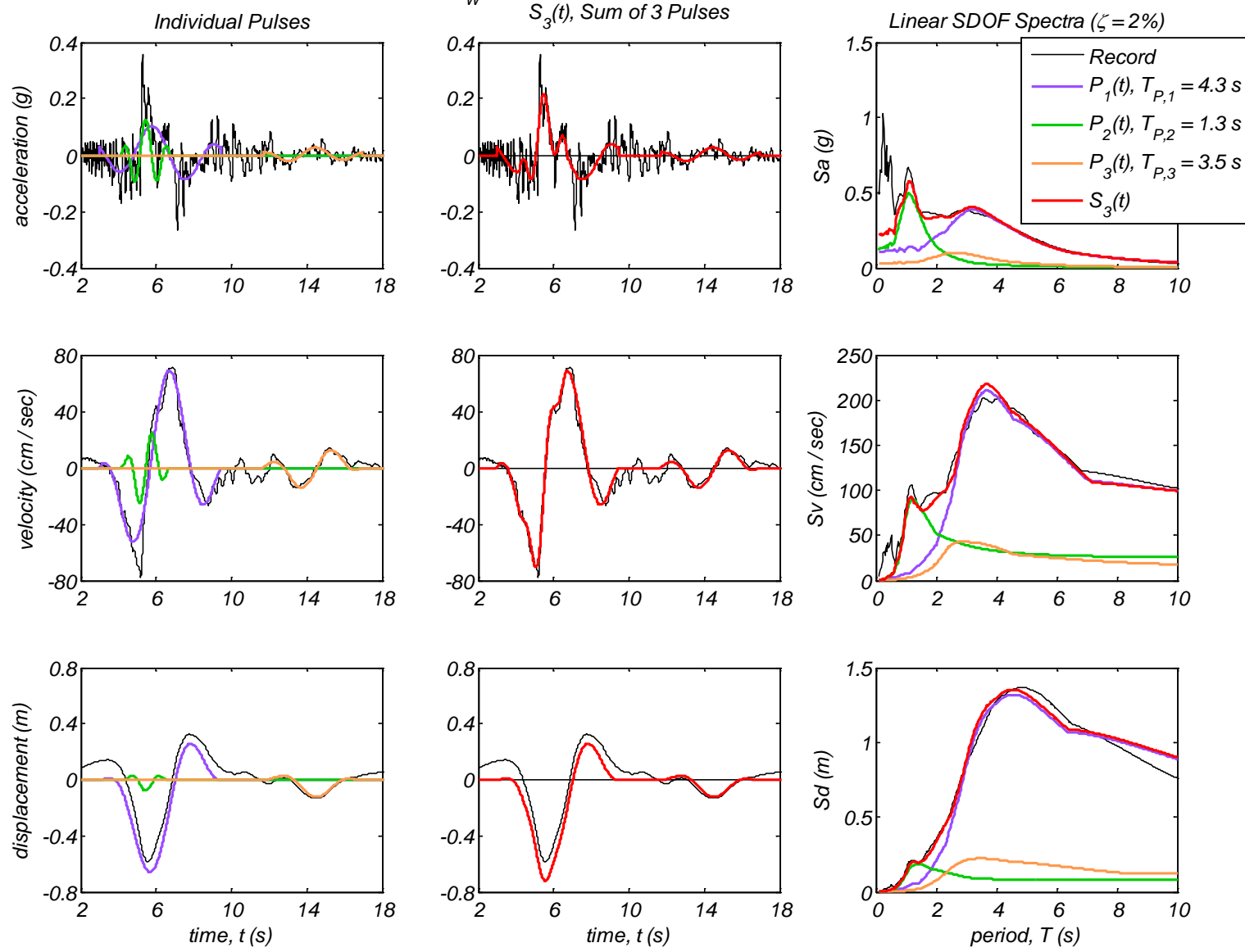


Appendix B2 – Time history and linear spectral response of three extracted pulses using the CPE<sub>V-EN</sub> method for 40 Motions



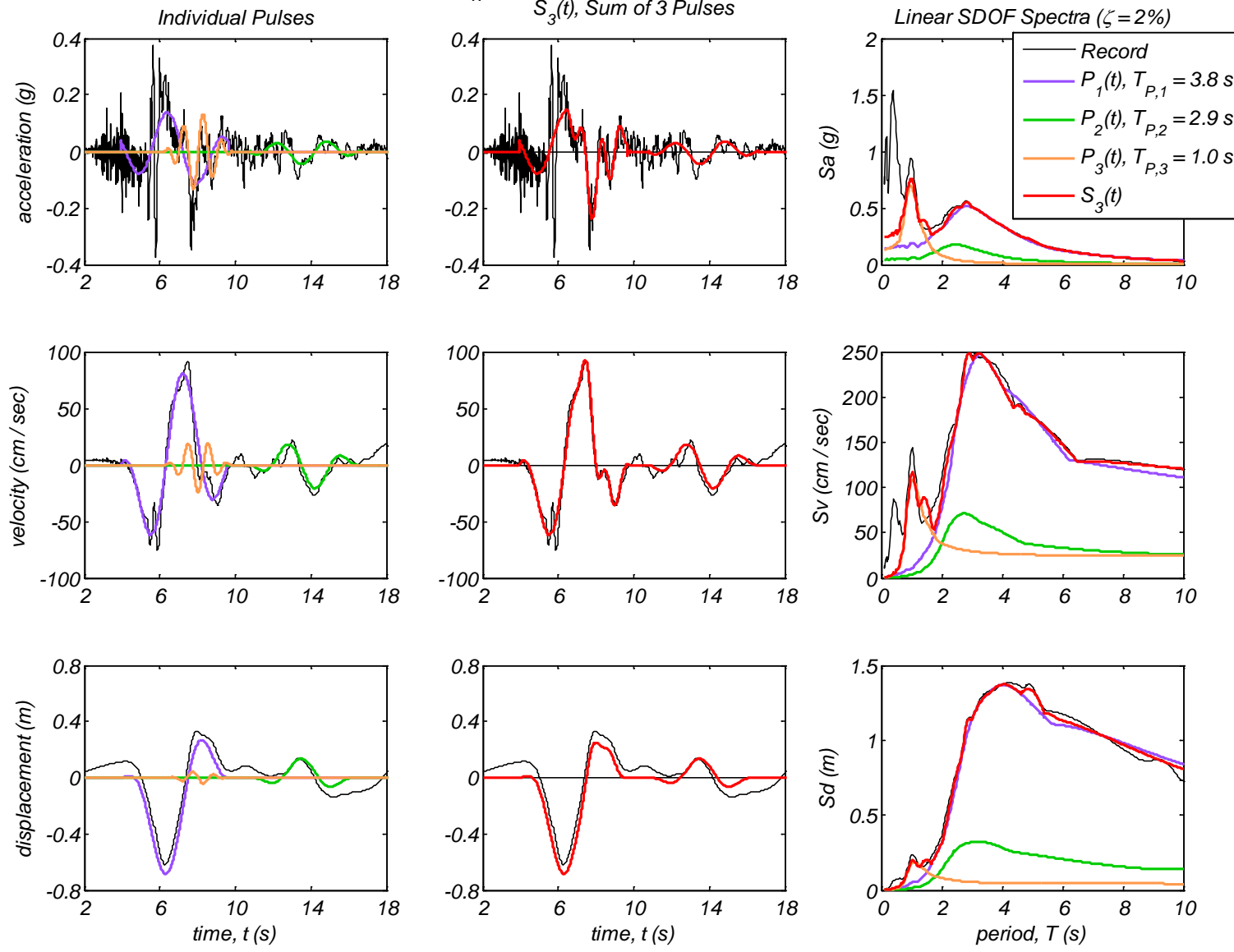
Appendix B2 – Time history and linear spectral response of three extracted pulses using the CPE<sub>V-EN</sub> method for 40 Motions

Record #4: El Centro Array #4, Imperial Valley, 1979,  $M_W 6.5$



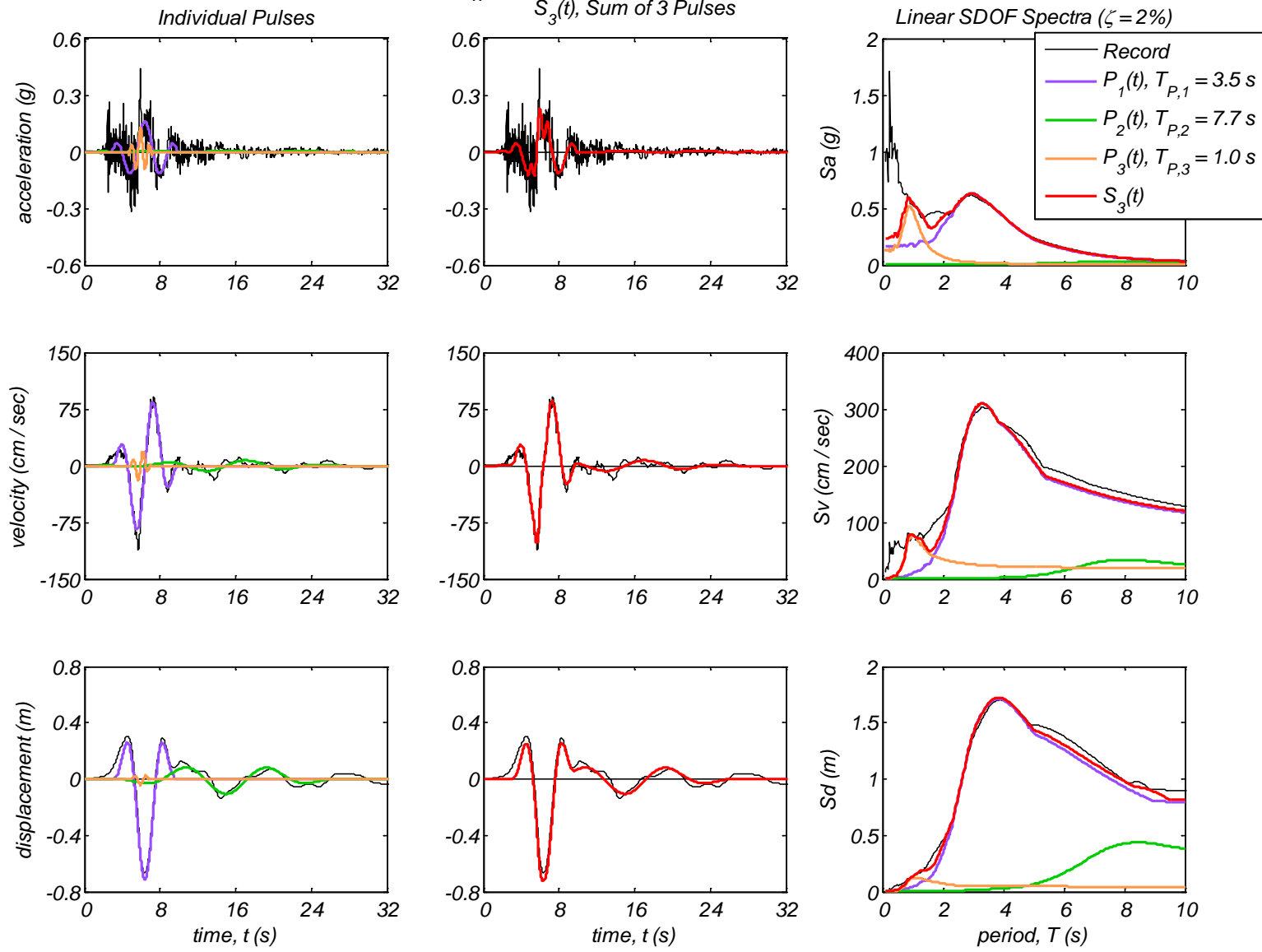
Appendix B2 – Time history and linear spectral response of three extracted pulses using the CPE<sub>V-EN</sub> method for 40 Motions

Record #5: El Centro Array #5, Imperial Valley, 1979,  $M_W 6.5$



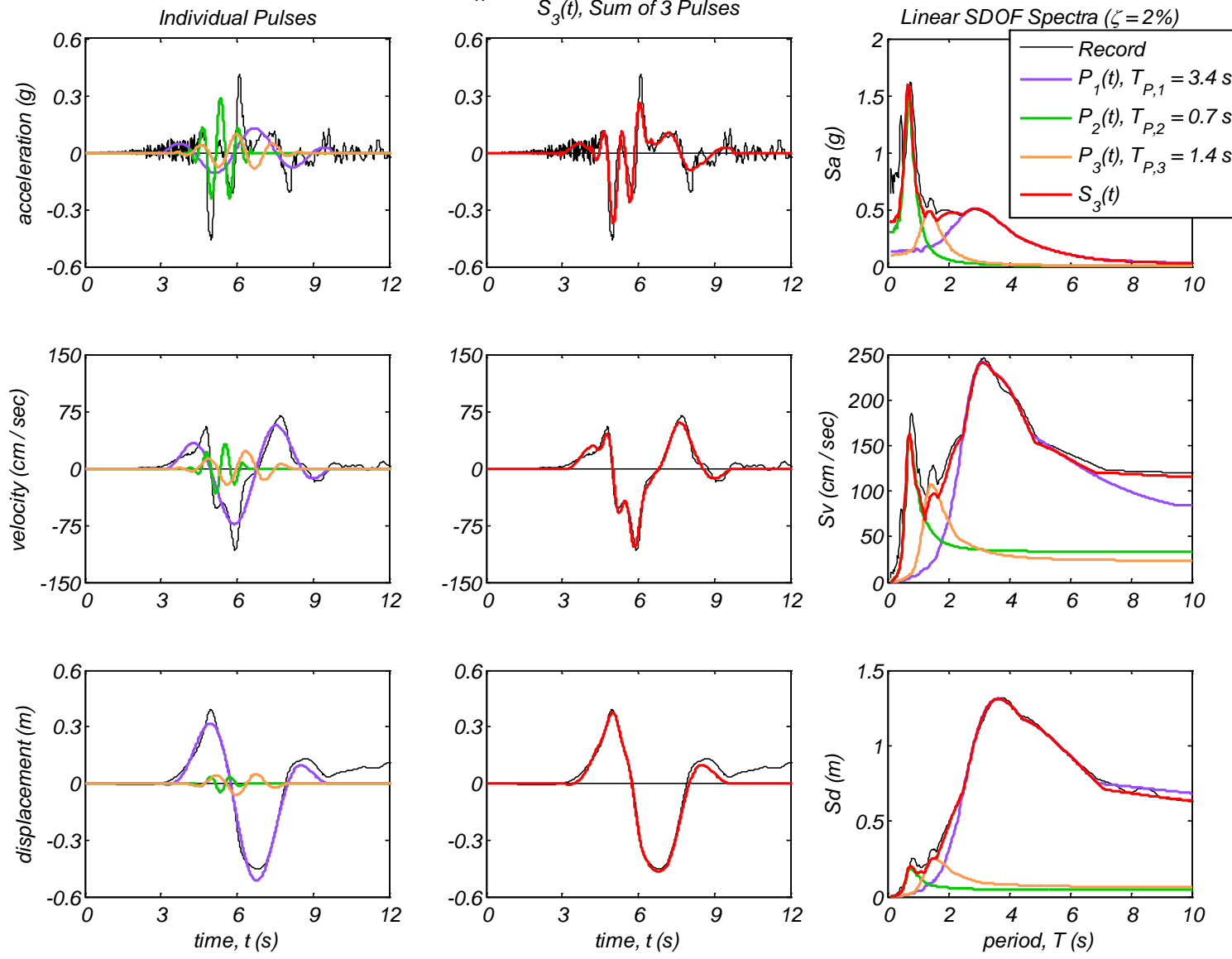
Appendix B2 – Time history and linear spectral response of three extracted pulses using the CPE<sub>V-EN</sub> method for 40 Motions

Record #6: El Centro Array #6, Imperial Valley, 1979,  $M_W 6.5$



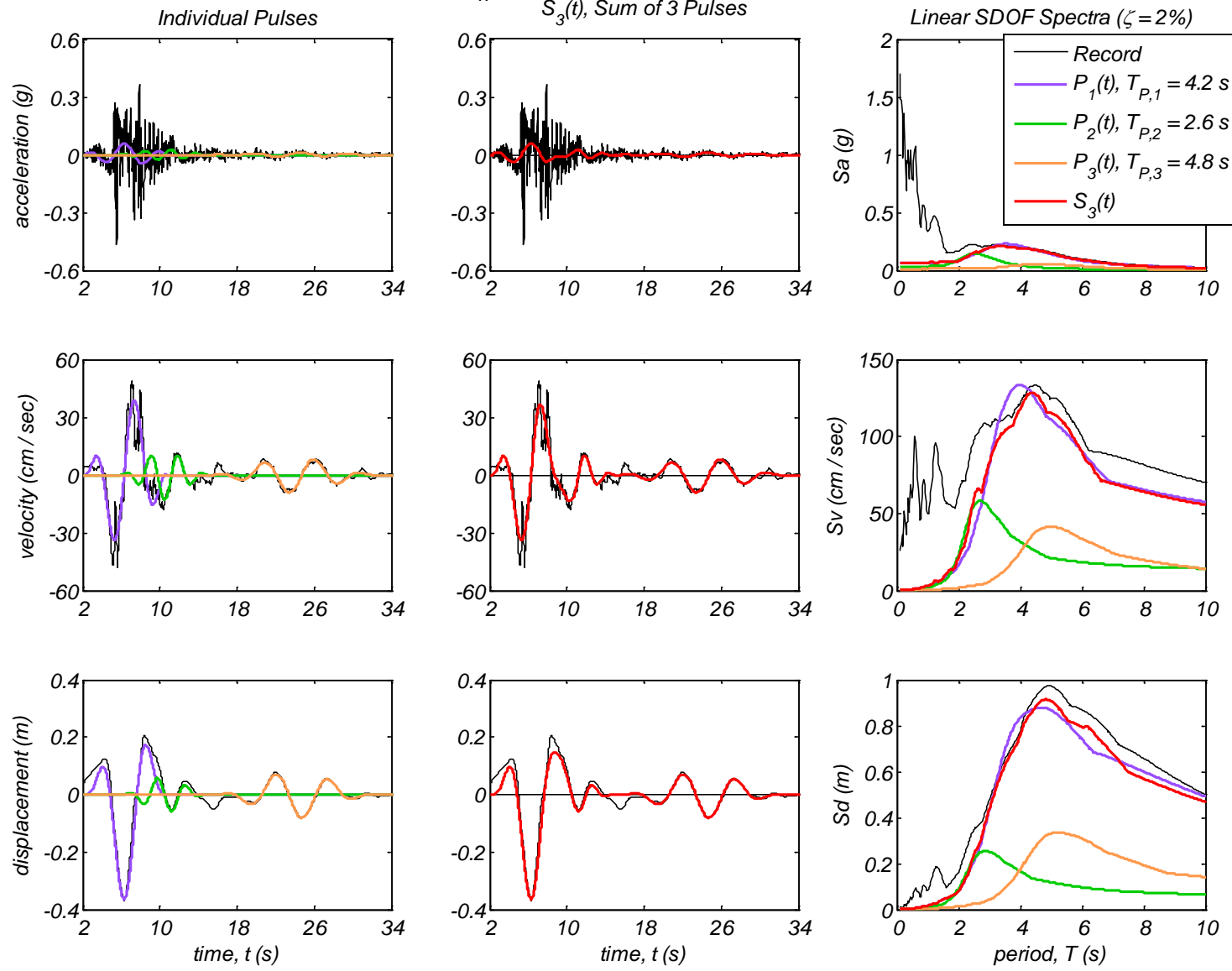
Appendix B2 – Time history and linear spectral response of three extracted pulses using the CPE<sub>V-EN</sub> method for 40 Motions

Record #7: El Centro Array #7, Imperial Valley, 1979,  $M_W 6.5$



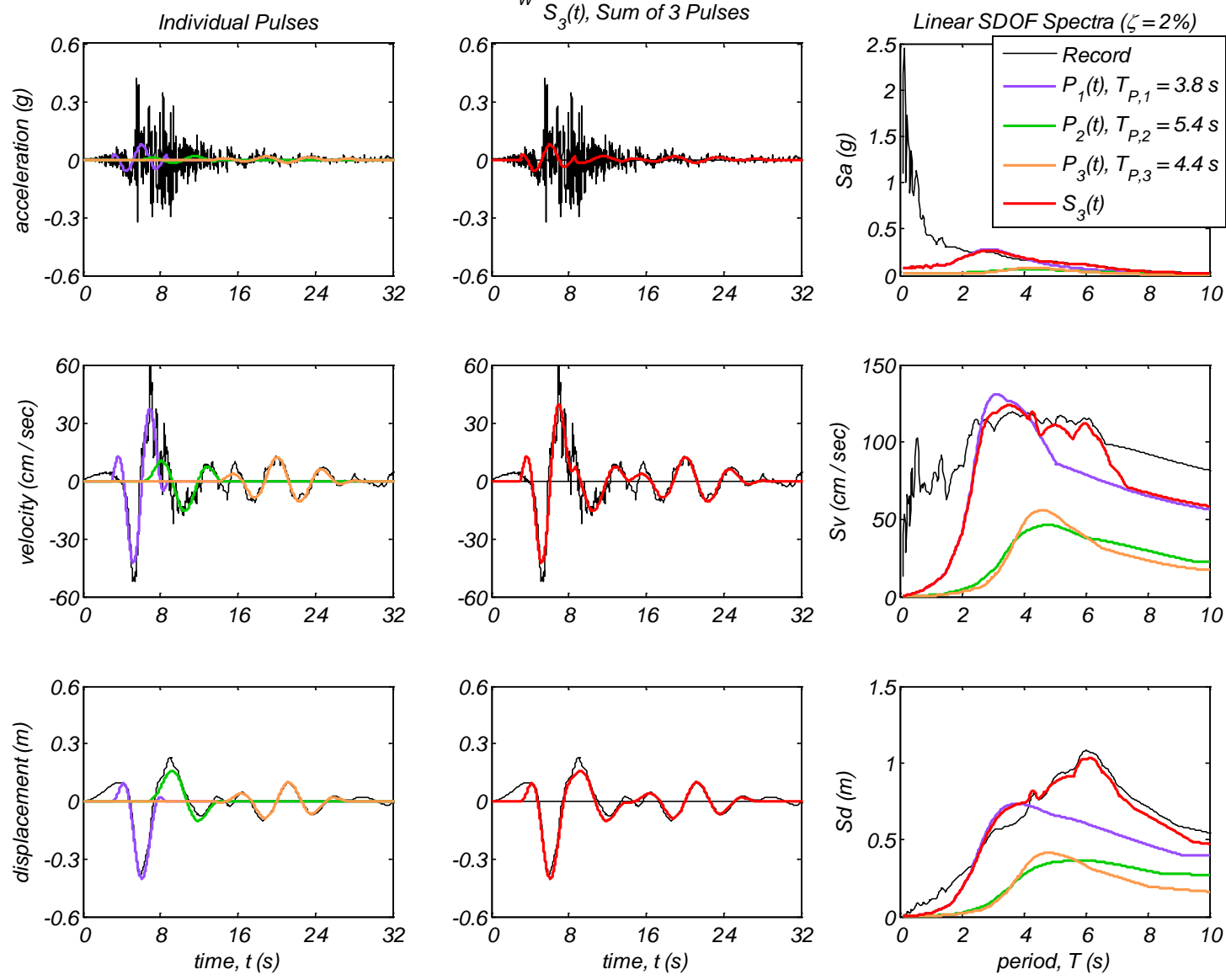
Appendix B2 – Time history and linear spectral response of three extracted pulses using the CPE<sub>V-EN</sub> method for 40 Motions

Record #8: El Centro Array #8, Imperial Valley, 1979,  $M_W 6.5$

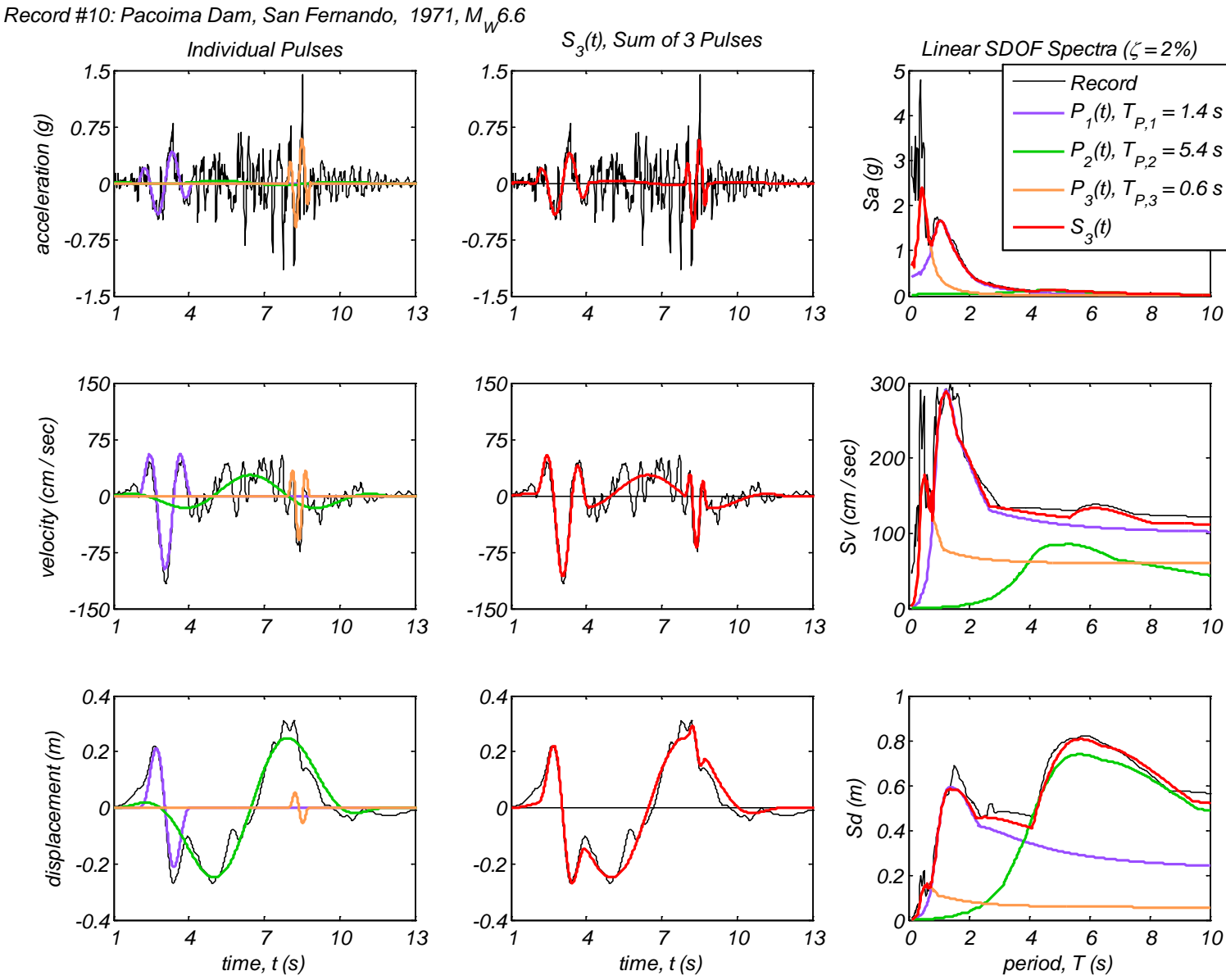


Appendix B2 – Time history and linear spectral response of three extracted pulses using the CPE<sub>V-EN</sub> method for 40 Motions

Record #9: El Centro Differential Array, Imperial Valley, 1979,  $M_W 6.5$

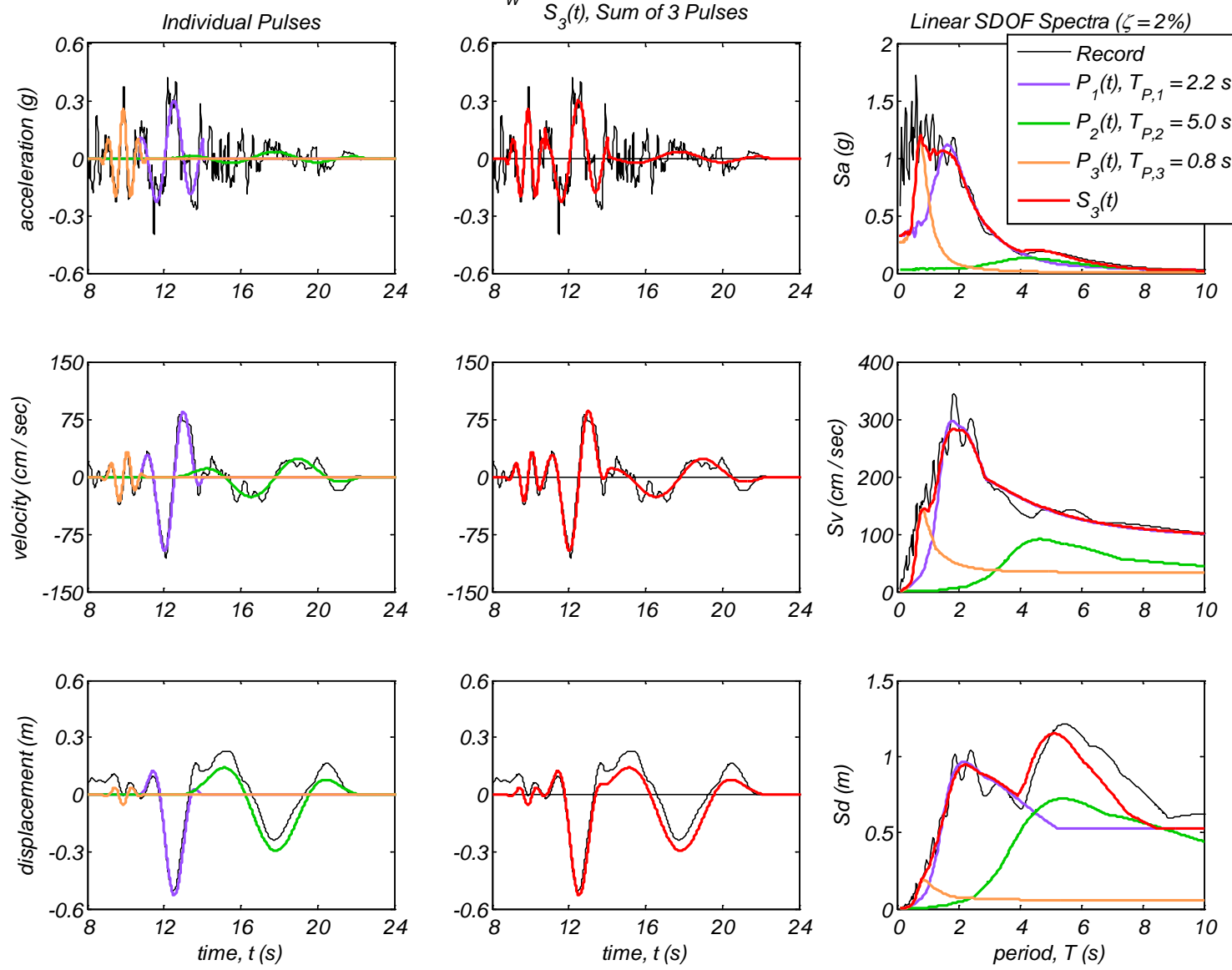


Appendix B2 – Time history and linear spectral response of three extracted pulses using the CPE<sub>V-EN</sub> method for 40 Motions



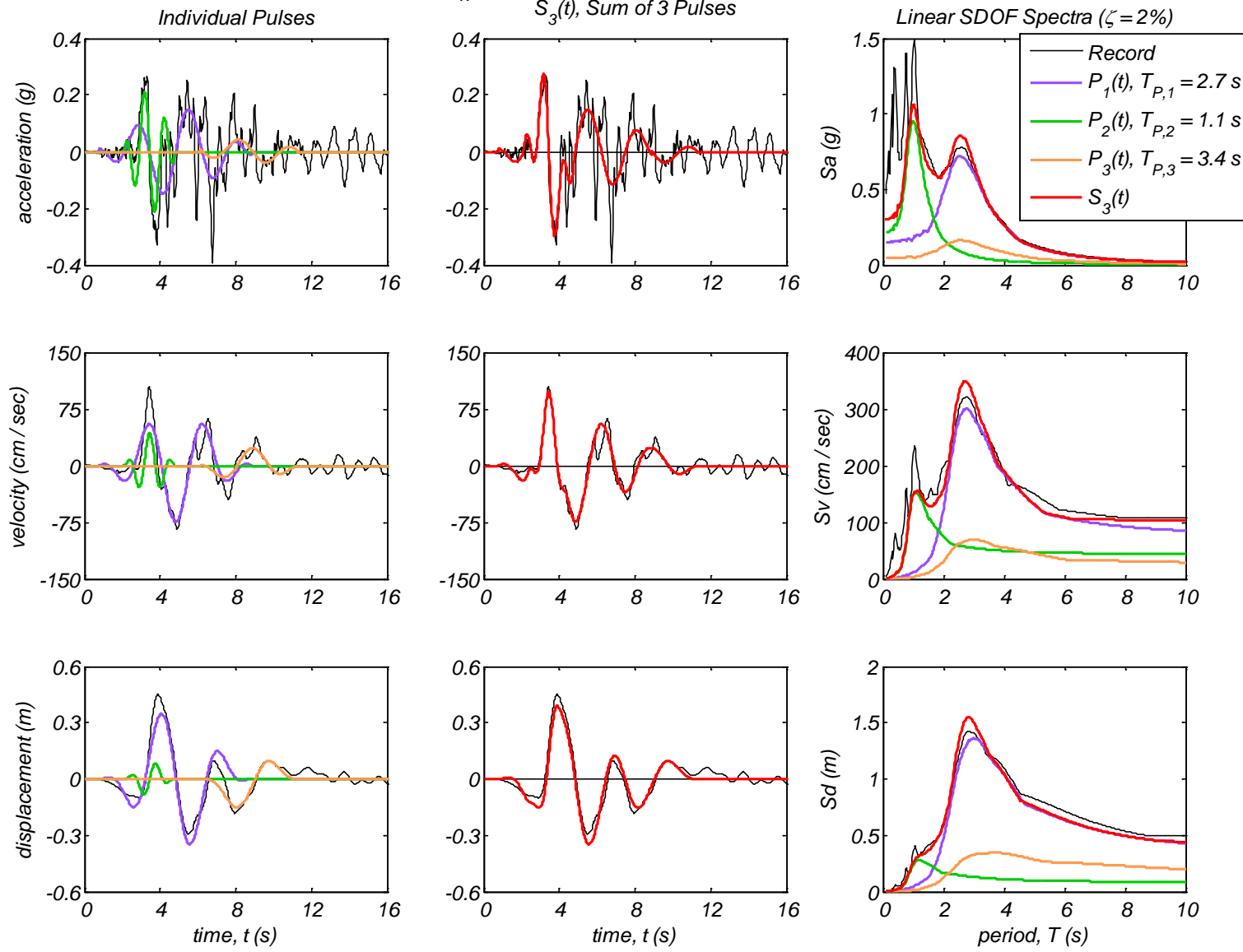
Appendix B2 – Time history and linear spectral response of three extracted pulses using the CPE<sub>V-EN</sub> method for 40 Motions

Record #11: Parachute Test Site, Superstition Hills(B), 1987,  $M_w 6.6$



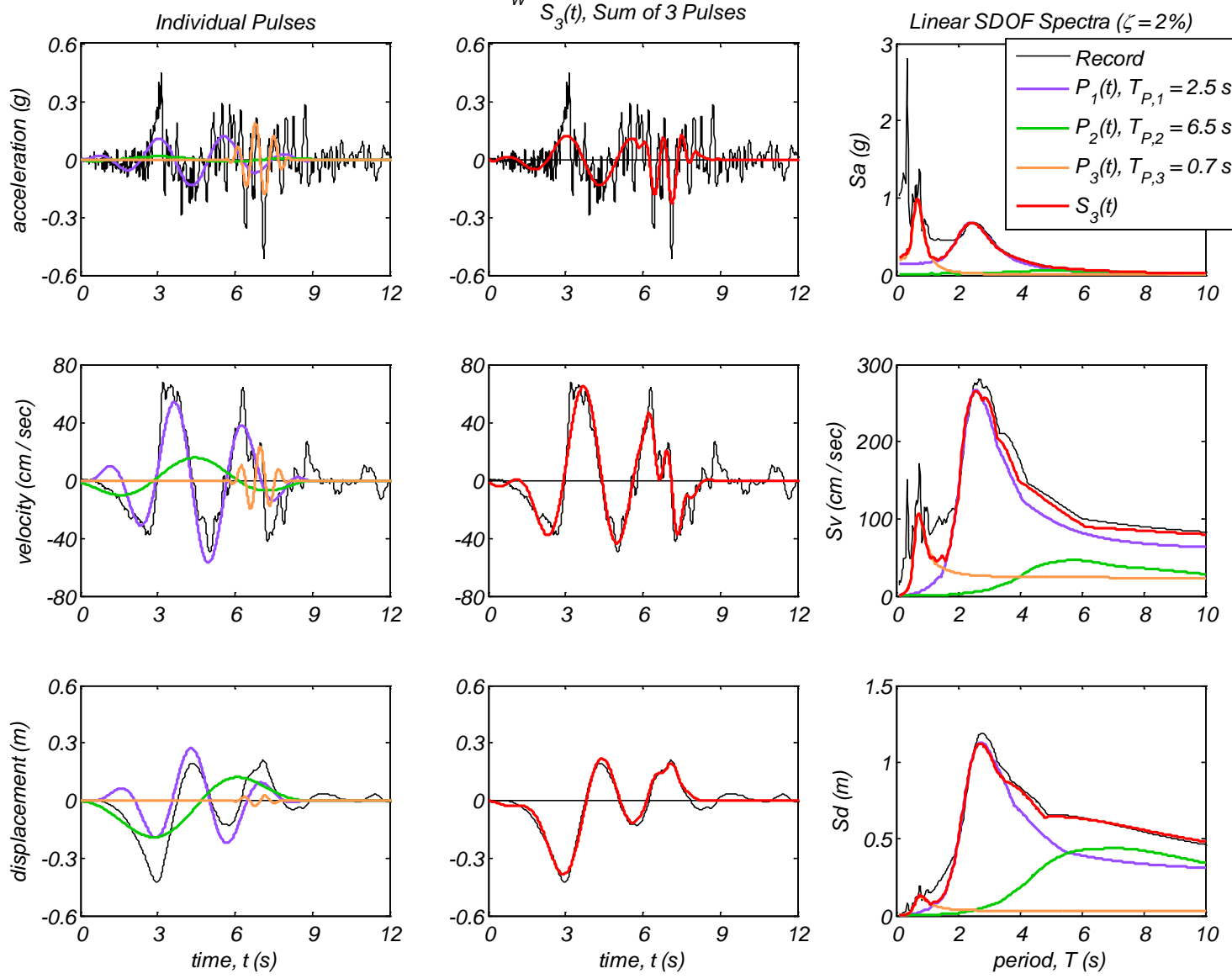
Appendix B2 – Time history and linear spectral response of three extracted pulses using the CPE<sub>V-EN</sub> method for 40 Motions

Record #12: Jensen Filter Plant, Northridge, 1994,  $M_W 6.7$

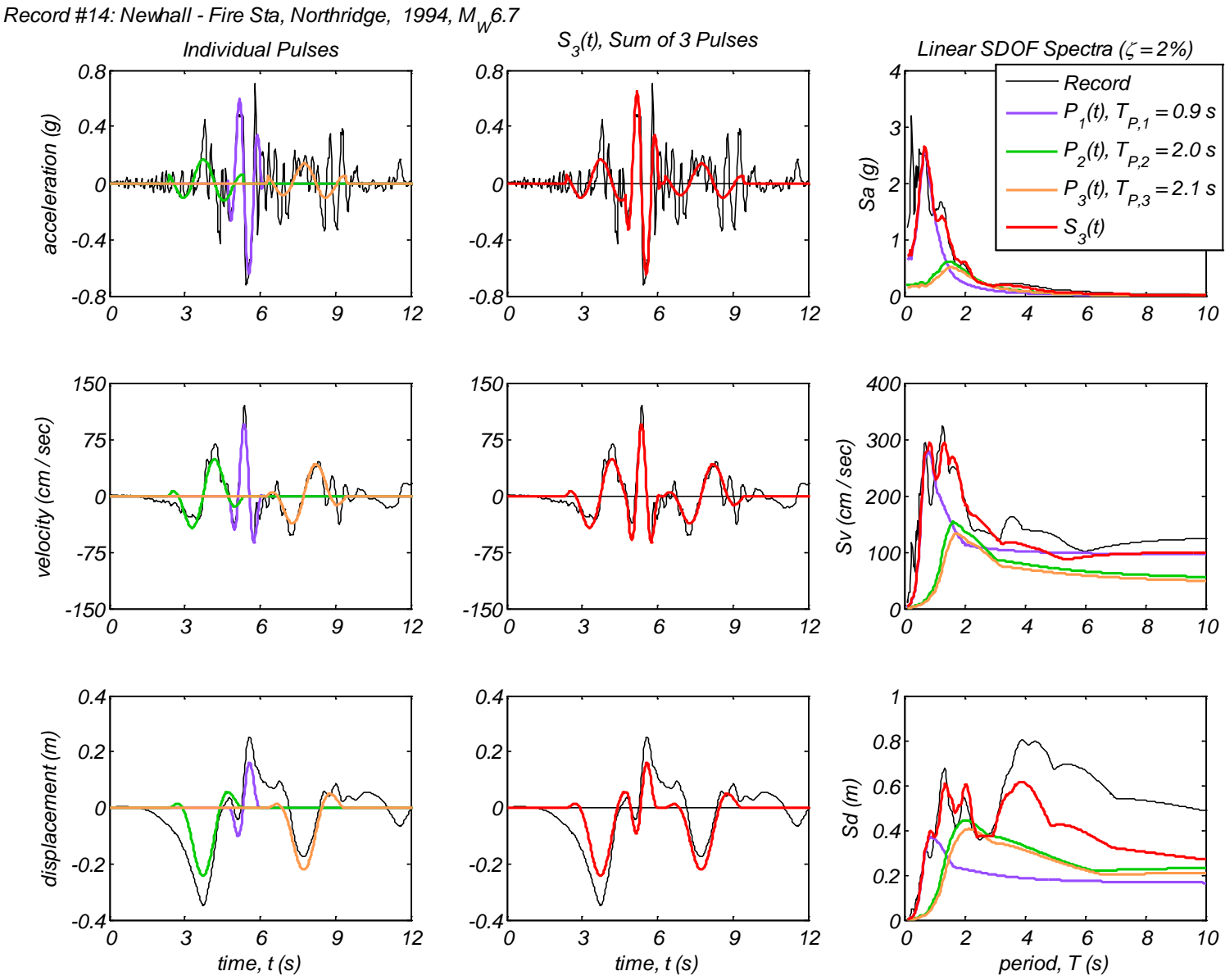


Appendix B2 – Time history and linear spectral response of three extracted pulses using the CPE<sub>V-EN</sub> method for 40 Motions

Record #13: Jensen Filter Plant Generator, Northridge, 1994,  $M_W 6.7$

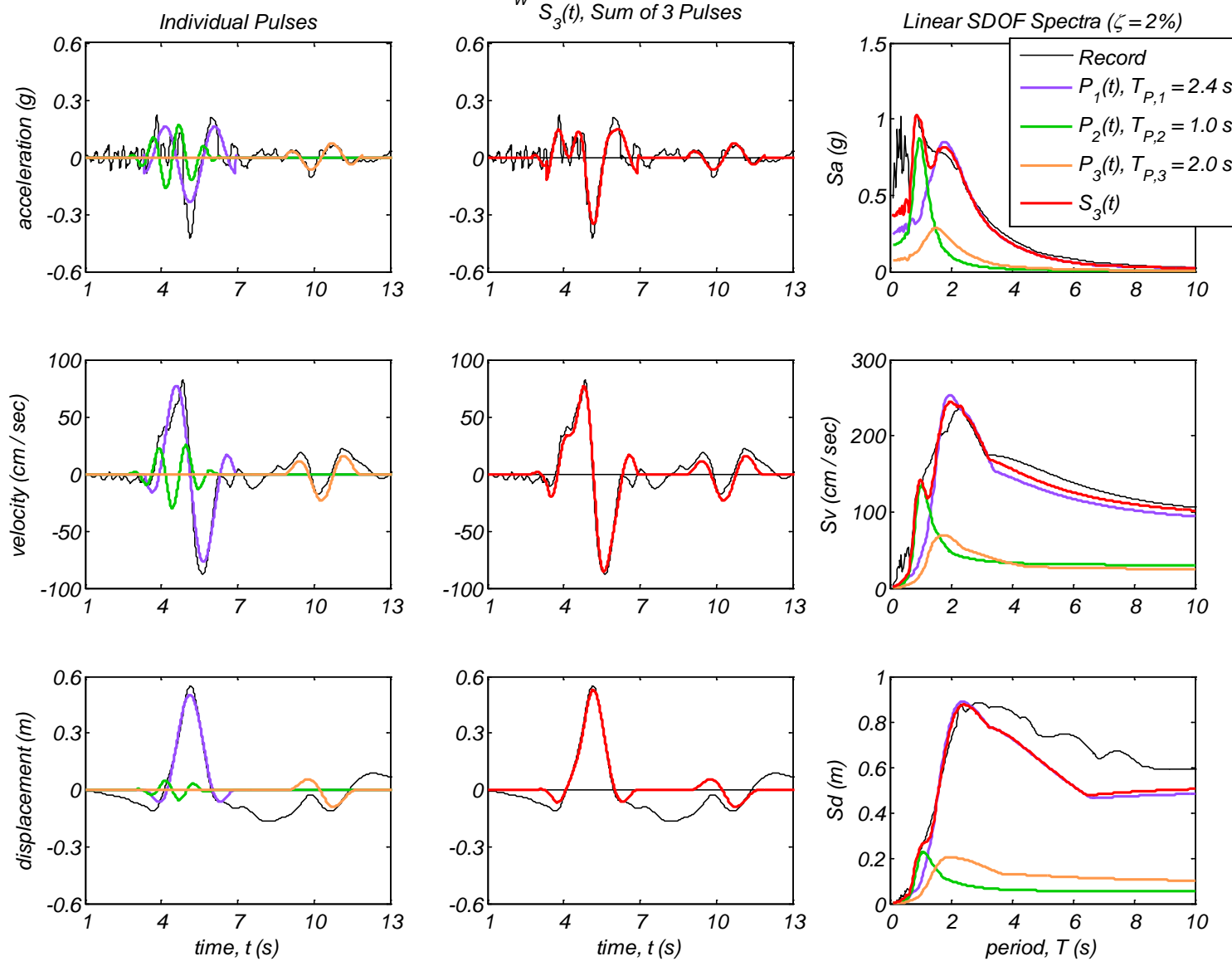


Appendix B2 – Time history and linear spectral response of three extracted pulses using the CPE<sub>V-EN</sub> method for 40 Motions

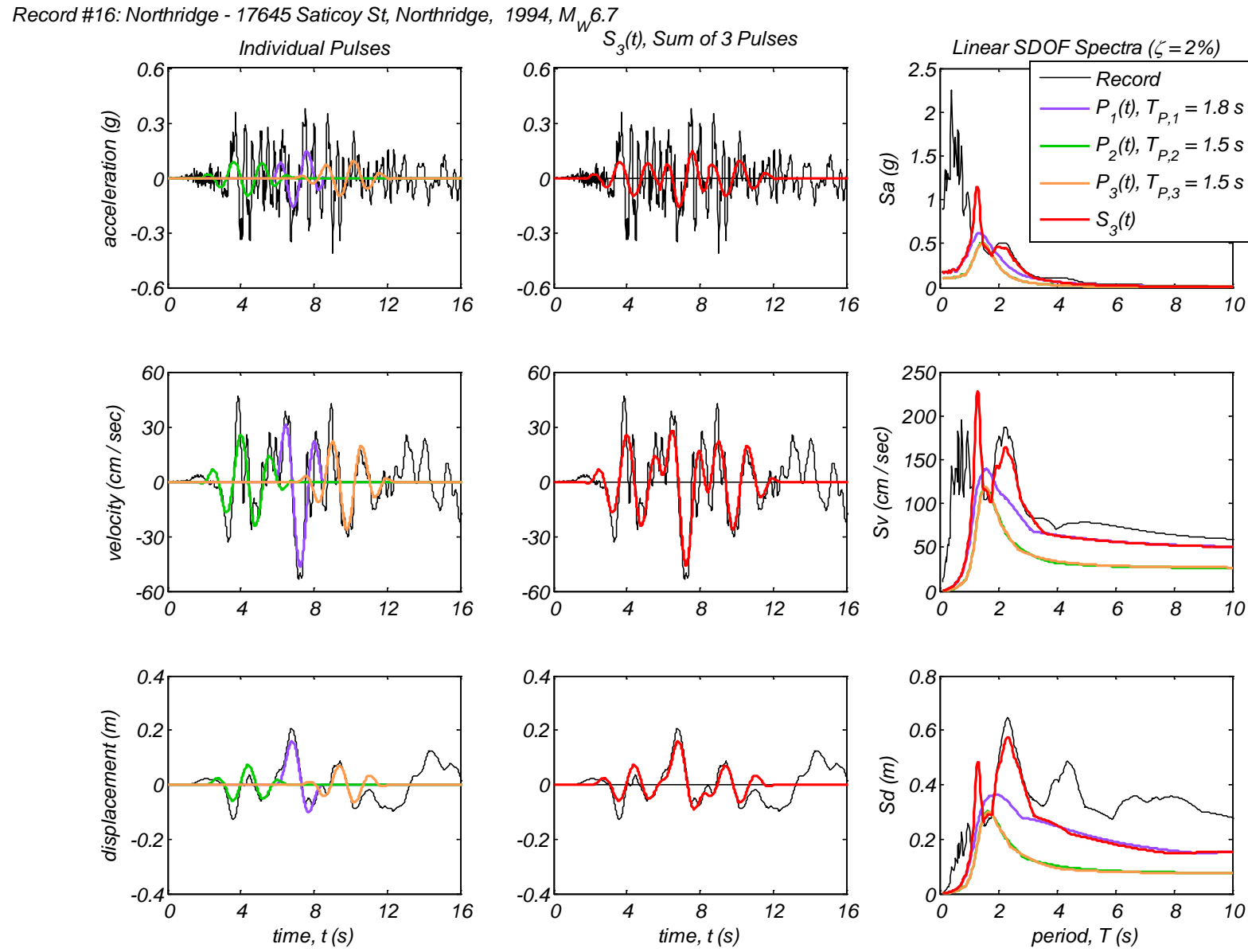


Appendix B2 – Time history and linear spectral response of three extracted pulses using the CPE<sub>V-EN</sub> method for 40 Motions

Record #15: Newhall - W. Pico Canyon Rd., Northridge, 1994,  $M_W 6.7$

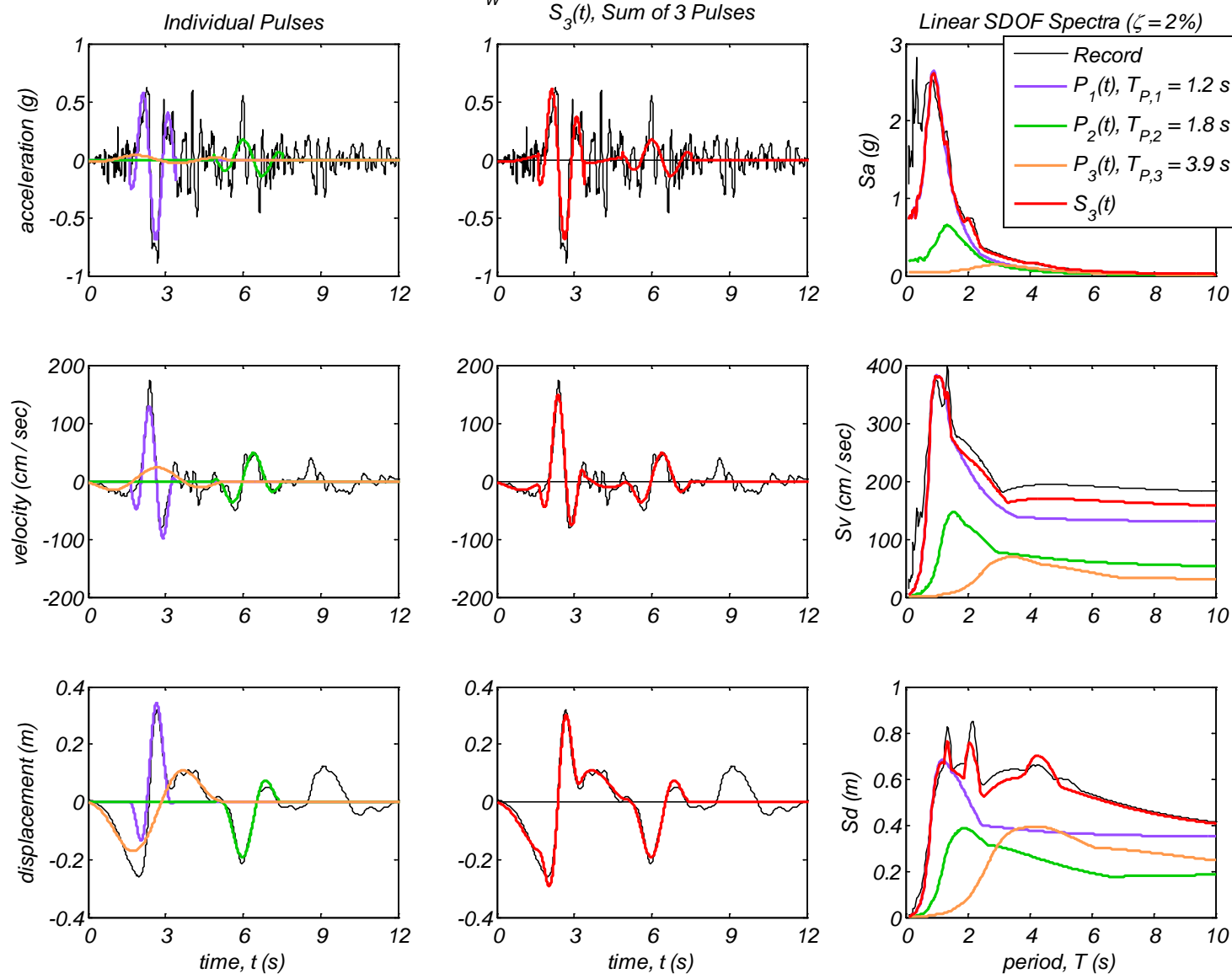


Appendix B2 – Time history and linear spectral response of three extracted pulses using the CPE<sub>V-EN</sub> method for 40 Motions

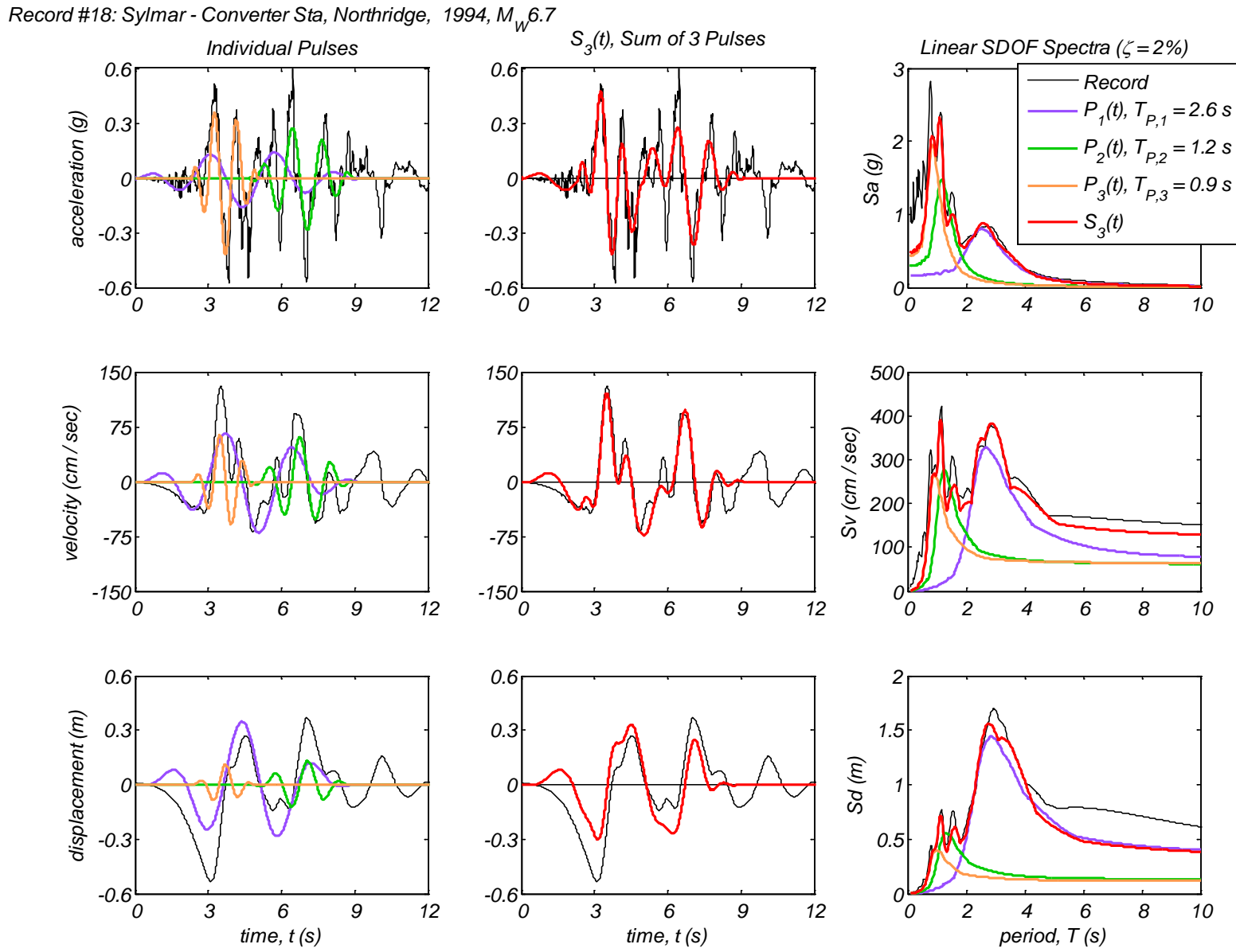


Appendix B2 – Time history and linear spectral response of three extracted pulses using the CPE<sub>V-EN</sub> method for 40 Motions

Record #17: Rinaldi Receiving Sta, Northridge, 1994,  $M_W 6.7$

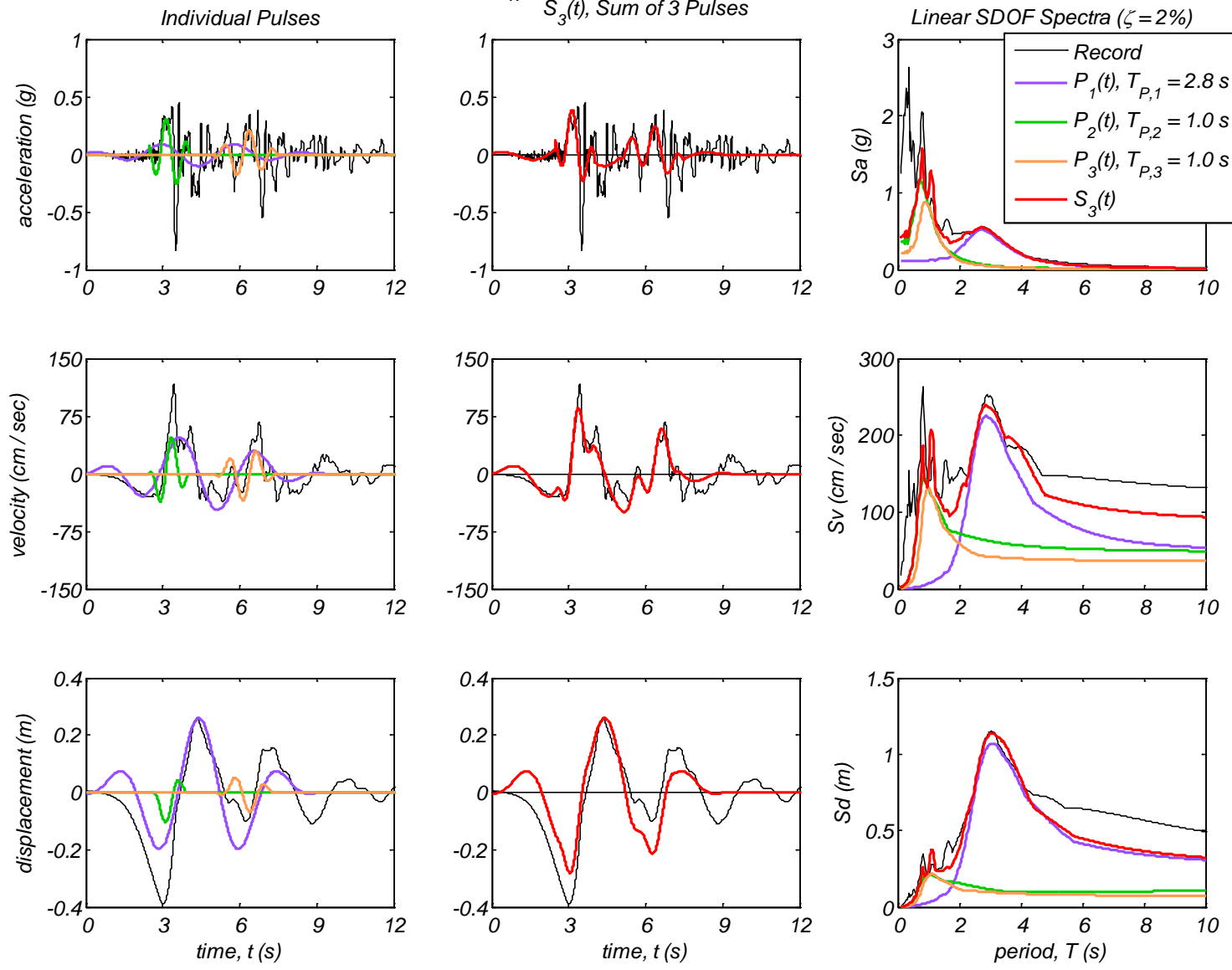


Appendix B2 – Time history and linear spectral response of three extracted pulses using the CPE<sub>V-EN</sub> method for 40 Motions



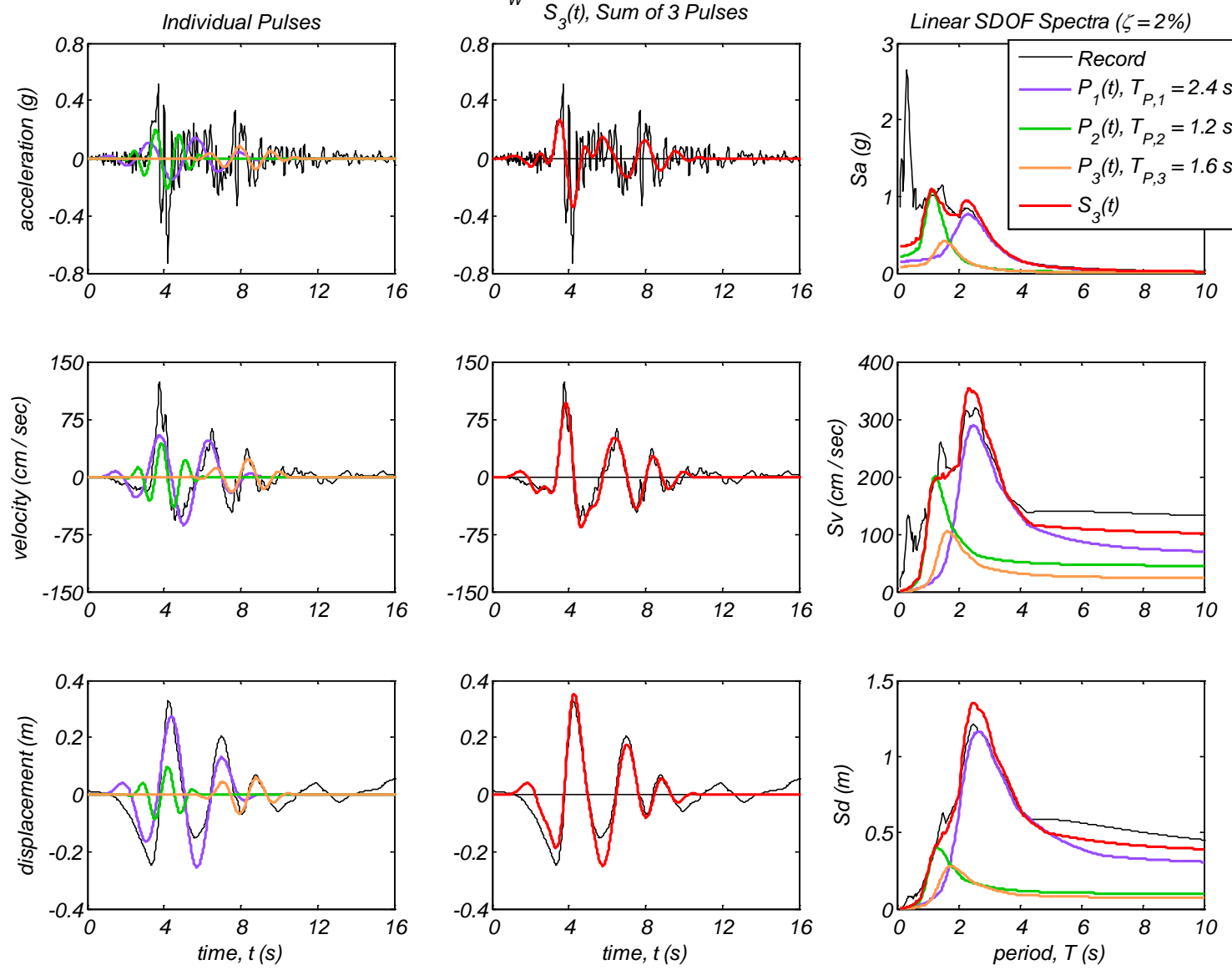
Appendix B2 – Time history and linear spectral response of three extracted pulses using the CPE<sub>V-EN</sub> method for 40 Motions

Record #19: Sylmar - Converter Sta East, Northridge, 1994,  $M_W$  6.7



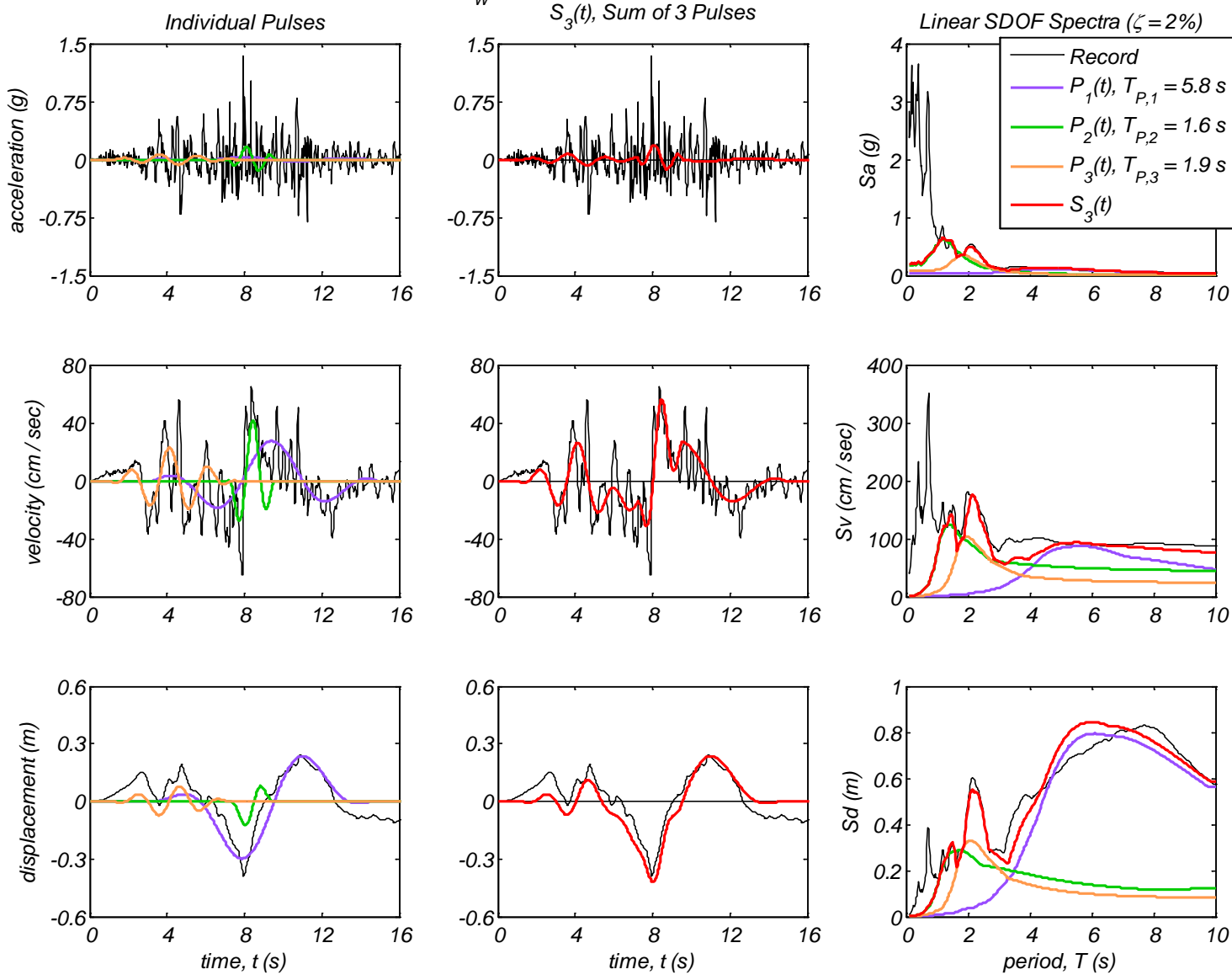
Appendix B2 – Time history and linear spectral response of three extracted pulses using the CPE<sub>V-EN</sub> method for 40 Motions

Record #20: Sylmar - Olive ViewMed FF, Northridge, 1994,  $M_W 6.7$

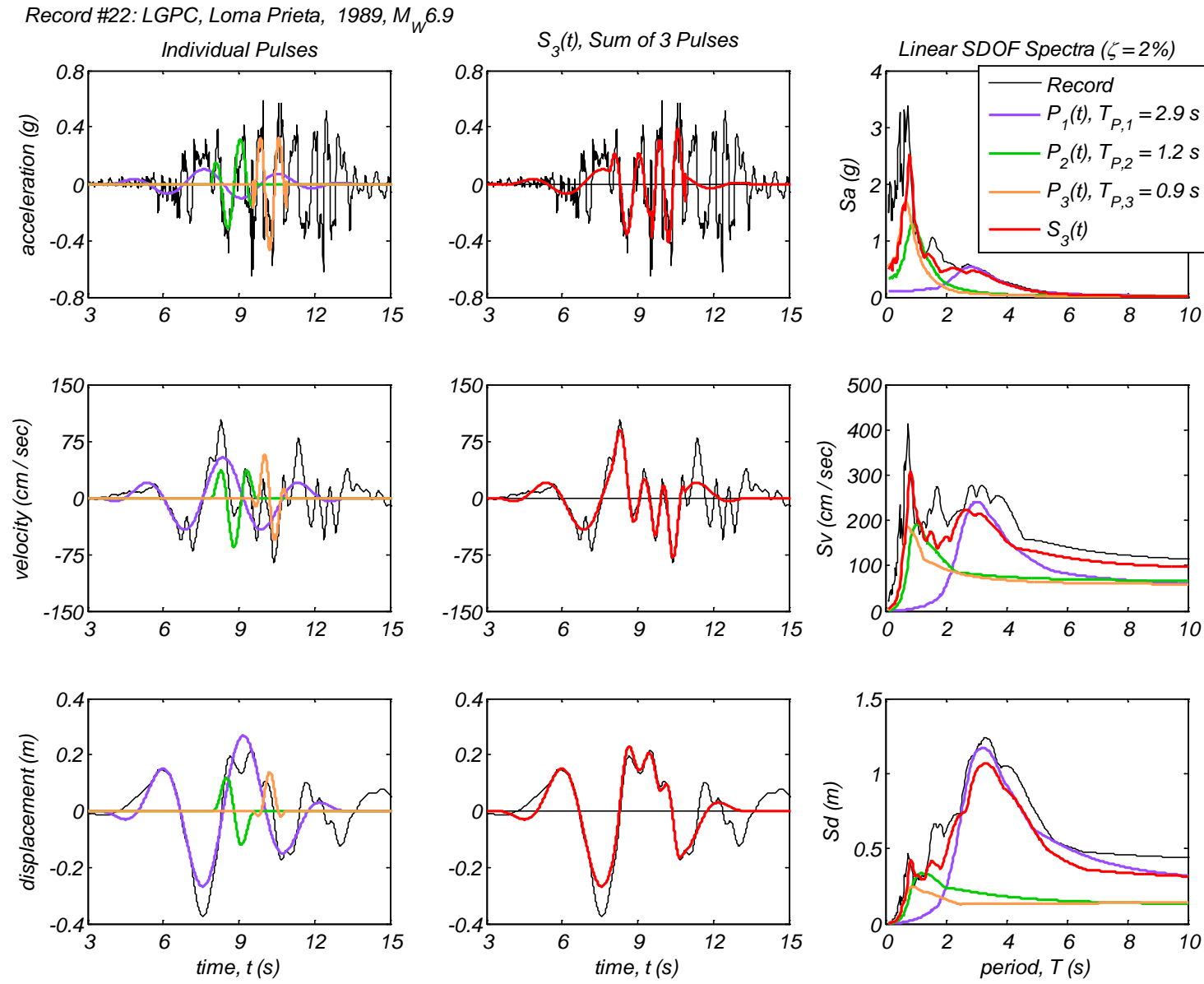


Appendix B2 – Time history and linear spectral response of three extracted pulses using the CPE<sub>V-EN</sub> method for 40 Motions

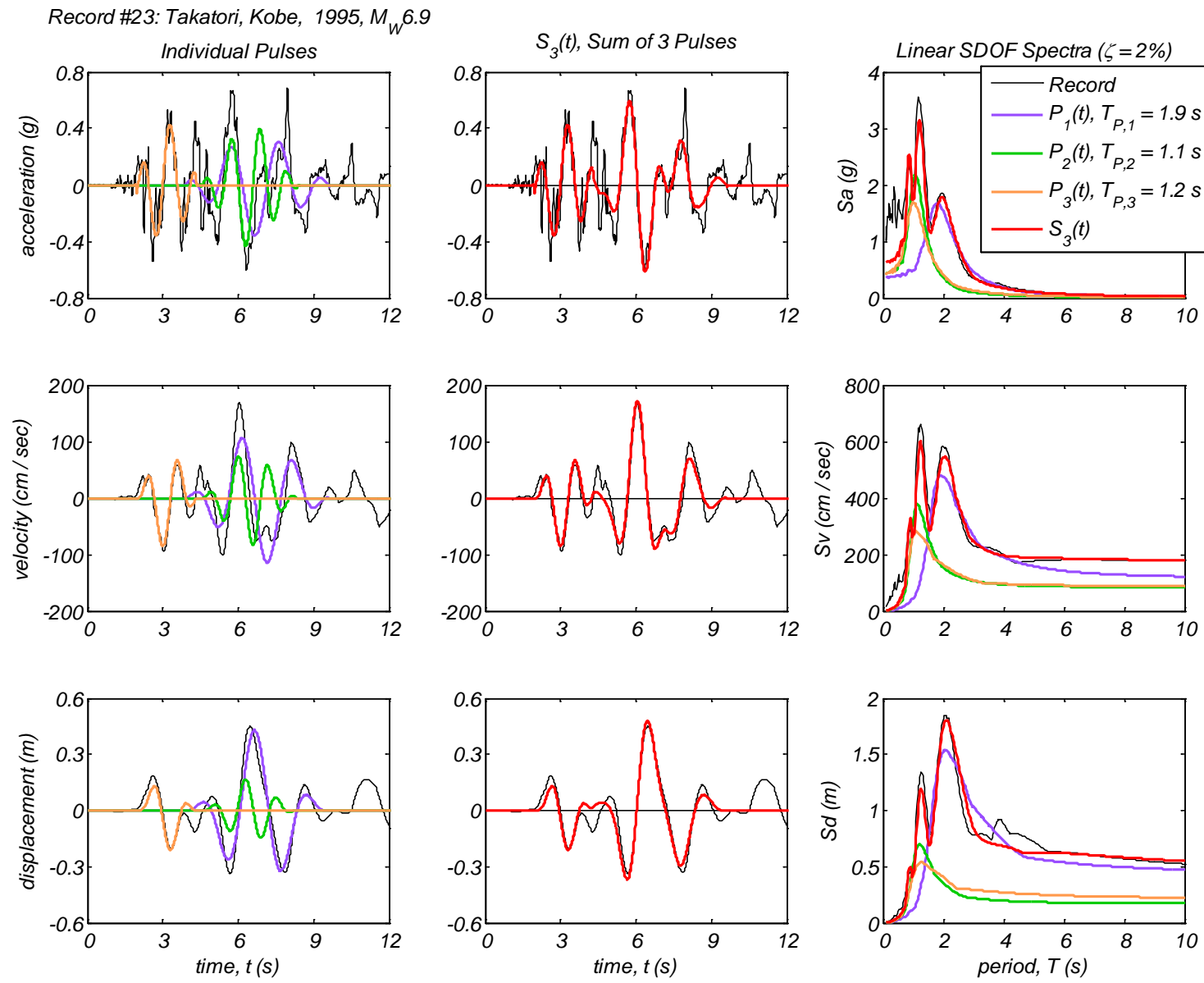
Record #21: Tarzana, Cedar Hill, Northridge, 1994,  $M_W 6.7$



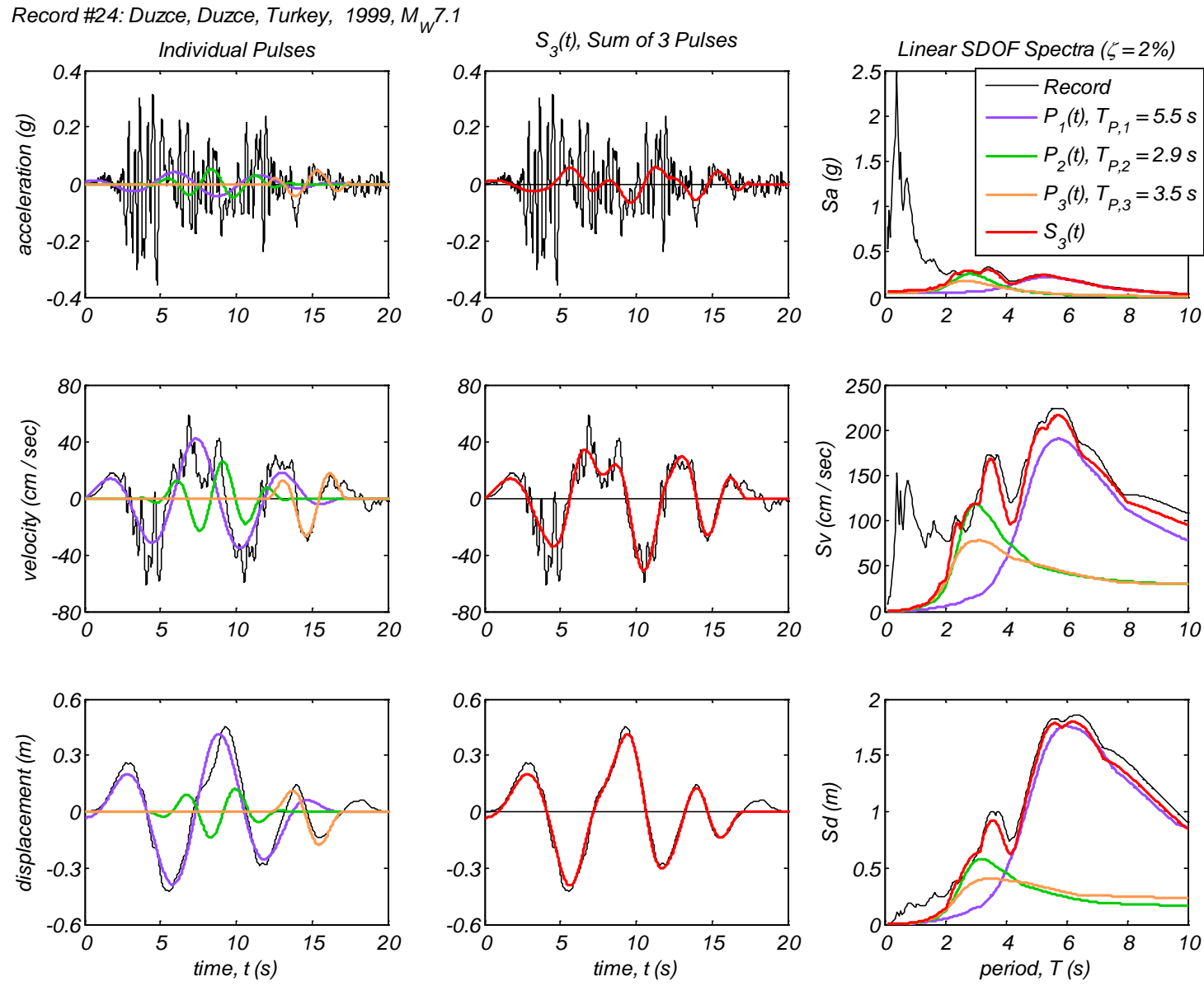
Appendix B2 – Time history and linear spectral response of three extracted pulses using the CPE<sub>V-EN</sub> method for 40 Motions



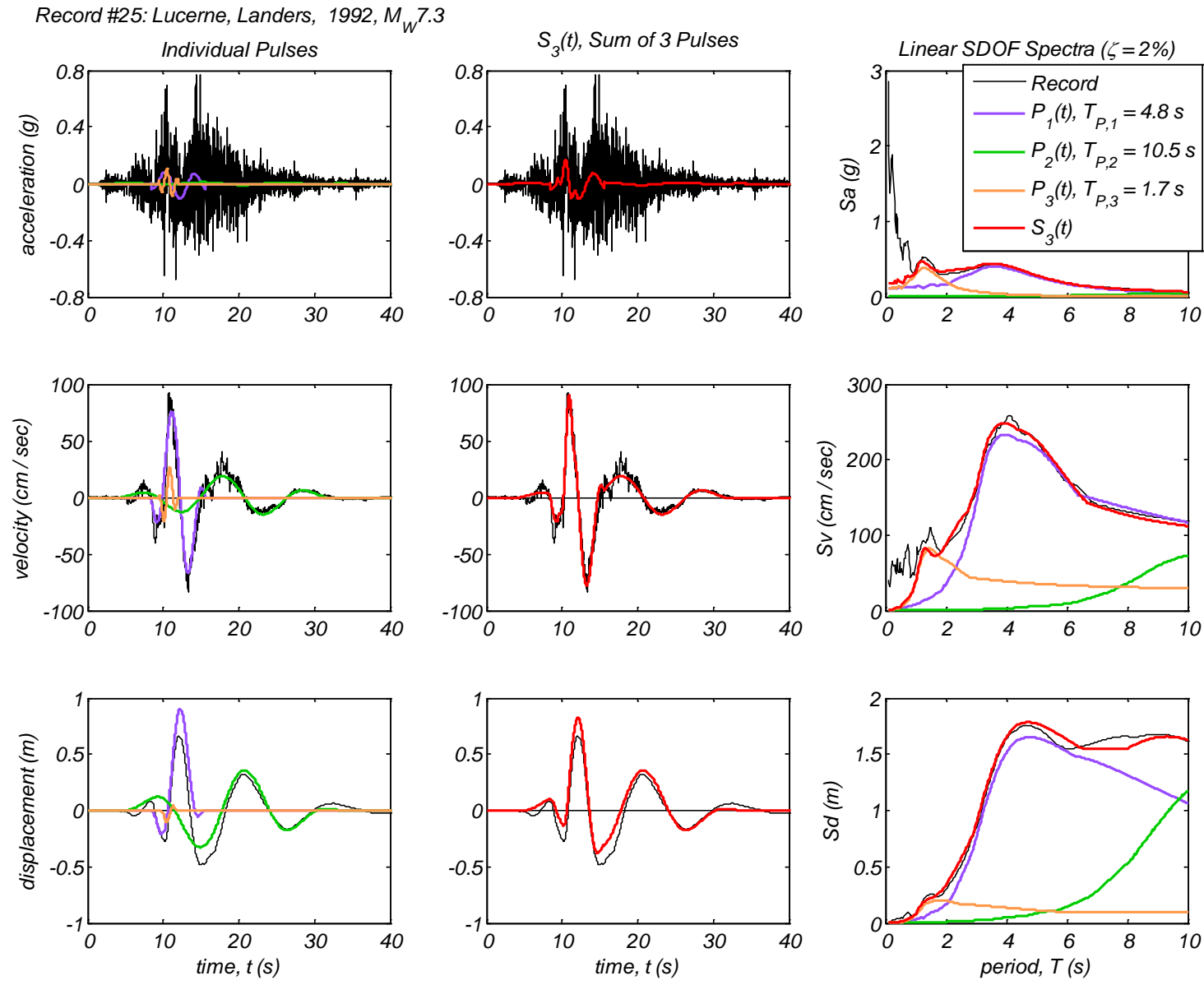
Appendix B2 – Time history and linear spectral response of three extracted pulses using the CPE<sub>V-EN</sub> method for 40 Motions



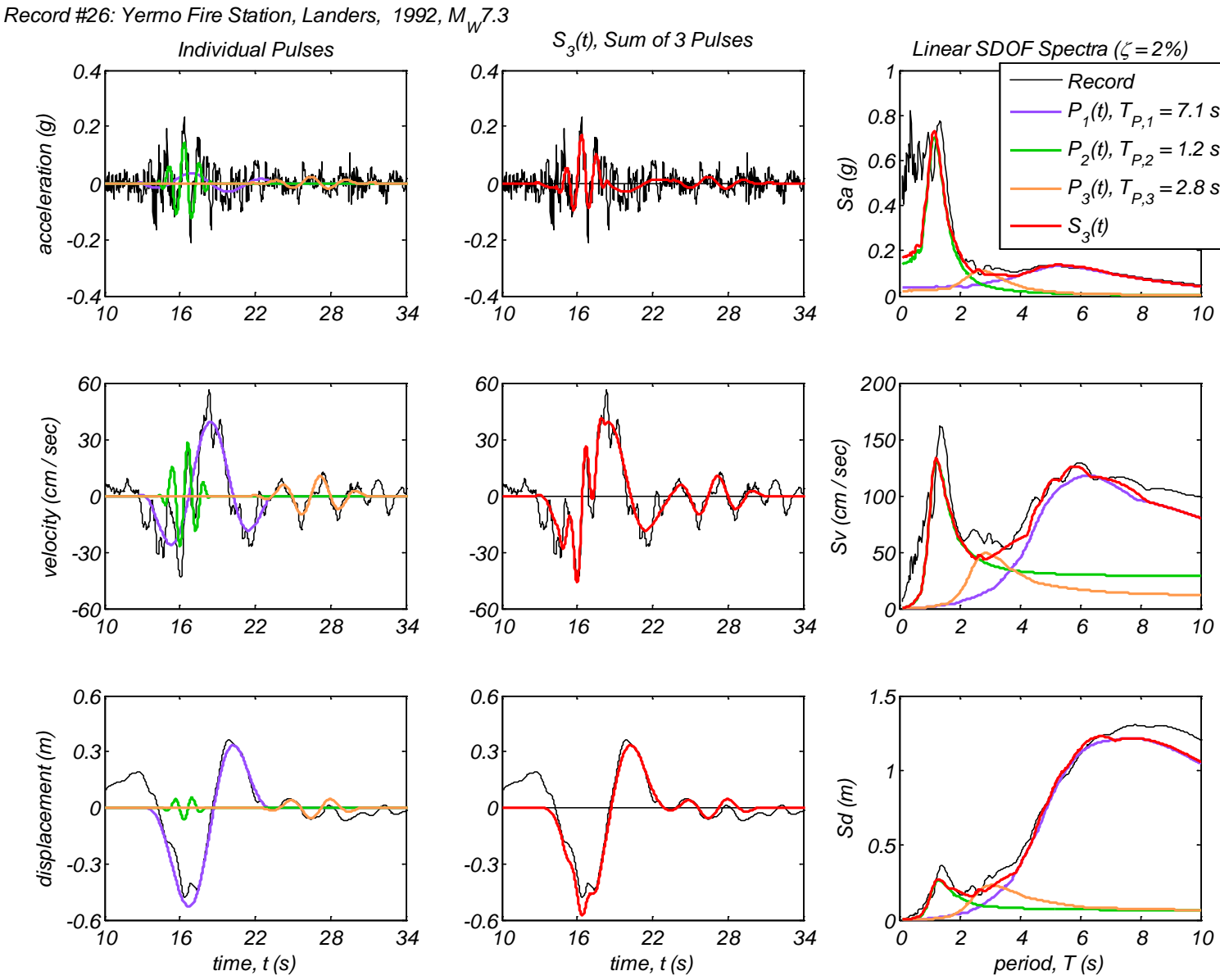
Appendix B2 – Time history and linear spectral response of three extracted pulses using the CPE<sub>V-EN</sub> method for 40 Motions



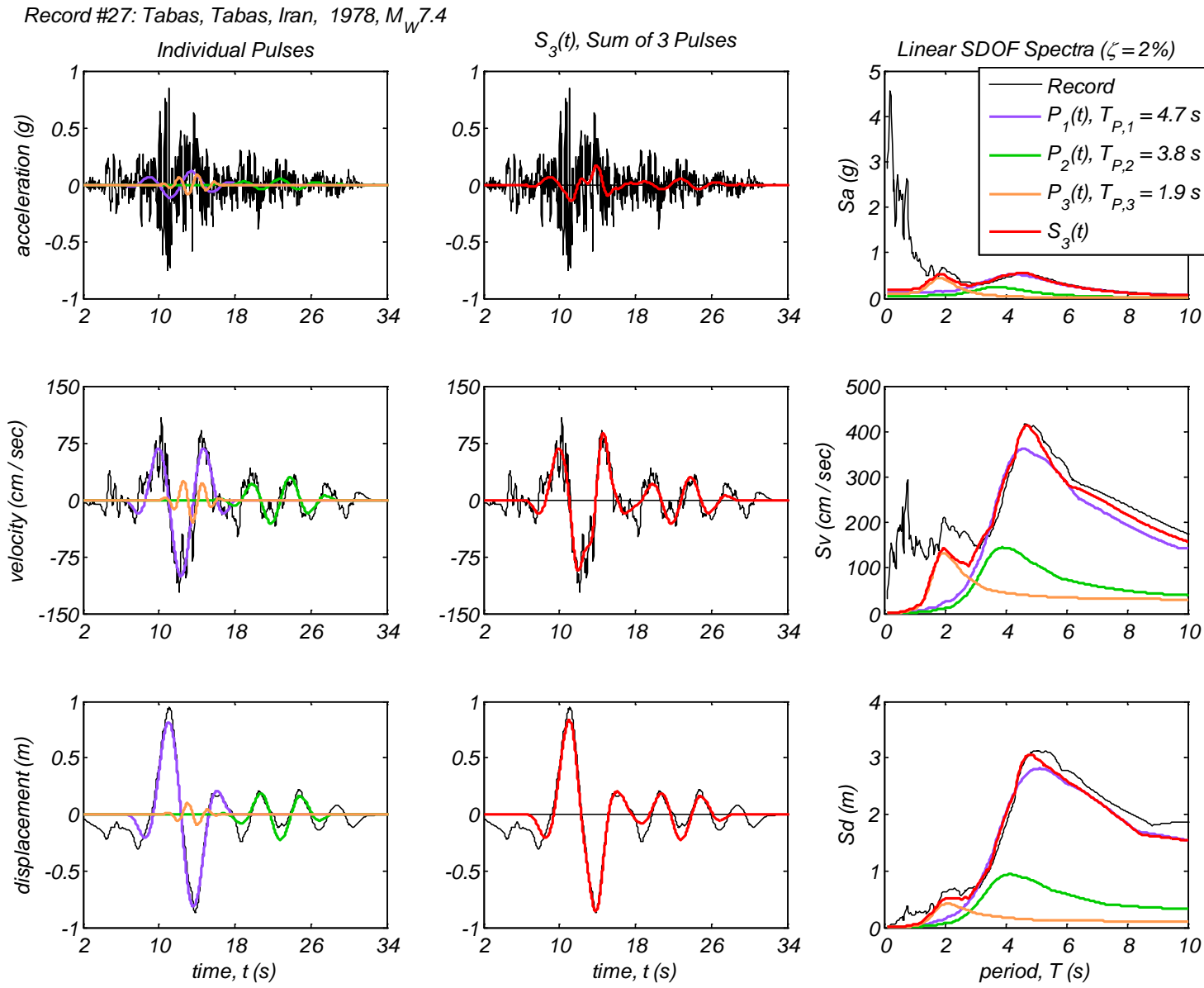
Appendix B2 – Time history and linear spectral response of three extracted pulses using the CPE<sub>V-EN</sub> method for 40 Motions



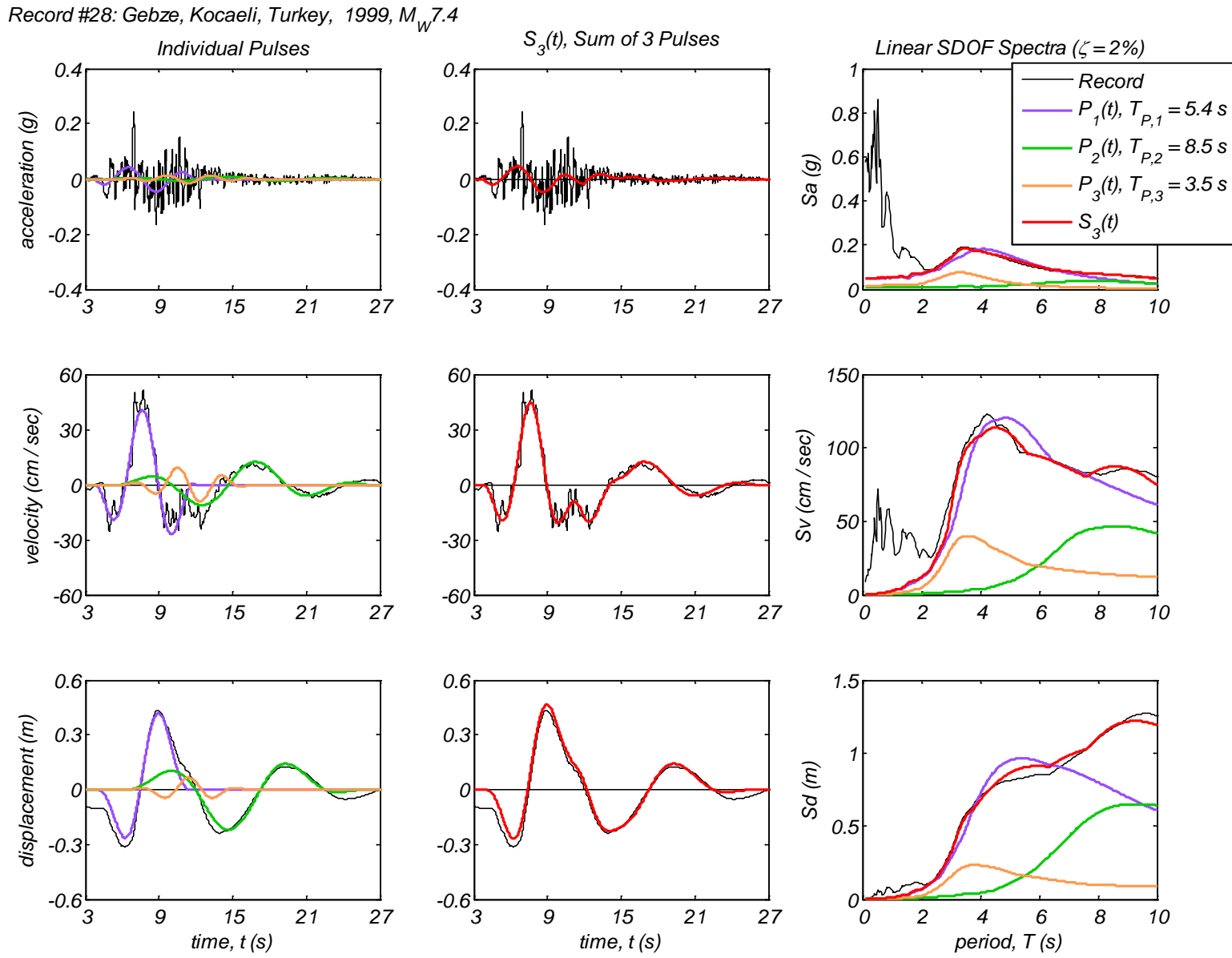
Appendix B2 – Time history and linear spectral response of three extracted pulses using the CPE<sub>V-EN</sub> method for 40 Motions



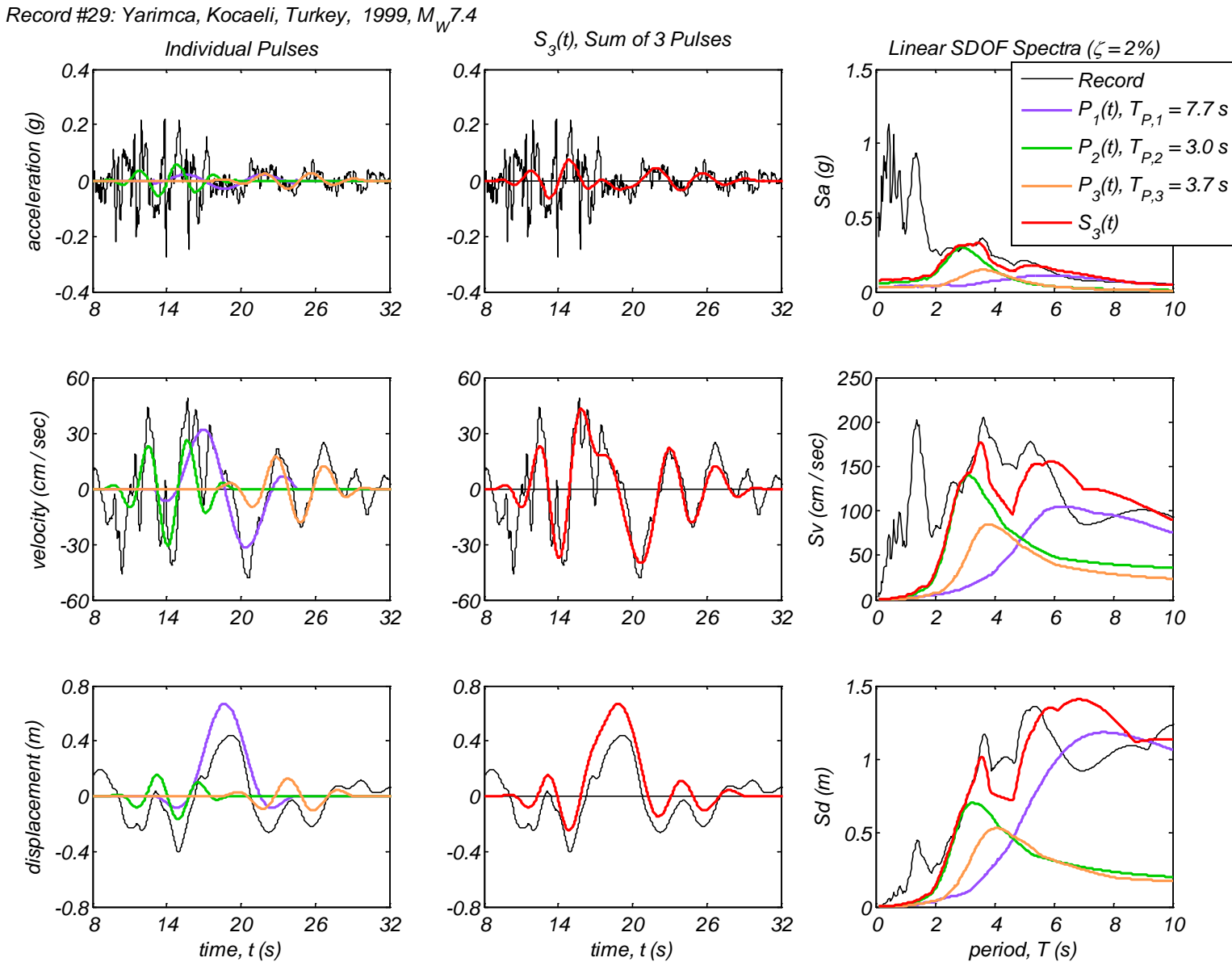
Appendix B2 – Time history and linear spectral response of three extracted pulses using the CPE<sub>V-EN</sub> method for 40 Motions



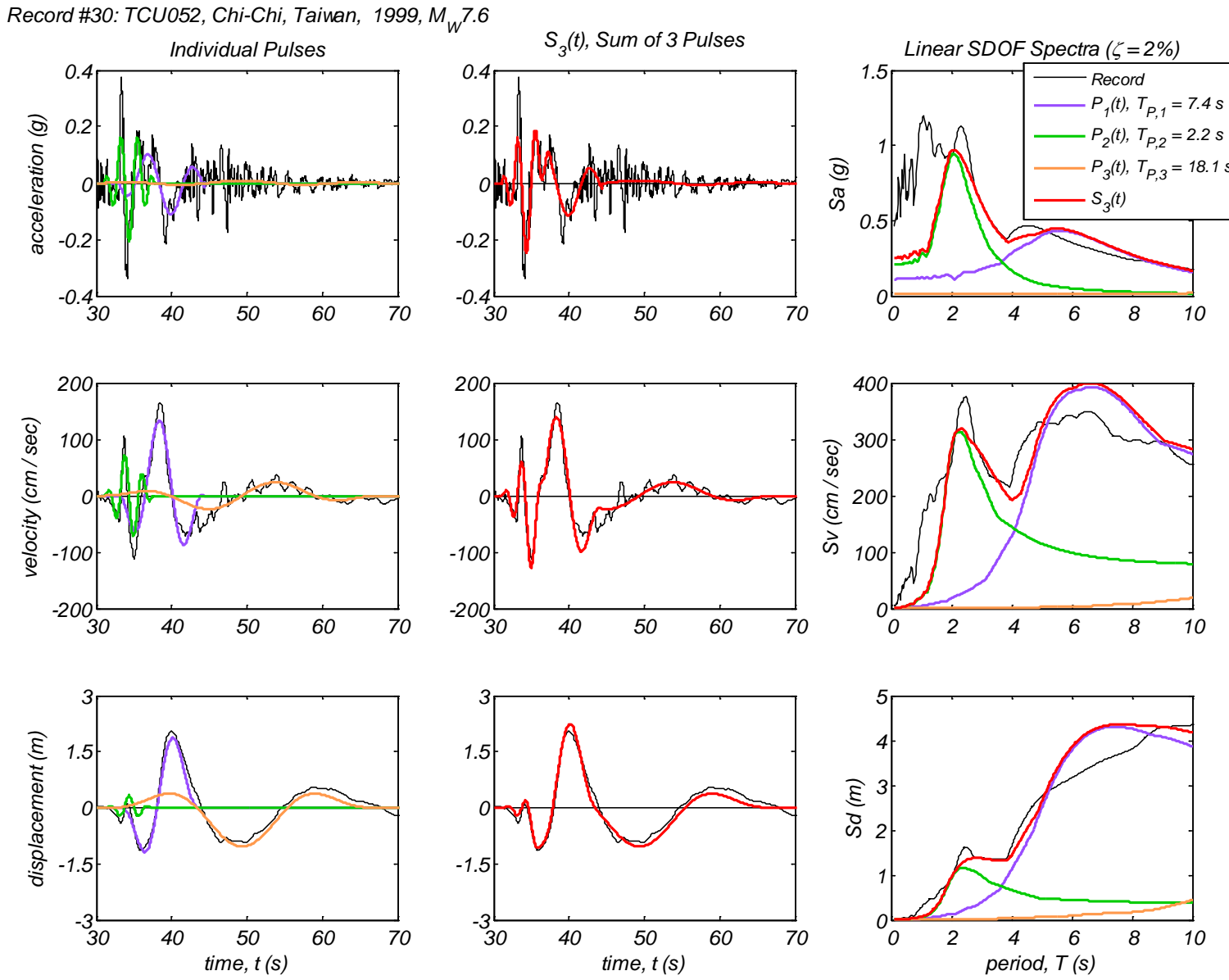
Appendix B2 – Time history and linear spectral response of three extracted pulses using the CPE<sub>V-EN</sub> method for 40 Motions



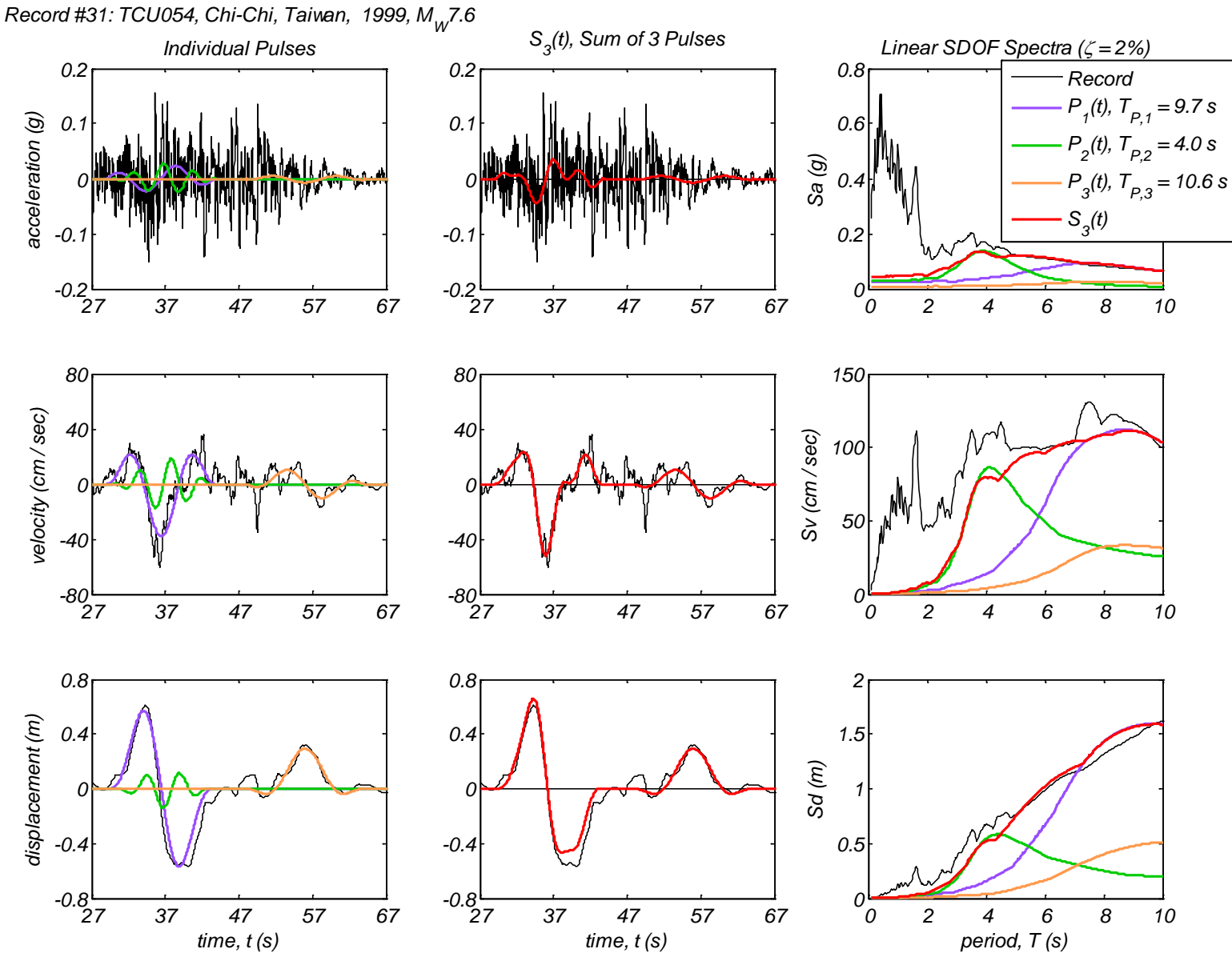
Appendix B2 – Time history and linear spectral response of three extracted pulses using the CPE<sub>V-EN</sub> method for 40 Motions



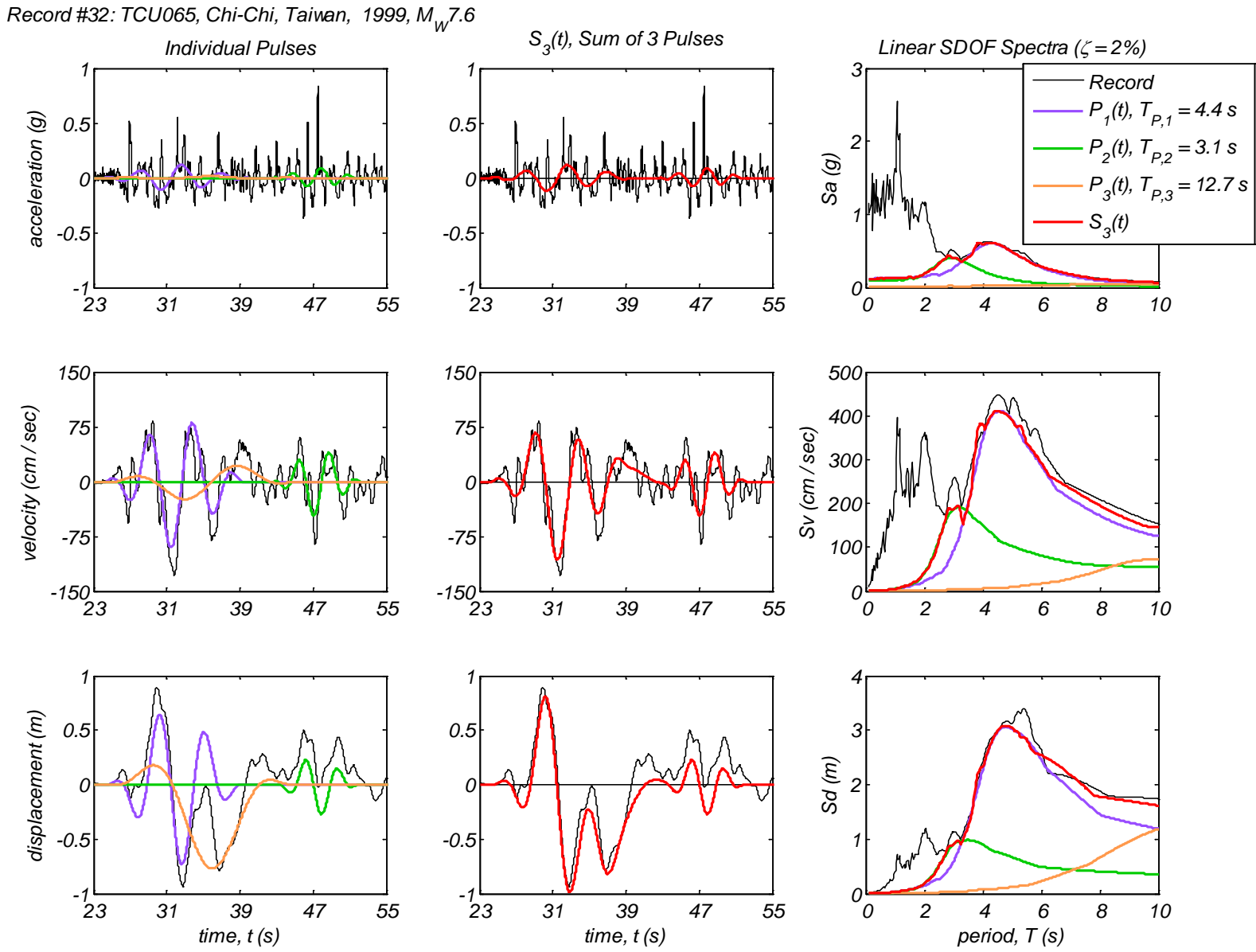
Appendix B2 – Time history and linear spectral response of three extracted pulses using the CPE<sub>V-EN</sub> method for 40 Motions



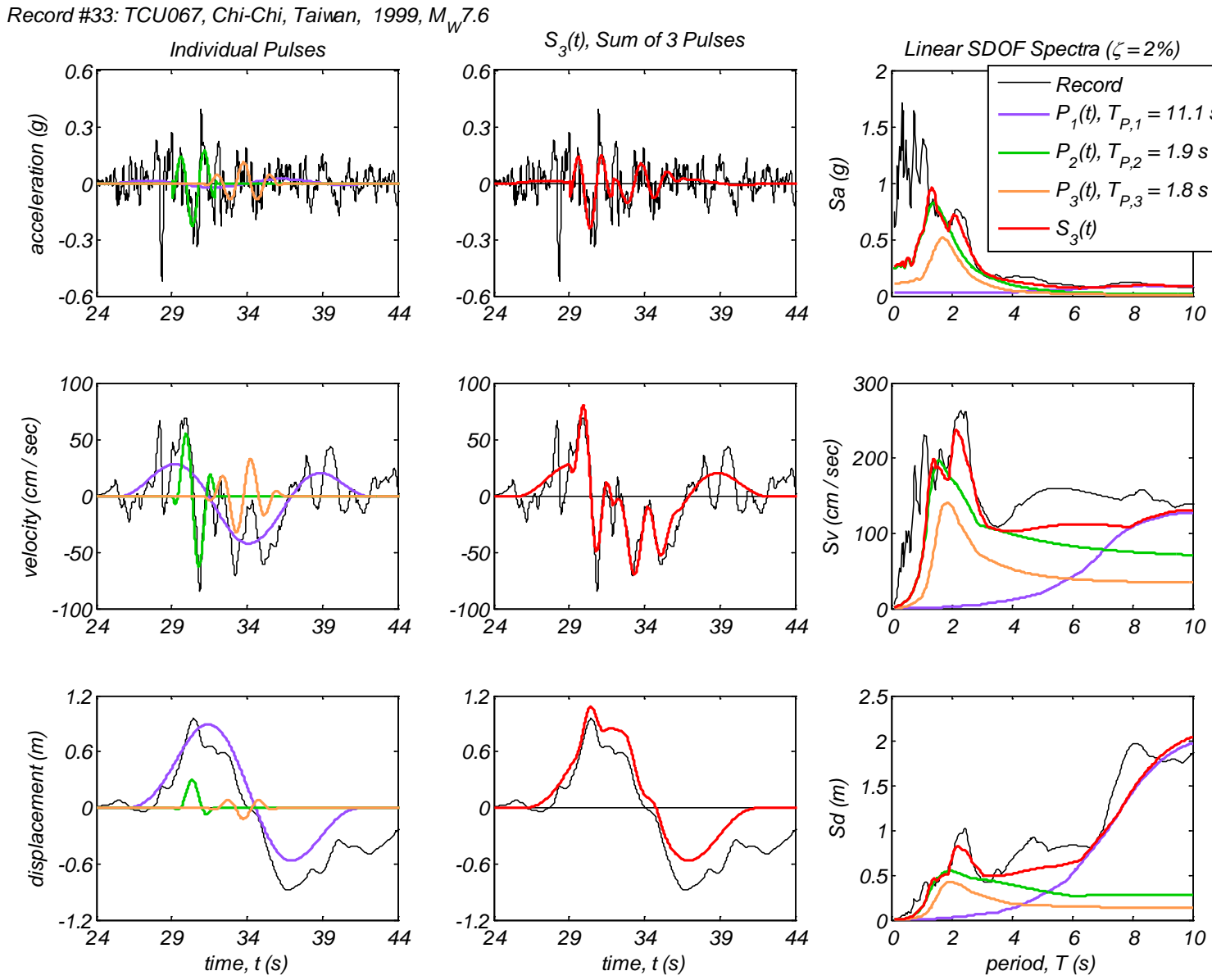
Appendix B2 – Time history and linear spectral response of three extracted pulses using the CPE<sub>V-EN</sub> method for 40 Motions



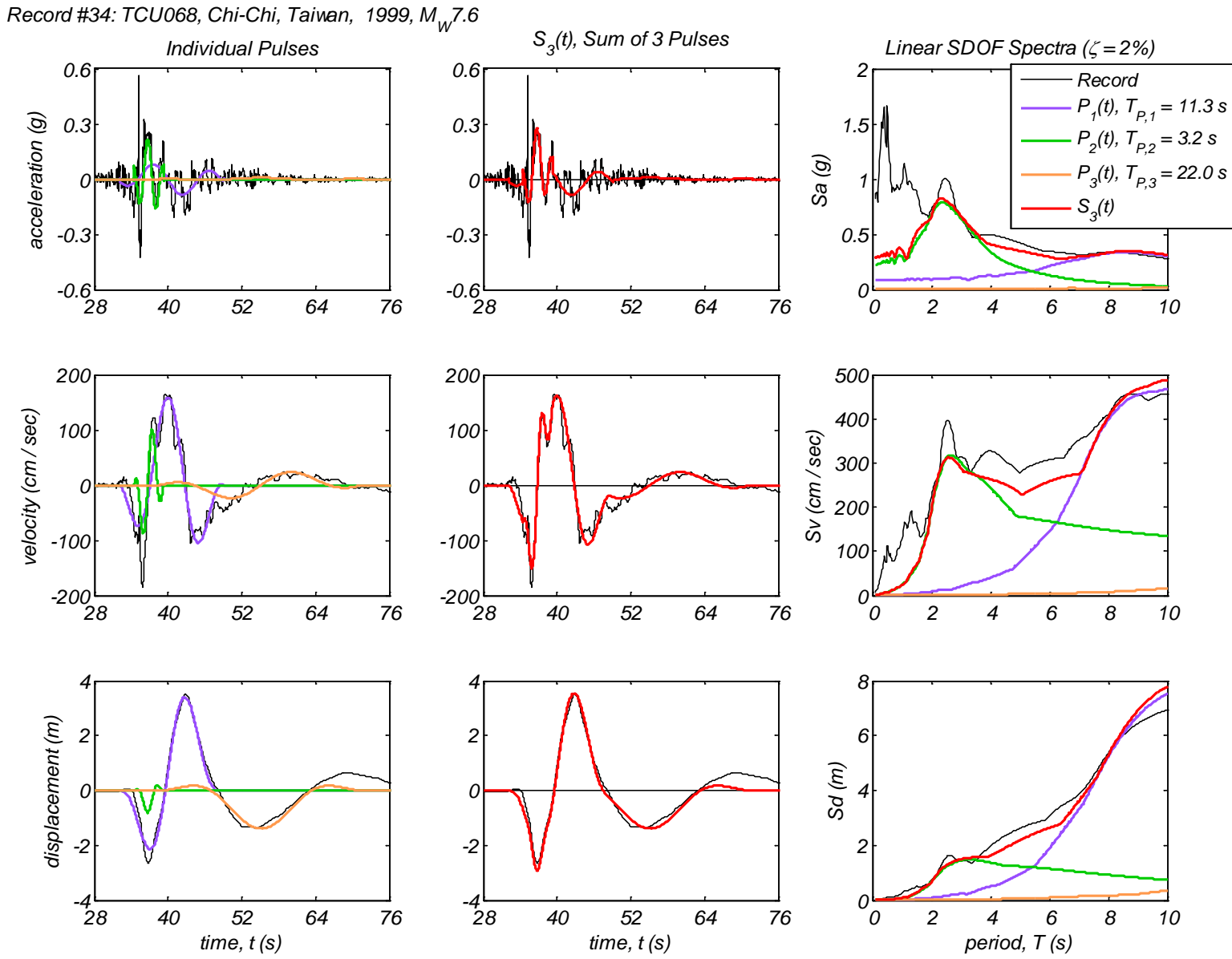
Appendix B2 – Time history and linear spectral response of three extracted pulses using the CPE<sub>V-EN</sub> method for 40 Motions



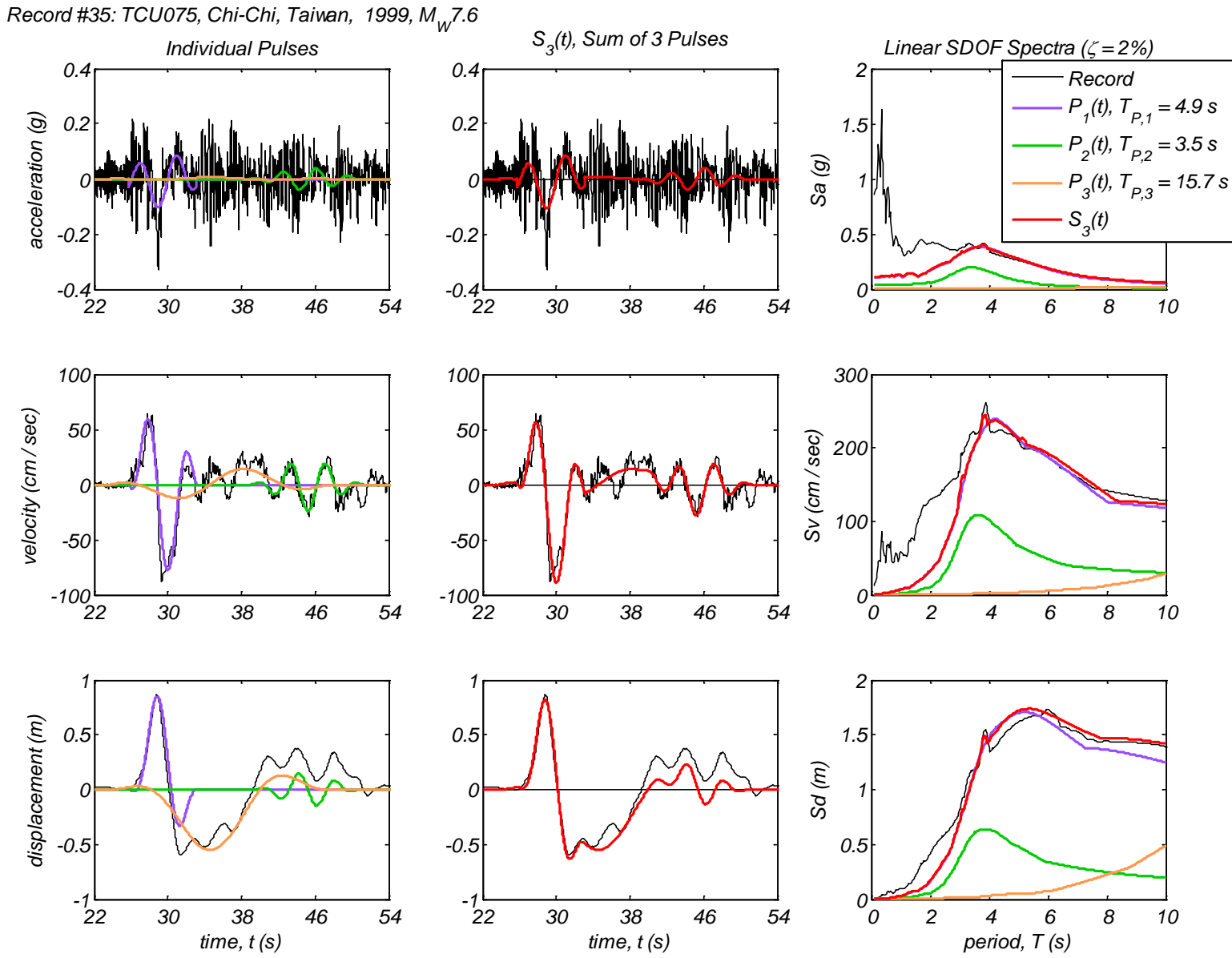
Appendix B2 – Time history and linear spectral response of three extracted pulses using the CPE<sub>V-EN</sub> method for 40 Motions



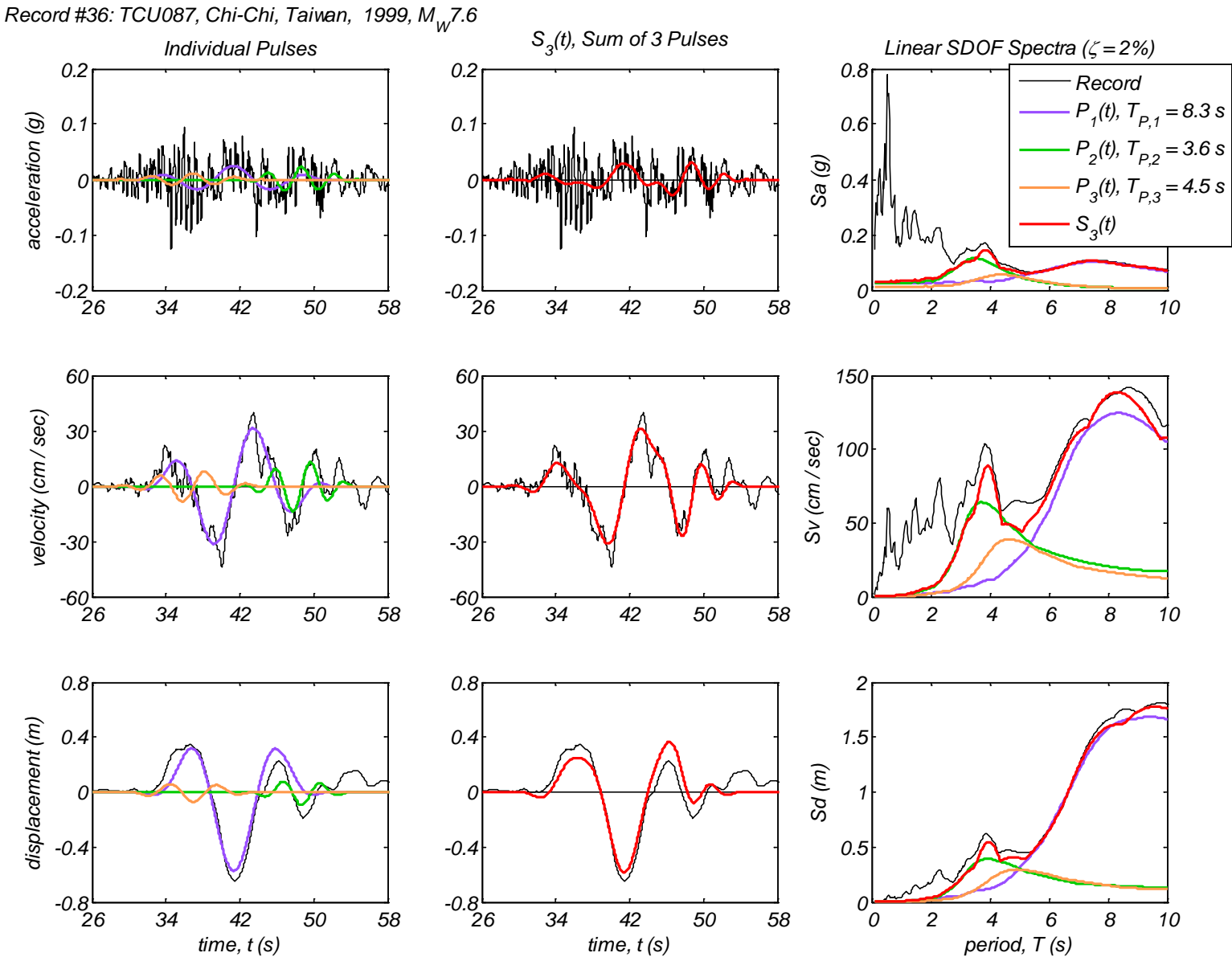
Appendix B2 – Time history and linear spectral response of three extracted pulses using the CPE<sub>V-EN</sub> method for 40 Motions



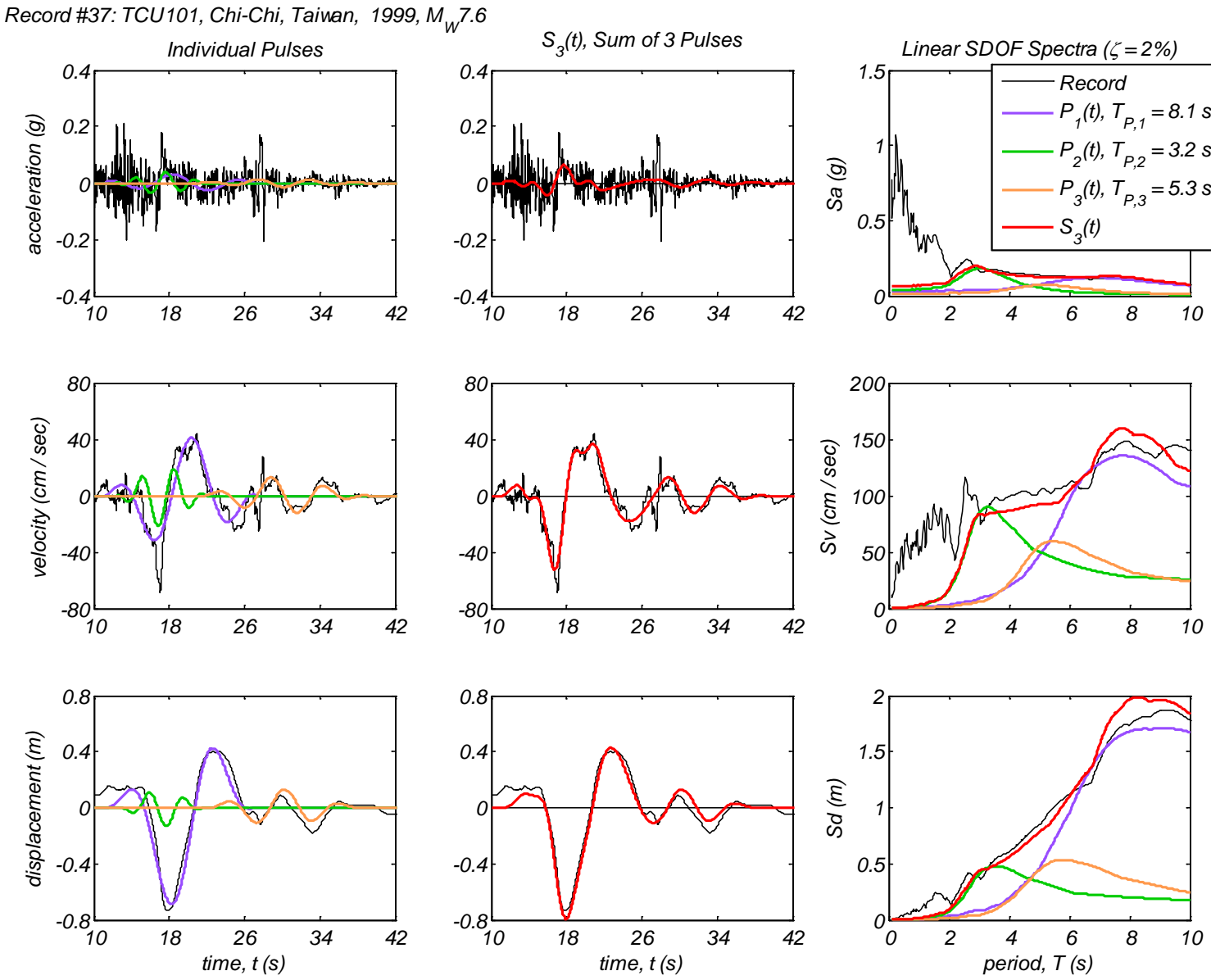
Appendix B2 – Time history and linear spectral response of three extracted pulses using the CPE<sub>V-EN</sub> method for 40 Motions



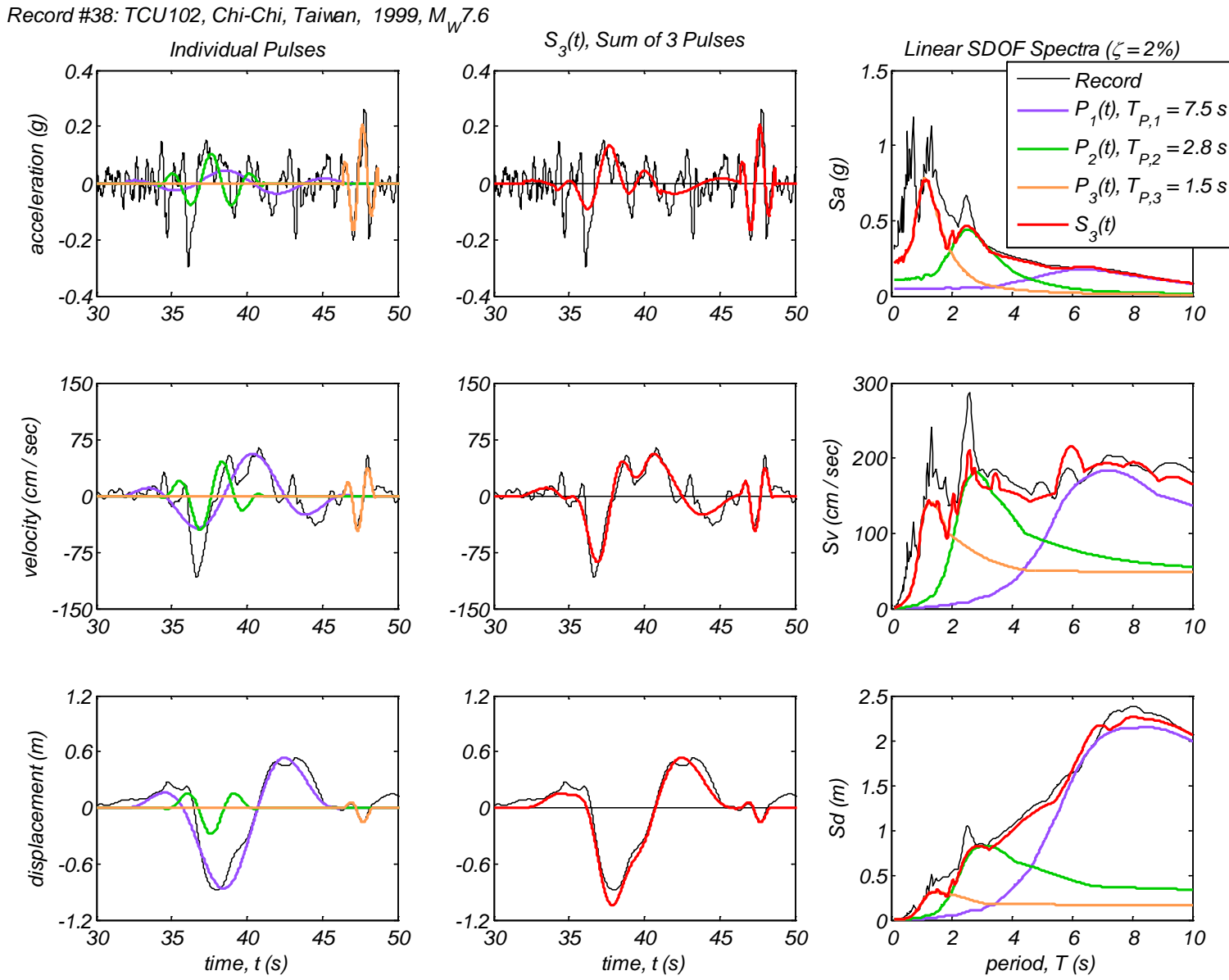
Appendix B2 – Time history and linear spectral response of three extracted pulses using the CPE<sub>V-EN</sub> method for 40 Motions



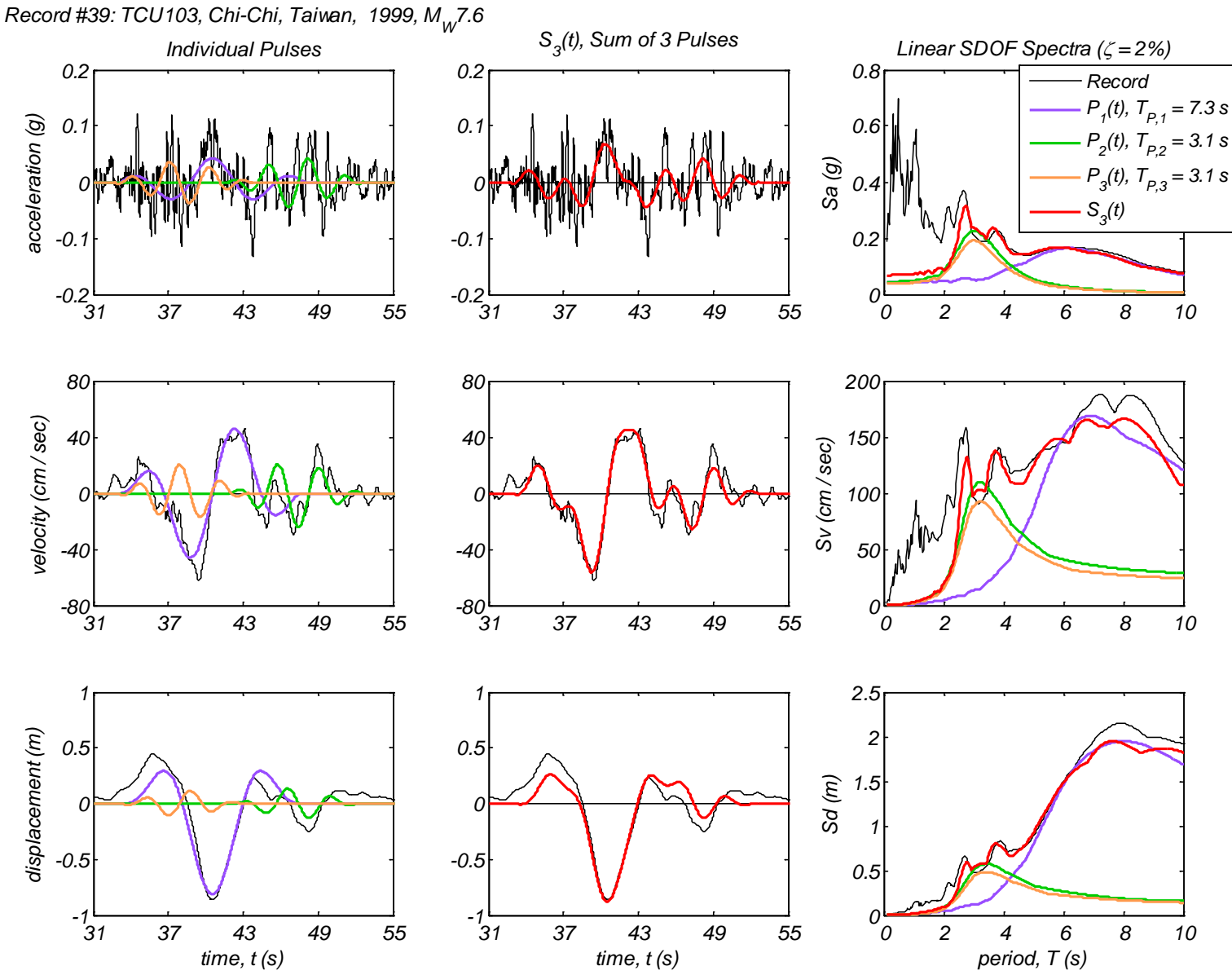
Appendix B2 – Time history and linear spectral response of three extracted pulses using the CPE<sub>V-EN</sub> method for 40 Motions



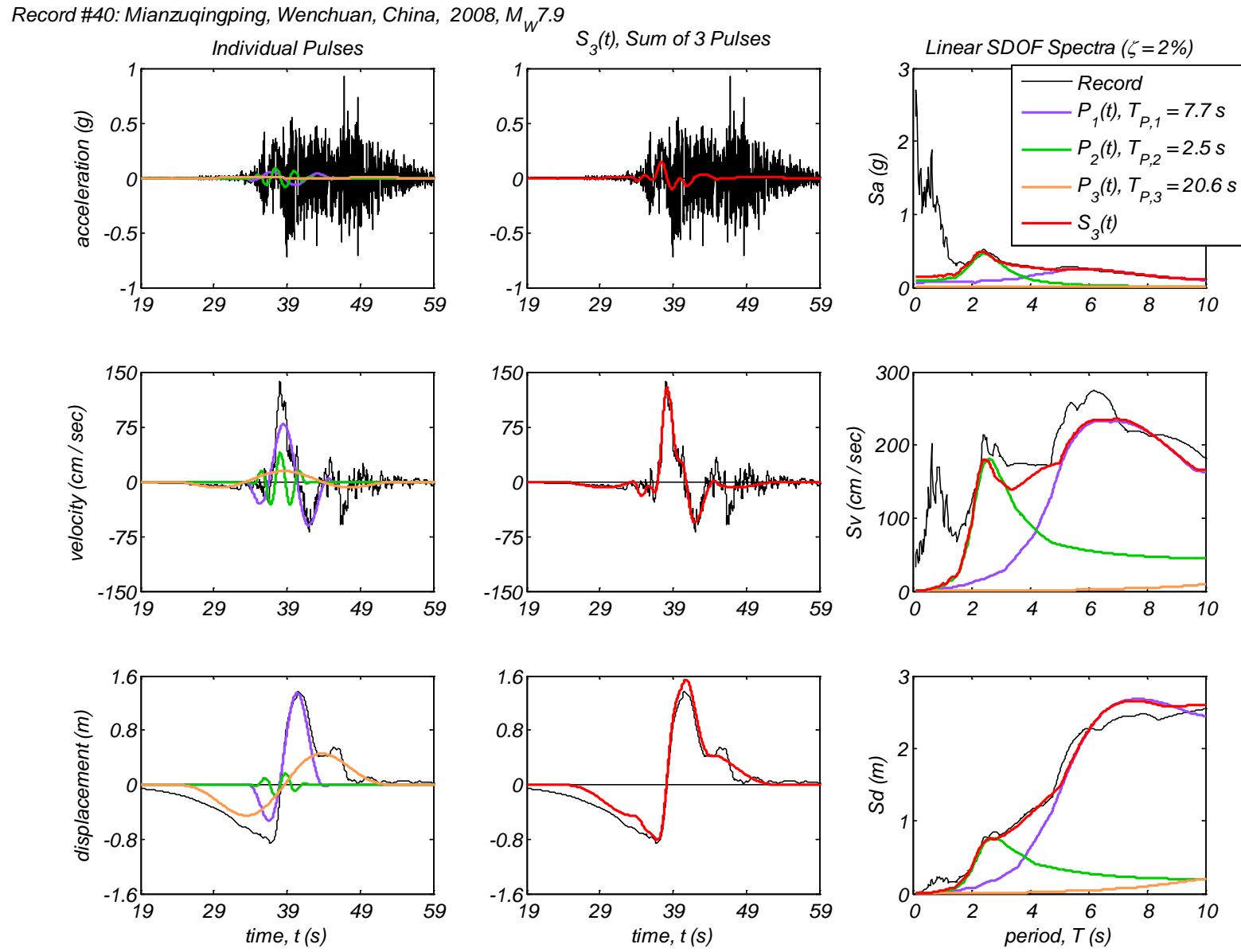
Appendix B2 – Time history and linear spectral response of three extracted pulses using the CPE<sub>V-EN</sub> method for 40 Motions



Appendix B2 – Time history and linear spectral response of three extracted pulses using the CPE<sub>V-EN</sub> method for 40 Motions

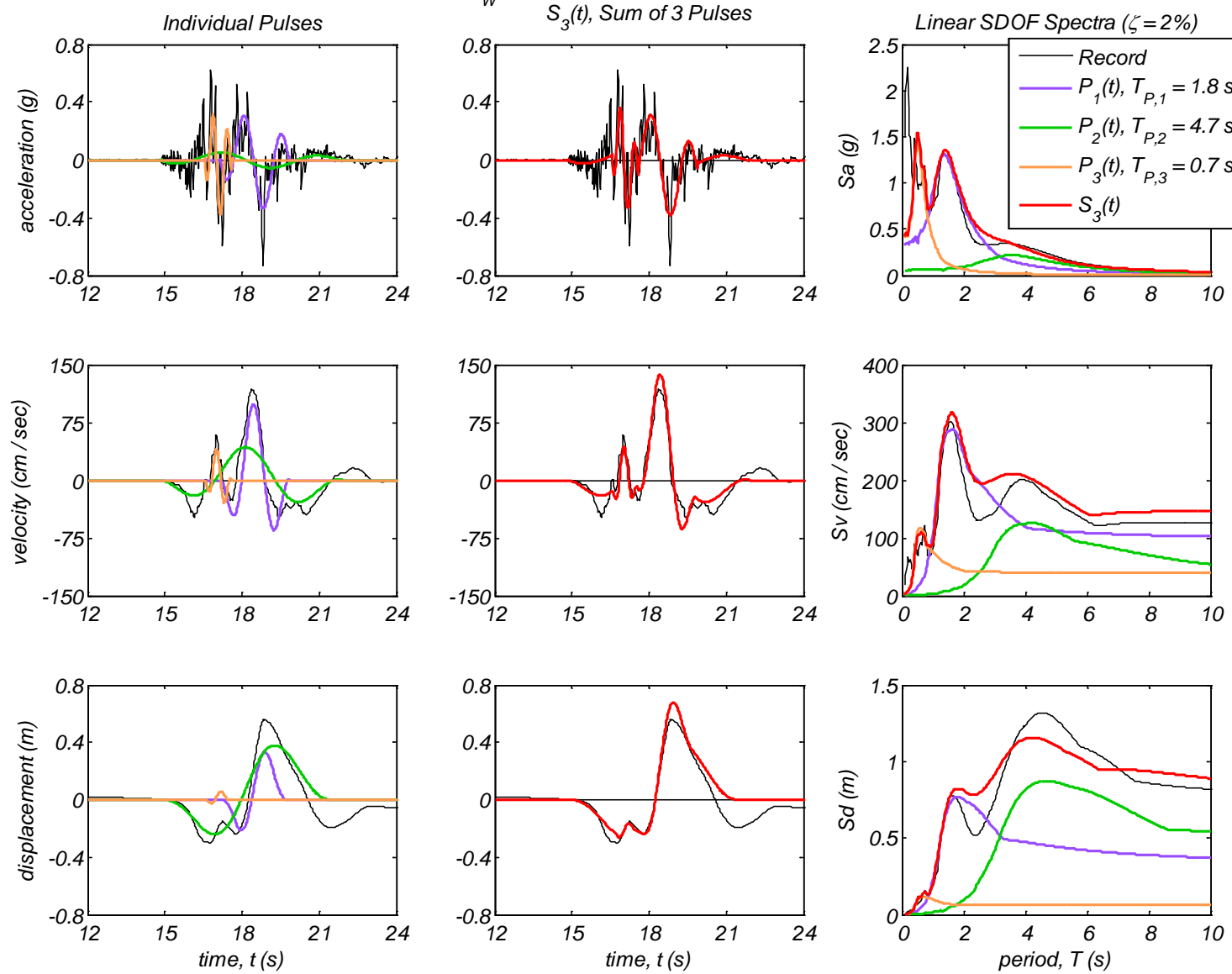


Appendix B2 – Time history and linear spectral response of three extracted pulses using the CPE<sub>V-EN</sub> method for 40 Motions



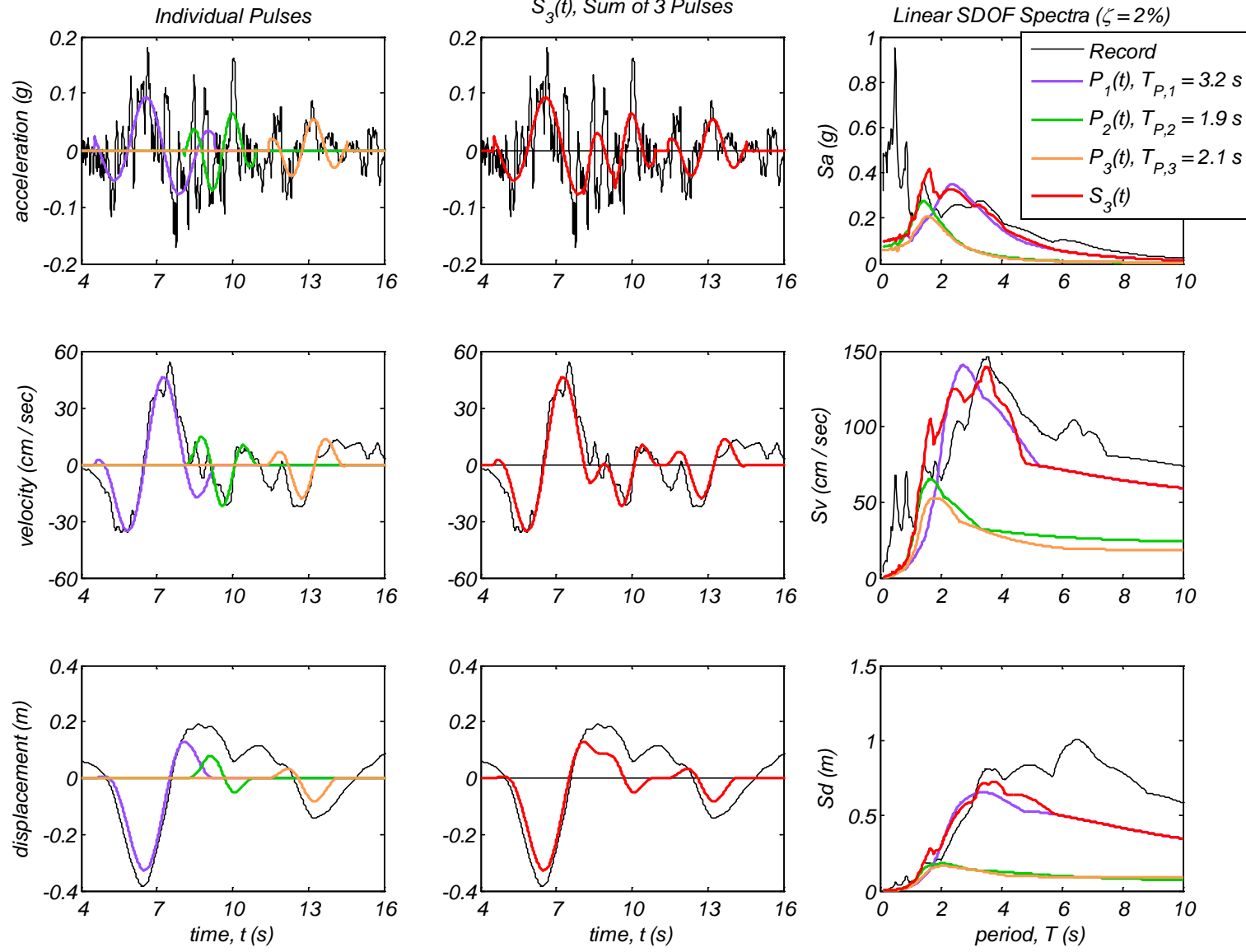
### Appendix B3: Time history and linear spectral response of three extracted pulses using the CPE<sub>V-AM</sub> method for 40 motions

Record #1: PRPC, Christchurch, New Zealand, 2011,  $M_W = 6.3$

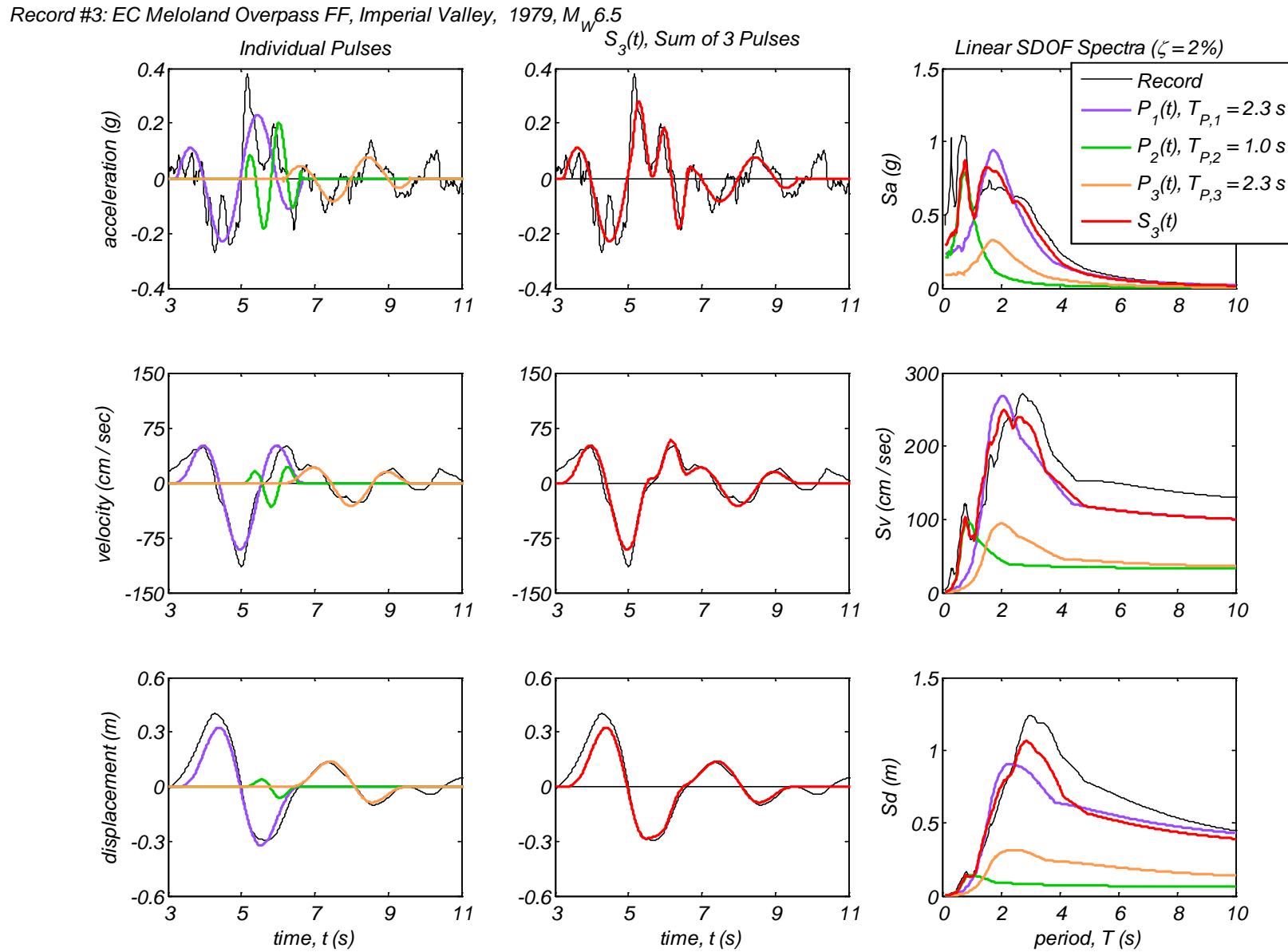


Appendix B3 – Time history and linear spectral response of three extracted pulses using the CPE<sub>V-AM</sub> method for 40 Motions

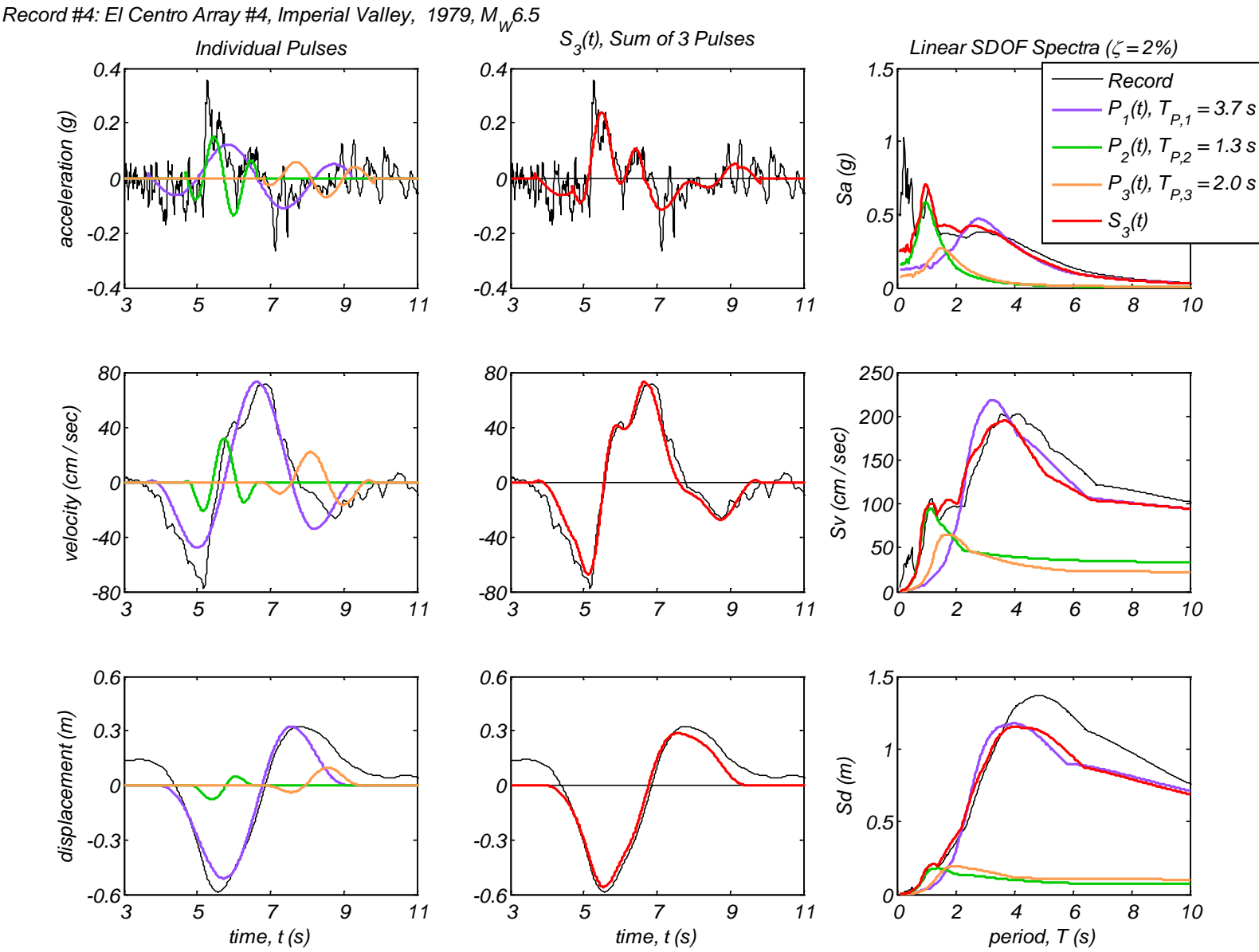
Record #2: EC County Center FF, Imperial Valley, 1979,  $M_W 6.5$



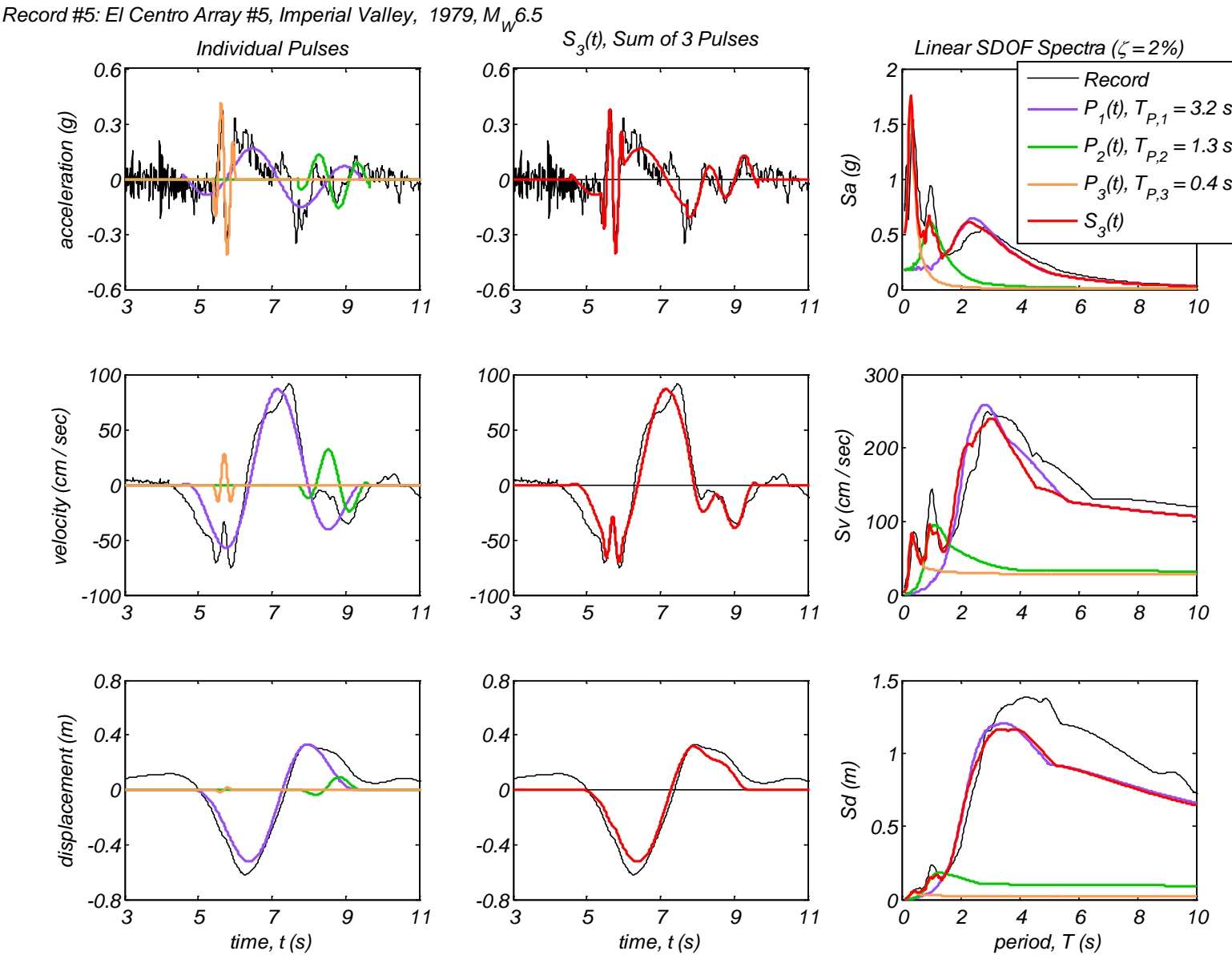
Appendix B3 – Time history and linear spectral response of three extracted pulses using the CPE<sub>V-AM</sub> method for 40 Motions



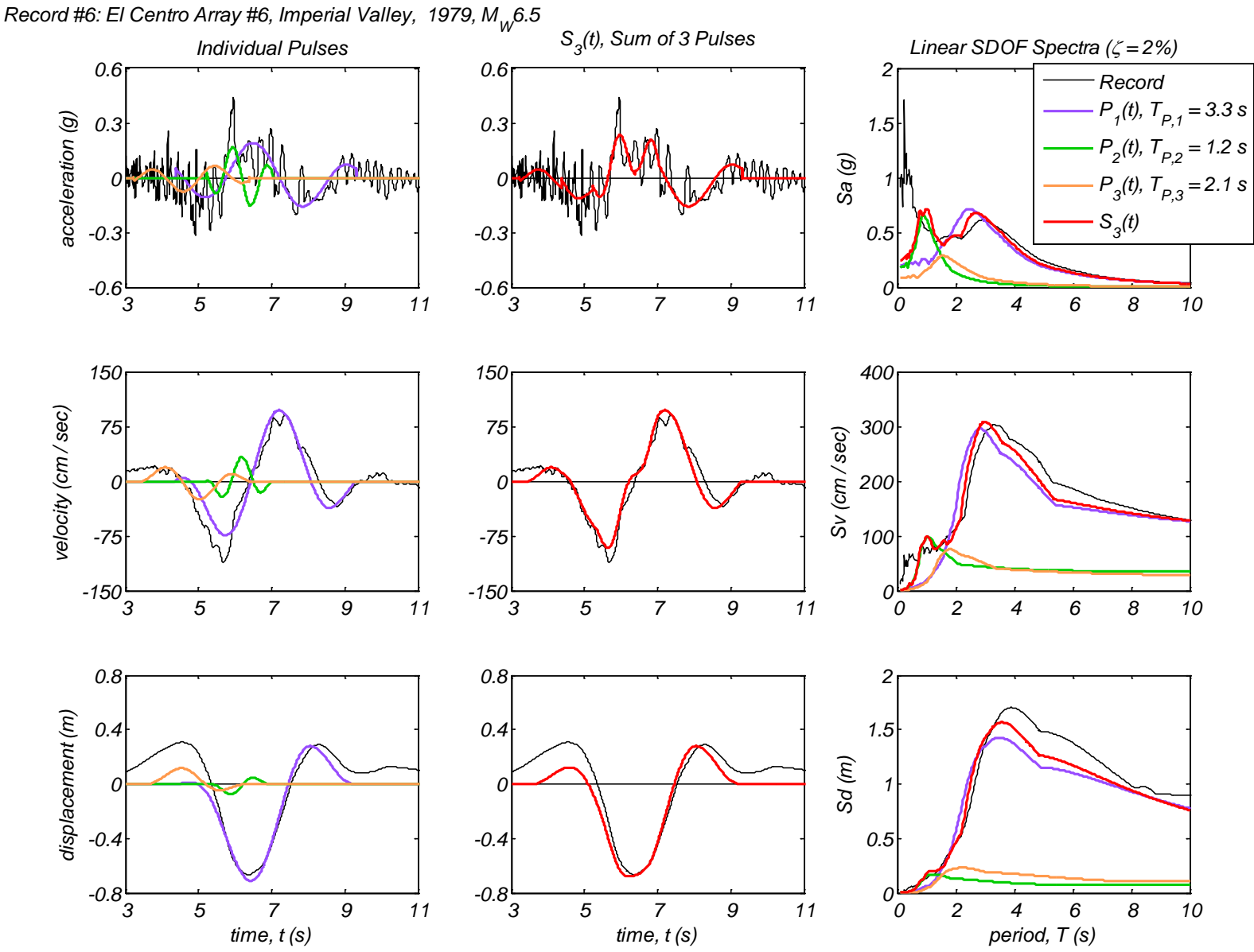
Appendix B3 – Time history and linear spectral response of three extracted pulses using the CPE<sub>V-AM</sub> method for 40 Motions



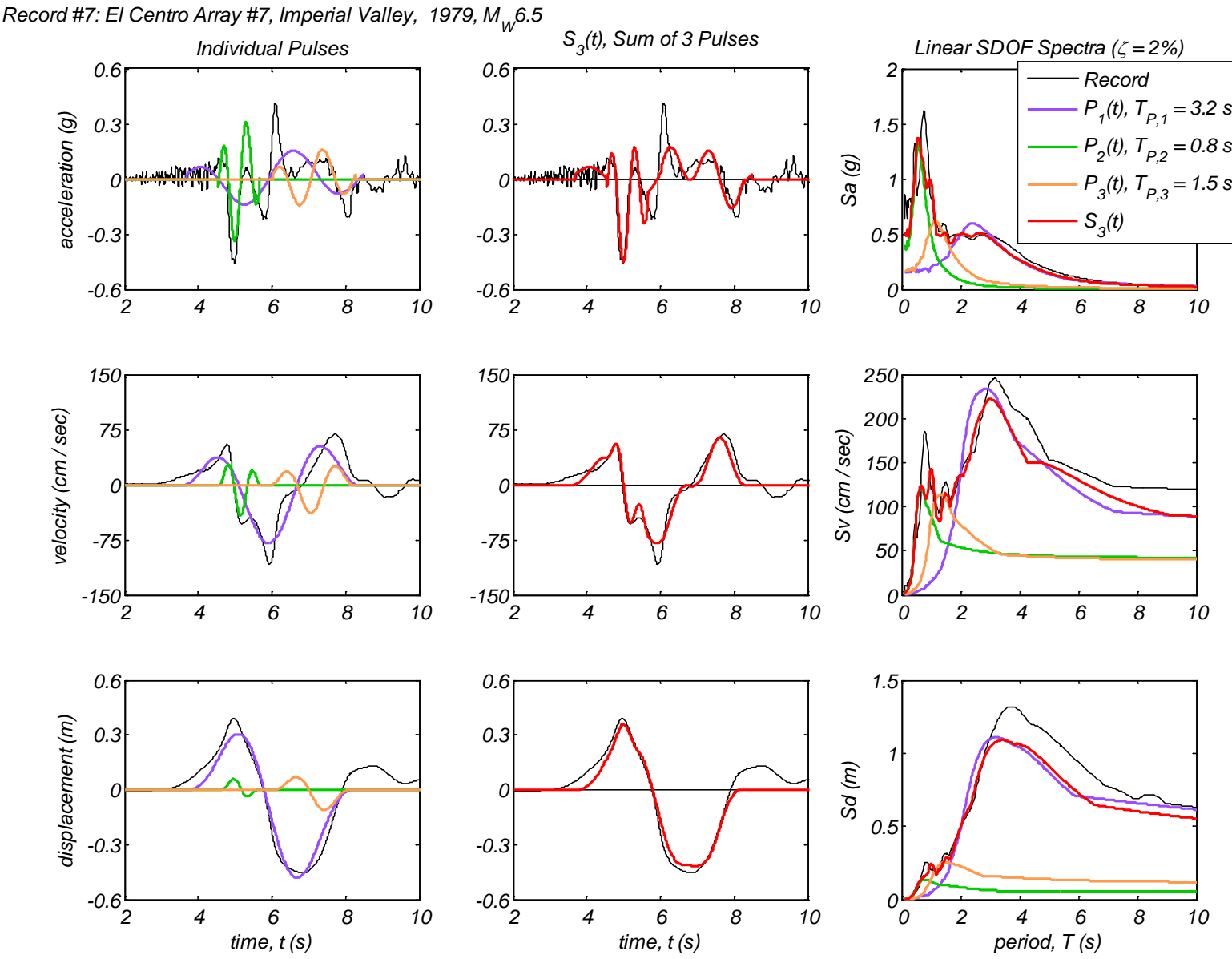
Appendix B3 – Time history and linear spectral response of three extracted pulses using the CPE<sub>V-AM</sub> method for 40 Motions



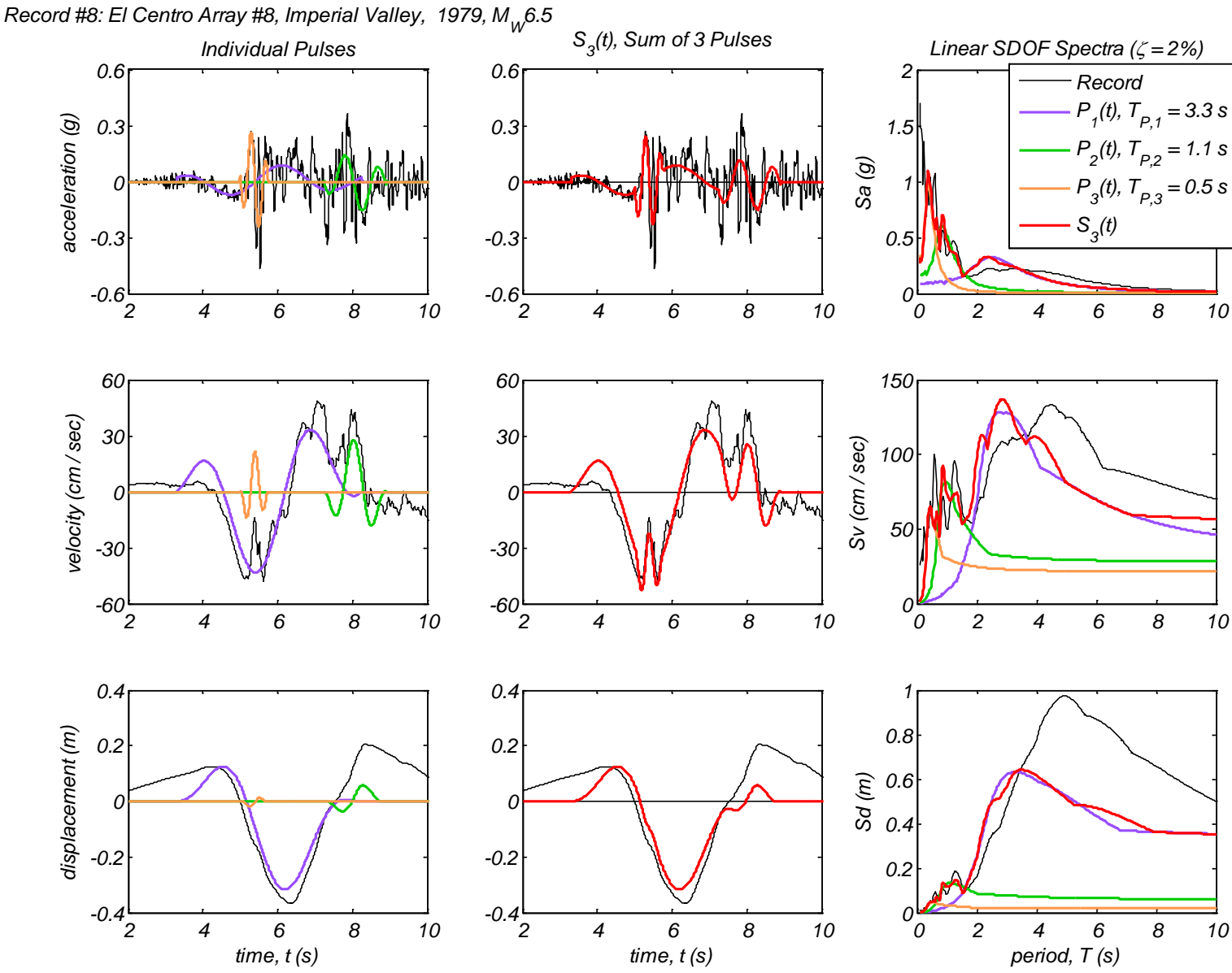
Appendix B3 – Time history and linear spectral response of three extracted pulses using the CPE<sub>V-AM</sub> method for 40 Motions



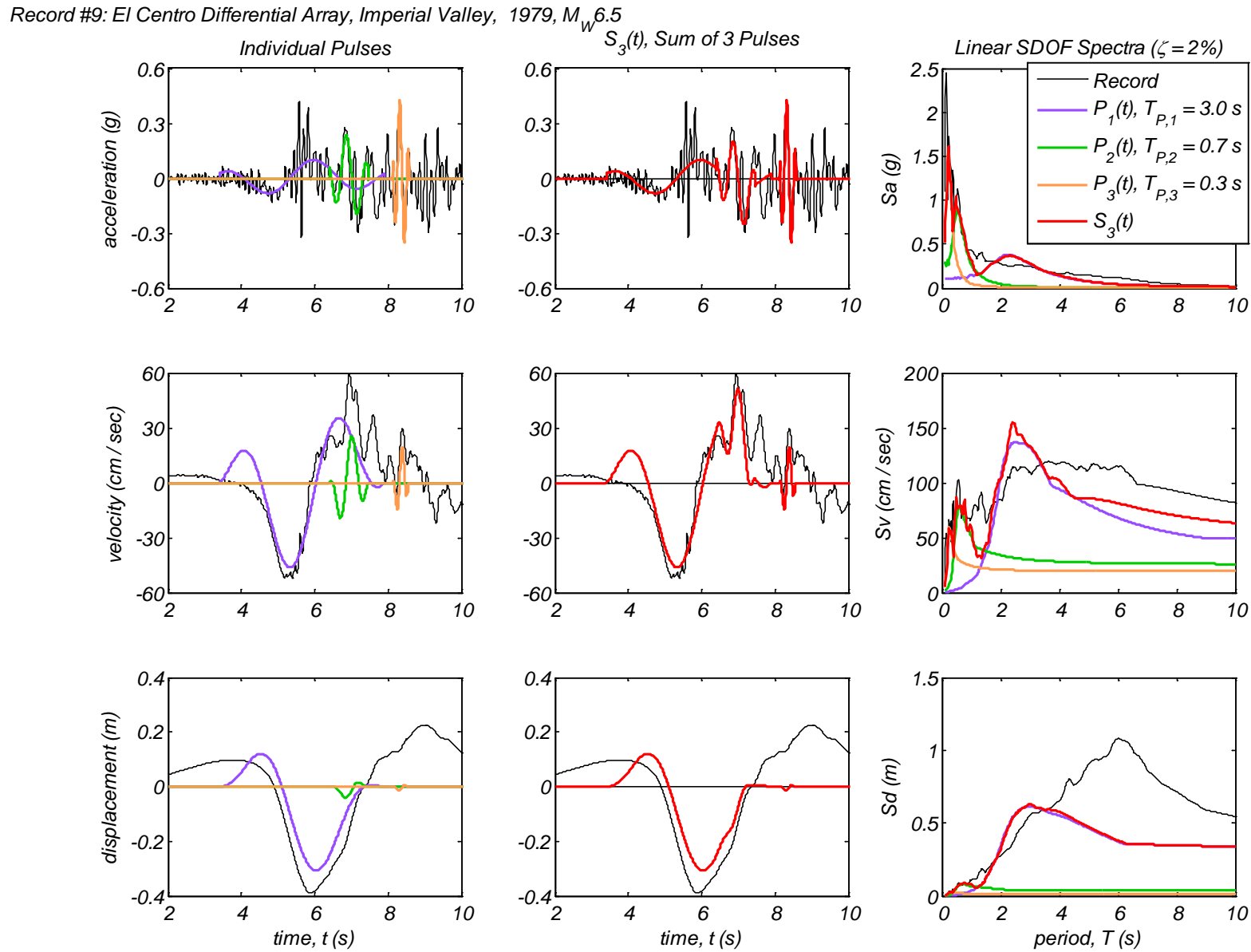
Appendix B3 – Time history and linear spectral response of three extracted pulses using the CPE<sub>V-AM</sub> method for 40 Motions



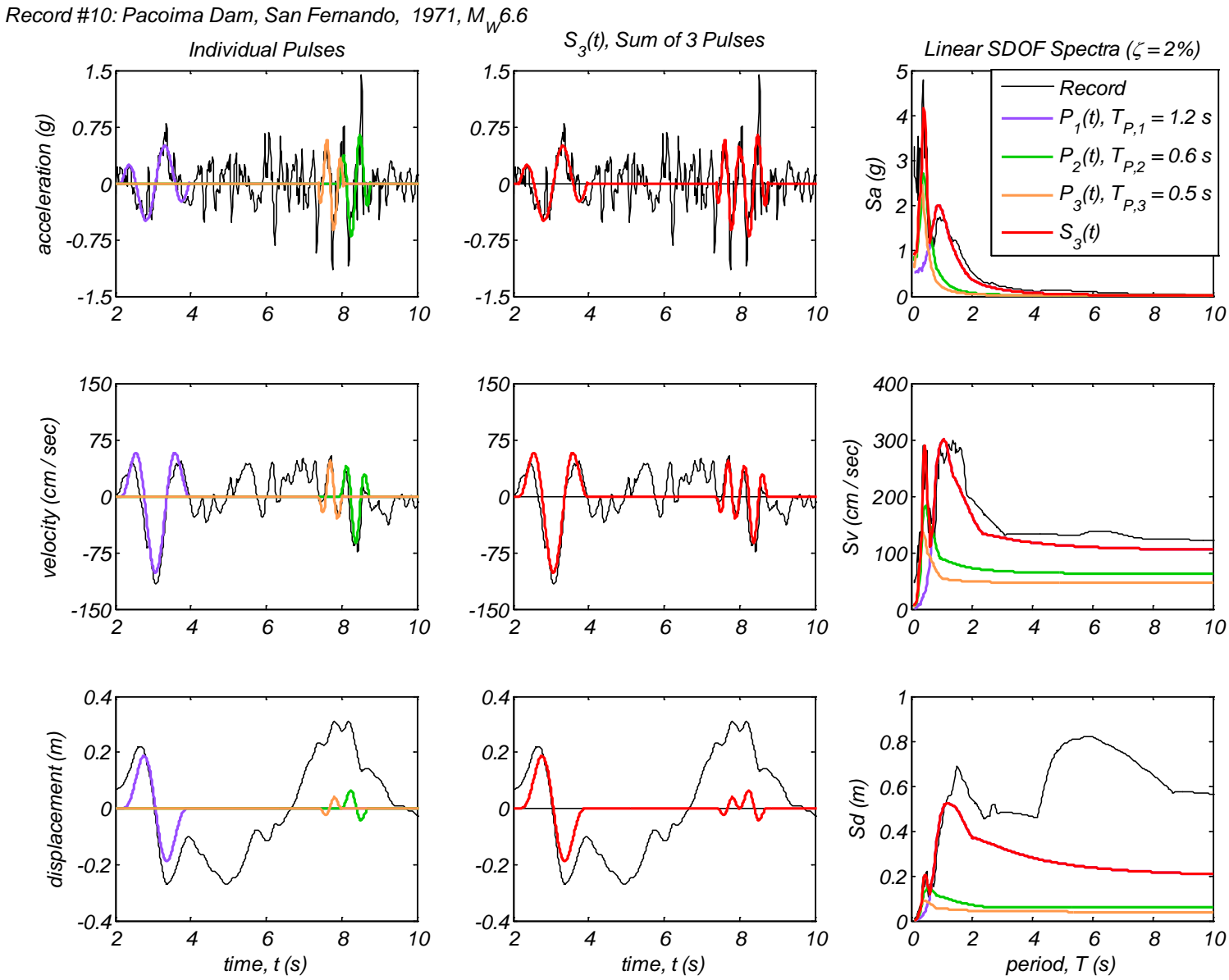
Appendix B3 – Time history and linear spectral response of three extracted pulses using the CPE<sub>V-AM</sub> method for 40 Motions



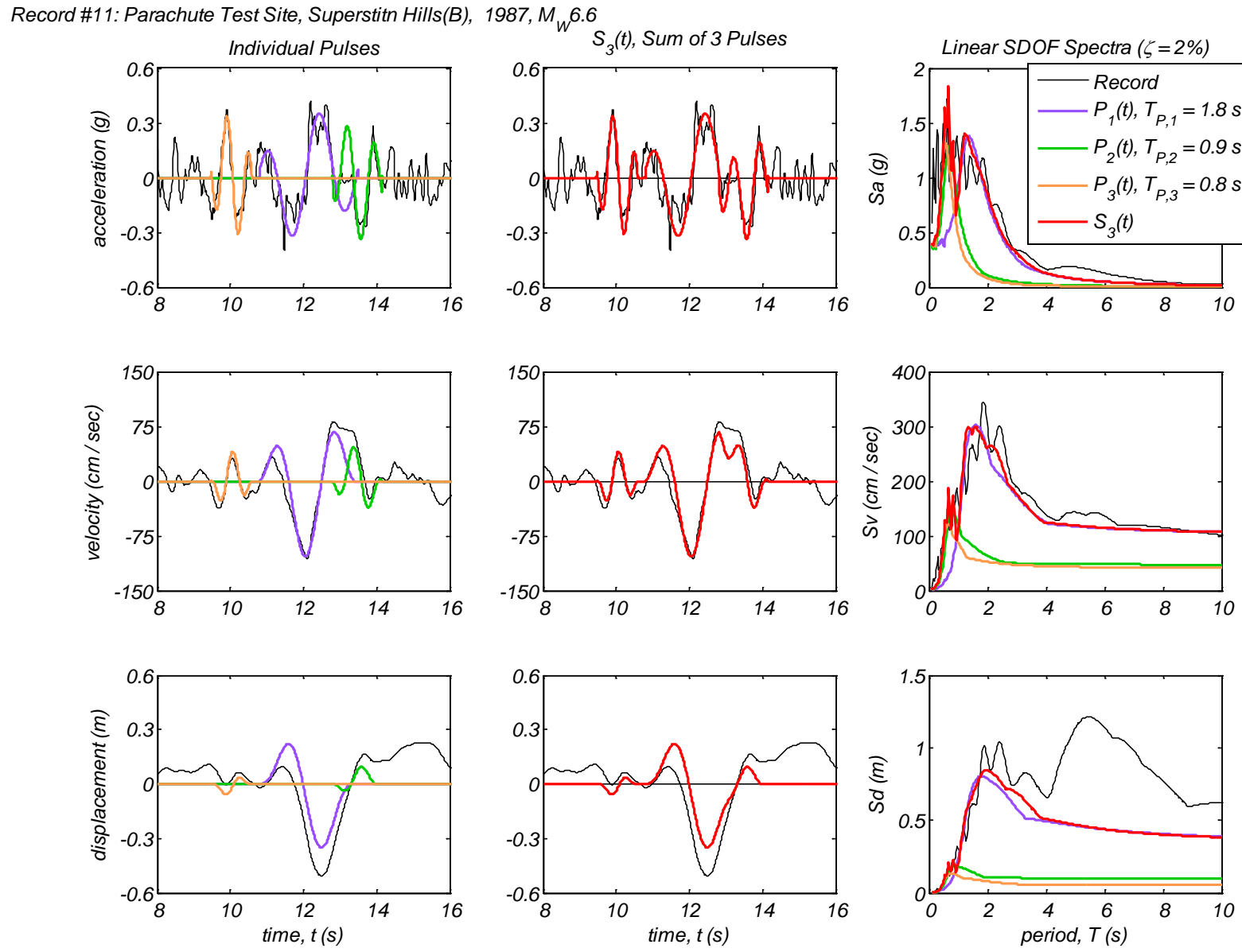
Appendix B3 – Time history and linear spectral response of three extracted pulses using the CPE<sub>V-AM</sub> method for 40 Motions



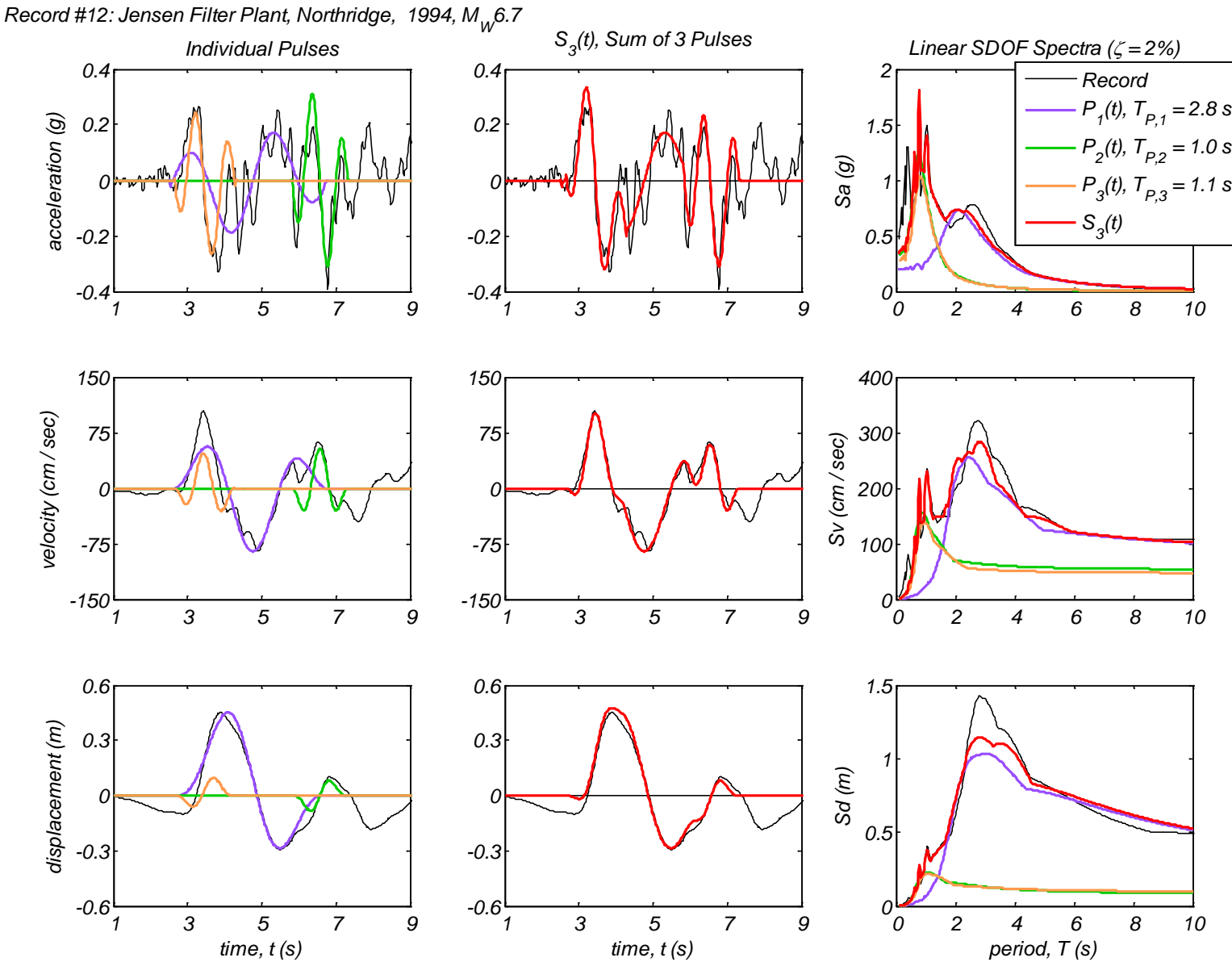
Appendix B3 – Time history and linear spectral response of three extracted pulses using the CPE<sub>V-AM</sub> method for 40 Motions



Appendix B3 – Time history and linear spectral response of three extracted pulses using the CPE<sub>V-AM</sub> method for 40 Motions

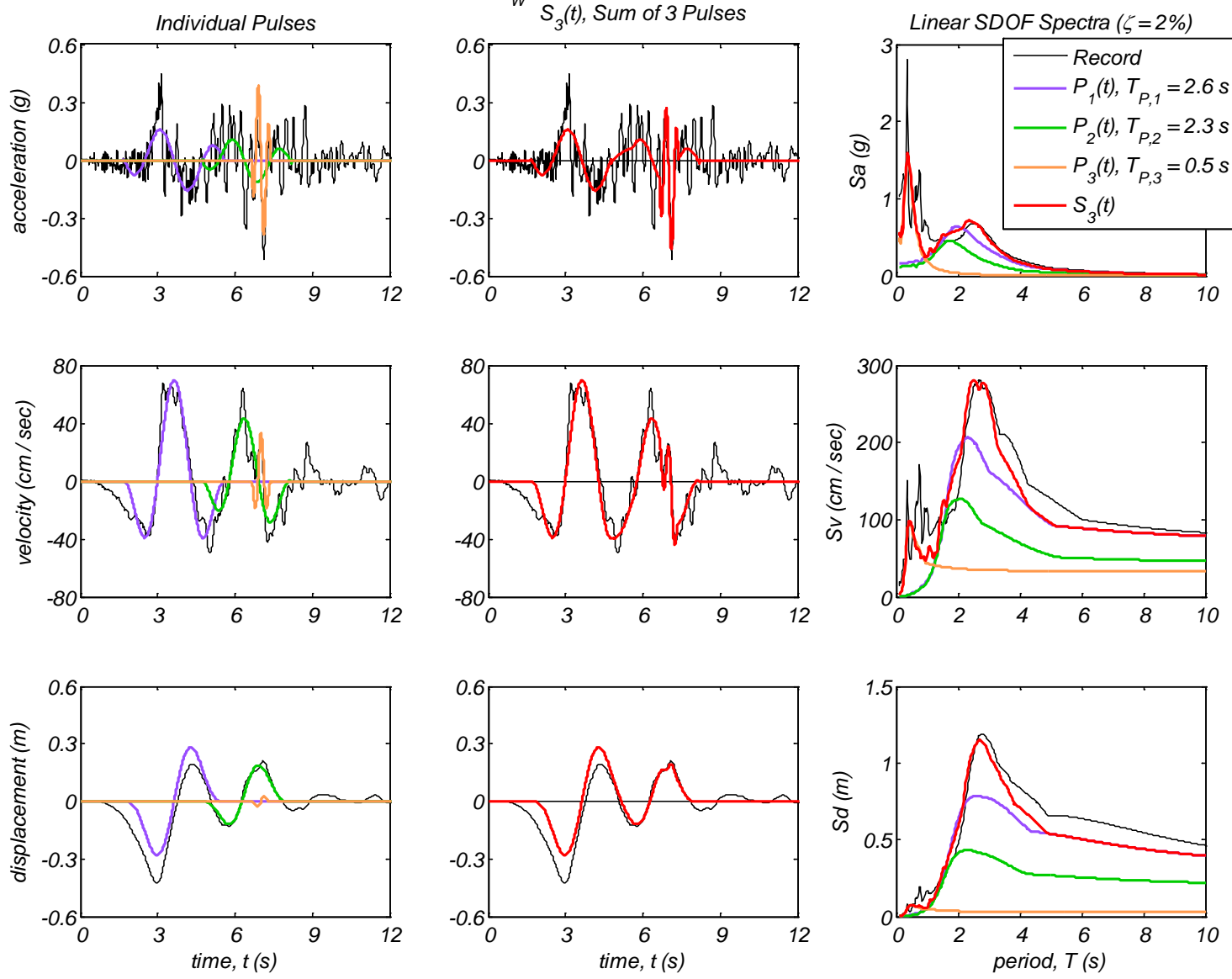


Appendix B3 – Time history and linear spectral response of three extracted pulses using the CPE<sub>V-AM</sub> method for 40 Motions

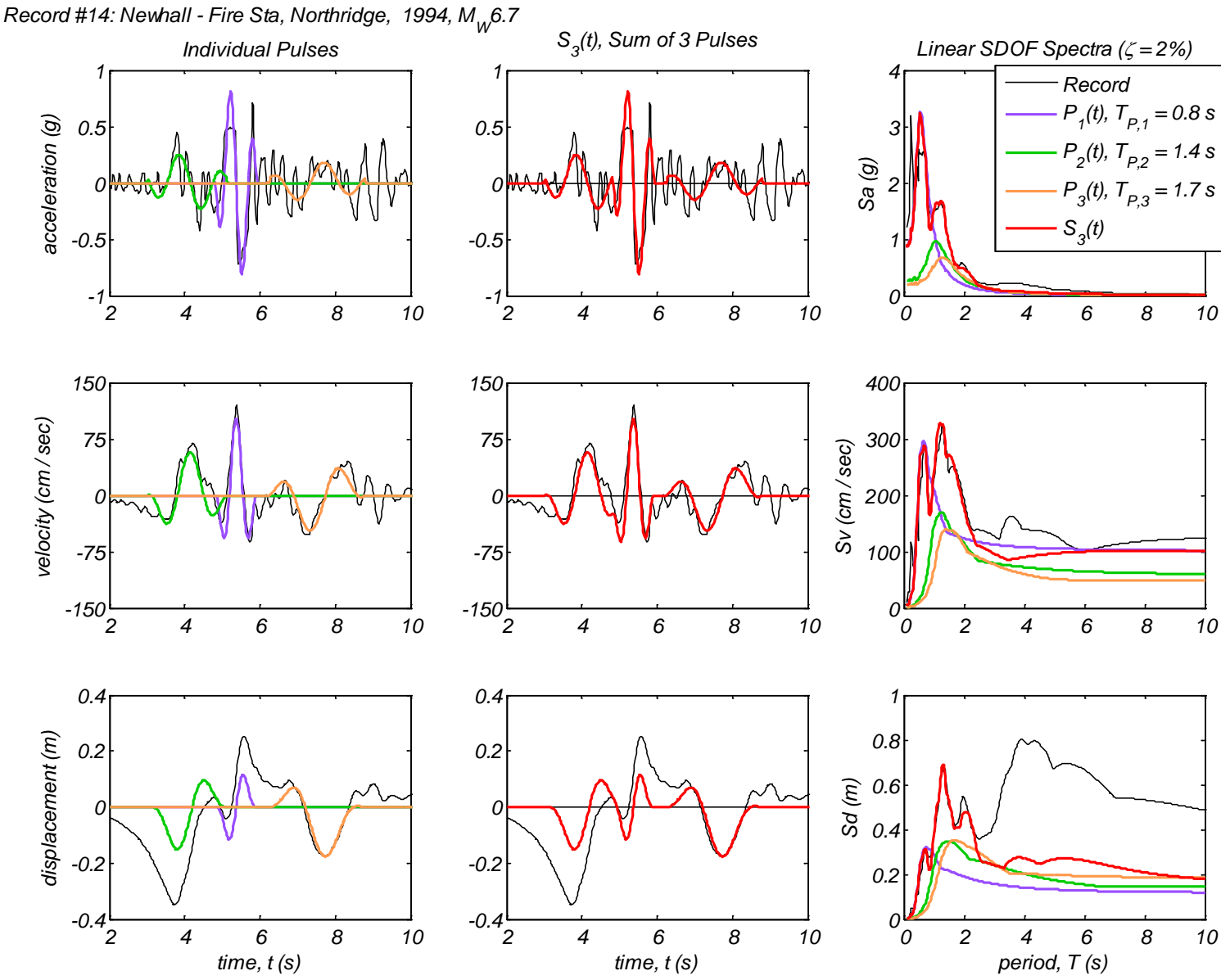


Appendix B3 – Time history and linear spectral response of three extracted pulses using the CPE<sub>V-AM</sub> method for 40 Motions

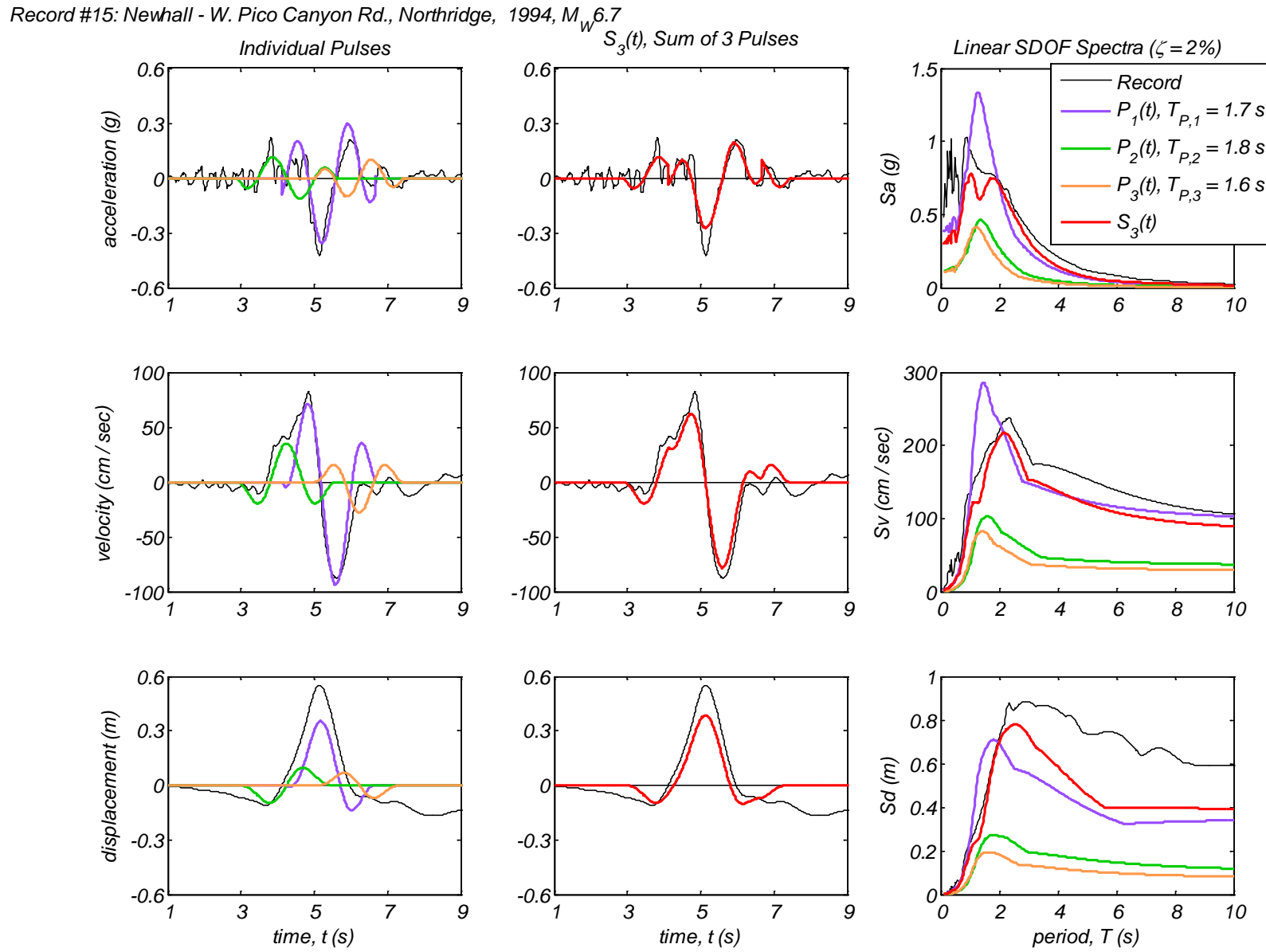
Record #13: Jensen Filter Plant Generator, Northridge, 1994,  $M_W 6.7$



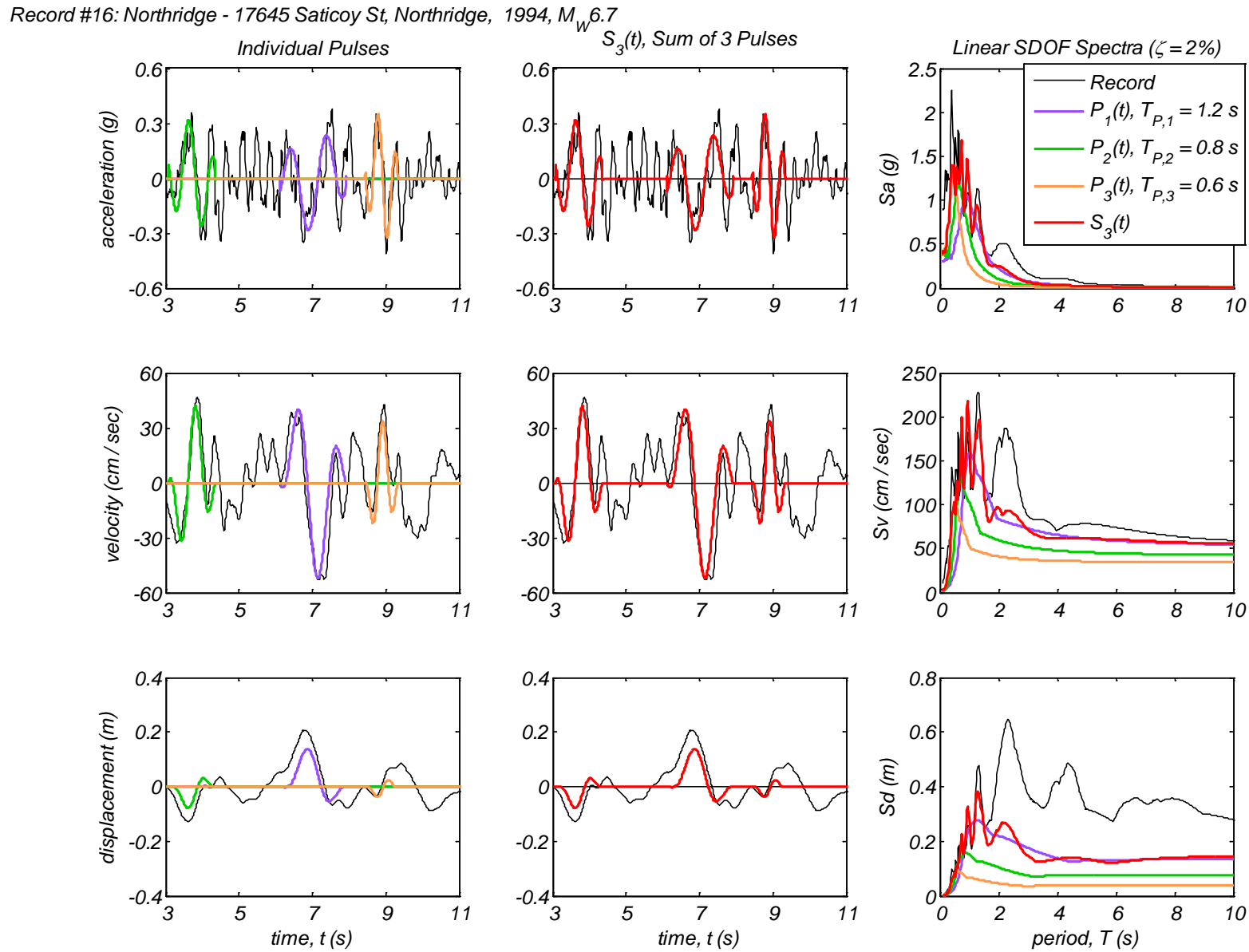
Appendix B3 – Time history and linear spectral response of three extracted pulses using the CPE<sub>V-AM</sub> method for 40 Motions



Appendix B3 – Time history and linear spectral response of three extracted pulses using the CPE<sub>V-AM</sub> method for 40 Motions

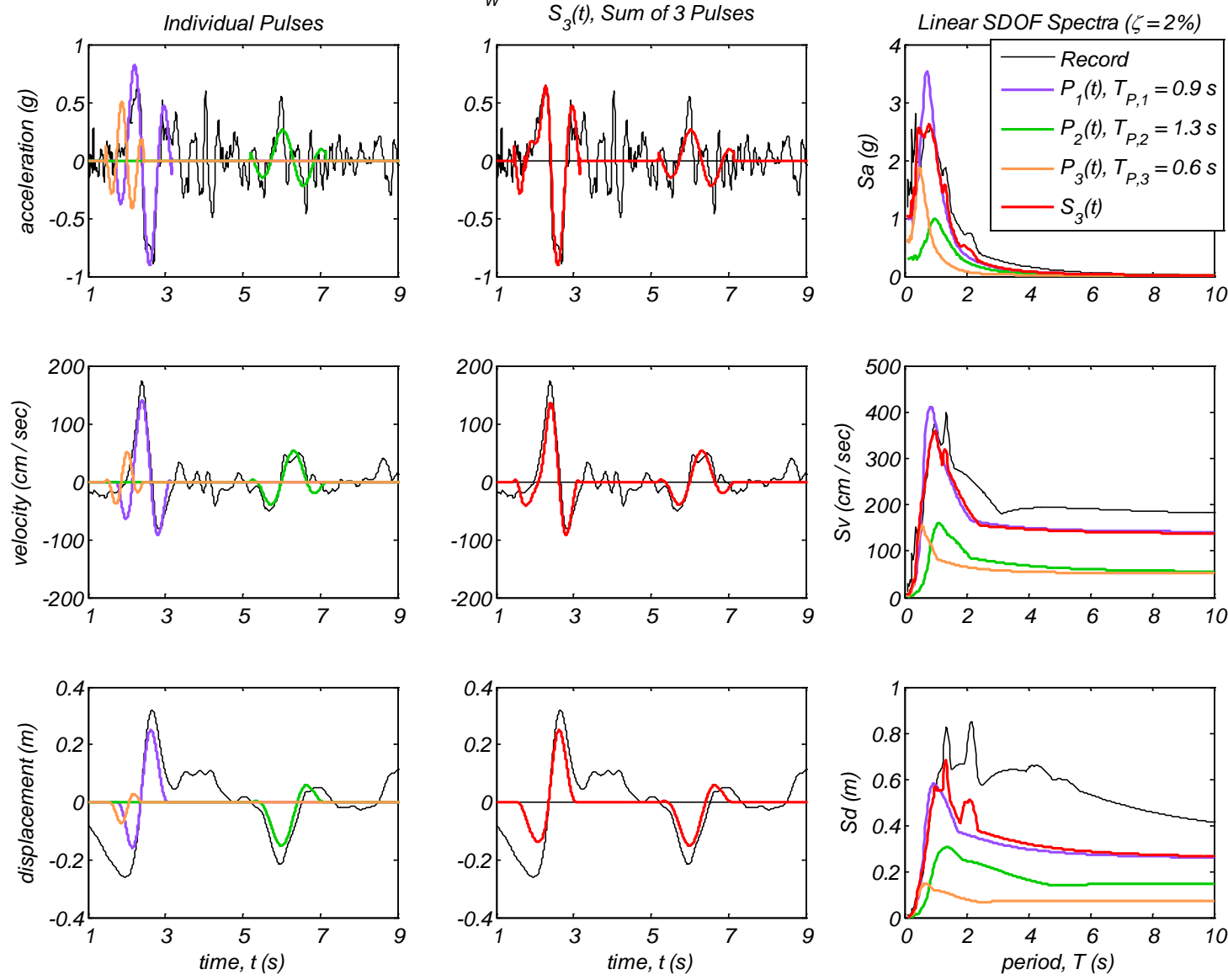


Appendix B3 – Time history and linear spectral response of three extracted pulses using the CPE<sub>V-AM</sub> method for 40 Motions



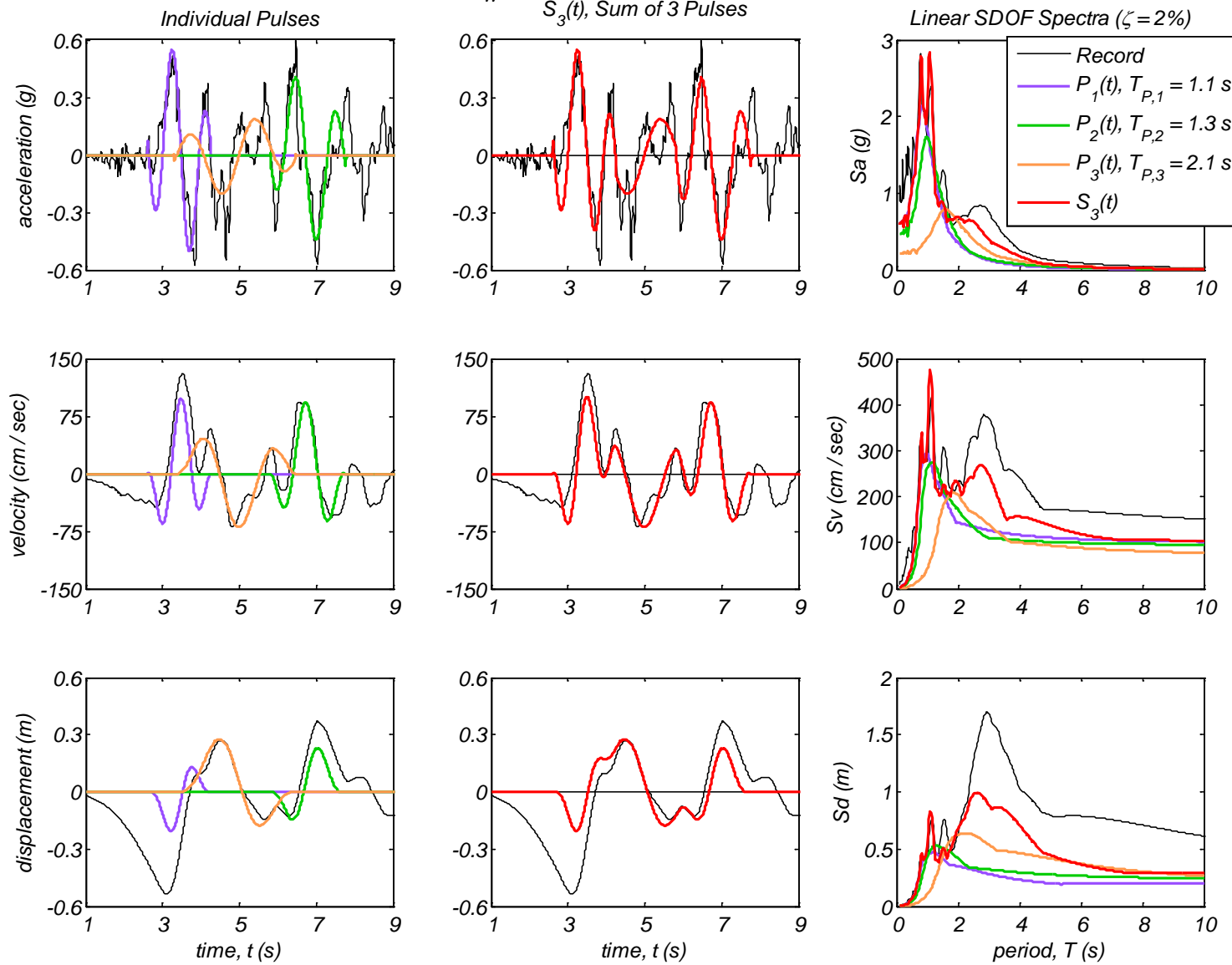
Appendix B3 – Time history and linear spectral response of three extracted pulses using the CPE<sub>V-AM</sub> method for 40 Motions

Record #17: Rinaldi Receiving Sta, Northridge, 1994,  $M_W 6.7$



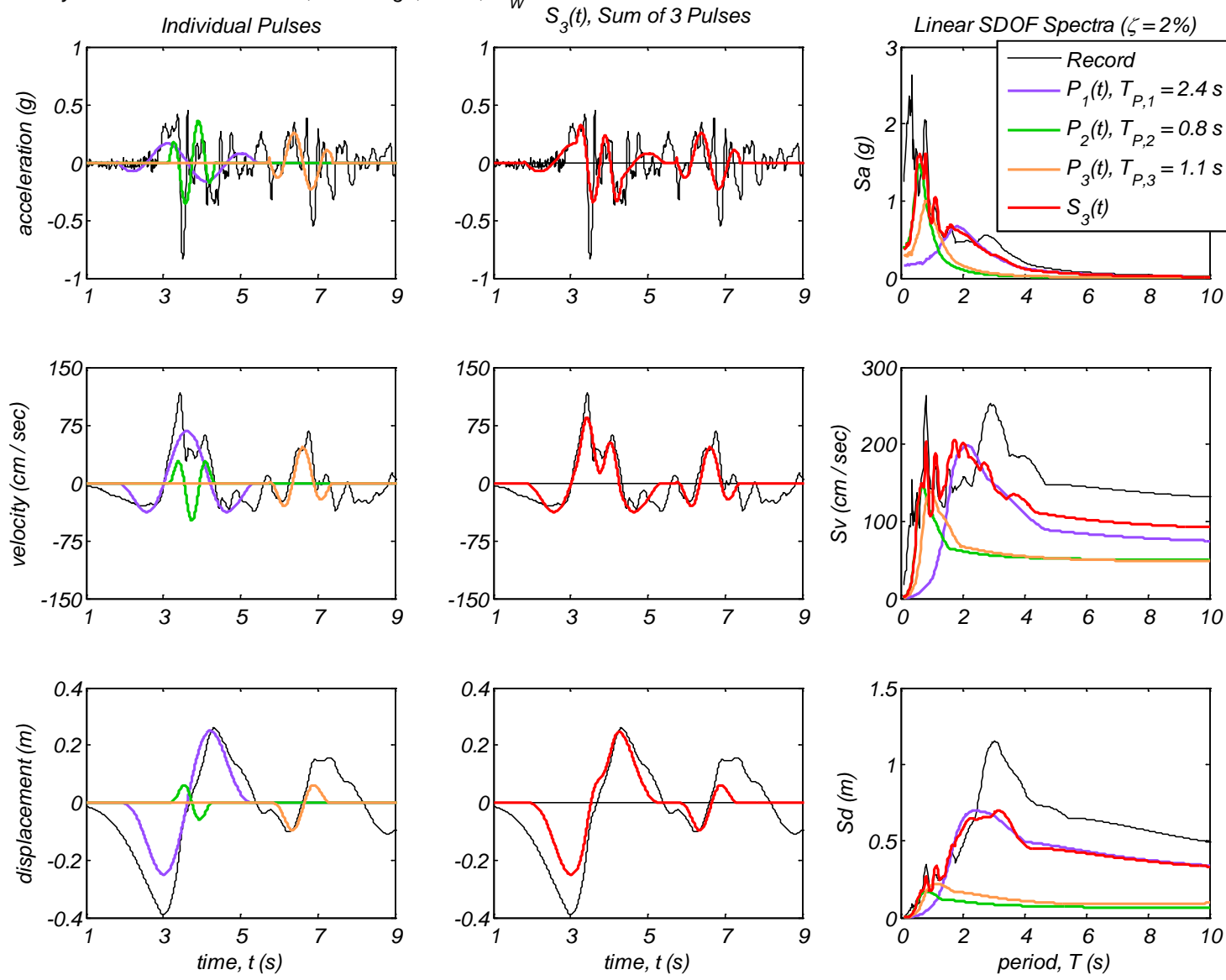
Appendix B3 – Time history and linear spectral response of three extracted pulses using the CPE<sub>V-AM</sub> method for 40 Motions

Record #18: Sylmar - Converter Sta, Northridge, 1994,  $M_w 6.7$



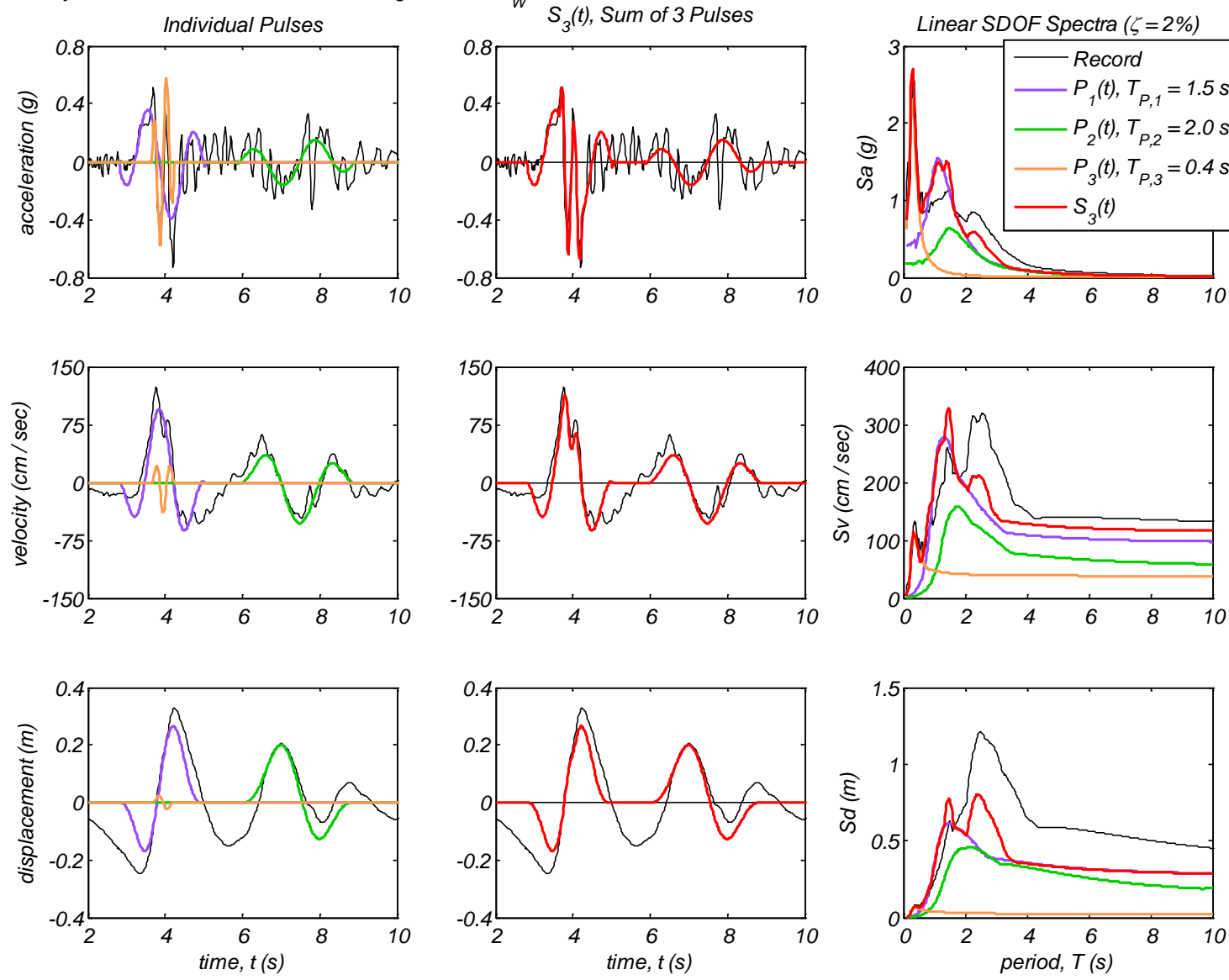
Appendix B3 – Time history and linear spectral response of three extracted pulses using the CPE<sub>V-AM</sub> method for 40 Motions

Record #19: Sylmar - Converter Sta East, Northridge, 1994,  $M_W 6.7$

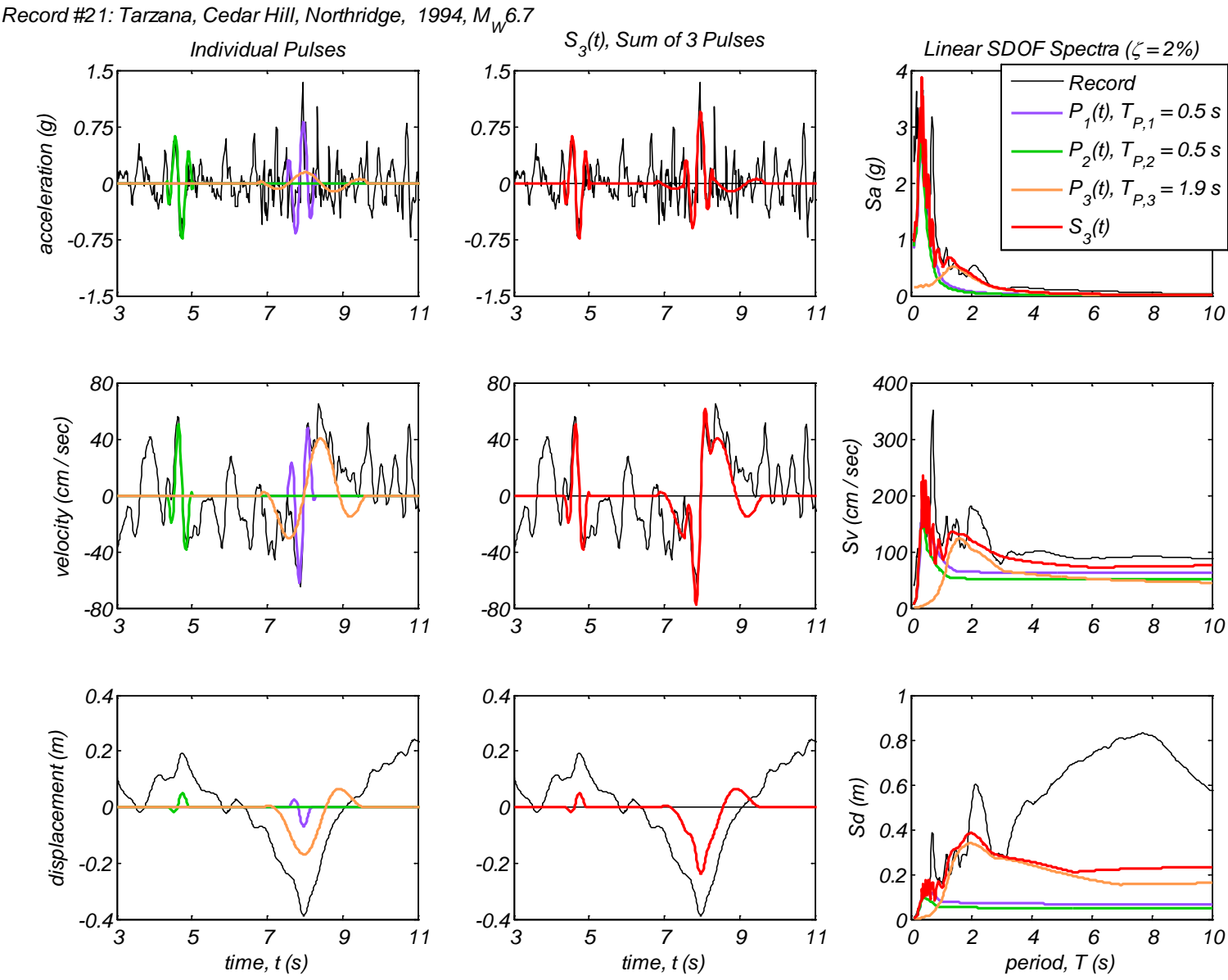


Appendix B3 – Time history and linear spectral response of three extracted pulses using the CPE<sub>V-AM</sub> method for 40 Motions

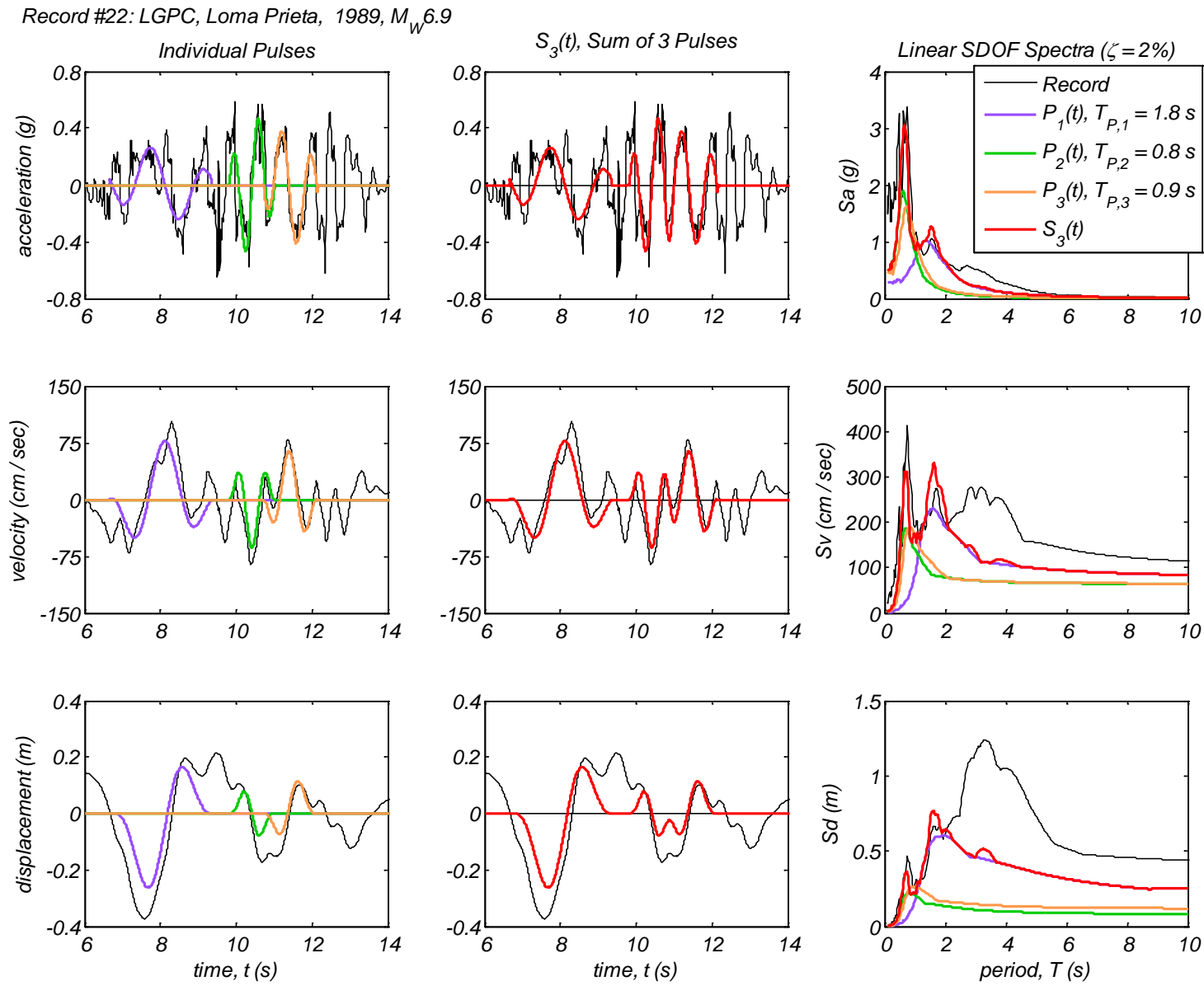
Record #20: Sylmar - Olive ViewMed FF, Northridge, 1994,  $M_w 6.7$



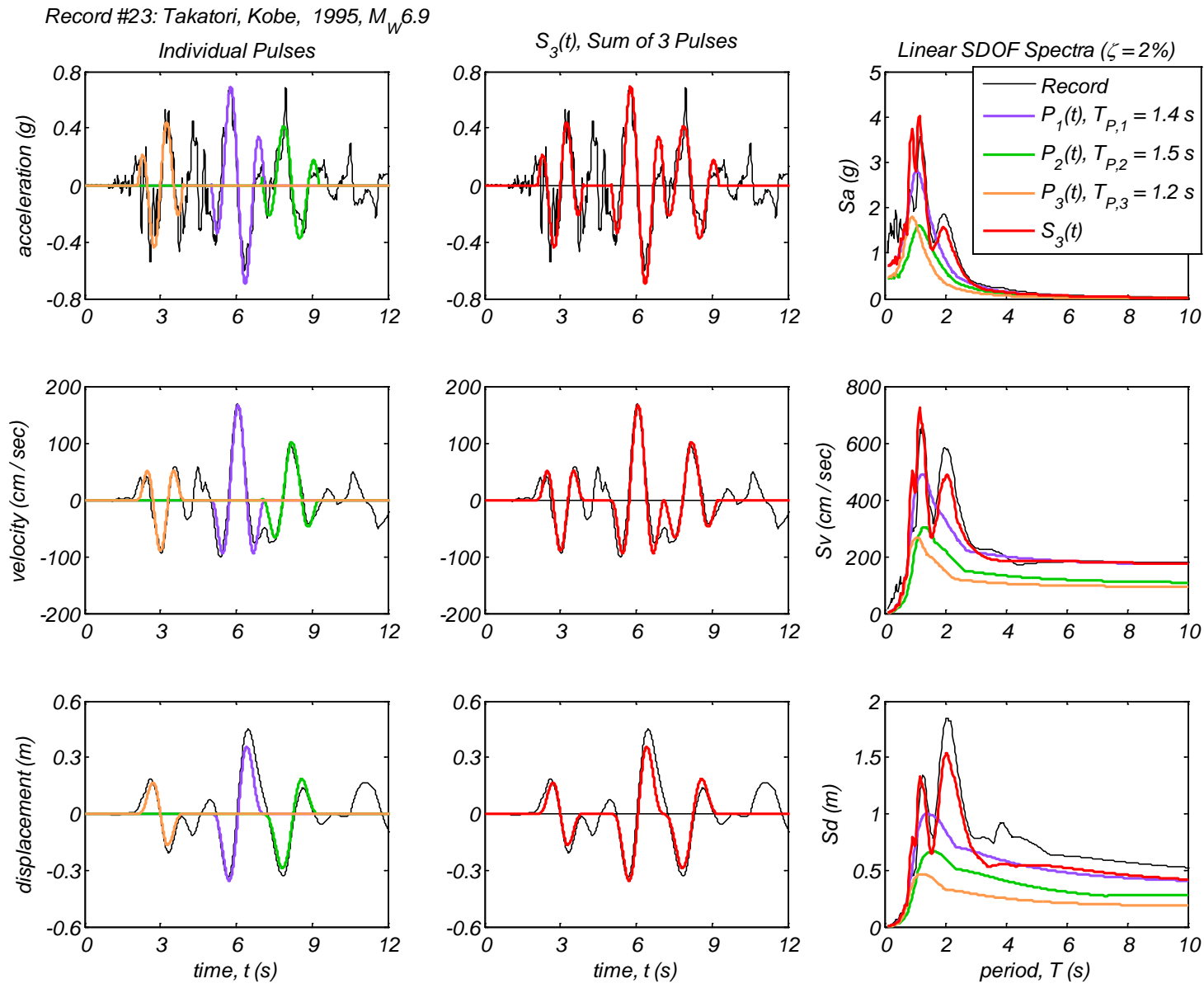
Appendix B3 – Time history and linear spectral response of three extracted pulses using the CPE<sub>V-AM</sub> method for 40 Motions



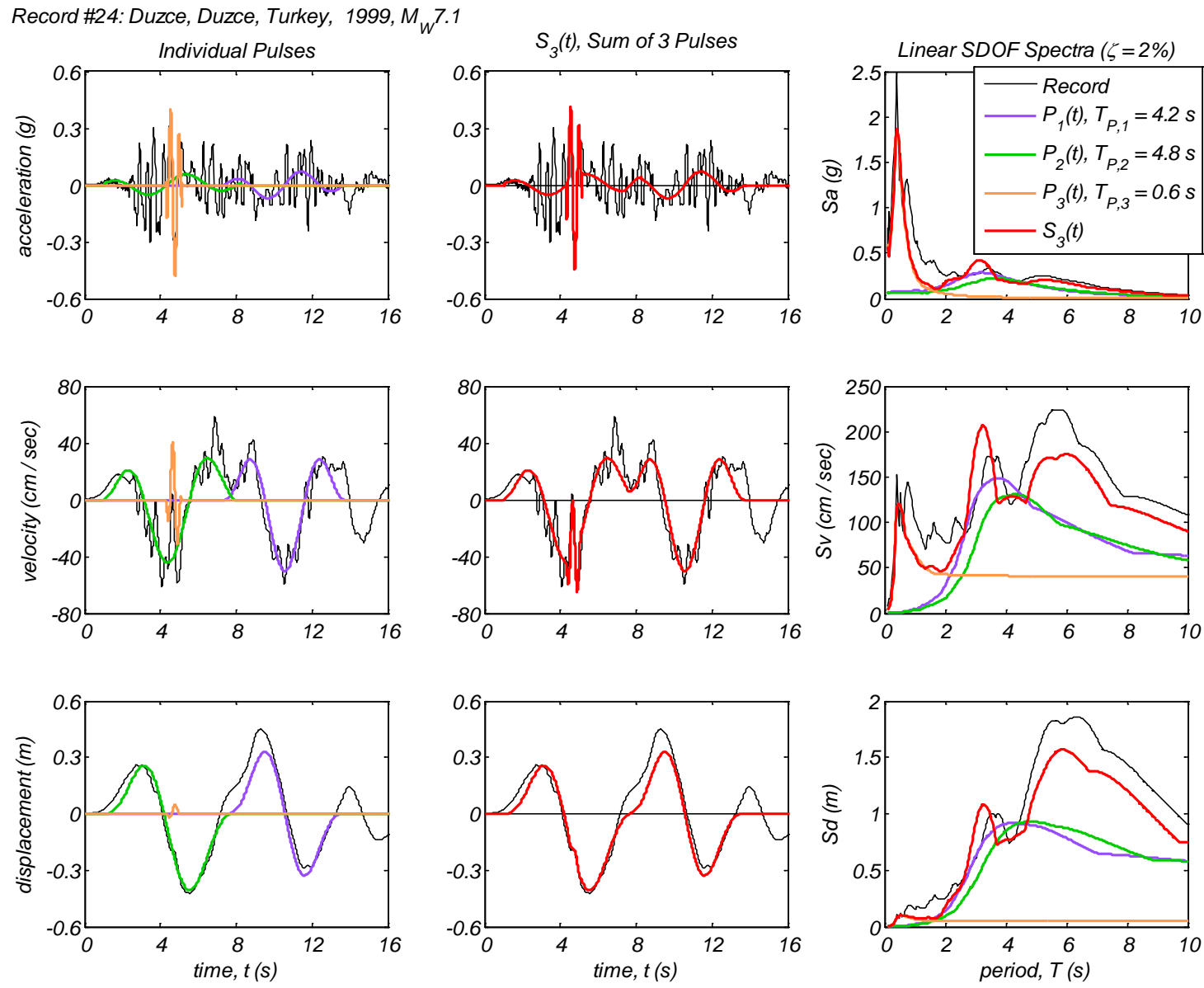
Appendix B3 – Time history and linear spectral response of three extracted pulses using the CPE<sub>V-AM</sub> method for 40 Motions



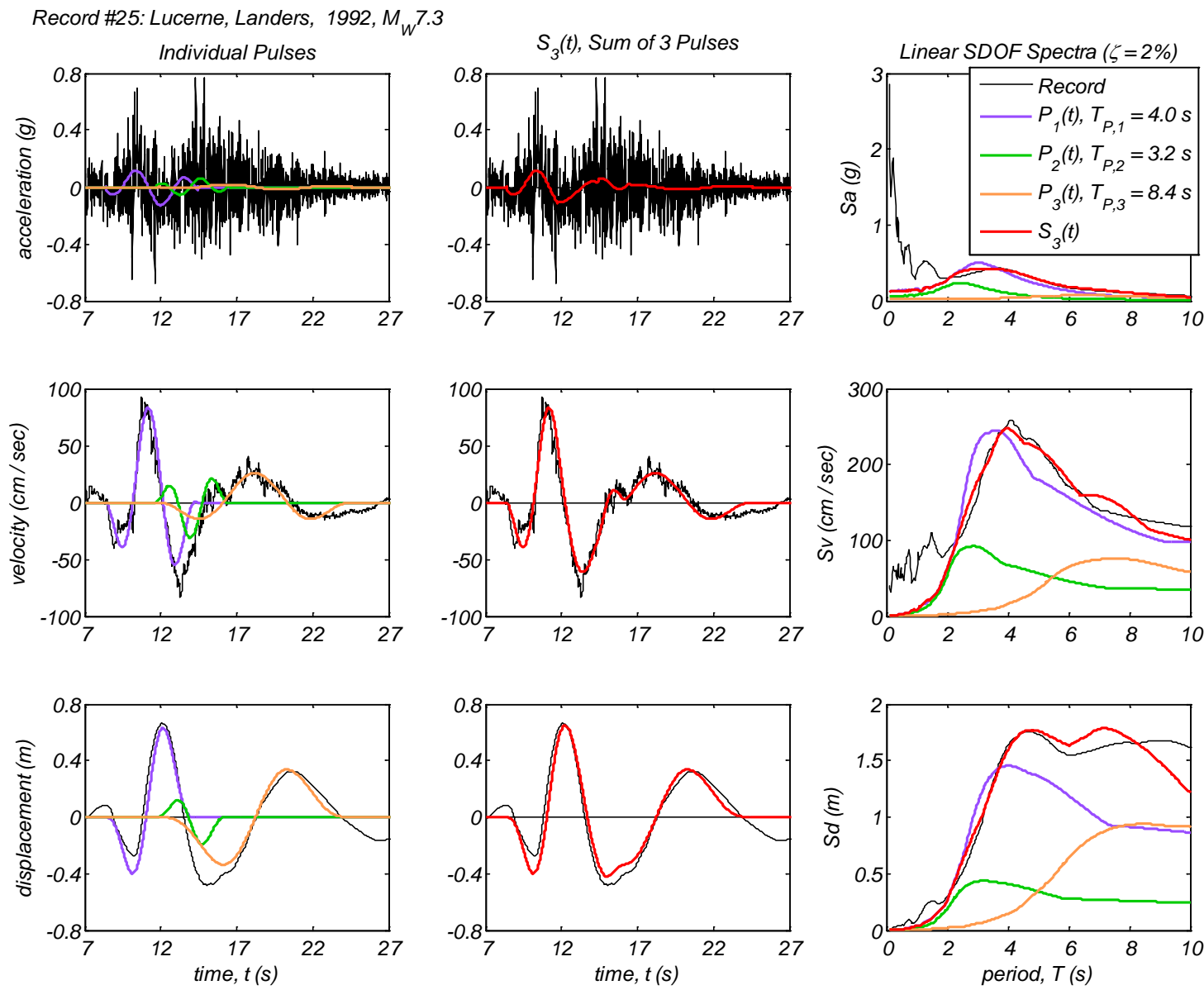
Appendix B3 – Time history and linear spectral response of three extracted pulses using the CPE<sub>V-AM</sub> method for 40 Motions



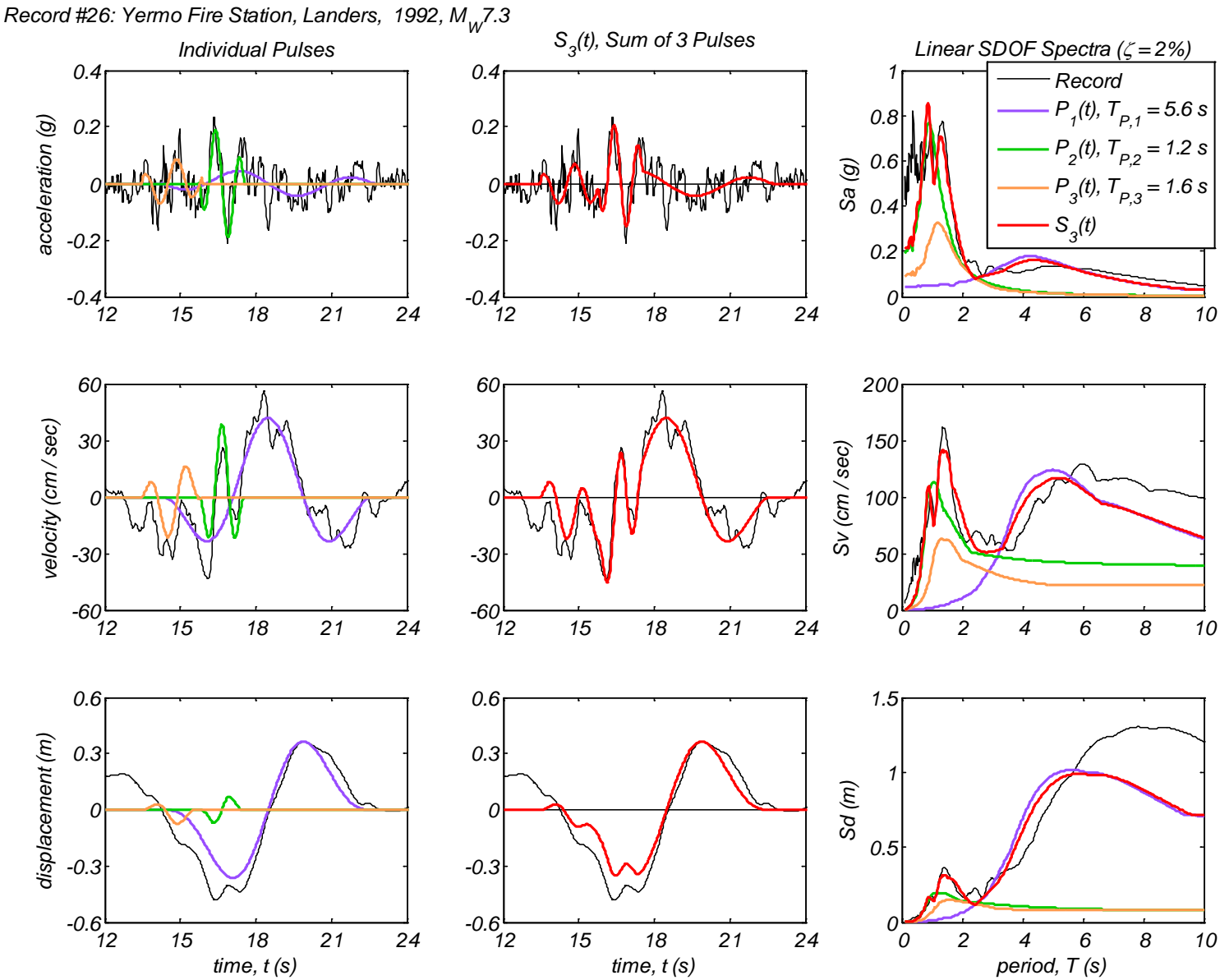
Appendix B3 – Time history and linear spectral response of three extracted pulses using the CPE<sub>V-AM</sub> method for 40 Motions



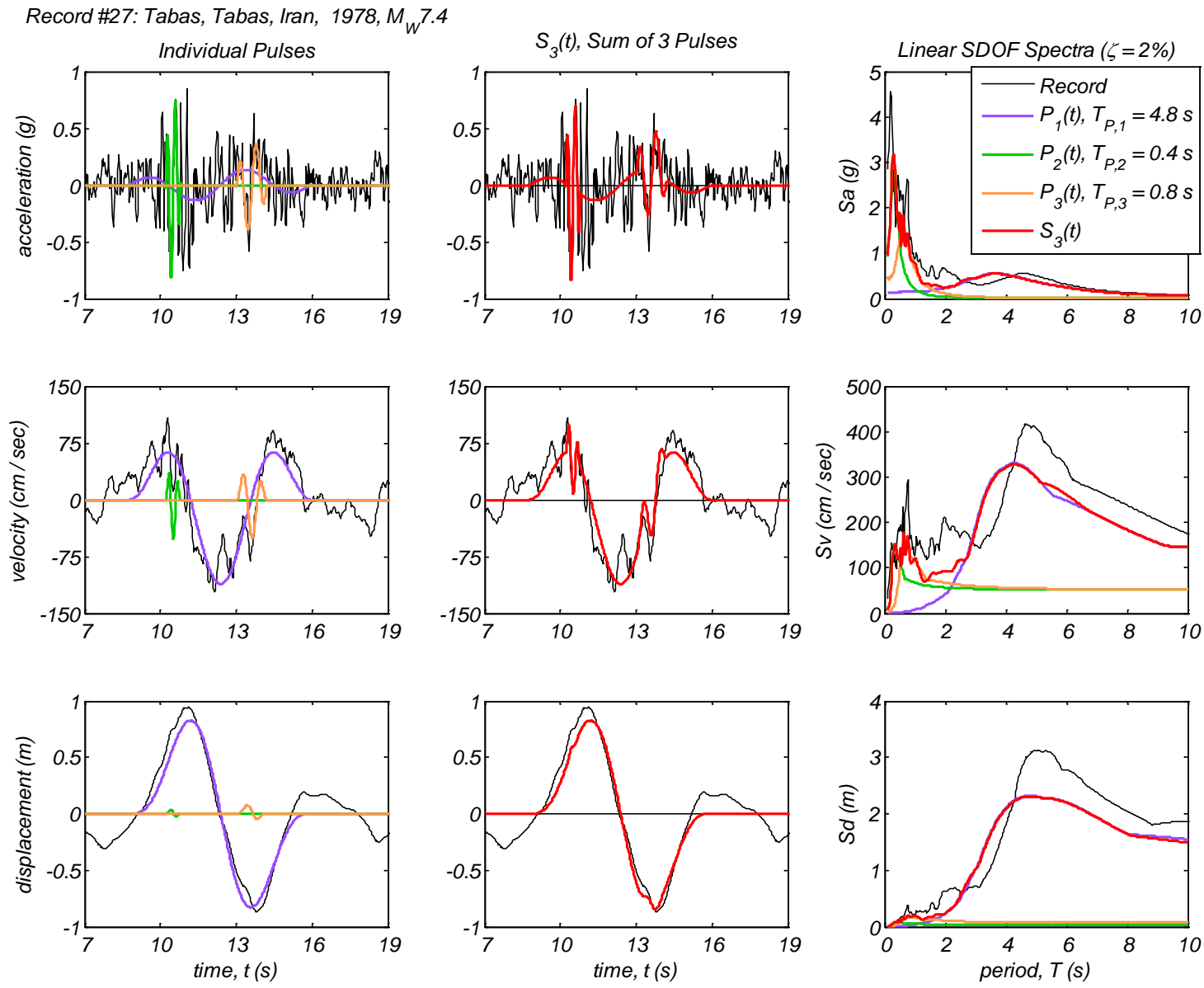
Appendix B3 – Time history and linear spectral response of three extracted pulses using the CPE<sub>V-AM</sub> method for 40 Motions



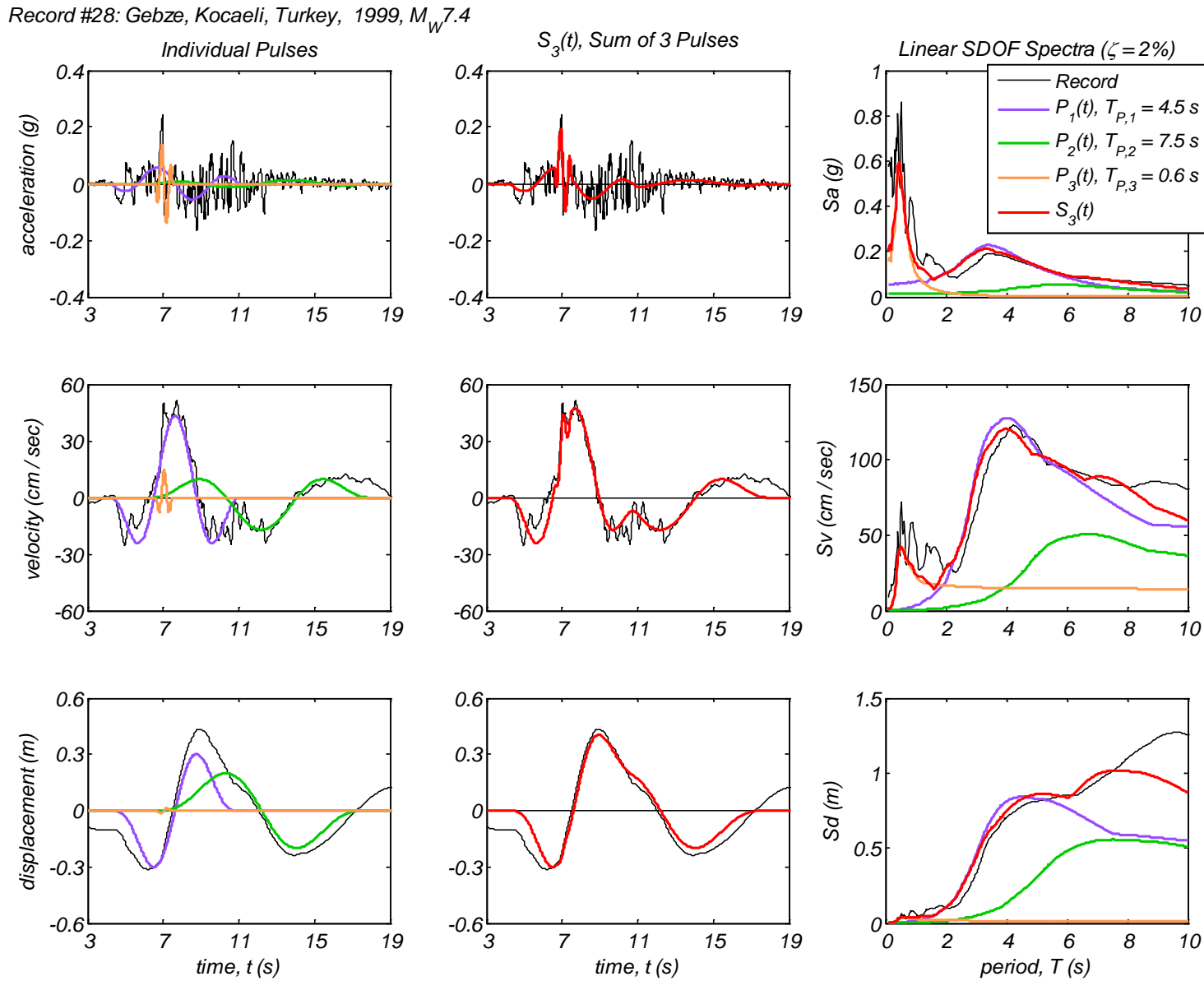
Appendix B3 – Time history and linear spectral response of three extracted pulses using the CPE<sub>V-AM</sub> method for 40 Motions



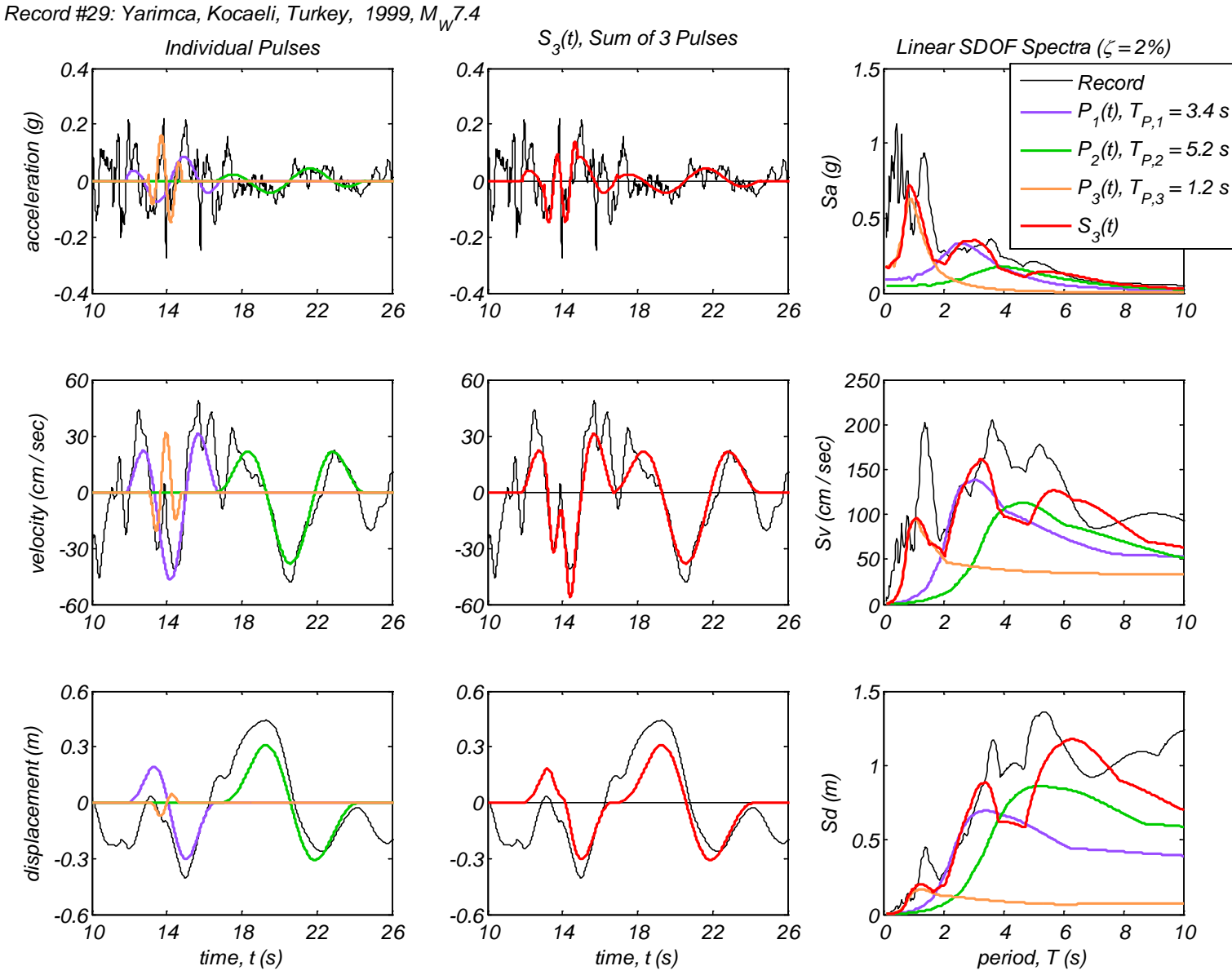
Appendix B3 – Time history and linear spectral response of three extracted pulses using the CPE<sub>V-AM</sub> method for 40 Motions



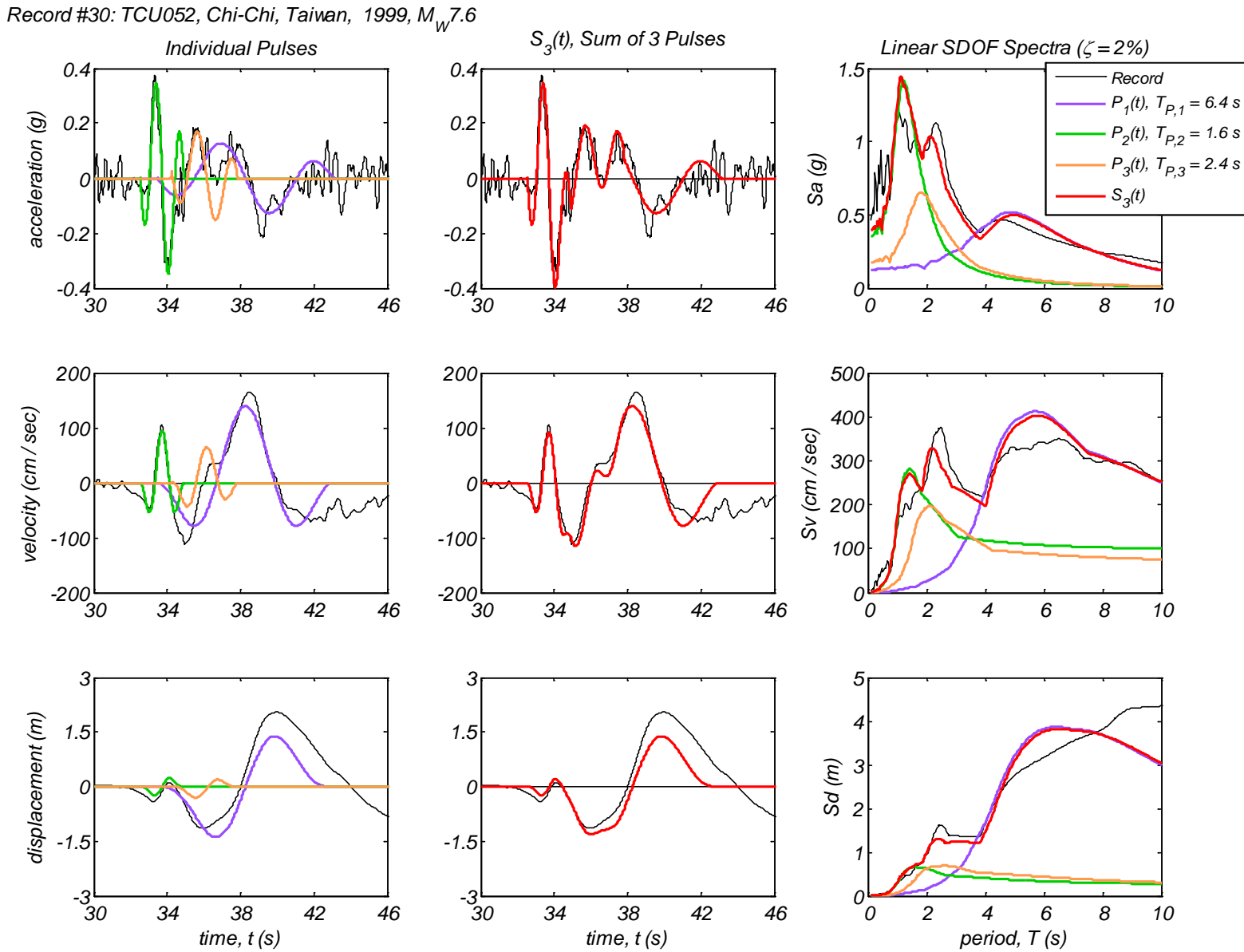
Appendix B3 – Time history and linear spectral response of three extracted pulses using the CPE<sub>V-AM</sub> method for 40 Motions



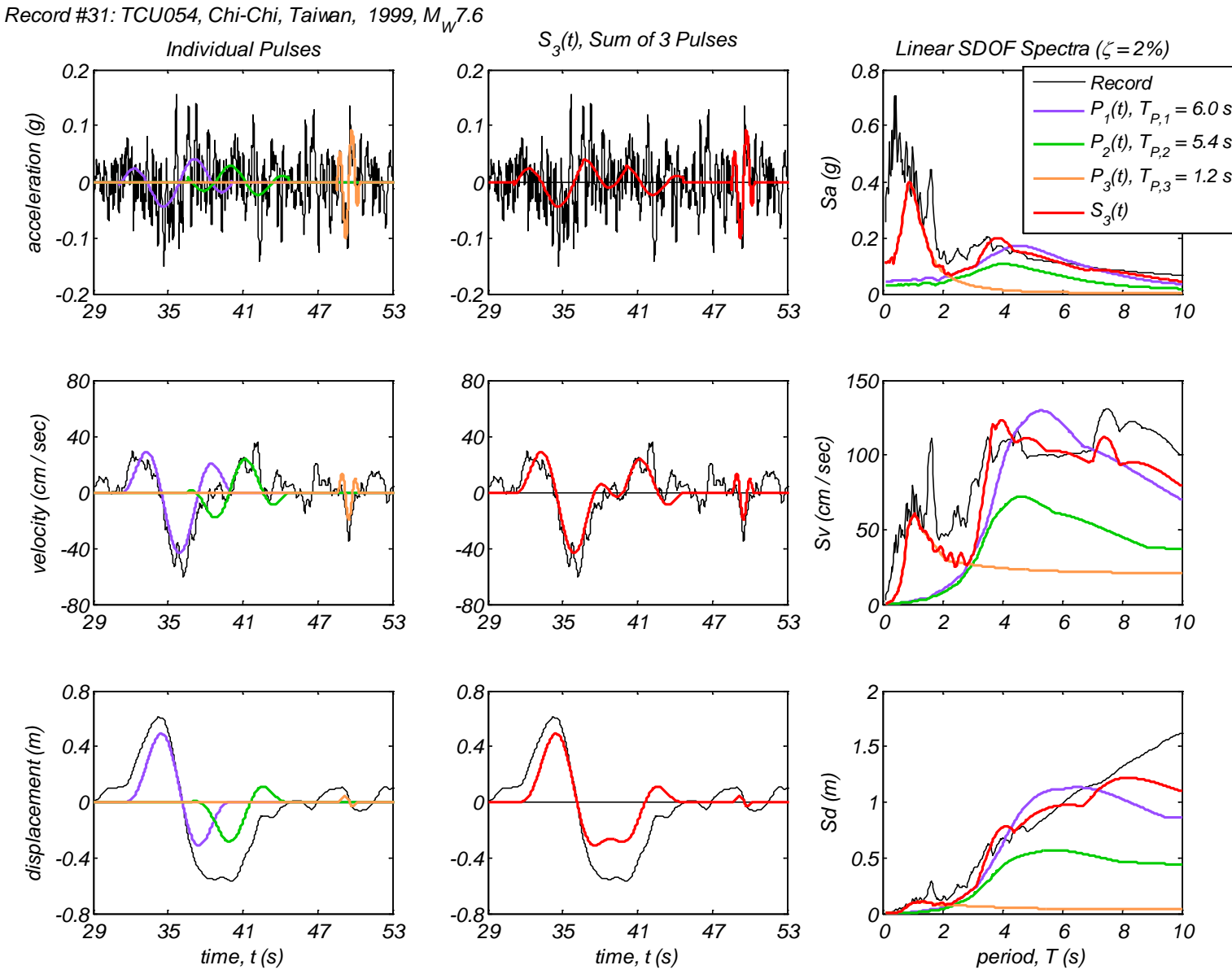
Appendix B3 – Time history and linear spectral response of three extracted pulses using the CPE<sub>V-AM</sub> method for 40 Motions



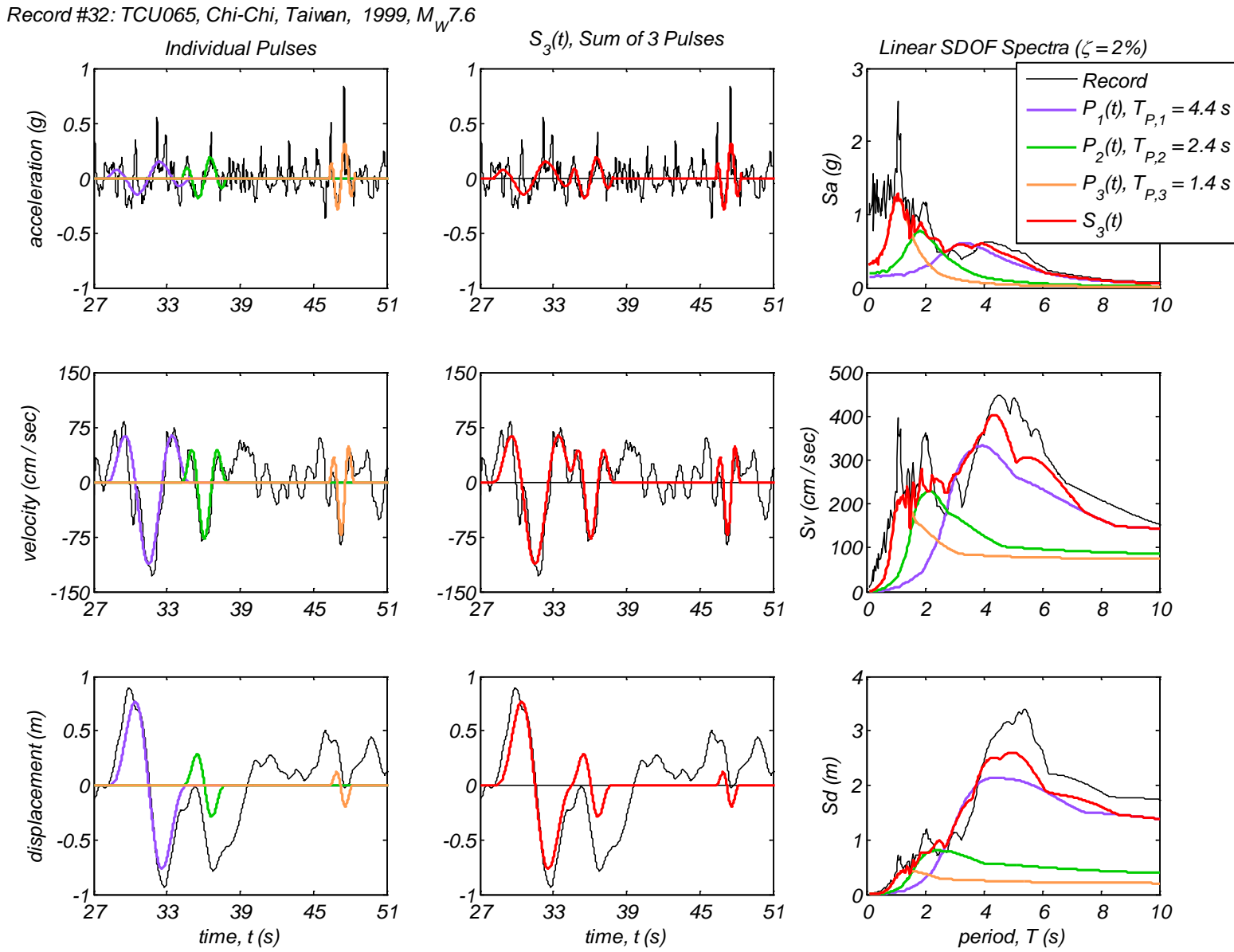
Appendix B3 – Time history and linear spectral response of three extracted pulses using the CPE<sub>V-AM</sub> method for 40 Motions



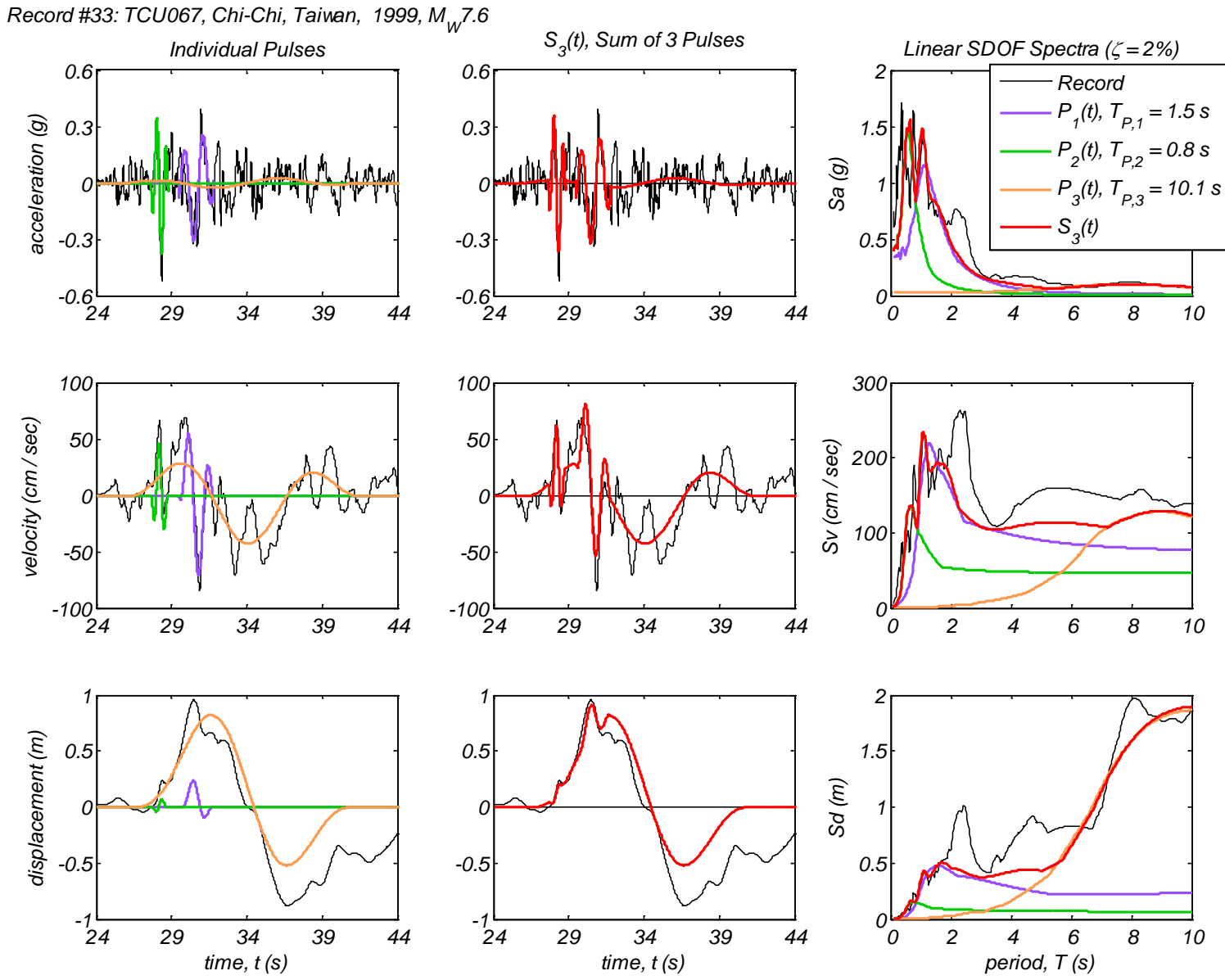
Appendix B3 – Time history and linear spectral response of three extracted pulses using the CPE<sub>V-AM</sub> method for 40 Motions



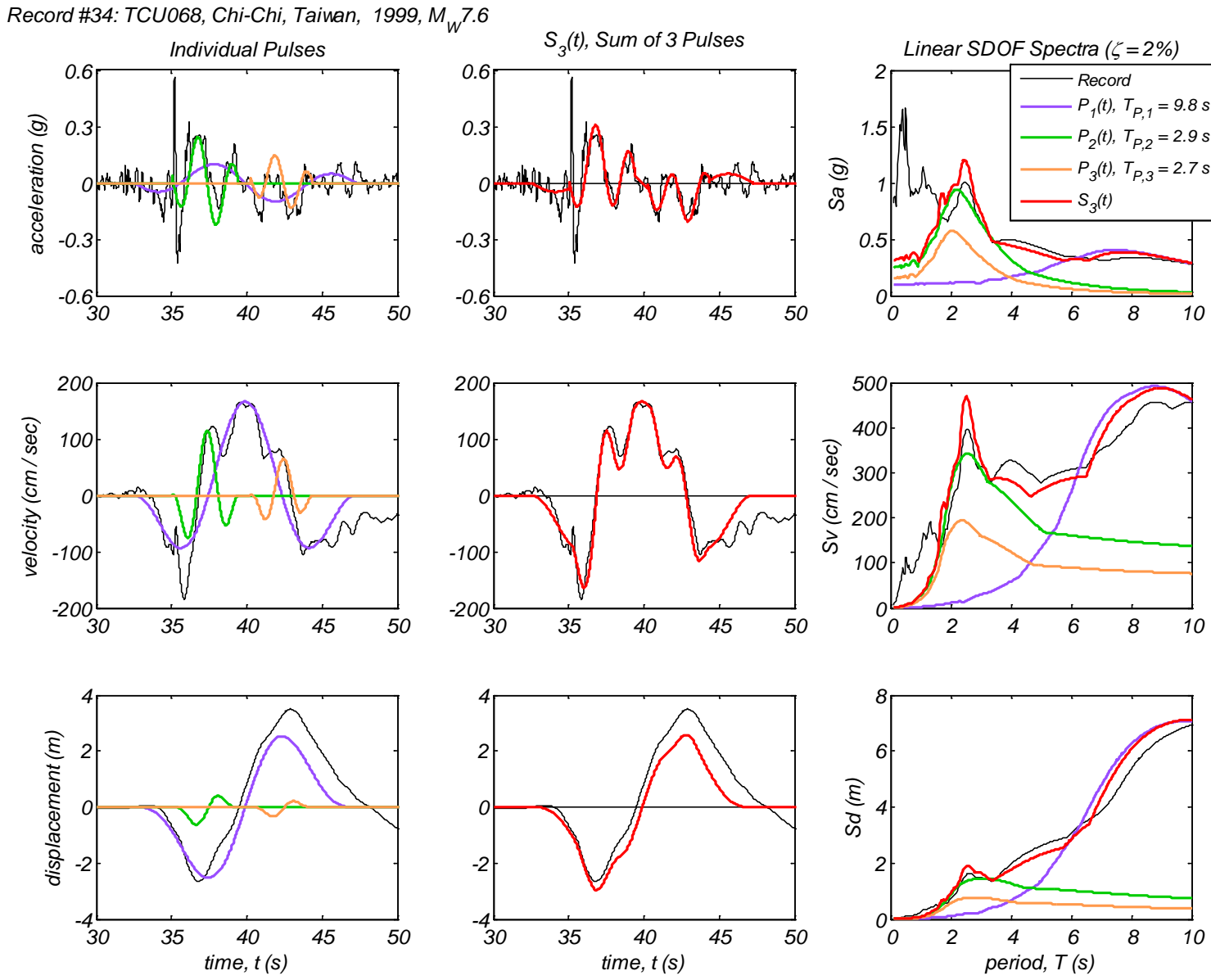
Appendix B3 – Time history and linear spectral response of three extracted pulses using the CPE<sub>V-AM</sub> method for 40 Motions



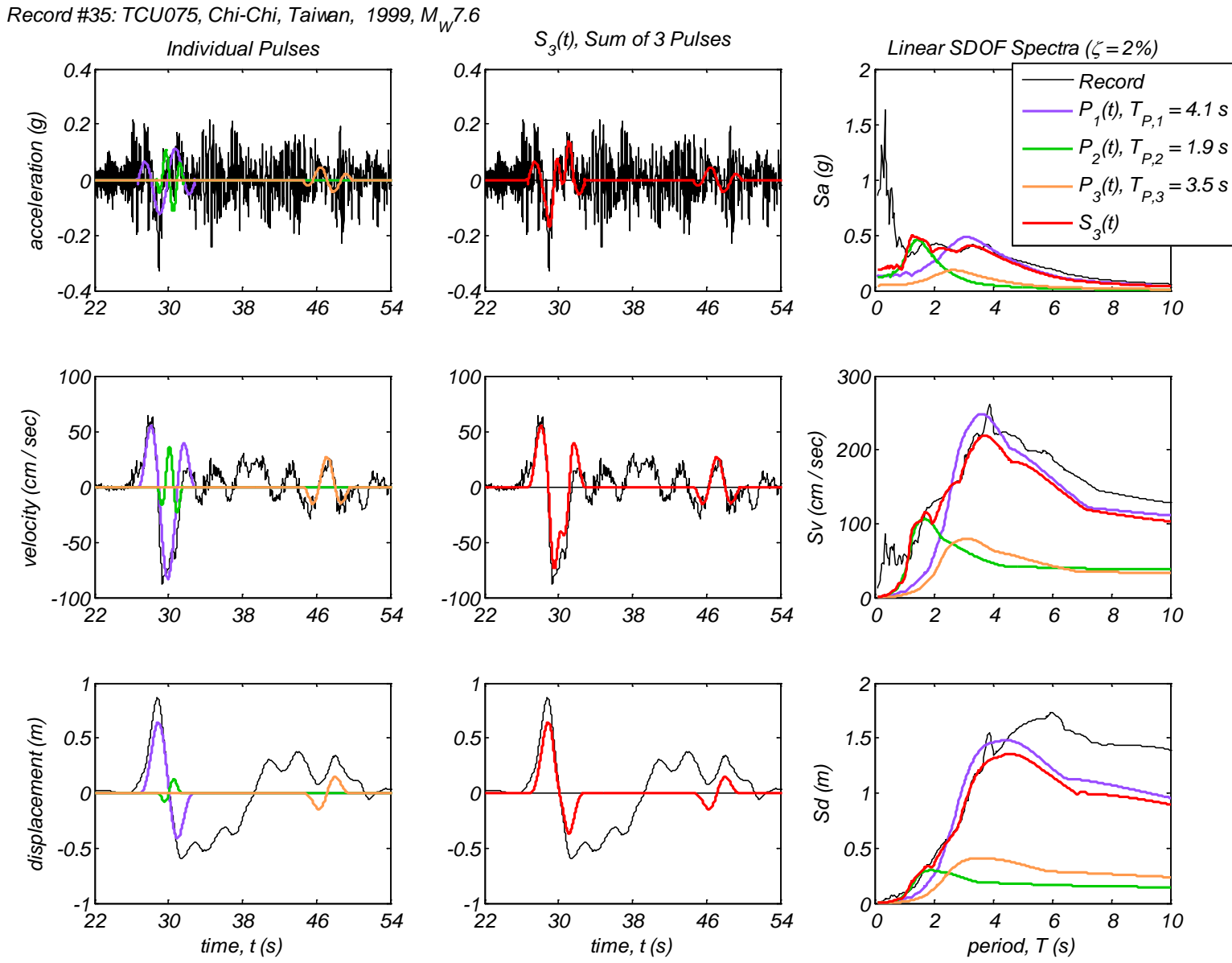
Appendix B3 – Time history and linear spectral response of three extracted pulses using the CPE<sub>V-AM</sub> method for 40 Motions



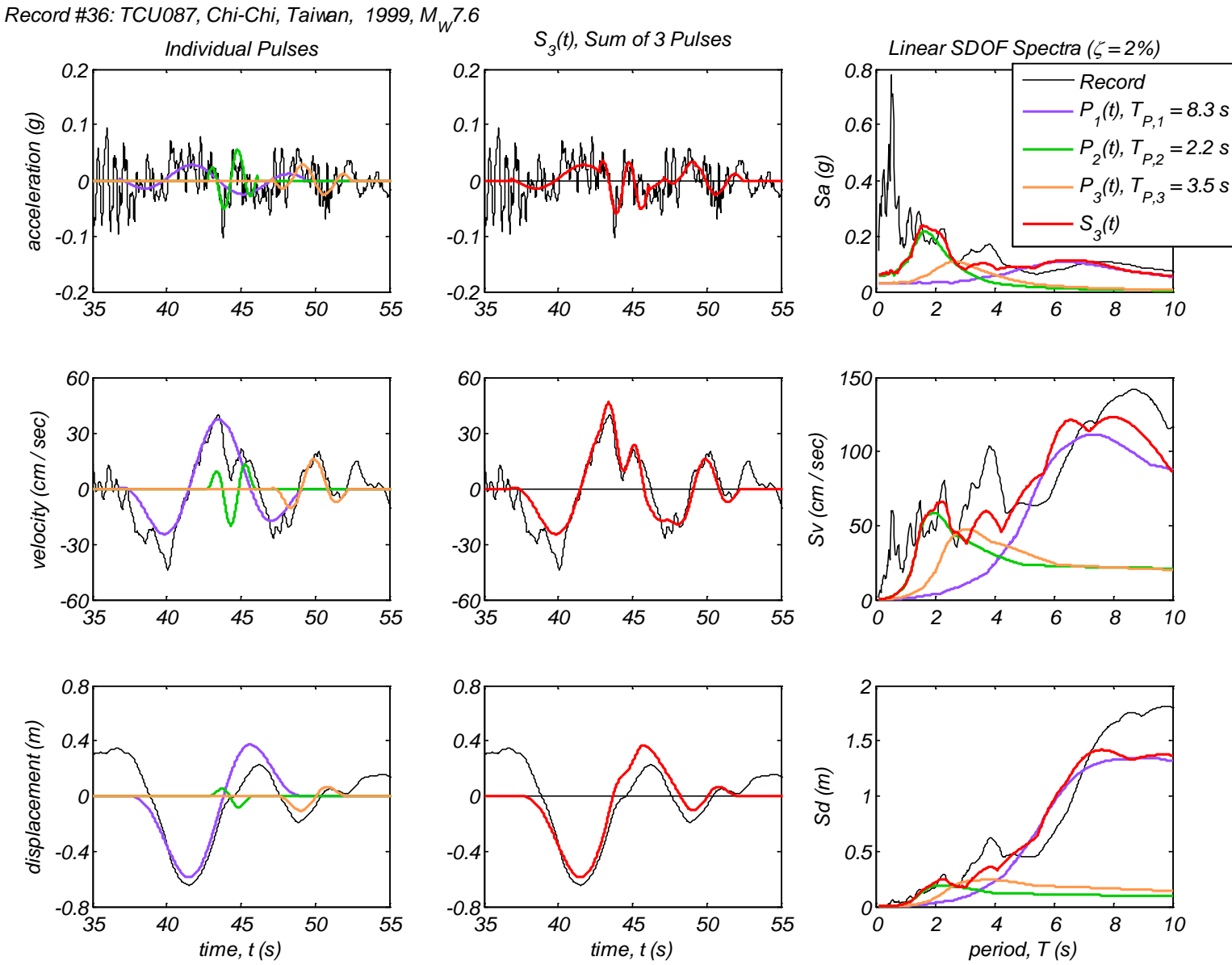
Appendix B3 – Time history and linear spectral response of three extracted pulses using the CPE<sub>V-AM</sub> method for 40 Motions



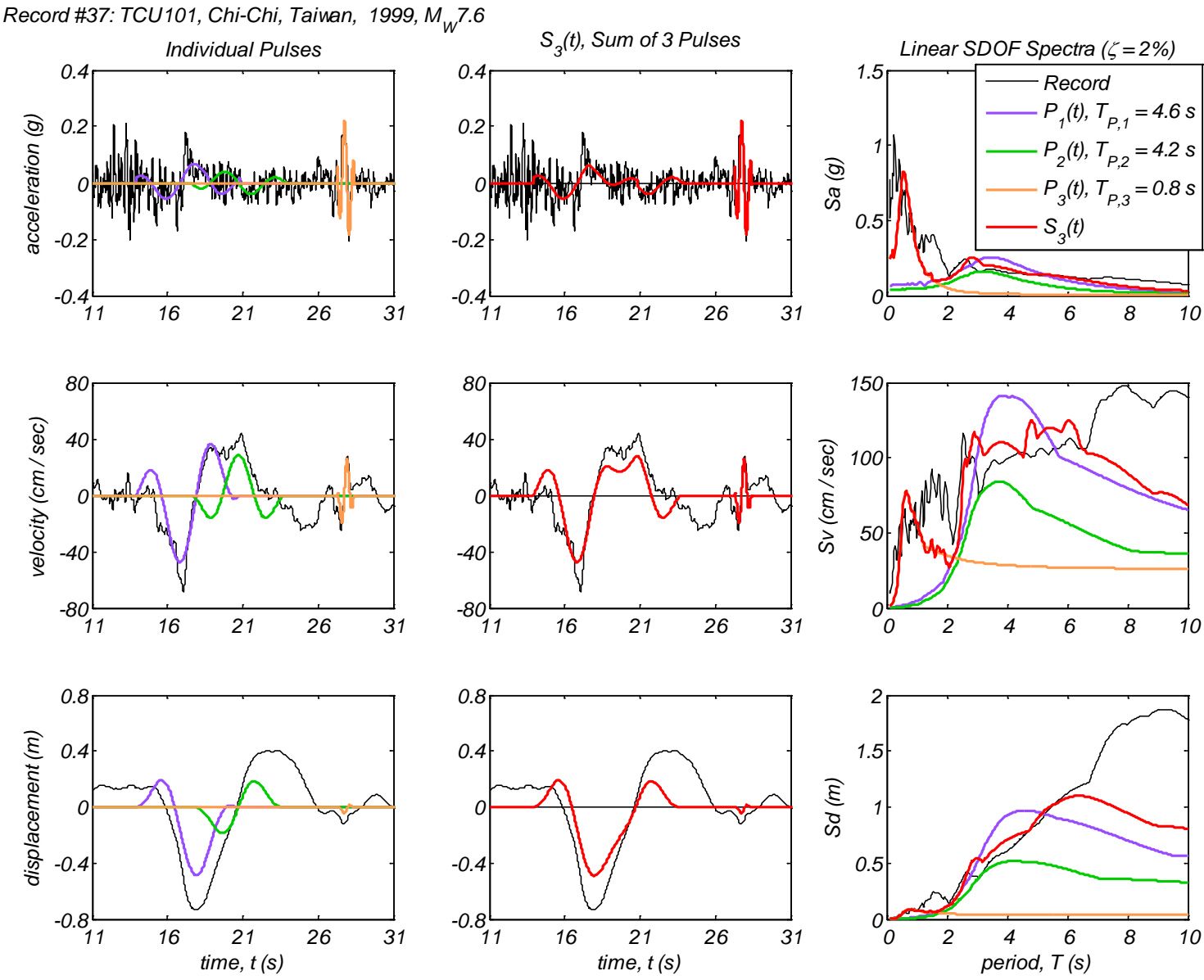
Appendix B3 – Time history and linear spectral response of three extracted pulses using the CPE<sub>V-AM</sub> method for 40 Motions



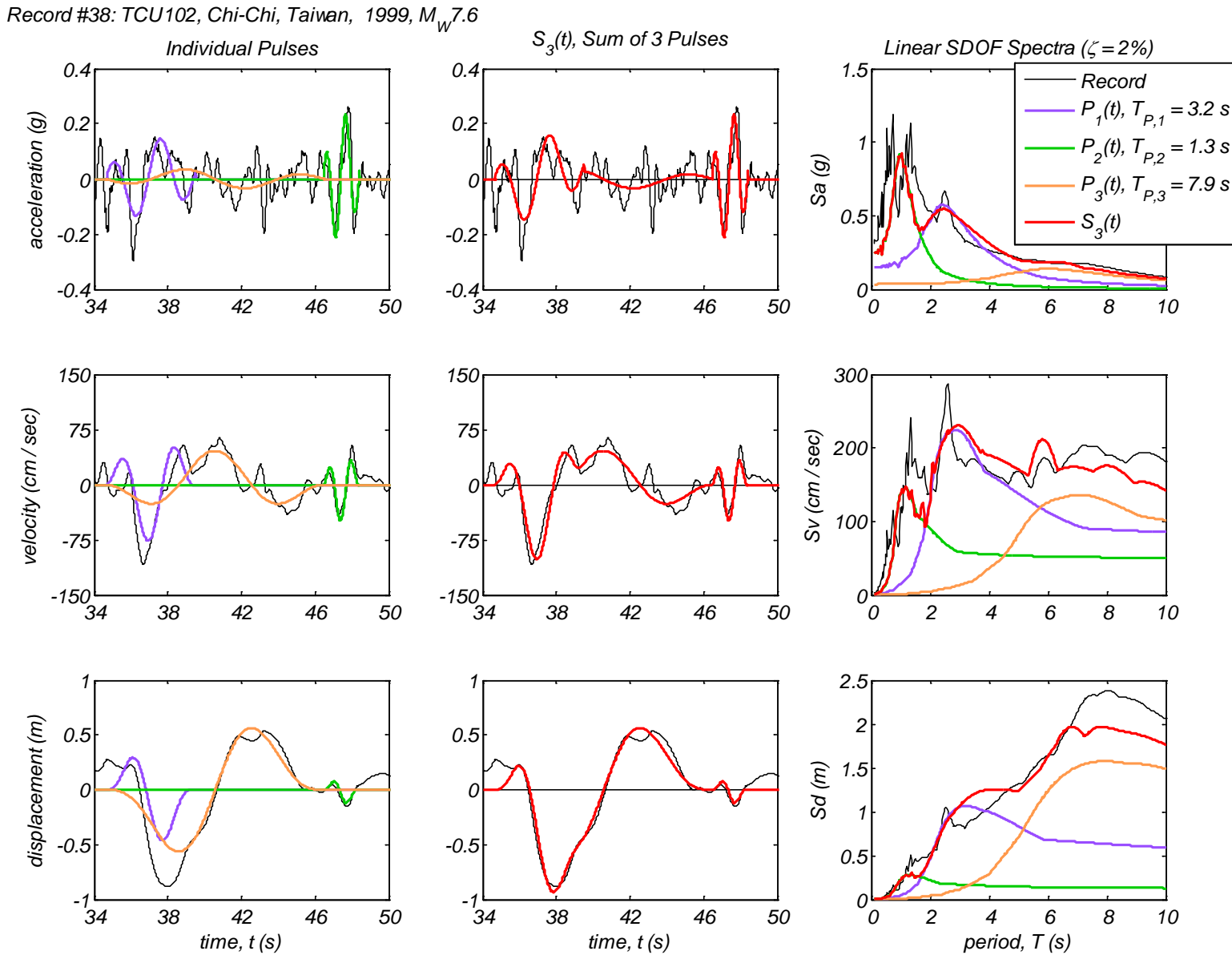
Appendix B3 – Time history and linear spectral response of three extracted pulses using the CPE<sub>V-AM</sub> method for 40 Motions



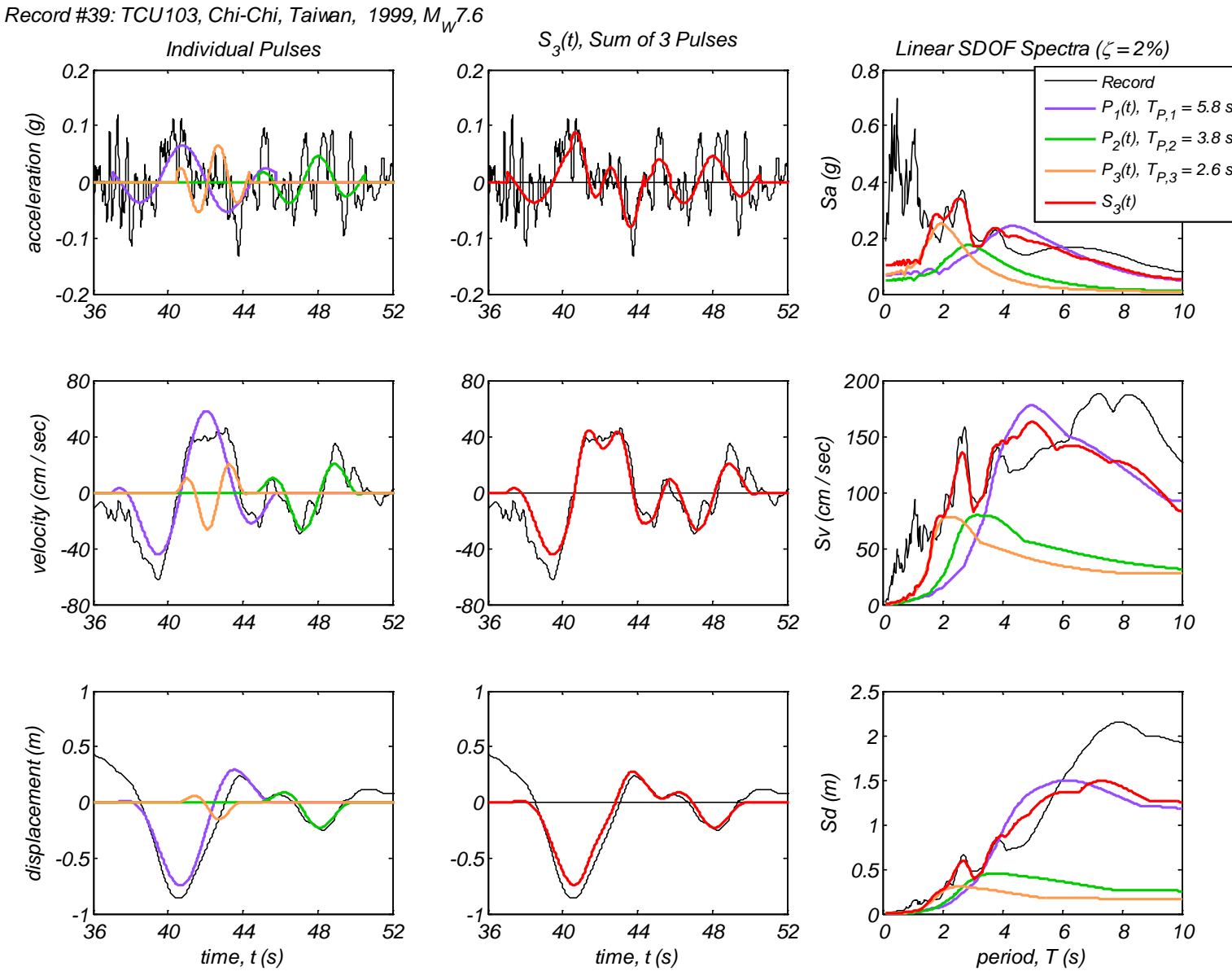
Appendix B3 – Time history and linear spectral response of three extracted pulses using the CPE<sub>V-AM</sub> method for 40 Motions



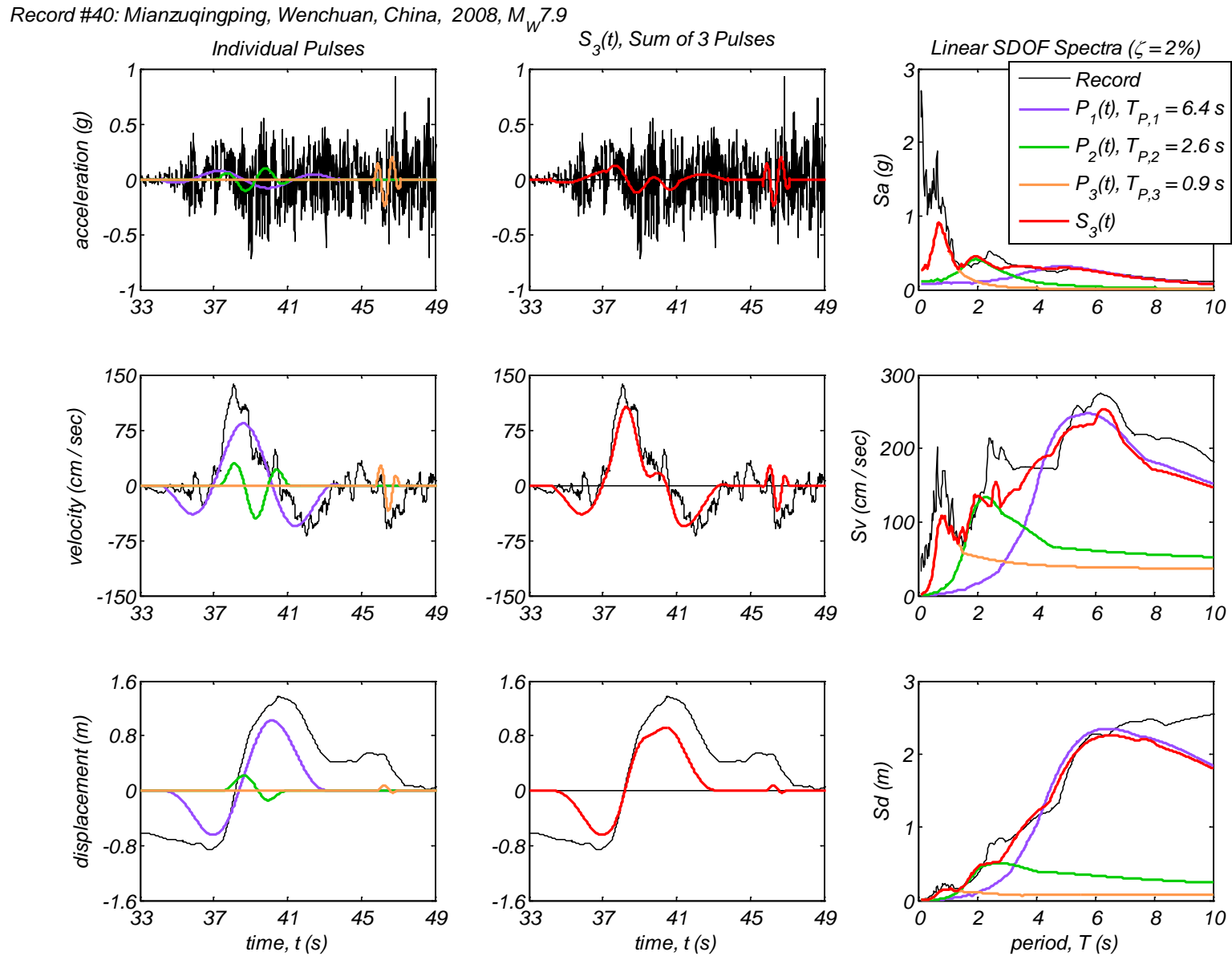
Appendix B3 – Time history and linear spectral response of three extracted pulses using the CPE<sub>V-AM</sub> method for 40 Motions



Appendix B3 – Time history and linear spectral response of three extracted pulses using the CPE<sub>V-AM</sub> method for 40 Motions

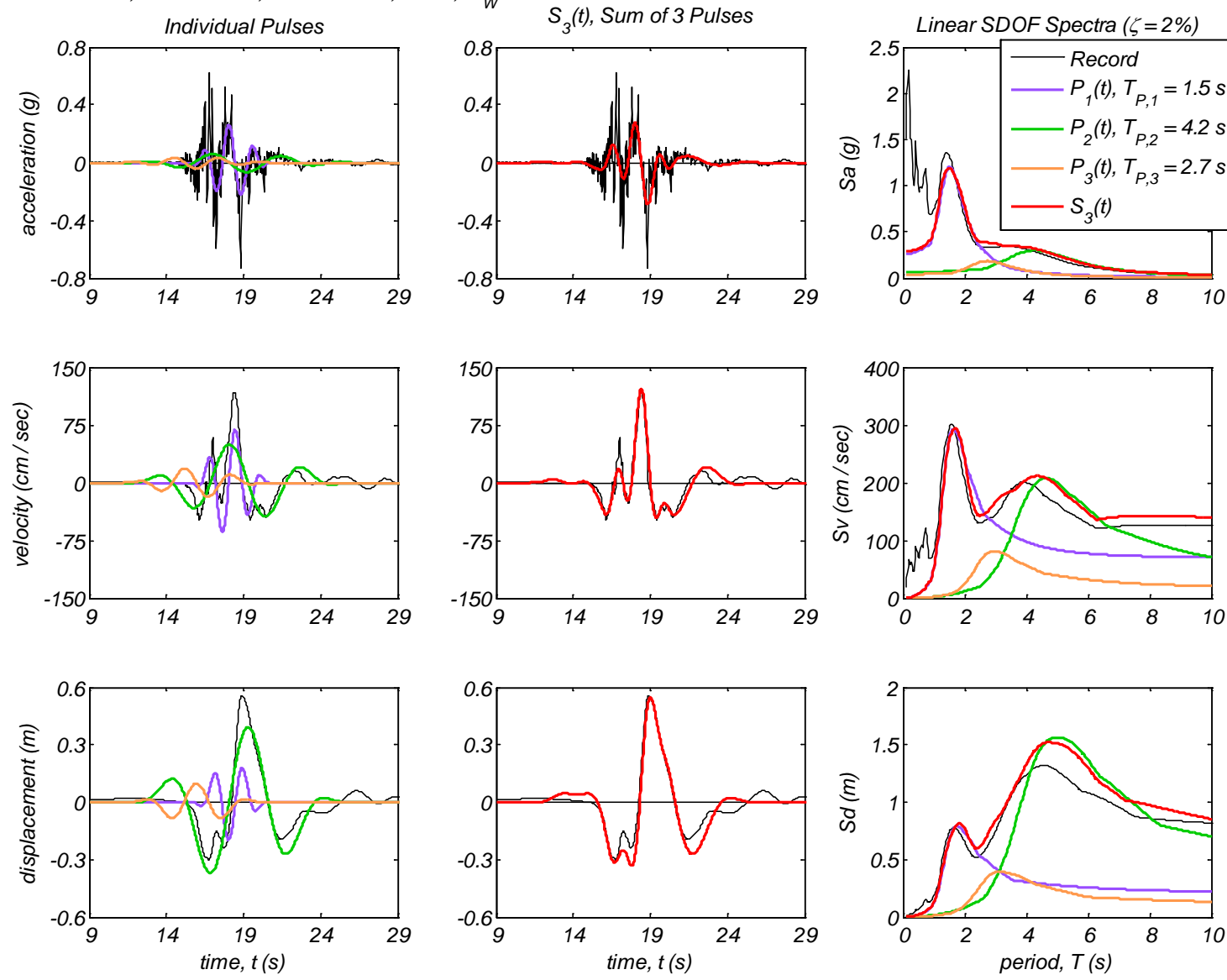


Appendix B3 – Time history and linear spectral response of three extracted pulses using the CPE<sub>V-AM</sub> method for 40 Motions



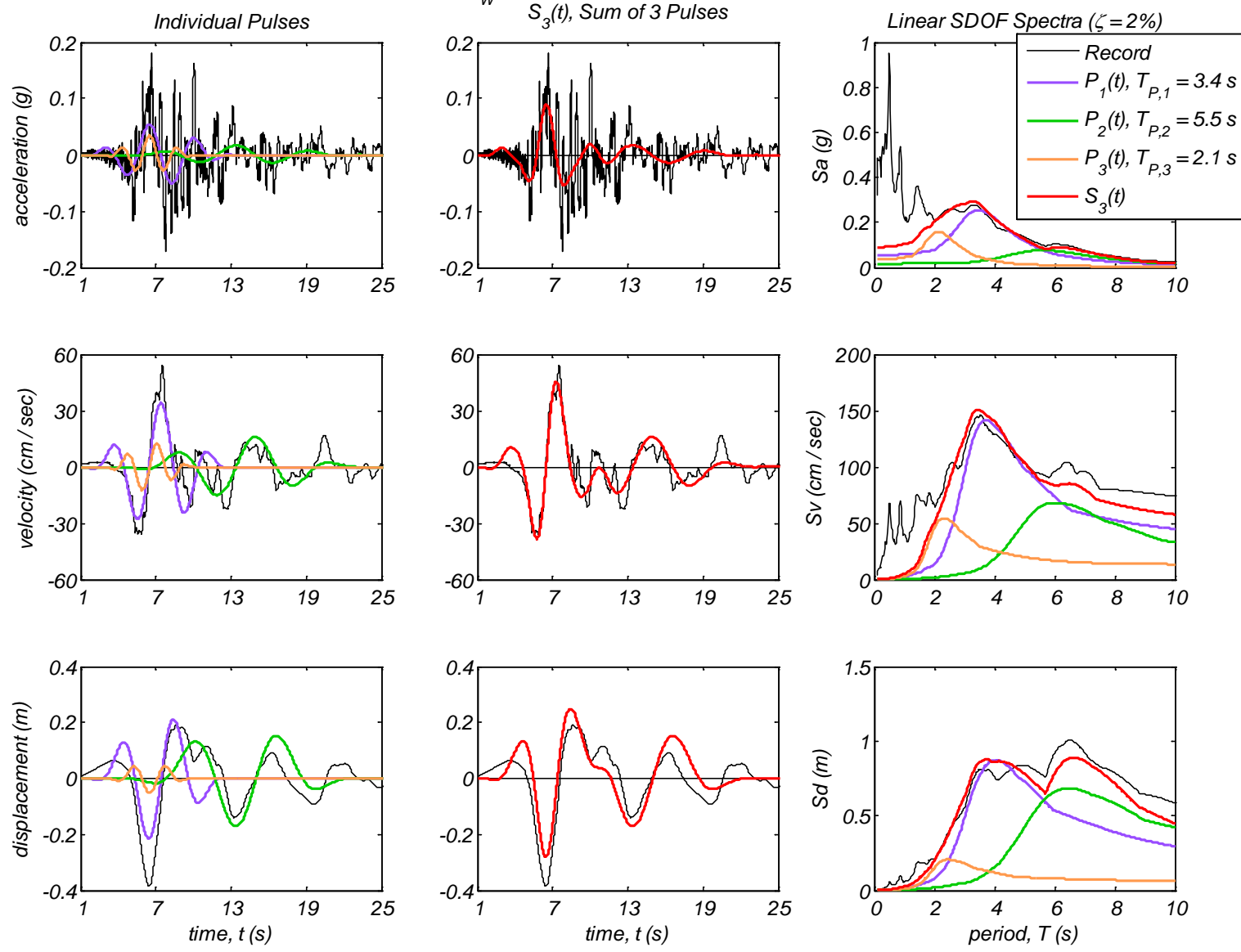
## Appendix B4: Time history and linear spectral response of three extracted pulses using the CPE<sub>A-AR</sub> method for 40 motions

Record #1: PRPC, Christchurch, New Zealand, 2011,  $M_W 6.3$

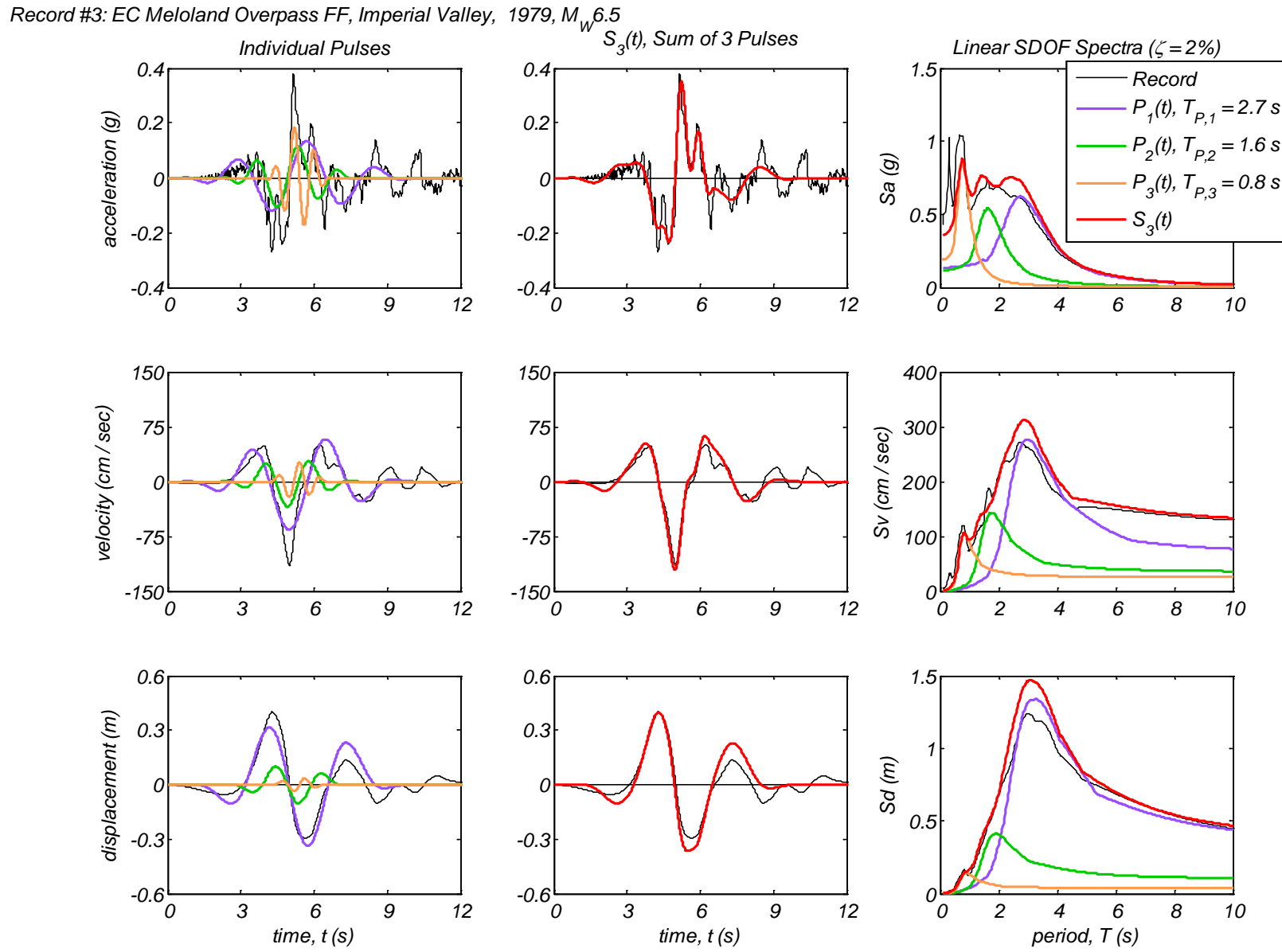


Appendix B4 – Time history and linear spectral response of three extracted pulses using the CPE<sub>A-AR</sub> method for 40 Motions

Record #2: EC County Center FF, Imperial Valley, 1979,  $M_W 6.5$

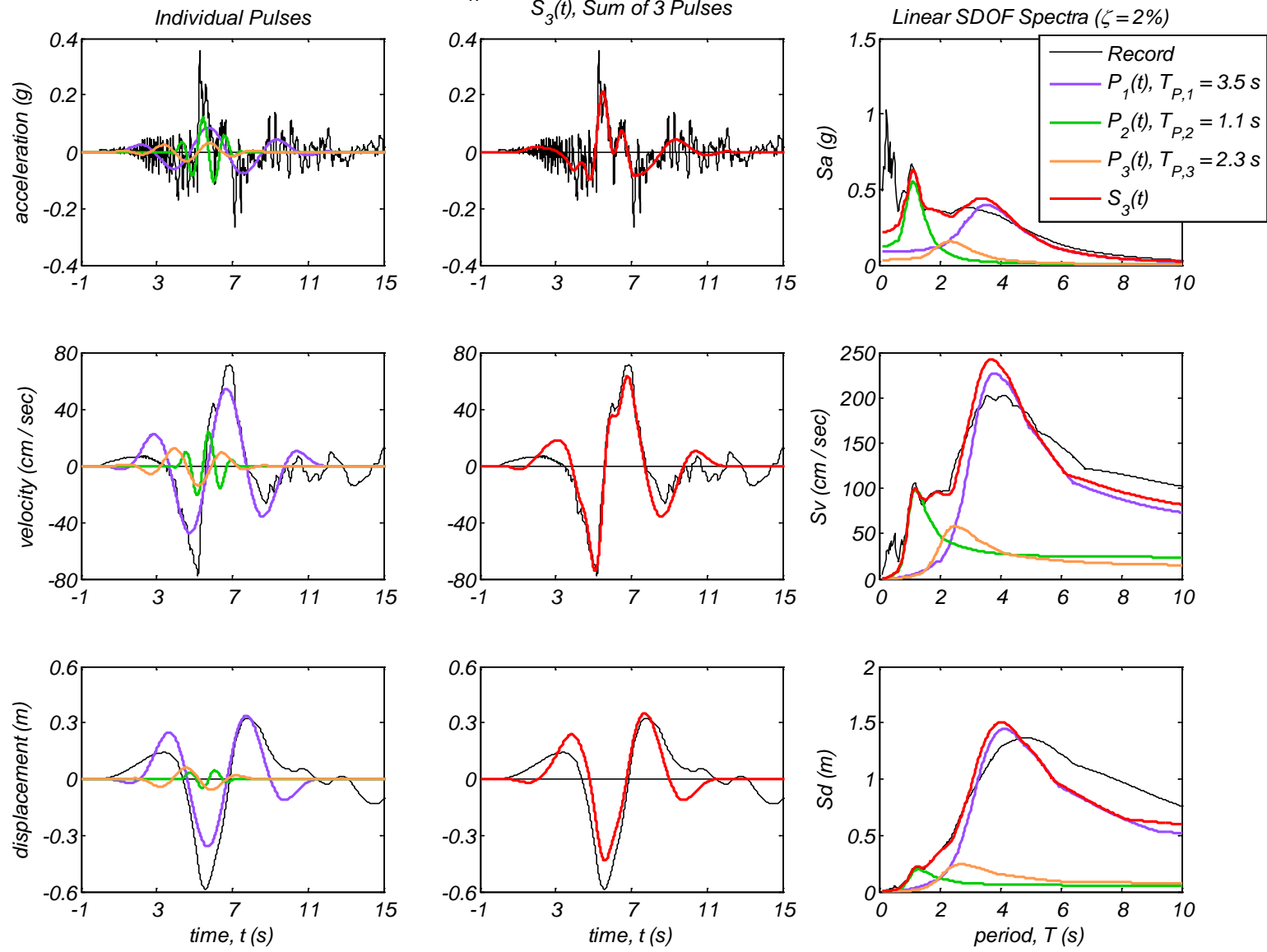


Appendix B4 – Time history and linear spectral response of three extracted pulses using the CPE<sub>A-AR</sub> method for 40 Motions



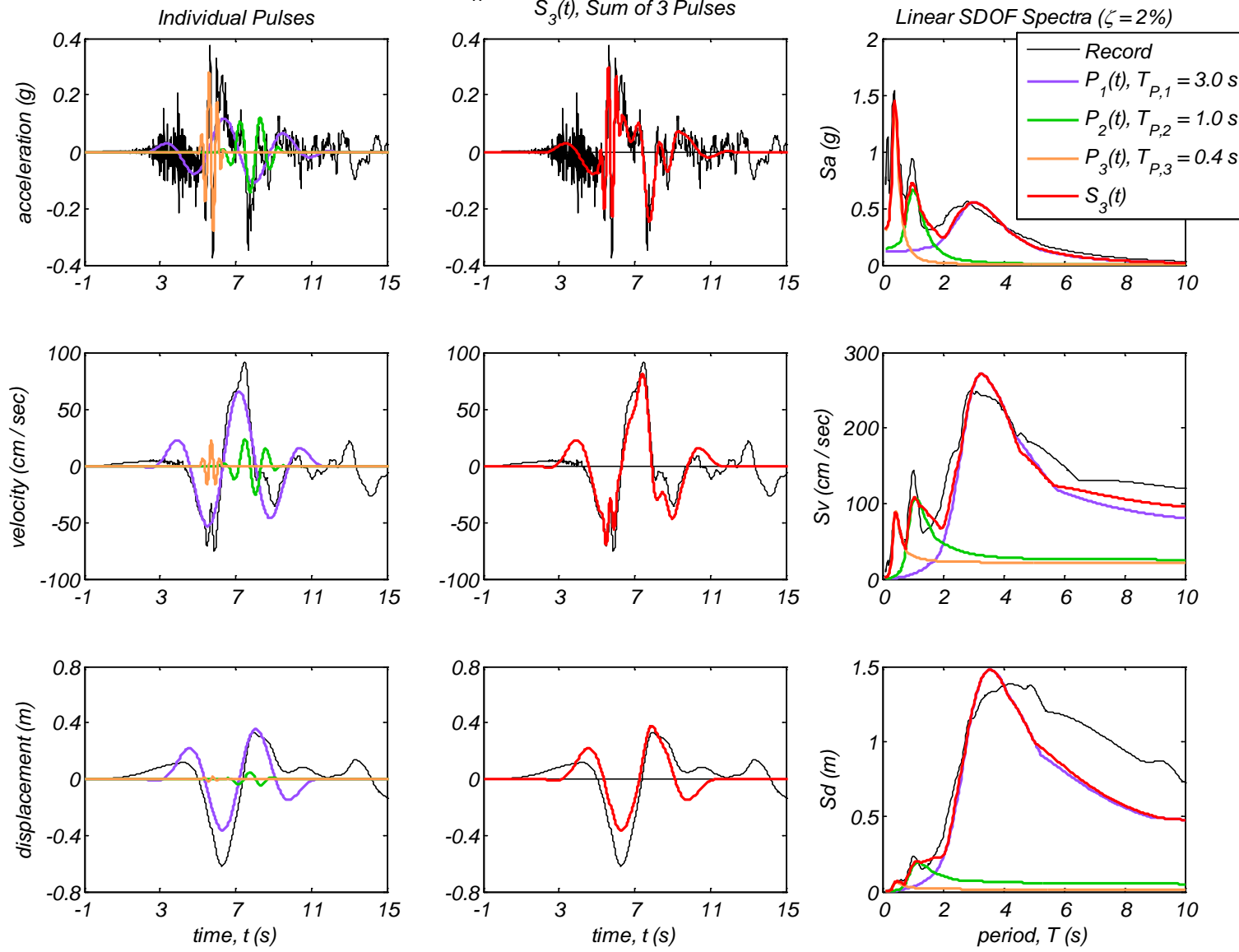
Appendix B4 – Time history and linear spectral response of three extracted pulses using the CPE<sub>A-AR</sub> method for 40 Motions

Record #4: El Centro Array #4, Imperial Valley, 1979,  $M_W 6.5$

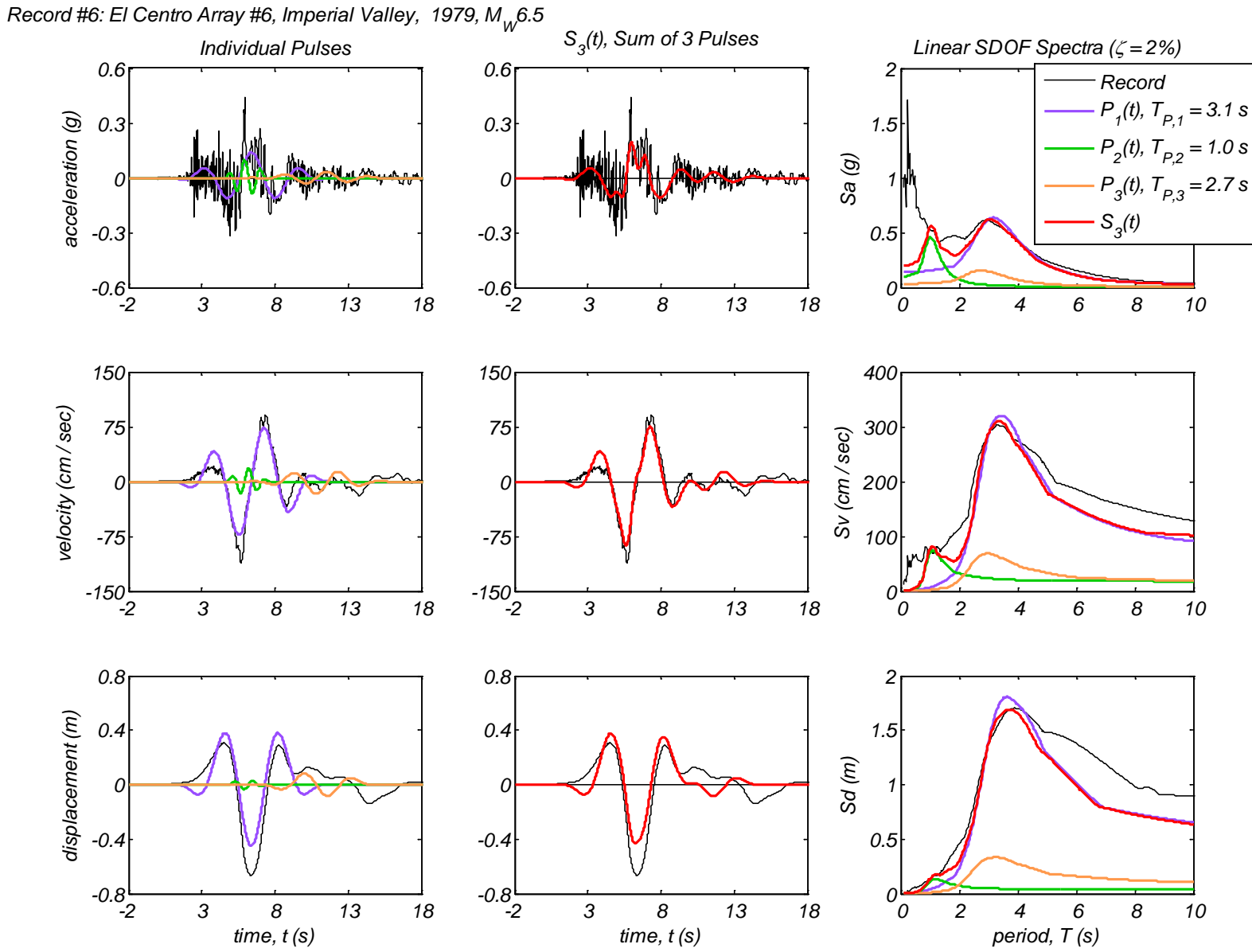


Appendix B4 – Time history and linear spectral response of three extracted pulses using the CPE<sub>A-AR</sub> method for 40 Motions

Record #5: El Centro Array #5, Imperial Valley, 1979,  $M_W 6.5$

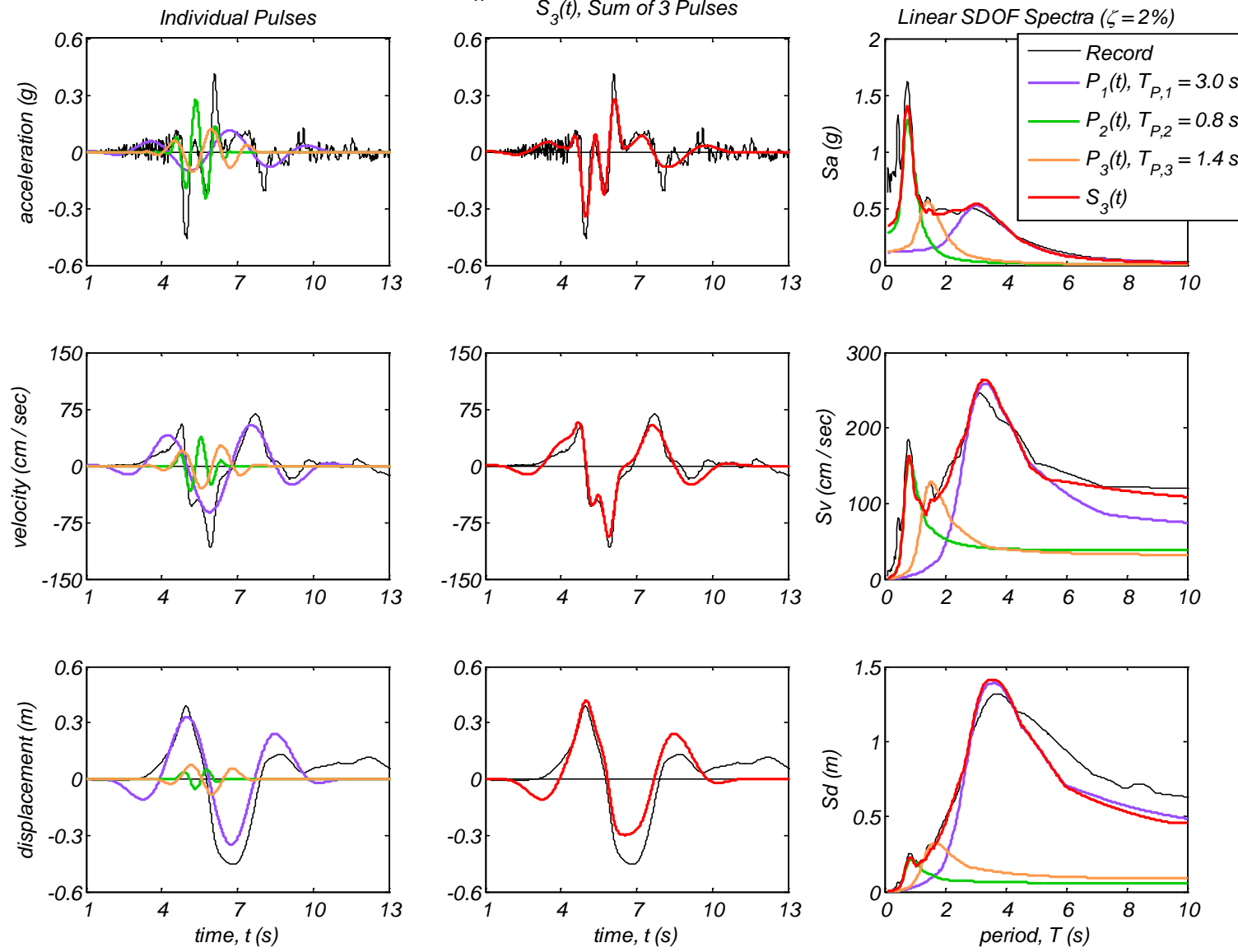


Appendix B4 – Time history and linear spectral response of three extracted pulses using the CPE<sub>A-AR</sub> method for 40 Motions

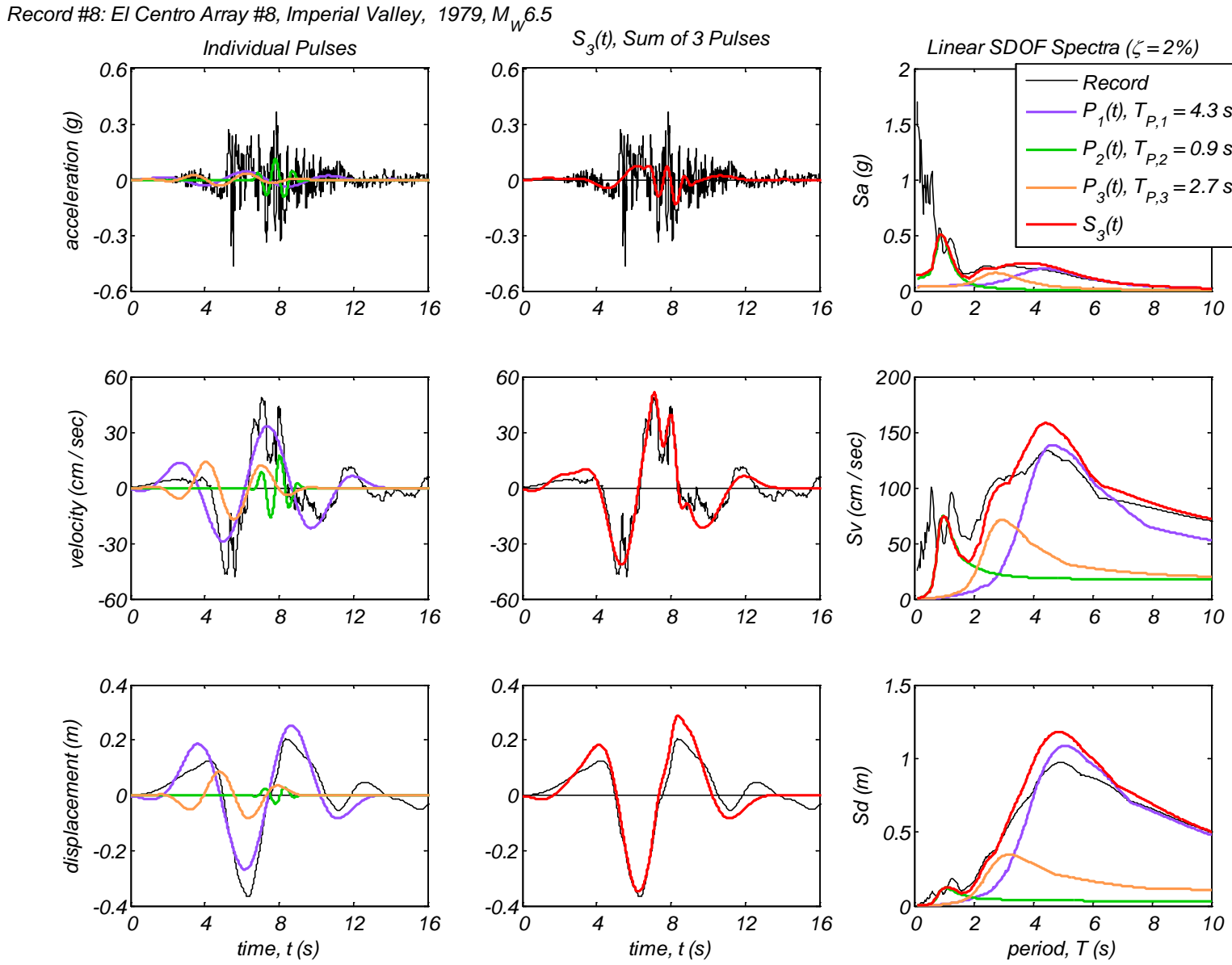


Appendix B4 – Time history and linear spectral response of three extracted pulses using the CPE<sub>A-AR</sub> method for 40 Motions

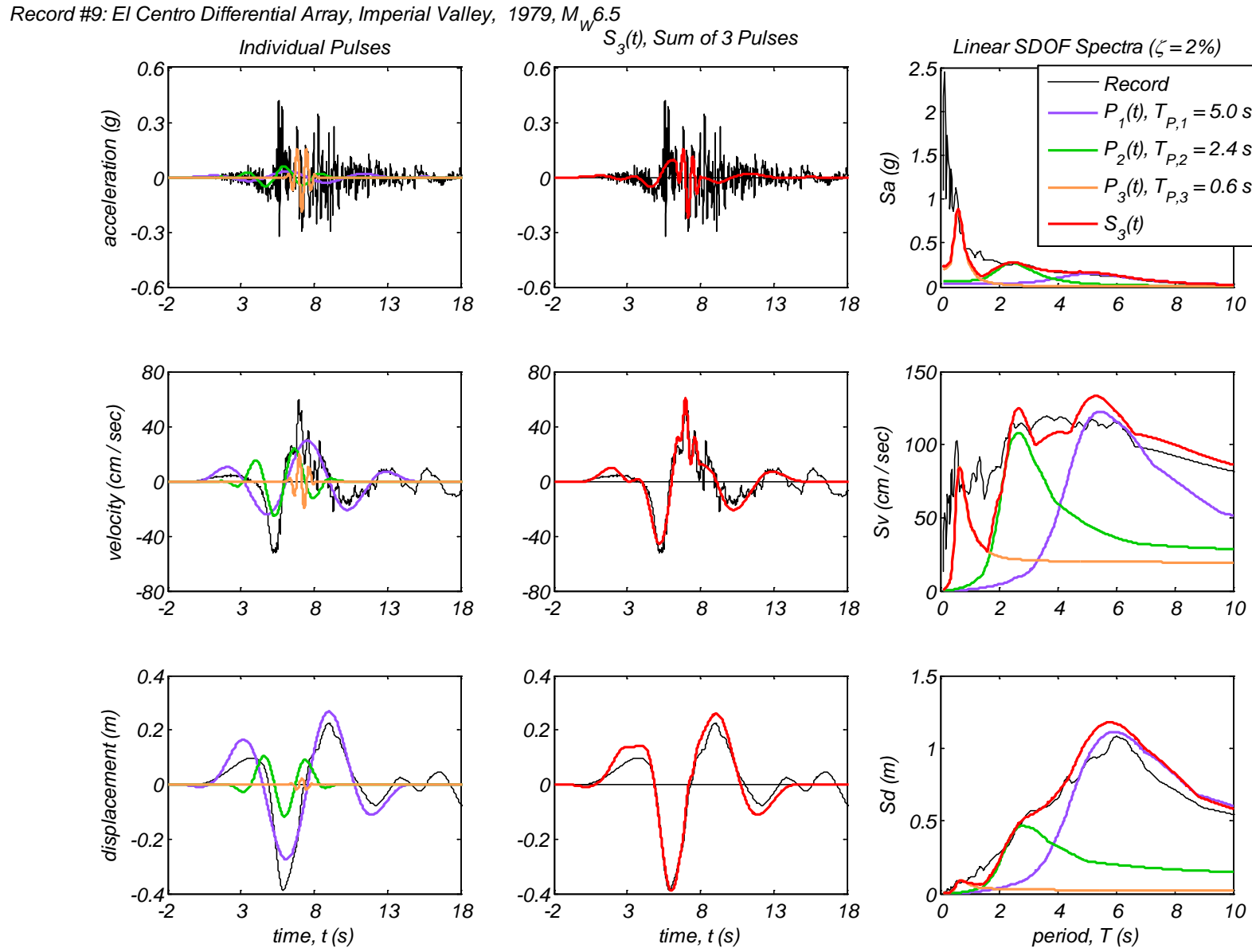
Record #7: El Centro Array #7, Imperial Valley, 1979,  $M_W 6.5$



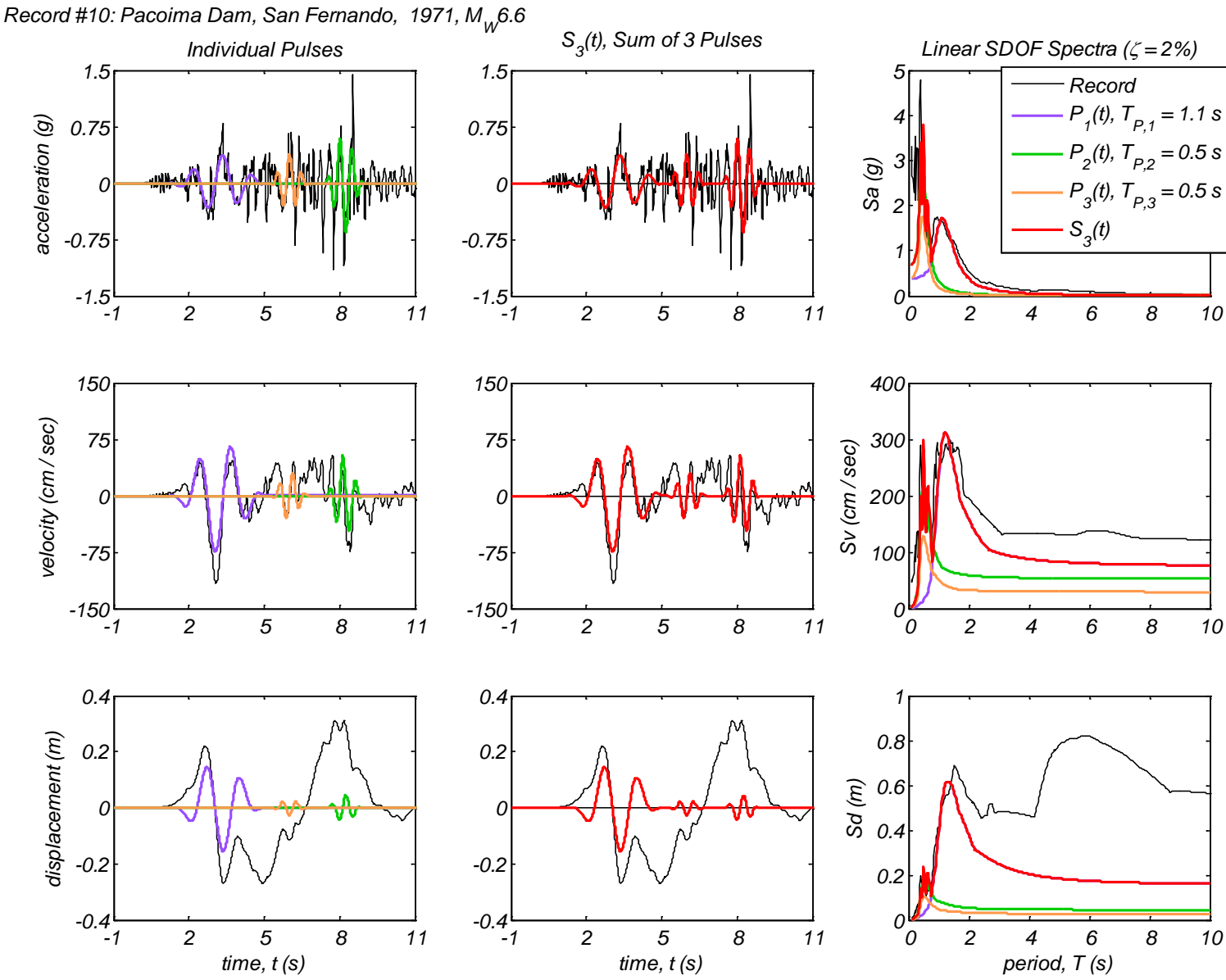
Appendix B4 – Time history and linear spectral response of three extracted pulses using the CPE<sub>A-AR</sub> method for 40 Motions



Appendix B4 – Time history and linear spectral response of three extracted pulses using the CPE<sub>A-AR</sub> method for 40 Motions

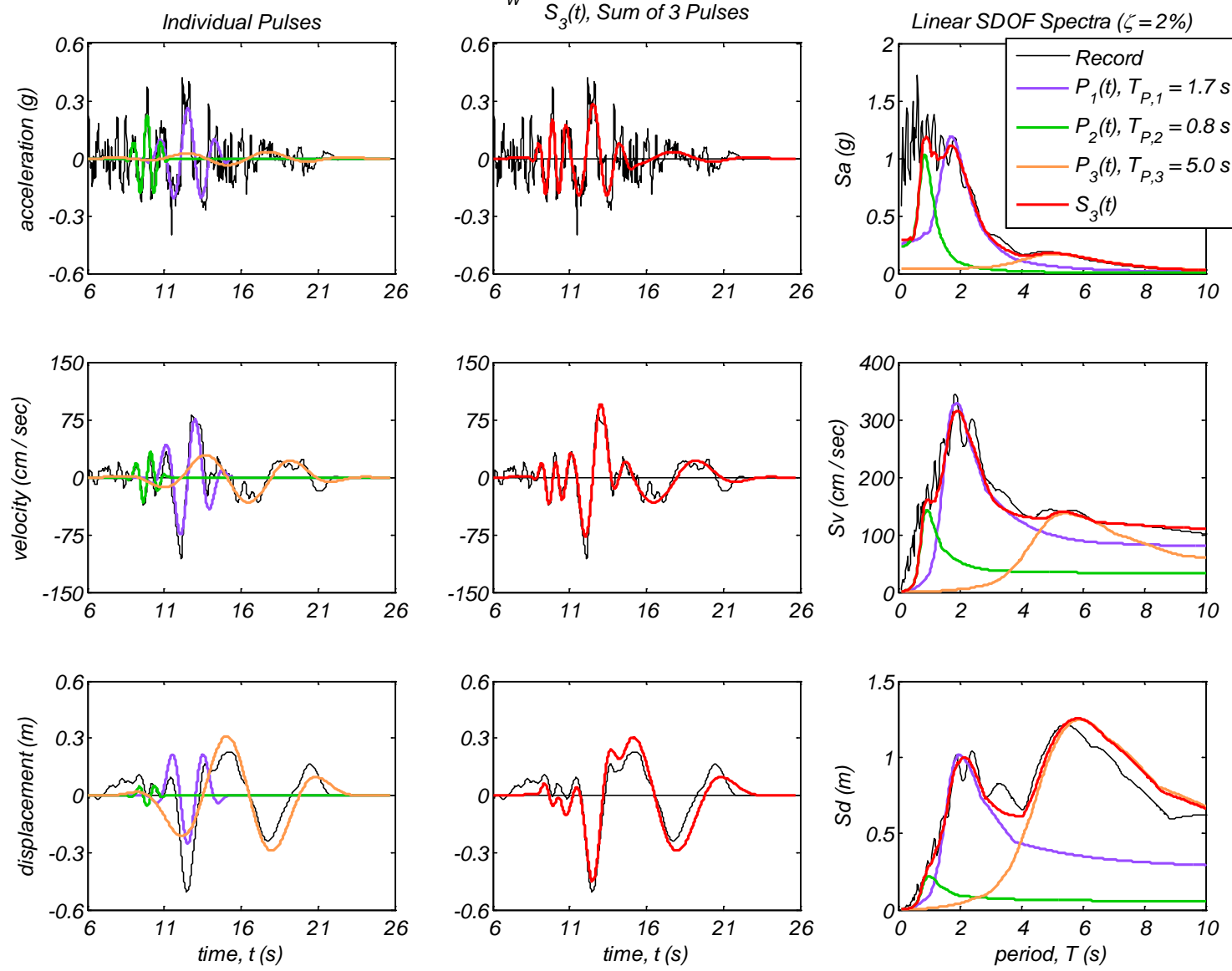


Appendix B4 – Time history and linear spectral response of three extracted pulses using the CPE<sub>A-AR</sub> method for 40 Motions

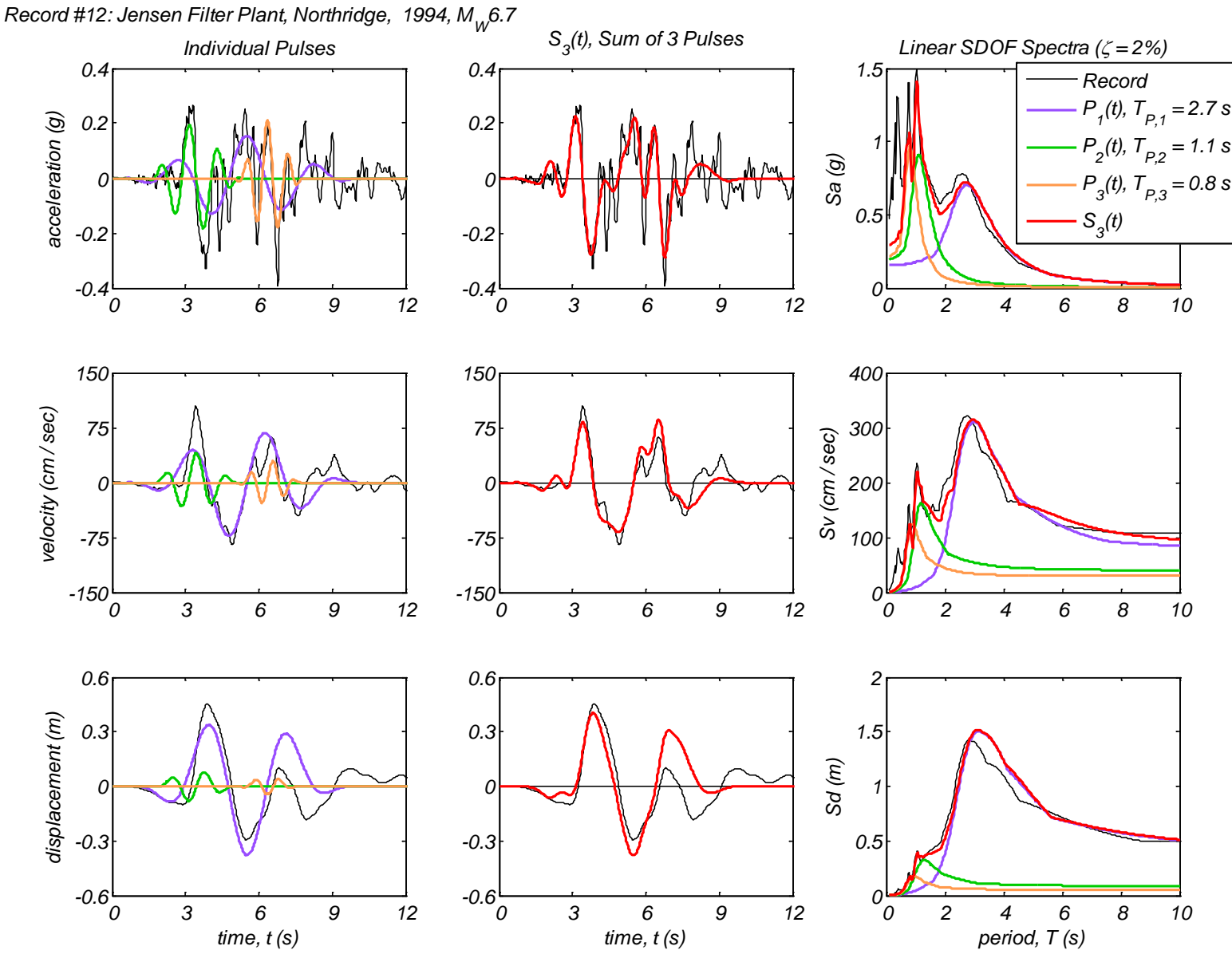


Appendix B4 – Time history and linear spectral response of three extracted pulses using the CPE<sub>A-AR</sub> method for 40 Motions

Record #11: Parachute Test Site, Superstition Hills(B), 1987,  $M_w 6.6$

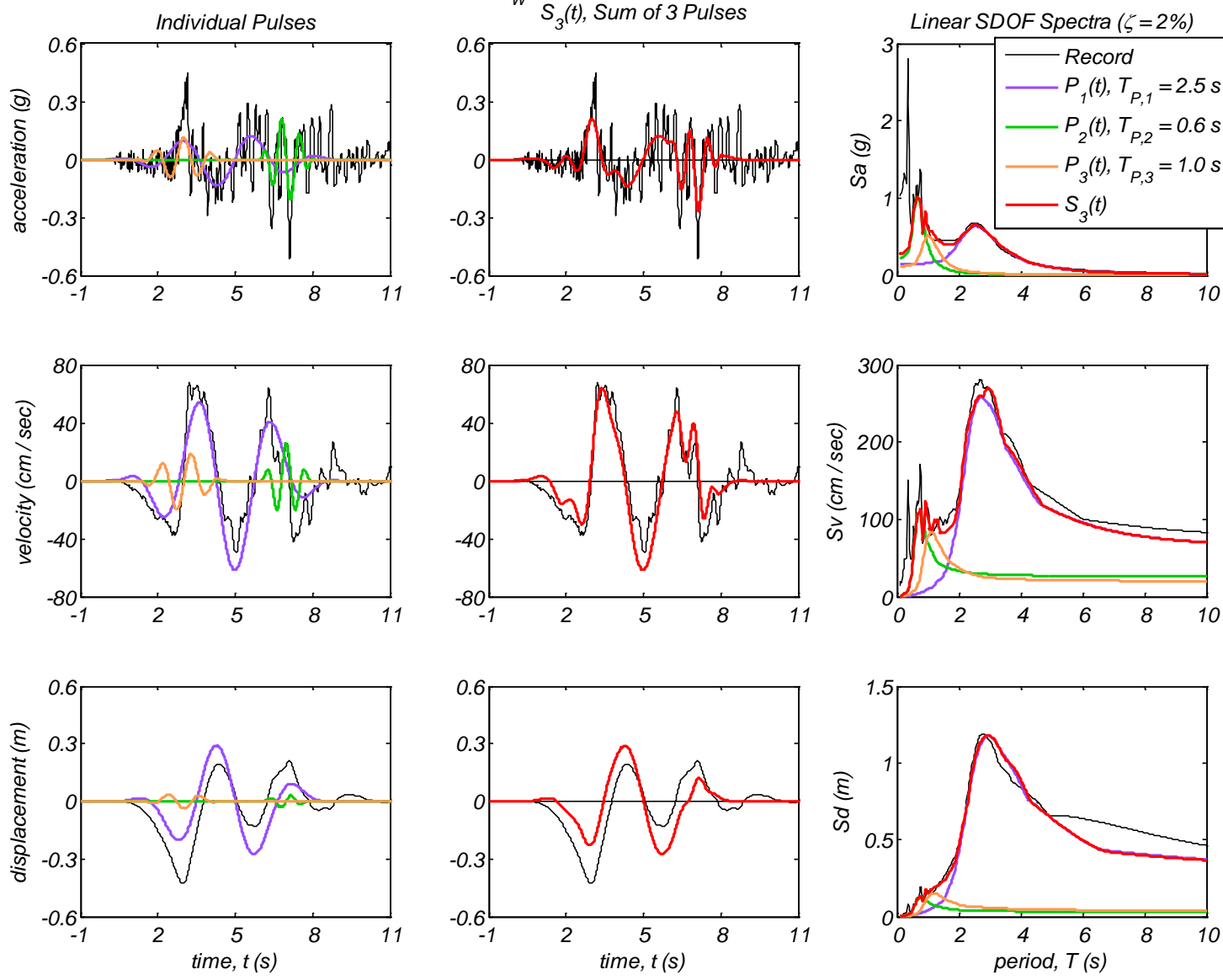


Appendix B4 – Time history and linear spectral response of three extracted pulses using the CPE<sub>A-AR</sub> method for 40 Motions

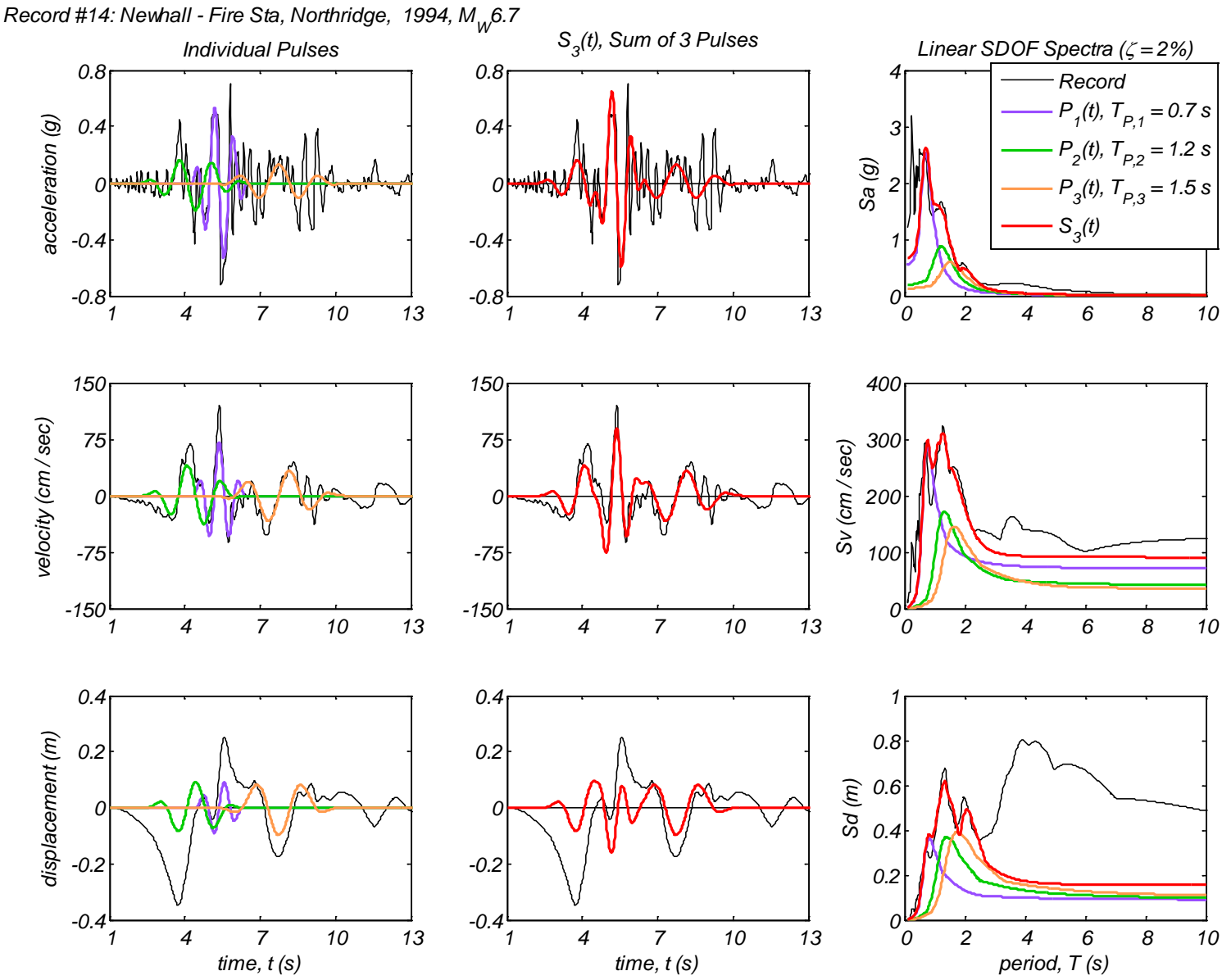


Appendix B4 – Time history and linear spectral response of three extracted pulses using the CPE<sub>A-AR</sub> method for 40 Motions

Record #13: Jensen Filter Plant Generator, Northridge, 1994,  $M_W 6.7$

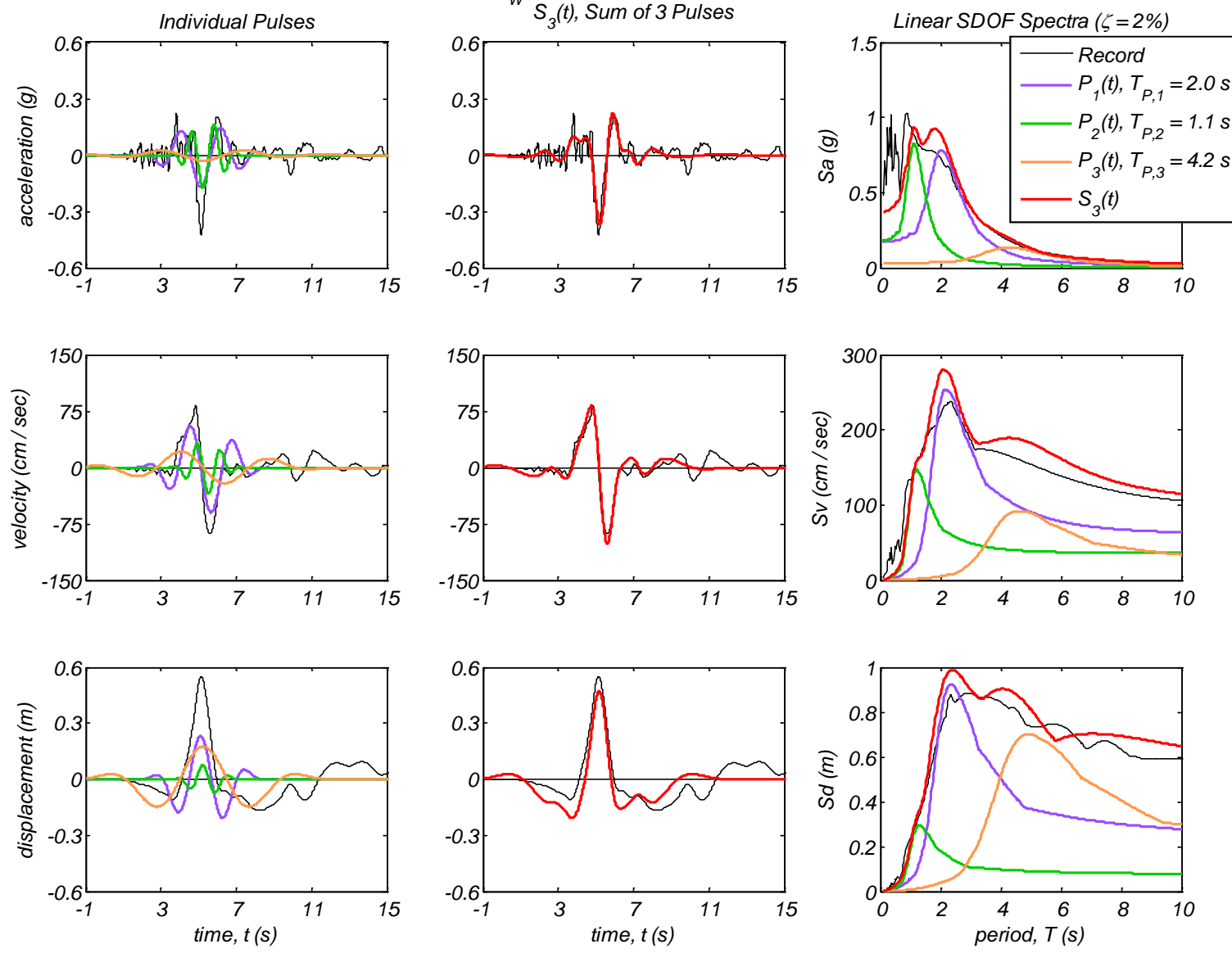


Appendix B4 – Time history and linear spectral response of three extracted pulses using the CPE<sub>A-AR</sub> method for 40 Motions



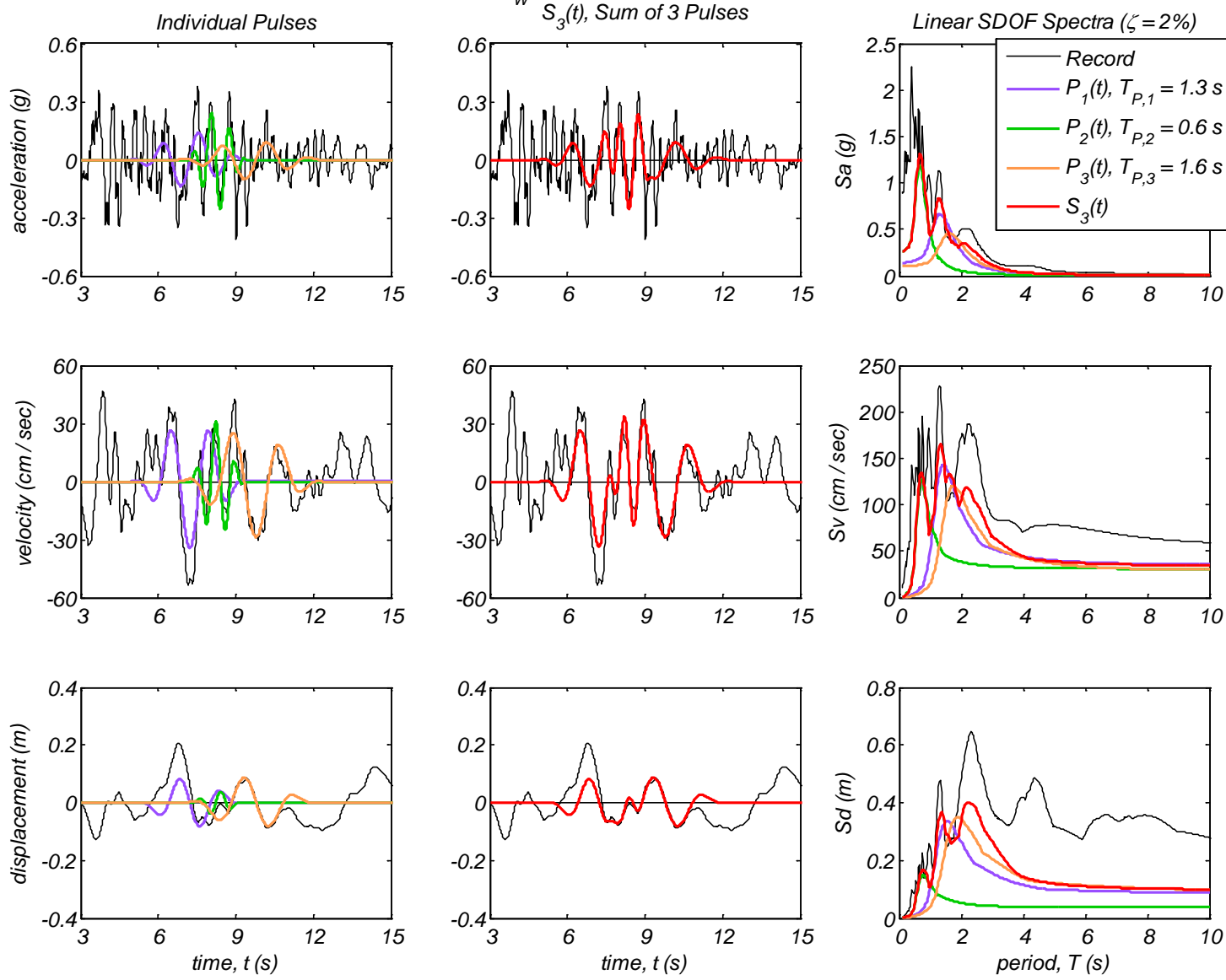
Appendix B4 – Time history and linear spectral response of three extracted pulses using the CPE<sub>A-AR</sub> method for 40 Motions

Record #15: Newhall - W. Pico Canyon Rd., Northridge, 1994,  $M_w 6.7$



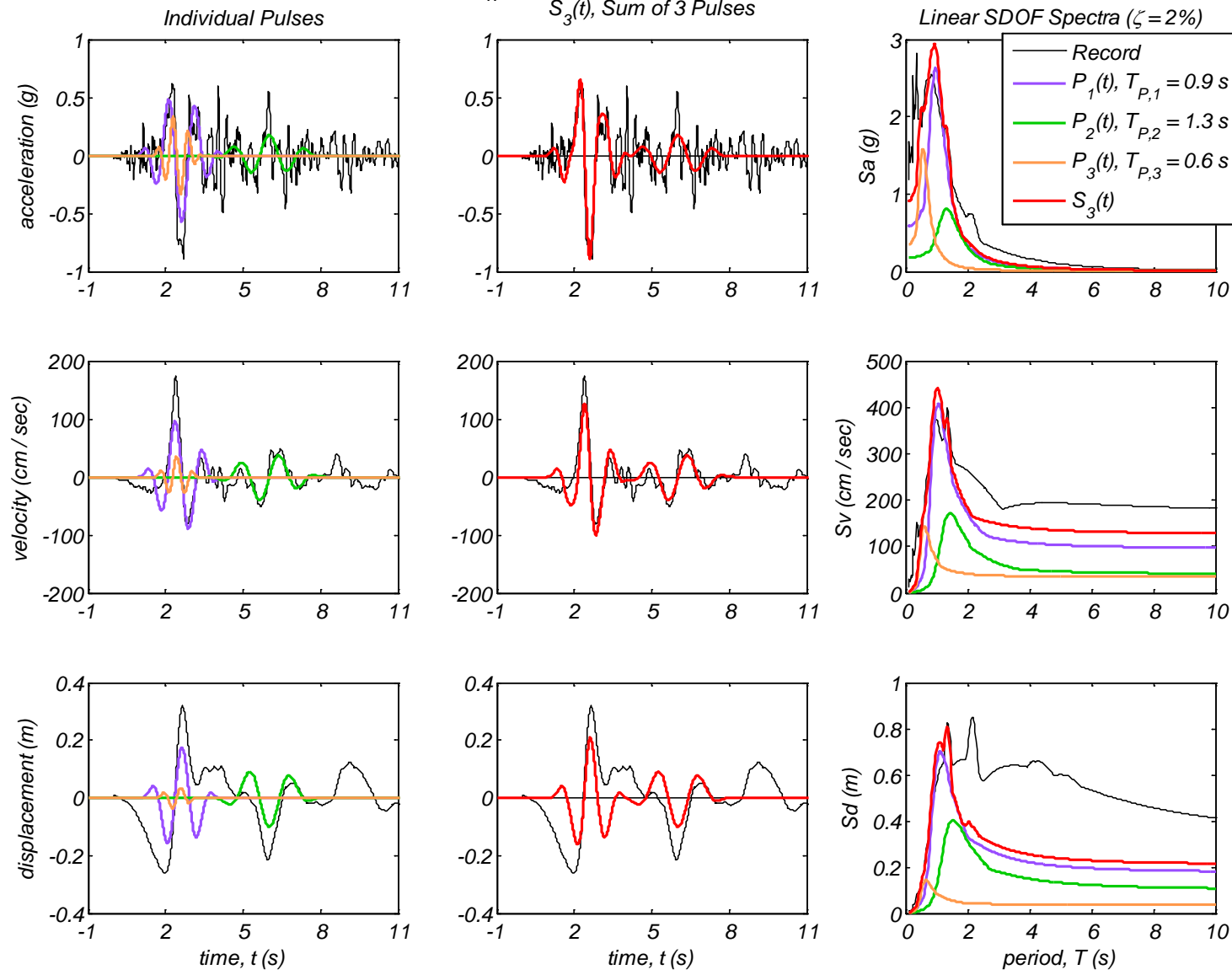
Appendix B4 – Time history and linear spectral response of three extracted pulses using the CPE<sub>A-AR</sub> method for 40 Motions

Record #16: Northridge - 17645 Saticoy St, Northridge, 1994,  $M_W 6.7$

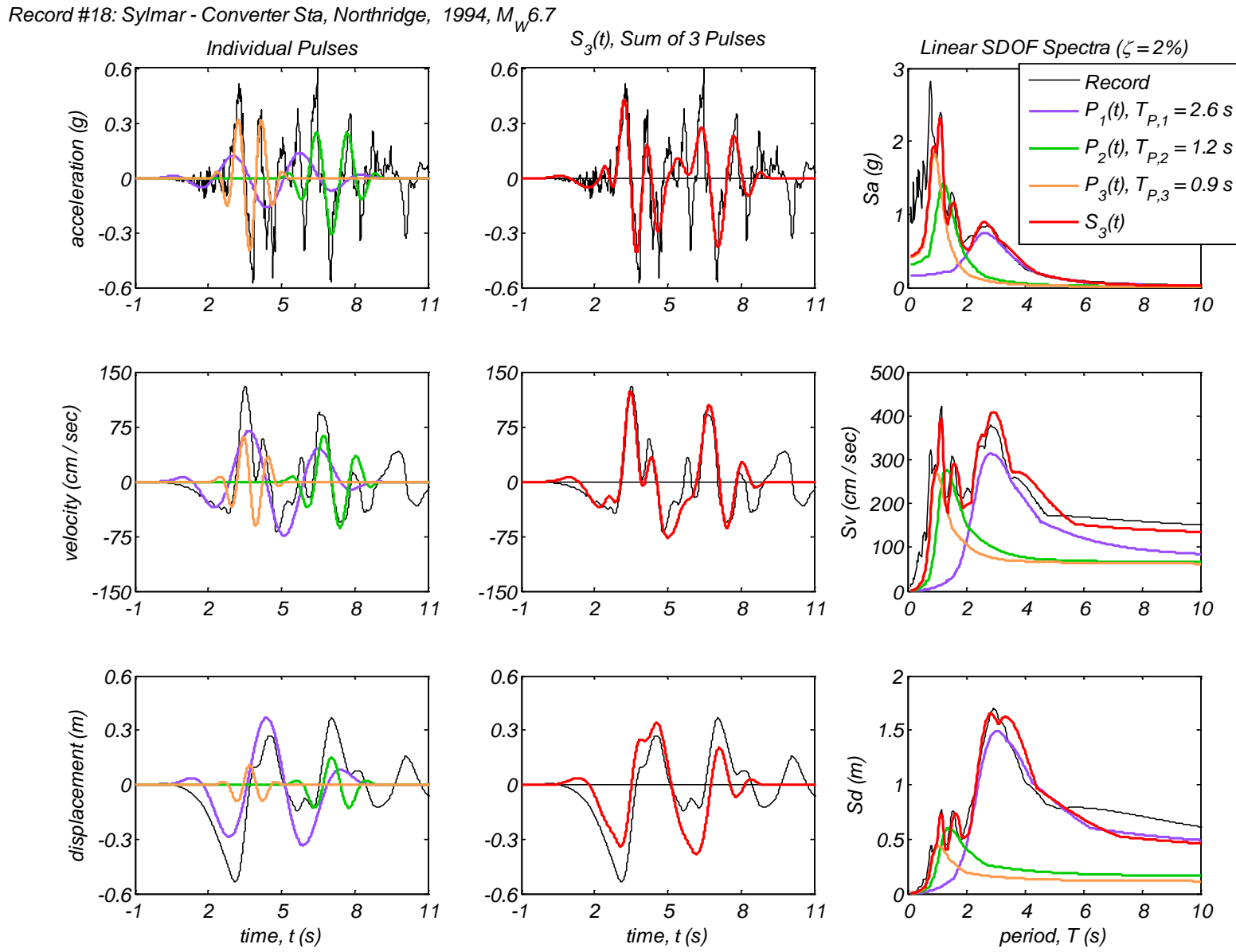


Appendix B4 – Time history and linear spectral response of three extracted pulses using the CPE<sub>A-AR</sub> method for 40 Motions

Record #17: Rinaldi Receiving Sta, Northridge, 1994,  $M_W 6.7$

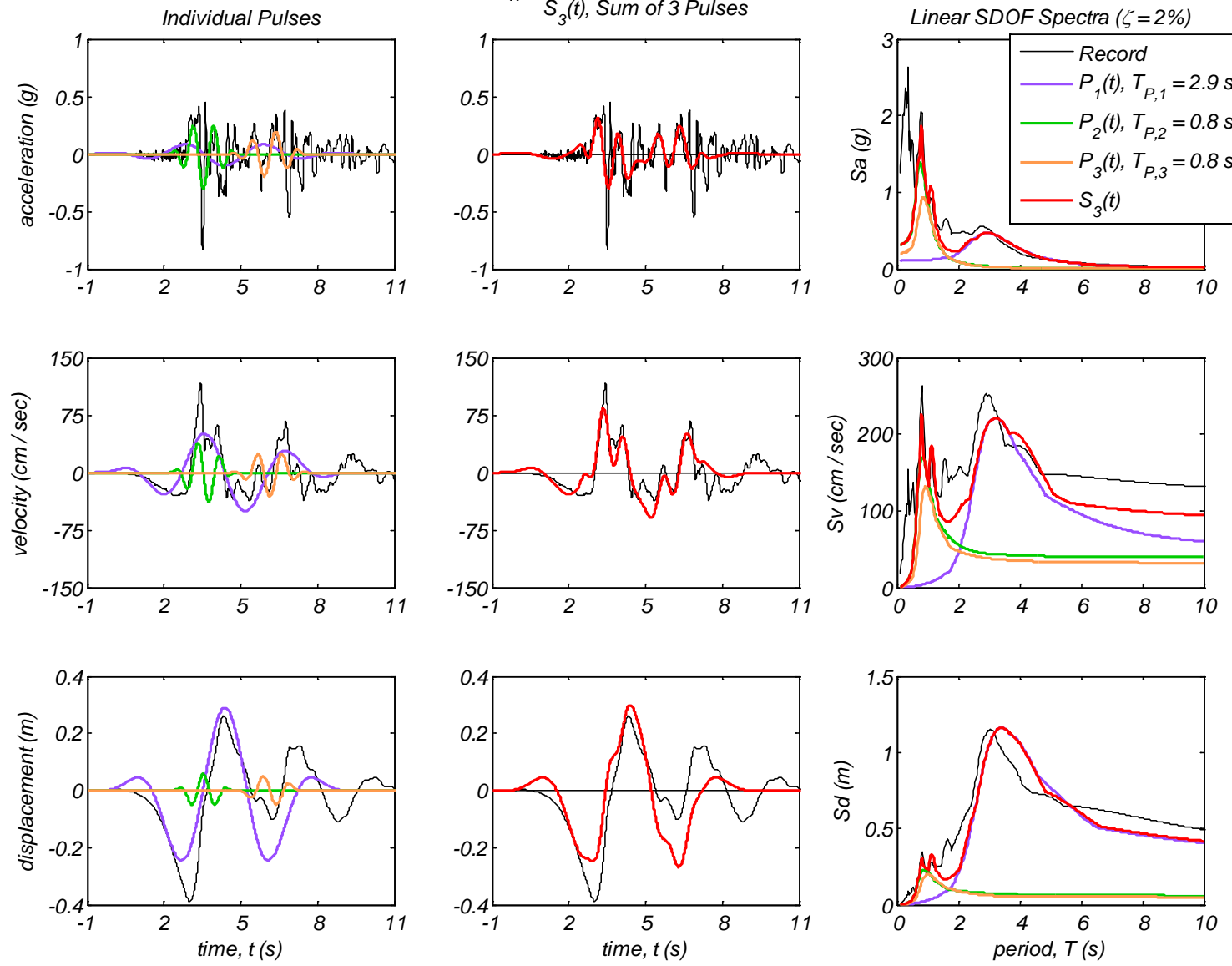


Appendix B4 – Time history and linear spectral response of three extracted pulses using the CPE<sub>A-AR</sub> method for 40 Motions



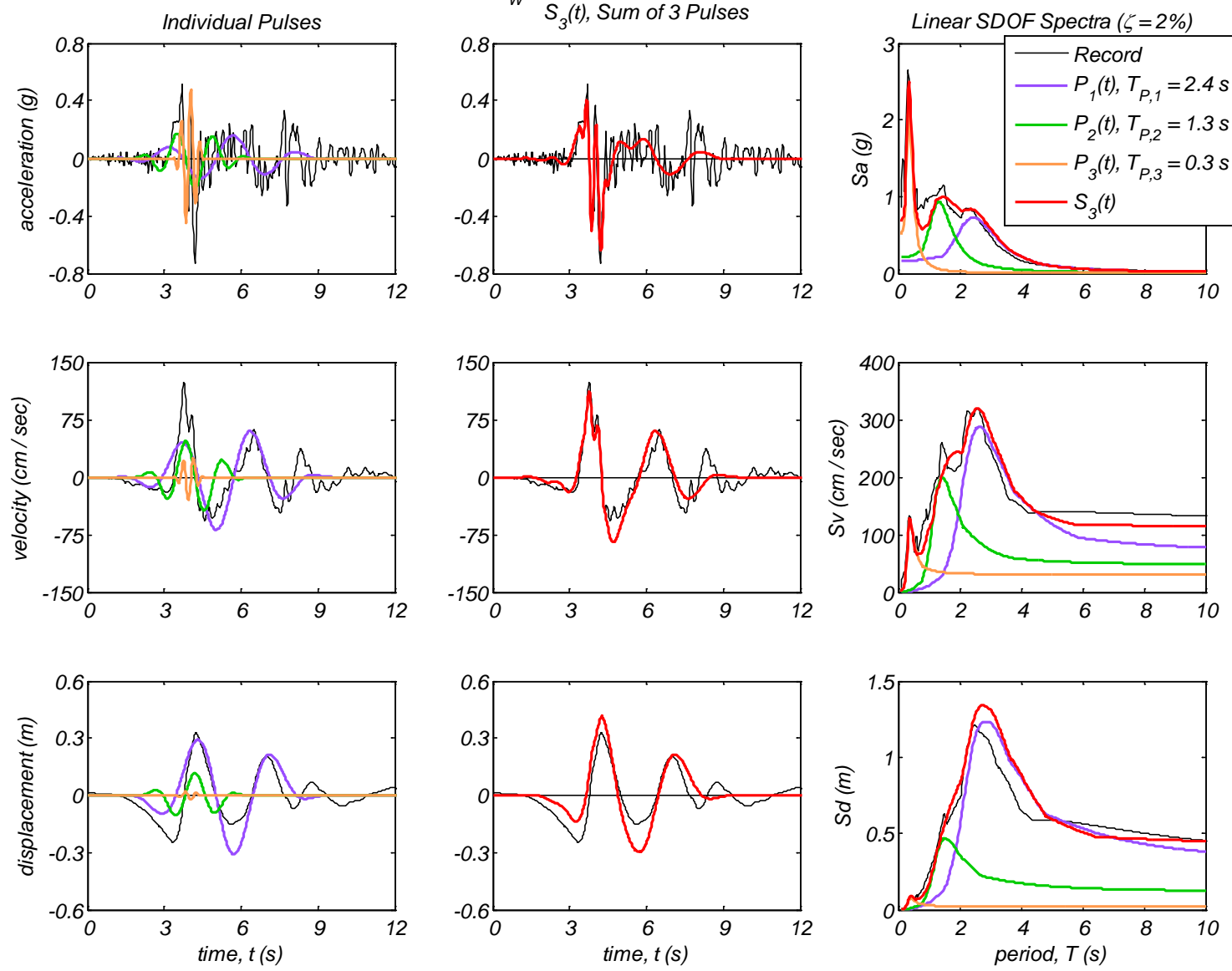
Appendix B4 – Time history and linear spectral response of three extracted pulses using the CPE<sub>A-AR</sub> method for 40 Motions

Record #19: Sylmar - Converter Sta East, Northridge, 1994,  $M_W$  6.7



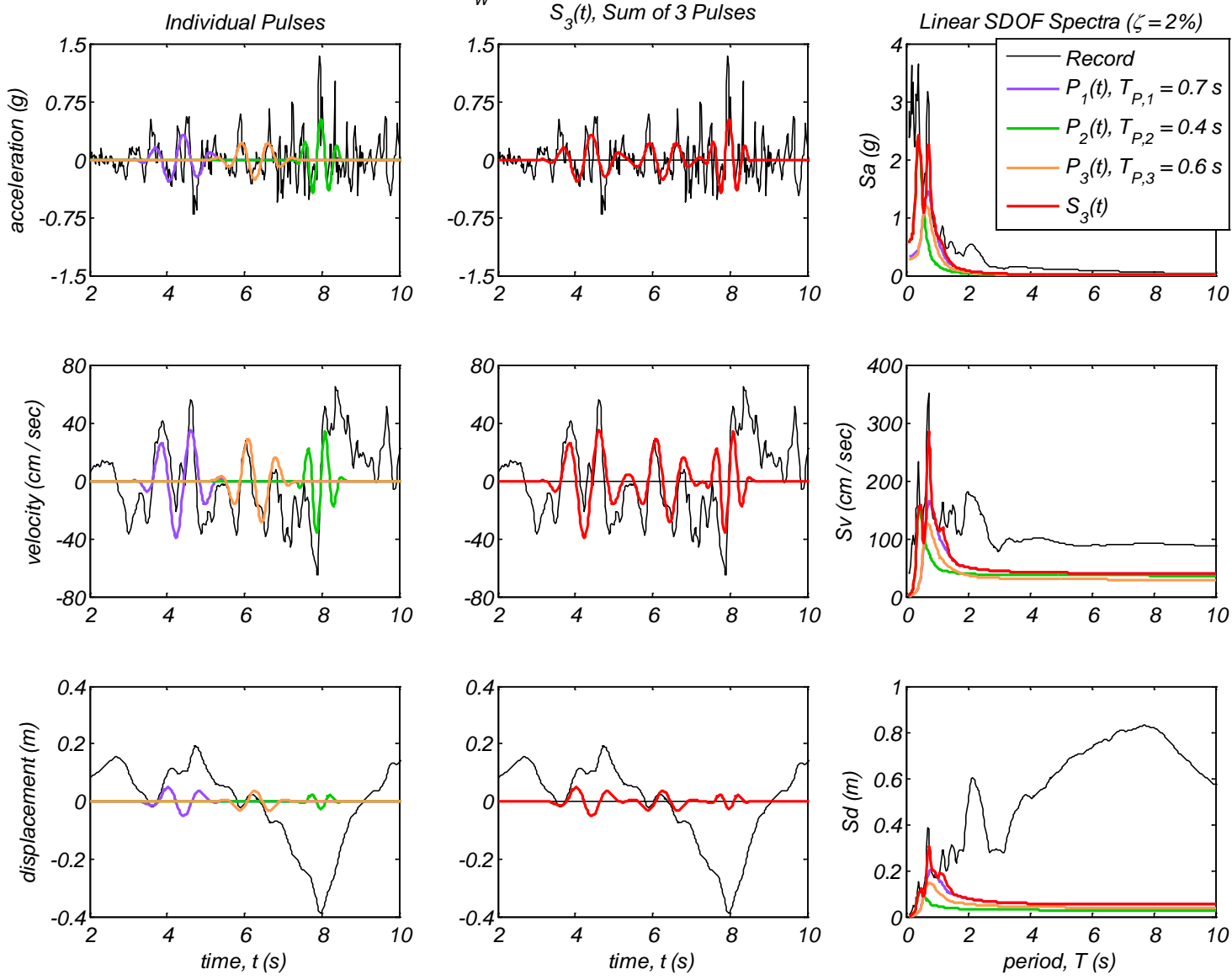
Appendix B4 – Time history and linear spectral response of three extracted pulses using the CPE<sub>A-AR</sub> method for 40 Motions

Record #20: Sylmar - Olive ViewMed FF, Northridge, 1994,  $M_W 6.7$

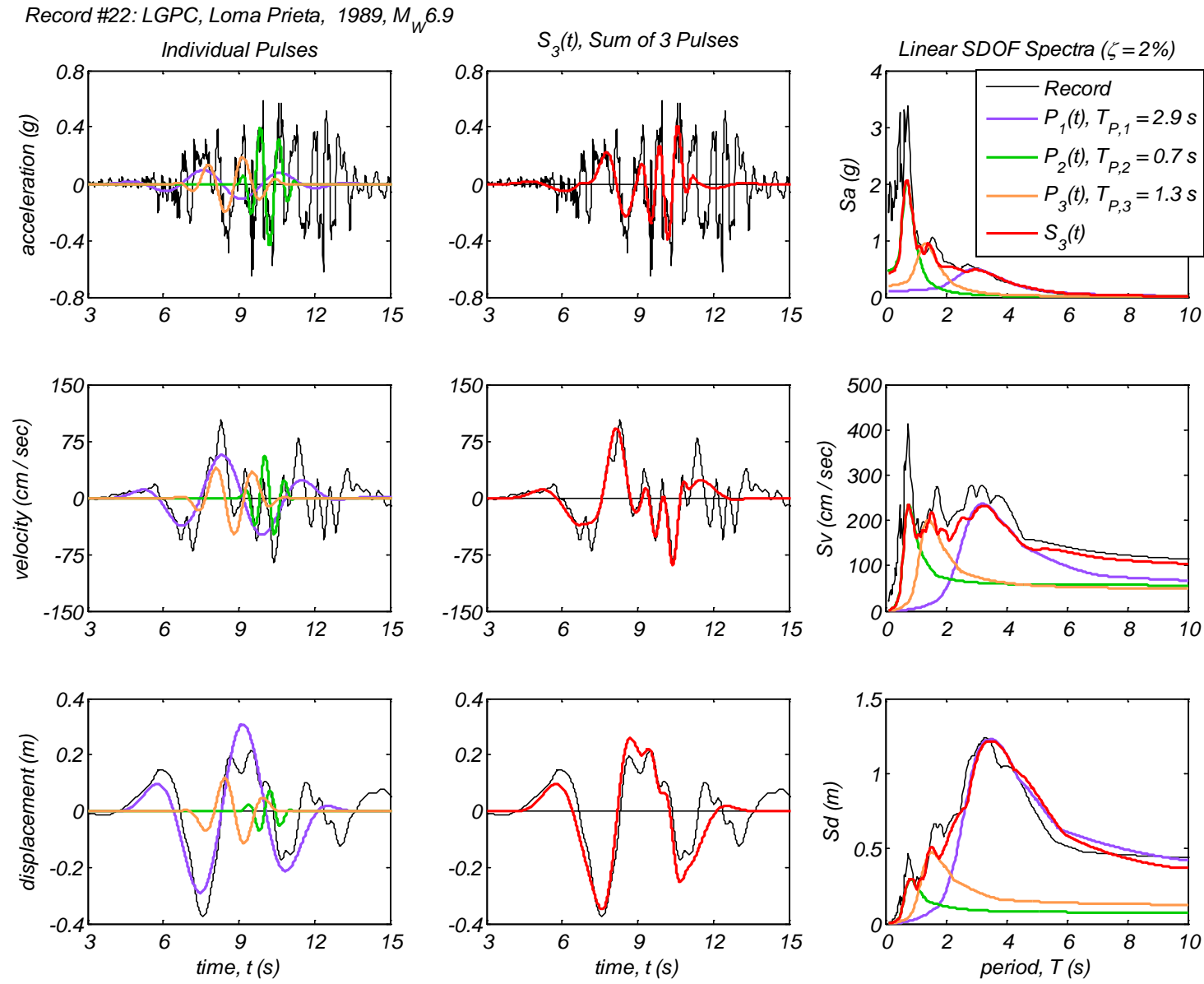


Appendix B4 – Time history and linear spectral response of three extracted pulses using the CPE<sub>A-AR</sub> method for 40 Motions

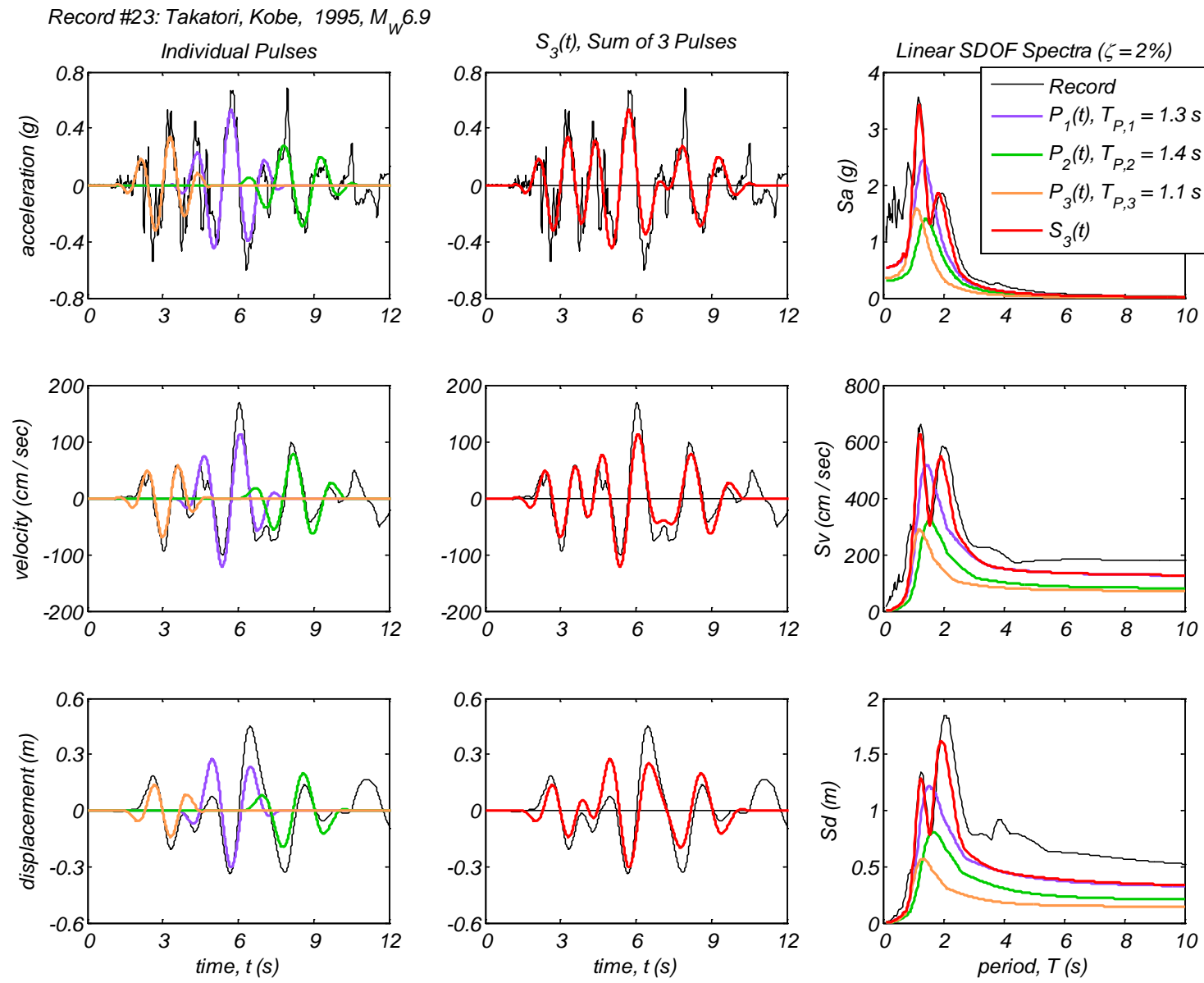
Record #21: Tarzana, Cedar Hill, Northridge, 1994,  $M_W 6.7$



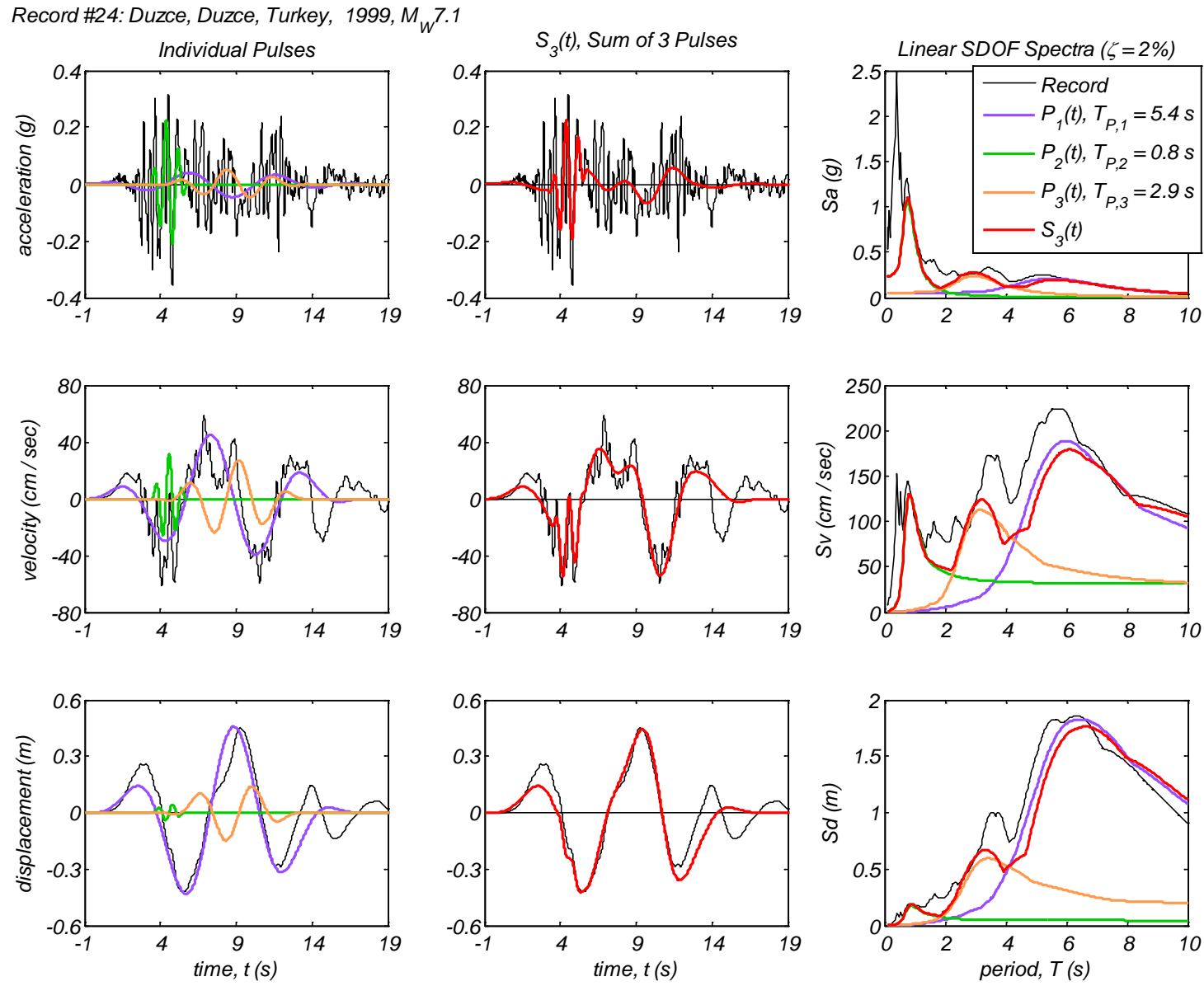
Appendix B4 – Time history and linear spectral response of three extracted pulses using the CPE<sub>A-AR</sub> method for 40 Motions



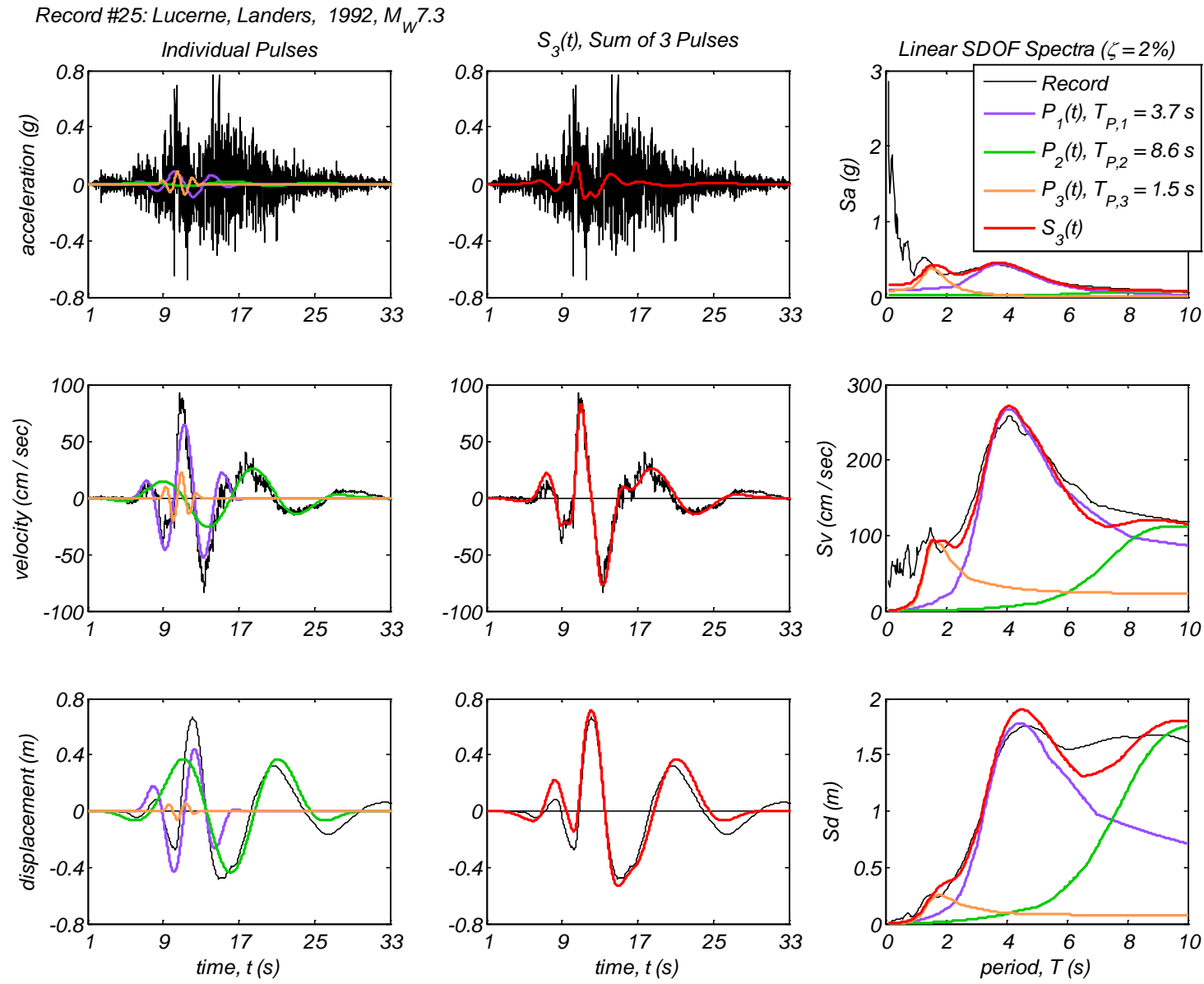
Appendix B4 – Time history and linear spectral response of three extracted pulses using the CPE<sub>A-AR</sub> method for 40 Motions



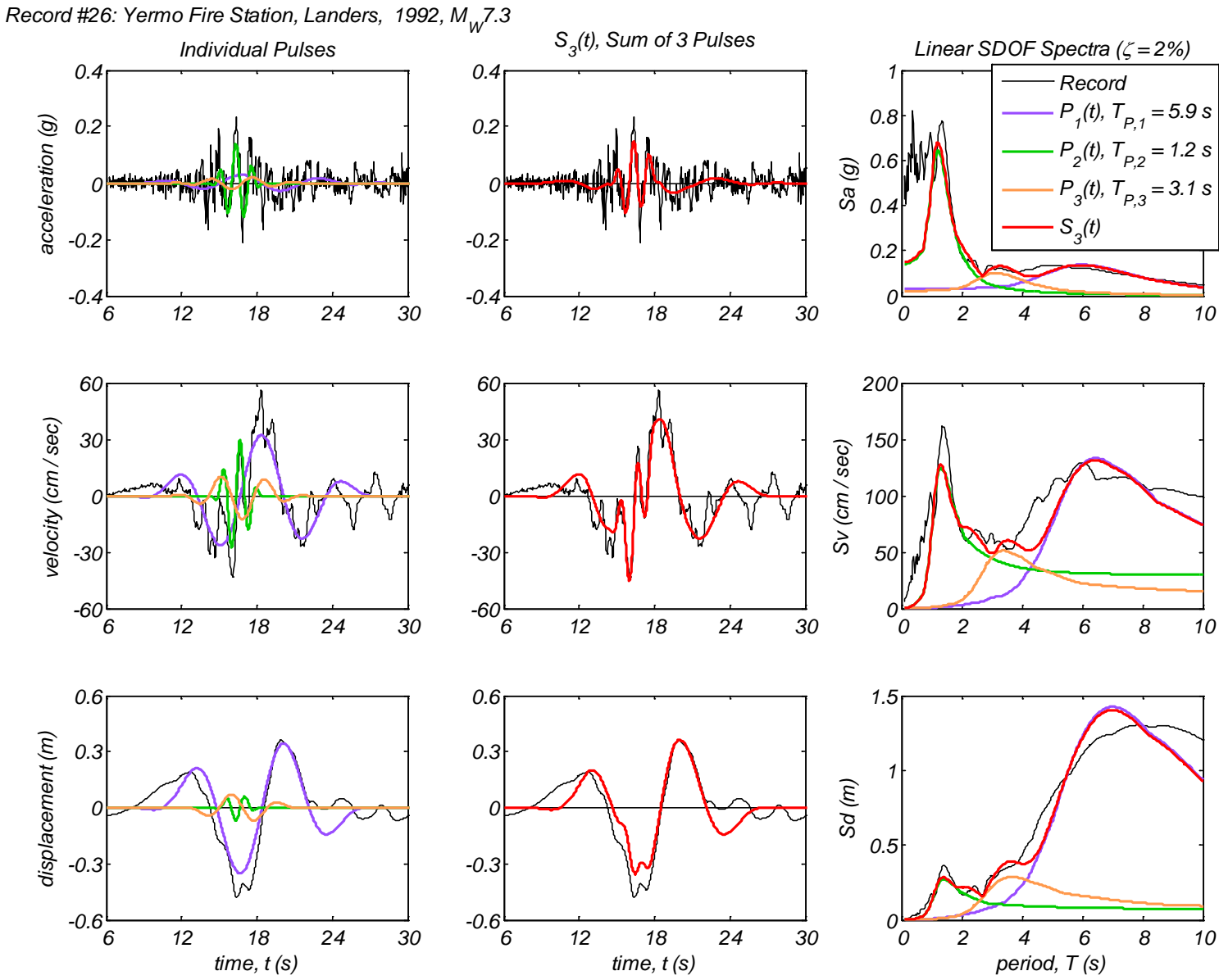
Appendix B4 – Time history and linear spectral response of three extracted pulses using the CPE<sub>A-AR</sub> method for 40 Motions



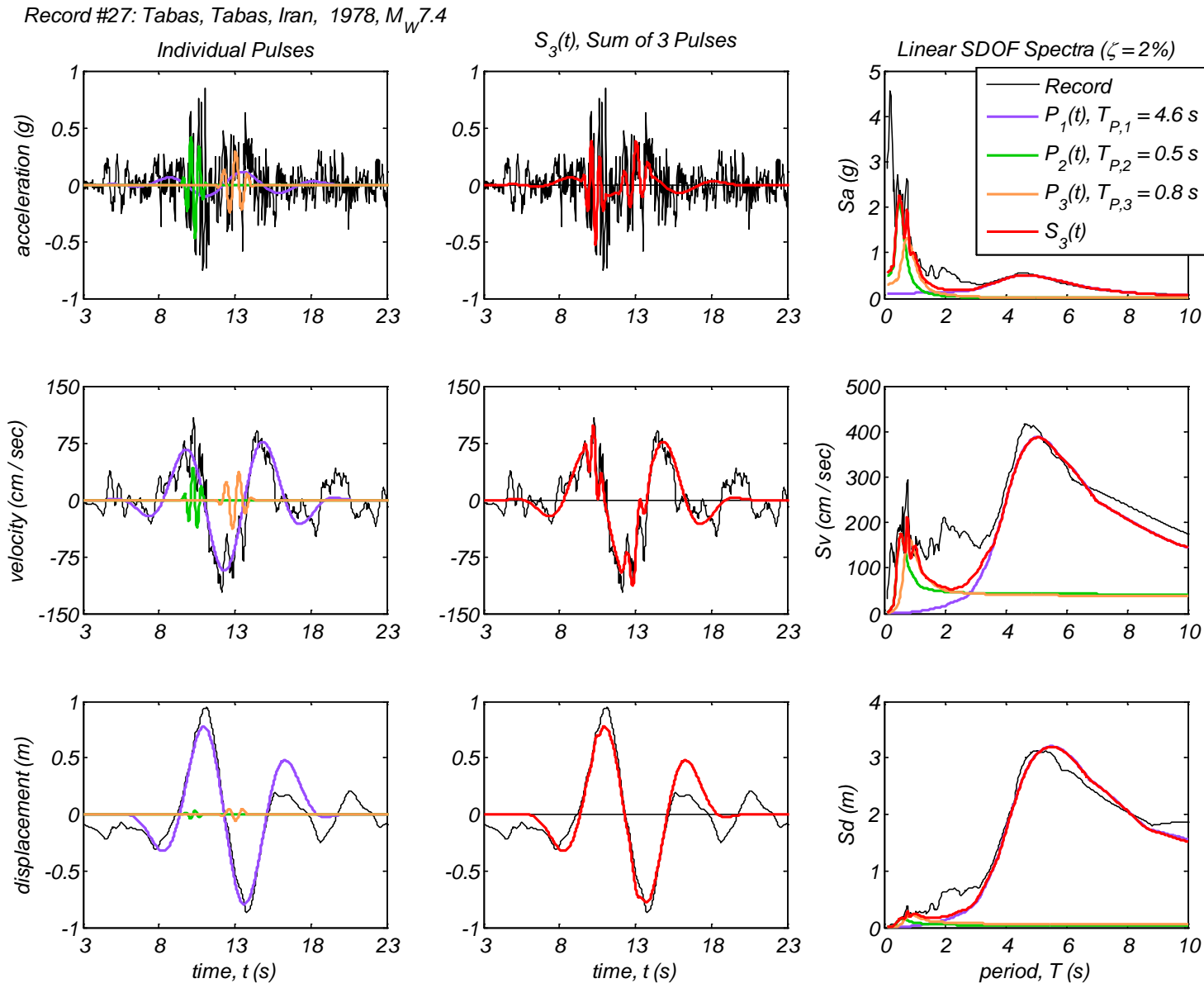
Appendix B4 – Time history and linear spectral response of three extracted pulses using the CPE<sub>A-AR</sub> method for 40 Motions



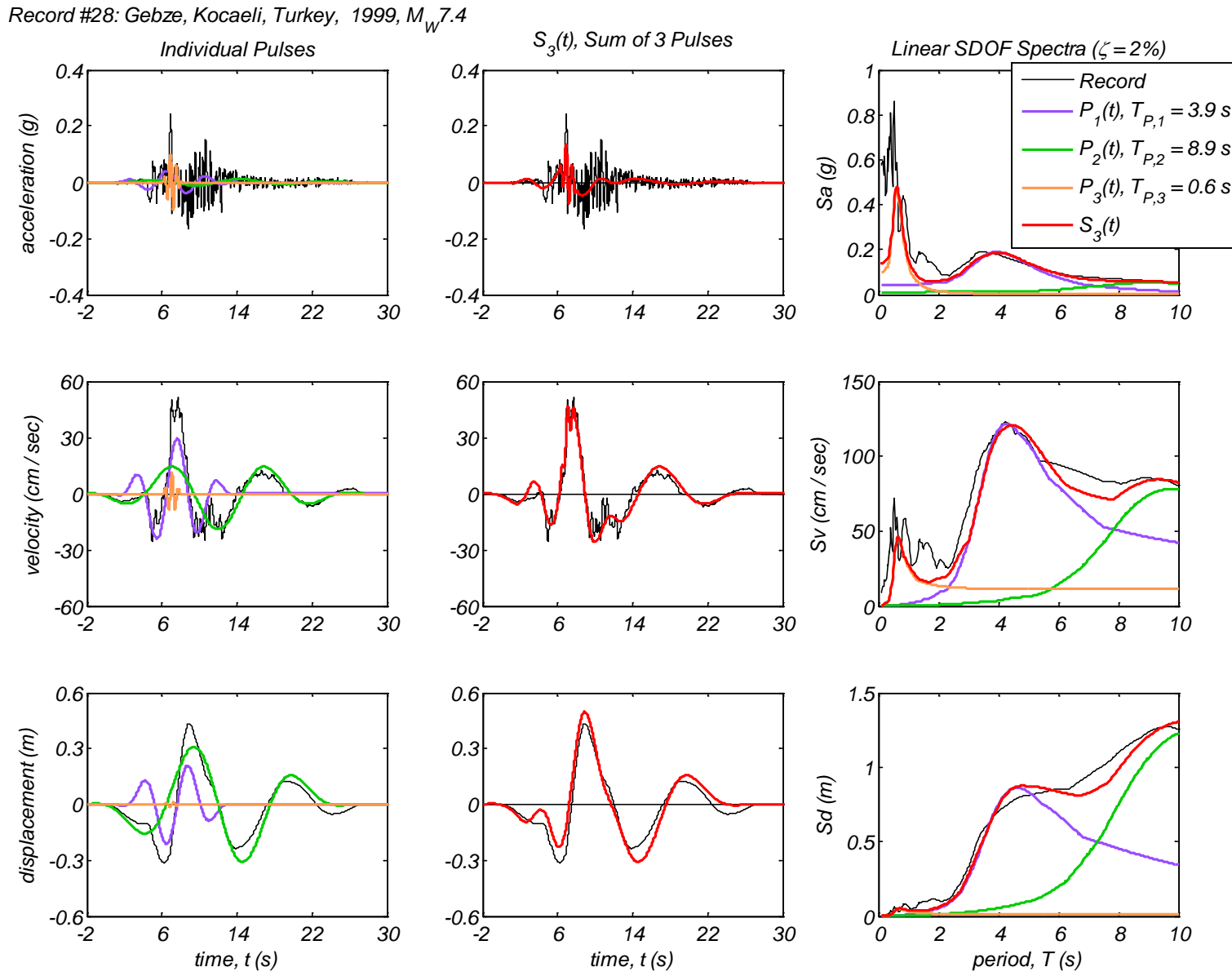
Appendix B4 – Time history and linear spectral response of three extracted pulses using the CPE<sub>A-AR</sub> method for 40 Motions



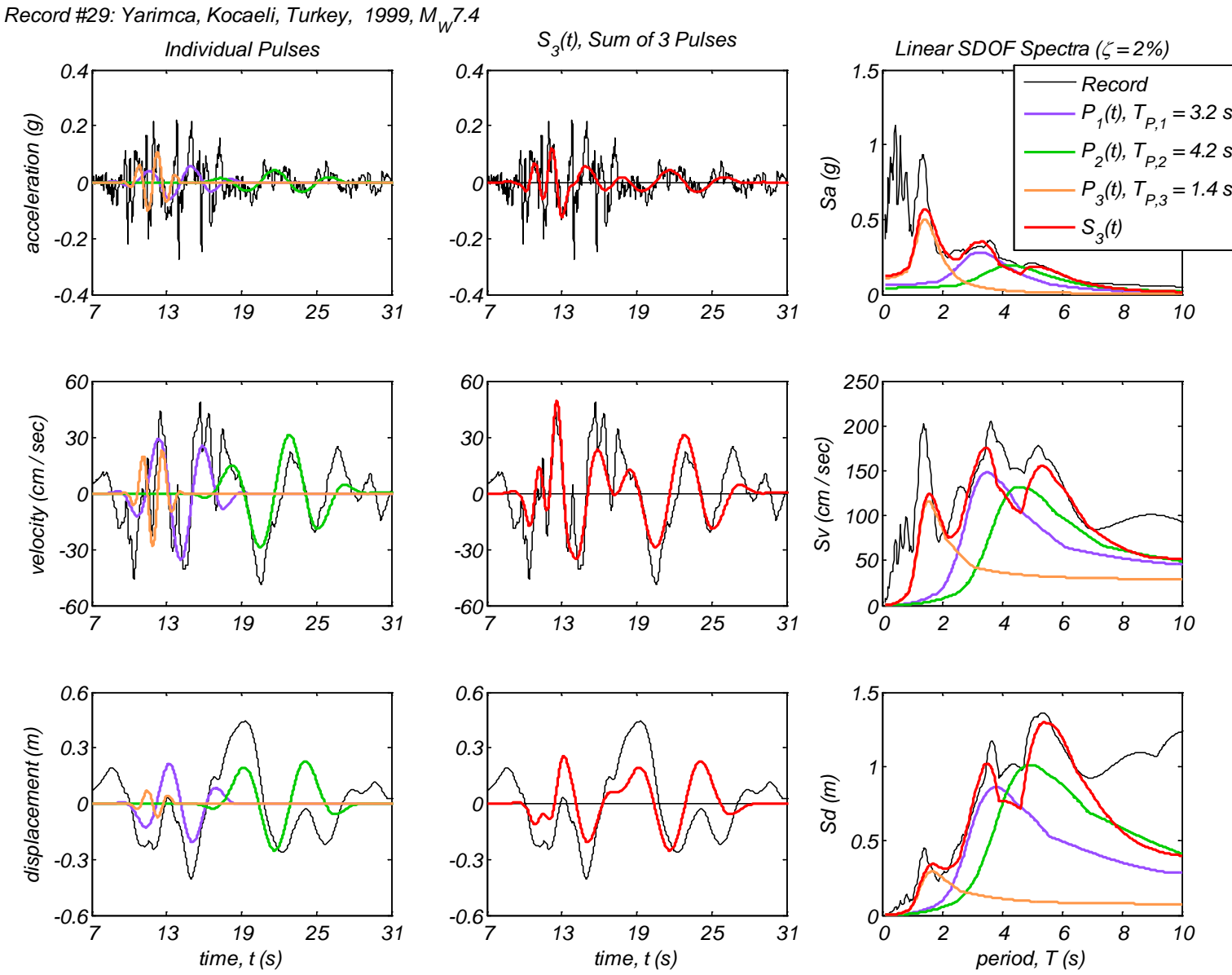
Appendix B4 – Time history and linear spectral response of three extracted pulses using the CPE<sub>A-AR</sub> method for 40 Motions



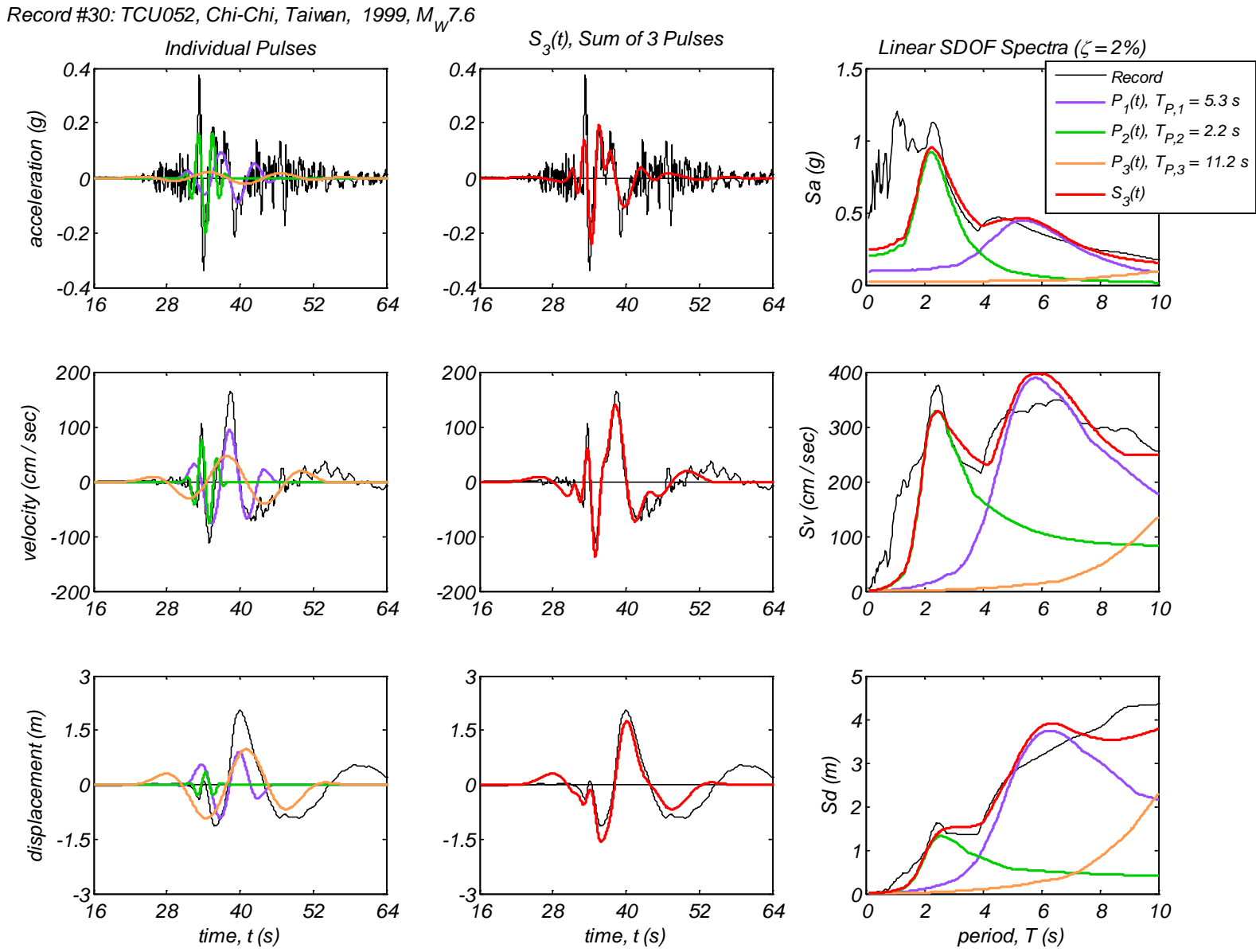
Appendix B4 – Time history and linear spectral response of three extracted pulses using the CPE<sub>A-AR</sub> method for 40 Motions



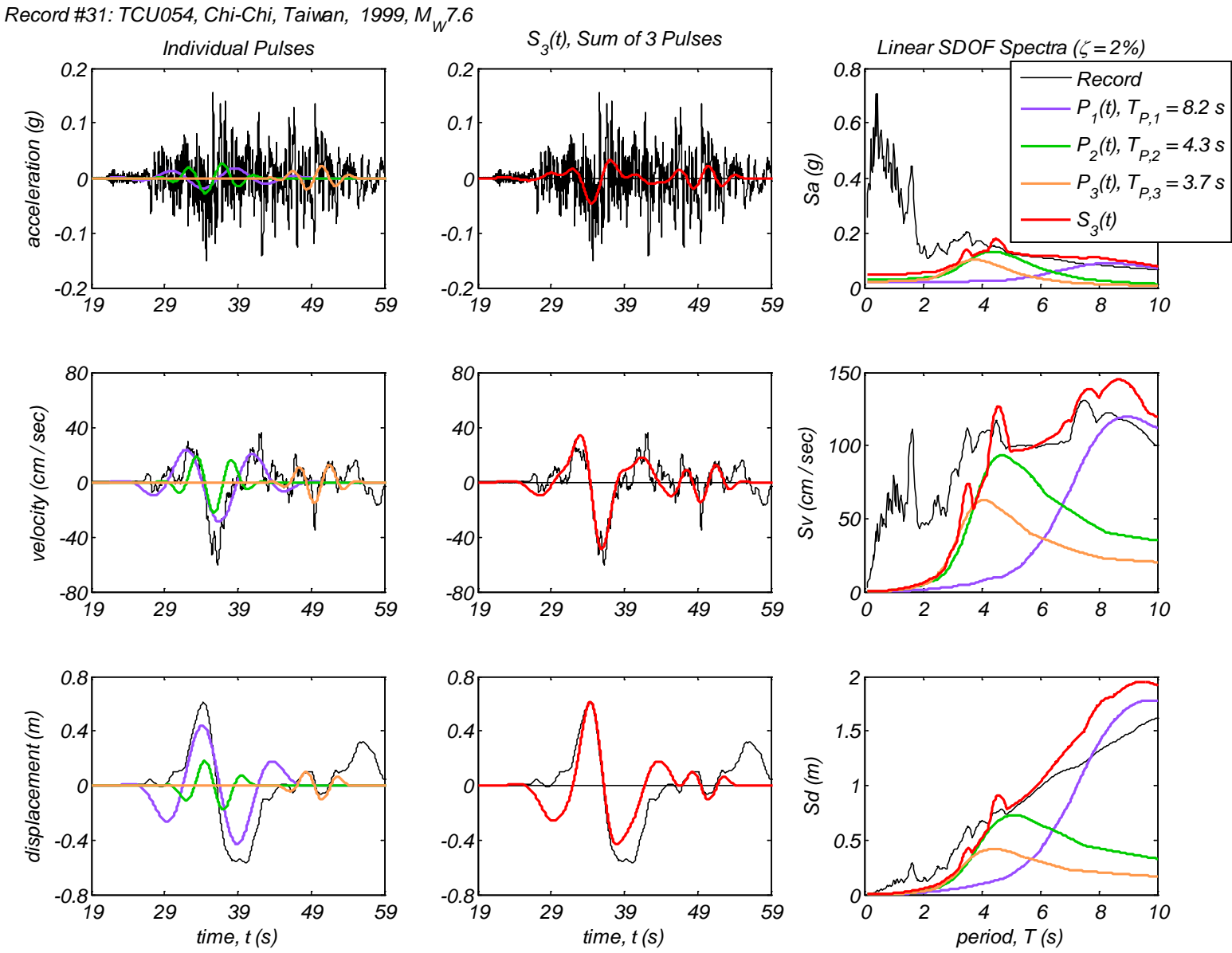
Appendix B4 – Time history and linear spectral response of three extracted pulses using the CPE<sub>A-AR</sub> method for 40 Motions



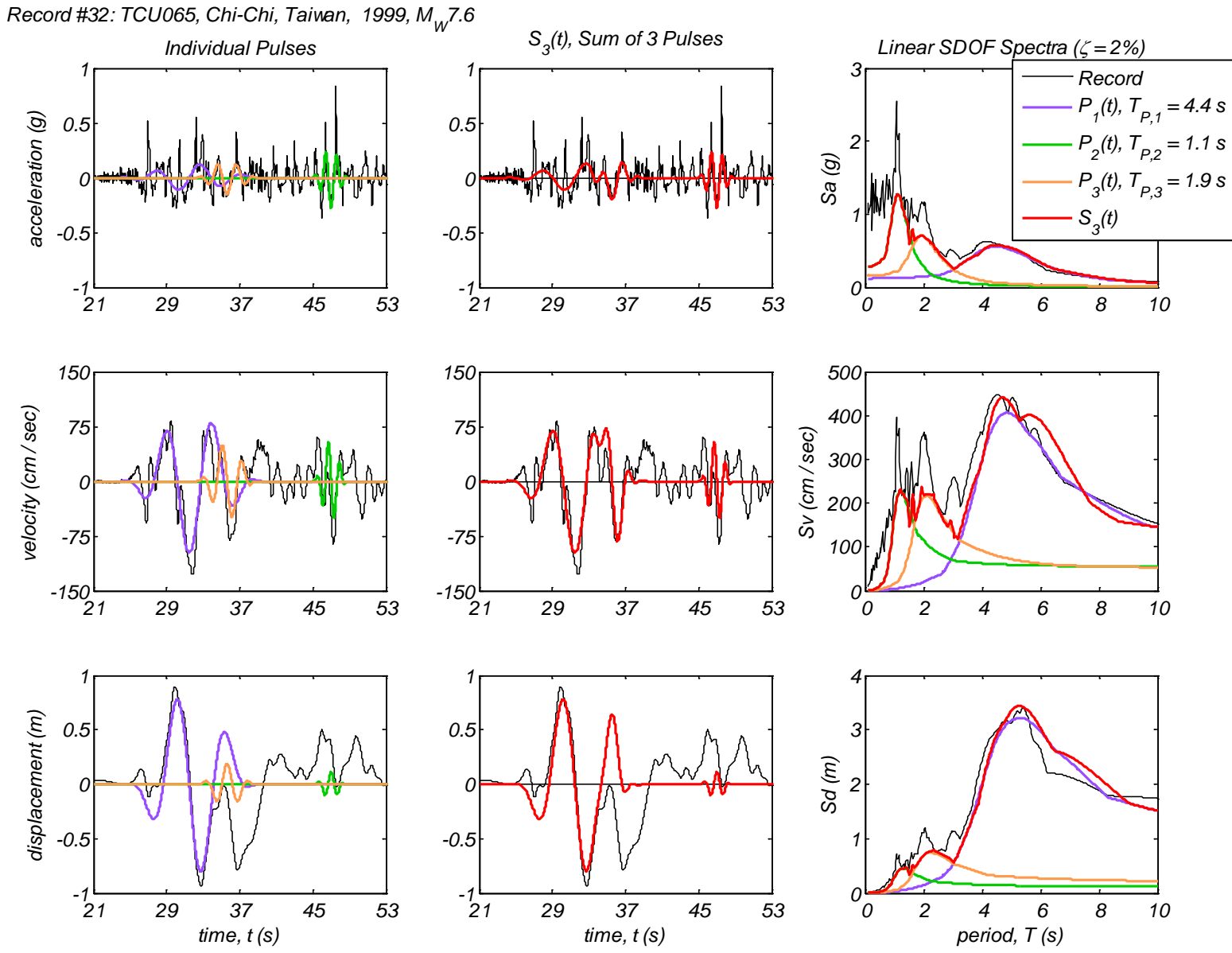
Appendix B4 – Time history and linear spectral response of three extracted pulses using the CPE<sub>A-AR</sub> method for 40 Motions



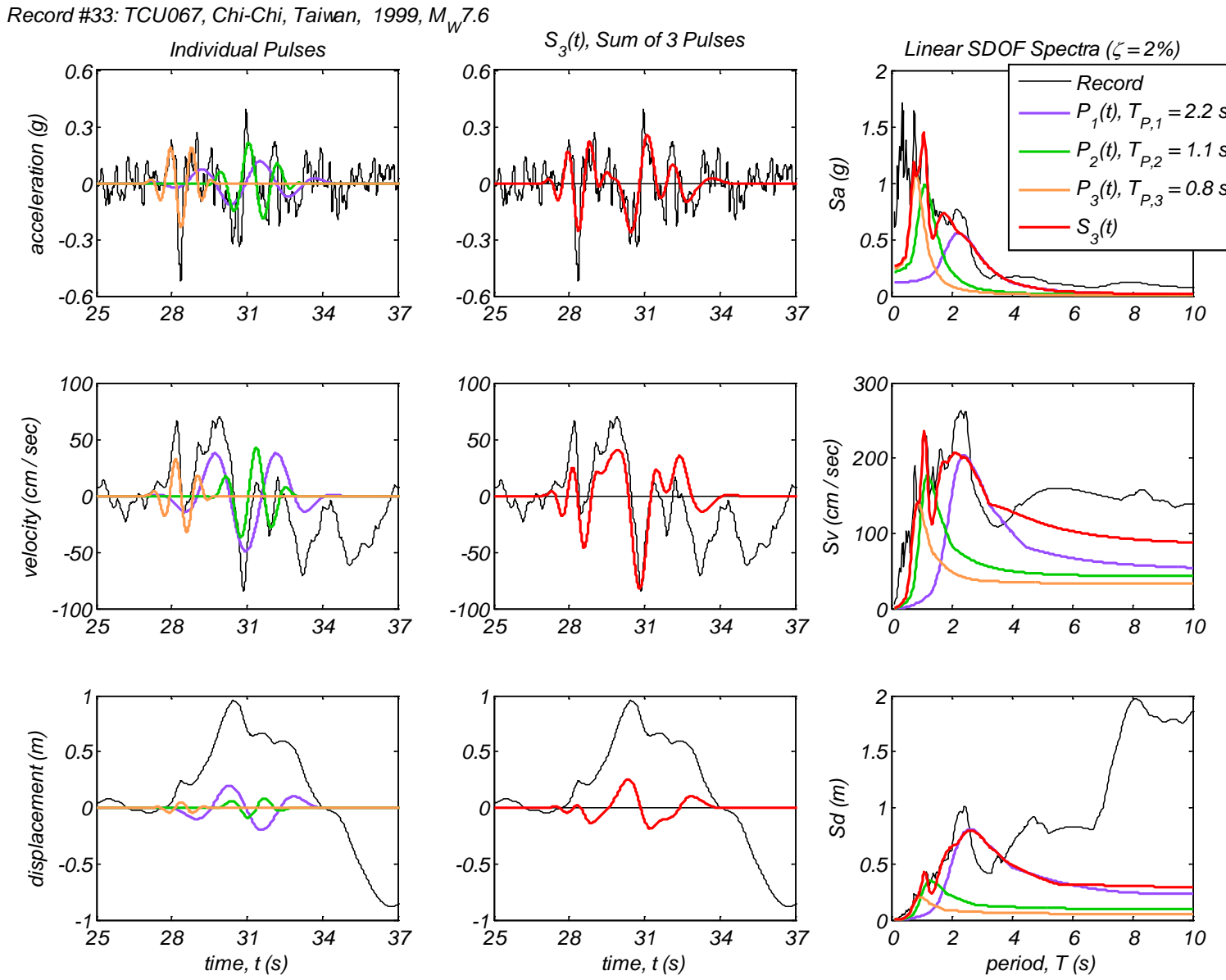
Appendix B4 – Time history and linear spectral response of three extracted pulses using the CPE<sub>A-AR</sub> method for 40 Motions



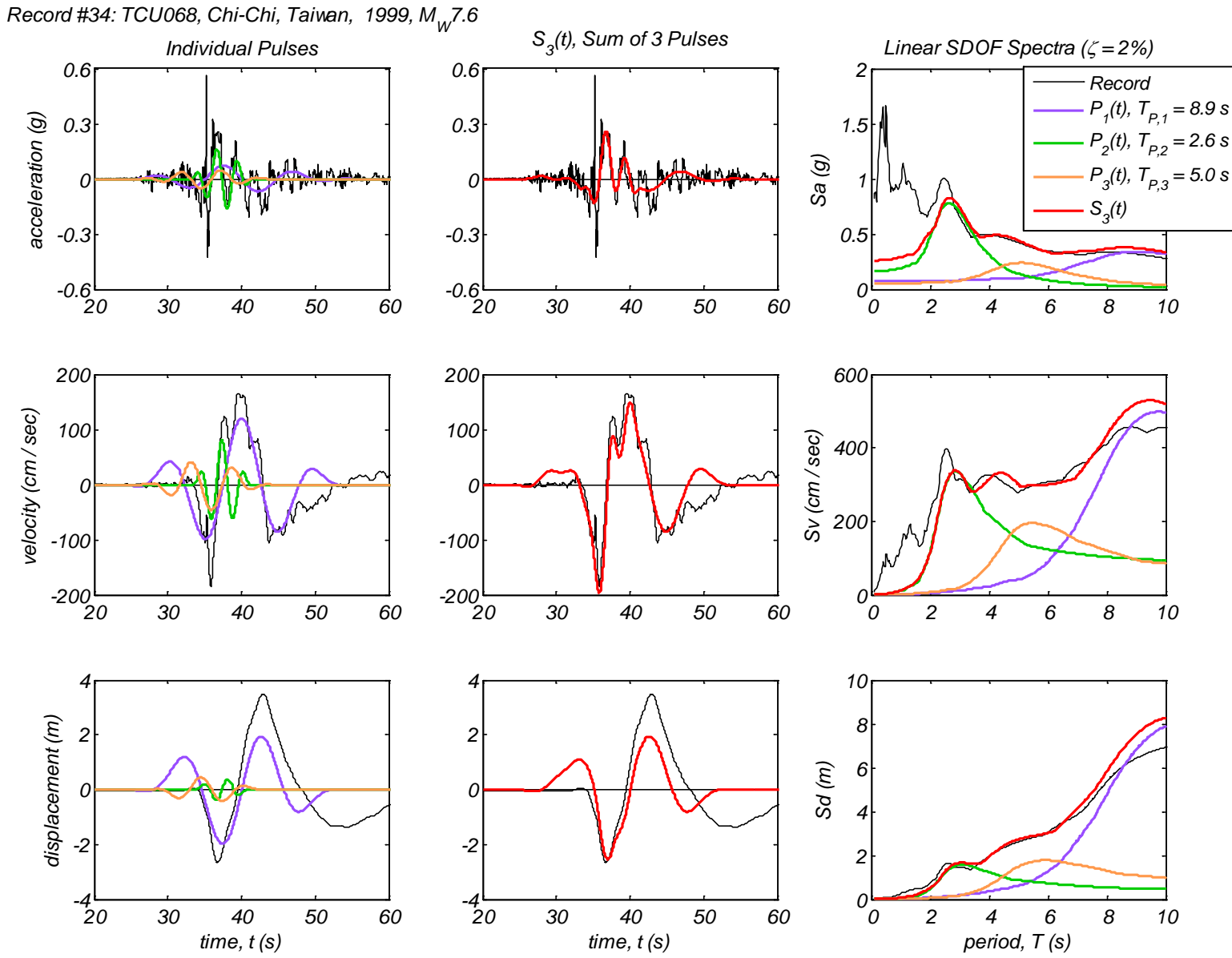
Appendix B4 – Time history and linear spectral response of three extracted pulses using the CPE<sub>A-AR</sub> method for 40 Motions



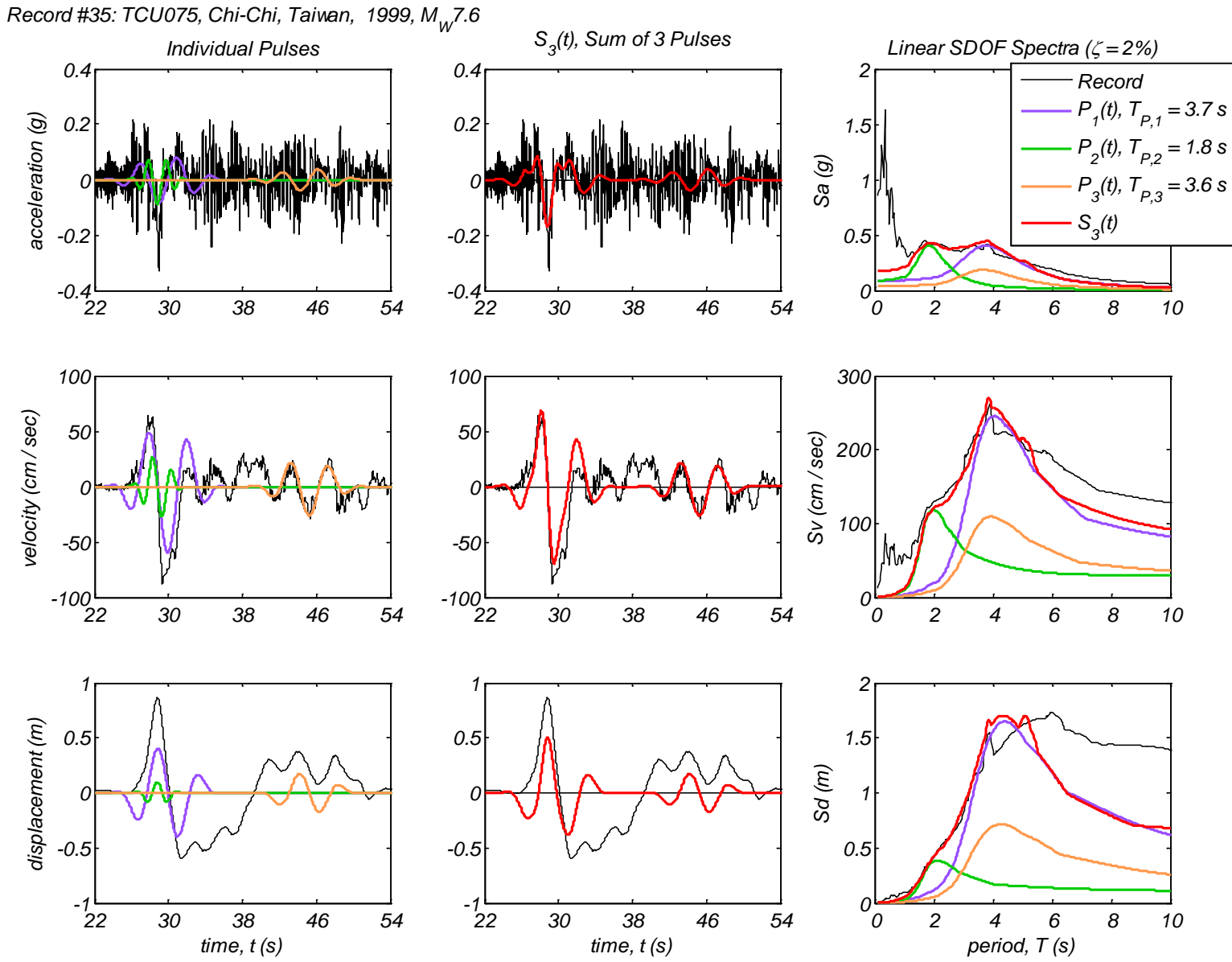
Appendix B4 – Time history and linear spectral response of three extracted pulses using the CPE<sub>A-AR</sub> method for 40 Motions



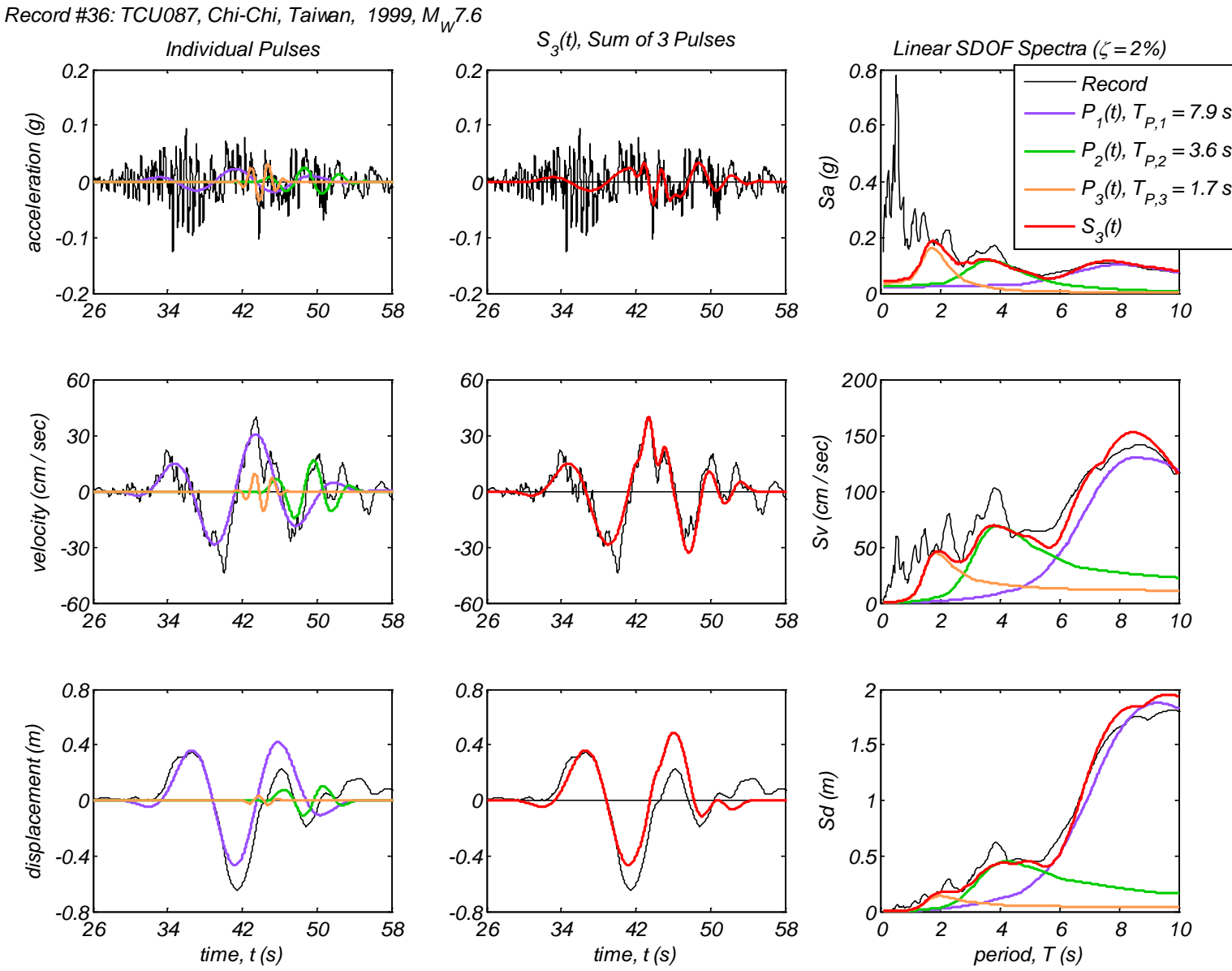
Appendix B4 – Time history and linear spectral response of three extracted pulses using the CPE<sub>A-AR</sub> method for 40 Motions



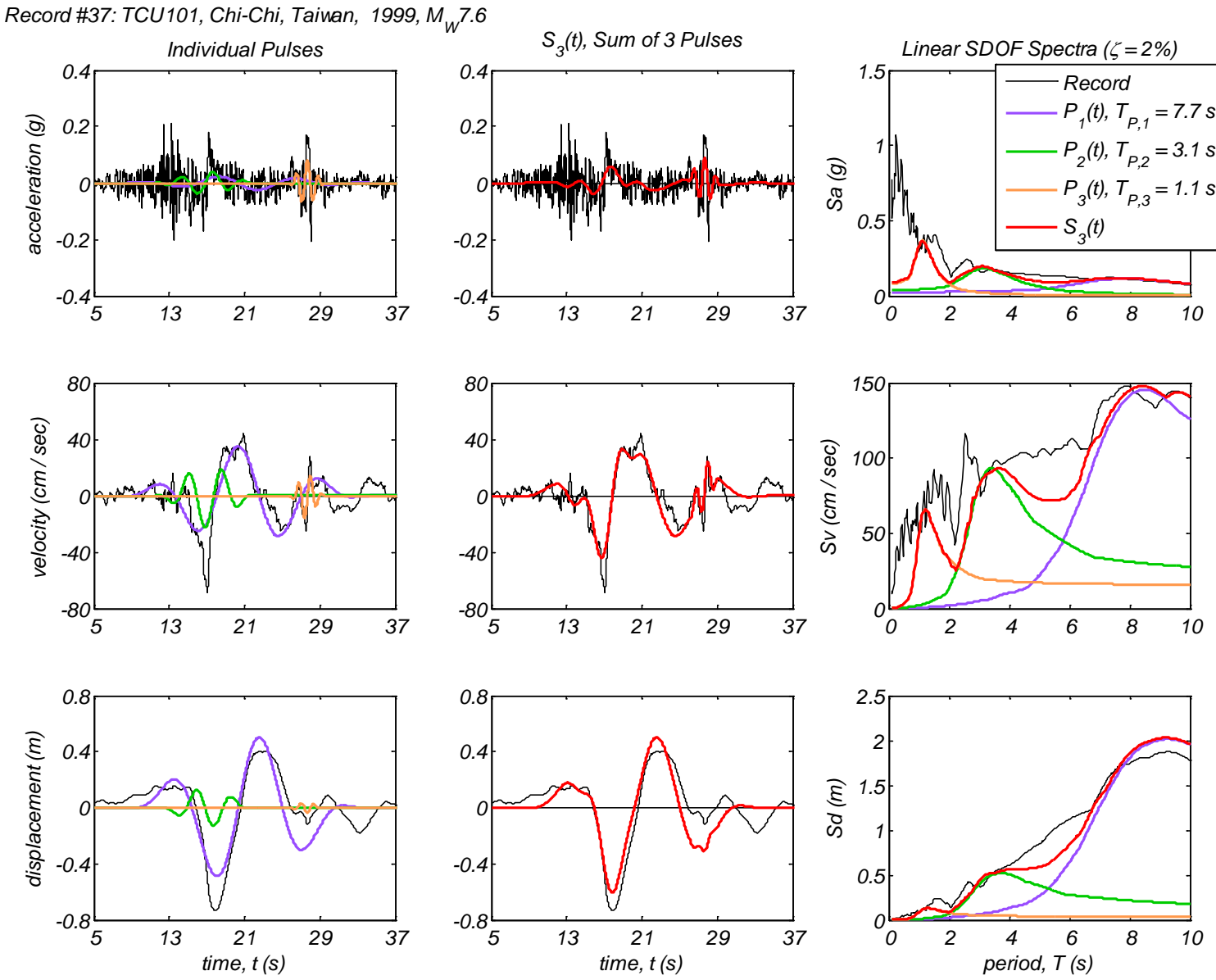
Appendix B4 – Time history and linear spectral response of three extracted pulses using the CPE<sub>A-AR</sub> method for 40 Motions



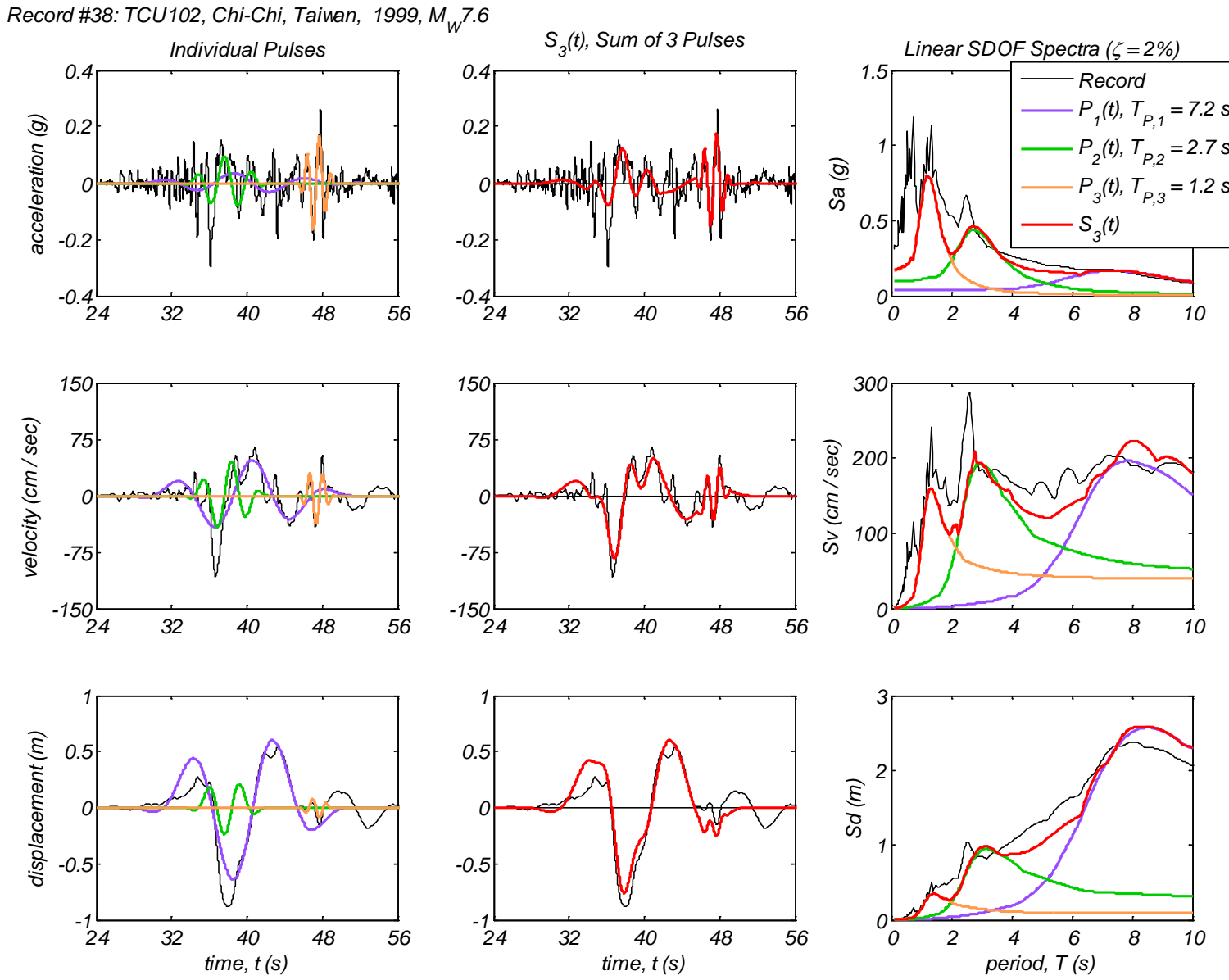
Appendix B4 – Time history and linear spectral response of three extracted pulses using the CPE<sub>A-AR</sub> method for 40 Motions



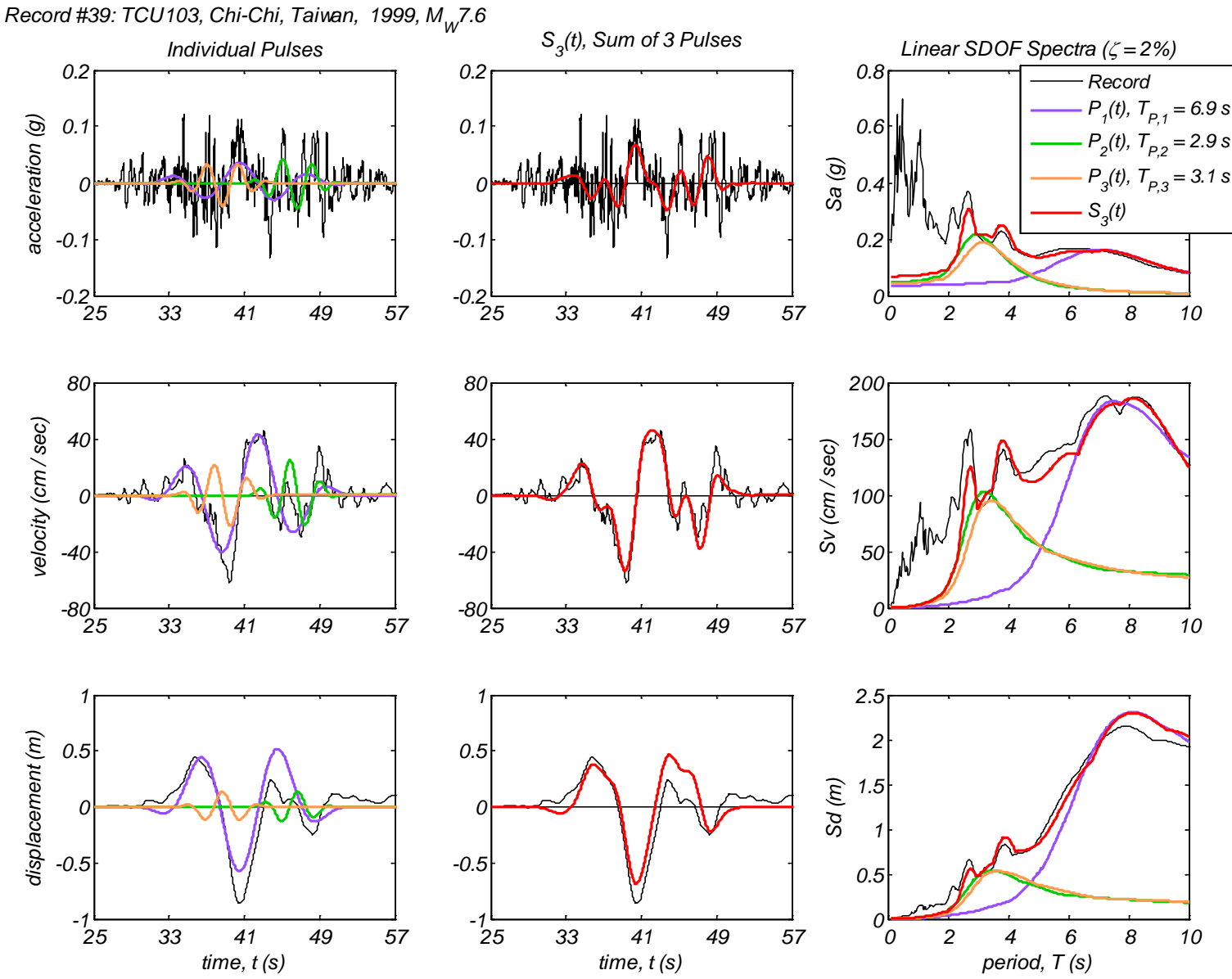
Appendix B4 – Time history and linear spectral response of three extracted pulses using the CPE<sub>A-AR</sub> method for 40 Motions



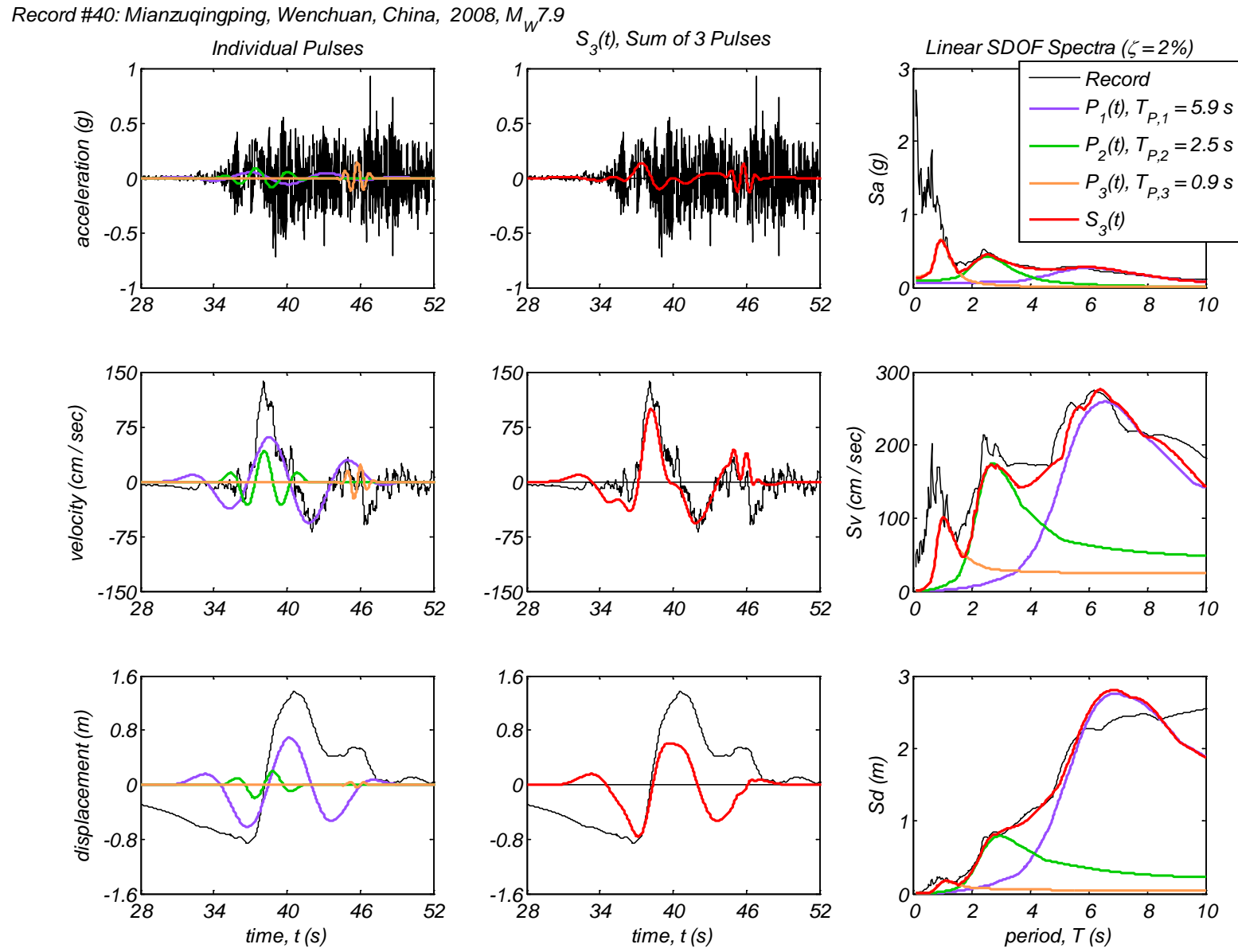
Appendix B4 – Time history and linear spectral response of three extracted pulses using the CPE<sub>A-AR</sub> method for 40 Motions



Appendix B4 – Time history and linear spectral response of three extracted pulses using the CPE<sub>A-AR</sub> method for 40 Motions

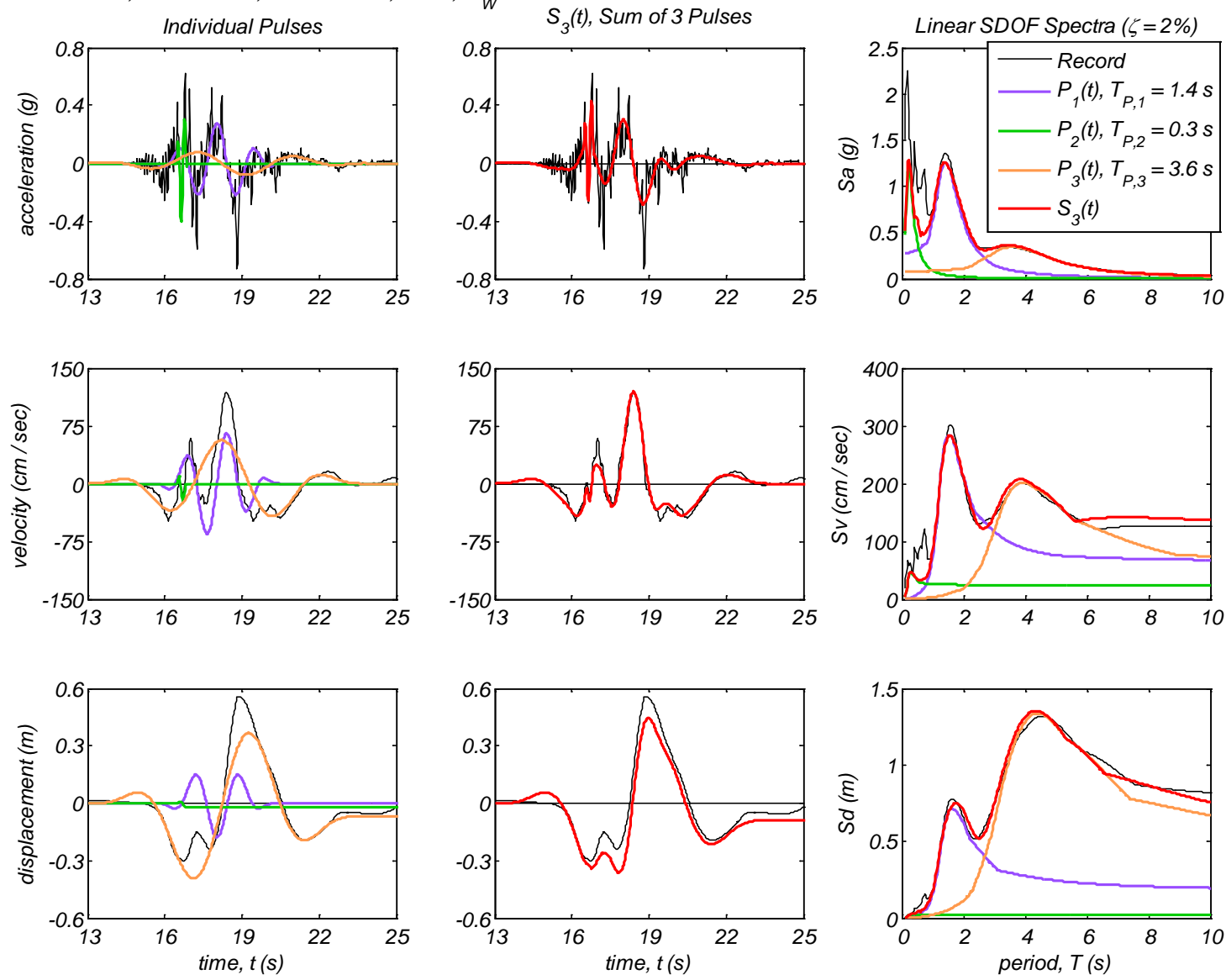


Appendix B4 – Time history and linear spectral response of three extracted pulses using the CPE<sub>A-AR</sub> method for 40 Motions



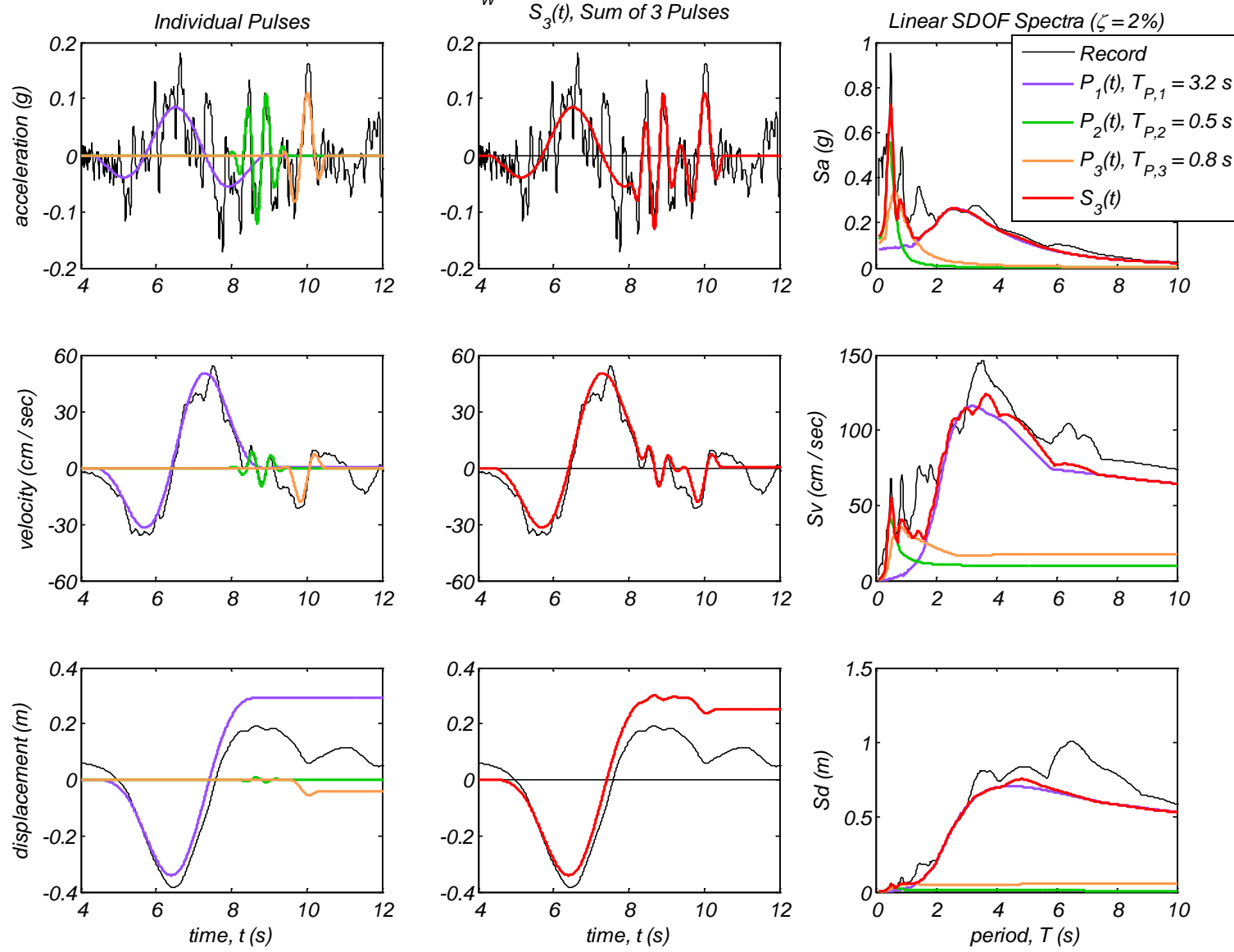
## Appendix B5: Time history and linear spectral response of three extracted pulses using the CPE<sub>A-EN</sub> method for 40 motions

Record #1: PRPC, Christchurch, New Zealand, 2011,  $M_W 6.3$

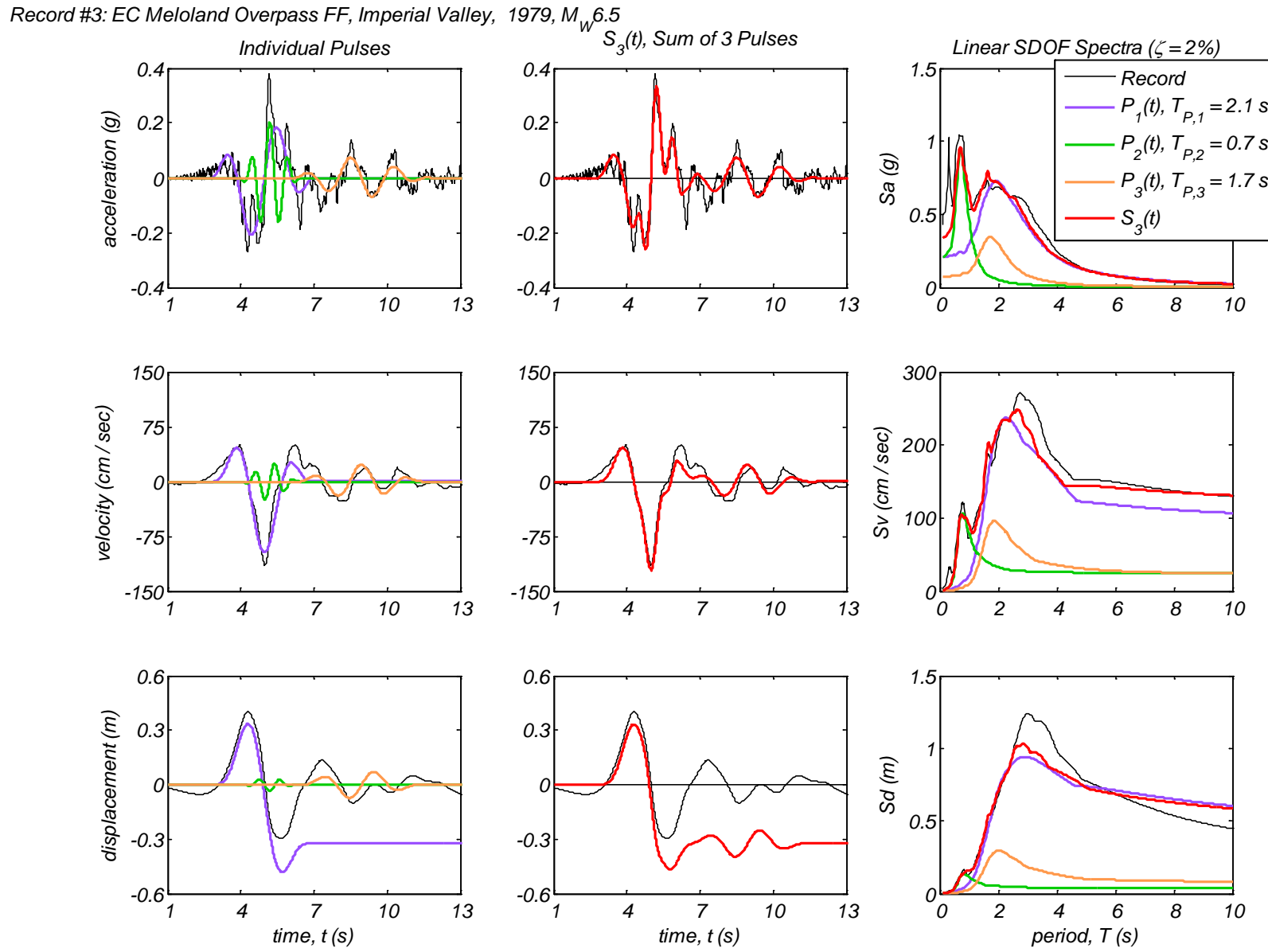


Appendix B5 – Time history and linear spectral response of three extracted pulses using the CPE<sub>A-EN</sub> method for 40 Motions

Record #2: EC County Center FF, Imperial Valley, 1979,  $M_W 6.5$

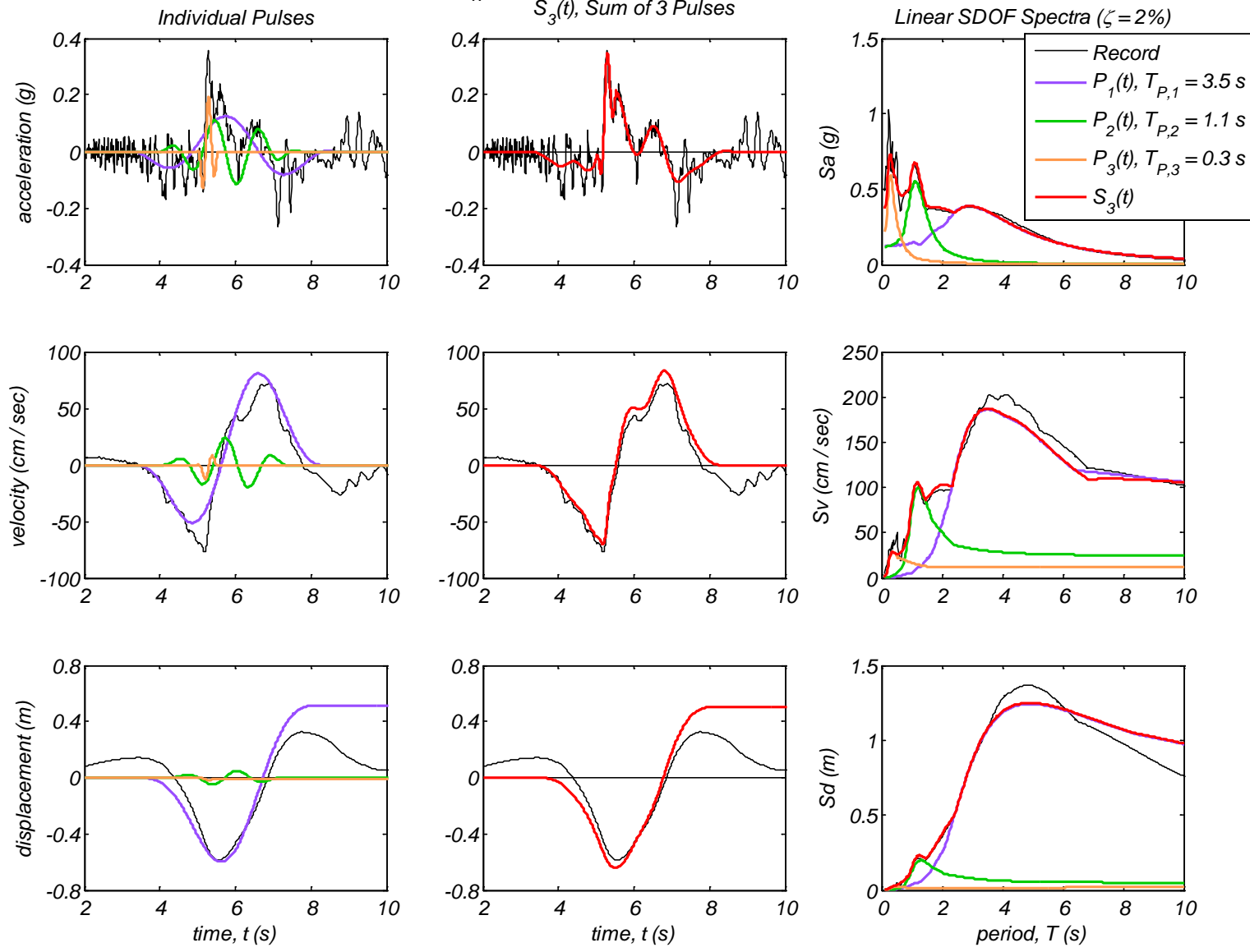


Appendix B5 – Time history and linear spectral response of three extracted pulses using the CPE<sub>A-EN</sub> method for 40 Motions



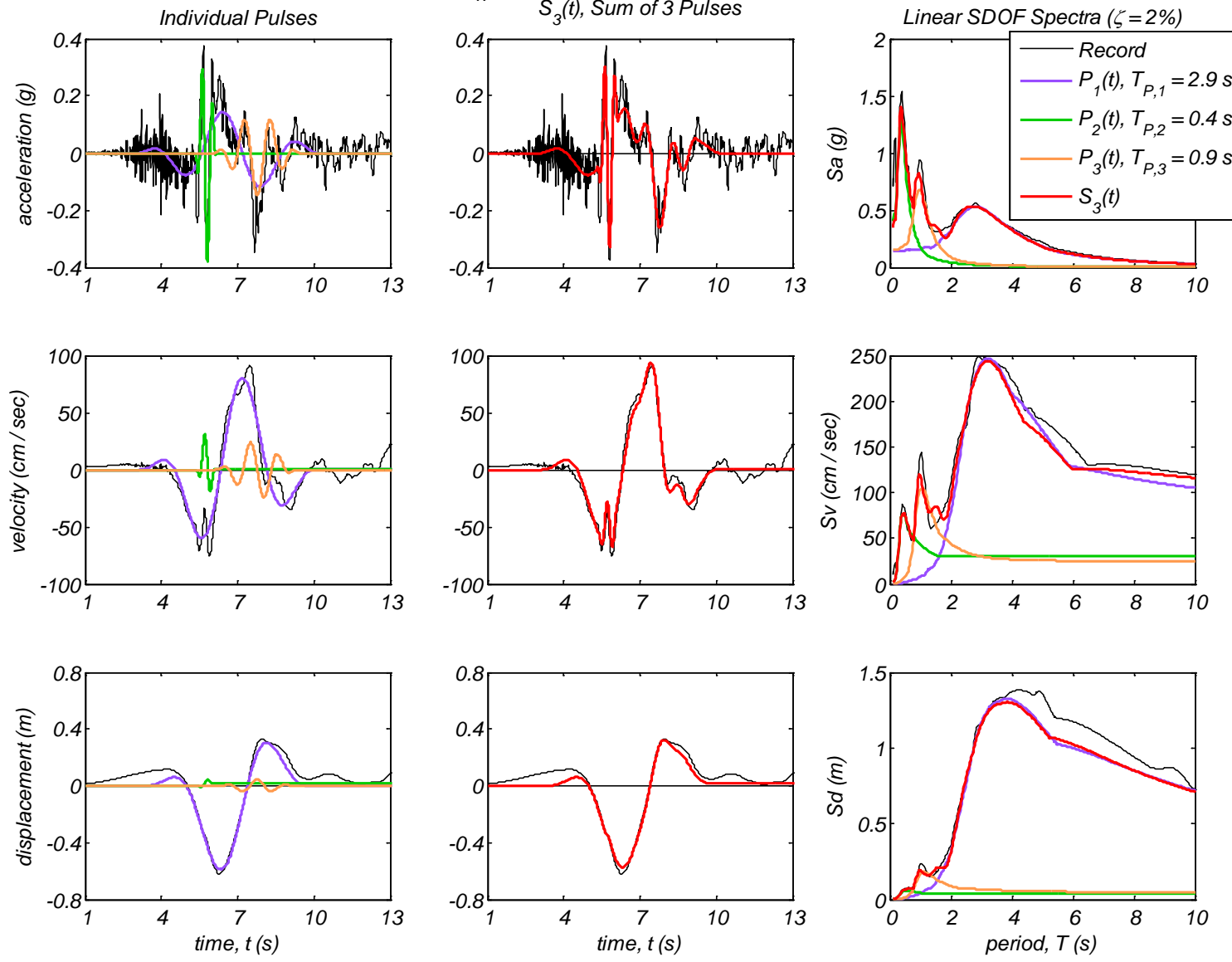
Appendix B5 – Time history and linear spectral response of three extracted pulses using the CPE<sub>A-EN</sub> method for 40 Motions

Record #4: El Centro Array #4, Imperial Valley, 1979,  $M_W 6.5$



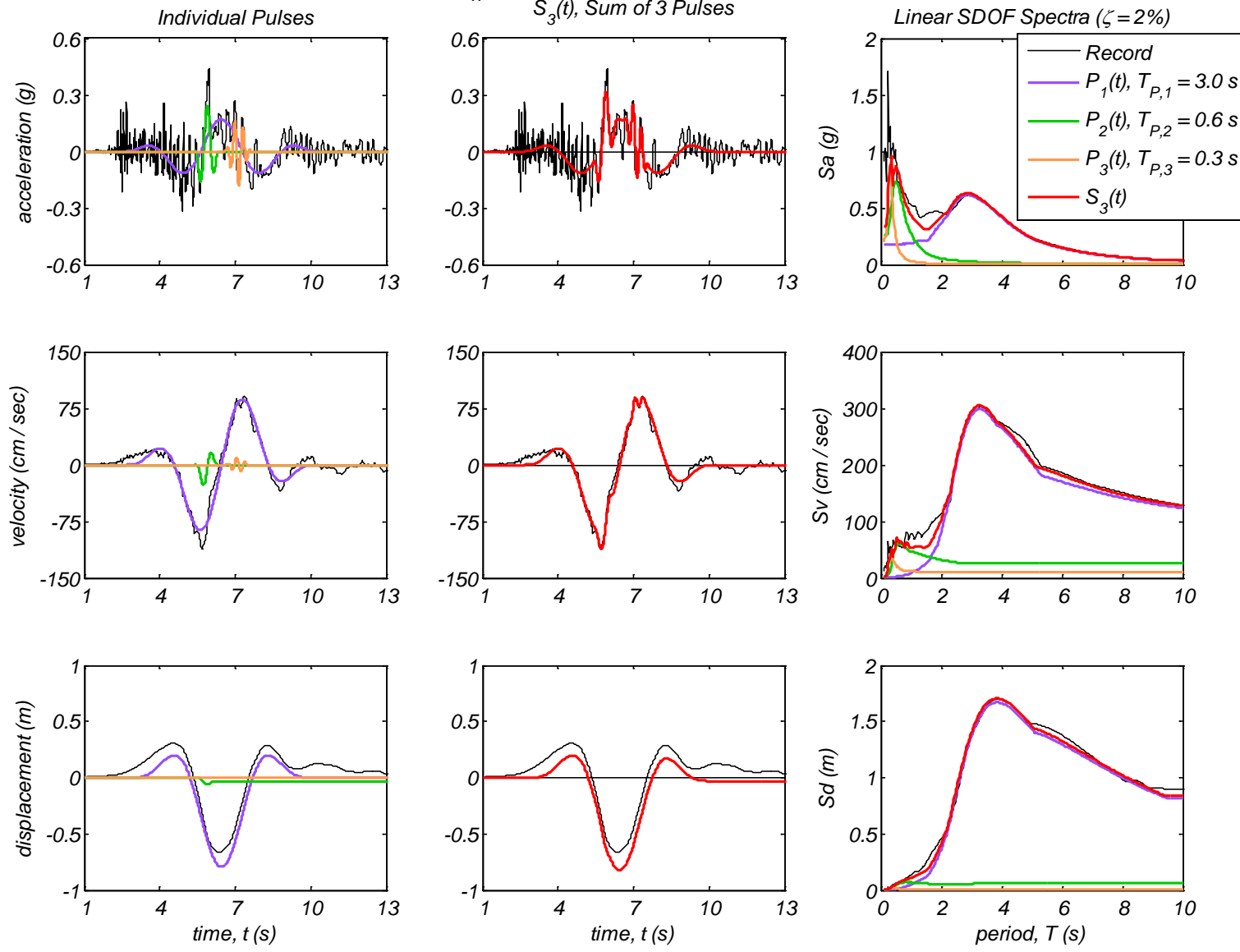
Appendix B5 – Time history and linear spectral response of three extracted pulses using the CPE<sub>A-EN</sub> method for 40 Motions

Record #5: El Centro Array #5, Imperial Valley, 1979,  $M_W 6.5$



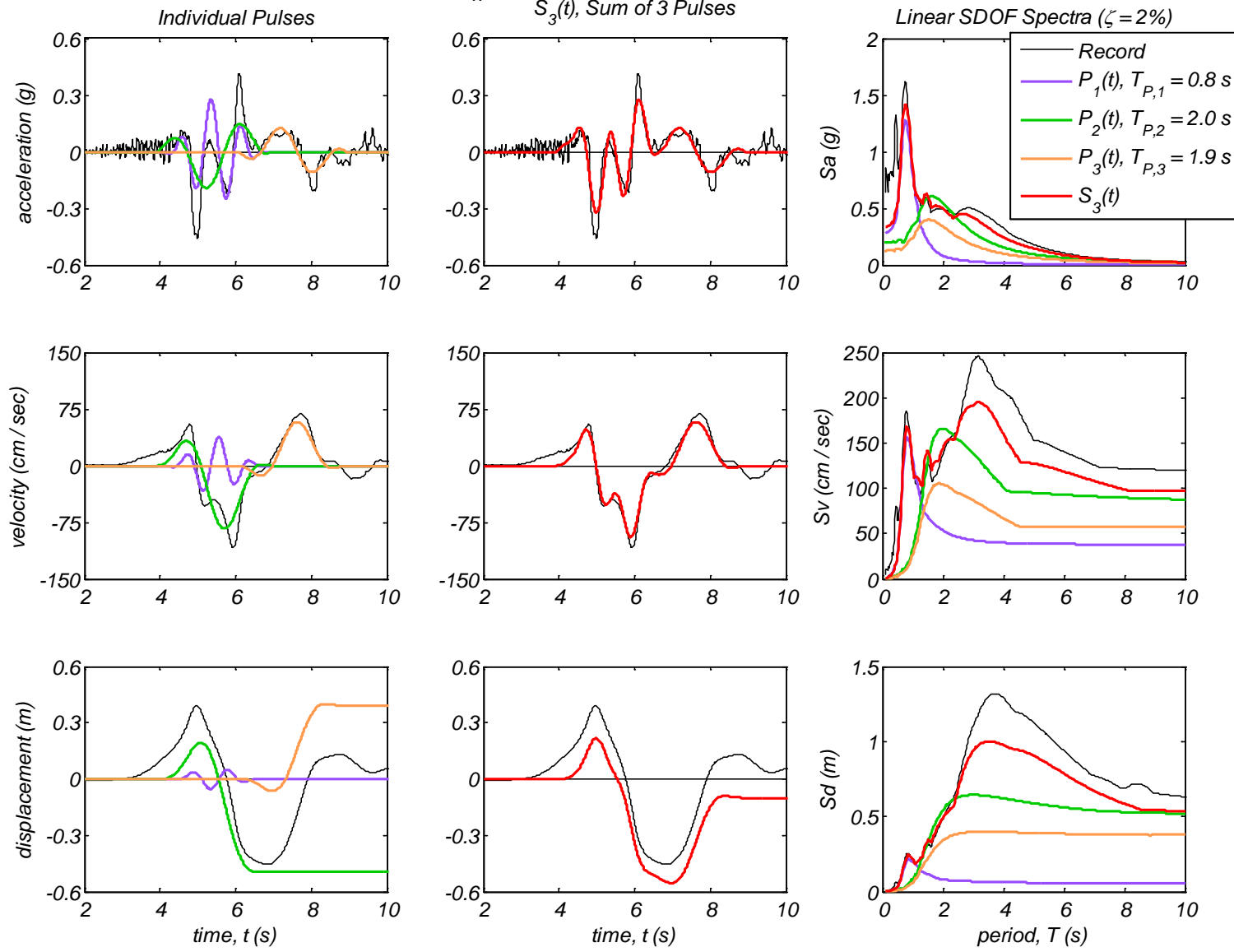
Appendix B5 – Time history and linear spectral response of three extracted pulses using the CPE<sub>A-EN</sub> method for 40 Motions

Record #6: El Centro Array #6, Imperial Valley, 1979,  $M_W 6.5$



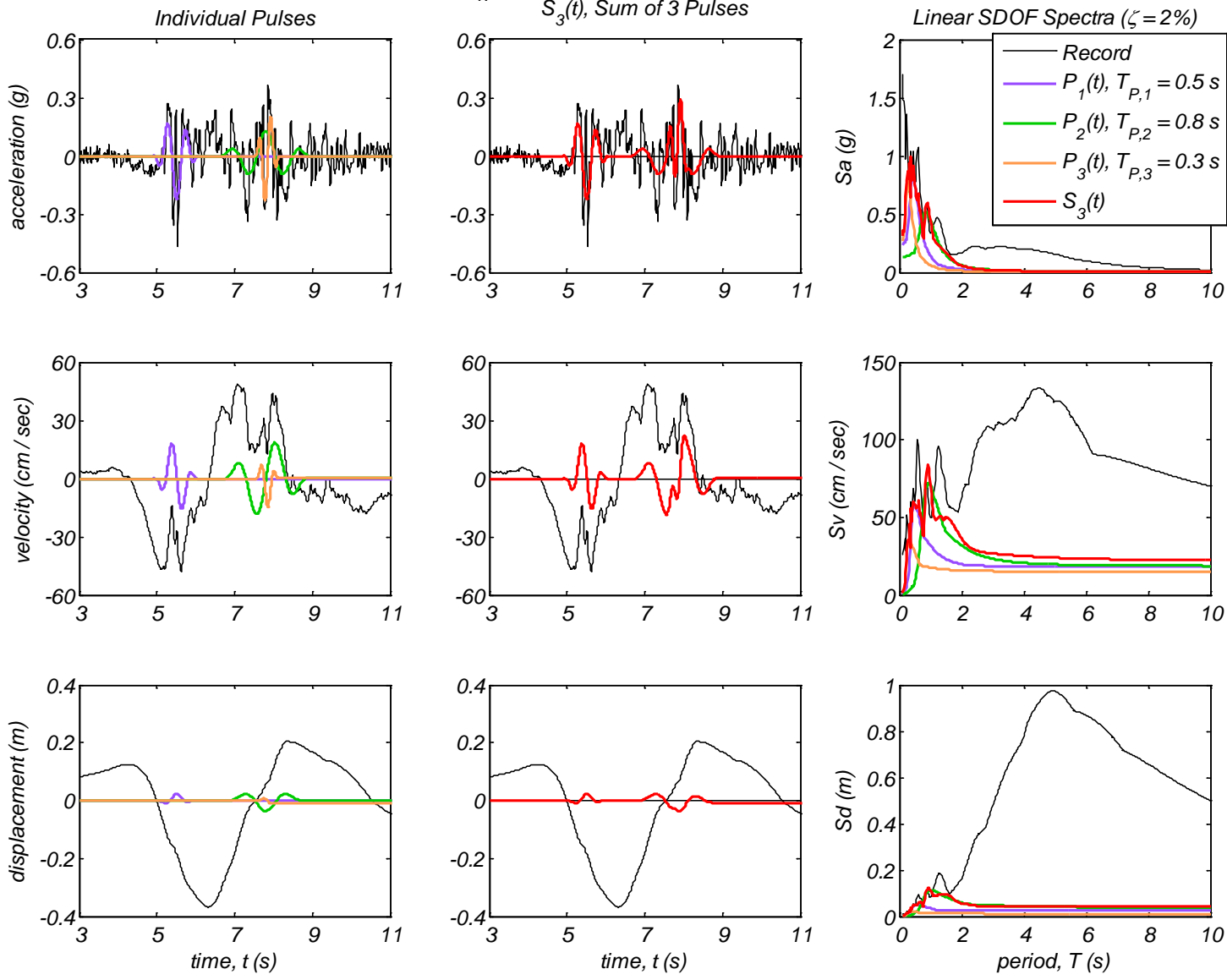
Appendix B5 – Time history and linear spectral response of three extracted pulses using the CPE<sub>A-EN</sub> method for 40 Motions

Record #7: El Centro Array #7, Imperial Valley, 1979,  $M_W 6.5$



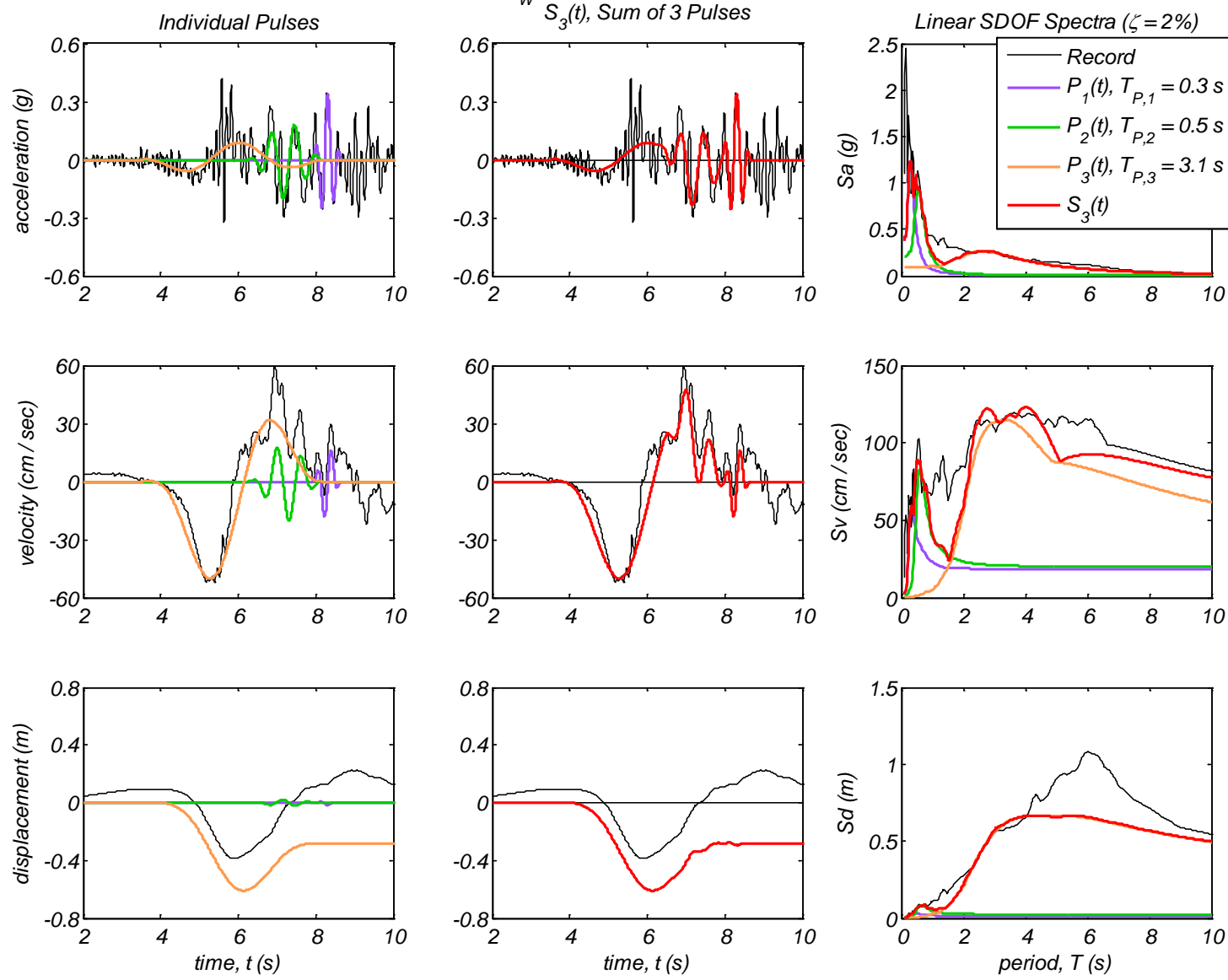
Appendix B5 – Time history and linear spectral response of three extracted pulses using the CPE<sub>A-EN</sub> method for 40 Motions

Record #8: El Centro Array #8, Imperial Valley, 1979,  $M_W 6.5$

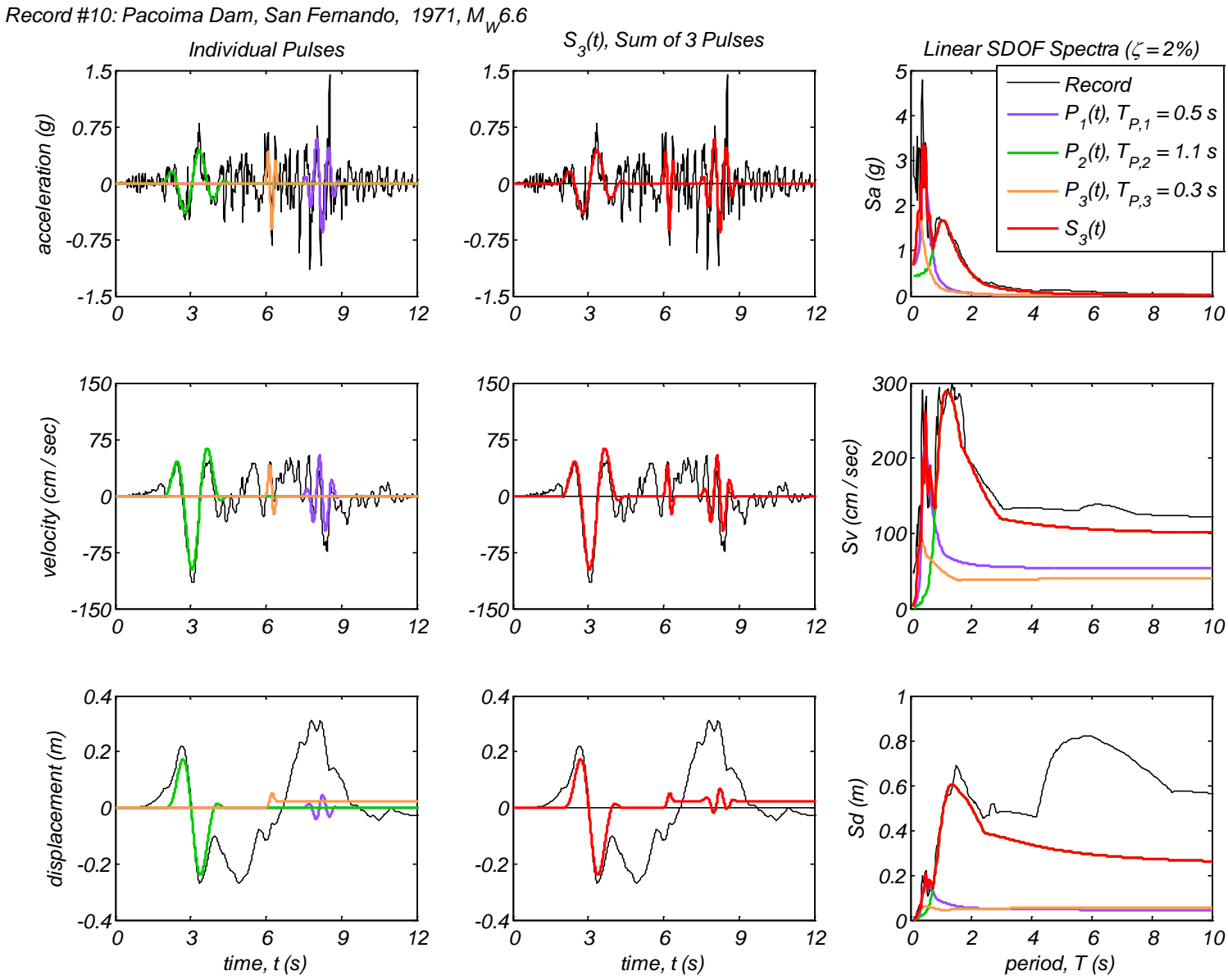


Appendix B5 – Time history and linear spectral response of three extracted pulses using the CPE<sub>A-EN</sub> method for 40 Motions

Record #9: El Centro Differential Array, Imperial Valley, 1979,  $M_w 6.5$

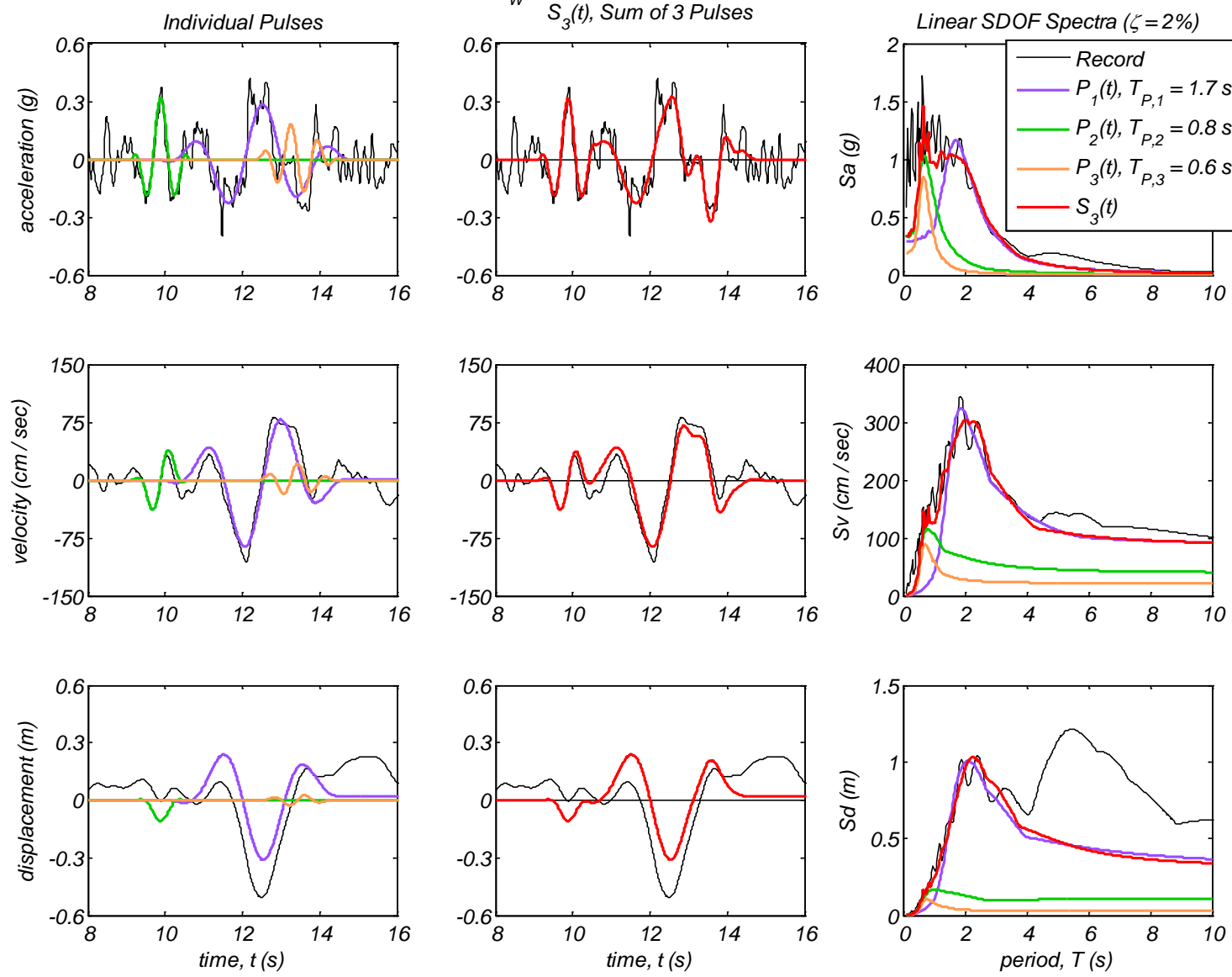


Appendix B5 – Time history and linear spectral response of three extracted pulses using the CPE<sub>A-EN</sub> method for 40 Motions

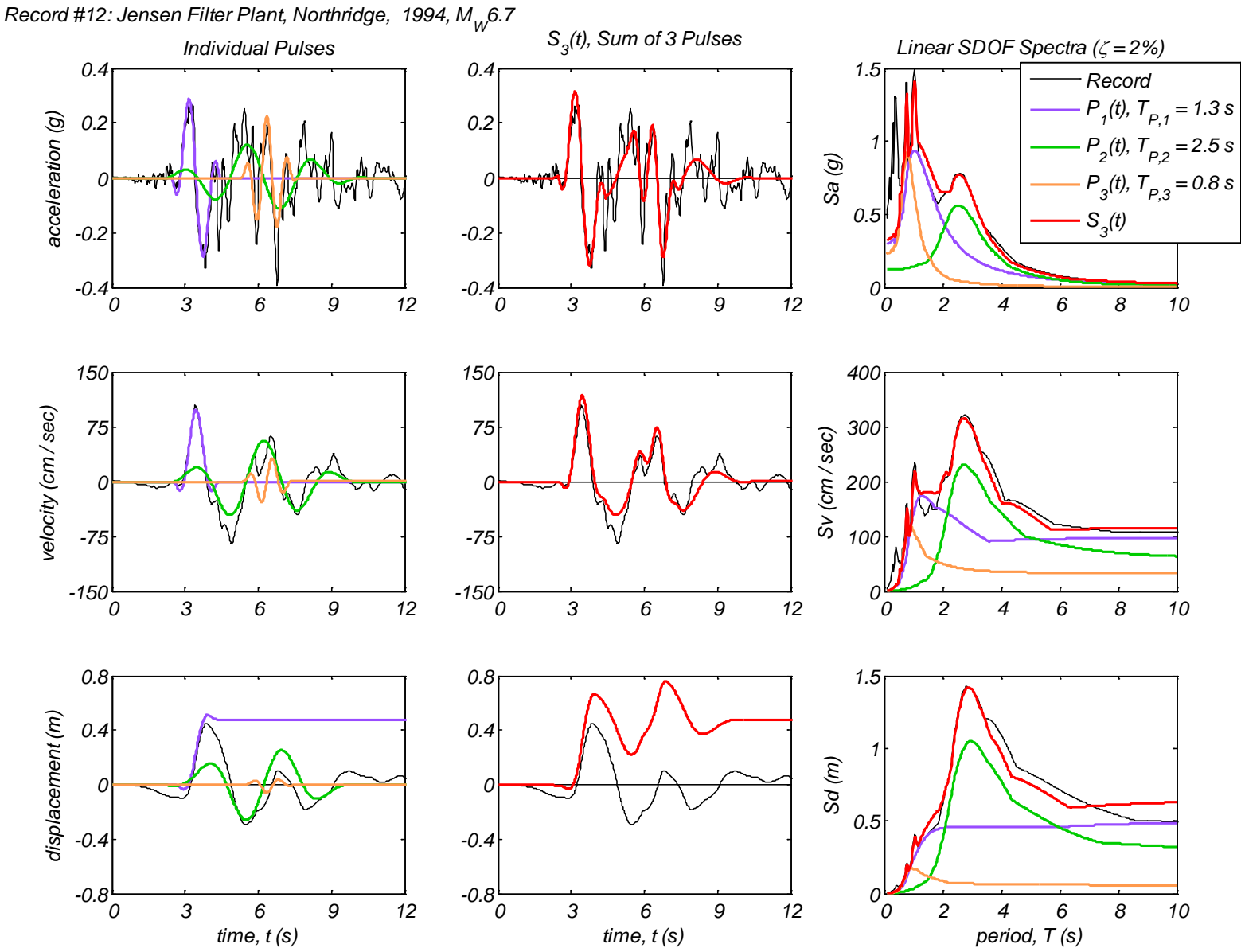


Appendix B5 – Time history and linear spectral response of three extracted pulses using the CPE<sub>A-EN</sub> method for 40 Motions

Record #11: Parachute Test Site, Superstition Hills(B), 1987,  $M_w 6.6$

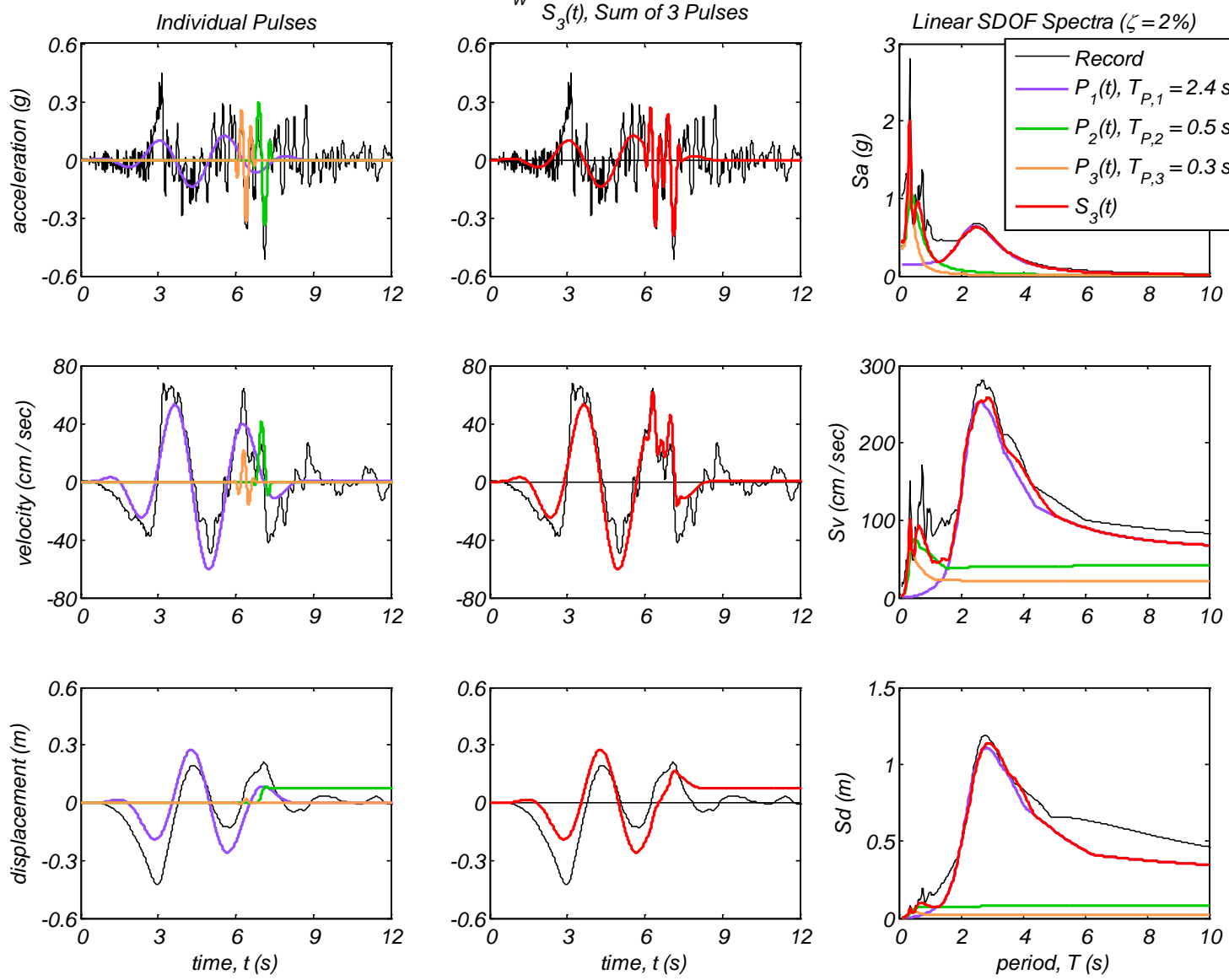


Appendix B5 – Time history and linear spectral response of three extracted pulses using the CPE<sub>A-EN</sub> method for 40 Motions



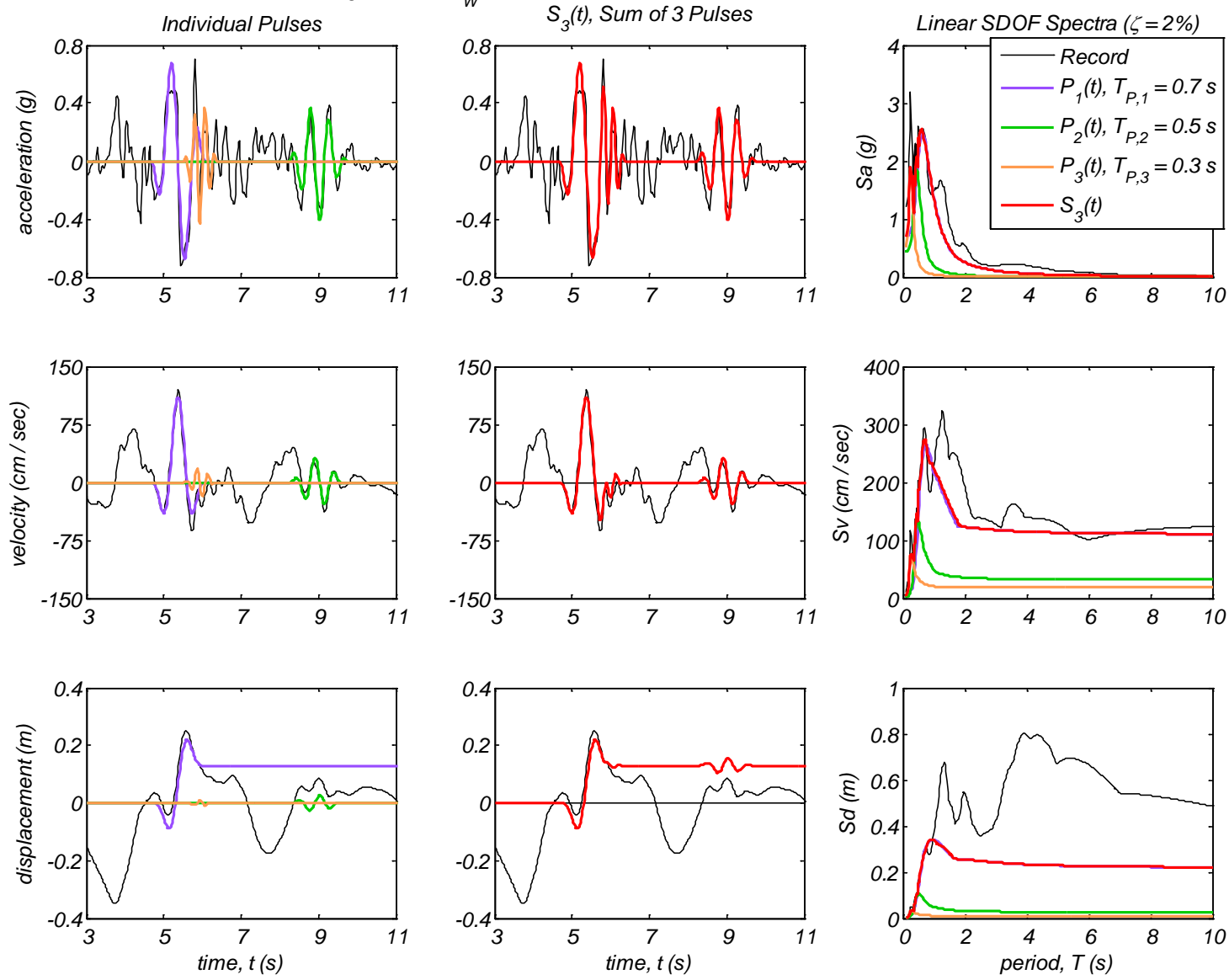
Appendix B5 – Time history and linear spectral response of three extracted pulses using the CPE<sub>A-EN</sub> method for 40 Motions

Record #13: Jensen Filter Plant Generator, Northridge, 1994,  $M_W 6.7$



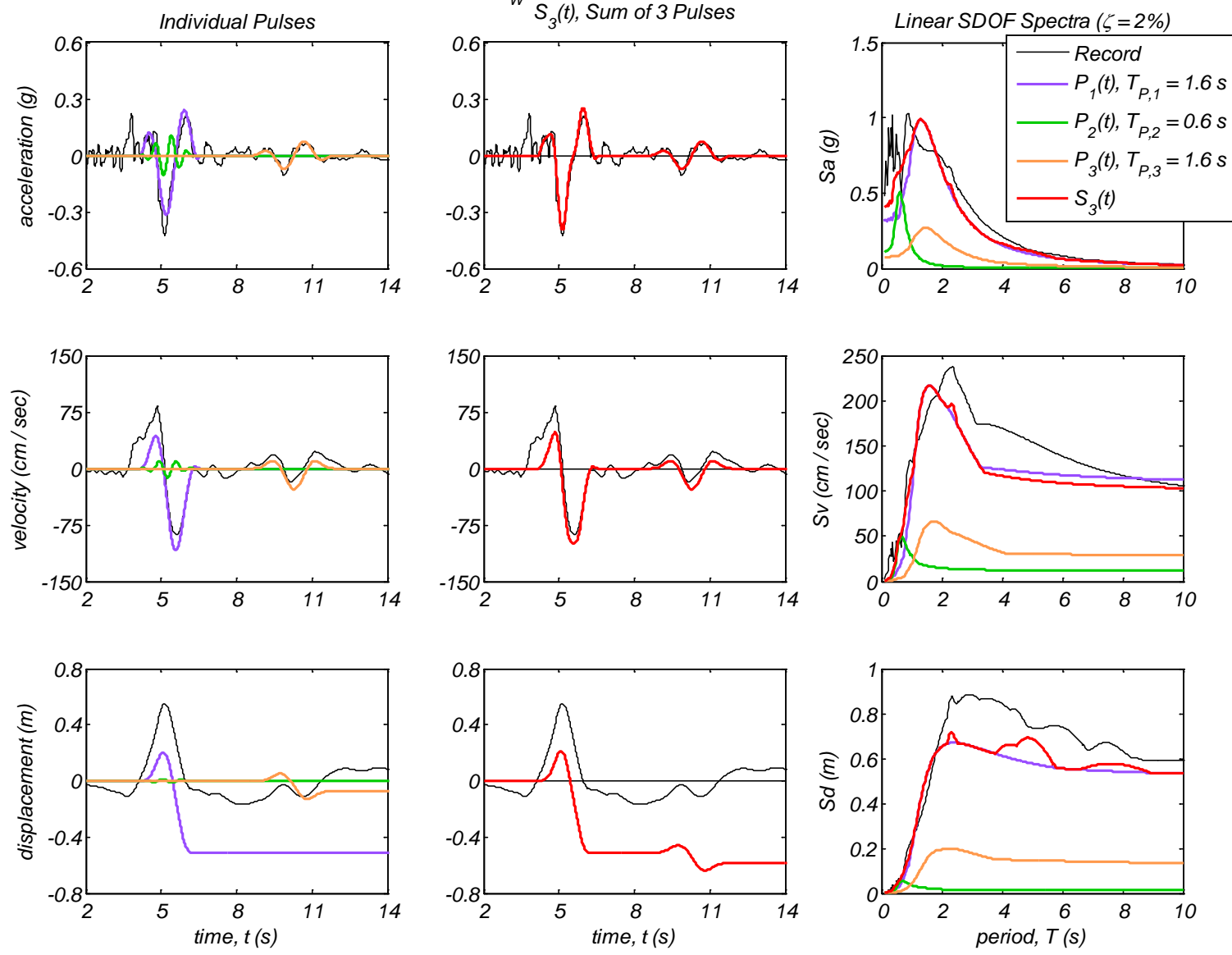
Appendix B5 – Time history and linear spectral response of three extracted pulses using the CPE<sub>A-EN</sub> method for 40 Motions

Record #14: Newhall - Fire Sta, Northridge, 1994,  $M_w 6.7$



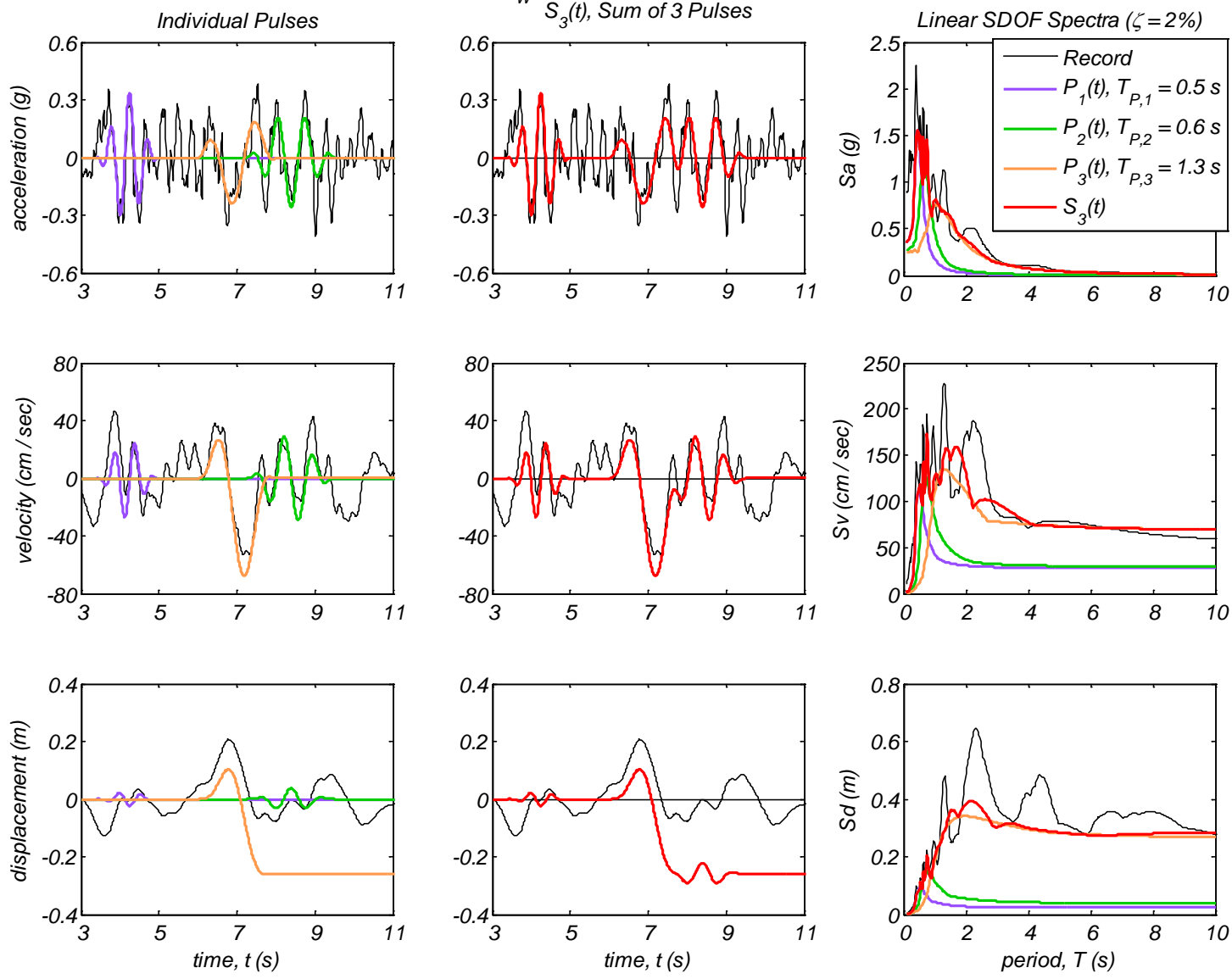
Appendix B5 – Time history and linear spectral response of three extracted pulses using the CPE<sub>A-EN</sub> method for 40 Motions

Record #15: Newhall - W. Pico Canyon Rd., Northridge, 1994,  $M_W$  6.7



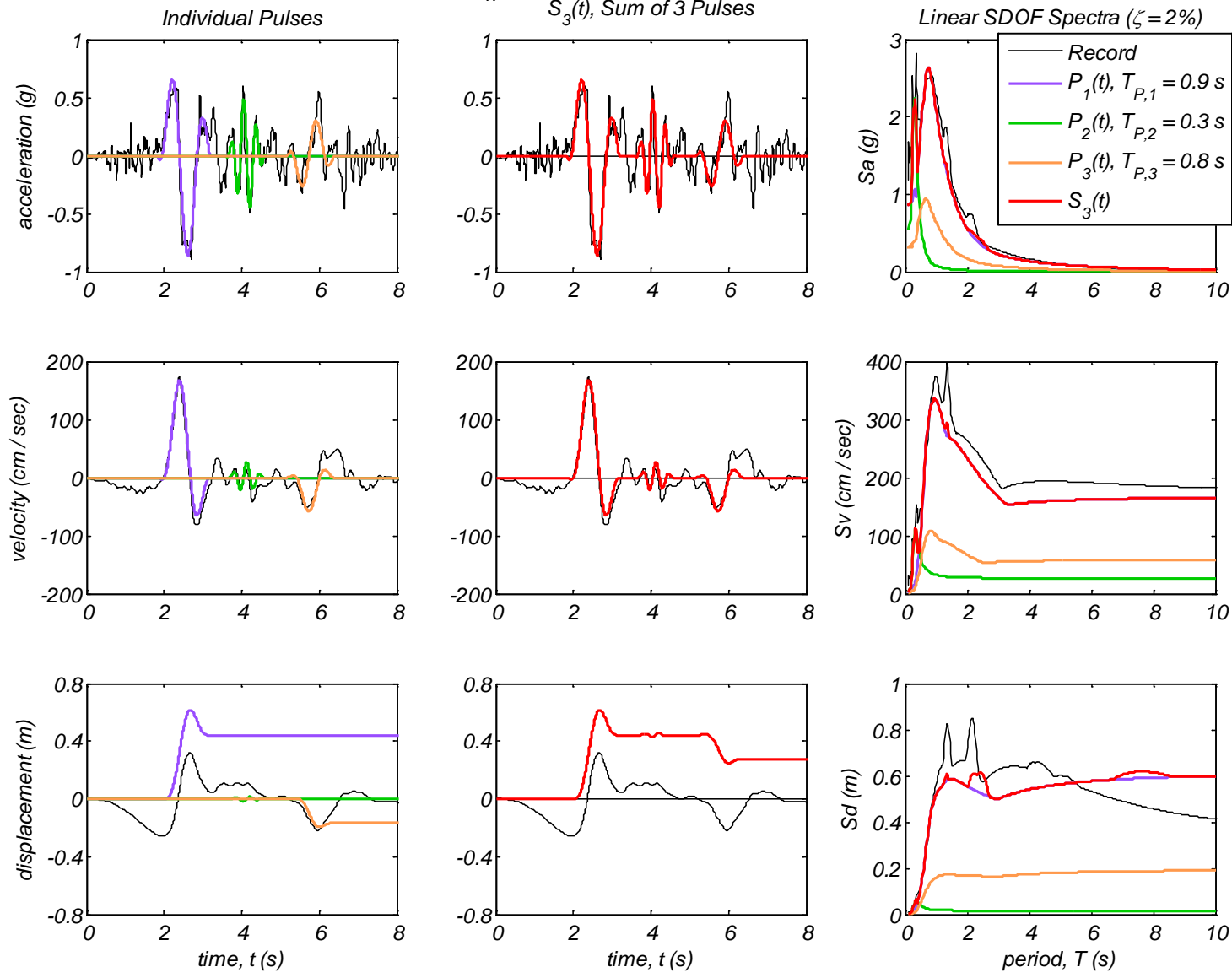
Appendix B5 – Time history and linear spectral response of three extracted pulses using the CPE<sub>A-EN</sub> method for 40 Motions

Record #16: Northridge - 17645 Saticoy St, Northridge, 1994,  $M_W 6.7$

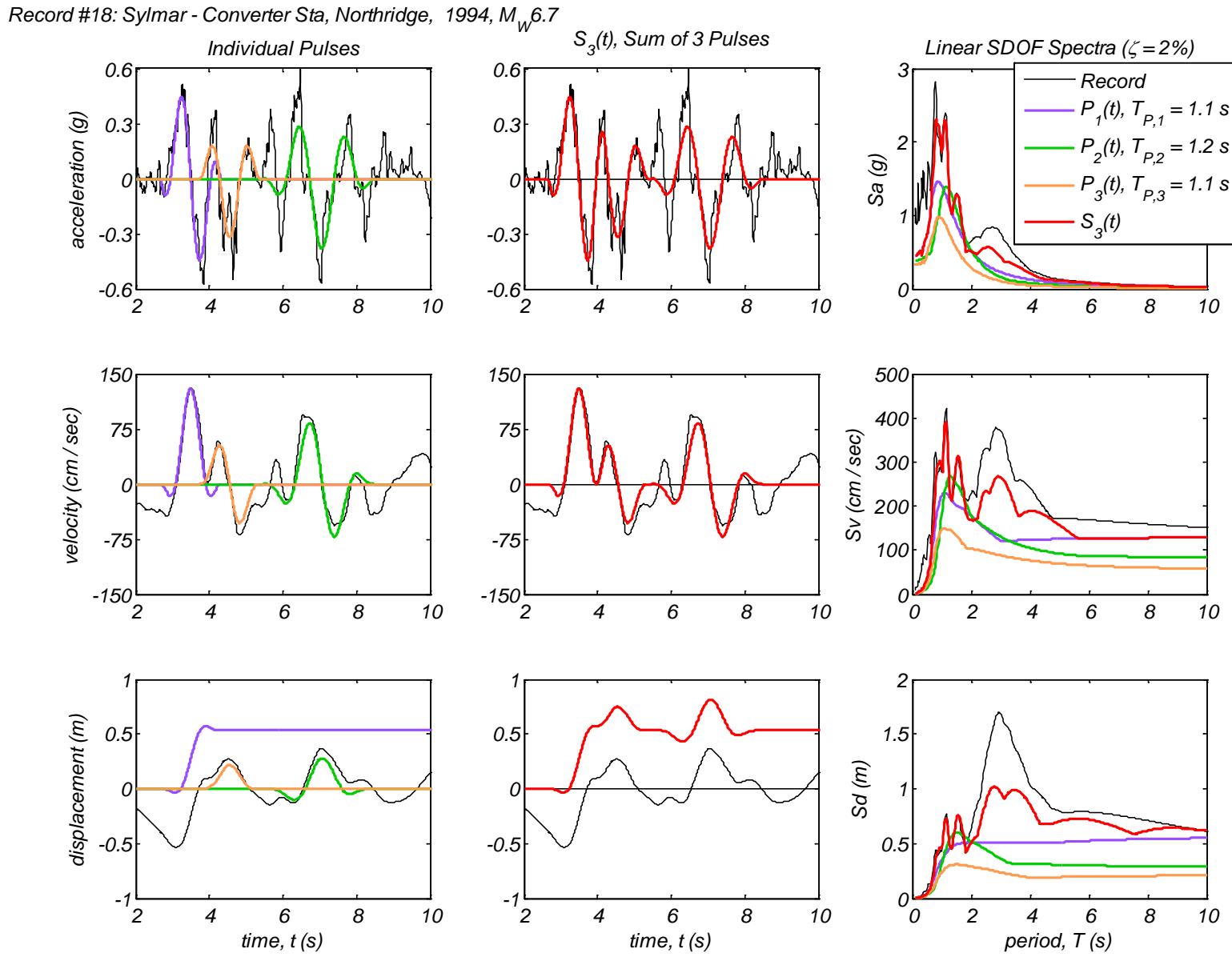


Appendix B5 – Time history and linear spectral response of three extracted pulses using the CPE<sub>A-EN</sub> method for 40 Motions

Record #17: Rinaldi Receiving Sta, Northridge, 1994,  $M_W 6.7$

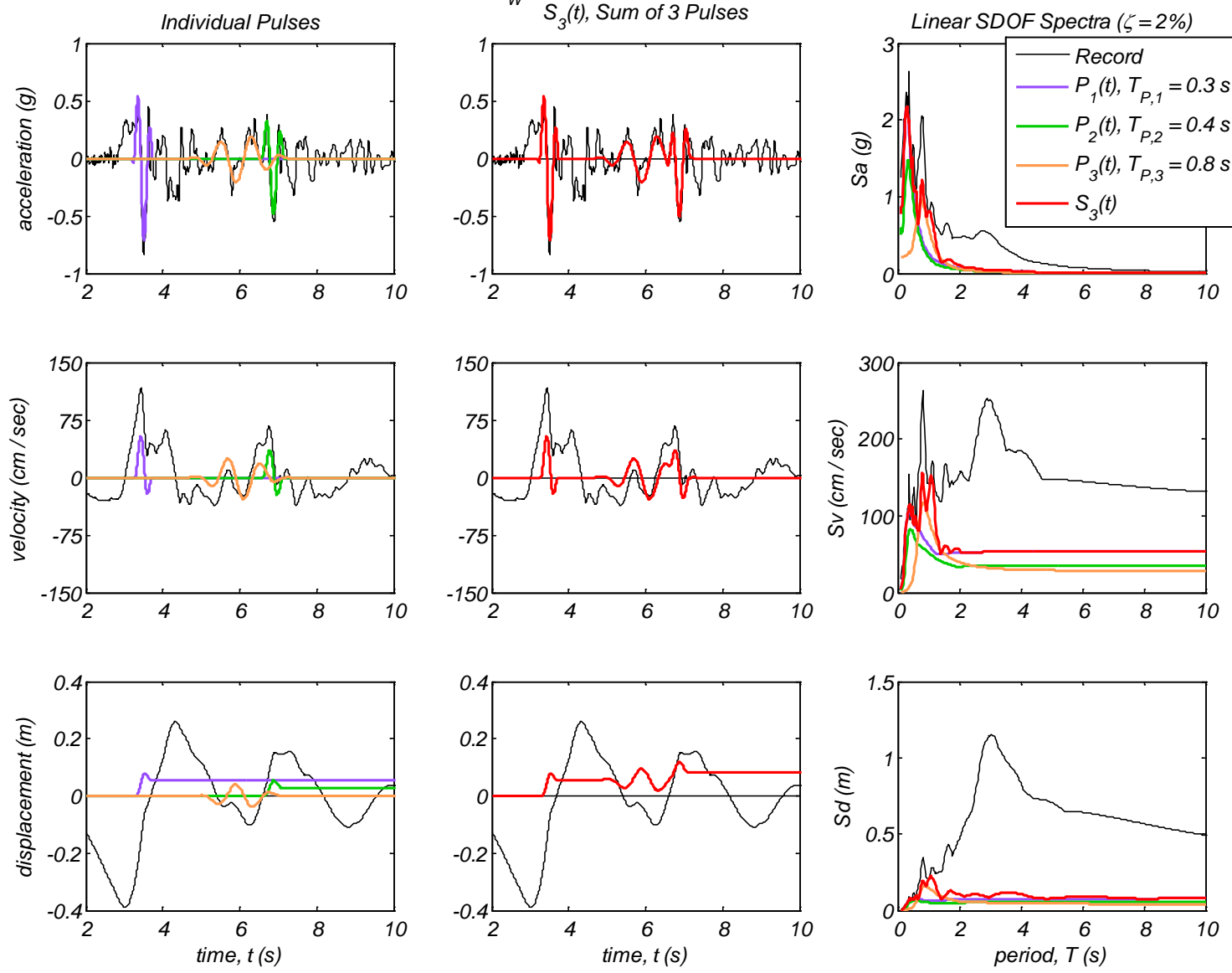


Appendix B5 – Time history and linear spectral response of three extracted pulses using the CPE<sub>A-EN</sub> method for 40 Motions



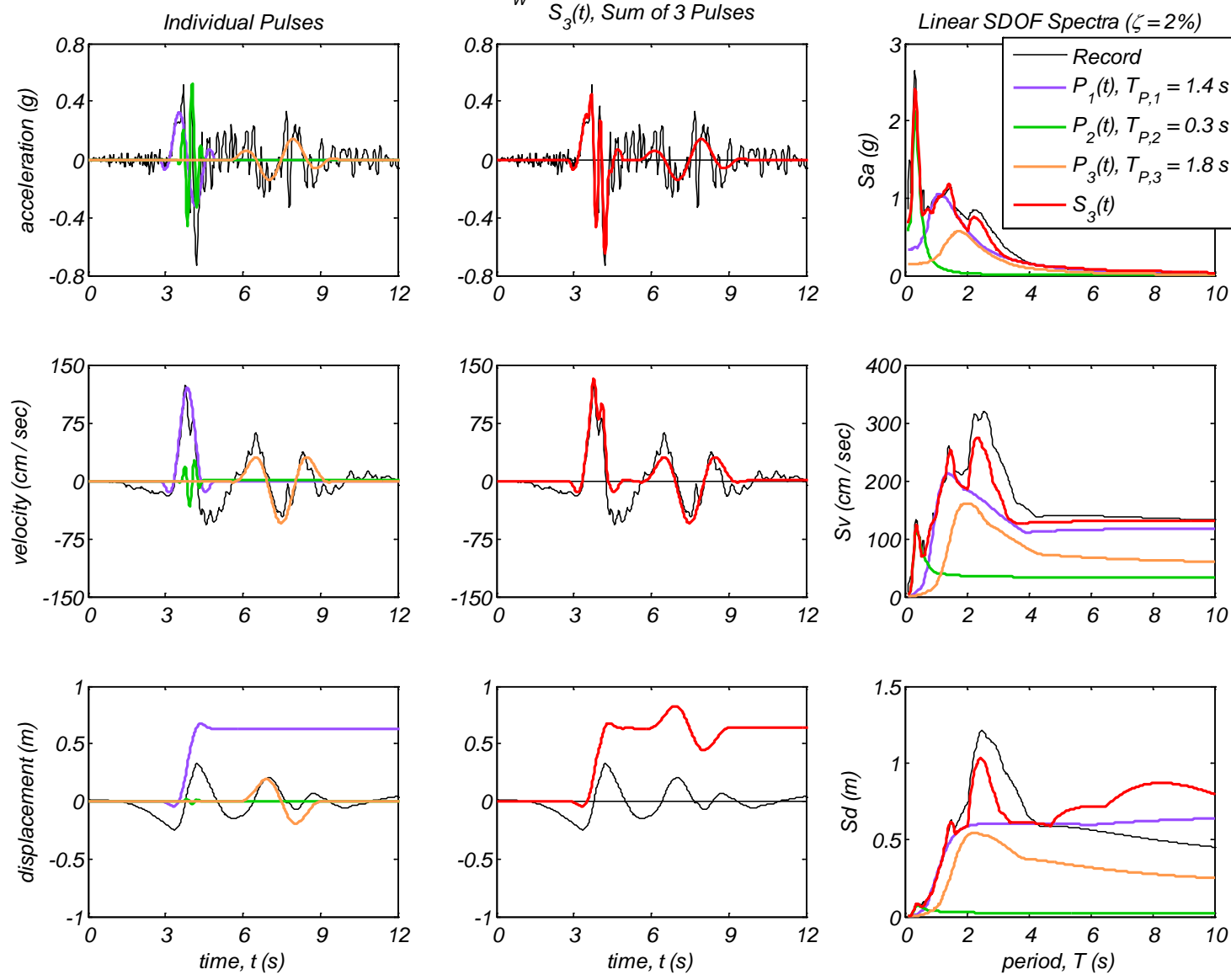
Appendix B5 – Time history and linear spectral response of three extracted pulses using the CPE<sub>A-EN</sub> method for 40 Motions

Record #19: Sylmar - Converter Sta East, Northridge, 1994,  $M_W 6.7$

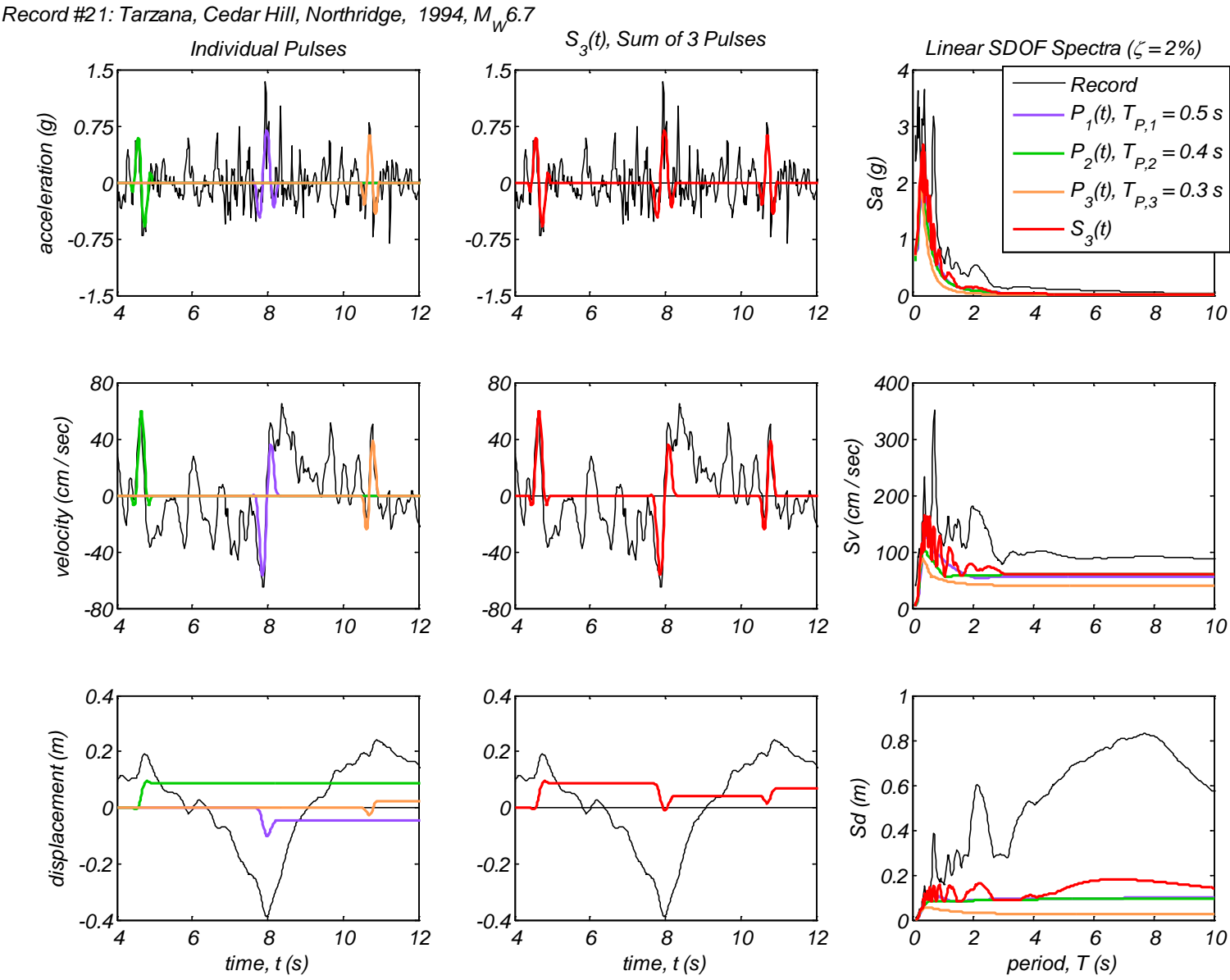


Appendix B5 – Time history and linear spectral response of three extracted pulses using the CPE<sub>A-EN</sub> method for 40 Motions

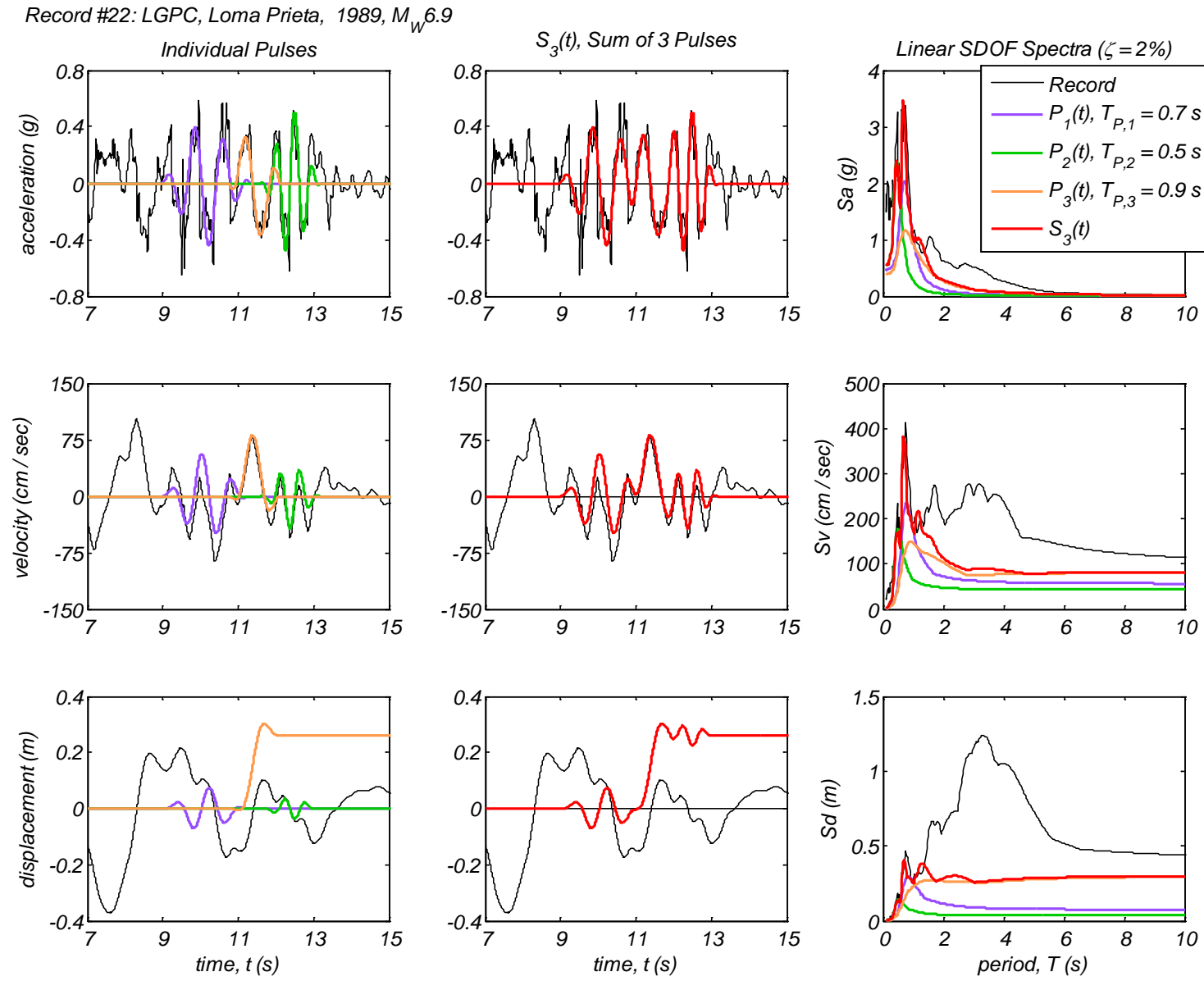
Record #20: Sylmar - Olive ViewMed FF, Northridge, 1994,  $M_W 6.7$



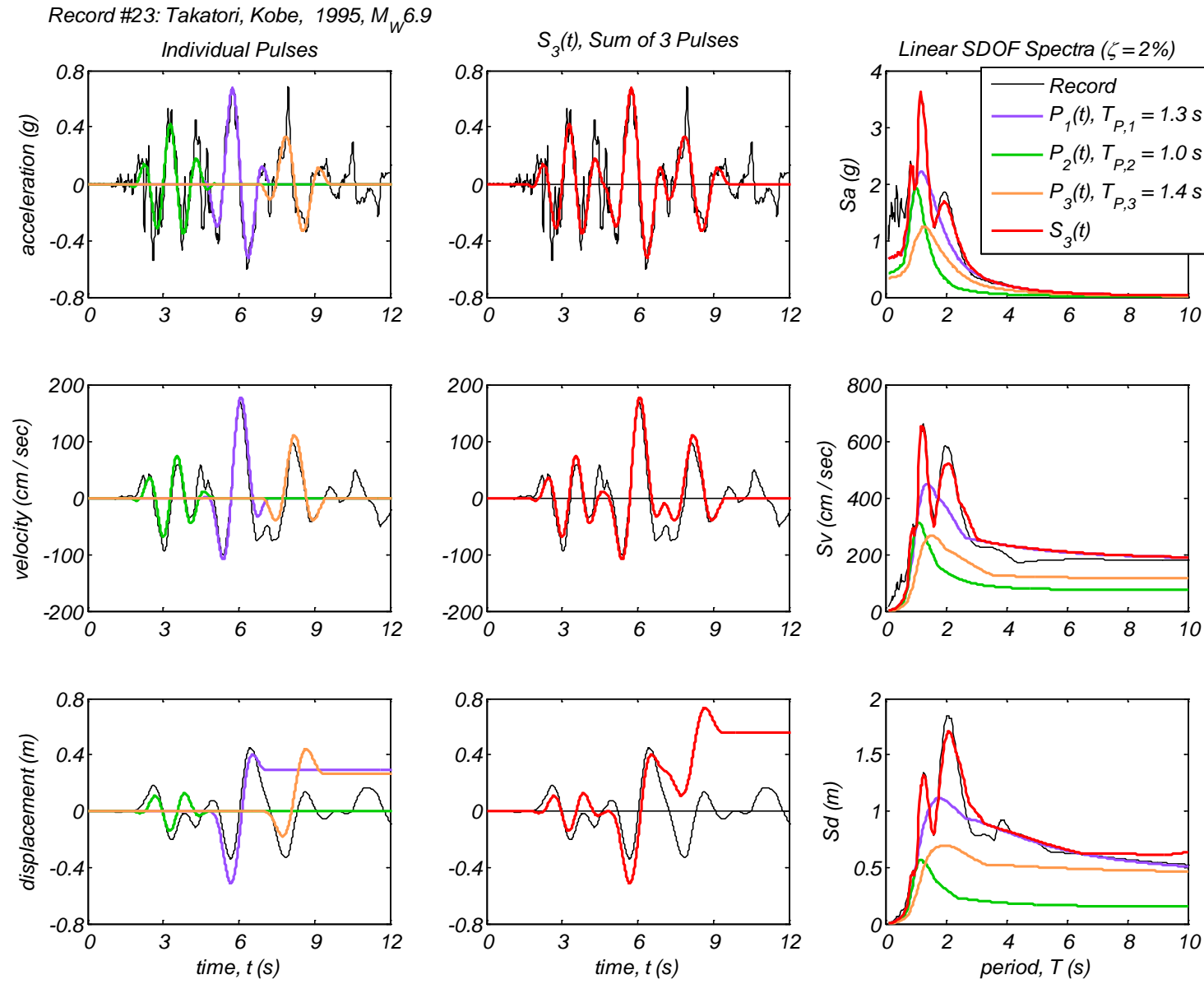
Appendix B5 – Time history and linear spectral response of three extracted pulses using the CPE<sub>A-EN</sub> method for 40 Motions



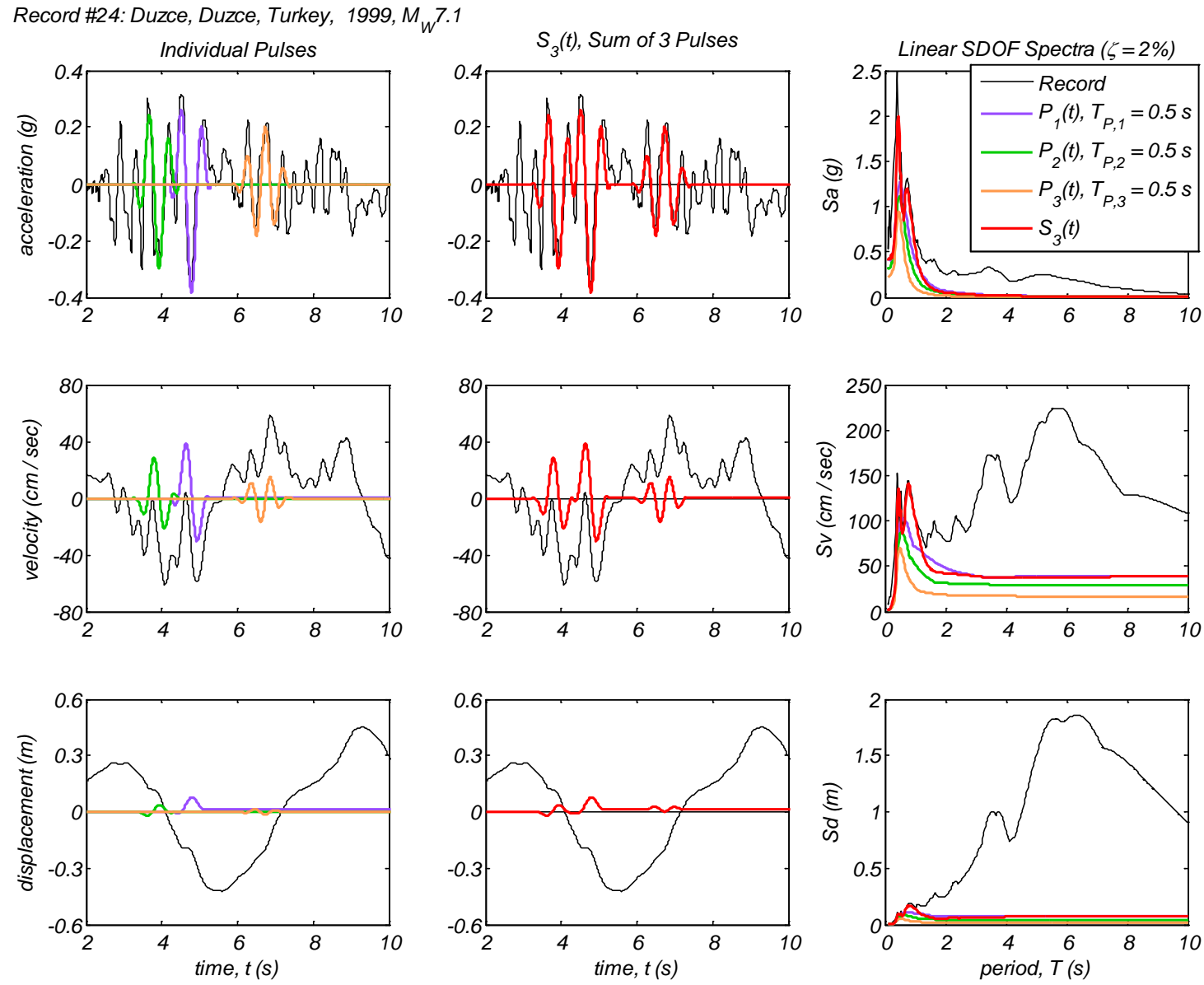
Appendix B5 – Time history and linear spectral response of three extracted pulses using the CPE<sub>A-EN</sub> method for 40 Motions



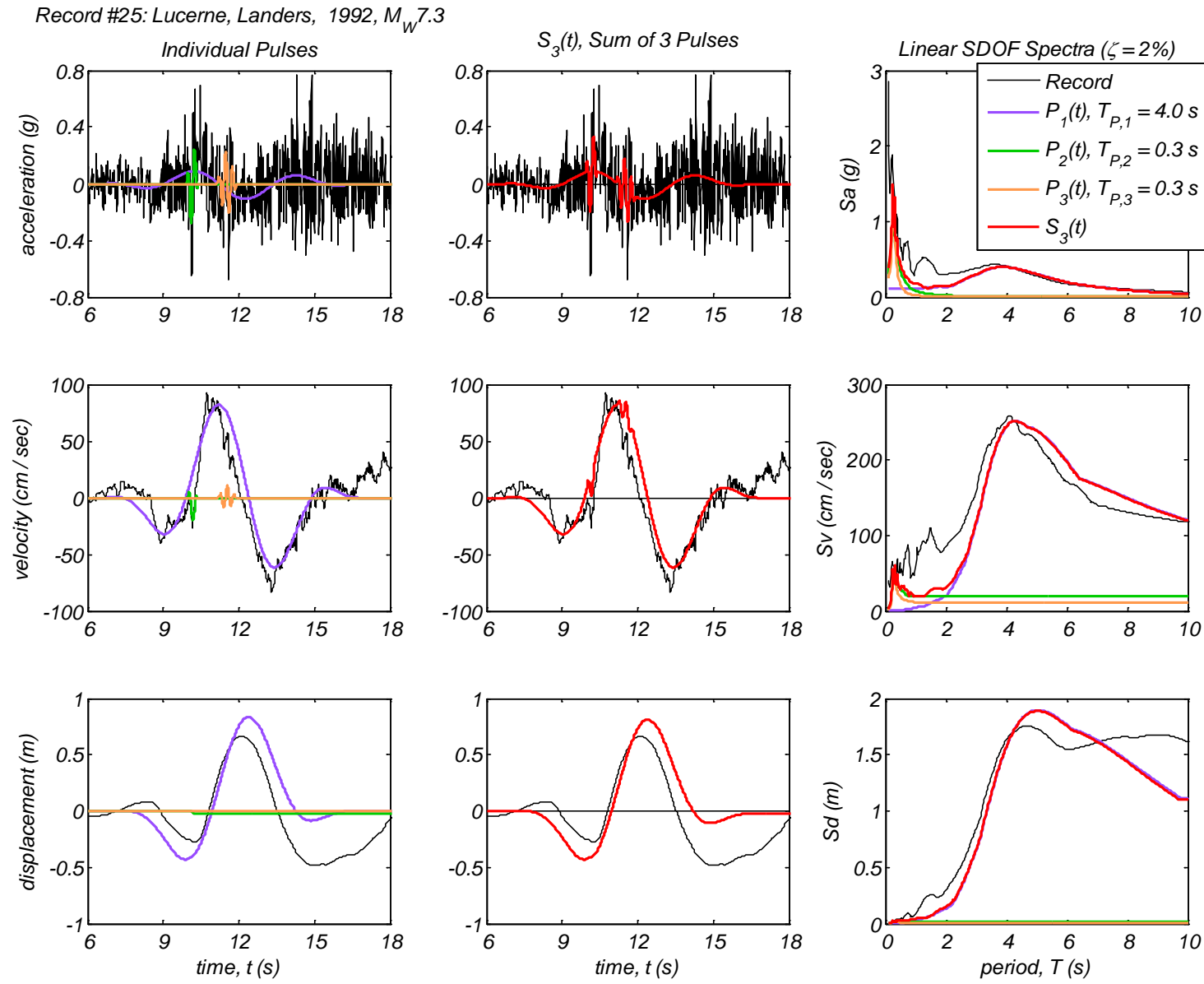
Appendix B5 – Time history and linear spectral response of three extracted pulses using the CPE<sub>A-EN</sub> method for 40 Motions



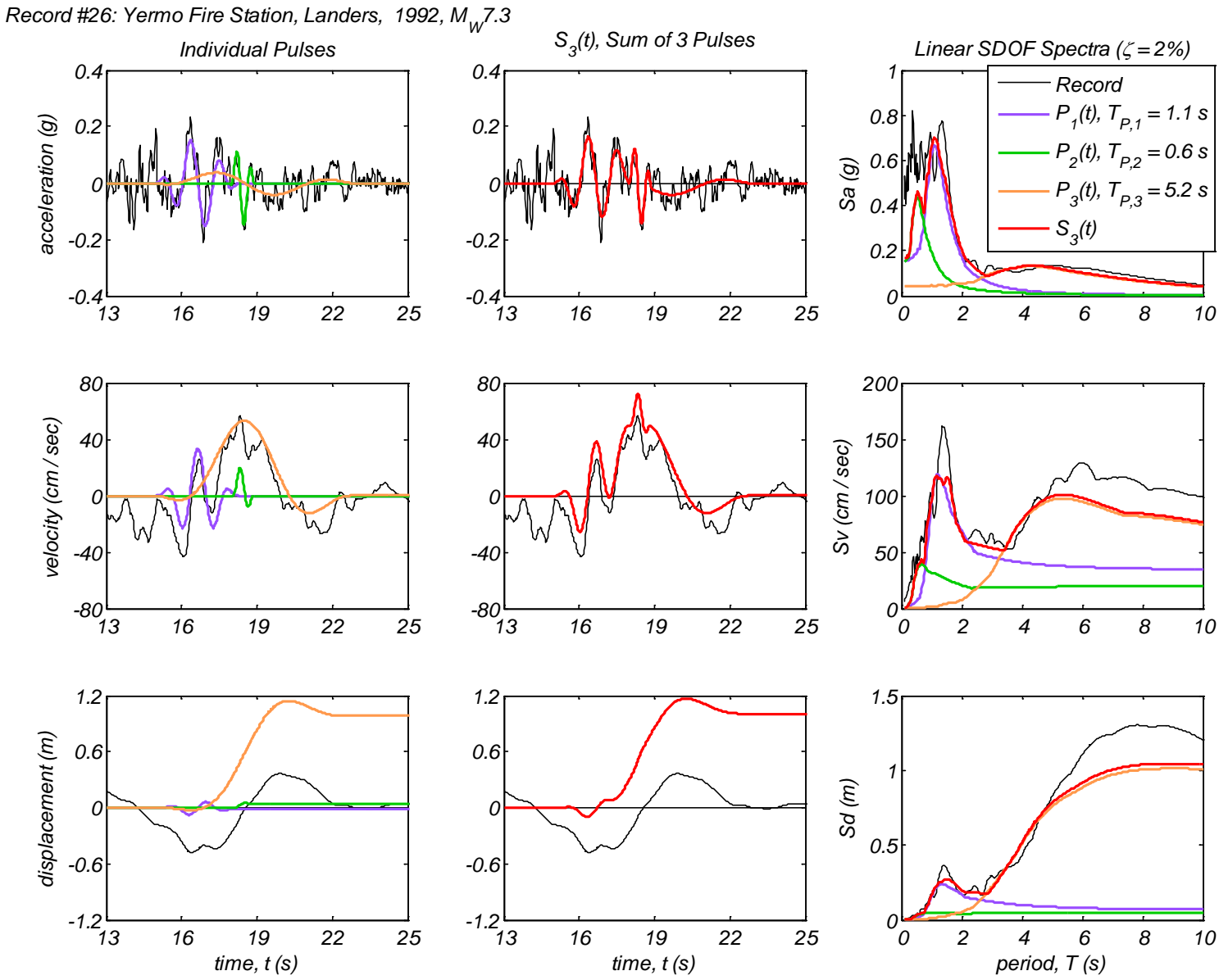
Appendix B5 – Time history and linear spectral response of three extracted pulses using the CPE<sub>A-EN</sub> method for 40 Motions



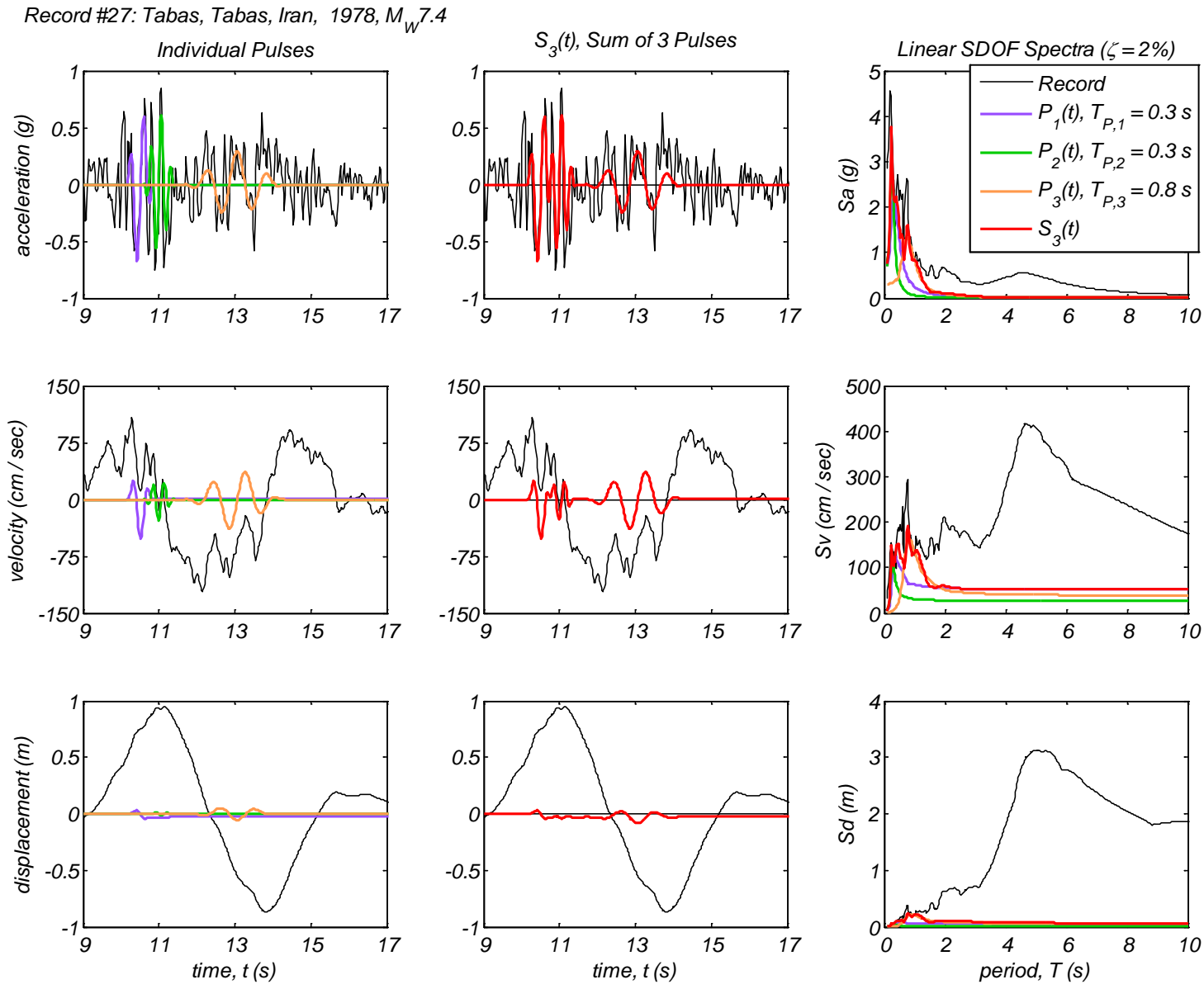
Appendix B5 – Time history and linear spectral response of three extracted pulses using the CPE<sub>A-EN</sub> method for 40 Motions



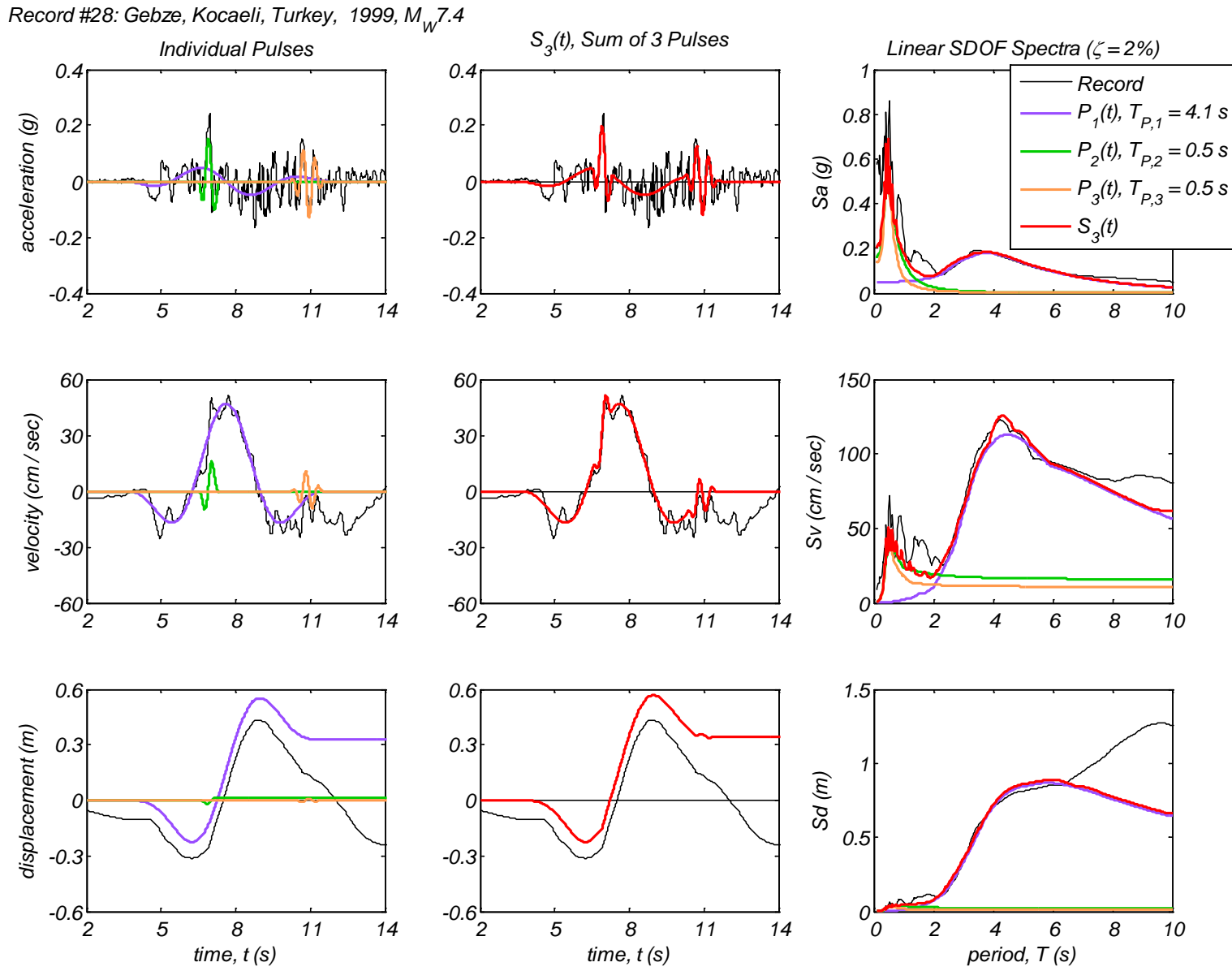
Appendix B5 – Time history and linear spectral response of three extracted pulses using the CPE<sub>A-EN</sub> method for 40 Motions



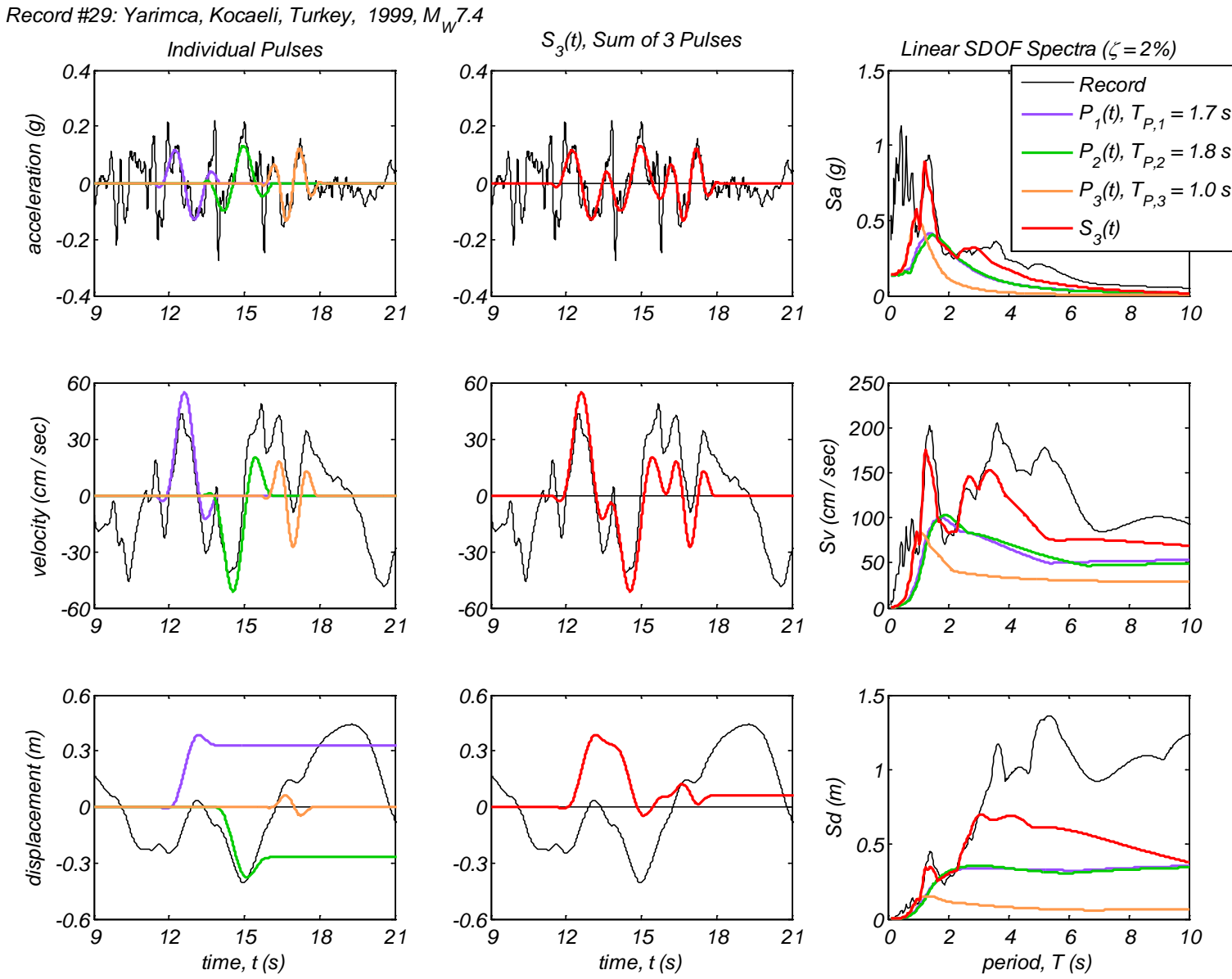
Appendix B5 – Time history and linear spectral response of three extracted pulses using the CPE<sub>A-EN</sub> method for 40 Motions



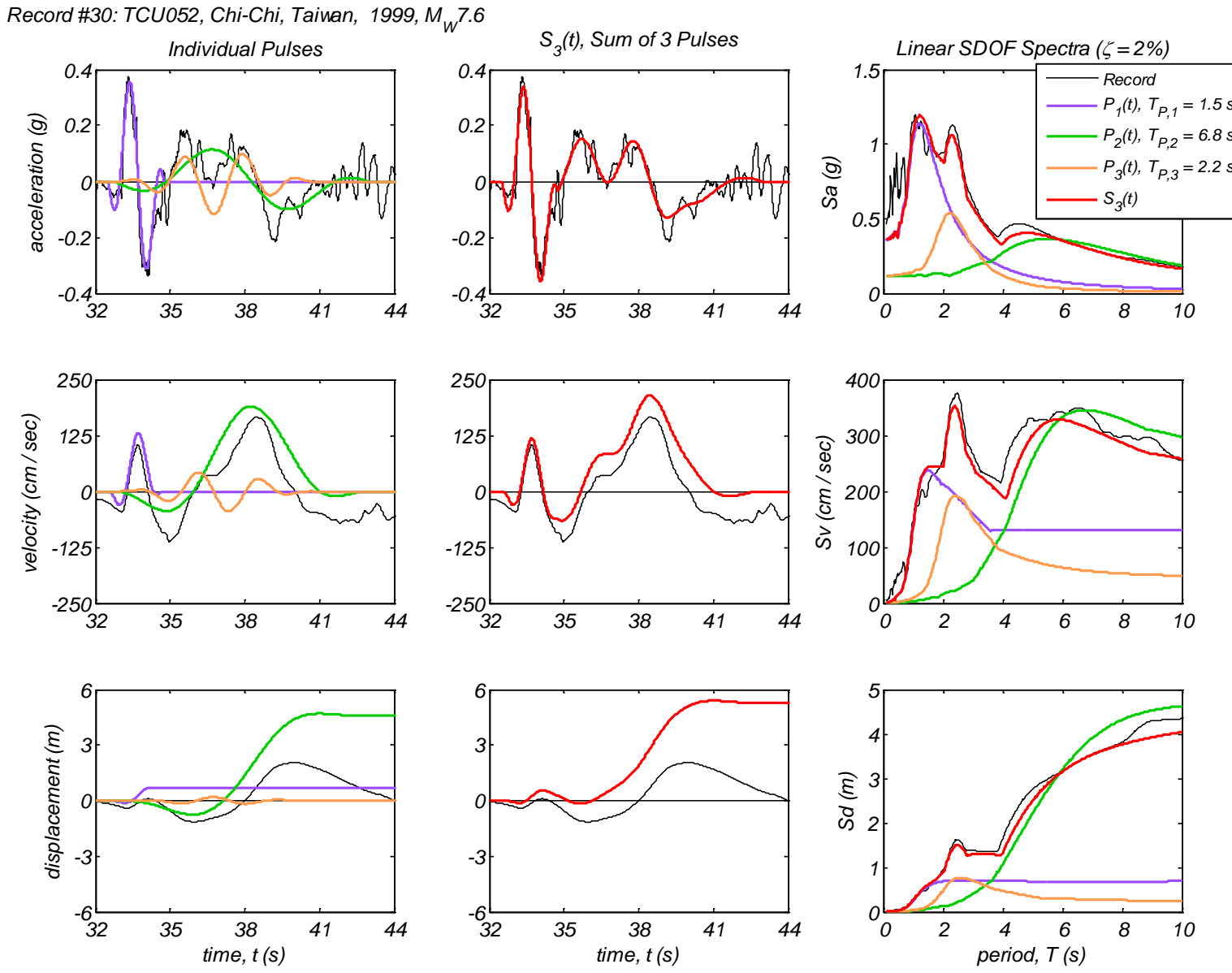
Appendix B5 – Time history and linear spectral response of three extracted pulses using the CPE<sub>A-EN</sub> method for 40 Motions



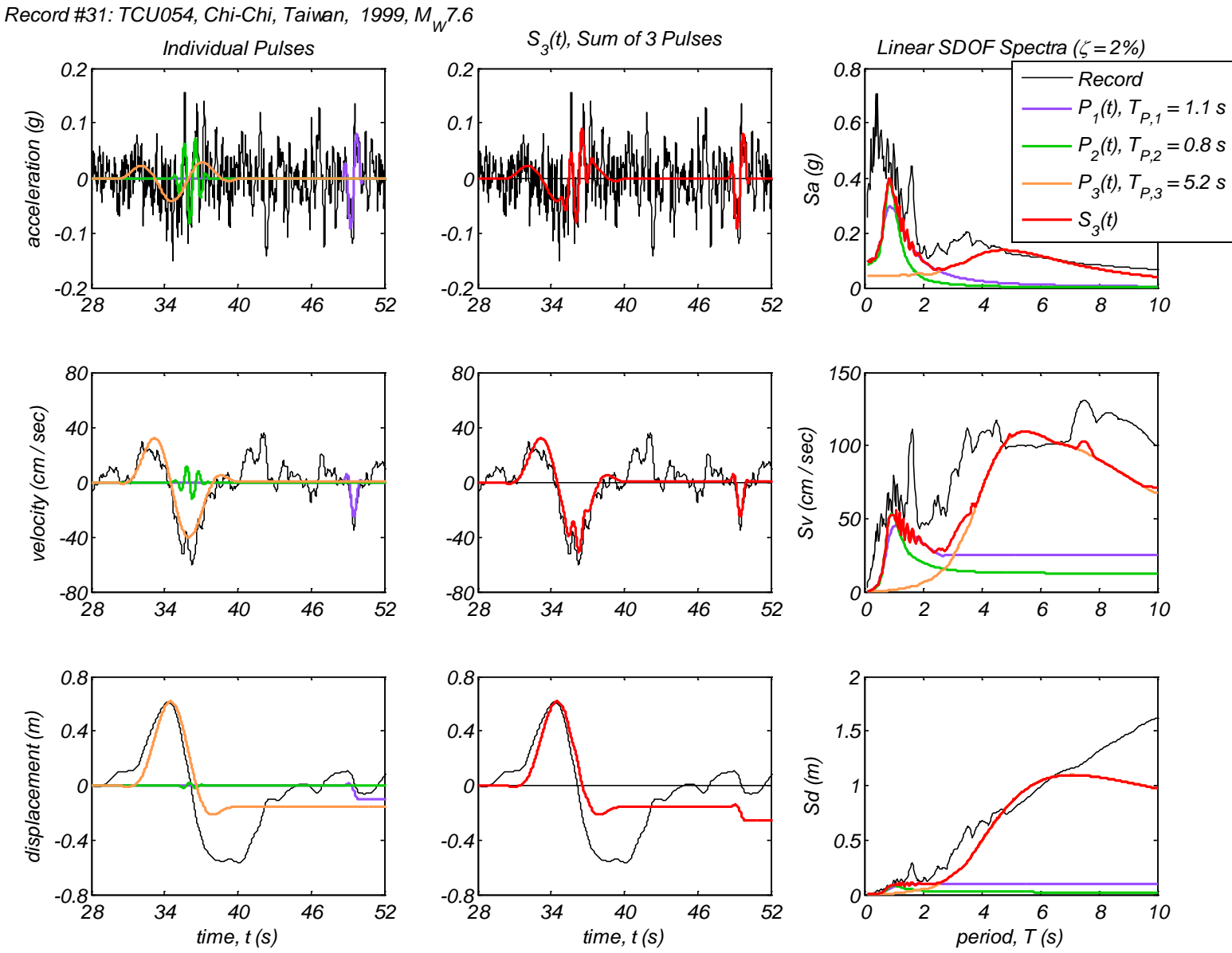
Appendix B5 – Time history and linear spectral response of three extracted pulses using the CPE<sub>A-EN</sub> method for 40 Motions



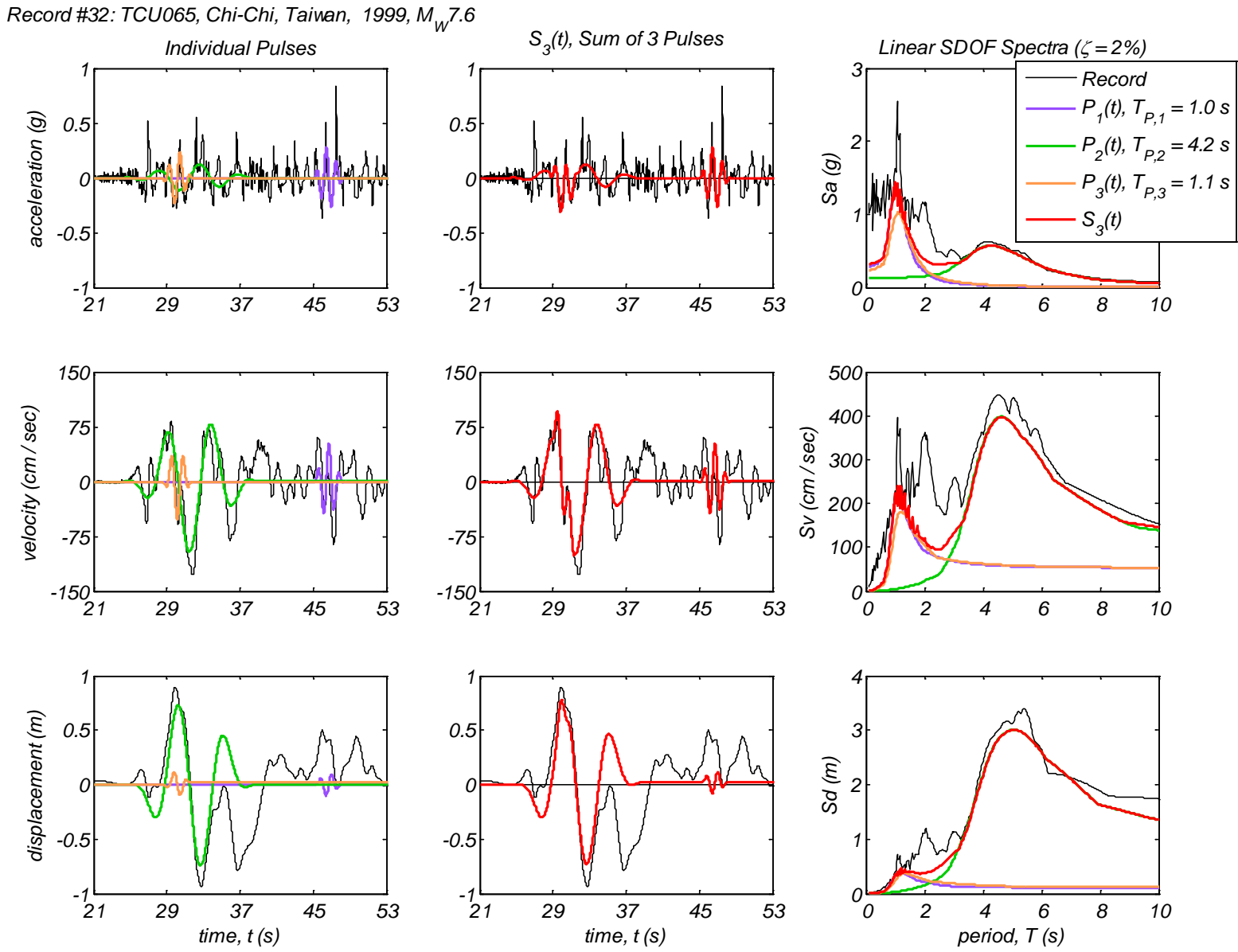
Appendix B5 – Time history and linear spectral response of three extracted pulses using the CPE<sub>A-EN</sub> method for 40 Motions



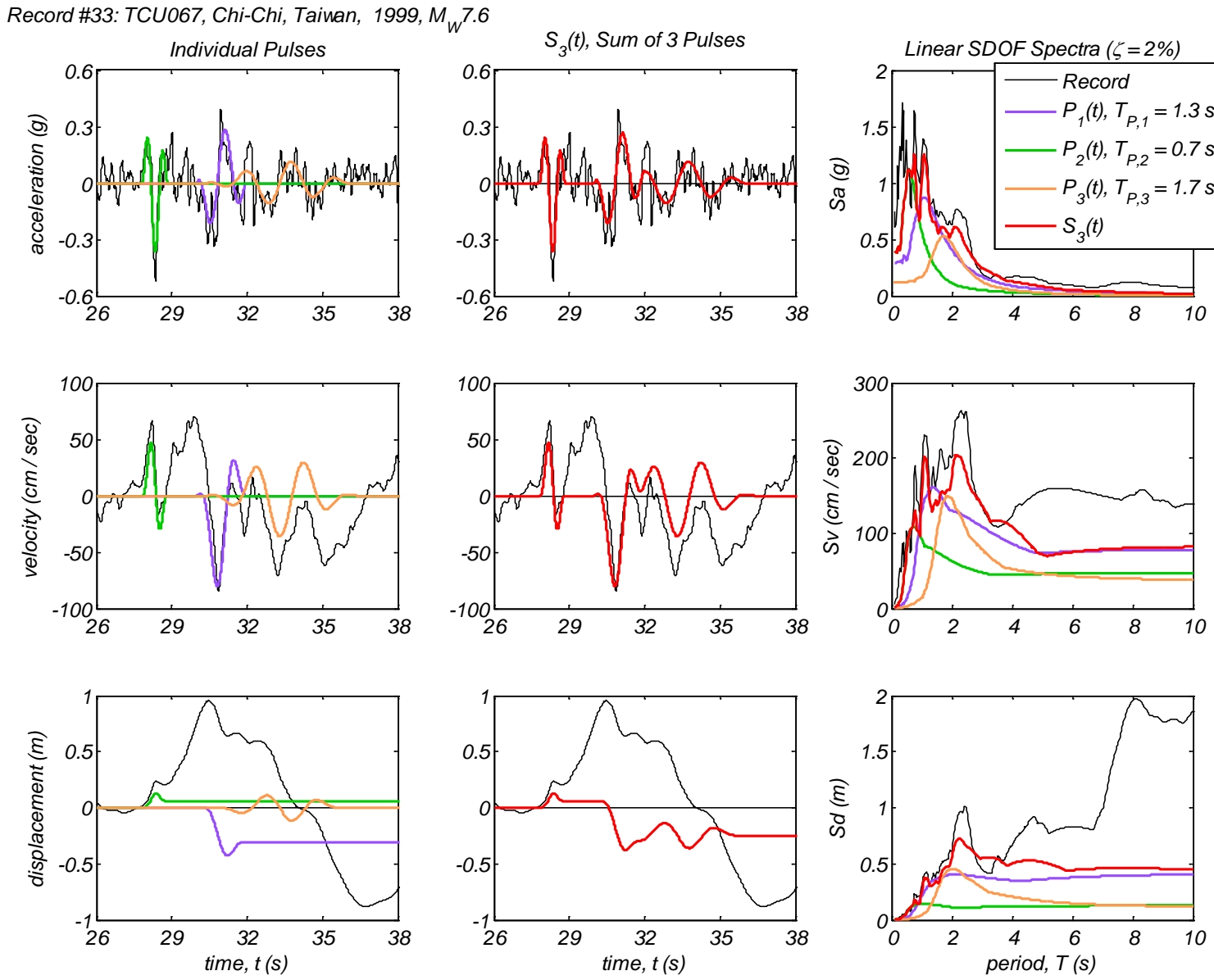
Appendix B5 – Time history and linear spectral response of three extracted pulses using the CPE<sub>A-EN</sub> method for 40 Motions



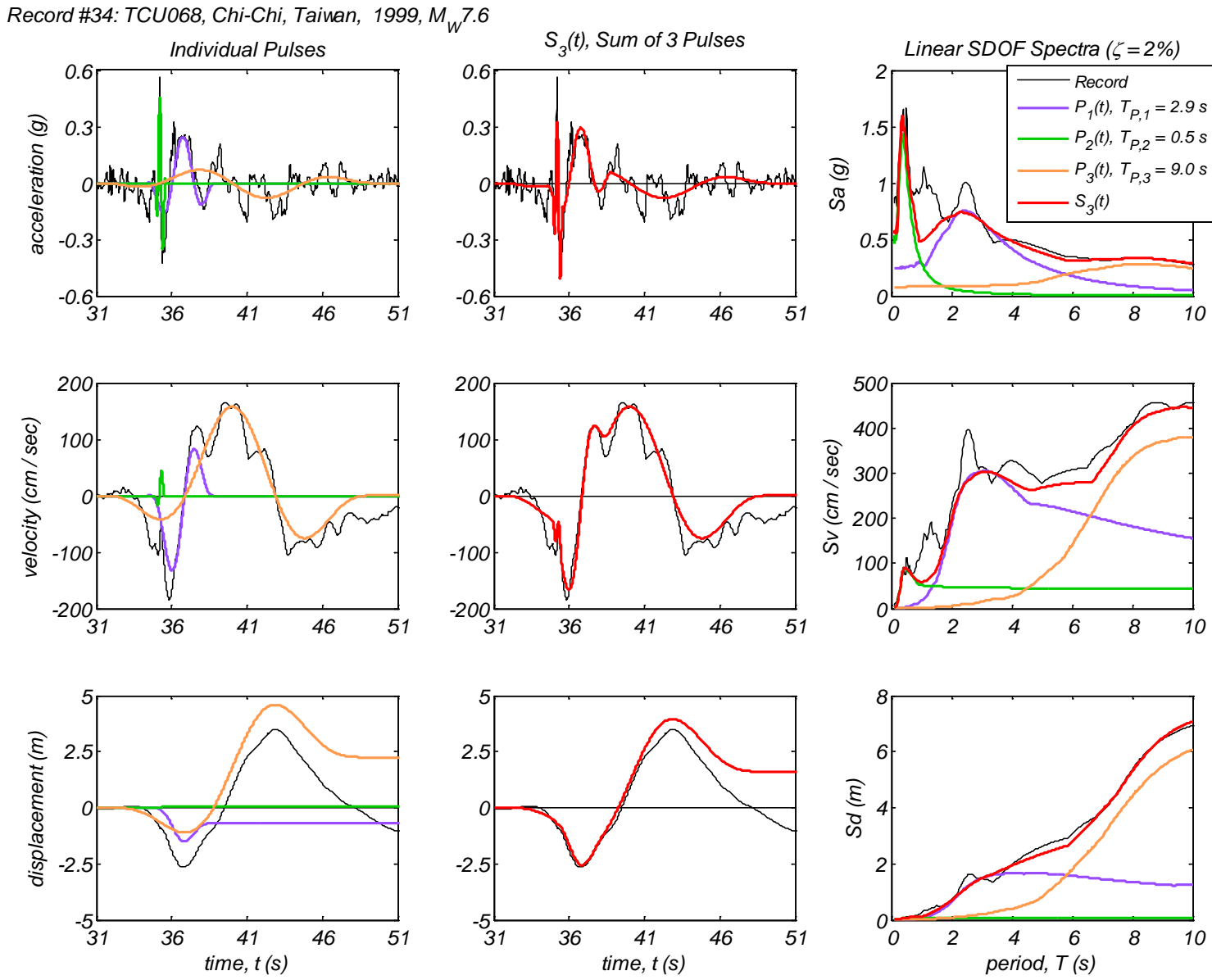
Appendix B5 – Time history and linear spectral response of three extracted pulses using the CPE<sub>A-EN</sub> method for 40 Motions



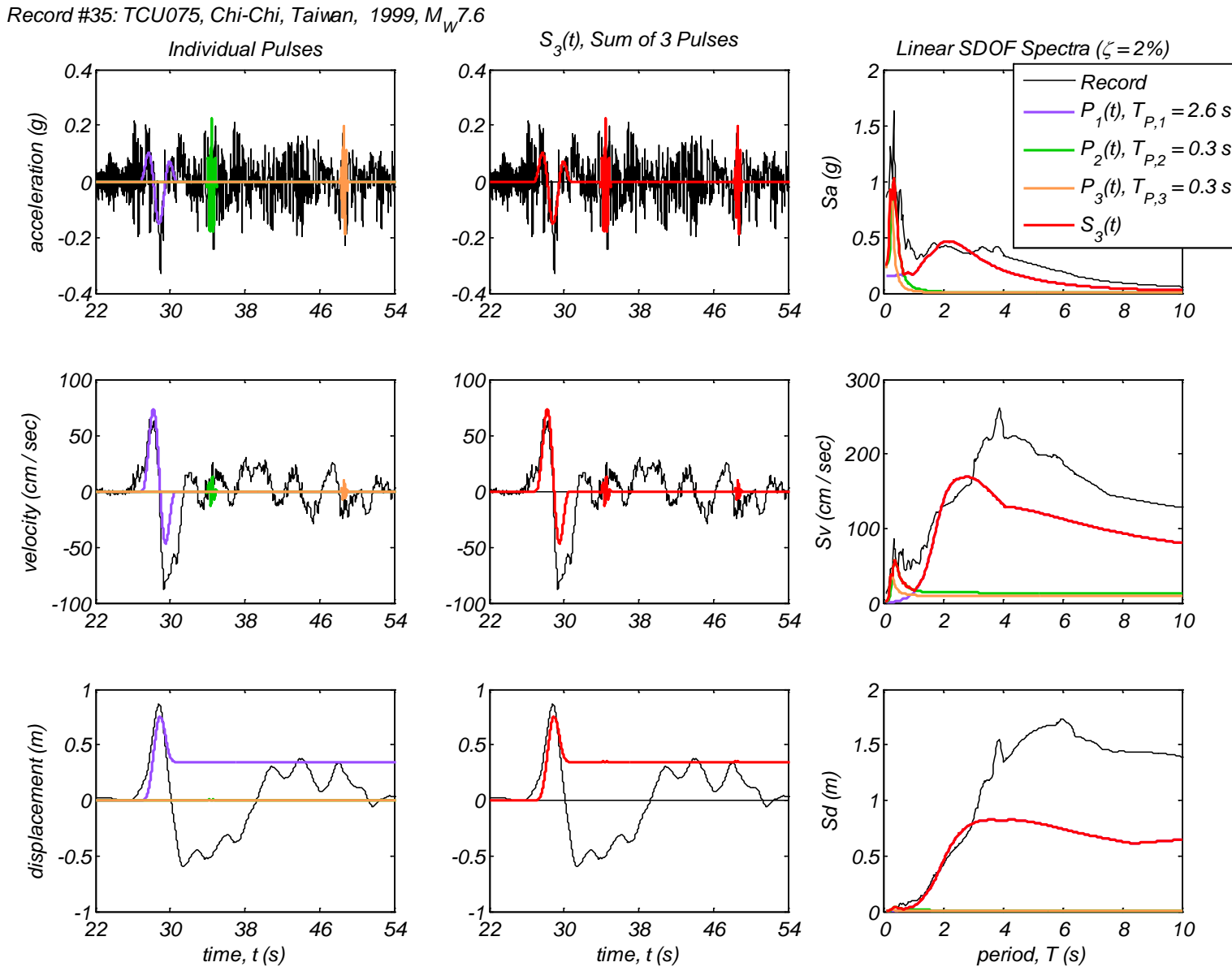
Appendix B5 – Time history and linear spectral response of three extracted pulses using the CPE<sub>A-EN</sub> method for 40 Motions



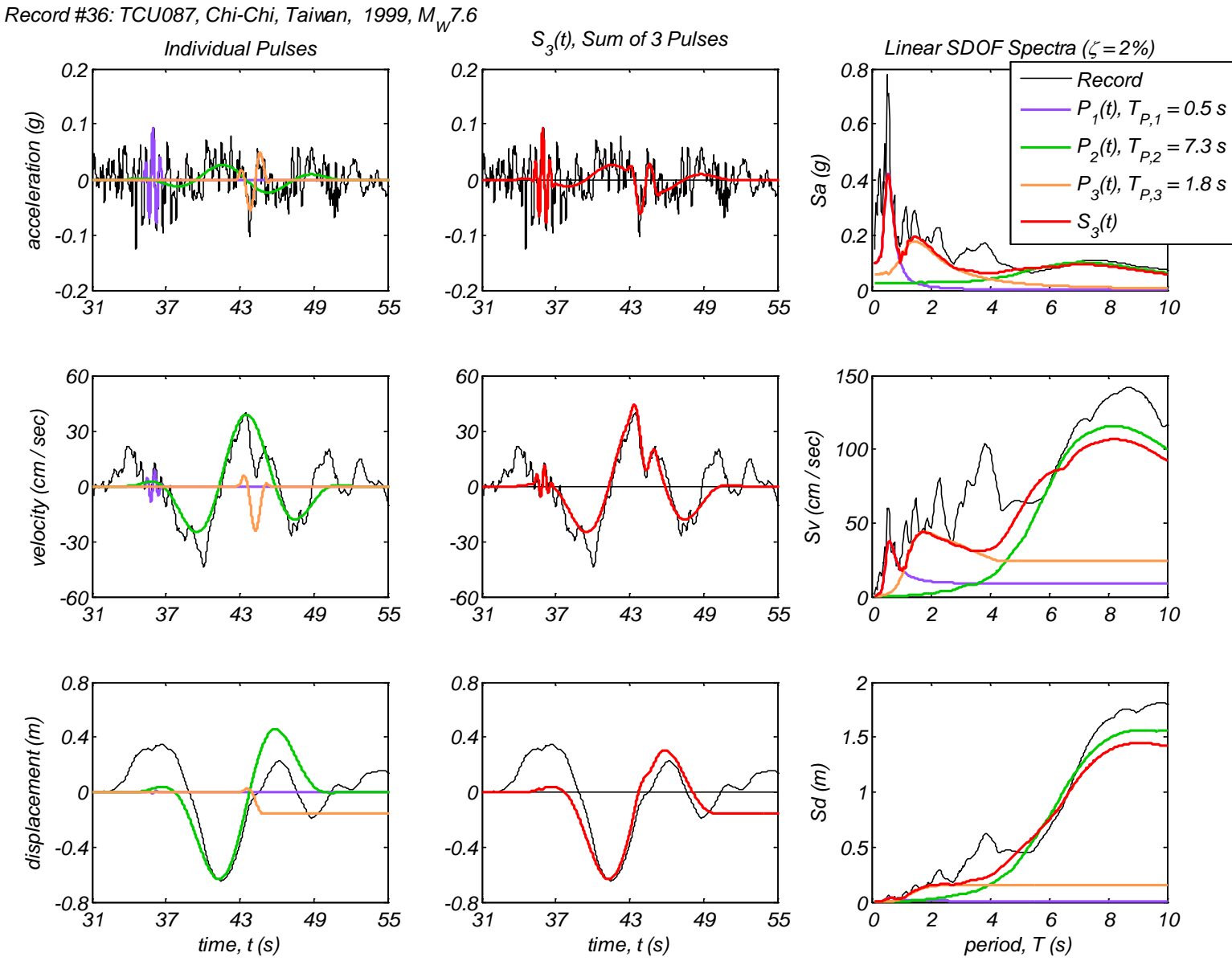
Appendix B5 – Time history and linear spectral response of three extracted pulses using the CPE<sub>A-EN</sub> method for 40 Motions



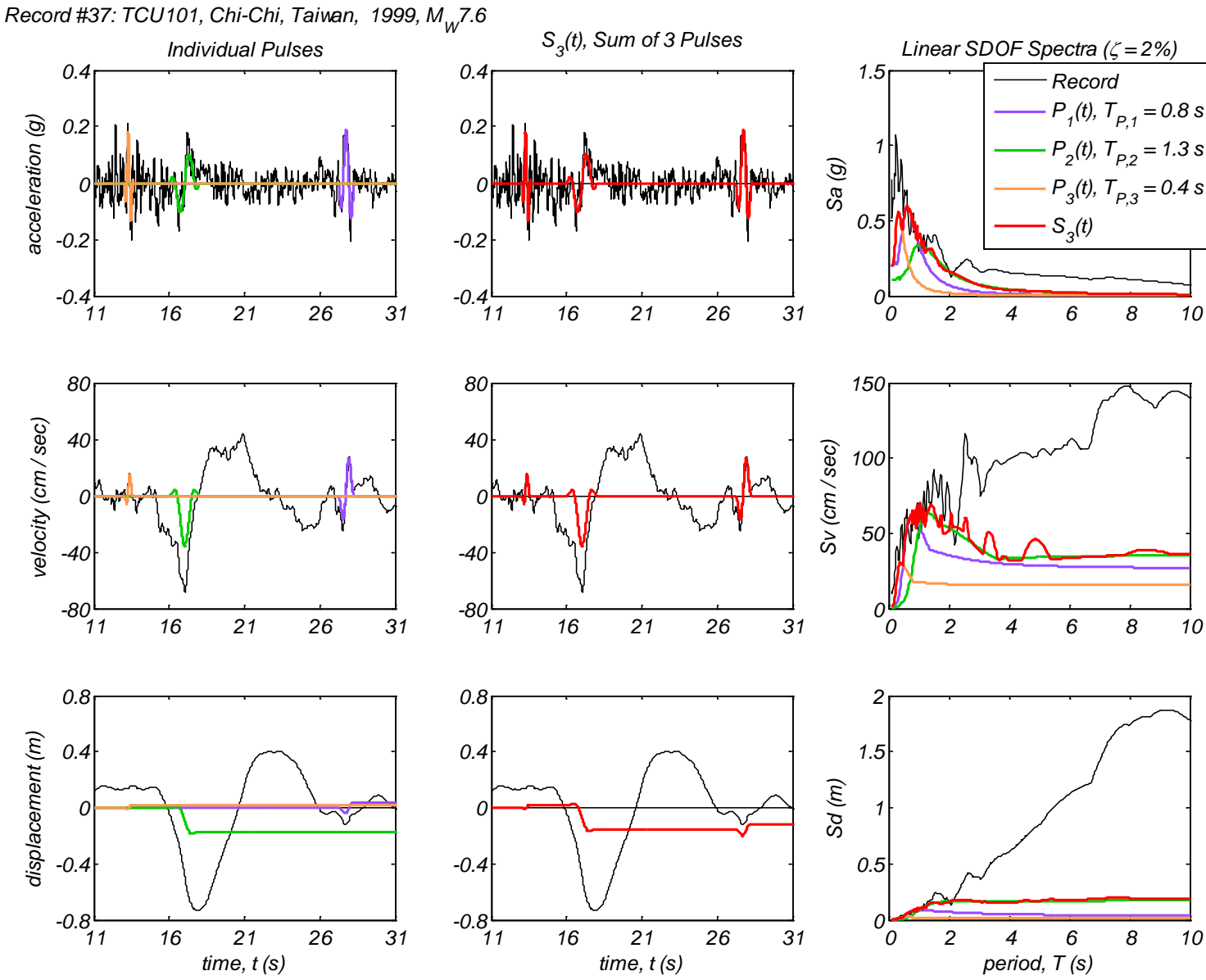
Appendix B5 – Time history and linear spectral response of three extracted pulses using the CPE<sub>A-EN</sub> method for 40 Motions



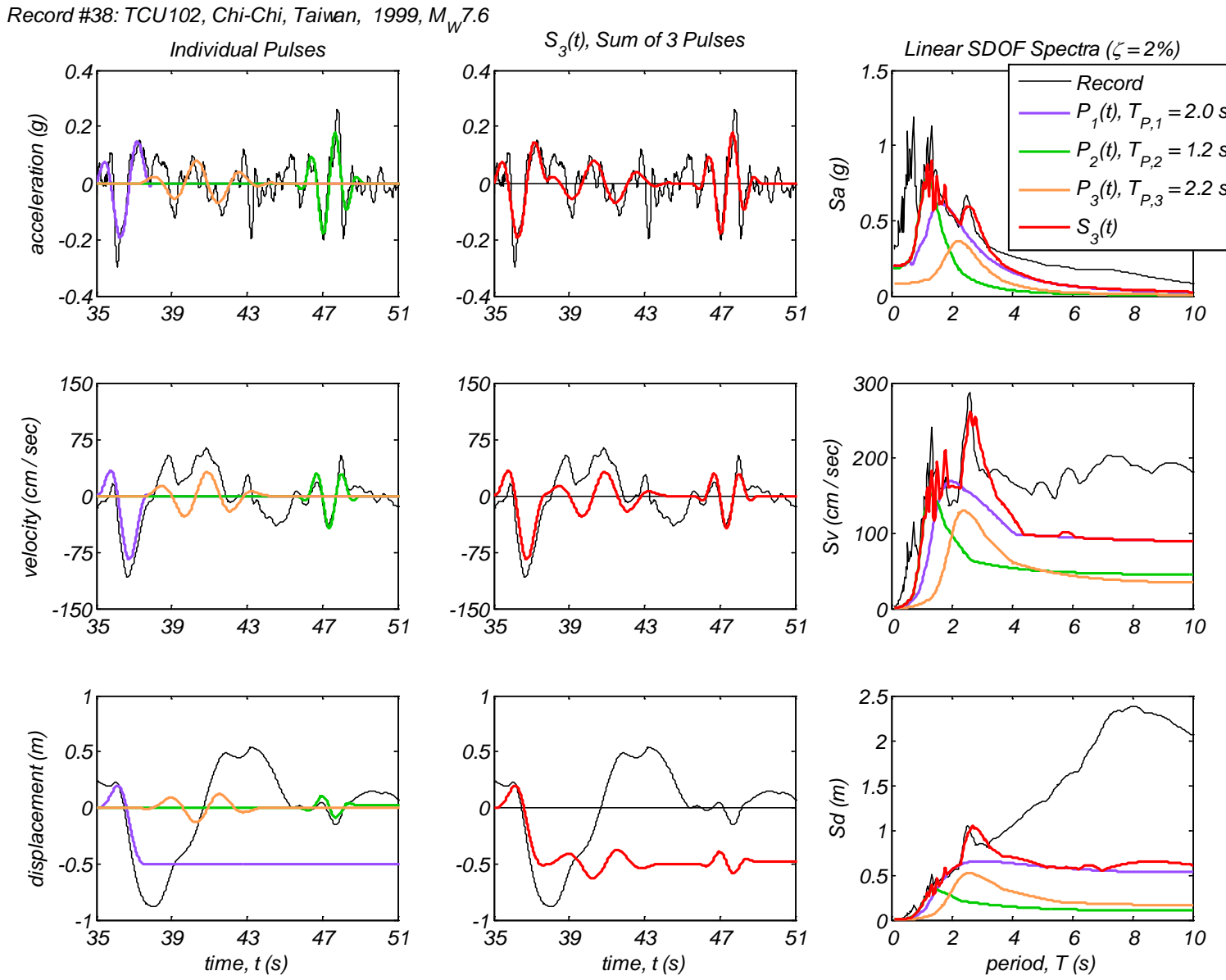
Appendix B5 – Time history and linear spectral response of three extracted pulses using the CPE<sub>A-EN</sub> method for 40 Motions



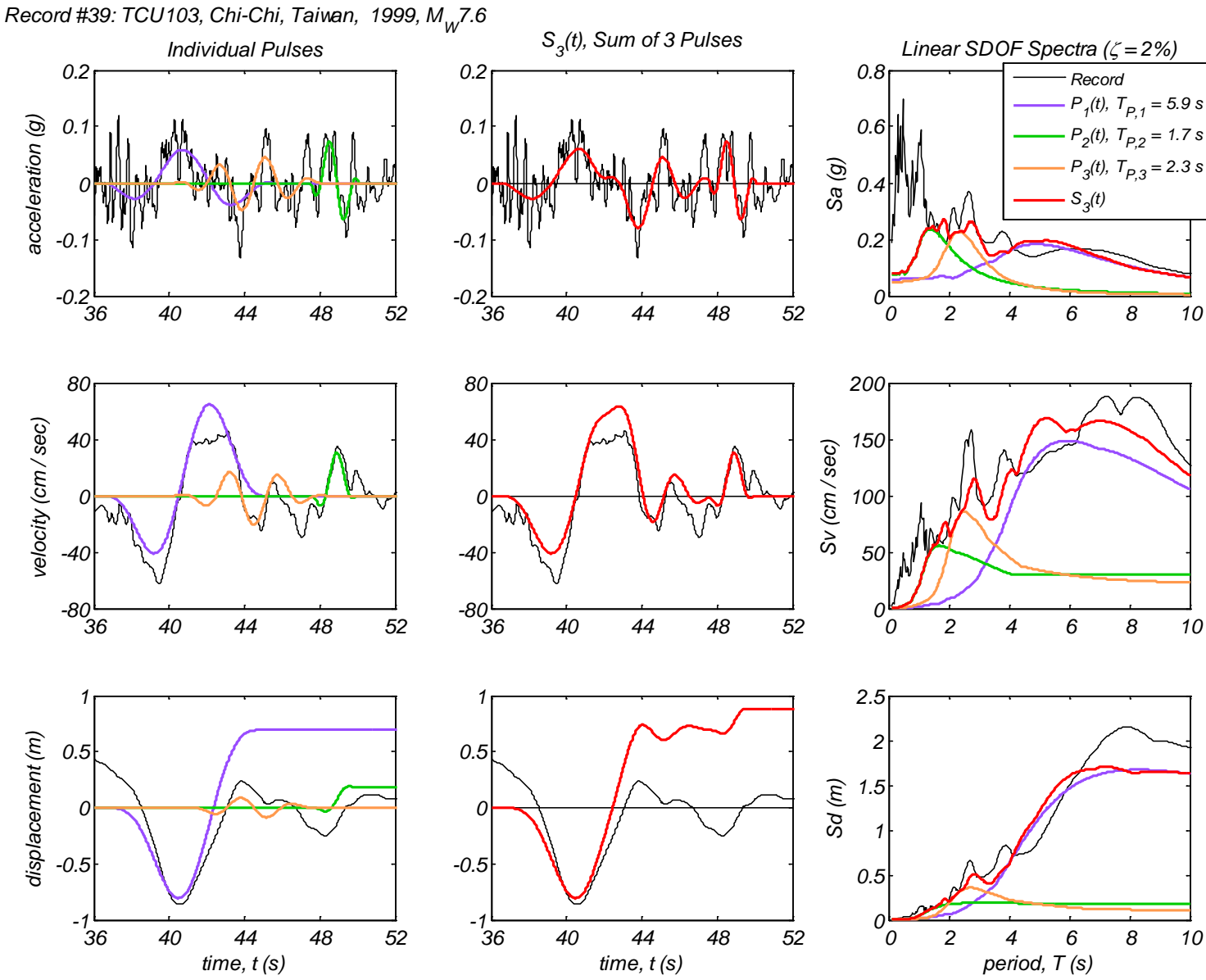
Appendix B5 – Time history and linear spectral response of three extracted pulses using the CPE<sub>A-EN</sub> method for 40 Motions



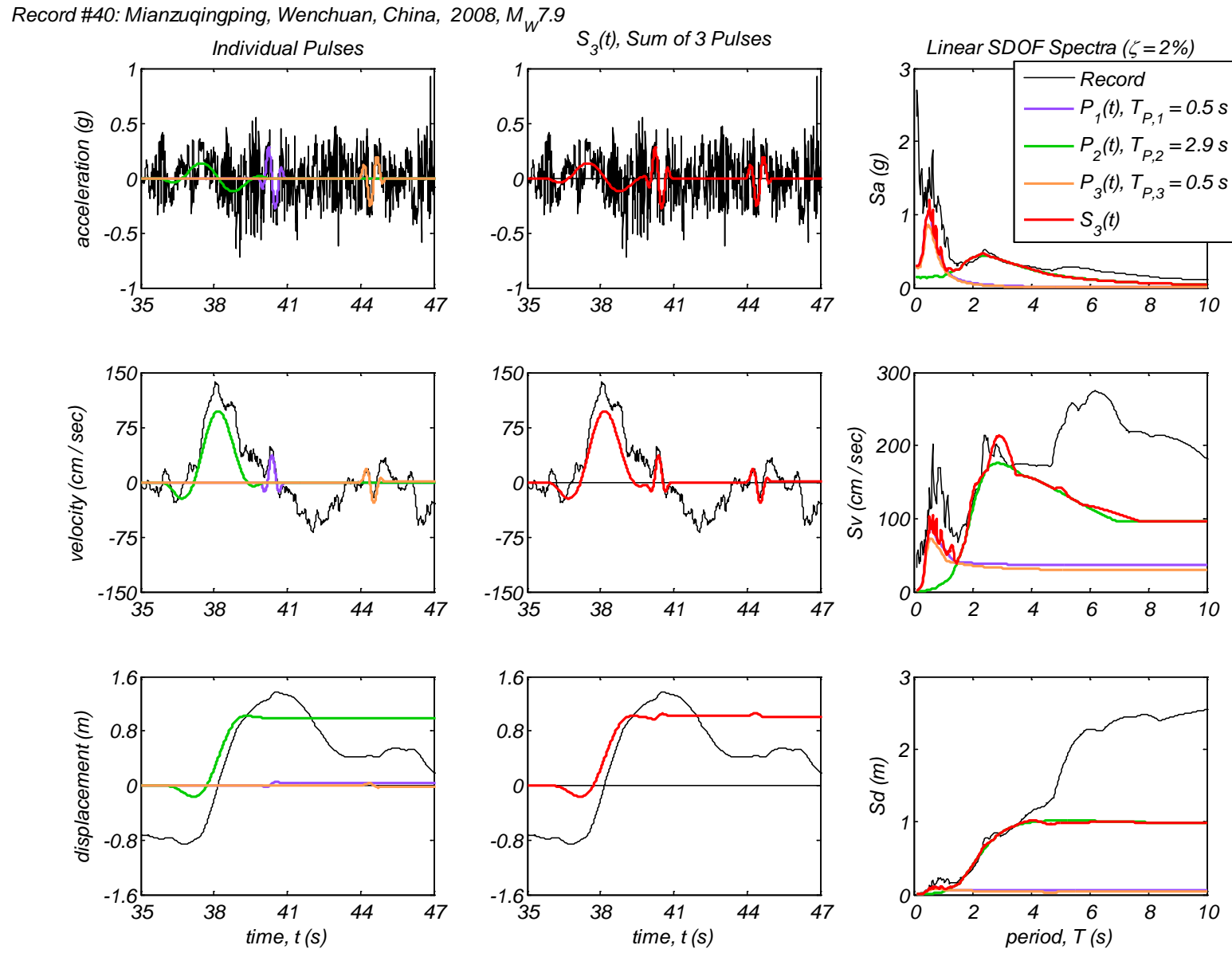
Appendix B5 – Time history and linear spectral response of three extracted pulses using the CPE<sub>A-EN</sub> method for 40 Motions



Appendix B5 – Time history and linear spectral response of three extracted pulses using the CPE<sub>A-EN</sub> method for 40 Motions

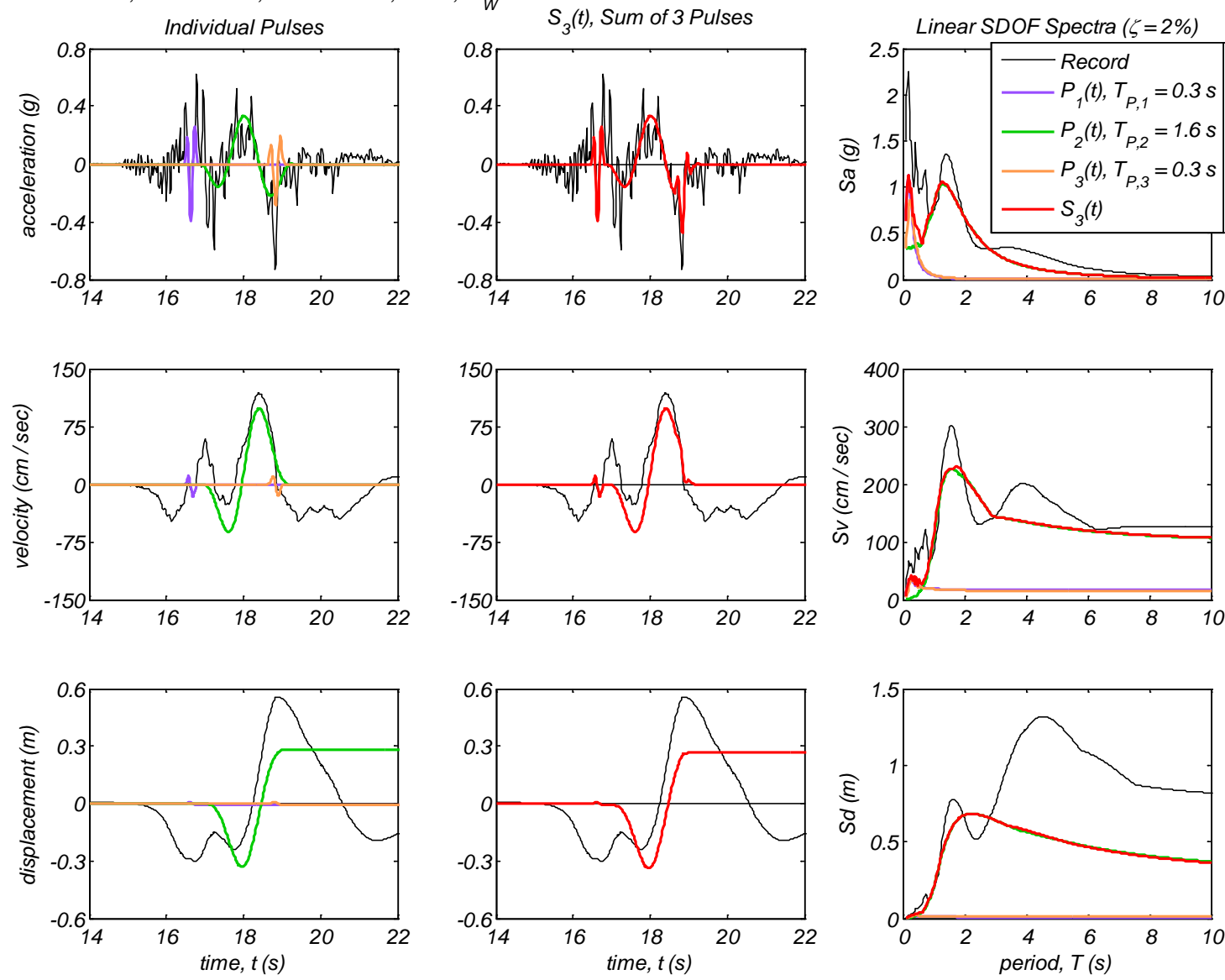


Appendix B5 – Time history and linear spectral response of three extracted pulses using the CPE<sub>A-EN</sub> method for 40 Motions



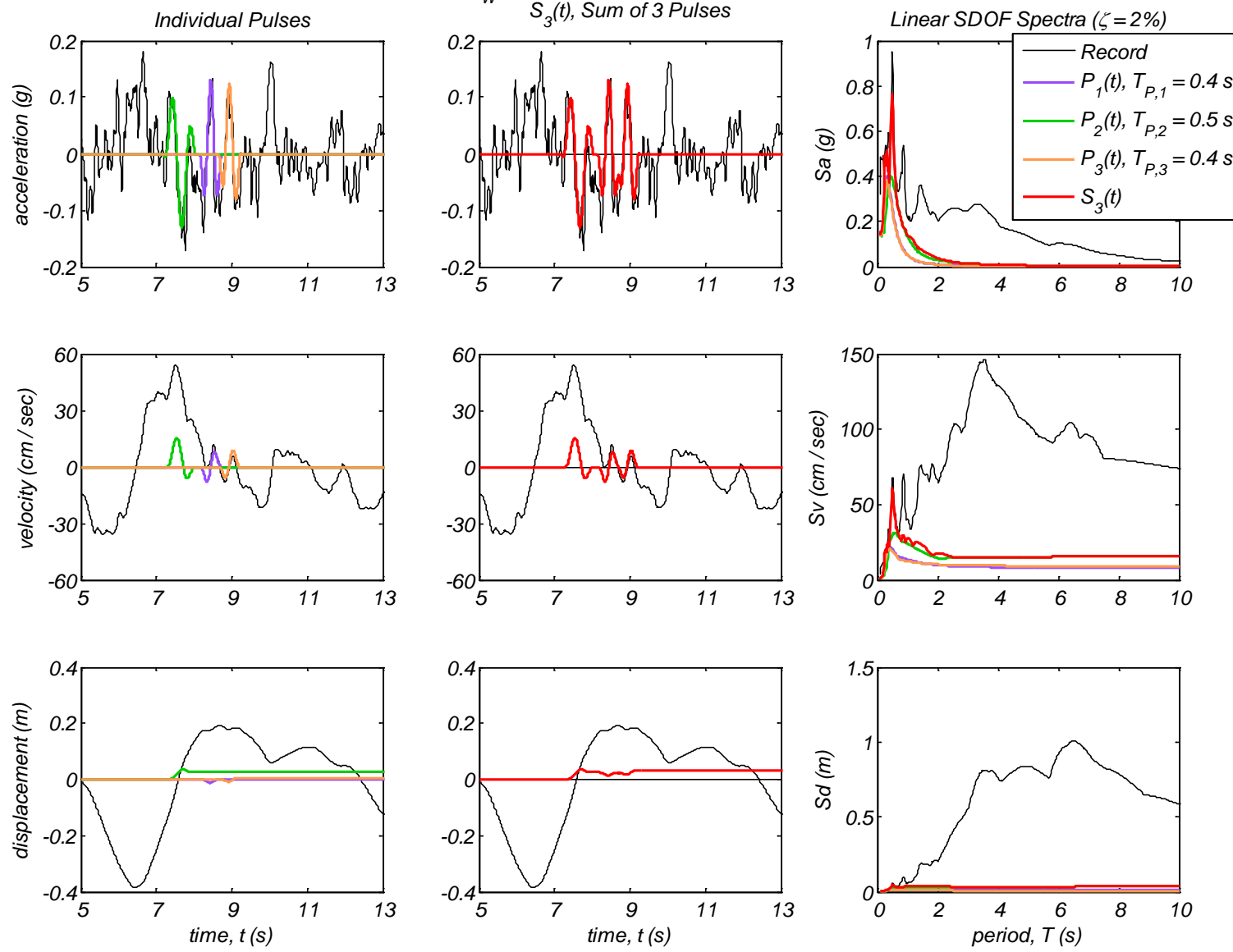
## Appendix B6: Time history and linear spectral response of three extracted pulses using the CPE<sub>A-AM</sub> method for 40 motions

Record #1: PRPC, Christchurch, New Zealand, 2011,  $M_W 6.3$

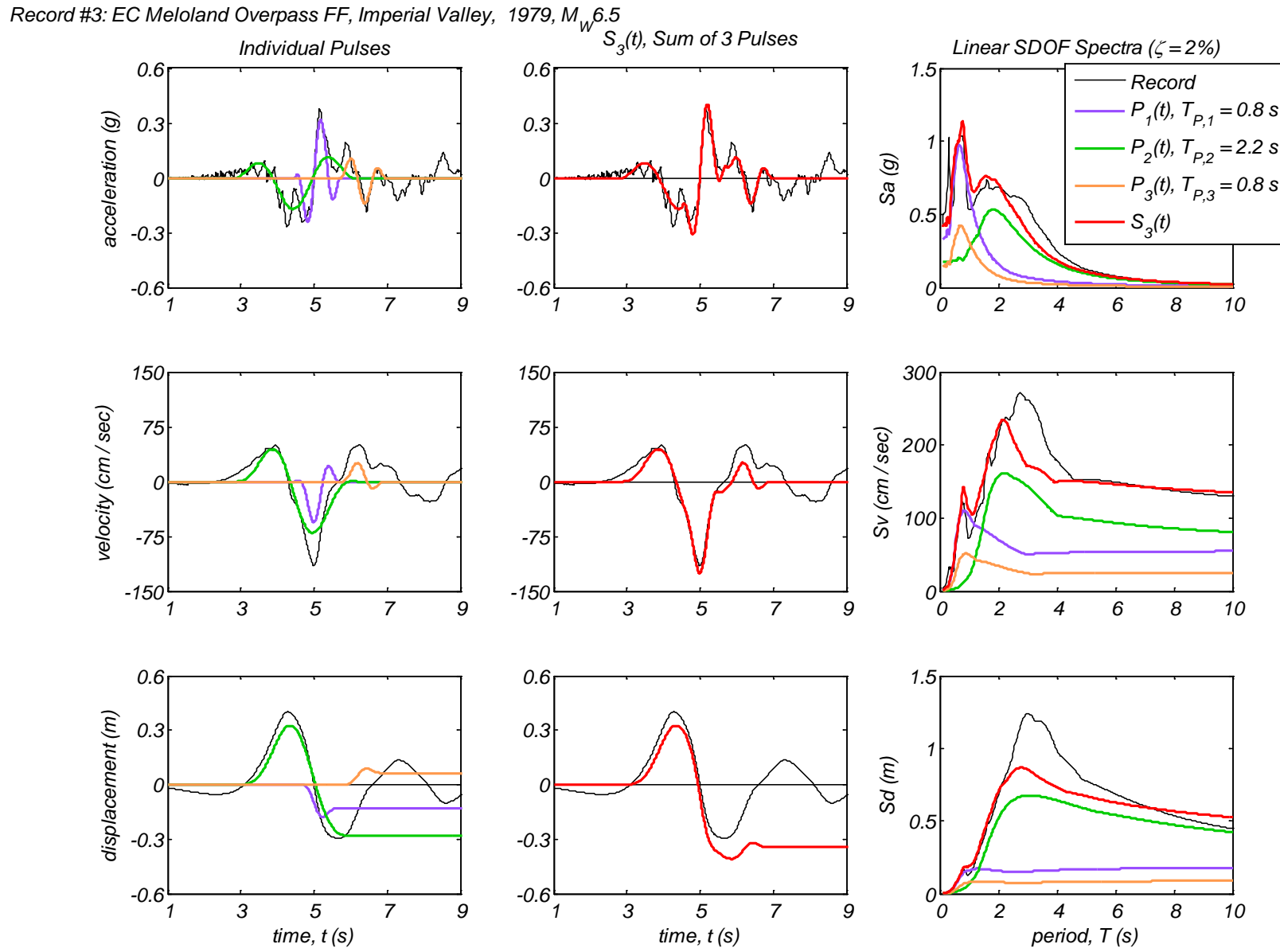


Appendix B6 – Time history and linear spectral response of three extracted pulses using the CPE<sub>A-AM</sub> method for 40 Motions

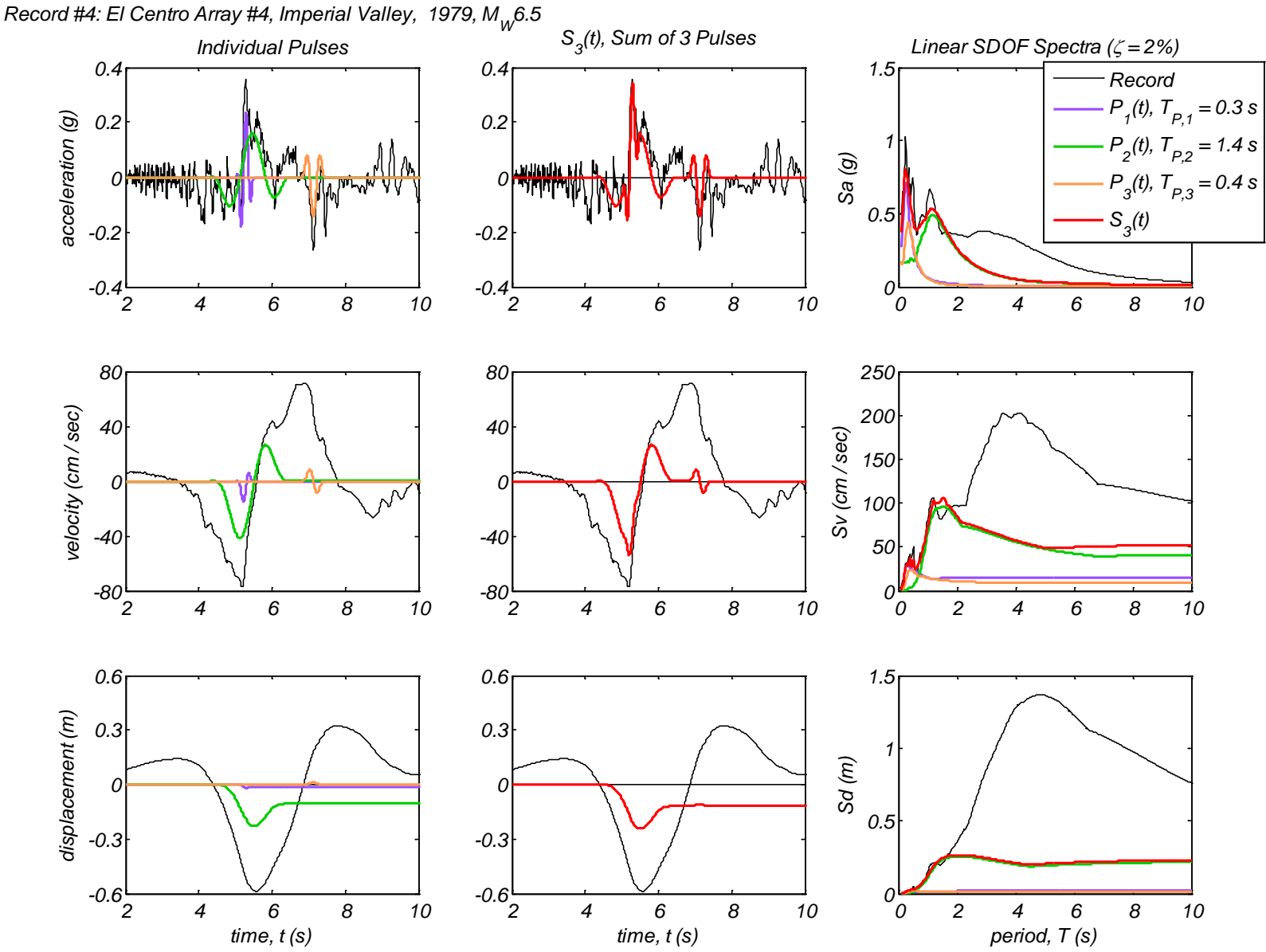
Record #2: EC County Center FF, Imperial Valley, 1979,  $M_W 6.5$



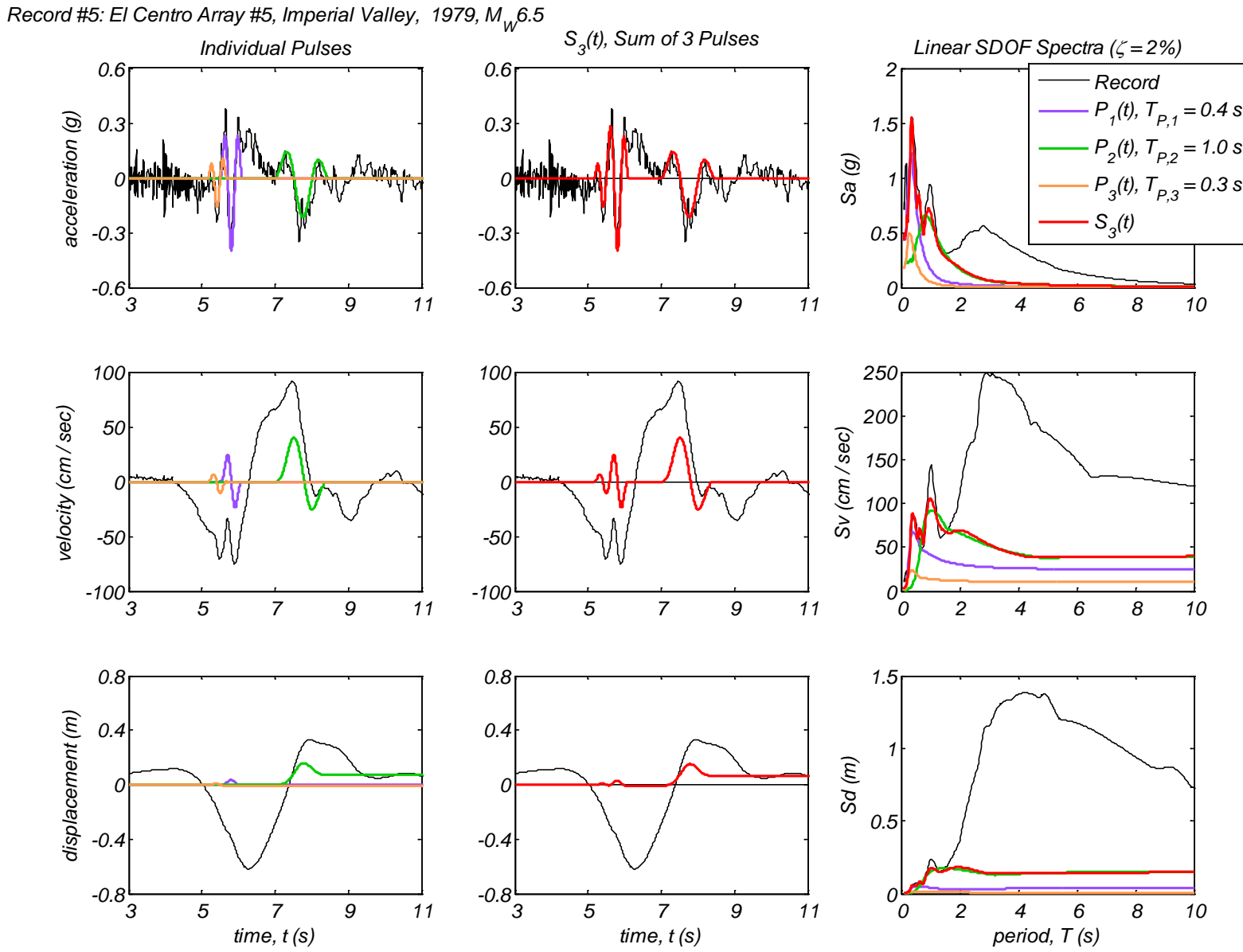
Appendix B6 – Time history and linear spectral response of three extracted pulses using the CPE<sub>A-AM</sub> method for 40 Motions



Appendix B6 – Time history and linear spectral response of three extracted pulses using the CPE<sub>A-AM</sub> method for 40 Motions

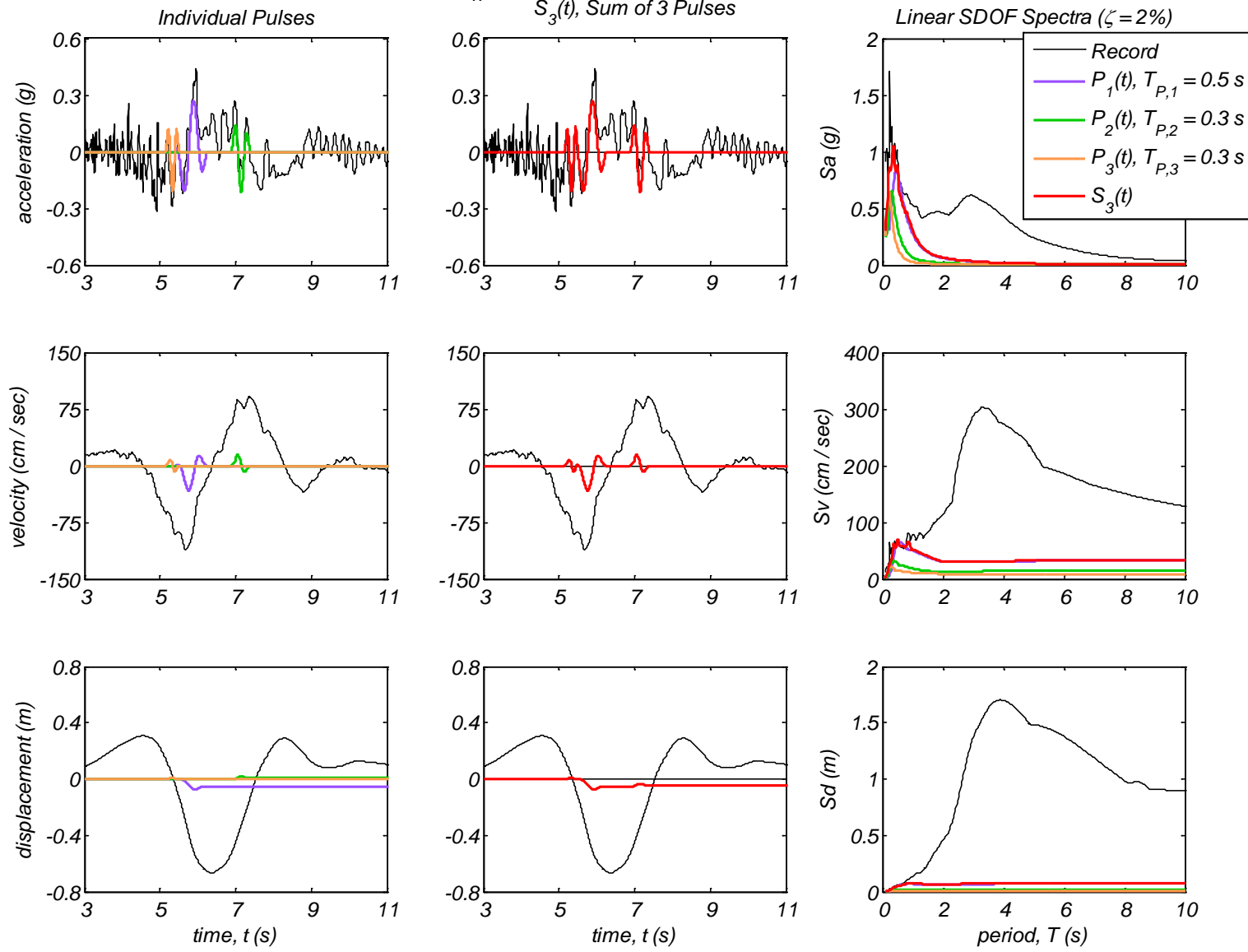


Appendix B6 – Time history and linear spectral response of three extracted pulses using the CPE<sub>A-AM</sub> method for 40 Motions

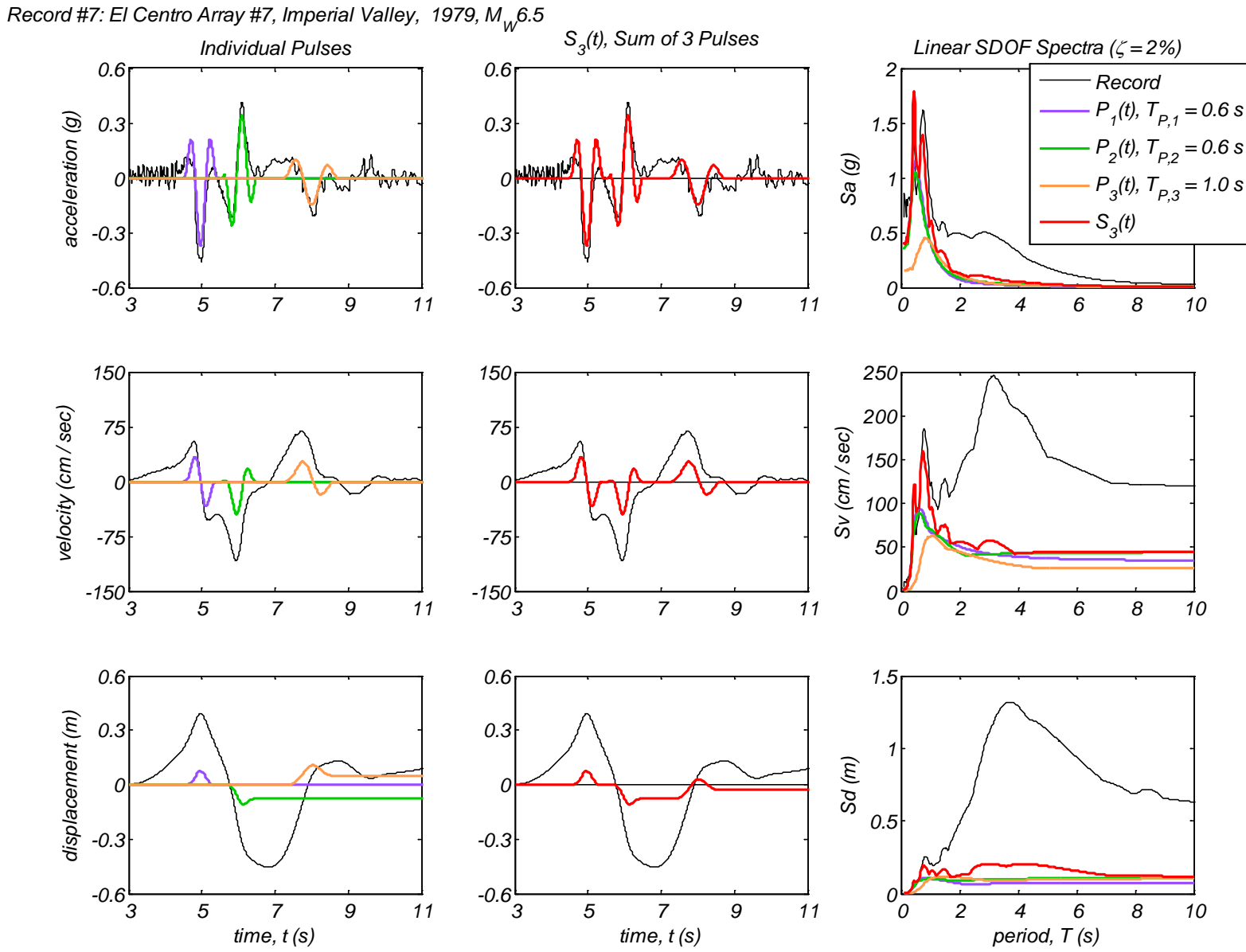


Appendix B6 – Time history and linear spectral response of three extracted pulses using the CPE<sub>A-AM</sub> method for 40 Motions

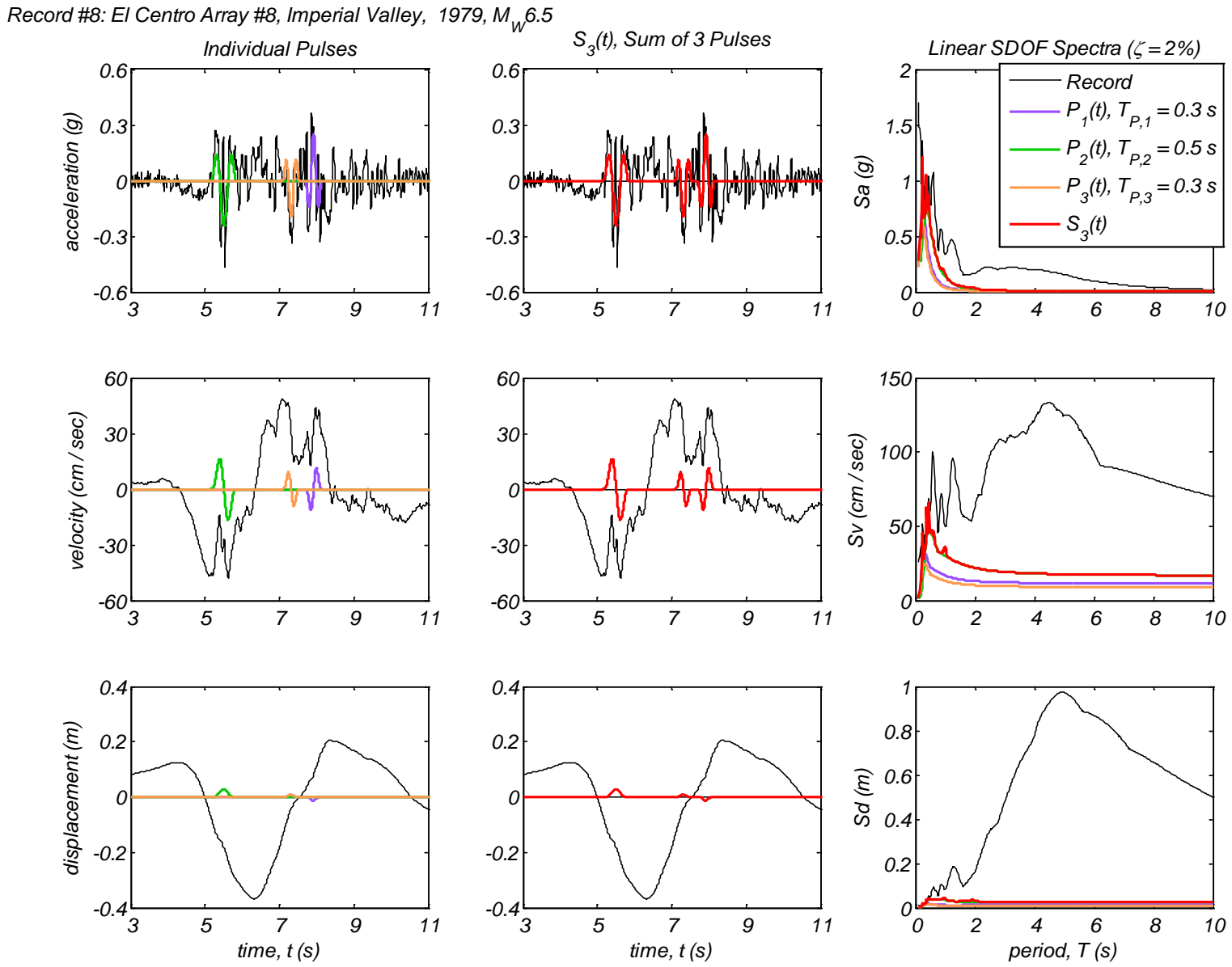
Record #6: El Centro Array #6, Imperial Valley, 1979,  $M_W 6.5$



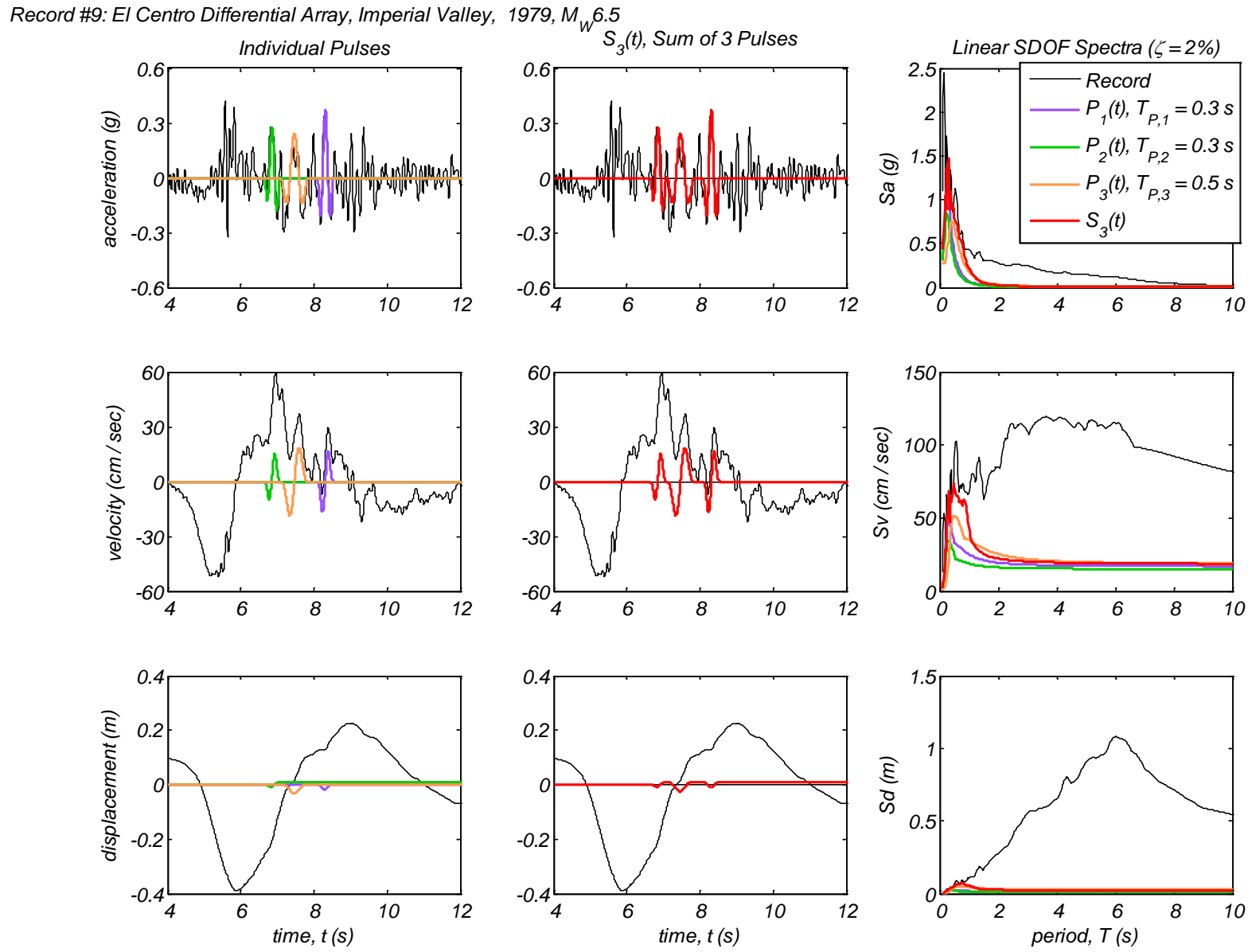
Appendix B6 – Time history and linear spectral response of three extracted pulses using the CPE<sub>A-AM</sub> method for 40 Motions



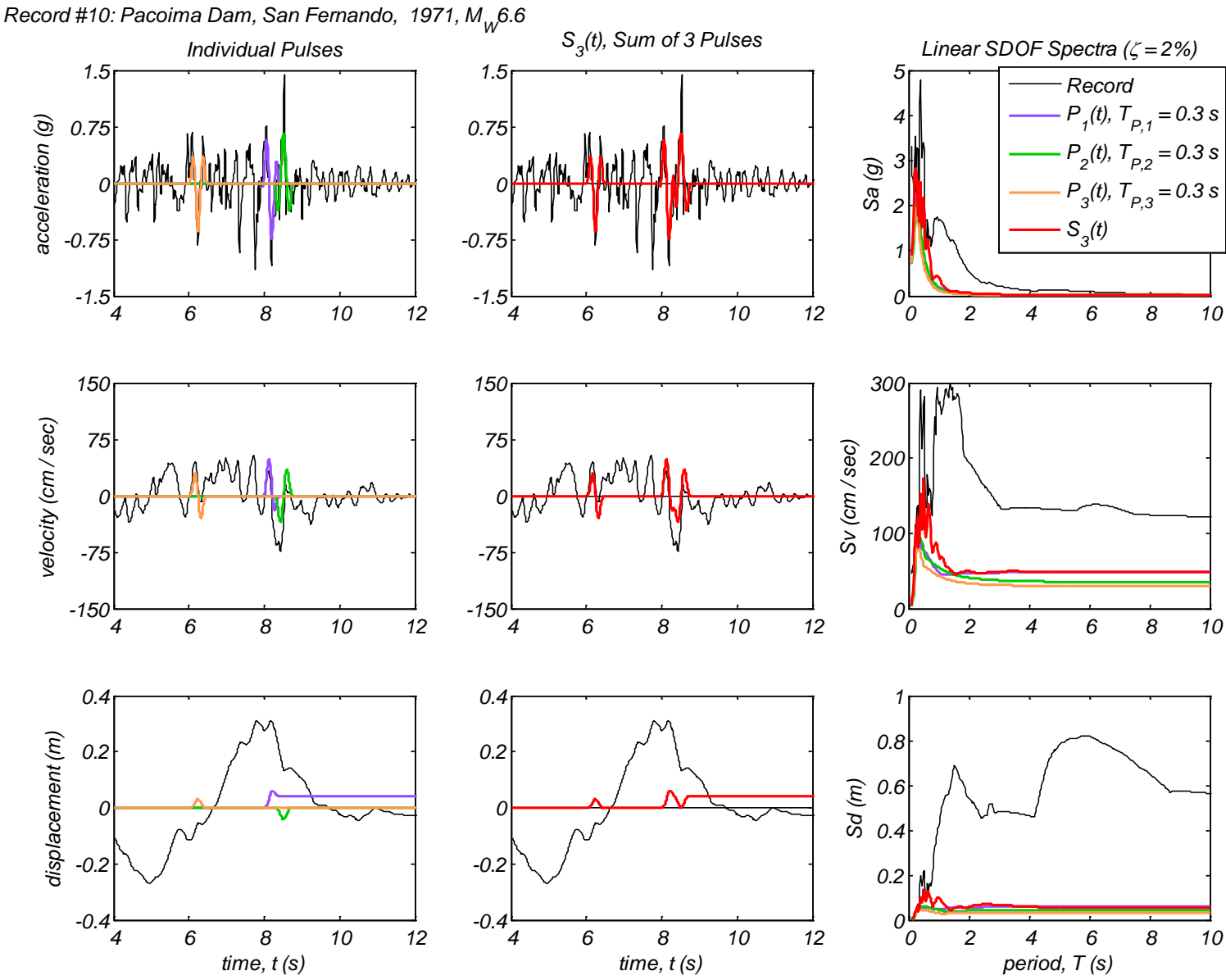
Appendix B6 – Time history and linear spectral response of three extracted pulses using the CPE<sub>A-AM</sub> method for 40 Motions



Appendix B6 – Time history and linear spectral response of three extracted pulses using the CPE<sub>A-AM</sub> method for 40 Motions

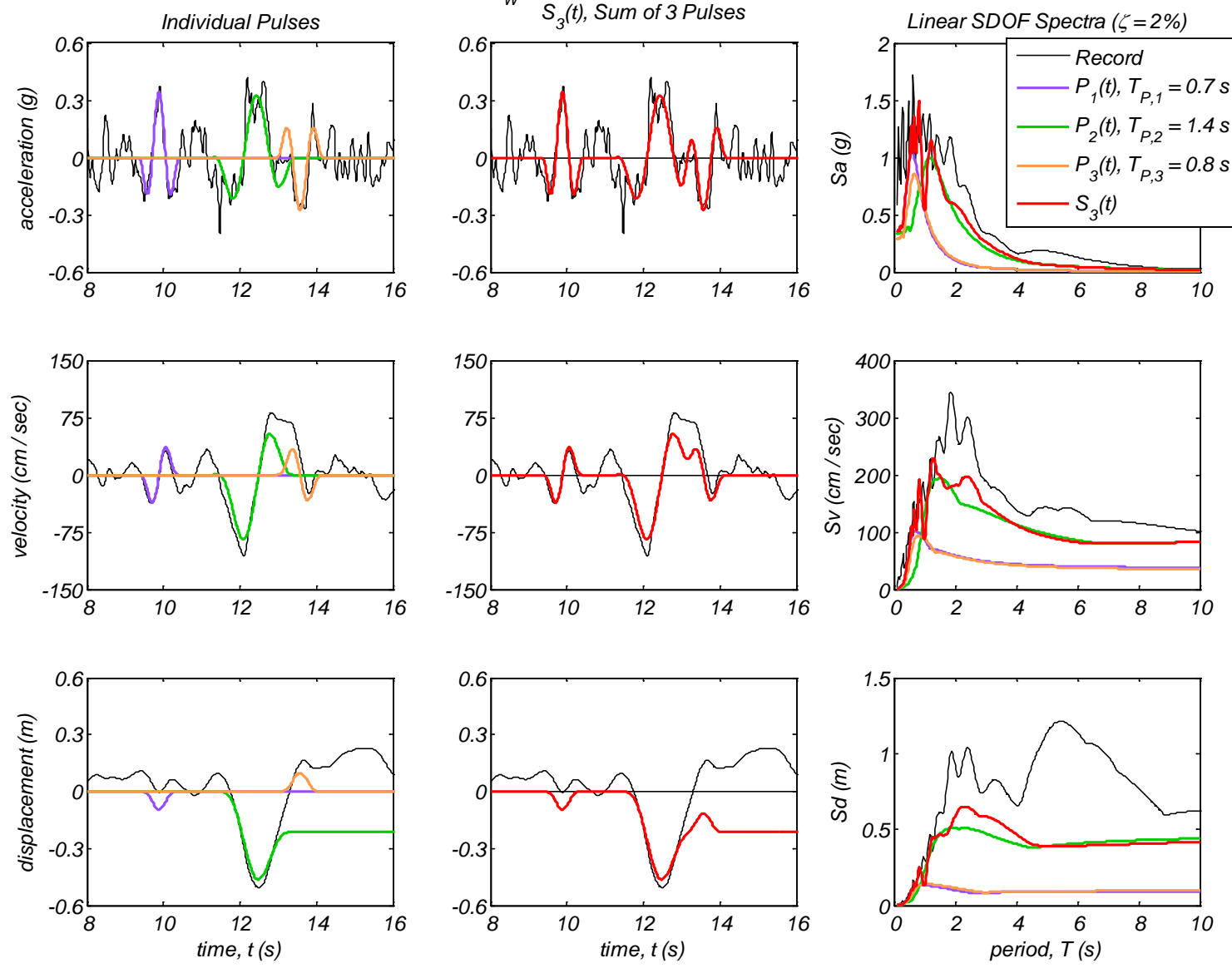


Appendix B6 – Time history and linear spectral response of three extracted pulses using the CPE<sub>A-AM</sub> method for 40 Motions



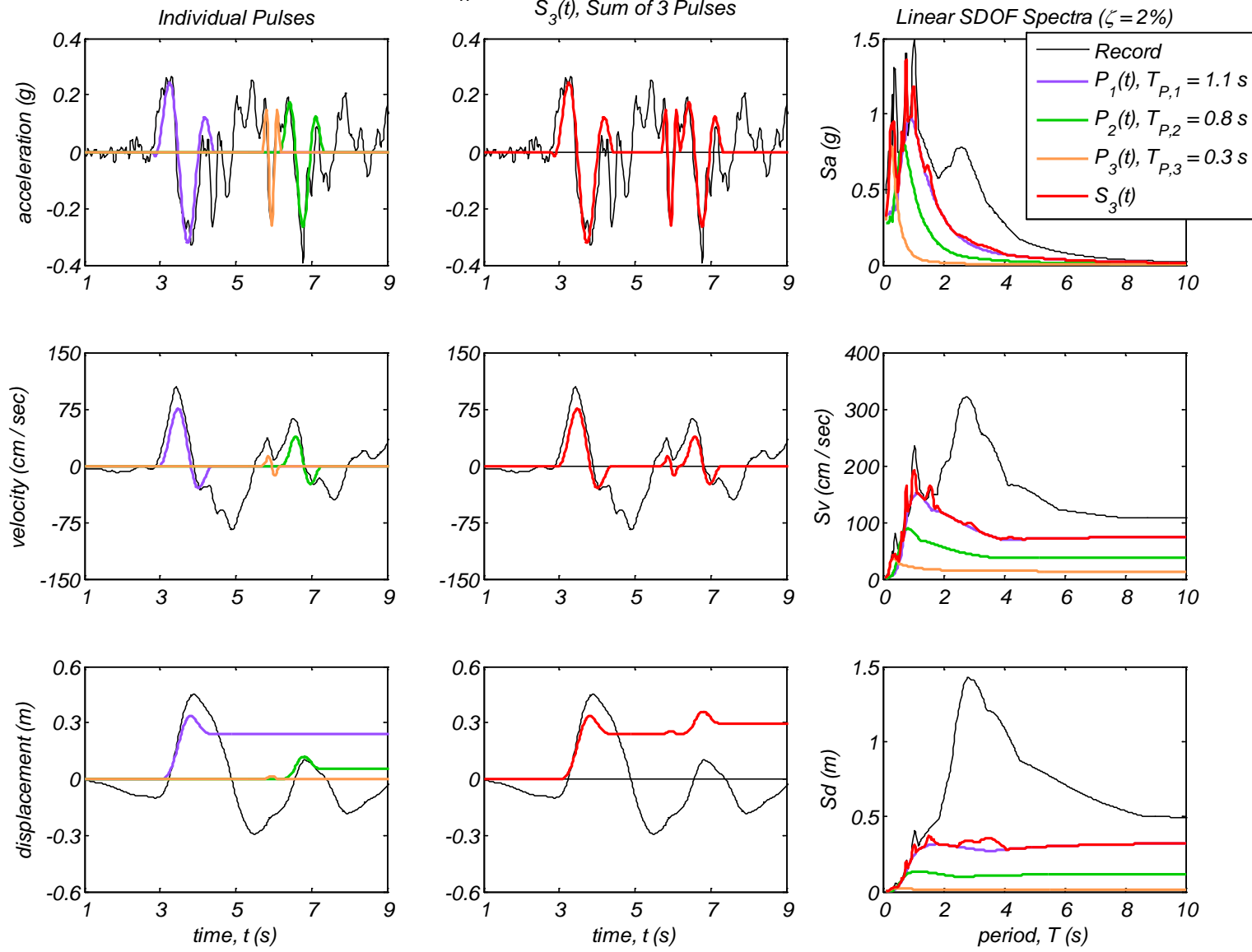
Appendix B6 – Time history and linear spectral response of three extracted pulses using the CPE<sub>A-AM</sub> method for 40 Motions

Record #11: Parachute Test Site, Superstition Hills(B), 1987,  $M_w 6.6$



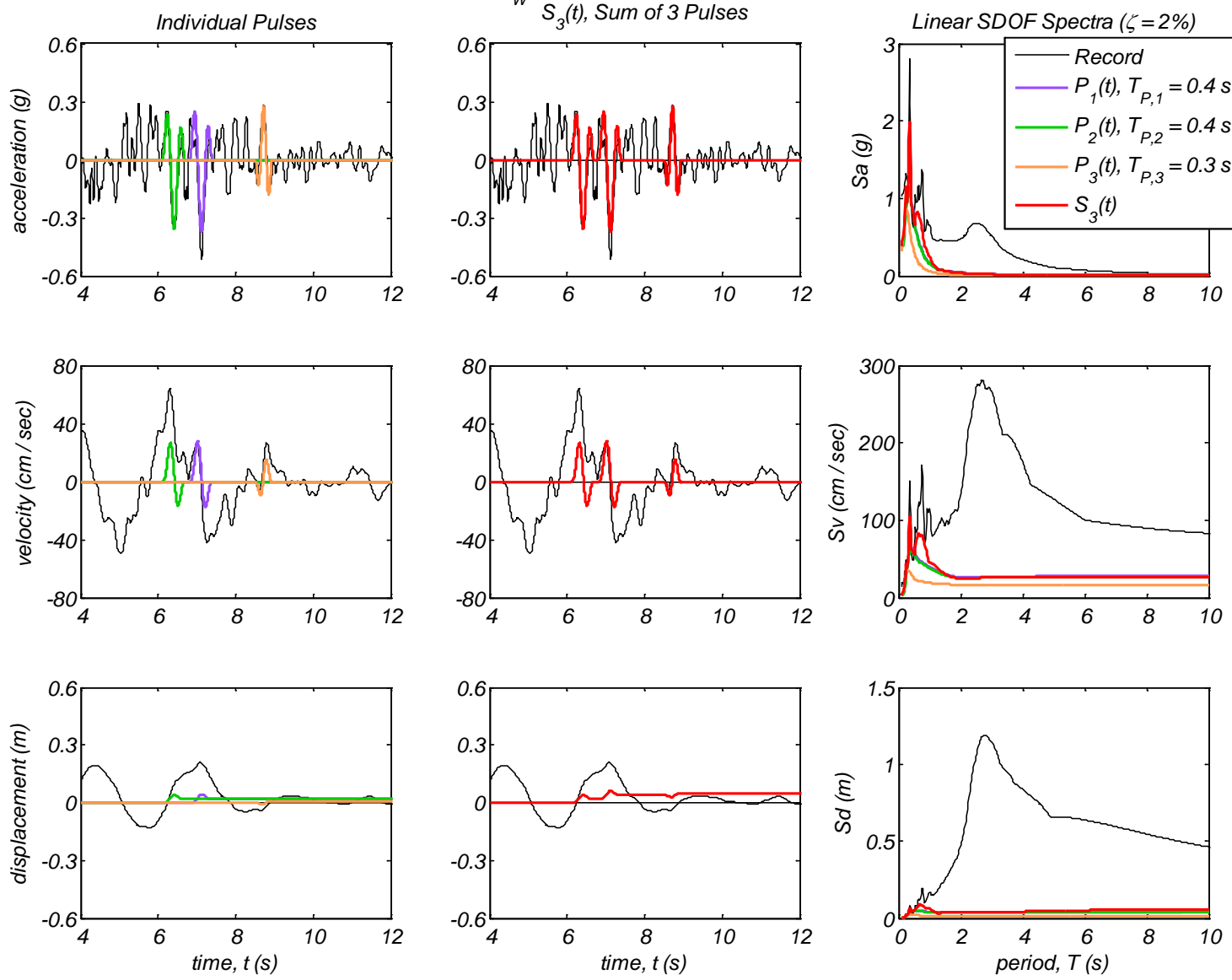
Appendix B6 – Time history and linear spectral response of three extracted pulses using the CPE<sub>A-AM</sub> method for 40 Motions

Record #12: Jensen Filter Plant, Northridge, 1994,  $M_W 6.7$

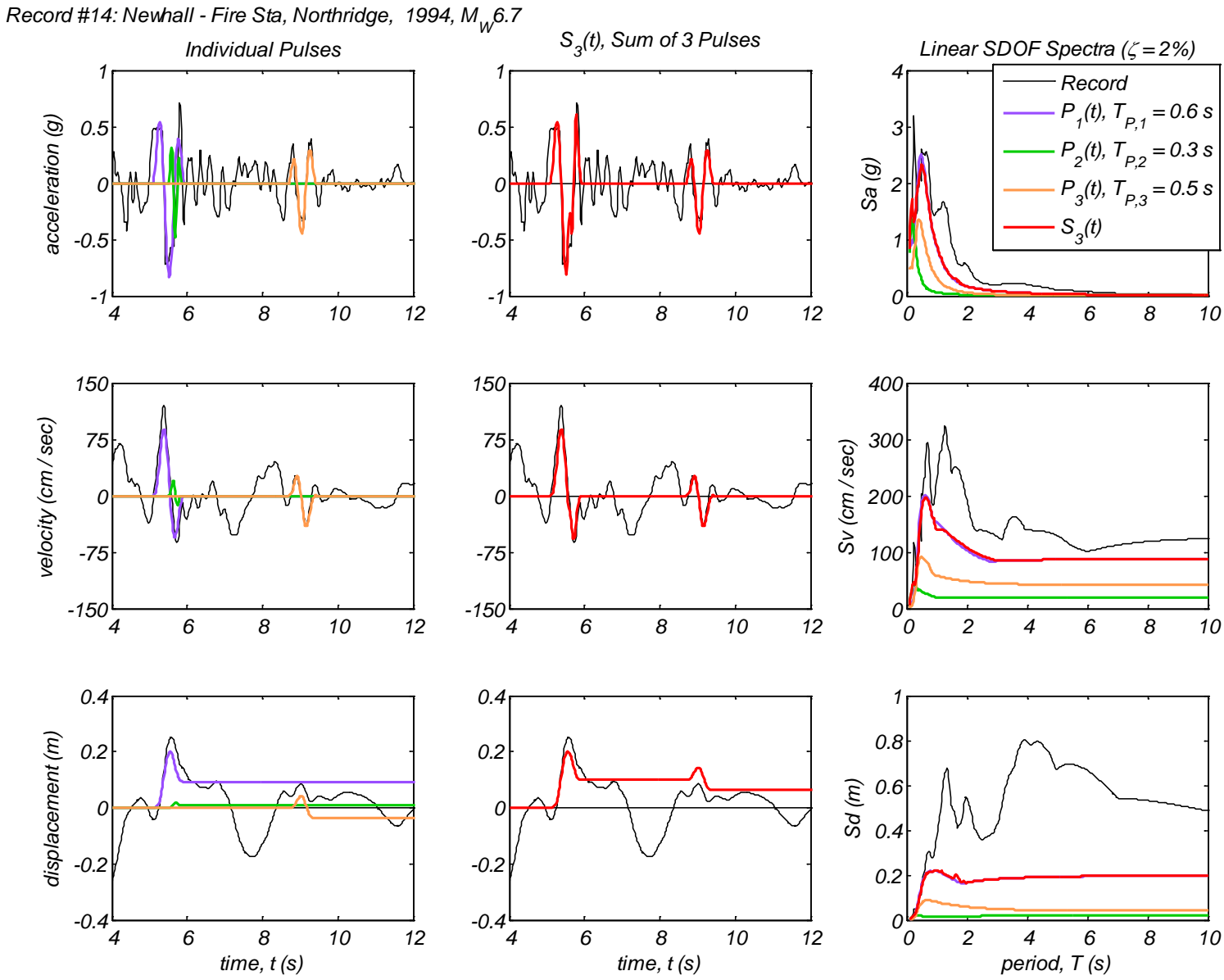


Appendix B6 – Time history and linear spectral response of three extracted pulses using the CPE<sub>A-AM</sub> method for 40 Motions

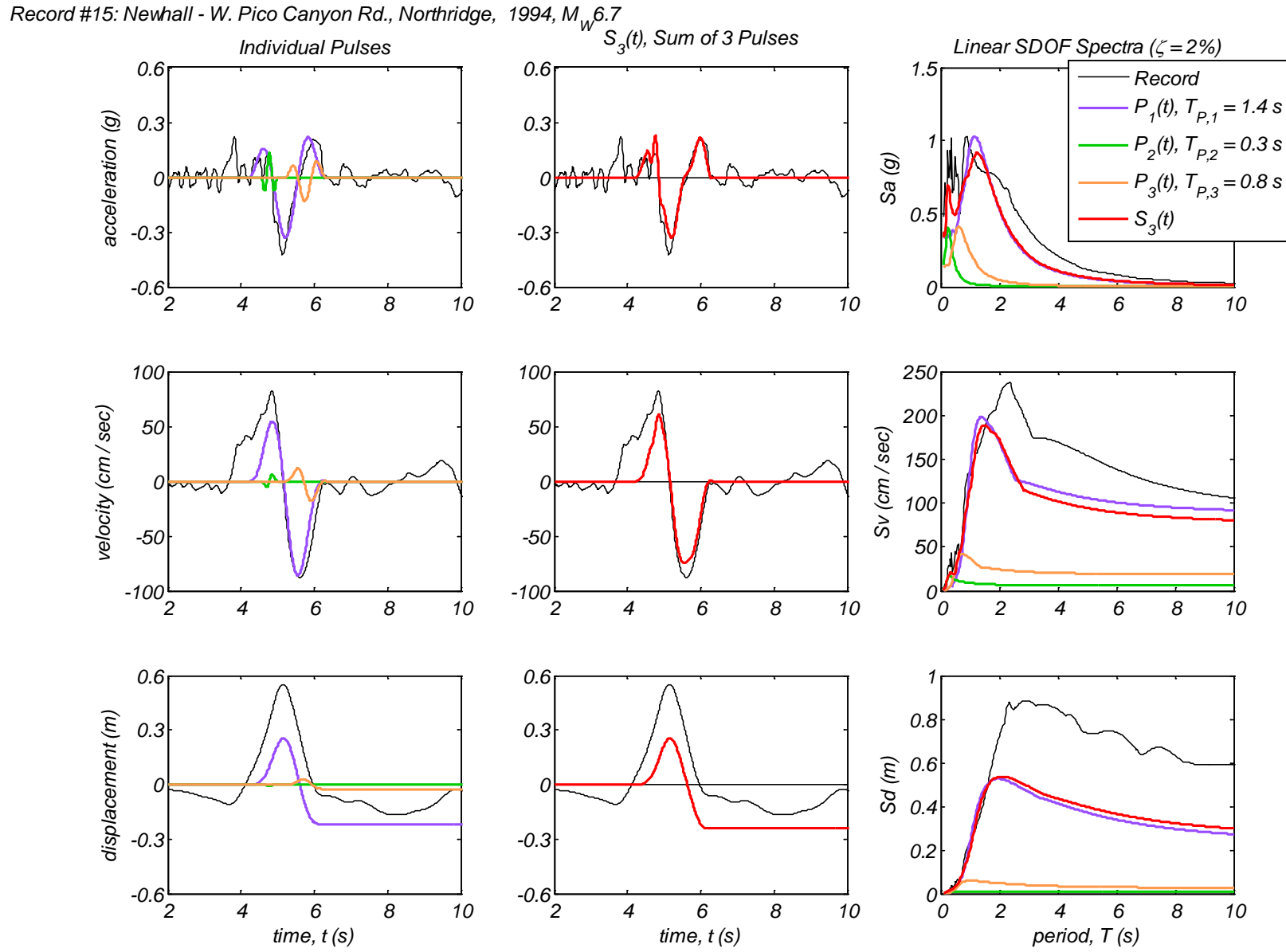
Record #13: Jensen Filter Plant Generator, Northridge, 1994,  $M_W 6.7$



Appendix B6 – Time history and linear spectral response of three extracted pulses using the CPE<sub>A-AM</sub> method for 40 Motions

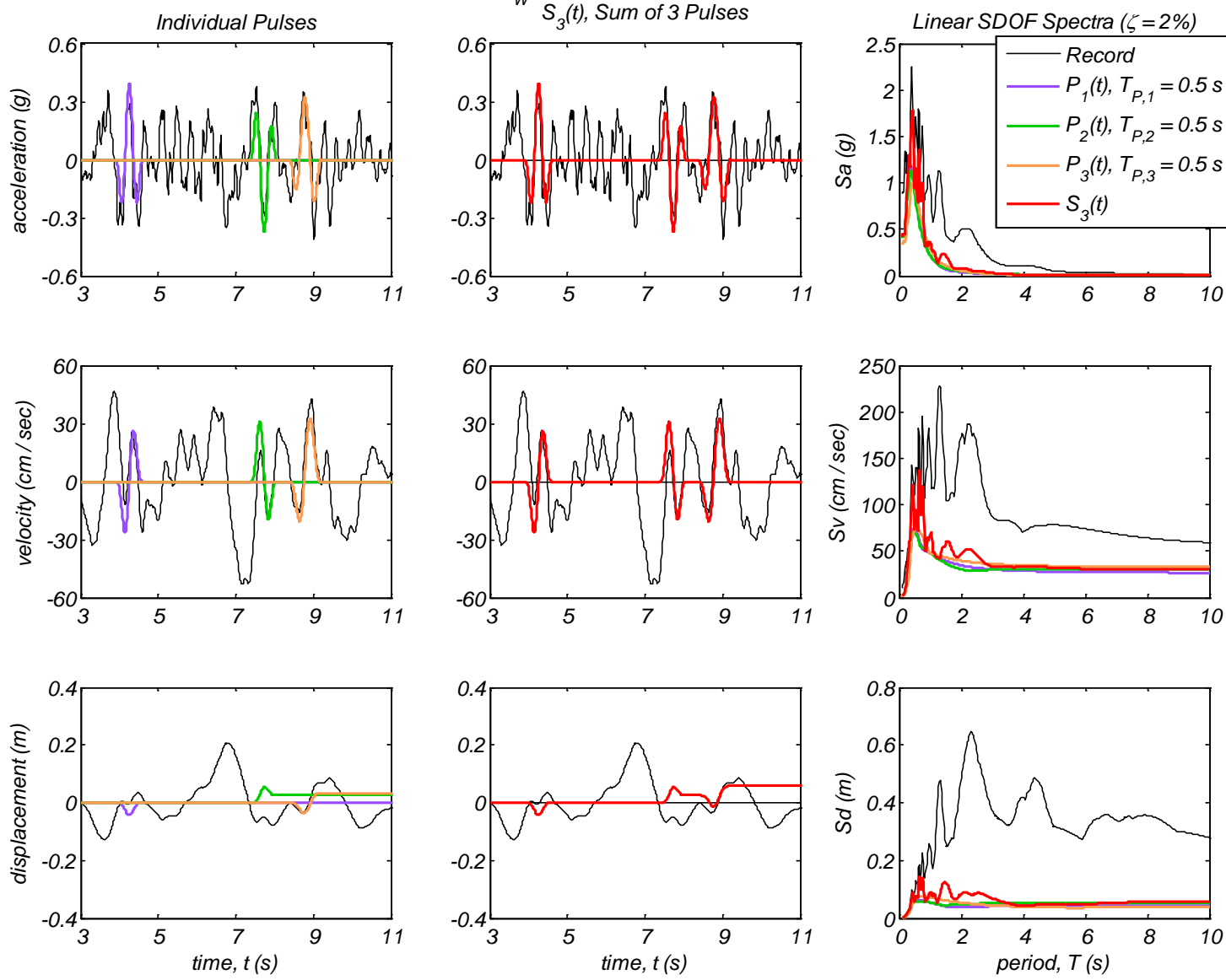


Appendix B6 – Time history and linear spectral response of three extracted pulses using the CPE<sub>A-AM</sub> method for 40 Motions



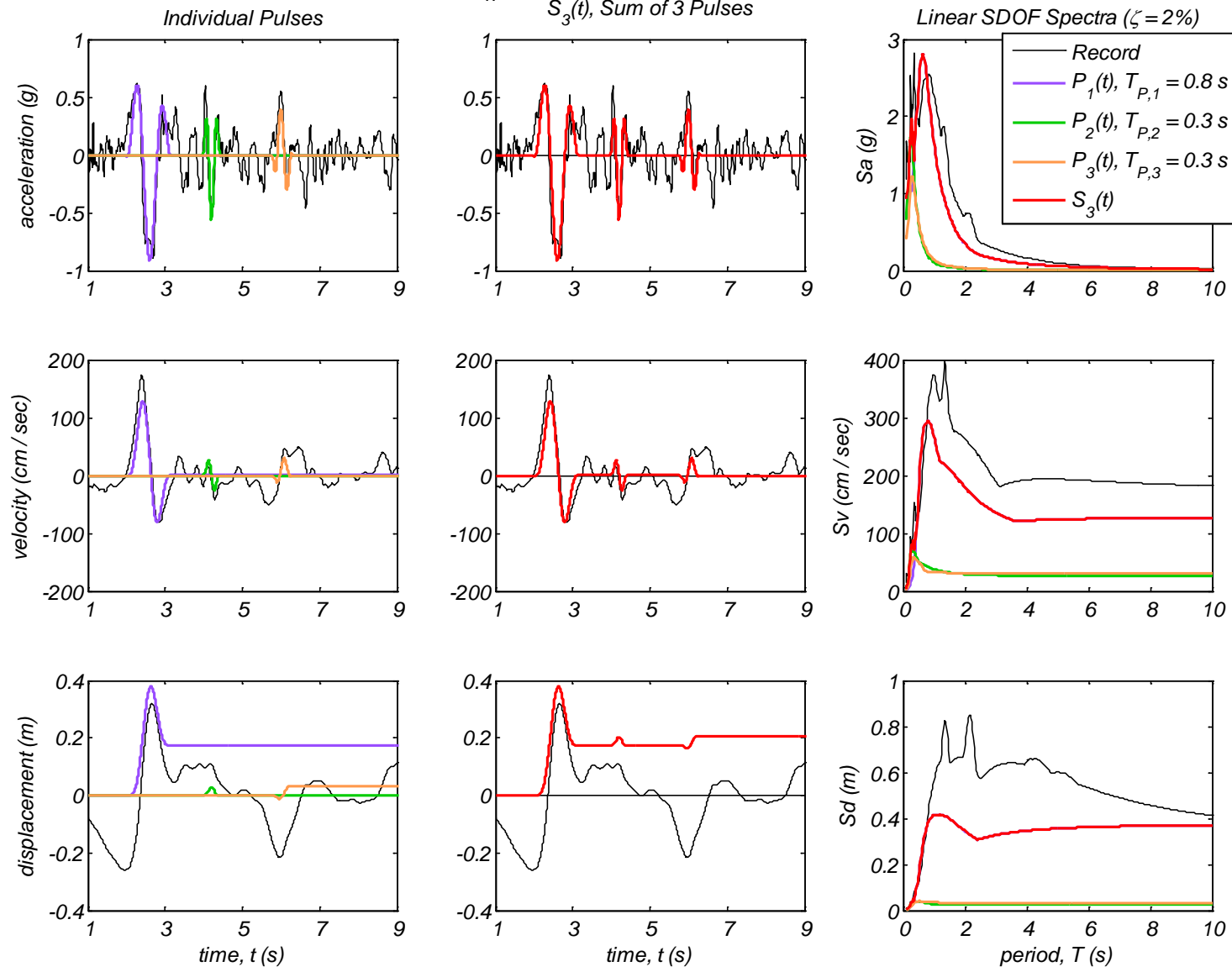
Appendix B6 – Time history and linear spectral response of three extracted pulses using the CPE<sub>A-AM</sub> method for 40 Motions

Record #16: Northridge - 17645 Saticoy St, Northridge, 1994,  $M_W 6.7$

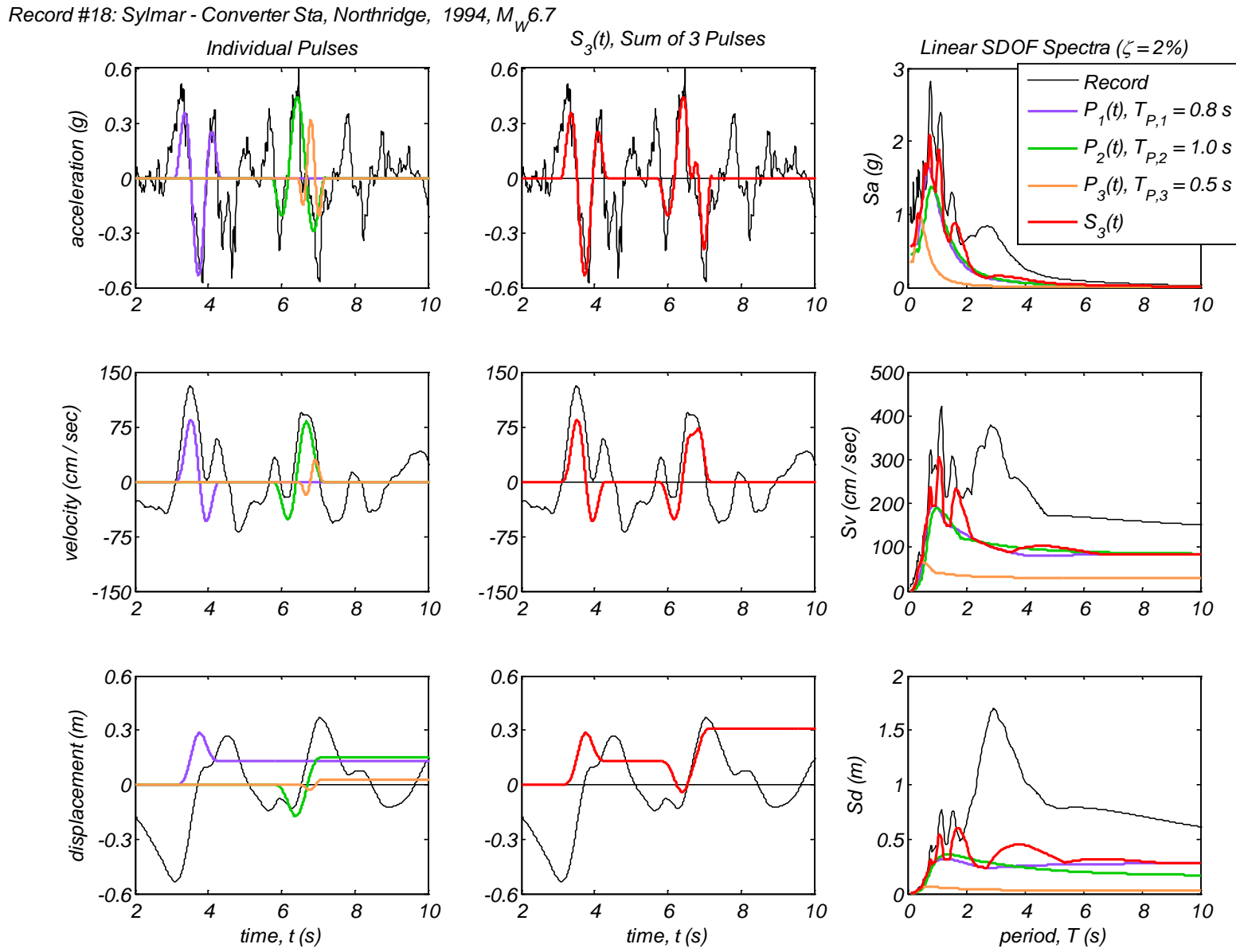


Appendix B6 – Time history and linear spectral response of three extracted pulses using the CPE<sub>A-AM</sub> method for 40 Motions

Record #17: Rinaldi Receiving Sta, Northridge, 1994,  $M_W 6.7$

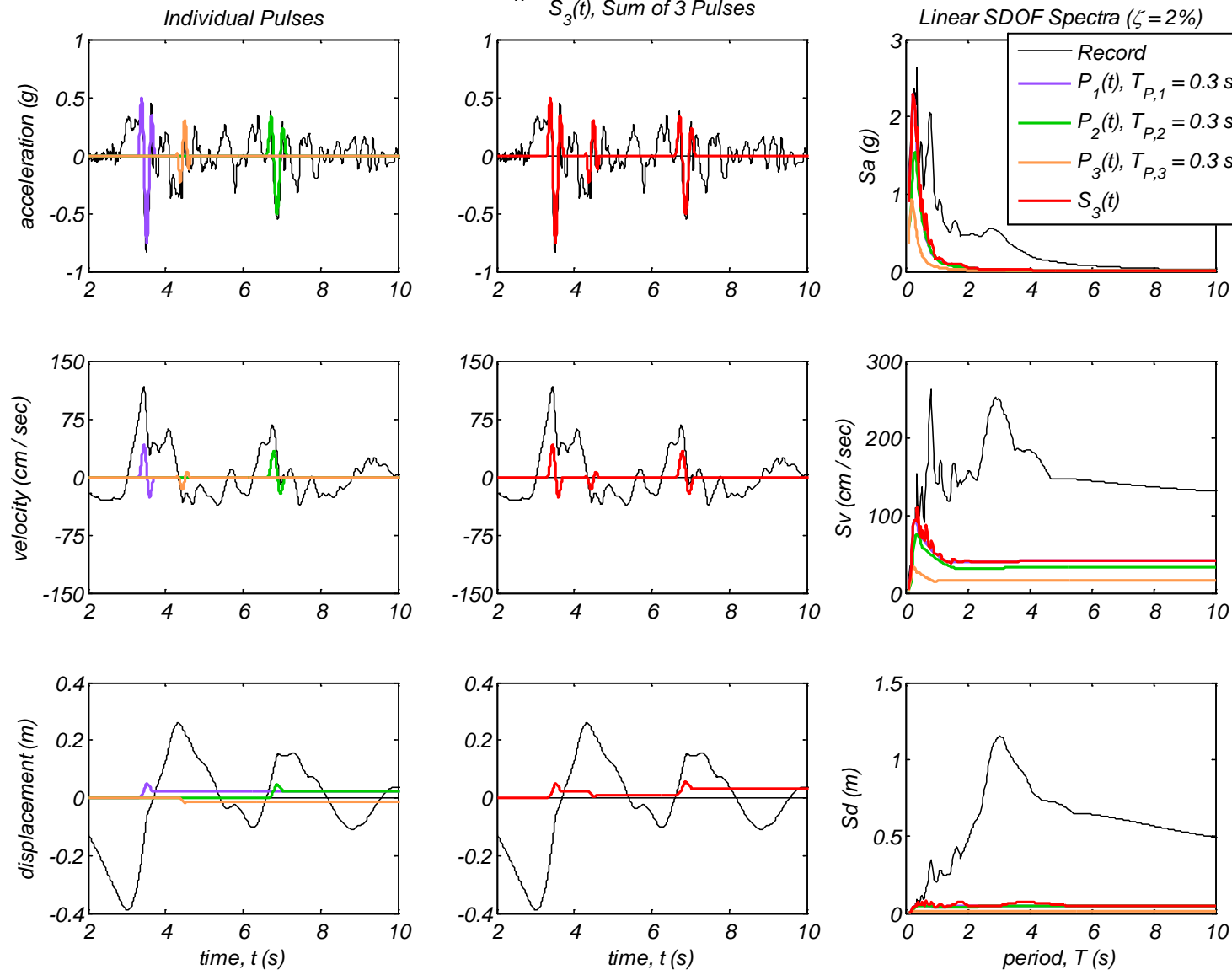


Appendix B6 – Time history and linear spectral response of three extracted pulses using the CPE<sub>A-AM</sub> method for 40 Motions



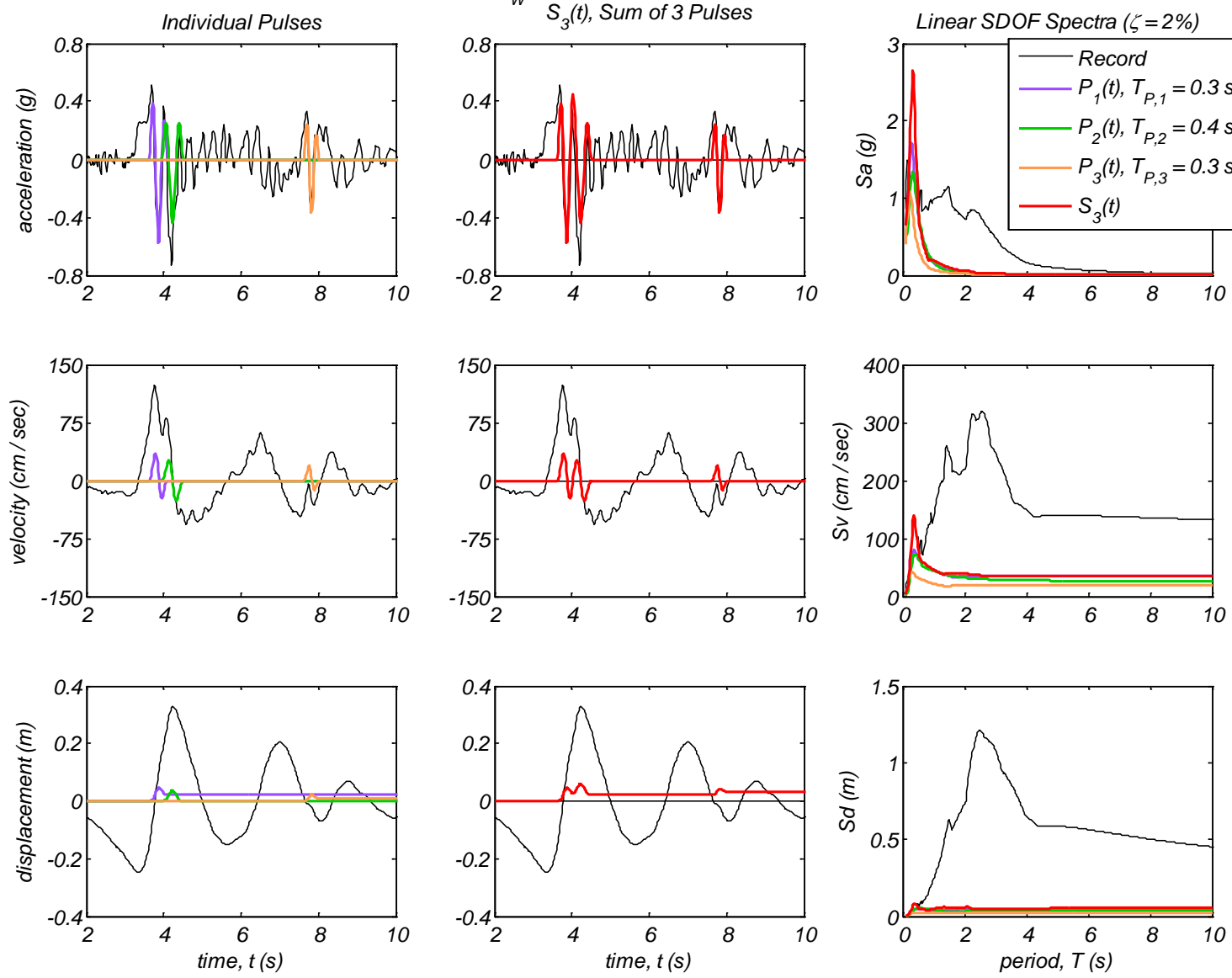
Appendix B6 – Time history and linear spectral response of three extracted pulses using the CPE<sub>A-AM</sub> method for 40 Motions

Record #19: Sylmar - Converter Sta East, Northridge, 1994,  $M_W$  6.7



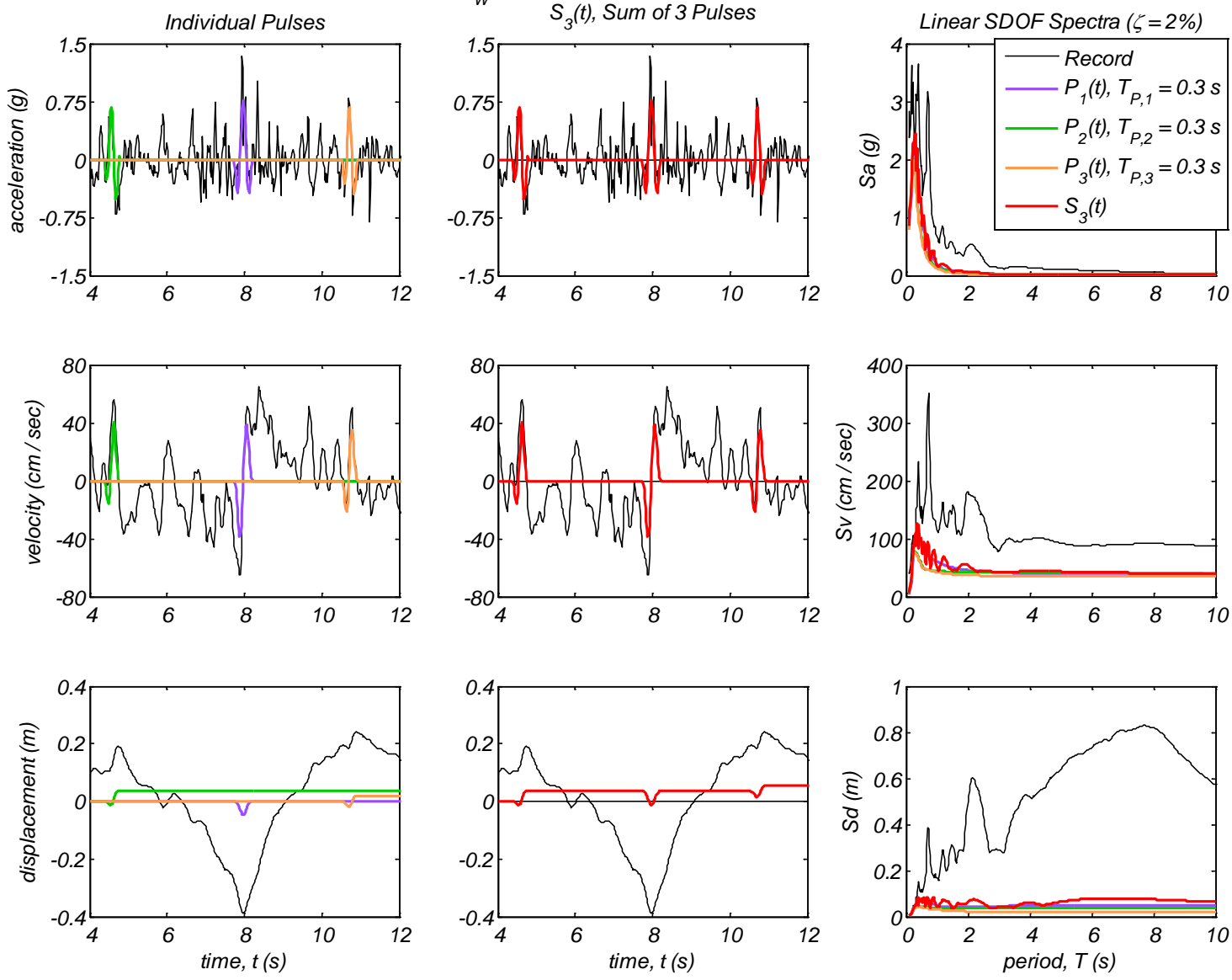
Appendix B6 – Time history and linear spectral response of three extracted pulses using the CPE<sub>A-AM</sub> method for 40 Motions

Record #20: Sylmar - Olive ViewMed FF, Northridge, 1994,  $M_W$  6.7

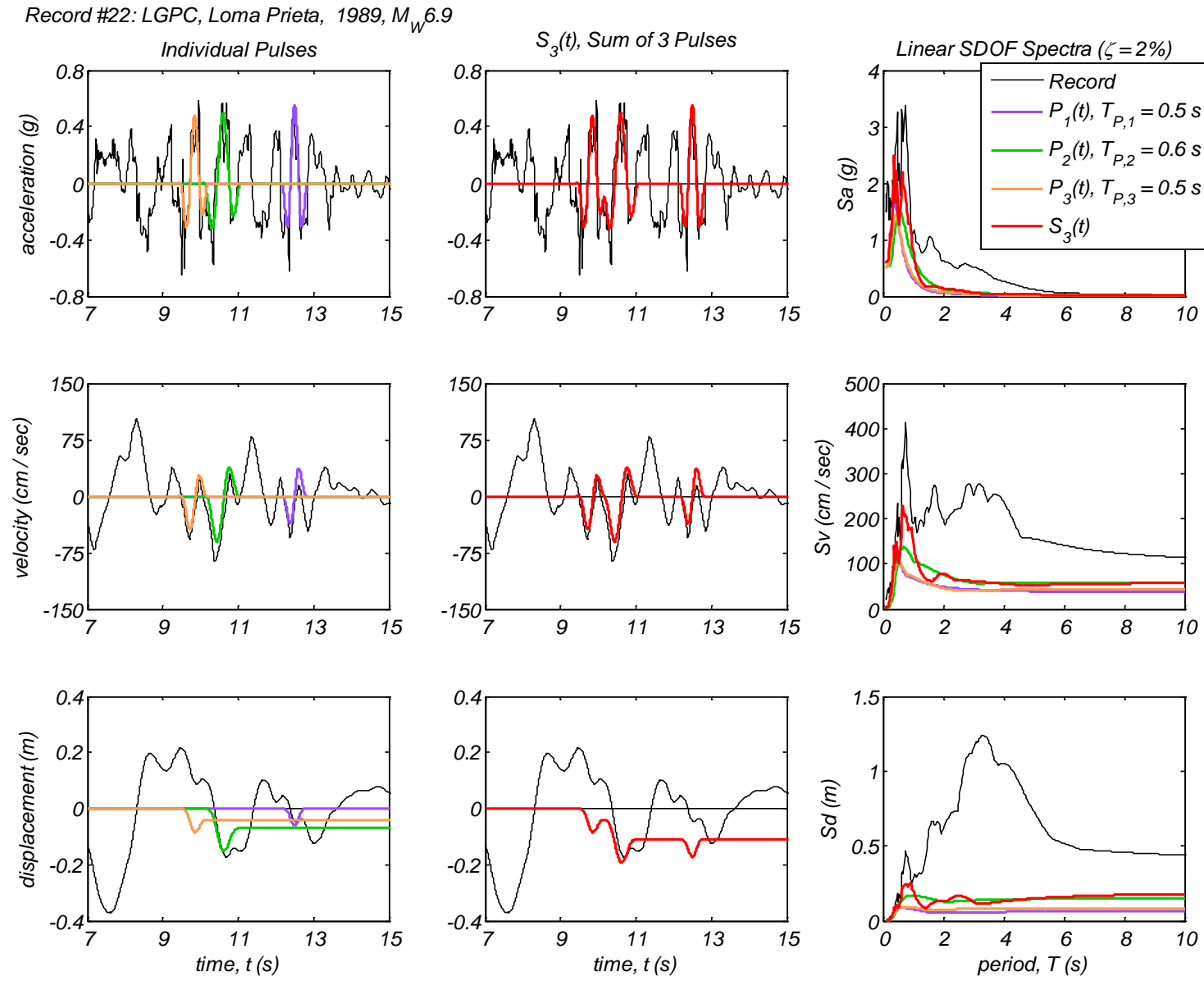


Appendix B6 – Time history and linear spectral response of three extracted pulses using the CPE<sub>A-AM</sub> method for 40 Motions

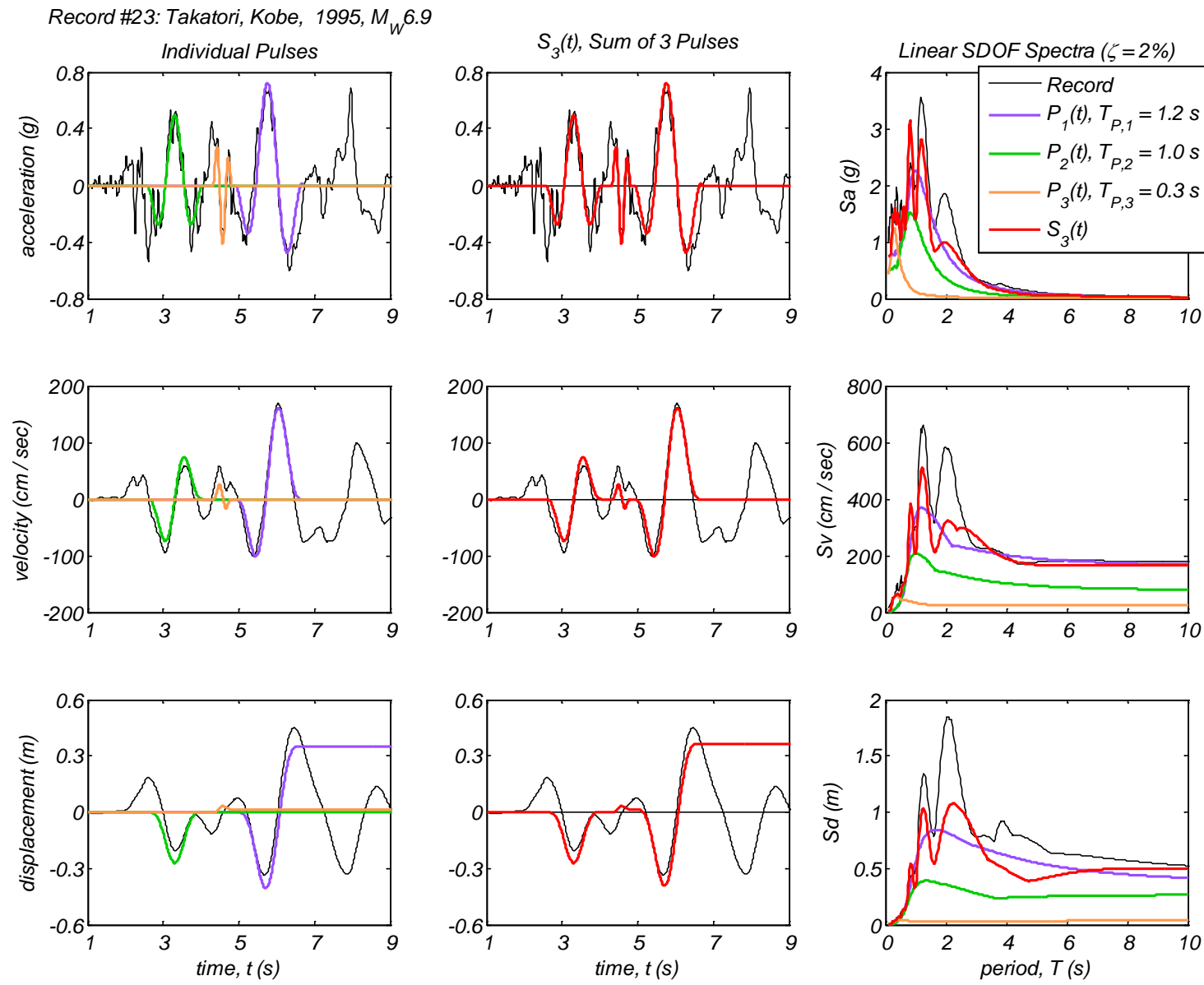
Record #21: Tarzana, Cedar Hill, Northridge, 1994,  $M_W 6.7$



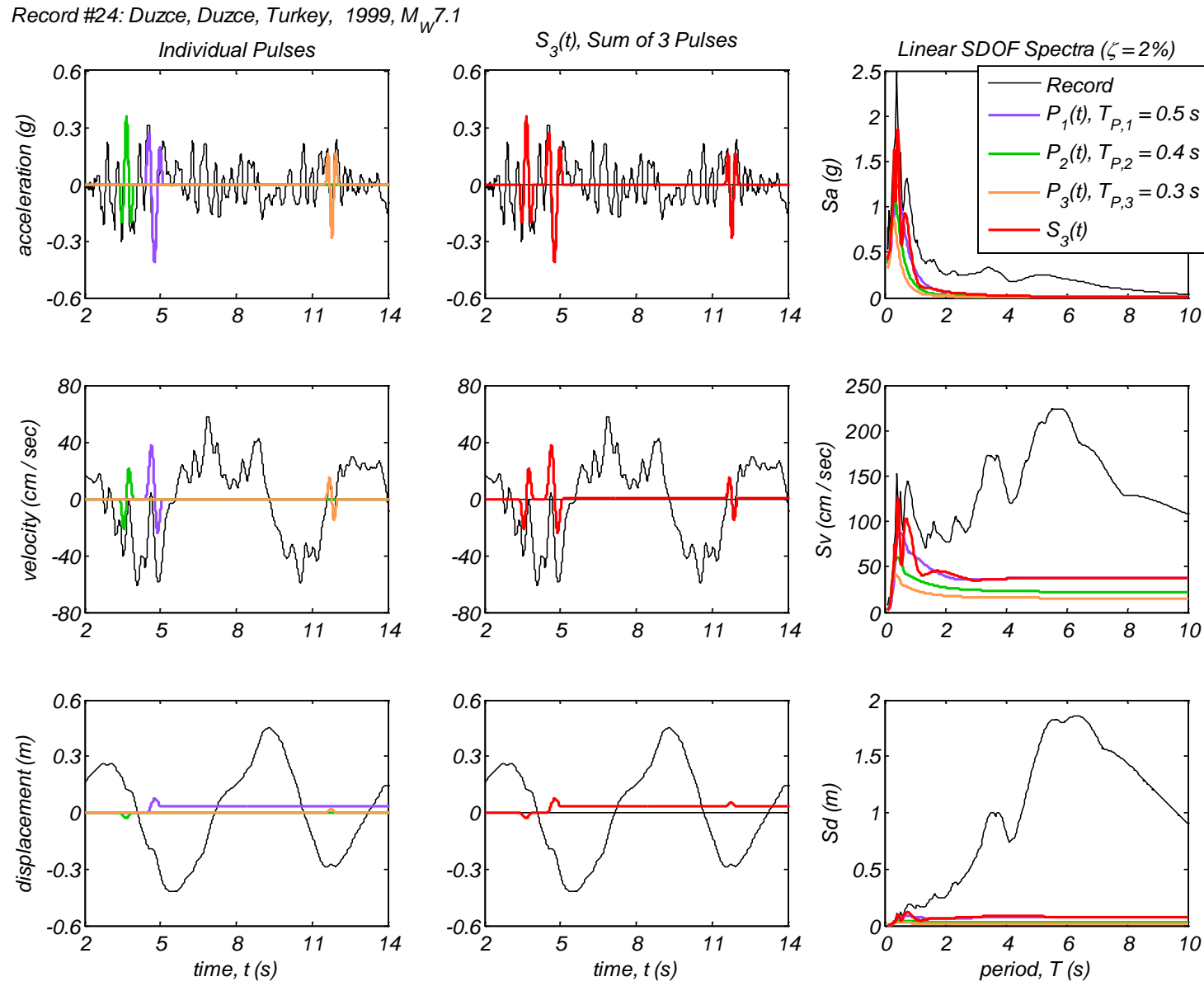
Appendix B6 – Time history and linear spectral response of three extracted pulses using the CPE<sub>A-AM</sub> method for 40 Motions



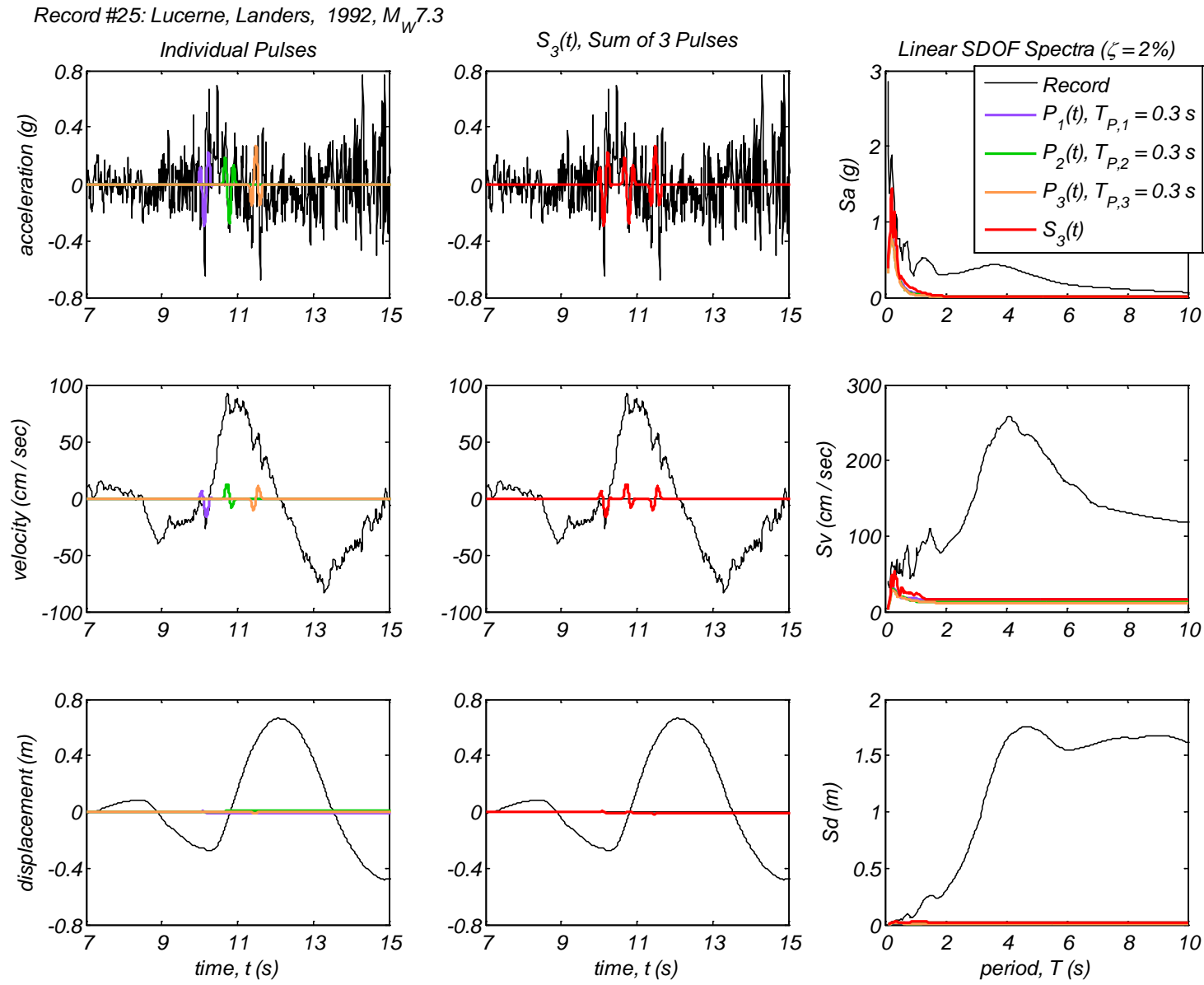
Appendix B6 – Time history and linear spectral response of three extracted pulses using the CPE<sub>A-AM</sub> method for 40 Motions



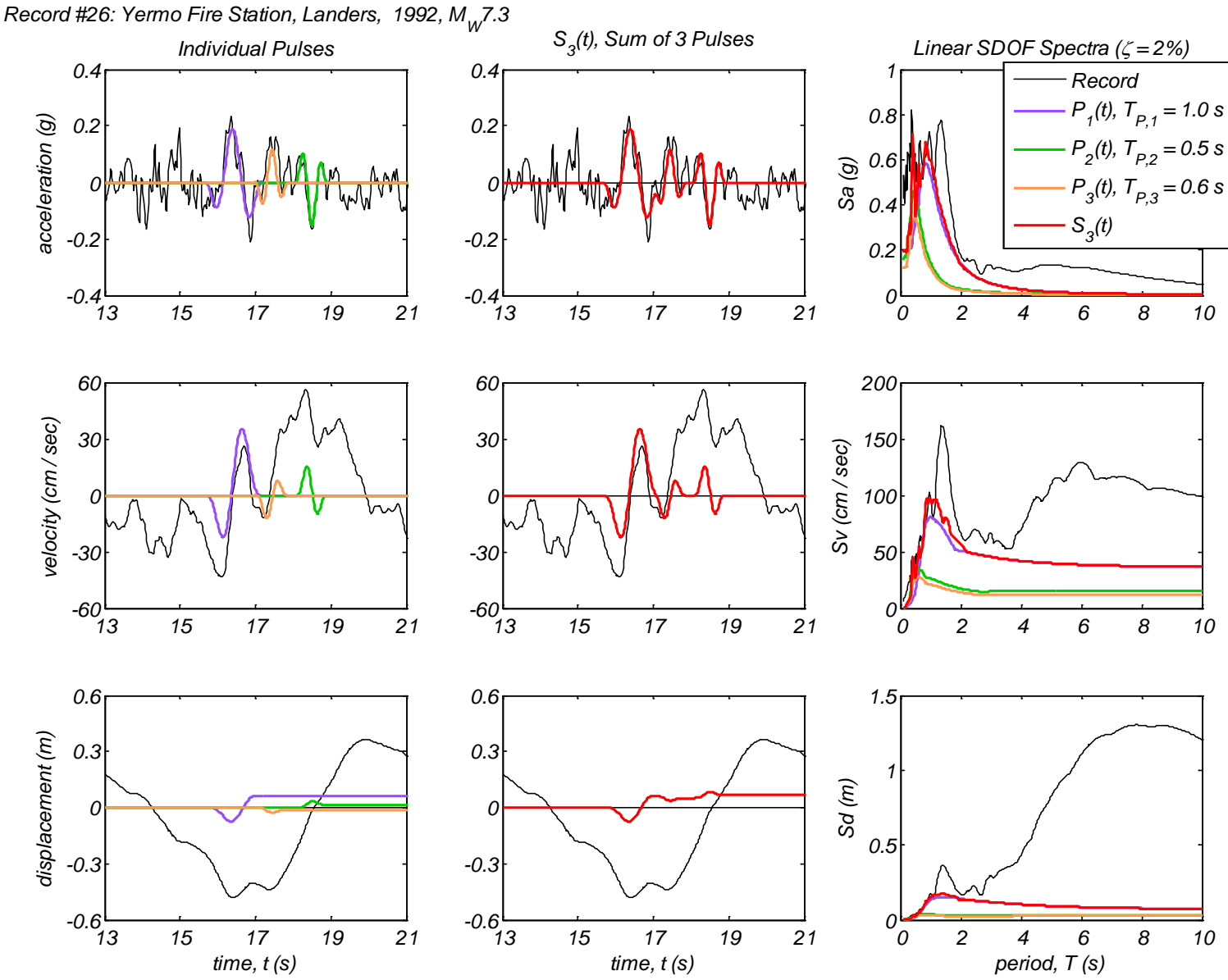
Appendix B6 – Time history and linear spectral response of three extracted pulses using the CPE<sub>A-AM</sub> method for 40 Motions



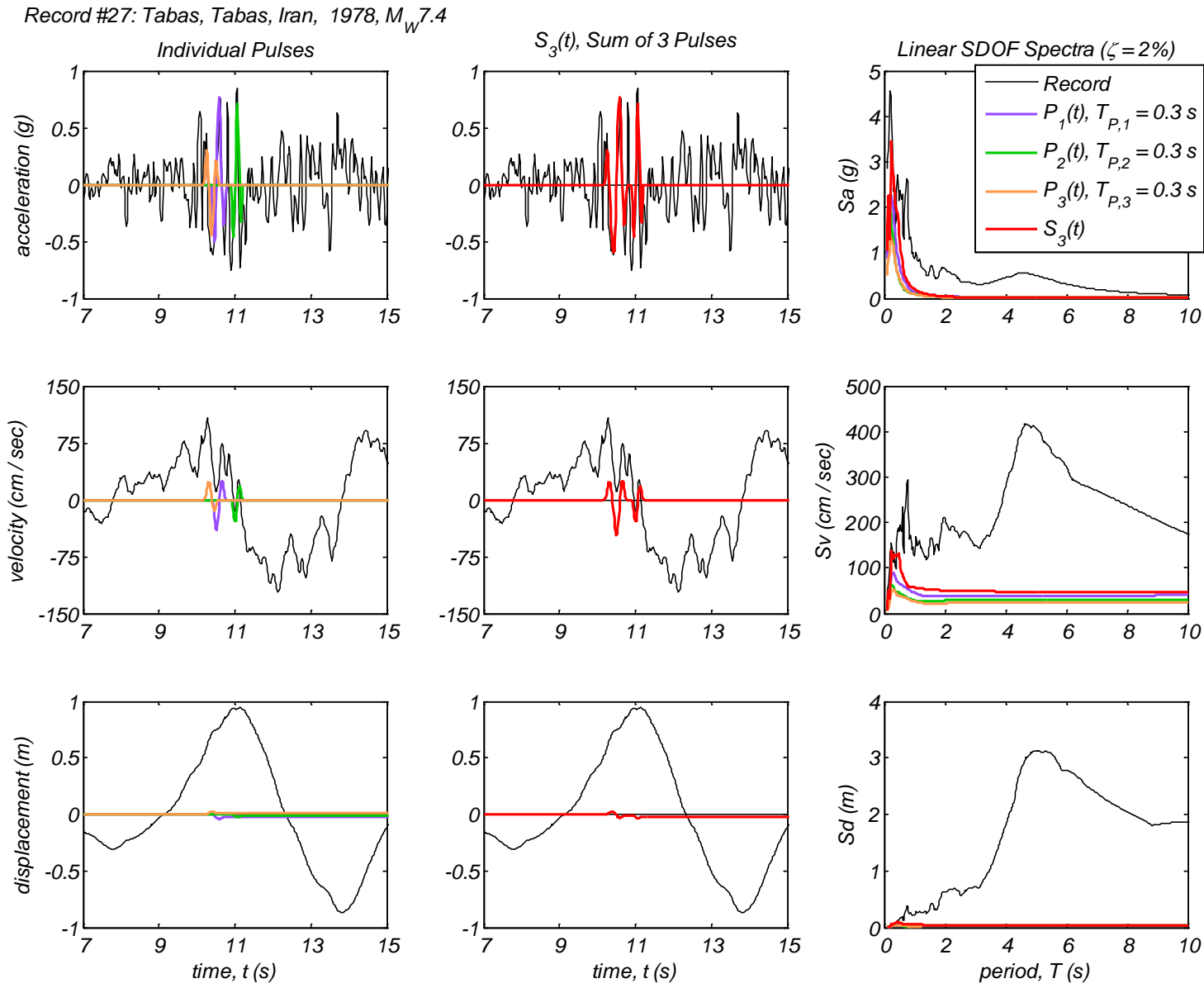
Appendix B6 – Time history and linear spectral response of three extracted pulses using the CPE<sub>A-AM</sub> method for 40 Motions



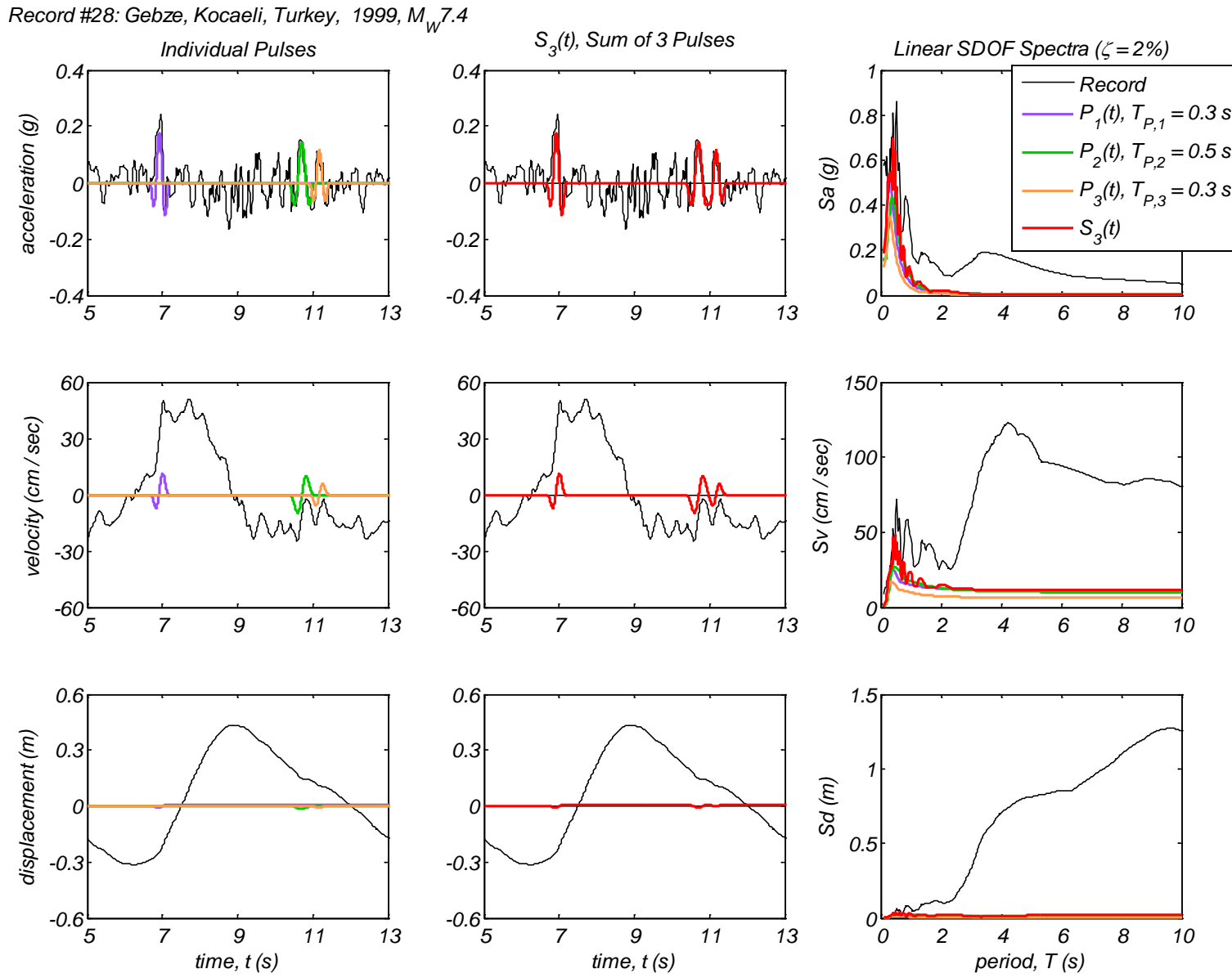
Appendix B6 – Time history and linear spectral response of three extracted pulses using the CPE<sub>A-AM</sub> method for 40 Motions



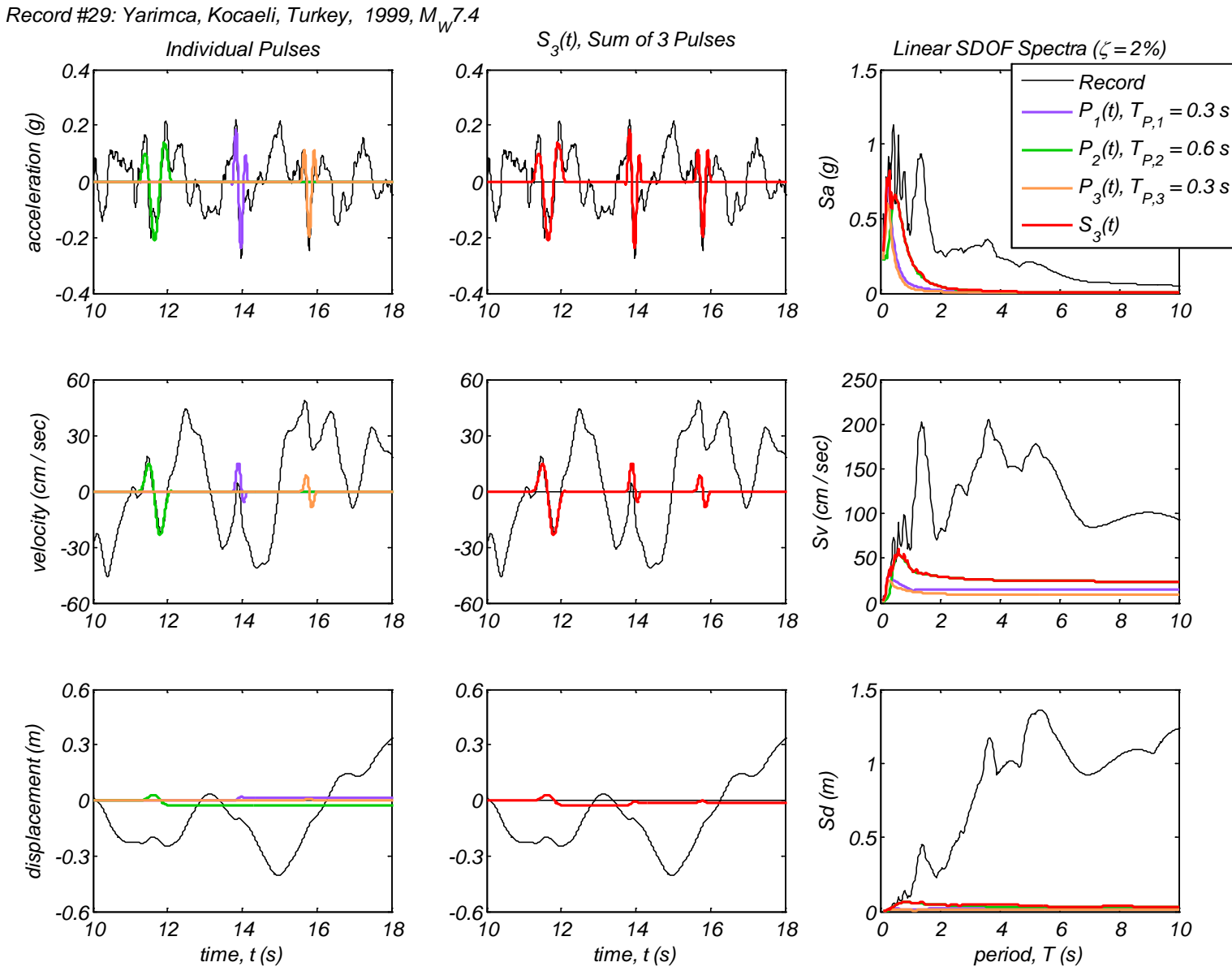
Appendix B6 – Time history and linear spectral response of three extracted pulses using the CPE<sub>A-AM</sub> method for 40 Motions



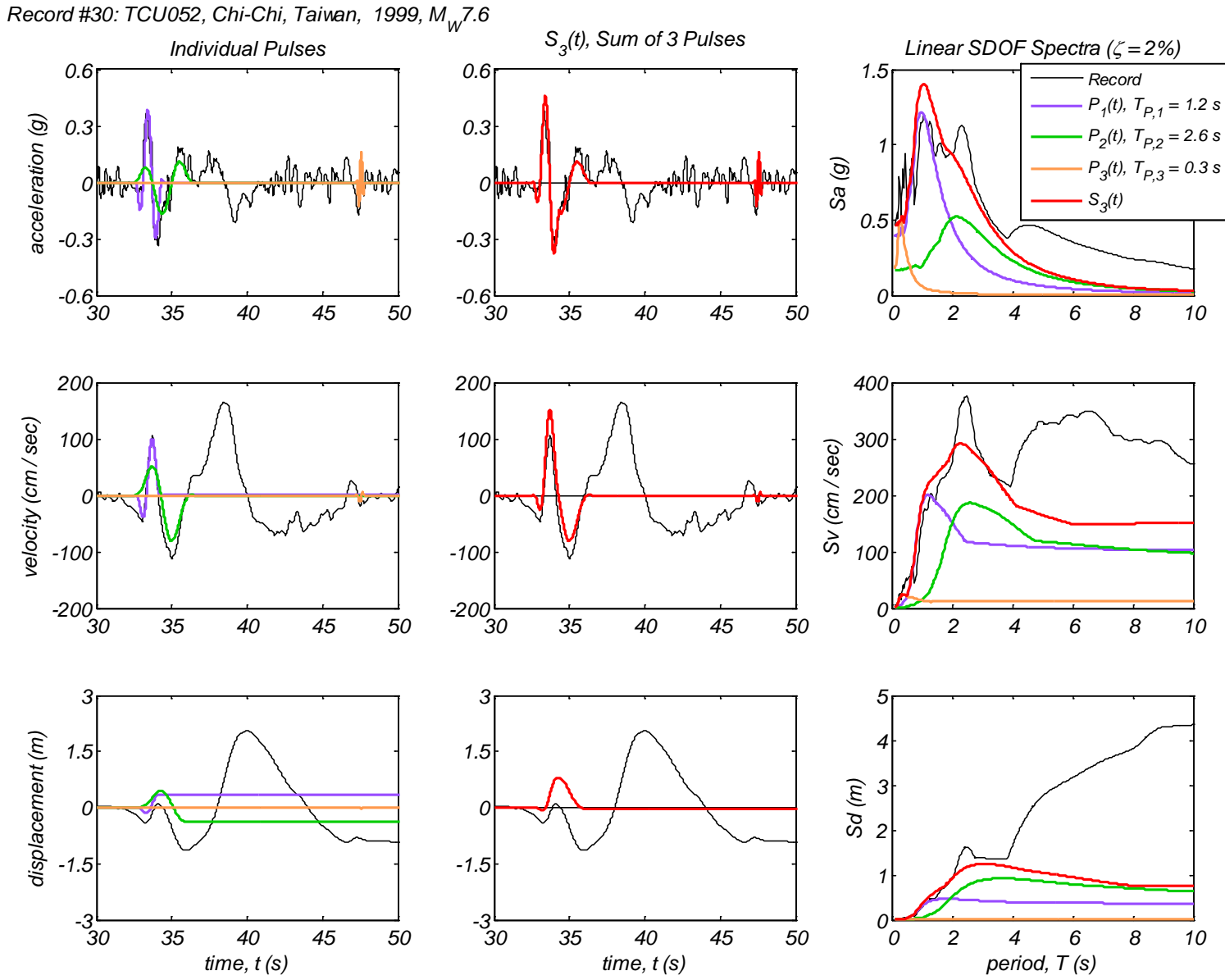
Appendix B6 – Time history and linear spectral response of three extracted pulses using the CPE<sub>A-AM</sub> method for 40 Motions



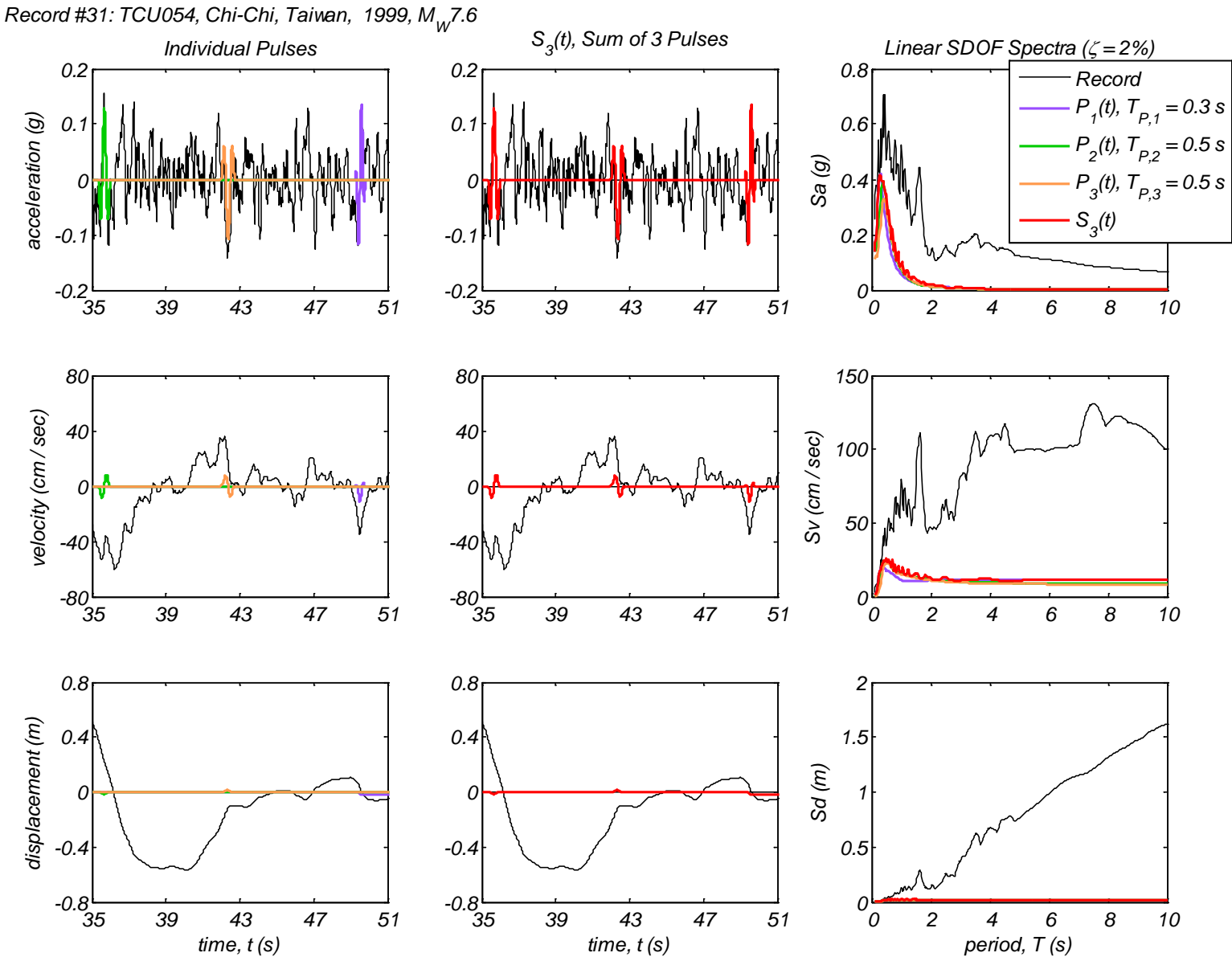
Appendix B6 – Time history and linear spectral response of three extracted pulses using the CPE<sub>A-AM</sub> method for 40 Motions



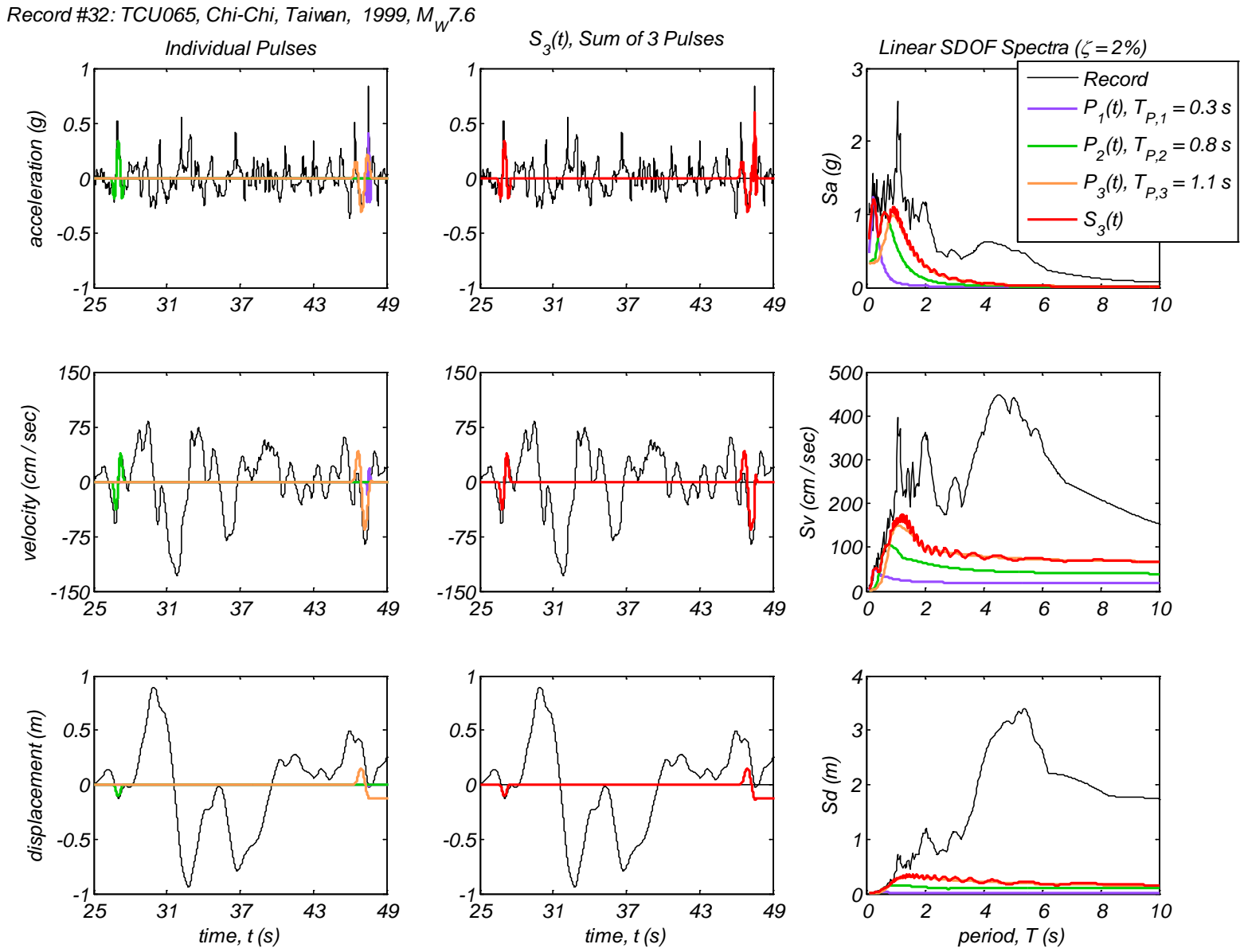
Appendix B6 – Time history and linear spectral response of three extracted pulses using the CPE<sub>A-AM</sub> method for 40 Motions



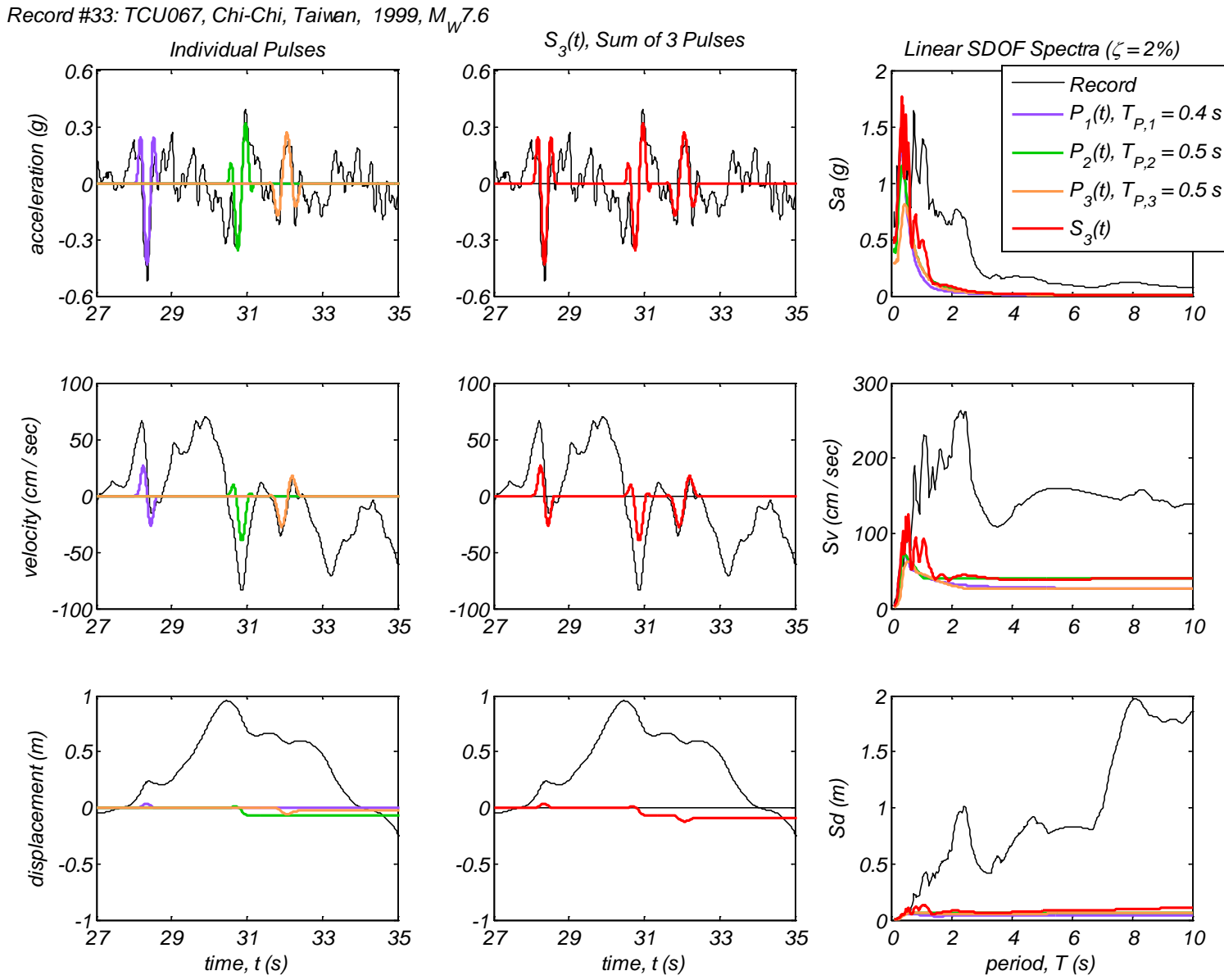
Appendix B6 – Time history and linear spectral response of three extracted pulses using the CPE<sub>A-AM</sub> method for 40 Motions



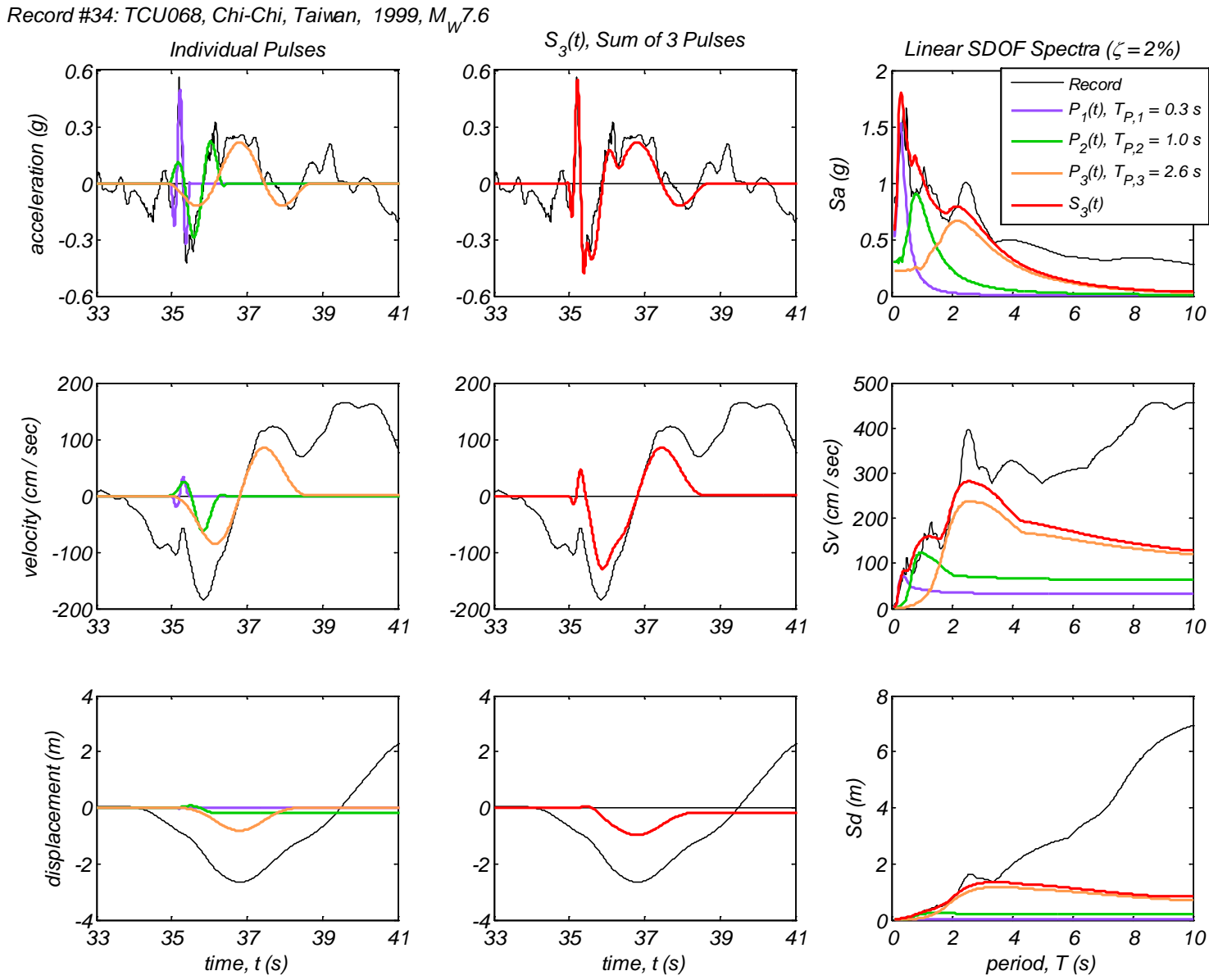
Appendix B6 – Time history and linear spectral response of three extracted pulses using the CPE<sub>A-AM</sub> method for 40 Motions



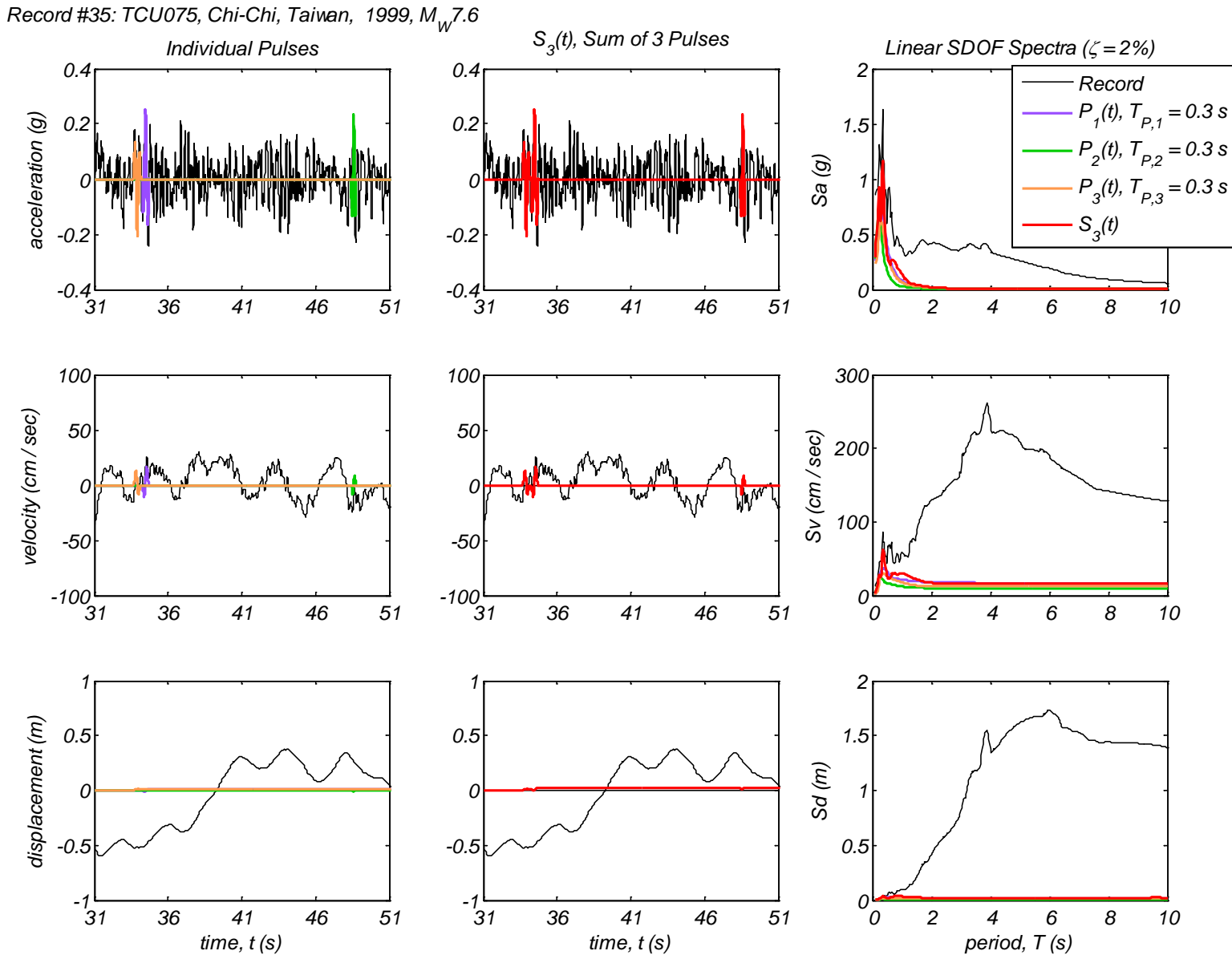
Appendix B6 – Time history and linear spectral response of three extracted pulses using the CPE<sub>A-AM</sub> method for 40 Motions



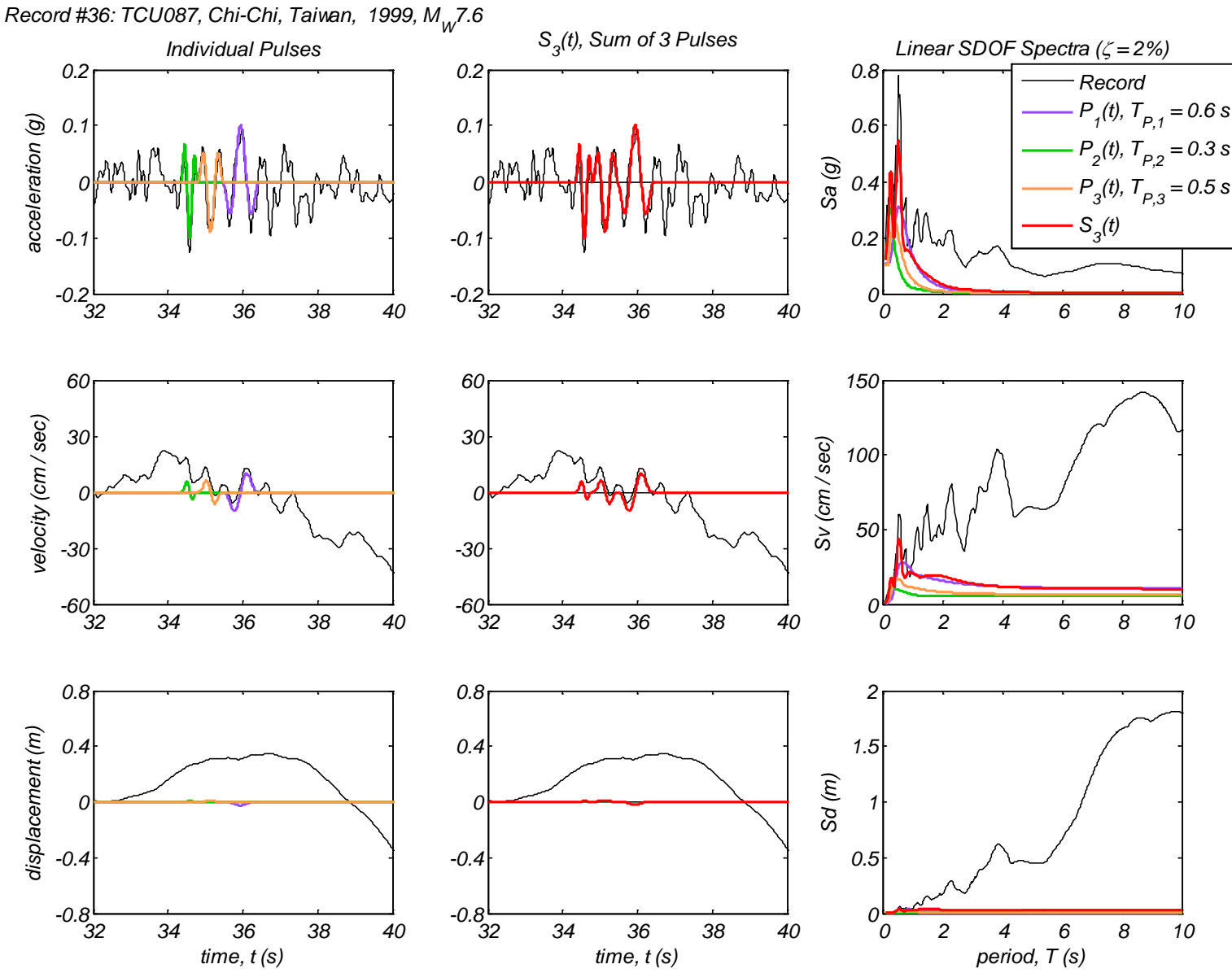
Appendix B6 – Time history and linear spectral response of three extracted pulses using the CPE<sub>A-AM</sub> method for 40 Motions



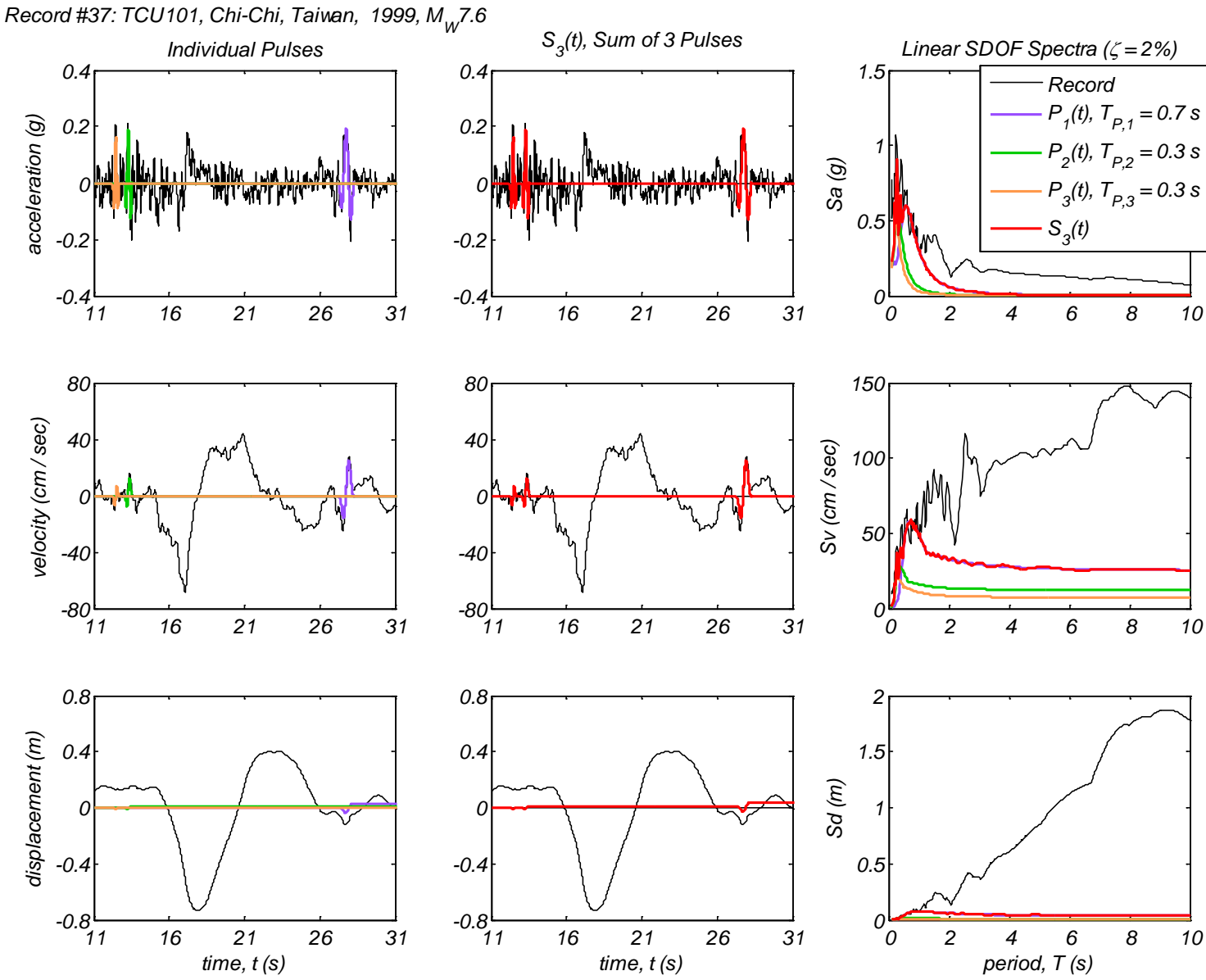
Appendix B6 – Time history and linear spectral response of three extracted pulses using the CPE<sub>A-AM</sub> method for 40 Motions



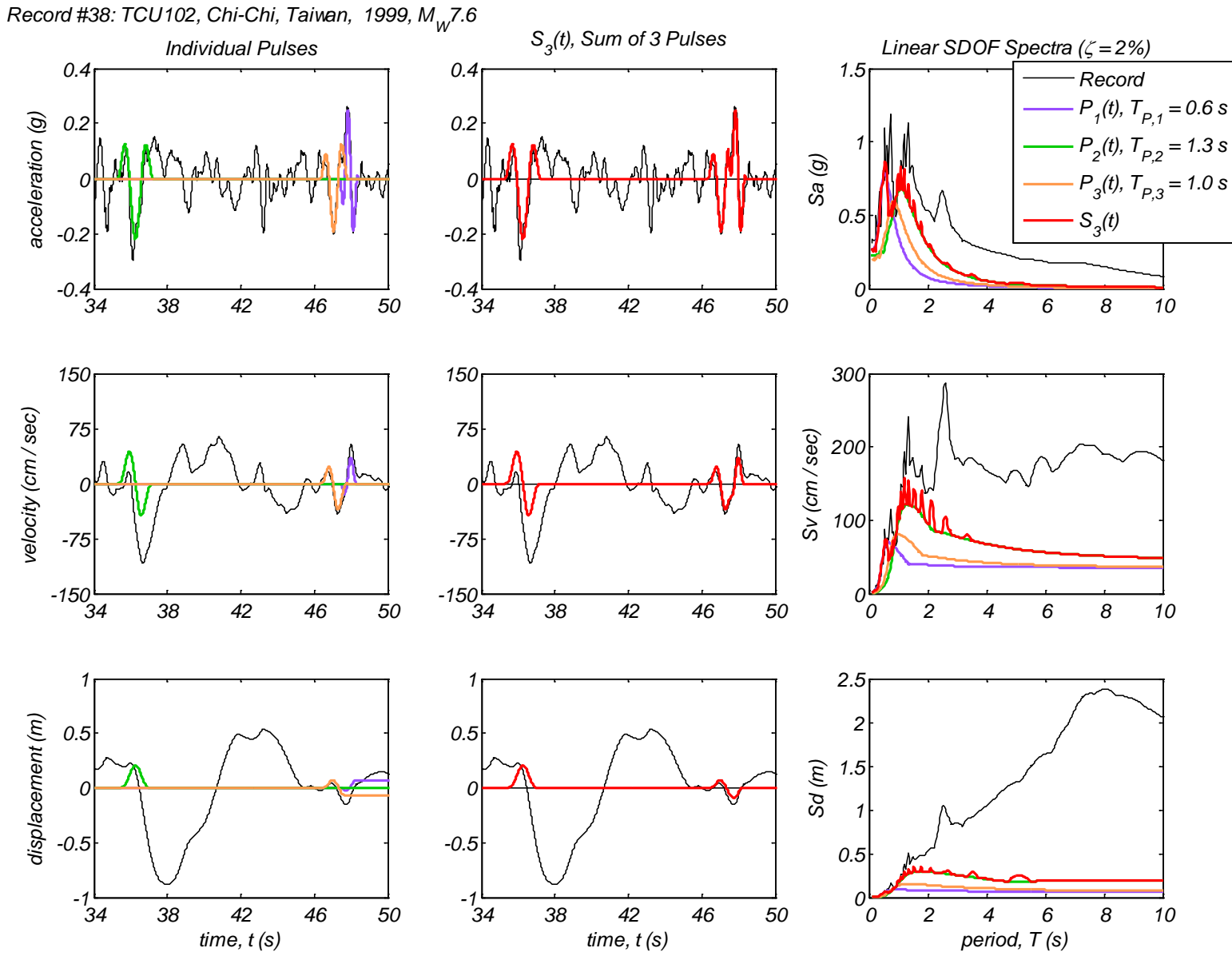
Appendix B6 – Time history and linear spectral response of three extracted pulses using the CPE<sub>A-AM</sub> method for 40 Motions



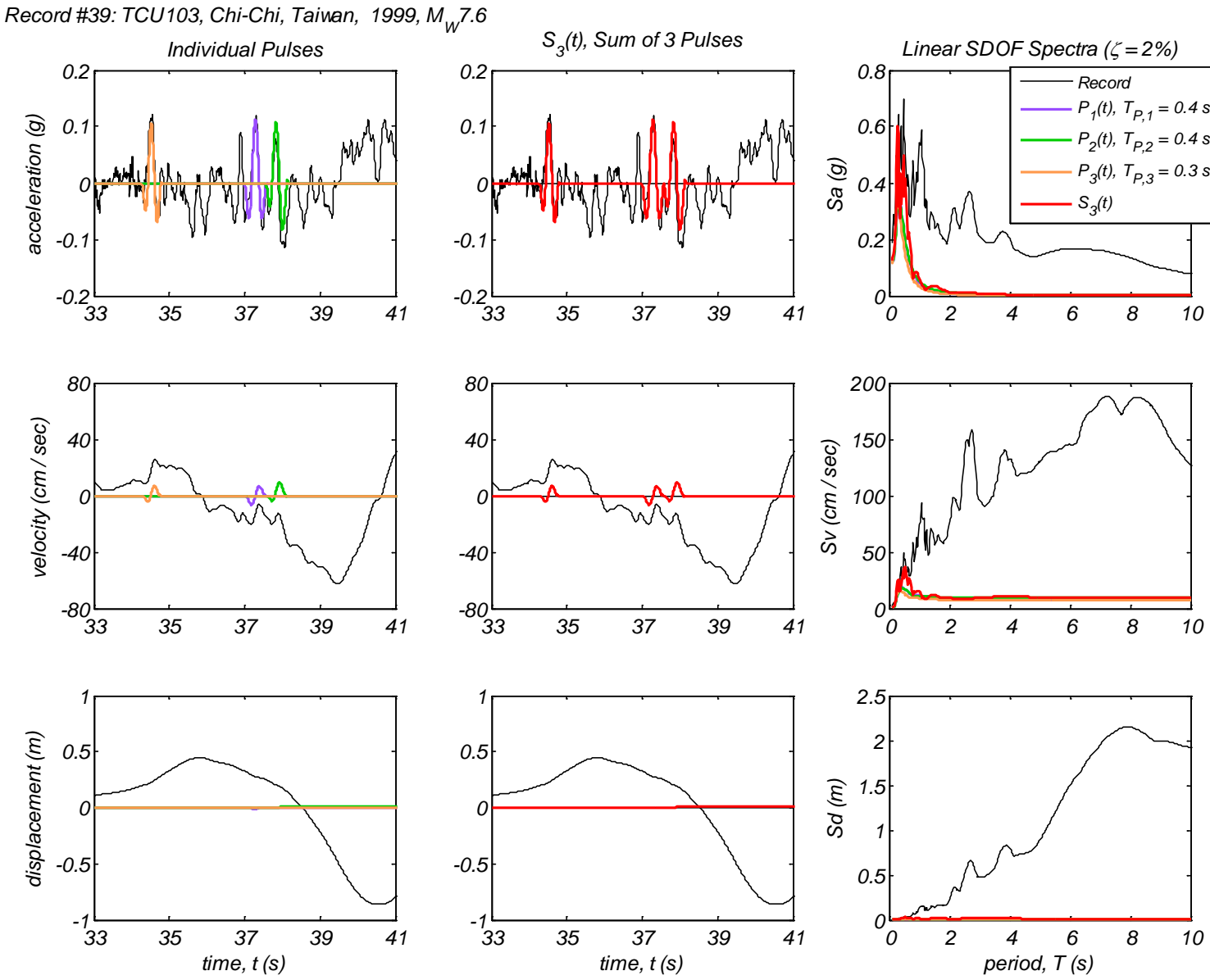
Appendix B6 – Time history and linear spectral response of three extracted pulses using the CPE<sub>A-AM</sub> method for 40 Motions



Appendix B6 – Time history and linear spectral response of three extracted pulses using the CPE<sub>A-AM</sub> method for 40 Motions



Appendix B6 – Time history and linear spectral response of three extracted pulses using the CPE<sub>A-AM</sub> method for 40 Motions



Appendix B6 – Time history and linear spectral response of three extracted pulses using the CPE<sub>A-AM</sub> method for 40 Motions

